Herpesvirus DNA

edited by
Yechiel Becker

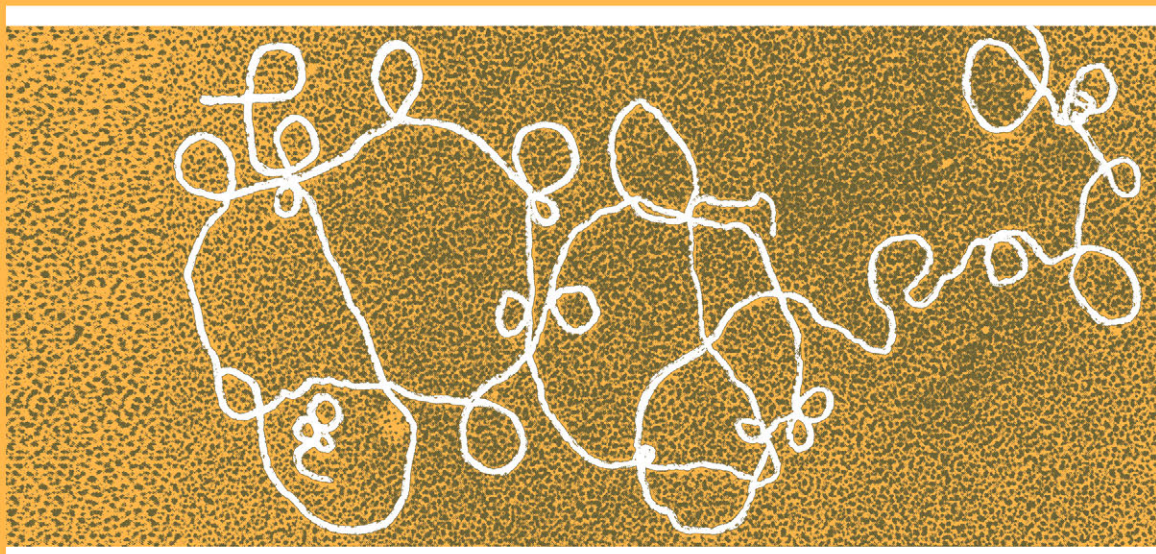

DEVELOPMENTS IN
MOLECULAR VIROLOGY · VOLUME 1

Springer-Science+Business Media, B.V.

HERPESVIRUS DNA

DEVELOPMENTS IN MOLECULAR VIROLOGY

VOLUME 1

Yechiel Becker, series editor

Series ISBN 90-247-2444-9

Herpesvirus DNA

Recent studies on the organization of viral genomes, mRNA transcription, DNA replication, defective DNA, and viral DNA sequences in transformed cells and bacterial plasmids

Edited by

YECHIEL BECKER
The Hebrew University of Jerusalem, Israel

1981

SPRINGER-SCIENCE+BUSINESS MEDIA, B.V.

ISBN 978-94-015-6899-9 ISBN 978-94-015-6897-5 (eBook)
DOI 10.1007/978-94-015-6897-5

PREFACE

Herpesviruses, classified in the family Herpesviridae, are important human and animal pathogens that can cause primary, latent or recurrent infections and even cancer. The major interest in research on herpesviruses today focuses on understanding the organization of the DNA genome, as well as on characterizing the viral genes in regard to their control and function. Modern techniques have allowed the viral DNA to become a molecular tool in the study of gene function, since it is now possible to implant the DNA into eukaryotic cells.

This book contains original studies on the structure and organization of the DNA of human and animal herpesviruses. The various chapters acquaint the reader with the organization of the viral DNA, the mRNA transcripts, the replicative intermediates of the viral DNA, defective DNA genomes and their mode of synthesis, analyses of the viral DNA sequences in transformed cells, and the relationship between the presence of viral DNA fragments in the cancer cells and the transformed state of the cells.

An attempt has been made to provide insight into the present experimental approach and to update the reader on the use of the most advanced molecular techniques like restriction enzyme analysis, blotting of viral nucleic acids, cloning of viral DNA fragments in bacterial plasmids, and transfection of cells with both cloned and uncloned viral DNA fragments. These studies will give the reader a clear perspective of the philosophy and technology of herpesvirus DNA research. The book will thus be of great value to all who are interested in understanding the molecular aspects of herpesvirus DNA and the biological properties of the viral genes.

I wish to thank all the contributors to this volume

which, I hope, will serve as a stimulus to scientists engaged in research on herpesviruses. To my regret, certain chapters which were promised did not arrive. The assistance of Dr. Julia Hadar with editing and indexing of the manuscripts and the excellent secretarial help of Mrs. Esther Herskovics are much appreciated.

Yechiel Becker
Jerusalem, January 1981

CONTENTS

ANIMAL HERPESVIRUSES

LIST OF CONTRIBUTORS

KEVIN P. ANDERSON,
Department of Molecular Biology
and Biochemistry,
University of California, Irvine
Irvine, California 92717, U.S.A.

SALLY S. ATHERTON,
Department of Microbiology,
University of Mississippi
Medical Center,
Jackson, Mississippi 39216, U.S.A.

K.F. BASTOW,
University of Cambridge,
Department of Pathology, Division
of Virology, Laboratories Block,
Addenbrooke's Hospital, Hills Road,
Cambridge CB2 2QQ, U.K.

YECHIEL BECKER,
Department of Molecular Virology,
The Hebrew University - Hadassah
Medical School,
Jerusalem, Israel

TAMAR BEN-PORAT,
Department of Microbiology,
Vanderbilt University School of
Medicine,
Nashville, Tennessee 37232, U.S.A.

J. BARKLIE CLEMENTS,
Institute of Virology,
University of Glasgow,
Glasgow, G11 5JR, Scotland, U.K.

ROBERT E. COSTA,
Department of Molecular Biology
and Biochemistry,
University of California, Irvine,
Irvine, California 92717, U.S.A.

DOLORES M. CUIFO,
Department of Pharmacology and
Experimental Therapeutics,
The Johns Hopkins University
Medical School,
725 North Wolfe Street,
Baltimore, Maryland 21205, U.S.A.

G. DARAI,
Institut für Medizinische Virologie
der Universität Heidelberg,
Im Neuenheimer Feld 324,
69 Heidelberg, F.R.G.

G. DARBY,
University of Cambridge,
Department of Pathology, Division
of Virology, Laboratories Block,
Addenbrooke's Hospital, Hills Road,
Cambridge CB2 2QQ, U.K.

STEVEN A. DAUENHAUER,
Department of Microbiology,
University of Mississippi Medical
Center,
Jackson, Mississippi 39216, U.S.A.

H. DELIUS,
European Molecular Biology
Laboratory,
Postfach 10.2209,
69 Heidelberg, F.R.G.

GAYATHRI B. DEVI,
Department of Molecular Biology
and Biochemistry,
University of California, Irvine,
Irvine, California 92717, U.S.A.

ANDREW J. EASTON,
Institute of Virology,
University of Glasgow,
Glasgow, G11 5JR, Scotland, U.K.

R.M. FLÜGEL,
Institut für Virusforschung am
Deutschen Krebsforschungszentrum,
Im Neuenheimer Feld 280,
69 Heidelberg, F.R.G.

NIZA FRENKEL,
The Brandecker Laboratories,
Department of Biology,
The University of Chicago,
Chicago, Illinois 60637, U.S.A.

ADAM FRIEDMAN,
Department of Genetics,
The Hebrew University,
Jerusalem, Israel

E.R. GAVIS,
Department of Embryology,
Carnegie Institution of Washington,
Baltimore, Maryland 21210, U.S.A.

BEVERLEY H. GAYLAND,
Department of Molecular Biology
and Biochemistry,
University of California, Irvine,
Irvine, California 92717, U.S.A.

J.L.M.C. GEELEN,
Laboratorium voor de Gezondheids-
leer, University of Amsterdam,
Amsterdam, The Netherlands

GARY S. HAYWARD,
Department of Pharmacology and
Experimental Therapeutics,
The Johns Hopkins University
School of Medicine,
725 North Wolfe Street,
Baltimore, Maryland 21205, U.S.A.

BERCH E. HENRY,
Department of Microbiology,
University of Mississippi
Medical Center,
Jackson, Mississippi 39216, U.S.A.

KANII HIRAI,
Eckerd College Biomedical
Research Institute, St. Petersburg,
Florida 33170, U.S.A.

IVAN HIRSCH,
Department of Experimental
Virology, Institute of Sera and
Vaccines,
101 03 Prague, Czechoslovakia

LOUIS E. HOLLAND,
Department of Molecular Biology
and Biochemistry,
University of California, Irvine,
Irvine, California 92717, U.S.A.

H.C. KAERNER,
Institute for Virus Research,
German Cancer Research Center,
Im Neuenheimer Feld 280,
6900 Heidelberg, F.R.G.

ALBERT S. KAPLAN,
Department of Microbiology,
Vanderbilt University School
of Medicine,
Nashville, Tennessee 37232, U.S.A.

JEFFREY M. LEIDEN,
The Brandecker Laboratories,
Department of Biology,
The University of Chicago,
Chicago, Illinois 60637, U.S.A.

HILLA LOCKER,
The Brandecker Laboratories,
Department of Biology,
The University of Chicago,
Chicago, Illinois 60637, U.S.A.

JOAN C.M. MACNAB,
Medical Research Council, MRC
Virology Unit, Institute of Virology,
Church Street,
Glasgow, G11 5JR, U.K.

T. MATSUO,
Department of Virology, Cancer
Institute, Hokkaido University
School of Medicine,
060 Sapporo, Japan

B. MATZ
Institut für Medizinische Virologie
der Universität Heidelberg,
Im Neuenheimer Feld 324,
69 Heidelberg, F.R.G.

S.L. MCKNIGHT,
Department of Embryology,
Carnegie Institution of Washington,
Baltimore, Maryland 21210, U.S.A.

A.C. MINSON,
University of Cambridge,
Department of Pathology, Division
of Virology, Laboratories Block,
Addenbrooke's Hospital, Hills Road,
Cambridge CB2 2QQ, U.K.

F. MIZUNO
Department of Bacteriology,
Asahikawa Medical College,
071-01 Asahikawa, Japan

M. NONOYAMA,
Life Sciences Biomedical Research
Institute, St. Petersburg,
Florida 33710, U.S.A.

DENNIS J. O'CALLAGHAN,
Department of Microbiology,
University of Mississippi
Medical Center,
Jackson, Mississippi 39216, U.S.A.

T. OSATO,
Department of Virology, Cancer
Institute, Hokkaido University
School of Medicine,
060 Sapporo, Japan

SAMUEL RABKIN,
Department of Molecular Virology,
The Hebrew University - Hadassah
Medical School,
Jerusalem, Israel

G.R. REYES,
Department of Pharmacology and
Experimental Therapeutics,
The Johns Hopkins University
School of Medicine,
725 North Wolfe Street,
Baltimore, Maryland 21205, U.S.A.

FRAZER J. RIXON,
Institute of Virology,
University of Glasgow,
Glasgow, G11 5JR, Scotland, U.K.

ROBIN A. ROBINSON,
Department of Microbiology,
University of Mississippi
Medical Center,
Jackson, Mississippi 39216, U.S.A.

YEHUDA SHTRAM,
Department of Molecular Virology,
Hebrew University - Hadassah
Medical School,
Jerusalem, Israel

JOHN STACZAK,
Department of Microbiology,
University of Mississippi
Medical Center,
Jackson, Mississippi 39216, U.S.A.

JAMES R. STRINGER,
Department of Molecular Biology
and Biochemistry, Cold Spring
Harbor Laboratories, Cold Spring
Harbor, New York, U.S.A.

WILLIAM C. SUMMERS,
Radiobiology Laboratories,
Yale University School of Medicine,
333 Cedar Street, New Haven,
Connecticut 06510, U.S.A.

A. TANAKE,
Life Sciences Biomedical Research
Institute, St. Petersburg,
Florida 33710, U.S.A.

LORI L. TRIBBLE,
Department of Molecular Biology
and Biochemistry,
University of California, Irvine,
Irvine, California 92717, U.S.A.

RALPH B. VANCE,
Department of Microbiology,
University of Mississippi
Medical Center,
Jackson, Mississippi 39216, U.S.A.

DON VLAZNY,
The Brandecker Laboratories,
Department of Biology,
The University of Chicago,
Chicago, Illinois 60637, U.S.A.

EDWARD K. WAGNER,
Department of Molecular Biology
and Biochemistry,
University of California, Irvine,
Irvine, California 92717, U.S.A.

MICHAEL J. WAGNER,
Radiobiology Laboratories,
Yale University School of Medicine,
333 Cedar Street, New Haven,
Connecticut 06510, U.S.A.

M.W. WESTSTRATE,
Laboratorium voor de Gezondheids-
leer, University of Amsterdam,
Amsterdam, The Netherlands

JOE H. WHARTON,
Department of Microbiology,
University of Mississippi
Medical Center,
Jackson, Mississippi 39216, U.S.A.

K. YAMAMOTO,
Department of Virology, Cancer
Institute, Hokkaido University
School of Medicine,
060 Sapporo, Japan

1. Introduction: Current trends in herpesvirus DNA research (a review)

Y. Becker

During the last ten years, marked progress has been made in the study of herpesviruses, particularly in elucidating the properties of the DNA genomes of various members of the Herpesviridae. New techniques for cleavage of DNA, cloning short fragments in bacterial plasmids and for DNA sequencing have considerably advanced our knowledge of the organization of the herpesvirus DNA genome which carries about 100 genes. The aim of the present review is not to cover all the publications in the field, but to indicate current trends in research on herpesvirus DNA and the direction in which present research is heading.

HERPESVIRUS GENOMES HAVE UNIQUE FEATURES

The viral DNA has a molecular weight of 100 x 10^6

The first study that revealed the molecular weight and properties of HSV-1 DNA was reported in 1968 (1); the DNA genome was found to be linear and double-stranded. These results were confirmed by studies from another laboratory (2, 3), and further investigations revealed that one of the two strands of HSV DNA is fragmented when treated with alkali (4). One interpretation of this phenomenon is the presence of ribonucleotides in the polydeoxyribonucleotide chain (5), although another possibility is the presence of gaps in the DNA chain of molecules obtained from purified virions (6). The exact reason for the alkali sensitivity of one of the DNA strands of HSV DNA is still not known.

HSV DNA has two unique sequences flanked by repeat sequences

Further insight into the organization of HSV DNA was contributed by Sheldrick and Berthelot (7). Studies on the

Y. Becker (ed), Herpesvirus DNA.

annealing properties of alkali-resistant single-stranded DNA revealed that the HSV DNA is made up of two covalently linked unique components, one large (L) and one small (S), each flanked by identical repeat sequences but with opposite orientation. The internal repeats of the two unique sequences are ligated, forming a linear DNA molecule of about 100 x 10^6 daltons. DNA genomes from other herpesviruses were found to differ in their internal organization. The organization of the joint region between the L and S components is described in this book by Wagner and Summers (Chap. 2).

There are three classes of herpesvirus DNA

Honess and Watson (8) suggested that the viral DNA genomes should be divided into three classes: the first class has only one unique DNA sequence, like the DNA of channel catfish herpesvirus or Epstein-Barr virus (EBV), the second class contains DNA genomes which have two unique sequences, but the terminal repeat sequence of the S component is absent, and the third class of DNA molecules contains the L and S unique components and the four repeat sequences. Cleavage with restriction enzymes showed that HSV DNA (class 3) has four molecular conformations in regard to the relative orientations of the L and S components (9). The molecular process which is involved in the formation of the four subpopulations of HSV DNA (class 3) is not yet known and various models have been proposed (10, 11, 12). Pseudorabies virus class 2 DNA, which lacks the terminal repeat sequences of the S component, appears in two molecular forms in which only the L unique component is inverted in relation to the S component (See Ben Porat and Kaplan, Chap. 18).

EBV DNA was found to resemble the L unique component of other herpesviruses, but at each molecular end there are analogous sequences (13). Similarly, Herpesvirus saimiri and H. ateles have genomes with a unique sequence of low G + C content that resembles the L component of class 3

viruses and is bounded on either side by reiterated sequences with a high G + C content (14, 15).

Detailed analyses are presented in this book on the organization and function of the DNA of cytomegalovirus (Geelen and Weststrate, Chap. 16), Tupaia monkey virus (Darai et al., Chap. 17), equine abortion virus (O'Callaghan et al., Chap. 19), Marek's disease virus and herpes turkey virus (Nonoyama and Hirai, Chap. 21).

Temperature sensitive (ts) mutants are essential for studying the gene arrangement in the viral DNA

Realizing the importance of ts mutants in the genetic analysis and gene mapping of herpesviruses, the research groups led by J.H. Subak-Sharpe and P.A. Schaffer independently investigated ts mutants of HSV-1 and HSV-2. (Some of the work done by these two groups can be found in refs. 16-20). Collaborative studies between these two groups (21) led to a better understanding of the genetic mapping of HSV, and studies by Roizman and his associates, using ts mutants of Schaffer and others (22-25) led to the presentation of a partial genetic map for HSV-1 and HSV-2 (26, 27). The fine mapping of the thymidine kinase and the DNA polymerase genes of HSV are discussed below.

RESTRICTION ENZYME CLEAVAGE PATTERNS IN PARENTAL AND RECOMBINANT DNA

The mode of recombination between herpesvirus DNA molecules is not known, and the viral and cellular enzymes involved in this process have yet to be elucidated. However, infection of cells with two strains of HSV gives rise to recombinants, and restriction enzyme analysis of recombinant viral DNA allows the determination of the origin of each DNA fragment (24, 28). Physical mapping of ts mutants, using intertypic marker rescue, was reported by Stow and Wilkie (29).

Mapping of viral mRNA on the viral genome

Establishment of the restriction enzyme cleavage maps for HSV (27,30,31) led to the use of sub-genomic fragments of DNA as probes. This approach, which allowed detailed analyses to be made of the mRNA transcription sites on the viral DNA, is presented by Clements et al. (Chap. 3) and Wagner et al. (Chap. 4).

Cloning of viral DNA fragments in bacterial plasmids

This technique has opened the way to preparing a library of cloned fragments that in the future will allow the genes present in each fragment to be analyzed at the level of nucleotide sequences. Approval of the E. coli plasmid pBR322 as a vector for P3-EK2 recombinant DNA research (32) has advanced studies on cloned herpesvirus DNA fragments even further. Cloned DNA fragments of HSV-1 and equine abortion virus were used in the studies by Clements et al. (Chap. 3) and O'Callaghan et al. (Chaps. 19 and 20), respectively. Colbere-Garapin et al. (33) cloned the HSV-1 DNA fragment containing the viral TK gene in the pBR322 plasmid and used it for transforming L(TK^-) mouse cells, while Enquist et al. (34) cloned DNA fragments isolated from defective and nondefective HSV-1 in EK-2 coliphage λgtWES·λB. Post et al. (35) have cloned all the restriction fragments of HSV-1 in the pBR322 plasmid. Other laboratories have also reported on the availability of cloned DNA (36). Since the means to amplify viral DNA fragments by growing them in bacterial cells is now available, it will soon be possible to elucidate the sequence organization of the major viral genes. Hayward et al. (Chap. 15) have indeed studied the structure of the HSV TK gene in detail.

Fine mapping of the HSV TK and DNA polymerase genes

Morse et al. (22) presented the localization of templates specifying HSV functions and polypeptides on the viral genome. The TK gene is mapped between the coordinates 0.25 to 0.35 and the phosphonoacetic acid resistant gene (the

DNA polymerase gene) between coordinates 0.42 to 0.52 map units. More recently, Halliburton et al. (36) mapped the HSV-1 TK gene at 0.300 to 0.309 map units and the HSV-2 TK gene at 0.295 to 0.315 map units. Smiley et al. (37) constructed a genetic map of the TK gene using a new technique for measuring the frequency of TK^+ virus in populations of TK^- mutants. The TK gene was oriented in respect to the DNA polymerase gene. The exact map location of the TK gene is provided by Hayward et al. (Chap. 15).

Studies by Parris et al. (38) using four ts mutants of HSV-1 which were mapped by marker rescue and two-factor crosses identified a DNA fragment which maps in the L region of the genome. The results coordinate with only one or two molecular arrangements of the viral DNA. The ts mutation affecting the HSV DNA polymerase has been located on the physical map of the viral genome (39). All the mutations were found to cluster in a 4.9-kilobase pair region between map units 38.6 to 41.8. The phosphonoacetic acid resistant mutation was mapped within a 2.9-kilobase region between map units 40 to 41.8. Similar studies on other genes will eventually provide the complete genetic map for HSV.

REPLICATION OF HERPESVIRUS DNA

Replicative intermediates of the viral DNA

A rolling circle model for the replication of HSV-1 DNA was proposed (27), according to which the viral DNA circularizes after entering the nucleus and replication is initiated at one or two sites on the molecule. DNA synthesis initially proceeds in both directions until nicks in the DNA template strand convert the replicating complex into a rolling circle which is excised to unit size molecules. Ben Porat and Kaplan (Chap. 18) describe a similar replication process for pseudorabies virus DNA. Hirsch (Chap. 5) has identified an initiation site for HSV DNA replication at the junction between the internal repeats of the unique L and S components of the viral DNA. In a

series of studies on HSV-1 DNA replication (40, 41), two initiation sites for HSV-1 DNA replication were suggested. Electron microscopy showed that replication of the viral DNA is semiconservative and the two initiation sites for DNA replication are internally located, one in the L and S junction, and the other in the center of the L component. Two replication forks move simultaneously, and replicative intermediates with "eyes" (or "loops") were observed. Since the initiation sites are not in the center of the DNA molecule, Y-shaped molecules were seen due to termination of synthesis by one of the replication forks having reached one of the molecular ends. The synthesis of the viral DNA resembles that of bacteriophage DNA genomes (42). In these studies, viral DNA molecules supporting the rolling circle model of HSV-1 DNA replication were not observed.

Defective DNA and its mode of replication

Defective HSV-1 DNA was found to be 0.008 g/ml more dense than the normal viral DNA (43). Defective DNA arises from the repeat sequence of the S component and is made up of repeats of the original sequence (44). Further studies (45; Chaps. 10,11) suggested that defective DNA replicates by the mechanism of rolling circles, thus leading to reiterations of the original sequence that arises from the repeat sequence of the S component. Studies by Cuifo and Hayward (Chap. 8) revealed a second type of defective HSV-1 DNA which arises from a sequence originally present in the center of the unique L component of the viral DNA. It is possible that both types of defective HSV-1 DNA arise from either of the two initiation sites for DNA replication: the first arises from the initiation site at the L junction between L and S, and the second from the initiation site at the center of the L component. It is possible that a mistake in the initiation of DNA synthesis leads to the appearance of a nucleotide sequence, which is replicated by the viral DNA polymerase by a mechanism resembling rolling circles (Chap. 11). A different type of defective viral DNA is described by Kaerner (Chap. 9).

HERPESVIRUS DNA SEQUENCES IN TRANSFORMED CELLS

Transformation of cells with inactivated herpesviruses

The study of Duff and Rapp (46) on in-vitro transformation of cells by uv-irradiated virus revealed that herpesviruses have an oncogenic potential under conditions where the lytic properties of the virus are changed. To prove that the cells were indeed transformed by the virus, it was mandatory to detect residual virus sequences in the genomes of such cells. Leiden and Frenkel (Chap. 12) have carefully analyzed the nature of the HSV DNA sequences in transformed cells. Viral DNA sequences were also found in the genome of cells transformed by equine abortion virus (Robinson and O'Callaghan, Chap. 20).

Transfection of cells with viral DNA

The first demonstration that an HSV-1 gene can be incorporated into mammalian cell DNA and even function in the new environment was that of Munyon et al. (47). It was shown that TK^- L cells (designated LTK^-) were converted into the TK^+ genotype by HSV-1. Transfection of cells with naked DNA (48) was used for the transformation of such cells by Wigler et al. (49). This 'biochemical' transformation of cells has been carefully analyzed by Darby et al. (Chap. 13). Macnab (Chap. 14) used HSV mutants to characterize the viral DNA fragments which can functionally complement the mutations.

STUDIES USING CLONED HERPESVIRUS DNA SEQUENCES

To summarize, the availability of cloned fragments of herpesvirus DNA has opened new avenues for studying the organization and function of the viral DNA. Studies using cloned viral DNA fragments as probes include:

a) Transfection of animal cells with cloned DNA to biochemically transform TK^- cells (Chaps. 13 and 15).
b) Identification of the sequences in HSV-1 DNA which activate an endogenous mouse retrovirus (50).

c) Identification of the HSV mRNA sequences (Chap. 3).

d) Identification of viral DNA sequences in transformed cells (Chaps. 12, 14 and Chap. 20).

e) Detailed mapping of EBV DNA (51).

Sequencing of the viral genes, which is in progress in a number of laboratories, will finally solve many of the problems concerning herpesvirus DNA.

REFERENCES

1. Becker, Y., Dym, H. and Sarov, I. Virology 36:184-192, 1968.
2. Frenkel, N. and Roizman, B. J. Virol. 8:591-593,1971.
3. Kieff, E.D., Bachenheimer, S.L. and Roizman, B. J. Virol. 8:125-132, 1971.
4. Wilkie, N.M. J. gen Virol. 21:453-467, 1973.
5. Hirsch, J. and Vonka, V. J. Virol. 13:1162-1168, 1974.
6. Frenkel, N. and Roizman, B. J. Virol. 10:565-572,1972
7. Sheldrick, P. and Berthelot, N. Cold Spring Harbor Symp. Quant. Biol. 39:667-678, 1974.
8. Honess, R.W. and Watson, D.H. J. gen. Virol. 37:15-37, 1977.
9. Hayward, G.S., Jacob, R.J., Wadsworth, S.C. and Roizman B. Proc. Natl. Acad. Sci. USA 72:4243-4247, 1975.
10. Roizman, B., Hayward, G., Jacob, R., Wadsworth, S., Frenkel, N., Honess, R.W. and Kozak, M. In: Oncogenesis and Herpesviruses II (Eds. G. de-Thé, M.A. Epstein and H. zur Hausen), IARC Scientific Publications No. 11, Lyon, 1975, pp. 3-38.
11. Becker Y. J. Theoret. Biol. 75:339-347, 1978.
12. Becker, Y. Persp. Biol. Med. 23:92-103, 1979.
13. Given, D. and Kieff, E. J. Virol. 28:524-542, 1978.
14. Bornkamm, G.W., Delius, H., Fleckenstein, B., Werner, F.J. and Mulder, C. J. Virol. 19:154-161, 1976.
15. Fleckenstein, B., Bornkamm, G.W., Mulder, C., Werner, F.J., Daniel, M.D., Falk, L.A. and Delius, H. J. Virol. 25:361-373, 1978.
16. Brown, S.M., Ritchie, D.A. and Subak-Sharpe, J.H. J. gen Virol. 18:329-346, 1973.
17. Hay, J. and Subak-Sharpe, J.H. J. gen. Virol. 31: 145-148, 1976.

18. Schaffer, P.A., Tevethia, M.J. and Benyesh-Melnick,M. Virology 58:219-228, 1974.

19. Parris, D.S., Courtney, R.J. and Schaffer, P.A. Virology 90:177-186, 1978.

20. Wilkie, N.M., Stow, N.D., Marsden, H.S., Preston, V., Cortini, R., Timbury, M.C. and Subak-Sharpe, J.H. In: Oncogenesis and Herpesviruses II (Eds. G. de-Thé, W. Henle and F. Rapp), IARC Scientific Publication No. 24, Lyon, 1978, pp. 11-31.

21. Timbury, M.C., Hendricks, M.L. and Schaffer, P.A. J. Virol. 18:1139-1142, 1976.

22. Morse, L.S., Pereira, L., Roizman, B. and Schaffer, P.A. J. Virol. 26:389-410, 1978.

23. Knipe, D.M., Ruyechan, W.T., Roizman, B. and Halliburton, I.W. Proc. Natl. Acad. Sci. USA 75:3896-3900, 1978.

24. Ruyechan, W.T., Morse, L.S., Knipe, D.M. and Roizman, B. J. Virol. 29:677-697, 1979.

25. Knipe, D.M., Ruyechan, W.T. and Roizman, B. J. Virol. 29:698-704, 1979.

26. Marsden, H.S., Stow, N.D., Preston, V.G., Timbury, M.C. and Wilkie, N.M. J. Virol. 28:624-655, 1978.

27. Roizman, B. Cell 16:481-494, 1979.

28. Preston, V.G., Davison, A.J., Marsden, H.S., Timbury, M.C., Subak-Sharpe, J.H. and Wilkie, N.M. J. Virol. 28:499-517, 1978.

29. Stow, N.D., and Wilkie, N.M. Virology 90:1-11, 1978.

30. Skare, J., Summers, W.P. and Summers, W.C. J. Virol. 15:726-732, 1975.

31. Wilkie, N.M. J. Virol. 20:222-233, 1976.

32. Sutcliffe, J.G. Nucleic Acids Res. 5:2721-2728,1978.

33. Colbere-Garapin, F., Chousterman, S., Horodniceanu,F., Kourilsky, P.and Garapin, A-C. Proc. Natl. Acad. Sci. USA 76:3755-3759, 1979.

34. Enquist, L.W., Madden, M.J., Schiop-Stansly, P. and Vande Woude, G.F. Science 203:541-544, 1979.

35. Post, L.E., Conley, A.J., Mocarski, E.S. and Roizman, B. Proc. Natl. Acad. Sci. USA 77:4201-4205, 1980.

36. Halliburton, I.W., Morse, L.S., Roizman, B. and Quinn, K.E. J. gen. Virol. 49:235-253, 1980.

37. Smiley, J.R., Wagner, M.J., Summers, W.P. and Summers, W.C. Virology 102:83-93, 1980.

38. Parris, D.S., Dixon, R.A.F. and Schaffer, P.A. Virology 100:275-287, 1980.

39. Chartrand, P., Crumpacker, C.S., Schaffer, P.A. and Wilkie, N.M. Virology 103:311-326, 1980.

40. Shlomai, J., Friedmann, A. and Becker, Y. Virology 69:647-659, 1976.

41. Friedmann, A., Shlomai, J. and Becker, Y. J. gen. Virol. 34:507-522, 1977.

42. Kornberg, A. DNA replication. W.H. Freeman & Co., San Francisco, 1980.

43. Wagner, M., Skare, J. and Summers, W.C. Cold Spring Harb. Symp. Quant. Biol. 39:683-686, 1974.

44. Frenkel, N., Locker, H., Batterson, W., Hayward, G.S. and Roizman, B. J. Virol. 20:527-531, 1976.

45. Becker, Y., Asher, Y., Weinberg-Zahlering, E., Rabkin, S., Friedman, S. and Kessler, E. J. gen. Virol. 40:319-335, 1978.

46. Duff, R. and Rapp, F. J. Virol. 12:209-217, 1973.

47. Munyon, W., Kraiselbund, E., Davis, D. and Mann, J. J. Virol. 7:813-820, 1971.

48. Graham, F.L. and van der Ebb, A.J. Virology 52: 456-467, 1973.

49. Wigler, M., Silverstein, S., Lee, L.S., Pellicer, A., Cheng, Y.C. and Axel, R. Cell 11:223-232, 1977.

50. Boyd, A.L., Enquist, L., Vande Woude, G.F. and Hampar, B. Virology 103:228-231, 1980.

51. Dambaugh, T., Beisel, C., Hummel, M., King, W., Fennewald, S., Cheung, A., Heller, M., Raab-Traub,N. and Kieff, E. Proc. Natl. Acad. Sci. USA 77:2999-3003, 1980.

2. Structure of HSV-1 DNA at the joint regions

Michael J. Wagner and William C. Summers

INTRODUCTION

Herpes simplex and several other members of the herpes group of viruses are unique among known animal viruses in having a genome composed of two segments which, while covalently linked in the virion, undergo a rearrangement during virus replication to produce a population of progeny genomes in which all four possible end to end orientations of the two segments are found (for a review, see Roizman,B., The structure and isomerization of herpes simplex virus genomes, Cell 16, 481-494, 1979). Thus, even plaque purified stocks of herpes simplex virus contain four isomeric forms of the viral genome. It is not known if all four forms are infectious, or what function genome rearrangement serves in the viral life cycle.

The point at which the two segments of the HSV genome are joined has been called the "joint." Sheldrick and Berthelot were the first to show that sequences at the ends of the genome are homologous to sequences at the joint (1). Specifically, the region of each segment next to the joint is an inverted repeat of the end of that segment. The events which result in genome isomerization must be occurring within or just adjacent to these inverted, repeated sequences at the ends and the joint. Also, these sequences must be involved in the formation of concatemers, which occurs during the replication of the HSV genome (2), and in the maturation of progeny DNA molecules from the concatemeric replicative intermediates.

We began investigation of the structure of the joint and the ends of herpes simplex virus DNA as a result of the observation, made in our laboratory, that the end of the long segment of the HSV genome was heterogeneous (3).

Y. Becker (ed), Herpesvirus DNA.

In restriction endonuclease digests of DNA from plaque purified virus, this end was represented by a group of fragments differing from one another by multiples of approximately 280 base pairs. We have constructed a fine structure map of restriction endonuclease sites in the joint region and at the ends, and have shown that the 280 base pair insertions occur both at the end of the L segment and at the joint, and that these insertions represent a tandem duplication of a region containing the terminal redundancy or its inverted repeat at the joint (4). Our results also have certain implications for the mechanisms of genome isomerization and concatemer formation and maturation.

EXPERIMENTAL

A digest of HSV-1 strain KOS DNA with EcoRI and HpaI restriction endonucleases contains a fragment of approximately 10.8 kilobases (1 kilobase = 1,000 base pairs) which spans the joint region (5,6). This fragment was isolated on an 0.7% agarose gel and redigested with HincII and AluI restriction endonucleases (Figure 1). In both cases, the sum of the molecular weights of the fragments produced was greater than 10.8 kilobases. Also, two fragments differing in molecular weight by 280 base pairs were produced in less than molar yield as compared to all of the other fragments. The fragments were ordered by isolation and recleavage of individual fragments and by analysis of partial digestion products. Figure 2 shows that the less than molar fragments (A and A*) map in the same place, and that the AluI-A and HincII-A fragments overlap. Thus the heterogeneity present at the end of the L segment is also present at the joint, with some DNA molecules containing an insertion of 280 base pairs. This insertion occurred somewhere within the region of overlap between HincII-A and AluI-A, a region of approximately 2800 base pairs which contains the joint.

The AluI-A fragment and the corresponding fragments

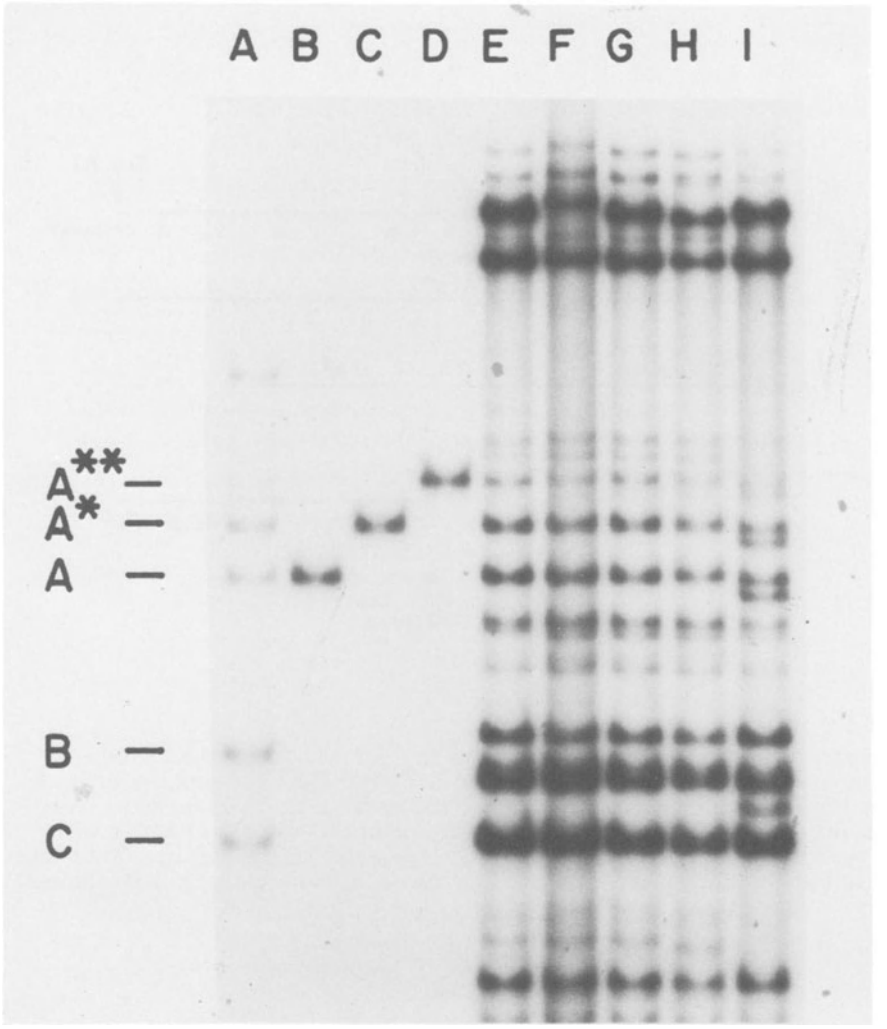

Figure 1. AluI fragments of the joint region and intact HSV DNA separated on a 0.7% agarose gel. Only the upper portion of the gel is shown. (A) AluI digest of the EcoRI-HpaI joint-spanning fragment. (B,C,D) Isolated AluI-A,A*, and A** fragments. (E-I) AluI digest of intact DNA from 5 plaque-purified stocks of HSV-1 strain KOS. These DNAs were used in the experiment shown in Figure 7.

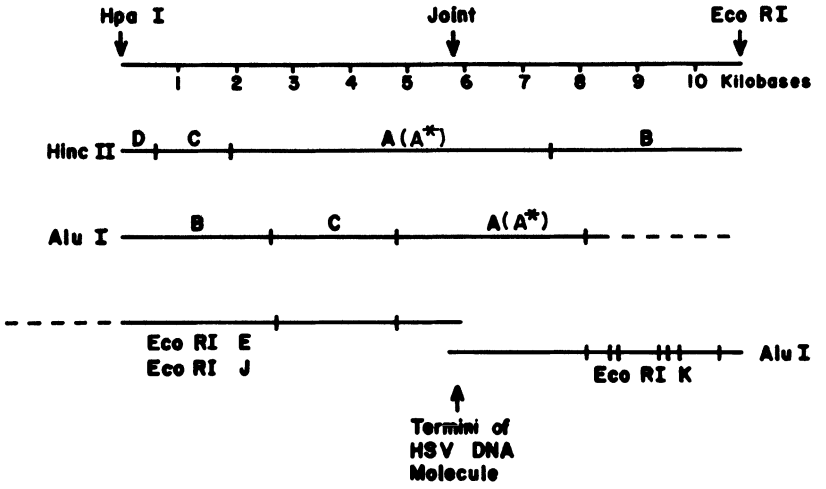

Figure 2. HincII and AluI cleavage maps of the EcoRI-HpaI joint-spanning fragments and of the termini of HSV DNA. Fragment A produced by both enzymes is heterogeneous. The maps of the termini have been inverted and aligned with the map of the joint region. EcoRI-E and J are the terminal fragments of the L segment in its two orientations; EcoRI-K is the terminal fragment of the S segment in both orientations.

with one or more insertions could be recovered directly from a total digest of HSV DNA (Figure 1) and these fragments were therefore chosen for further study. Figure 3 shows HinfI, BglI, and SmaI digests of AluI-A, A*, and A**. (We designate fragments containing insertions with asterisks, the number of which corresponds to the number of repetitions of the insertion.) The A fragments produced by HinfI and BglI again appear to exist in multiple forms differing by 280 base pairs. No such heterogeneous fragment can be found in SmaI digests, since the patterns obtained with this enzyme for AluI-A,A*, and A** appear identical. SmaI fragments were ordered by recleavage of SmaI partial digestion products (Figure 4), and HinfI, BglI and TaqI sites were also located by redigestion of isolated fragments. (Figure 5).

As can be seen from Figure 4, SmaI-F and F*, which differ in molecular weight by 10 base pairs, map in the same place. These two fragments were also found to be present in half molar yield as compared to all the other SmaI fragments (Figure 6). Thus, there is a previously undetected heterogeneity in this region, with approximately half of the molecules containing SmaI fragment F and half containing fragment F*. To determine whether this heterogeneity is always generated during virus growth, as is the 280 base pair heterogeneity, the virus stock was plaque purified. DNA was prepared from five different plaque purified stocks and AluI-A fragments were isolated from each and redigested with SmaI. Figure 7 shows that one virus stock contained only SmaI-F at the joint, indicating that the generation of fragment F* is not obligatory for HSV-1 growth. However, Figure 7 also shows that SmaI fragment A varies in size among the different stocks. Heterogeneities, probably comprising small insertions and deletions, seem to occur frequently in this region of the genome.

The 280 base pair heterogeneity seemed to disappear upon SmaI digestion. However, densitometer tracings of the autoradiograms revealed that the molar yields of SmaI

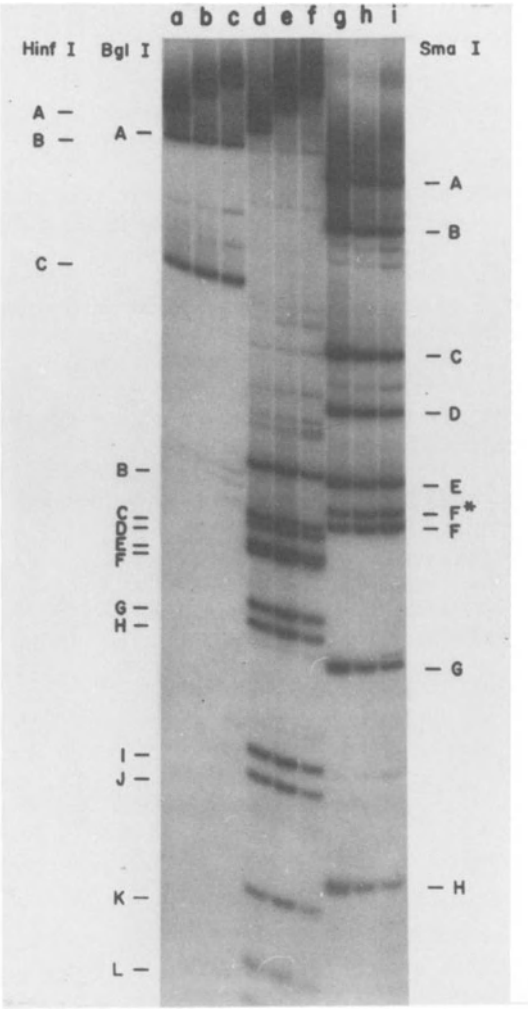

Figure 3. HinfI, BglI, and SmaI digests of AluI joint-spanning fragments separated on a 5% acrylamide gel. (a,b,c) HinfI digests of AluI-A,A*,andA**, respectively. (d,e,f) BglI digests of AluI-A,A* and A**, respectively. (g,h,i) SmaI digests of AluI-A,A*,and A** respectively.

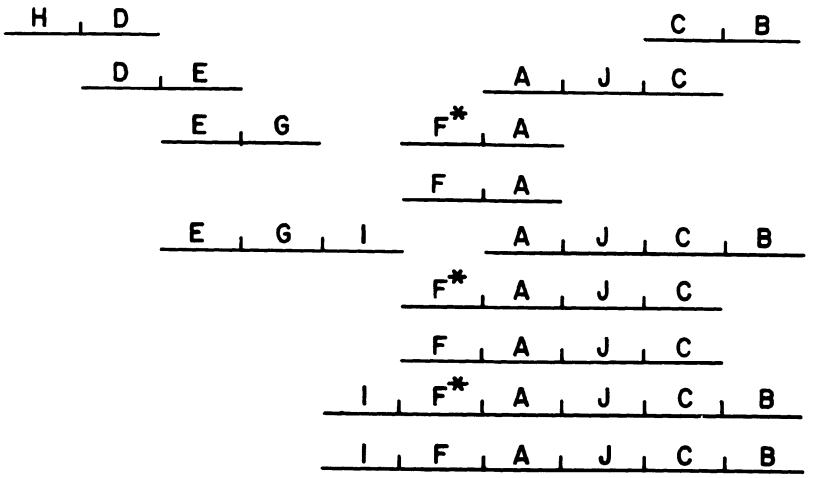

Figure 4. Composition and orientation of SmaI partial digestion products of AluI-A. Partial digestion products were isolated from an agarose gel and redigested with SmaI to determine their composition. The only self-consistent orientation of all the partial products, shown here, places fragments F and F* at the same position.

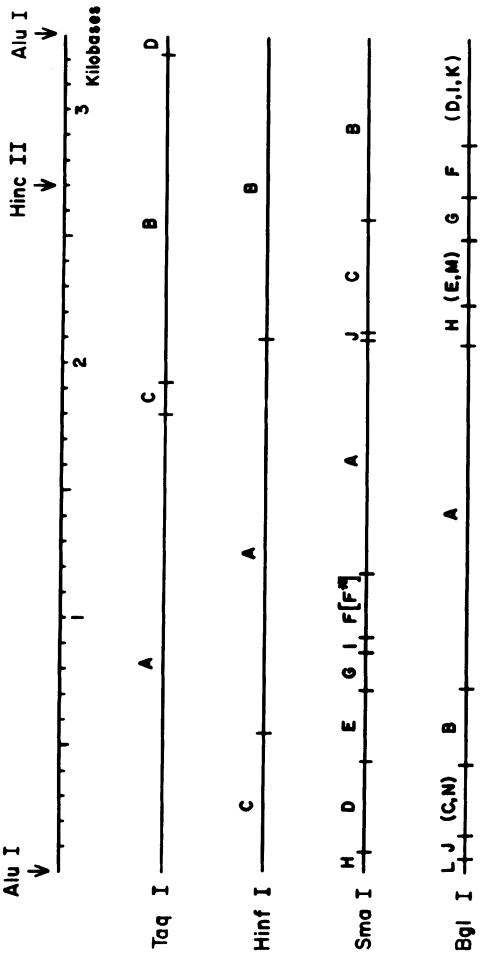

Figure 5. Map of TaqI, HinfI, SmaI, and BglI cleavage sites within the AluI joint spanning fragment containing no insertions (AluI-A). The relative order of fragments in parentheses has not been determined.

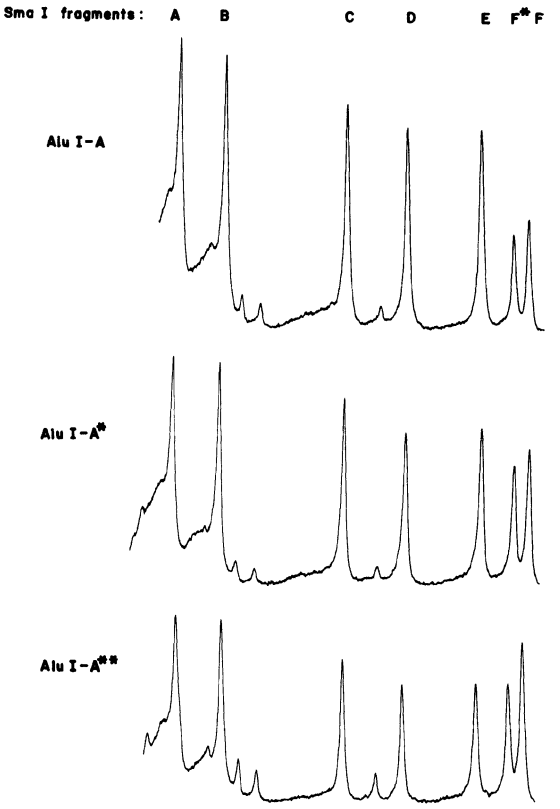

Figure 6. Densitometer tracings of autoradiographs of 5% acrylamide gels containing separated SmaI fragments of AluI-A, A*, and A**.

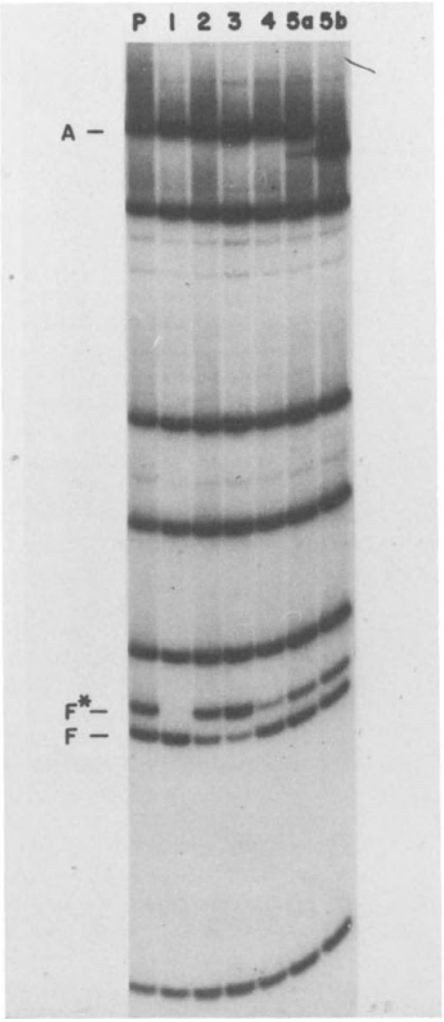

Figure 7. SmaI digestions of AluI-A fragments isolated from the DNA of five stocks of HSV-1 derived from single plaques. (P) is the parental stock, and (1) through (5) are the plaque purified stocks derived from (P). AluI-A occurred as a doublet in stock 5 (see Figure 1, track i). The two fragments were isolated and digested separately and are labeled 5a and 5b.

fragments F and F* increased with increasing numbers of 280 base pair insertions (Figure 6). An analysis of the molecular weights and compositions of the SmaI partial digestion products of HinfI fragments A and A* showed that HinfI-A* contained a tandem duplication of SmaI fragments I and F or F*. The sum of the molecular weights of these fragments (I = 42 base pairs, F = 230 base pairs) accounts for essentially the entire 280 base pair heterogeneity.

The precise location of the joint can be determined by comparing the termini with the joint region, since the termini are inverted repeats of sequences on either side of the joint. When terminal AluI fragments of HSV DNA are digested with SmaI, the fragments produced are consistent with the termini being inverted repeats of sequences at the joint. However, in those molecules containing only one copy of SmaI fragments I and F at the joint (i.e., molecules containing AluI-A), the inverted repeats of the termini must overlap, since SmaI-F and most of SmaI-I are present at both ends of the molecule (Figure 8). There is no single point which can be called the joint. Rather, this region of overlap is the true joint. The overlap also defines the terminal redundancy of the HSV-1 DNA molecule. For our strain (KOS), the terminal redundancy must therefore be 265 to 295 base pairs.

DISCUSSION

We have shown that two types of heterogeneity exist in the joint region of the DNA of HSV-1 strain KOS. The first type is due to the presence of a variable number of copies of a 280 base pair sequence which represents the joint between the L and S segments and closely corresponds to the terminal redundancy of the viral DNA molecule. This heterogeneity is present in all plaque purified virus stocks at both the joint and the terminus of the L segment, and the generation of this specific heterogeneity appears therefore to be an obligatory part of the virus life cycle. Locker and Frenkel have recently shown that a similar type

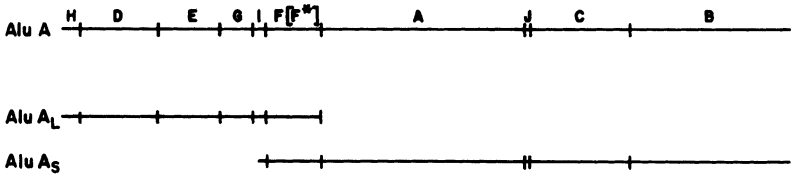

Figure 8. SmaI cleavage maps of the AluI joint-spanning fragment (AluI-A) and the terminal AluI fragments. The maps of the termini have been inverted and aligned with the map of the joint region. Alu-A_L is the terminal fragment from the L segment; Alu-A_S is the terminal fragment from the S segment.

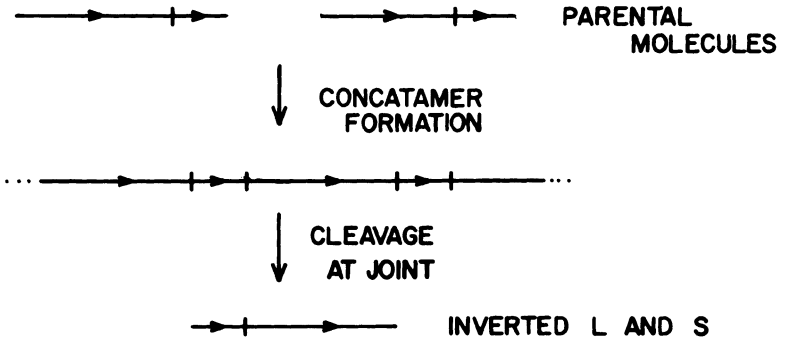

Figure 9. Proposed model for segment inversion. Parental molecules, with L and S segments in identical orientations, are joined head-to-tail to form a concatemer. Cleavage of the concatemer at the parental "joints" results in the production of progeny molecules in which both segments are inverted with respect to the parental molecules.

of heterogeneity is present in the DNAs of HSV-1 strains Justin and F, although the size of the reiterated sequence varies somewhat between strains (7). The second type of heterogeneity is due to the presence of small insertions and deletions within or adjacent to the joint. These insertions and deletions vary in size and location and are not present in all plaque purified virus stocks, indicating that they probably have no specific role in the virus life cycle. Perhaps the mechanism which duplicates and deletes the 280 base pair insertions also creates a hot spot for non-specific insertions and deletions.

The genome of herpes simplex virus is terminally redundant, that is, a short sequence at one terminus is directly repeated at the other terminus (8). Our analysis of restriction endonuclease sites at the termini of HSV-1 strain KOS indicate that this sequence must be limited to 265 to 295 base pairs. Further, it is this sequence which is tandemly reiterated in molecules containing 280 base pair insertions at the joint or at the terminus of the L segment. Insertions are not found at the terminus of the S segment, although the same sequences are present there as at the terminus of the L segment. We speculate that some feature of the DNA adjacent to the terminal redundancy in the L segment is necessary to produce duplications of the terminal redundancy.

If the two segments that make up the HSV genome are each viewed as having complete inverted repetitions at their ends (including an inverted repetition of the terminal redundancy) and are further viewed as being abutted end to end to make a complete genome, it would be expected that there would be a tandem duplication of the inverted terminal redundancy at the joint. This is indeed true of those DNA molecules having 280 base pair insertions at the joint. However, a large fraction of the molecules have only one copy of the 280 base pair sequence at the joint, and thus only one copy of the inverted terminal redundancy. In these molecules, the L and S segments overlap at the joint, and the joint itself must be

considered to be the region of overlap, as there is no single point where the two segments meet.

It is worth considering how these structures at the joint and termini may be involved in the processes of genome isomerization and concatemer formation and maturation. Genome isomerization is the result of inversion of the unique portions of the L and S segments. As first suggested by Sheldrick and Berthelot (1), this inversion could occur by intramolecular recombination between the inverted repeats at the ends of the segments. We have found that the frequency of recombination between HSV genomes is sufficient to account for the observed rapid rate of isomerization by this mechanism (9). The duplication of the 280 base pair sequence at the ends of the L segment could be a byproduct of the recombinational event which causes segment inversion. However, since the S segment also inverts but never contains 280 base pair insertions at its terminus, this hypothesis, in its simplest form, seems unlikely.

Replication of herpes simplex virus DNA appears to proceed through a concatemeric intermediate which is processed (presumably by cleavage at the junction between L and S segments) to produce unit size progeny genomes. Concatemer formation most likely requires a recombination event within the terminal redundancy, whether it is an intramolecular recombination to form a circular DNA molecule, followed by rolling circle replication to form a concatemer, or whether it is intermolecular recombination to form concatemers directly. If a process of homologous recombination occurs, the junction between L and S segments thus formed will be identical to the joint. It may contain one or more copies of the 280 base pair sequence, depending on how many copies were present at the terminus of the L segment of the parental molecules which formed the concatemer. If the concatemer is cleaved at the joint rather than the junction of the termini, the resulting progeny DNA molecules will have both L and S segments inverted with respect to the parental DNA molecules (Figure 9). If

concatemer formation occurs by intermolecular recombination, another round of concatemer formation and cleavage will result in the production of all four isomers of the HSV genome. Alternatively, the other two isomers can be formed by intermolecular recombination between the first two isomers within the repeated sequences at the joint. Thus, genome isomerization could occur simply as a result of the structure of the joint region and the role of concatemers in HSV replication.

The presence of the 280 base pair insertions at the joint and the left terminus may also be due to the role of concatemers in HSV replication. If the ends of two DNA molecules, each containing a copy of the terminal redundancy, are joined to form a concatemer by recombination within the terminal redundancy, one copy of the terminal redundancy will be lost. When the concatemers are cleaved to mature progeny DNA molecules, some mechanism must be provided to duplicate the sequences at the cleavage site so that each progeny molecule has a copy of the terminal redundancy. This mechanism may also be responsible for the accumulation of extra copies of the terminal redundancy at the end of the L segment and within the identical sequences at the joint, thus leading to the presence of variable numbers of 280 base pair insertions at those locations. That this may be a general feature of herpesvirus DNA replication is indicated by the fact that Herpesvirus saimiri and Epstein-Barr virus DNAs also have variable numbers of copies of a short sequence at their termini (10,11,12).

REFERENCES

1) Sheldrick, P. and Berthelot, N. Cold Spring Harbor Symp. Quant. Biol. 39:667-678 (1974).
2) Jacob, R. J., Morse, L. S., and Roizman, B. J. Virol. 29:448-457 (1979).
3) Summers, W.C. and Skare, J. In "DNA insertion elements, plasmids, and episomes" pp. 471-476. Bukhari, A. I., Shapiro, J. A., and Adhya, S., eds. Cold Spring Harbor Laboratory, Cold Spring Harbor, New York. (1977).

4) Wagner, M. J. and Summers, W. C. J. Virol. 27:374-387 (1978).
5) Skare, J. and Summers, W. C. Virology 76:581-595 (1977).
6) Wilkie, N. M. J. Virol. 20:222-233 (1976).
7) Locker, H. and Frenkel, N. J. Virol. 32:429-441 (1979).
8) Grafstrom, R. H., Alwine, J. C., Steinhart, W. L., and Hill, C. W. Cold Spring Harbor Symp. Quant. Biol. 39:679-681 (1974).
9) Smiley, J., Wagner, M., Summers, W. P. and Summers, W. C. Virology. In press.
10) Bornkamm, G. W., Delius, H., Fleckenstein, B., Werner, F. J., and Mulder, C. J. Virol. 19:154-161 (1976).
11) Kintner, C. R., and Sugden, B. Cell 17:661-671 (1979).
12) Given, D., Yee, D., Griem, K., and Kieff, E. J. Virol. 30:852-862 (1979).

3. Immediate-early transcription of HSV-1 and HSV-2

J. Barklie Clements, Andrew J. Easton and Frazer J. Rixon

THE IMMEDIATE-EARLY REPLICATION PHASE

Infection of permissive cells with HSV in the presence of protein synthesis inhibitors (1, 2) or infection at non-permissive temperature with certain temperature-sensitive mutants (3) results in the accumulation of a restricted set of virus mRNAs which map within certain regions of the virus genome only (1, 4). This restricted set of RNA sequences is transcribed by a pre-existing α-amanitin-sensitive RNA polymerase (5) and has been termed immediate-early (IE) RNA. We have shown for HSV-1 that progression from the IE to the early stage, where much more of the genome is transcribed, (1, 6) requires the continuous function of at least one IE polypeptide (7).

The polypeptides specified by IE mRNA form a sub-set of the virus polypeptides made during productive infection (8, 9). These polypeptides are phosphorylated, preferentially accumulate in the nucleus (10) and have DNA binding properties *in vitro*.

Hence, study of the IE replication phase and of the switch involved in the transition to the early phase has the potential to provide information on eukaryotic gene transcription by RNA polymerase II, and on how virus-coded polypeptides may act to modify this transcription.

Here we report on the properties of HSV-1 and HSV-2 IE mRNA's. We also describe our experiments with end-labelled DNA probes designed to elucidate the fine structures of several IE mRNA's and present DNA sequence data for the 3'-end of one IE mRNA.

Y. Becker (ed), Herpesvirus DNA.

GENOME MAP LOCATIONS, ORIENTATIONS, SIZES AND POLYPEPTIDES ENCODED BY IE mRNA's

Blot hybridizations (1, 11, 12, 13) of *in vivo* and *in vitro* labelled IE RNA to virus DNA fragments generated with various restriction endonucleases, together with a similar analysis of labelled cDNA specific to 3'-ends of mRNA's, has allowed the genome locations and orientations of 6 major IE mRNA's to be determined (Figure 1 and Table 1). IE mRNA orientations have been further confirmed using specific 5'- and 3'-end-labelled DNA probes (see below).

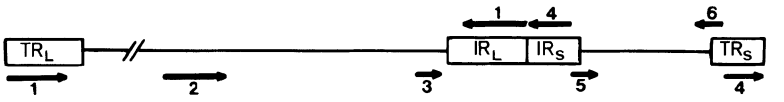

Figure 1. Genome locations and orientations of the major HSV IE mRNAs on the prototype orientation of the virus DNA.

Polyadenylated IE mRNA's were separated by electrophoresis in CH_3HgOH denaturing gels into 3 main virus-specific bands and the genome locations of the different size classes have been determined (13). The polypeptides encoded by IE mRNA's were determined directly by *in vitro* translation of the various size classes (13) and by analyses of polypeptides expressed by intertypic recombinants between HSV-1 and HSV-2 (9).

The major IE mRNA's map primarily in or adjacent to both sets of repetitive DNA regions which flank the two unique DNA regions, and the orientations indicate that there are at least two distinct IE promoters. HSV-1 and HSV-2 IE mRNA's were separated on CH_3HgOH gels to give three bands. The HSV-2 bands were similar but not identical in size to those found with HSV-1 and these size differences may be related to differences in size of the equivalent HSV-1 and HSV-2 IE polypeptides. In contrast to the other IE mRNA's, the IE mRNA 6 is much larger than required for its coding sequences.

Table 1. Genome map locations, sizes and the polypeptides specified by the major HSV-1 and HSV-2 IE mRNA's.

HSV-1 IE mRNA SPECIES	SIZE (kb)	GENOME LOCATIONS	POLYPEPTIDE SPECIFIED ($MW \times 10^{-3}$)
1	3.0	0.00 - 0.04 (TR_L) 0.79 - 0.83 (IR_L)	110
2	5.1	0.54 - 0.59 (U_L)	136
3	2.0	0.74 - 0.76 (U_L)	63
4	4.7	0.83 - 0.87 (IR_S) 0.96 - 1.00 (TR_S)	175
5	2.0	0.87 - 0.90 (IR_S/U_S)	68
6	2.0	0.94 - 0.96 (TR_S/U_S)	12
HSV-2 IE mRNA SPECIES			
1	3.4	0.00 - 0.04 (TR_L) 0.77 - 0.82 (IR_L)	118
2	-	0.54 - 0.60 (U_L)	142
3	1.75	0.73 - 0.74 (U_L)	65
4	4.7	0.82 - 0.86 (IR_S) 0.96 - 1.00 (TR_S)	182
5	1.75	0.85 - 0.88 (IR_S/U_S)	-
6	1.75	0.94 - 0.97 (TR_S/U_S)	12.3

HSV-1 IE mRNA's mapped to genome regions equivalent to those of the respective HSV-2 mRNA's of a similar size, and the data indicates a close similarity in the IE transcription phase between HSV-1 and HSV-2. This is not surprising as at least some HSV-1 and HSV-2 gene products are functionally interchangeable (14) and genetic exchanges have been demonstrated by the production of intertypic recombinants (9, 15, 16, 17). Analysis of intertypic recombinants has demonstrated the colinearity of equivalent genes on the two DNAs (18).

Our studies provide no evidence to support the claim,

based on liquid hybridization studies, by Frenkel et al (19), of a radically different transcriptional programme for HSV-2 as compared to HSV-1. The blot hybridization studies showed no major differences in the hybridization patterns of IE nuclear and cytoplasmic RNA's. This is inconsistent with liquid hybridization data which indicated that 50% (2) to 30% (4) of the HSV-1 genome was represented in IE nuclear RNA whereas only 13% was represented in the cytoplasm (4); 45% of the genome was represented in total HSV-2 IE mRNA (19). Our current knowledge of the genome map locations, sizes and polypeptides specified by both HSV-1 (9, 11, 13) and HSV-2 IE mRNAs (12), together with the molecular weights of those IE polypeptides shown to be unrelated due to breakdown (D. MacDonald and H.S. Marsden, personal communication), indicates that at least 20% of the HSV genome must be represented in the cytoplasm at the immediate-early stage.

No additional IE nuclear sequences were detected with DNAase-treated RNA samples which were not fractionated on Cs_2SO_4 gradients prior to blotting, or with cytoplasmic IE RNA labelled in vitro (12). These controls therefore demonstrate that the restricted hybridization patterns of both nuclear and cytoplasmic IE RNA are not due to artefacts introduced by the methods of RNA isolation or purification.

FINE STRUCTURE ANALYSIS OF HSV IE mRNA's

The rationale of RNA structure analysis using 5'-and 3'-end-labelled DNA probes (20) is shown in Figure 2 for a RNA with a single splice (encoded by one strand of a linear duplex DNA). The procedure uses restriction endonuclease cleaved fragments of HSV-1 and HSV-2 DNA's cloned under UK Category II containment using pAT 153 as the cloning vector and E.coli K12 HB101 as the host bacterium. DNA fragments were 5'-^{32}P-end-labelled using T4 polynucleotide kinase and γ-^{32}P ATP, after dephosphorylation with alkaline phosphatase (20). Fragments containing recessed 3'-ends were 3'-end-labelled using T4 DNA polymerase and one or more α-^{32}P-deoxynucleoside triphosphates (21) to fill out the restriction site. The end-labelled probes were normally cleaved with a

single cut restriction enzyme and the two fragments each containing a single labelled end were used in hybridization.

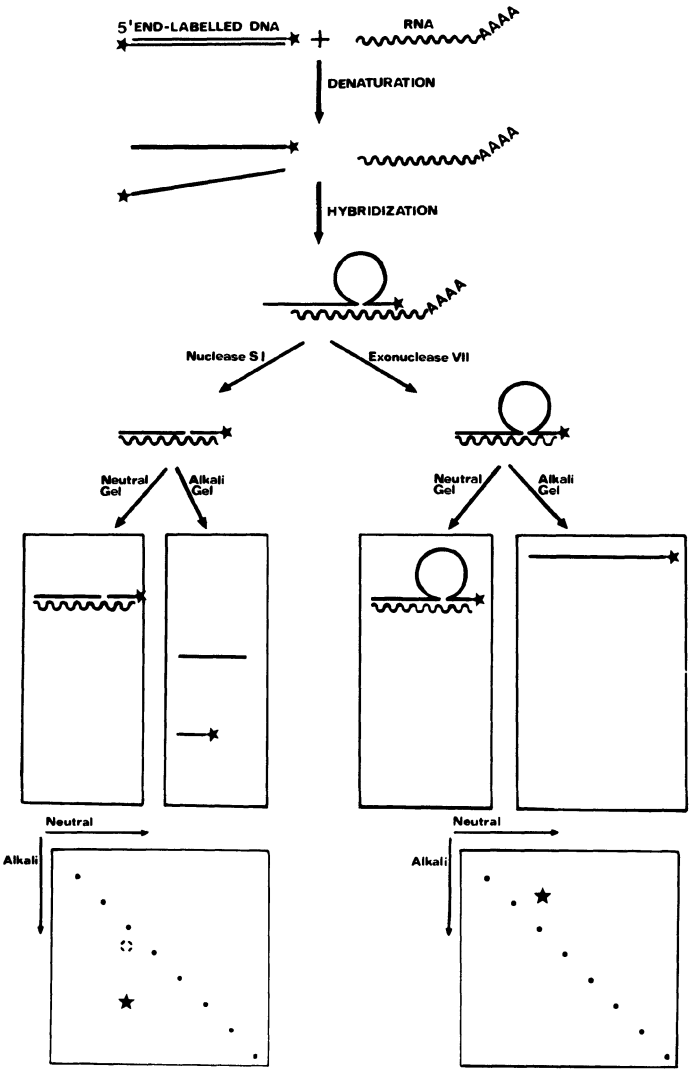

Figure 2. Rationale of RNA structure analysis using a 5'-end-labelled DNA probe to analyse the structure of an mRNA with a single splice.

Excess of end-labelled DNA probes were mixed with infected cell cytoplasmic IE RNA preparations in a solvent containing 90% formamide. After heating to denature the

DNA, hybridizations were performed at temperatures favouring DNA-RNA hybridization and minimising DNA reassociation (22). After hybridization, the non-homologous RNA and the non-hybridized DNA was removed with nuclease S1. The S1-resistant DNA-RNA hybrid consists of a continuous RNA strand with a complementary DNA strand having a specific nick at the site where the loop was excised; in a small proportion of molecules, S1 will also cut through the RNA opposite the nick to form two hybrid molecules, only one of which will be end-labelled.

As a consequence of the polarity of the RNA and DNA strands in a hybrid, the orientation of the RNA with respect to the physical map of the genome can be determined. A 5'-end-labelled DNA probe will only form a S1-resistant labelled hybrid with sequences at the 5'-end of the RNA while a 3'-end-labelled probe will hybridize only with 3'-end sequences of the RNA.

S1-resistant hybrids were electrophoresed in neutral and in alkaline agarose gels. Using end-labelled DNA probes, in both types of gels, only a single band is labelled (Figure 2). If the size of the labelled DNA in alkali gels differs from the value obtained with neutral gels, this indicates that the RNA is spliced. With end-labelled probes on alkaline gels, the size of the labelled DNA fragment determines the distance from the point of labelling to the end of an unspliced RNA, or to the position of the first splice point.

DNA-RNA hybrids were further fractionated using a two-dimensional procedure (23) with electrophoresis in a neutral buffer in the first dimension, and in alkaline buffer in the second dimension. The continuous DNA strands generated by unspliced RNAs will have the same relative mobility in both dimensions and will fall along a diagonal line. A single-spliced RNA will be resolved by the alkaline dimension into two DNA species only one of which will be end-labelled, with both spots vertically aligned below the diagonal. A vertical line through these spots bisects the diagonal at a point equivalent to the sum of the lengths of the component DNA single strands. With the 5'-end-

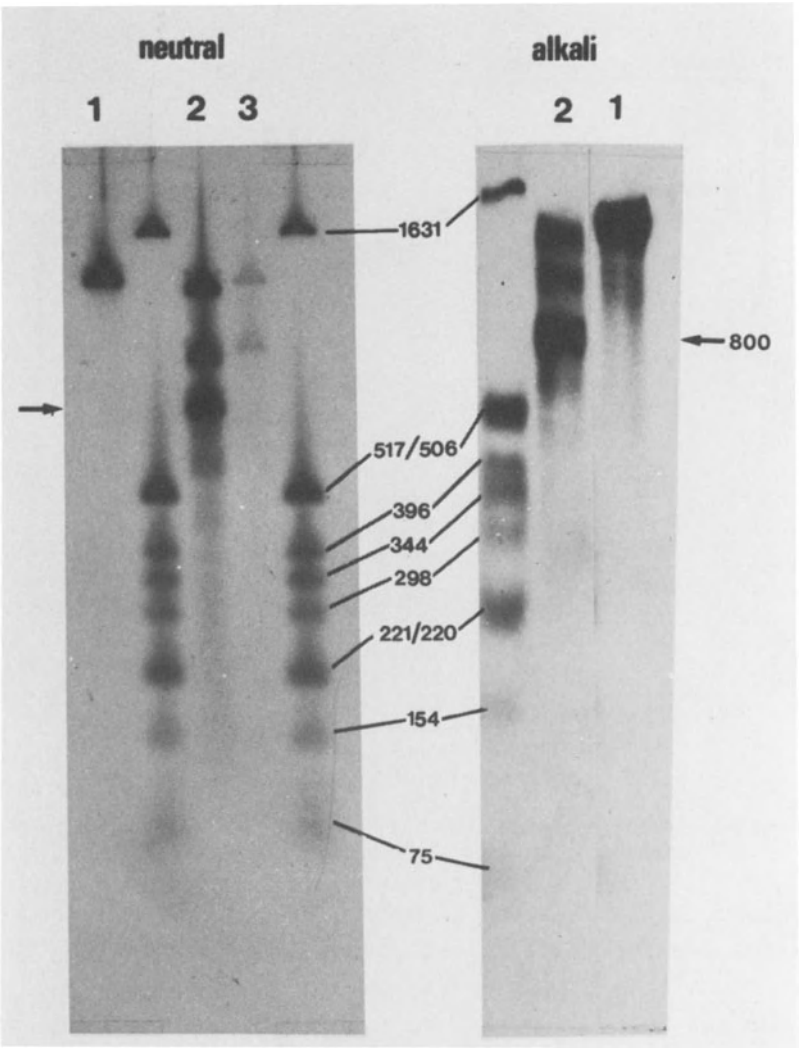

Figure 3. Structure of HSV-2 IE mRNA 3 analysed on neutral and alkaline gels using a 3'-end-labelled Hing III o fragment probe. Sample 1 is the unhybridized fragment probe. Sample 2 is the fragment probe hybridized to 10 µg HSV-2 IE cytoplasmic RNA. Sample 3 is the fragment probe hybridized to 10 µg yeast RNA. Samples were treated with nuclease S1.

labelled DNA probe, the spliced RNA generates a single spot corresponding to the distance from the labelled site to the splice point.

The S1 analyses demonstrate the presence of splices but do not provide direct information on their size. Exonuclease VII (24, 25) can be used instead of S1 to digest hybrids. This enzyme degrades single-stranded DNA but does

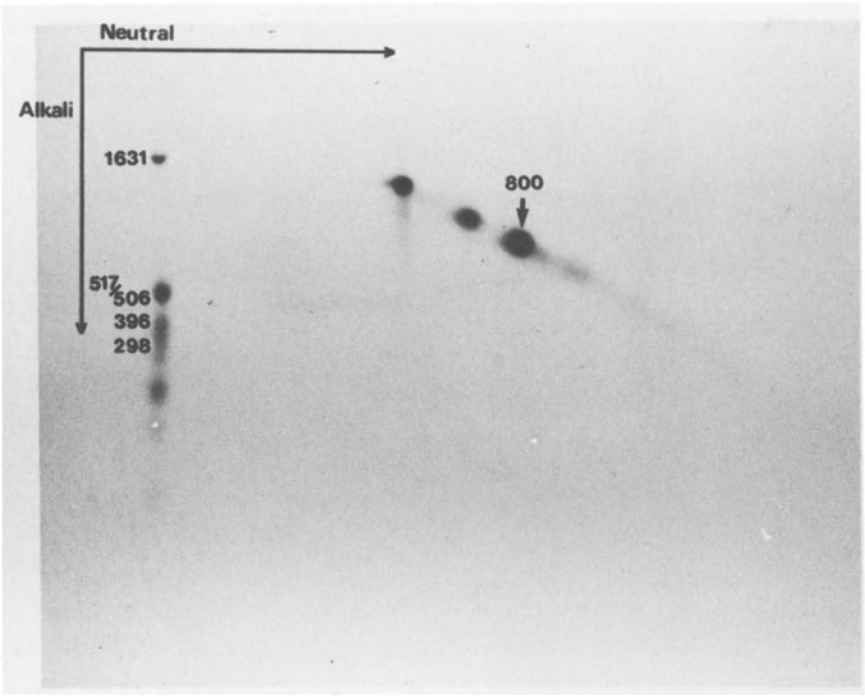

Figure 4. Structure of HSV-2 IE mRNA 3 anaysed by two-dimensional agarose gel electrophoresis using a 3'-end-labelled Hind III o fragment probe. The sample used was lO µg HSV-2 IE cytoplasmic RNA. After hybridization the sample was treated with nuclease Sl.

not cleave internal loops in hybrids (Figure 2). Hence, on alkaline gels, exonuclease VII generates a single labelled band with a size equivalent to that of the RNA plus the spliced out DNA sequences. On two-dimensional gels the end-labelled DNA spot should migrate above the diagonal and the splice length can be estimated.

HSV-2 IE mRNA 3

IE mRNA 3 lies entirely within the U_L region, and has its 3'-end in the Hind III o fragment (l2, Figure 7). To analyse the structure of this message, the cloned Hind III o fragment was 3'-end-labelled then cleaved with Pvu II (Figure 7) and the two labelled fragments isolated. These fragments were hybridized individually with HSV-2 IE cytoplasmic RNA and with yeast RNA.

Only the larger fragment directed formation of a DNA-

RNA hybrid, and under the hybridization conditions used two DNA reassociation products were seen with both the IE RNA and yeast RNA control IE (Figure 3, samples 2 and 3). A third band of 800 nucleotides was present only with the infected cell RNA (Figure 3, sample 2). This band was of similar size on neutral and alkaline gels, and furthermore lay on the diagonal after two-dimensional gel electrophoresis (Figure 4). This indicated that the 3'-end of IE mRNA 3 was unspliced for 800 nucleotides from the Hind III site as indicated in Figure 7. This data also confirms the orientation and location of the 3' end of IE mRNA 3 as determined previously (12).

The 5'-end of the RNA was analysed using cloned HSV-2 Bam HI fragment f, which contains the Hind III o fragment (Figure 7). Bam HI f was digested with Hind III, and the resultant ends were 5'-end-labelled. The mixture of 5'-end-labelled fragments was used in the hybridization procedure, and after S1 treatment, only one DNA-RNA hybrid was seen (Figure 5) with a DNA size in alkali of 840 nucleotides. After electrophoresis on a two-dimensional gel, the radioactivity lay on the diagonal (Figure 5) indicating that the RNA was not spliced at the 5'-end for 840 nucleotides from the Hind III site. Since both the 5'- and 3'-ends of this mRNA were studied by labelling at the same Hind III site, the total size of HSV-2 IE mRNA 3 would appear to be the sum of the size of the two DNA-RNA hybrids, 1640 nucleotides (Figure 7). An approximate estimate of the size of polyadenylated IE mRNA 3 on CH_3HgOH gels was 1750 nucleotides.

Nucleotide sequence at the 3'-end of HSV-2 IE mRNA 3

The DNA sequence at the 3'-end of IE mRNA 3 was determined using cloned Hind III o. The intact plasmid containing Hind III o was digested with Xma I which cleaves once within the insert (Figure 7). The two free ends were then 3'-end-labelled using α^{32}P-dCTP. The labelled DNA was cleaved with Hind III and the larger labelled fragment isolated by gel electrophoresis. This DNA fragment was sequenced by the method of Maxam and Gilbert (26), and the S1-resistant

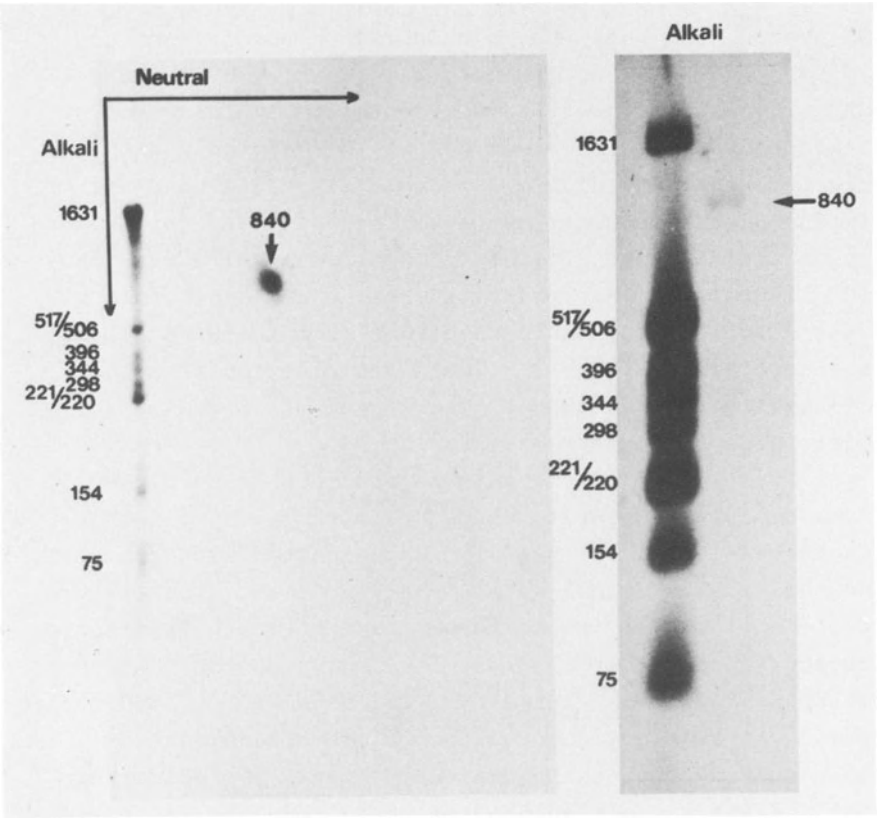

Figure 5. Structure of HSV-2 IE mRNA 3 analysed by two-dimensional and alkaline gel electrophoresis using a 5'-end-labelled Hind III digested Bam HI f fragment probe. The sample was 10ug HSV-2 IE cytoplasmic RNA. Following hybridization the sample was treated with nuclease S1.

DNA-RNA hybrid generated by this fragment was co-electrophoresed on the sequencing gels (Figure 6). This indicated the point at which transcription of IE mRNA 3 terminated on the DNA. The DNA sequence determined was of the strand complementary to the RNA. The sequence given in Figure 7 is that of the DNA strand with the same sequence as the RNA.

The location(s) of the 3'-end shown by the arrows in Figure 7 is not precisely defined as the sequence at which the DNA-RNA hybrid finishes contains two A residues. It is unclear if these are transcriptional or post-transcriptional additions.

The RNA contains the sequence 5'-AAUAAA-3' at 10 to 13 nucleotides upstream from the poly A tail. This sequence

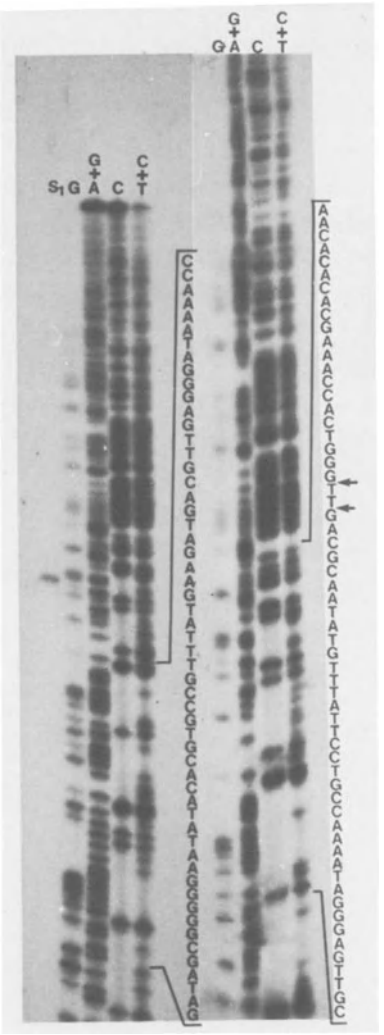

Figure 6. Autoradiogram of sequencing gels showing 3'-end of HSV-2 IE mRNA 3. The lanes are labelled according to the nomenclature of Maxam and Gilbert The 3'-end of the mRNA is determined by co-electrophoresing the nuclease S1-resistant DNA-RNA hybrid produced by hybridizing the 3'-end-labelled fragment probe to be sequenced to 10 µg of HSV-2 IE cytoplasmic RNA. The region in which the RNA terminates is indicated by arrows.

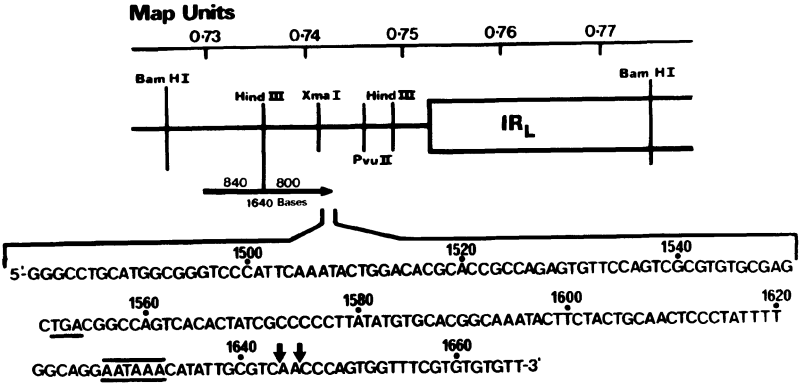

Figure 7. Summary showing the genome map location, size and 3'-end sequence of HSV-2 IE mRNA 3. Arrows indicate the 3'-end of the mRNA.

is present at the 3'-end of all known polyadenylated eukaryotic mRNA's and may serve as a signal for addition of the poly A (27).

Apart from the UAA stop codon present in the AAUAAA sequence, there is only one other stop codon (UGA) in the sequenced region which is not in phase with the UAA stop. The sequences at the 3'-end of IE mRNA 3 therefore appear to conform to those found at the 3'-end of other eukaryotic mRNA's.

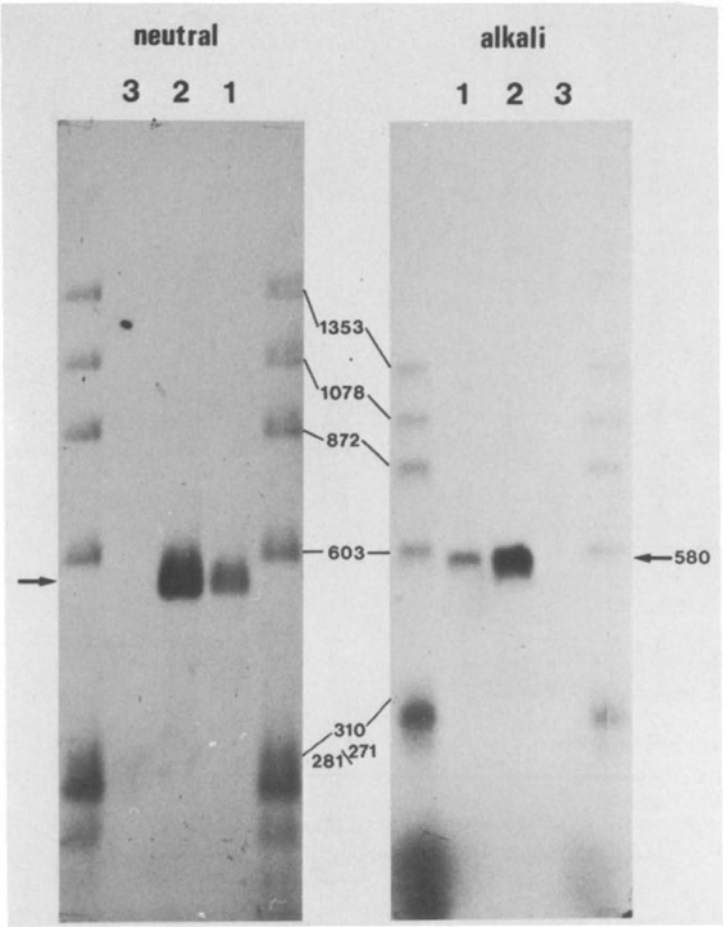

Figure 8. Structure of HSV-1 IE mRNA 6 analysed on neutral and alkaline gels using a 3'-end-labelled fragment probe labelled at Bam HI site a (Figure 12). Sample 1 is the fragment probe hybridized to 5 µg HSV-1 IE cytoplasmic RNA. Sample 2 is the fragment probe hybridized to 15 µg HSV-1 IE cytoplasmic RNA. Sample 3 is the fragment probe hybridized to 15 µg yeast RNA. Following hybridization the samples were treated with nuclease S1.

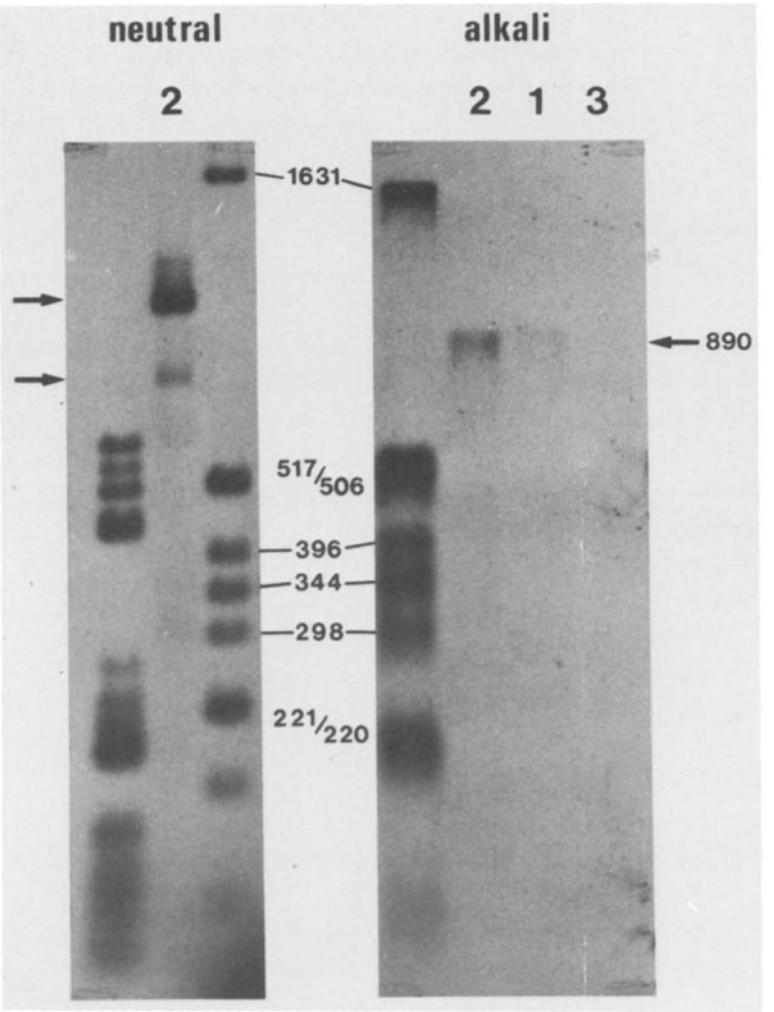

Figure 9. Structure of HSV-1 mRNA 6 analysed on neutral and alkaline gels using a 5'-end-labelled fragment probe labelled at Bam HI site b (Figure 12). Sample 1 is the fragment probe hybridized to 5 µg HSV-1 IE cytoplasmic RNA. Sample 2 is the fragment probe hybridized to 15 µg HSV-1 IE cytoplasmic RNA. Sample 3 is the fragment probe hybridized to 15 µg yeast RNA. Following hybridization, samples were treated with nuclease S1.

HSV-1 IE mRNA's 5 and 6

These mRNA's span the two junctions between IR_S and TR_S with U_S (Figure 1), and 5'-ends of both lie within IR_S and TR_S indicating that these mRNA's have common 5' sequences. Figure 8 shows S1 end-label protection analysis with a 3'-end-label at Bam HI site a (Figure 12). A single band was

detected in both neutral and alkaline gels and this had a size of 580 nucleotides in alkali. The apparent size increase of the band on denaturing gels was an effect consistently found and this was more marked the larger the hybrid. All sizes given are estimated from alkaline gels. Analysis of the hybrid by two-dimensional electrophoresis (Figure 10) shows a spot just above the diagonal formed by the marker fragments. This indicates that the 3'-end is unspliced for 580 nucleotides beyond the site.

The 5'-end of IE mRNA 6 was located using Bam HI site b (Figure 12) at 890 nucleotides from the labelled site. However, on neutral gels two bands with apparent sizes of 1000 and 785 base pairs were detected (Figure 9). These are due to cut-through at a single splice point located near the 5'-end and the smaller band is equivalent to the 890 nucleotide band. The presence of this splice was confirmed by two-dimensional gel electrophoresis (Figure 10), where the major spot (equivalent to the apparent 1000 base pair band on non-denaturing gels) was shifted well below the diagonal to 890 nucleotides.

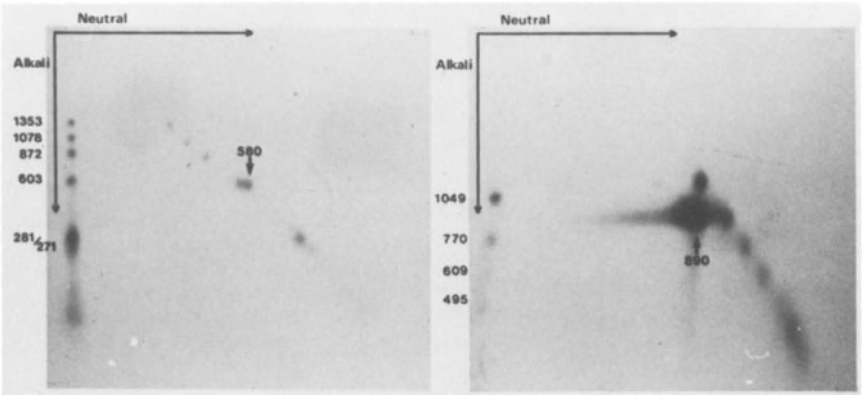

Figure 10. Structure of HSV-1 IE mRNA 6 analysed by two-dimensional gel electrophoresis using 3'-end 5'-end-labelled fragment probes. The fragment probes were 3'-end-labelled at Bam HI site a and 5'-end labelled at Bam HI site b (Figure 12). The fragment probes were hybridized to 15 µg HSV-1 IE cytoplasmic RNA. Following hybridization the samples were treated with nuclease S1.

To determine the size of the splice, the DNA-RNA hybrid formed with a 5'-label at the Bam HI site was treated with exonuclease VII and a labelled band of 1330 nucleotides was detected on alkaline gels as compared to the 890 nucleotide band generated with S1 (Figure 11). The 240 nucleotide stretch from the 5'-end to the splice point was estimated from the cut-through sizes and included a correction for the larger sizes obtained from alkaline gels. Subtraction of 890 plus 240 from 1330 gives a splice of 200 nucleotides.

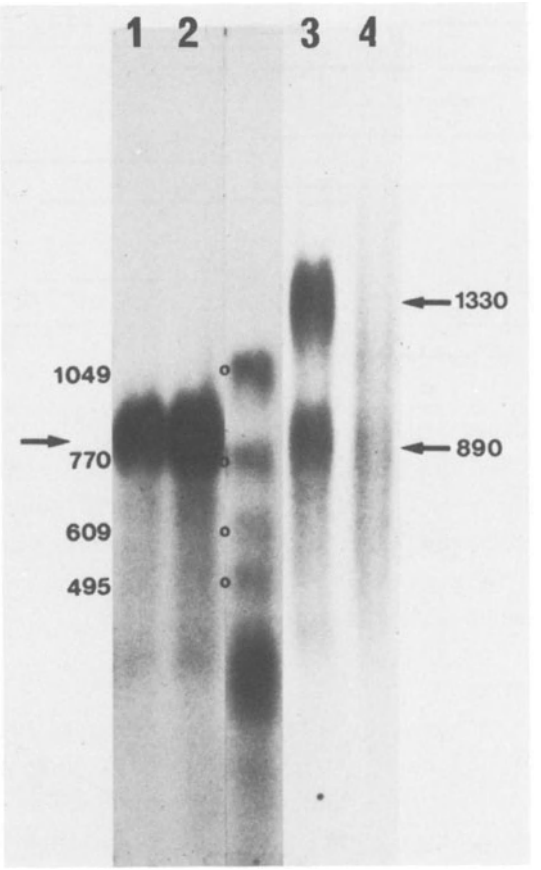

Figure 11. Structure of HSV-1 IE mRNA 6 analysed by electrophoresis on an alkali gel using a 5'-end-labelled fragment probe labelled at Bam HI site b (Figure 12). Sample 1 is the fragment probe hybridized to 5 µg HSV-1 IE cytoplasmic RNA followed by digestion with nuclease S1. Sample 2 is the fragment probe hybridized to 15 µg HSV-1 IE cytoplasmic RNA followed by digestion with nuclease S1. Sample 3 is the fragment probe hybridised to 15 µg HSV-1 IE cytoplasmic RNA followed by digestion with exonuclease VII. Sample 4 is the fragment probe hybridised to 15 µg yeast RNA followed by digestion with exo. VII.

Similarly, the structure of IE mRNA 5 was examined using 5'- and 3'-end-labelled DNA at the Hind III site in Bam HI n. These results are summarized in Figure 12 and show that IE mRNA 5 has a similar splice in IR_S to that of IE mRNA 6 in TR_S. The main body of IE mRNA 5 is approximately 1525 nucleotides,some 100 nucleotides smaller than the body of IE mRNA 6.

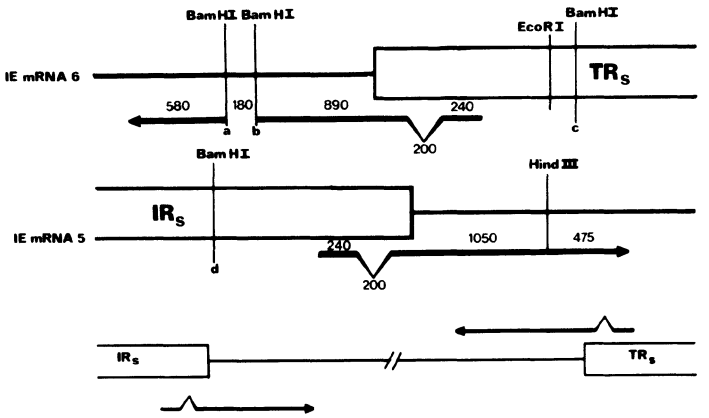

Figure 12. Summary showing genome locations, sizes, and structures of HSV-1 IE mRNAs 5 and 6.

Our data on the structures of these two mRNAs directly confirms similar structures recently described by Watson (28) who showed that both had identical splices at their 5'-ends. This data showed that IE mRNA 6 was continuous through Bam HI sites a and b (Figure 12).

OVERALL CONCLUSIONS

The data presented here for HSV-2, together with other information for HSV-1, suggests that IE mRNA 3 is unspliced. By contrast, HSV-1 IE mRNAs 5 and 6 appear to have a single splice. Adenovirus type 2 specifies an unspliced mRNA (29) as well as the various spliced species (30). The methodology used here may not detect small splices of 50 nucleotides or less which are located at the ends of mRNAs and this is determined by the sensitivities of the gel electrophoretic procedures used.

One would like the precise information on RNA structures that is obtained by comparison of mRNA sequences

with the relevant DNA sequences. Even this information however may not shed much light on the mechanism involved in synthesis of the mRNAs.

REFERENCES

1. Clements, J.B., Watson, R.J. and Wilkie, N.M. (1977). Cell 12, 275-285.

2. Kozak, M. and Roizman, B. (1974). Proc. Natl. Acad. Sci. USA., 71, 4322-4326.

3. Watson, R.J. and Clements, J.B. (1978). Virology 91, 364-379.

4. Jones, P.C. and Roizman, B. (1979). J. Virol. 31, 299-314.

5. Costanzo, F., Campadelli-Fuime, A., Foà-Tomasi, L., and Cassai, E. (1977). J. Virol. 21, 996-1001.

6. Swanstrom, R., and Wagner, E. (1974). Virology 60, 522-533.

7. Watson, R.J. and Clements, J.B. (1980). Nature 285, 329-330.

8. Honess, R.W. and Roizman, B. (1975). Proc. Natl. Acad. Sci. USA., 72, 1276-1280.

9. Preston, V.G., Davison, A.J., Marsden, H.S., Timbury, M.C., Subak-Sharpe, J.H. and Wilkie, N.M. (1978). J. Virol. 28, 499-517.

10. Pereira, L., Wolff, M.H., Fenwick, M. and Roizman, B. (1977). Virology 77, 733-749.

11. Clements, J.B., McLauchlan, J. and McGeoch, D.J. (1979) Nucleic Acids Res. 7, 77-91.

12. Easton, A. and Clements, J.B. (1980). Nucleic Acids Res. 8, 2627-2645.

13. Watson, R.J., Preston, C.M. and Clements, J.B. (1979) J. Virol. 31, 42-52.

14. Stow, N.D. and Wilkie, N.M. (1978). Virology 90, 1-11.

15. Timbury, M.C. and Subak-Sharpe, J.H. (1973). J. gen. Virol. 18, 347-357.

16. Morse, L.S., Buchman, T.G., Roizman, B. and Schaffer, P.A. (1977). J. Virol. 24, 231-248.

17. Marsden, H.S., Stow, N.D., Preston, V.G., Timbury, M.C. and Wilkie, N.M. (1978). J. Virol. 28, 624-642.

18. Wilkie, N.M., Davison, A.J., Chartrand, P., Stow, N.D., Preston, V.G. and Timbury, M.C. (1979). Cold Spring Harbor Symp. Quant. Biol. 43, 827-840.

19. Frenkel, N., Silverstein, S., Cassai, E. and Roizman, B. (1973). J. Virol. 11, 886-892.

20. Weaver, R.F. and Weissmann, C. (1979). Nucleic Acids Res. 7, 1175-1193.

21. Wu, R. (1970). J. Mol. Biol. 51, 501-521.

22. Casey, J. and Davidson, N. (1977). Nucleic Acids Res. 4, 1539-1552.

23. Favaloro, F., Treisman, R. and Kamen, R., (1980) in "Methods in Enzymology" 65, pp 718-49. Academic Press, L. Grossman and K. Moldave eds.

24. Chase, J.W. and Richardson, C.C. (1974). J. Biol. Chem. 249, 4553-4561.

25. Berk,A.J. and Sharp, P.A. (1978). Proc. Natl. Acad. Sci. USA., 75, 1274-1278.

26. Maxam, A.R. and Gilbert, W. (1980) in "Methods in Enzymology" 65, pp 499-580. Academic Press, L. Grossmann and K. Moldave, eds.

27. Benoist, C., O'Hara, K. and Chambon, P. (1980). Nucleic Acids Res. 8, 127-142.

28. Watson, R.J. (1980). RNA Workshop communication at the International Conference on Human Herpesviruses March 17-21, Atlanta.

29. Alestrom, G.A., Pessicaudet, M., Matthews, M.B., Klessig, D.F. and Pettersson, U. (1980). Cell, 19, 671-681.

30. Chow, L.T., Broker, T.R. and Lewis, J.B. (1979). J. Mol. Biol. 134, 265-302.

4. Isolation and characterization of HSV-1 mRNA

Edward K. Wagner, Kevin P. Anderson, Robert E. Costa, Gayathri B. Davi, Beverley H. Gaylord, Louis E. Holland, James R. Stringer*, and Lori L. Tribble

SUMMARY

We have reviewed our methods for the isolation, mapping, and characterization of HSV-1 mRNA abundant at the three stages of infection. The complexity of viral mRNA increases with each stage of infection. By use of HSV-1 DNA restriction fragments bound to cellulose, we have been able to examine in some detail the time of appearance and properties of viral mRNA homologous to specific regions of the genome.

INTRODUCTION

We, as well as workers in other laboratories, have been engaged in investigating the properties of HSV-1 mRNA as a general model for herpesvirus mRNA for a number of years. HSV-1 mRNA shares general properties with host cell mRNA; i.e., it is synthesized in the nucleus, is polyadenylated on the 3' end and capped on the 5' end, and is internally methylated (1-6).

There are three stages of HSV-1 replication, each characterized by an increasing complexity of viral mRNA expressed. The first stage, immediate-early, is comprised of those RNA species that can be expressed abundantly without *de novo* protein synthesis; i.e., with an unmodified host cell RNA polymerase (7, 8). Abundant members of this class of mRNA are quite limited, map in regions of the HSV-1 genome at or near the long (L_R) and short (S_R) repeat

Y. Becker (ed), Herpesvirus DNA.

regions, and encode only a limited number of polypeptides *in vivo* and *in vitro* (9-17).

Following expression of one or several immediate-early HSV-1 proteins, a more complex population of viral mRNA is abundant prior to viral DNA replication (18-23). This early viral mRNA maps throughout the HSV-1 genome in non-contiguous regions; but only a limited number of readily resolvable species are found (16, 24-26). Many of these early viral mRNAs are involved with priming the cell for viral DNA replication. We, as well as other workers, have shown that, without viral DNA replication, the early viral mRNA and protein population appears to persist (19, 21, 23, 27, 28). Recently, we have shown that, in the absence of viral DNA replication, the specific viral mRNA species and the polypeptides they encode *in vitro* are virtually indistinguishable from kinetically early ones (29).

Concomitant with viral DNA replication is the appearance of late HSV-1 mRNA (19, 20). These mRNA species encode a large number of polypeptides (29), many of which presumably are structural proteins of the virion.

The size and complexity of the HSV-1 genome has made the detailed characterization of individual HSV-1 mRNA species difficult. We have developed methods for the preparative isolation of HSV-1 mRNA homologous to specific restriction fragments of the viral genome (16, 17, 30, 31). Below, we have reviewed our basic methods for the isolation and characterization of viral mRNA abundant at different stages of infection of HSV-1. With the availability of recombinant DNA techniques, we are hopeful that workers on other--even more demanding--herpesviruses will be able to adapt some of these methods to their systems.

EXPERIMENTAL RESULTS

Experimental Approach

We have described our methods for the isolation of HSV-1

specific mRNA and nuclear RNA at the three stages of infection (16, 17, 29-31). Briefly, all infections are with the KOS strain of HSV-1 in HeLa cells at a MOI of 10 PFU/cell. Immediate-early RNA is isolated from cells infected and maintained in the presence of 200 μg/ml cycloheximide for 6 hours post-infection (hpi). Early RNA is isolated at 2 hpi or, alternatively, at 6 hpi from cells infected and maintained in the presence of 1.5×10^{-4} M adenine arabinoside (ara-A) and the adenine deaminase inhibitor pentostatin (3.5×10^{-6} M), or 1.9×10^{-4} M thymine arabinoside (ara-T). Late RNA is isolated from cells from 6 to 8 hpi. Viral DNA replication is maximal at 5 to 6 hpi.

HSV-1 specific, or restriction fragment specific, viral RNA is preparatively isolated by hybridization to viral DNA bound to cellulose. The procedures for such binding and hybridization have been described (30, 31). It has been our observation that hybridization in high percentages of formamide (70-80%) at or near the Tm of the DNA is vital for the elimination of non-specific RNA binding to the cellulose.

We have used the restriction endonucleases *Hind*III, *Bgl*II, and *Xba*I, singly and in concert, to isolate various sized pure restriction fragments of HSV-1 DNA for binding to cellulose. Further, we have available a number of *Eco*RI fragments cloned in phage λ WES·B, which were kindly supplied to us by L. Enquist and G. Van de Woude (32). Taken together, we have bound to cellulose fragments spanning the entire genome. The locations of the available restriction fragments are shown in Figure 1.

Purified viral mRNA has been further fractionated on methylmercury agarose gels (30, 33) or on sucrose gradients (31). Viral mRNA has been used as a template for the synthesis of 3' and total cDNA for localization of 3' ends to determine the direction of transcription (16, 17, 31). Further, such purified mRNA species have been translated *in vitro* to determine the size of the polypeptides encoded by them (17, 31).

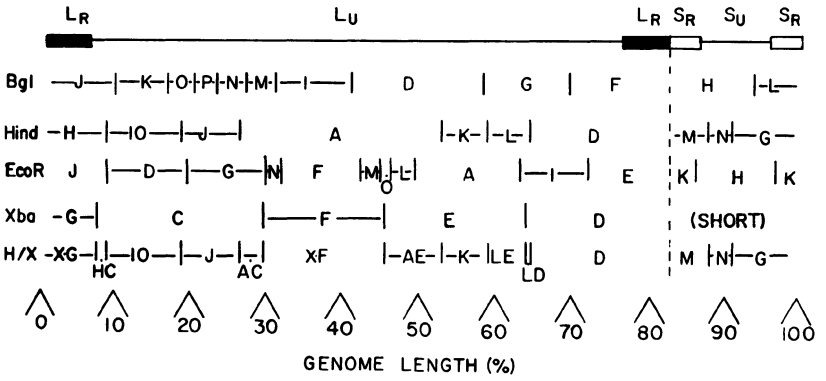

FIGURE 1. Location of restriction endonuclease sites for the KOS strain of HSV-1. The sites for cleavage by BglII, HindIII, Eco RI, XbaI, and HindIII/XbaI (H/X) double-digests are shown. The basis for the location of these sites for our strain (KOS) of HSV-1 has been described in detail (16, 24, 30). Submolar bands are: BglII A (F + H), B (J + H), C (F + L), and E (J + L). HindIII B (D + G), C (D + M), E (H + G), and F (H + M). EcoRI B (E + K), C (J + K). XbaI A (D + short) and B (G + short). In the H/X double-digests, submolar fragments HindIII B (D + G), HindIII C (D + M), H/X E (Xba G + Hind G), and H/X F (Xba G + Hind M) are obtained. Terminology for double-digest fragments has been discussed in detail (16).

Populations of HSV-1 mRNA Abundant at Different Stages of Infection

Total HSV-1 polyribosomal poly(A+) RNA, after labeling for one hour with [^{3}H]uridine, was isolated from cells at 5 hpi in the absence of protein synthesis, at 2 hpi and at 6 hpi under normal conditions of infection. Viral RNA synthesized under these regimes is, respectively: immediate-early RNA, early RNA, and late RNA. Preparative amounts of these three classes of viral mRNA were obtained by hybridizing total poly(A) RNA to HSV-1 DNA bound to cellulose. The size distributions of these classes of viral RNA are shown in Figure 2. It is apparent that abundant immediate-early HSV-1 RNA is found in only three size classes: 4.2, 2.8, and 1.8-2 kb, as determined from the migration of 28S rRNA

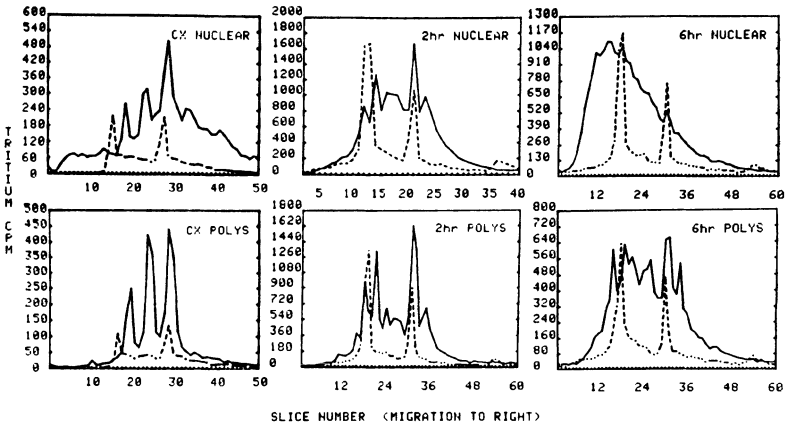

FIGURE 2. Size distribution of HSV-1 RNA abundant at the three stages of infection. HeLa cells infected under conditions to yield immediate-early, early, or late RNA, were labeled for one hour with [^{3}H]uridine. Nuclear and poly(A+) polyribosomal RNA were isolated as described (16, 31), and aliquots (4 to 5 µg) were hybridized separately in high formamide to 25 µg HSV-1 DNA bound to cellulose (31). Hybridized RNA was eluted and fractionated on methylmercury agarose gels (33). The dashed lines are the positions of ^{32}P-labeled 28S and 18S rRNA included as a marker.

and 18S rRNA (5.2 kb and 2.0 kb; 34, 35). A virtually identical size distribution was seen when HSV-1 poly(A) mRNA was isolated from cells infected at 39°C with a temperature-sensitive mutant of HSV-1 (*ts* B2) known to over-produce immediate-early proteins at 39°C (16). The size distribution of early viral mRNA is considerably more complex, with RNA species ranging from 1.5 to at least 5.2 kb being abundant. The pattern with late viral mRNA is even more complex. The most notable apparent addition being the marked increase in viral mRNA >5 kb in size. These size distributions suggest that the complexity of viral mRNA expression increases with each succeeding stage of viral replication.

In the nucleus, viral RNA shows a similar increase in complexity with stage of infection; thus, the three major size classes of immediate-early RNA are readily

detectable and the greater number of early species also are seen. It is clear in the case of immediate-early nuclear viral RNA, however, that there is readily detectable heterogeneously migrating RNA in addition to the major species. Late after infection, the size distribution of nuclear viral RNA shows a marked increase in the relative proportion of large species. The full significance of these patterns of nuclear RNA is currently being studied in detail.

The increase in complexity of viral mRNA species with progression of infection is graphically demonstrated by translation of the viral mRNA isolated from these three stages (Figure 3). Immediate-early RNAs are an efficient template for four major discrete polypeptides of 170,000 d, 120,000 d, 68,000 d, and 64,000 d. Other less prominant ones are also present. Total early viral mRNA is a template for polypeptides of the same size as these. In addition, nine other distinct sized polypeptides ranging from 140,000 d to 41,000 d are clearly discernible. Late viral mRNA is a template for *in vitro* translation of an even more complex population of viral polypeptides: 24 discrete sized polypeptides ranging from 155,000 d to 22,000 d or less. It is significant that at least one of the immediate-early polypeptides (170,000 d) is not efficiently translated with viral mRNA from cells at this stage of infection. Although the specific numbers of viral polypeptides encoded early and late probably are significant under-estimates of the total numbers encoded at the early and late stages of infection, the value of preparative isolation of viral mRNA is readily apparent even with this very cursory examination of the complexity of HSV-1 mRNA.

Mapping HSV-1 mRNA Abundant at Different Stages of Infection

Although, in principle, HSV-1 mRNA can be mapped on the viral genome by use of specific restriction fragments bound to cellulose, such probes are better suited for isolation

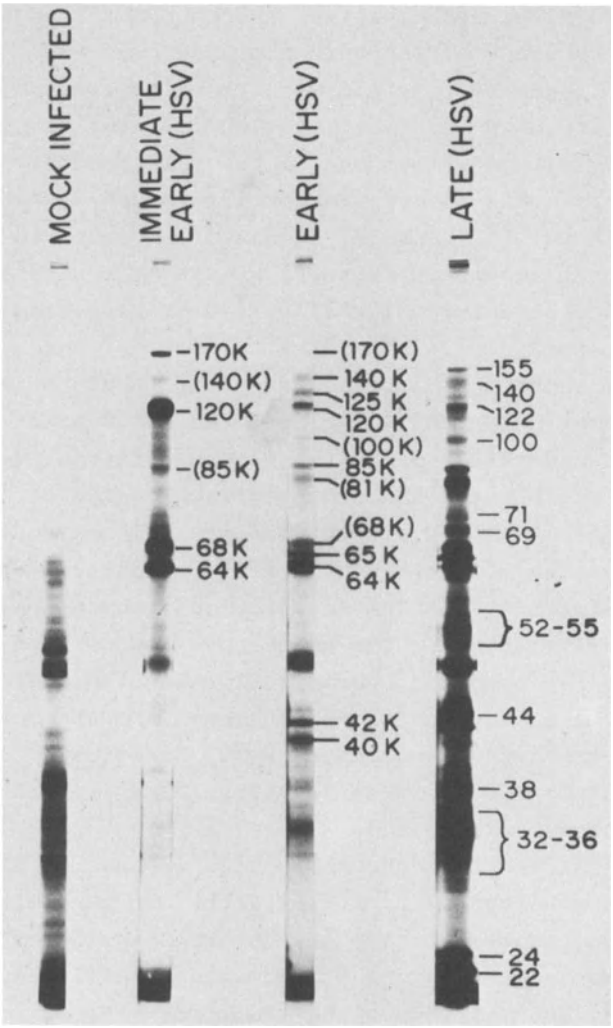

FIGURE 3. In vitro translation products of immediate-early, early, and late HSV-1 mRNA. Aliquots (0.3 to 0.6 μg) of HSV-1 poly(A+) mRNA isolated from the three stages of infection were purified by hybridization to DNA cellulose, as described in Figure 2; were translated in a commercial reticulocyte system (17, 29, 31); and fractionated on 9% polyacrylamide-SDS gels (36). Sizes of polypeptides, indicated in thousands of daltons, were determined from the migration of adenovirus markers. The heavy band of material migrating at 50,000 d is endogenous to the system.

of specific viral mRNA species. We have utilized the speed, ease, and accuracy of Southern blots (37) of HSV-1 DNA restriction fragments combined with the high resolution and reversibility of denaturing methylmercury gel electrophoresis of poly(A+) polyribosomal RNA of infected cells to provide a rapid means of mapping specific sized mRNA species abundant at the three stages of HSV-1 infection to specific restriction fragments. Further, by use of several different restriction enzyme blots, limited overlap information can be obtained.

The experimental procedure is to label total poly(A) polyribosomal RNA with ^{32}P in infected cells maintained so that immediate-early, early, or late RNA is the predominant species. The poly(A) RNA is size-fractionated on methylmercury gels, the gels sliced, and each slice (containing a specific size of RNA) is hybridized to a strip of a Southern blot of HSV-1 DNA restriction fragments made from a horizontal slab gel. The strips are reassembled in order of size of RNA used for hybridization and radioautographed, providing in essence a "two-dimensional" Southern blot hybrid of the size-fractionated RNA. Examples of such two-dimensional maps for immediate-early, early, and late viral mRNA are shown in Figure 4.

It is seen that the three size classes of immediate-early mRNA observed (4.2, 2.8, 1.8 kb) map to different restriction fragments. The 4.2 kb mRNA maps to all restriction fragments bearing the S_R segment (*Hind*III fragments B, C, E, F, G, and M), indicating that this mRNA is located in this region. Similarly, the 2.8 kb mRNA hybridizes efficiently to all fragments bearing the L_R sequence (*Hind*III fragments B, C, D, E, F, and H). The situation with the 1.8 kb mRNA is more complex, hybridizing to fragments containing sequences from both the L_R and S_R regions. Further, in data not shown, one 1.8 kb species hybridizes to *Hpa*I fragment T (0.74-0.76). This indicates that one 1.8 kb immediate-early mRNA maps in the L_U region. In addition to these major species, at least some viral mRNA of $\sim$5 kb in

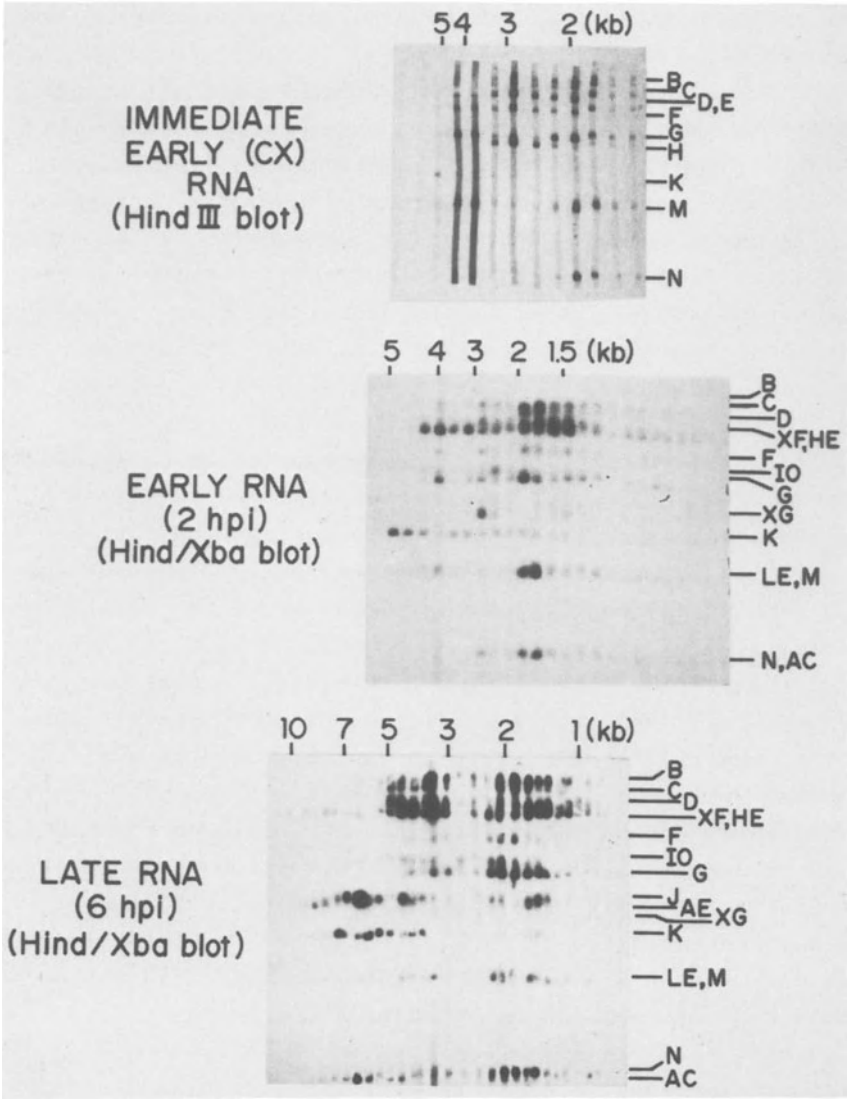

FIGURE 4. Southern blots of size-fractionated immediate-early, early, and late HSV-1 mRNA. As detailed elsewhere (16, 17, 30), poly(A+) polyribosomal RNA from cells labeled for 4 h with (^{32}P)orthophosphate (or for 2 h for early RNA), was size-fractionated on methylmercury agarose gels. The gels were sliced into 3 mm slices and each slice incubated with a strip from a Southern blot of either a HindIII or HindIII/XbaI double-digest of HSV-1 DNA. After hybridization, the strips were reassembled in order of size of RNA for radioautography. Size of RNA was determined by the migration of 28S and 18S rRNA in parallel gels. Only the restriction fragments bearing significant radioactivity are indicated.

size, mapping in *Hind*III fragment K, and ∿3 kb, mapping in fragment G, is seen.

These immediate-early mRNA species also are seen when early mRNA is mapped (cf., the 4.2 kb RNA mapping in *Hind*III fragment G and the 2.8 kb species in *Xba*I fragment G). In addition, other major early mRNA species are seen, such as the 5.2 kb mRNA in *Hind*III fragment K, 1.8 kb mRNA in *Hind*III fragment L (resolved on *Hind*III blots of HSV-1 DNA, not shown), 2.5 kb mRNA in *Hind*III fragment IO; and others described fully elsewhere (16, 29). It is clear that, as seen in Figure 2, little viral mRNA larger than 5.2 kb is seen at this time after infection. There are regions of the genome where discrete species of early HSV-1 mRNA are rare, such as *Hind*III fragment J and *Hind*III/*Xba*I fragments AC and AE. This latter region was found to be essentially free of R-loops when total early viral RNA was used to map the location of early regions of the viral genome (24).

Late after infection, a very much more complex pattern of viral mRNA is seen. Regions, such as *Hind*III fragment J, where early RNA is rare, now show several abundant species (i.e., 6 kb, 5 kb, and 1.8 kb). Other regions, such as *Hind*III fragment K, show additional mRNA species compared to those seen early (i.e., 7 kb and 3.8 kb). In at least two cases, the mRNAs of 4.2 and 2.8 kb mapping in the L_R and L_U, respectively, it is clear that the levels of immediate-early mRNA are reduced at this time after infection. A full description of such two-dimensional maps of late HSV-1 mRNA is found elsewhere (30).

The changes in complexity of viral mRNA homologous to a given region of the genome with stage of infection, as well as variations in the complexity in neighboring regions of the viral genome, are also shown in Figures 5 and 6. The experimental approach is to label infected cells with [^{3}H]uridine for one hour under conditions where immediate-early, early, or late viral mRNA is expressed. Polyribosomal poly(A+) RNA then is hybridized with excess HSV-1 DNA

restriction fragments bound to cellulose and the fragment specific mRNA then is size-fractionated on methylmercury agarose gels.

Shown in Figure 5 are: (i) The viral mRNA species homologous to the L_R region (*Xba*I fragment G) when immediate-early and early mRNA predominate. It is seen that 2 kb and 1.5 kb mRNA are found early in addition to the immediate-early 2.8 kb mRNA. (ii) The viral mRNA species homologous to 0.26 to 0.29 (*Hind*III/*Xba*I fragment AC), when early mRNA predominates, shows only heterogeneously migrating material. When late mRNA is present, 6 kb, 3.2 kb, and 2 kb mRNA species are prominant. (iii) The viral mRNA species homologous to 0.53 to 0.59 (*Hind*III fragment K), when early mRNA predominates, shows mainly a 5.2 kb mRNA species. Late viral mRNA homologous to this same region shows this to continue to be in abundance. But further 7, 3.8, and 1.8 kb species also are prominant. (iv) There is a complex pattern of viral mRNA species homologous to *Bgl*II fragment P (0.20-0.23) late after infection with abundant species 6, 4.5, 3, 2, 1.8, and 1.5 kb clearly resolvable. In contrast, the region neighboring this fragment, *Bgl*II fragment N (0.23-0.27), encodes only one major mRNA species, a 6 kb one (as described below, this mRNA species has its 3' terminus in *Bgl*II fragment P).

In Figure 6 are shown two other striking examples of changes in mRNA complexity in the transition from early to late. (i) *Eco*RI fragment N (0.3 to 0.315) contains sequences homologous to HSV-1 thymidine kinase (TdRK), an early protein (38, 39). Early after infection, one major mRNA species (1.5 kb) is homologous to this region; the size of this mRNA is in good agreement with the size of the TdRK mRNA reported by Cremer et al. (40). Late after infection, a number of other mRNA species ranging from 5 to 2 kb are isolable in comparable yields. (ii) *Eco*RI fragment M (0.42-0.45) contains the regions where the 149,000 d HSV-1 specific DNA polymerase has been located (41, 42). Early after infection, a major mRNA species 4.4 kb in size is

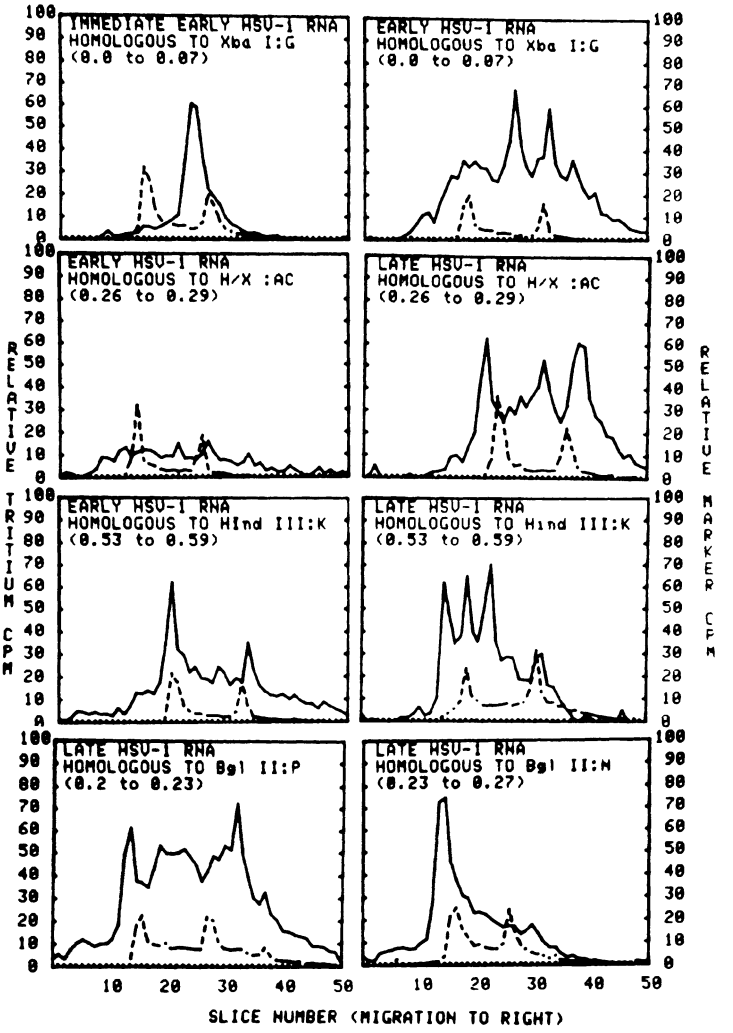

FIGURE 5. Size distribution of HSV-1 mRNA homologous to selected regions of the viral genome abundant at various times after infection. As described in Figure 2, poly(A+) polyribosomal RNA from cells where immediate-early, early, or late viral RNA is abundant was hybridized with HSV-1 DNA restriction fragments bound to cellulose. RNA samples of 5-10 µg were incubated with 25 µg equivalents of specific restriction fragments (31). Tritium radioactivity scales are between 500 and 1,000 CPM in various experiments. The dashed lines indicate the position of 28S and 18S rRNA included as size markers.

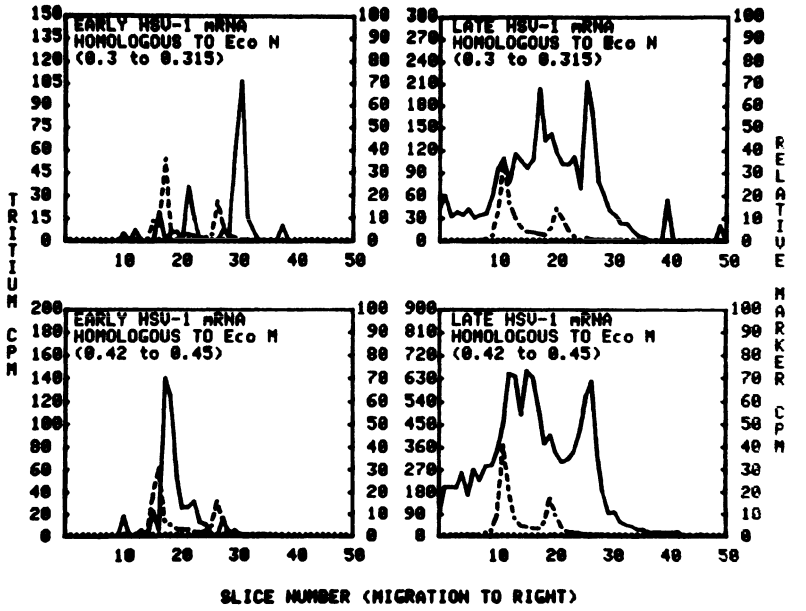

FIGURE 6. Size distribution of HSV-1 mRNA homologous to EcoRI fragments N and M early and late after infection. As described in Figures 2 and 5, poly(A+) polyribosomal RNA from cells where early or late viral RNA is abundant was hybridized with HSV-1 DNA restriction fragments bound to cellulose. The dashed lines indicate the position of 28S and 18S rRNA included as size markers.

seen homologous to this region, while late major species 3.5 and 1.6 kb also are seen.

Isolation and Characterization of Specific HSV-1 mRNA Species

The use of HSV-1 DNA restriction fragments bound to cellulose allows the isolation of a manageable number of viral mRNA species for further analysis (17, 31). Our protocol for analysis is simple: polyribosomal poly(A) mRNA is isolated from cells at the desired stage of replication. Viral

mRNA specific to a given region of the viral genome is isolated via preparative hybridization. Individual mRNA species can be obtained by size-fractionation on denaturing agarose gels, or by sucrose density gradient centrifugation. Such mRNA then can be used as a template for the synthesis of 3' cDNA via the use of reverse transcriptase, and the 3' end cDNA probes can be hybridized to Southern blots of restricted HSV-1 DNA. If the mRNA maps in two or more neighboring restriction fragments while the 3' probe cDNA maps in only one, a direction of transcription can be inferred. Size-fractionated mRNA also can be used for *in vitro* translation. Several examples of our approach are given below.

Size-fractionation of immediate-early HSV-1 mRNA on sucrose gradients gives a size distribution essentially the same as that seen in Figure 2. Translation of this mRNA indicates that the 4.2 kb species encodes the 170,000 d polypeptide, the 2.8 kb mRNA encodes the 120,000 d polypeptide, and the 1.8 kb mRNA encodes both a 68,000 d and a 64,000 d polypeptide. The translation products of size-fractionated 2.8 and 1.8 kb mRNA are shown in Figure 7. One immediate-early 1.8 kb mRNA species maps in *Hind*III fragments M (0.83-0.88) and N (0.88-0.91). It encodes the 68,000 d polypeptide since immediate-early *Hind*III fragment N cellulose-specific mRNA encodes this species. Its direction of synthesis is from M to N because, in addition to *Hind*III fragment N cellulose, the 2 kb mRNA can be preparatively isolated using any HSV-1 DNA restriction fragment bound to cellulose which contains the S_R region (i.e., *Hind*III fragments M or G, etc.); and yet, its 3' end maps mainly in *Hind*III fragment N (Figure 8). The directions of transcription of other immediate-early mRNA species are shown in Figure 9 (see Discussion).

Late mRNA specific to *Hind*III fragment K (0.53-0.59) is a template for the synthesis of polypeptides 140,000 d, 122,000 d, 54,000 d in size, and minor species 86,000 d and ~65,000 d also are seen. Early mRNA specific to this

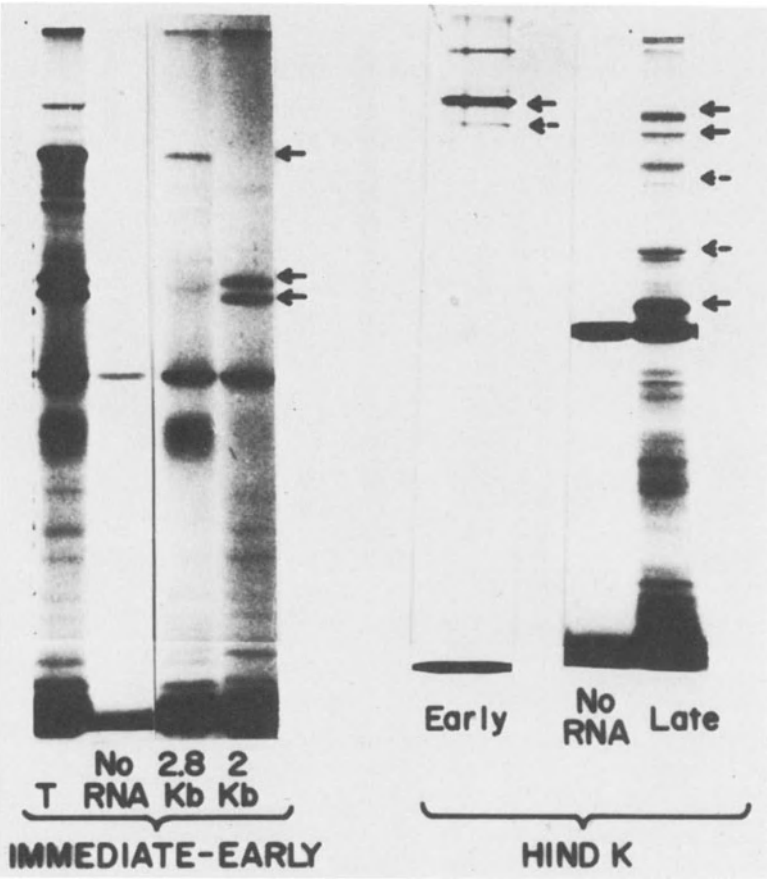

FIGURE 7. In vitro translation of isolated specific HSV-1 mRNA species. On the left are shown the size distributions of the translation products of total immediate-early HSV-1 RNA and the sizes of polypeptides encoded by 2.8 kb and 1.8 kb immediate-early RNA fractionated on sucrose gradients. The sizes of the polypeptides marked are (from the top) 120,000 d, 68,000 d, and 64,000 d. Bands of material migrating at the bottom of the gel were not reproducibly present. On the right are shown the products of in vitro translation of early and late HSV-1 mRNA homologous to HindIII fragment K. Also shown is the NO RNA CONTROL. Arrows indicate polypeptides of (from top) 140,000 d, 122,000 d, 85,000 d, 65,000 d, and 54,000 d. The dashed arrows indicate minor species reproducibly found. The band of material >200,000 d in the early RNA experiment is an artifact of the gel. The band at 50,000 d is seen with the NO RNA CONTROL; thus, it is endogenous to the system (31). Details are as described in Figure 3.

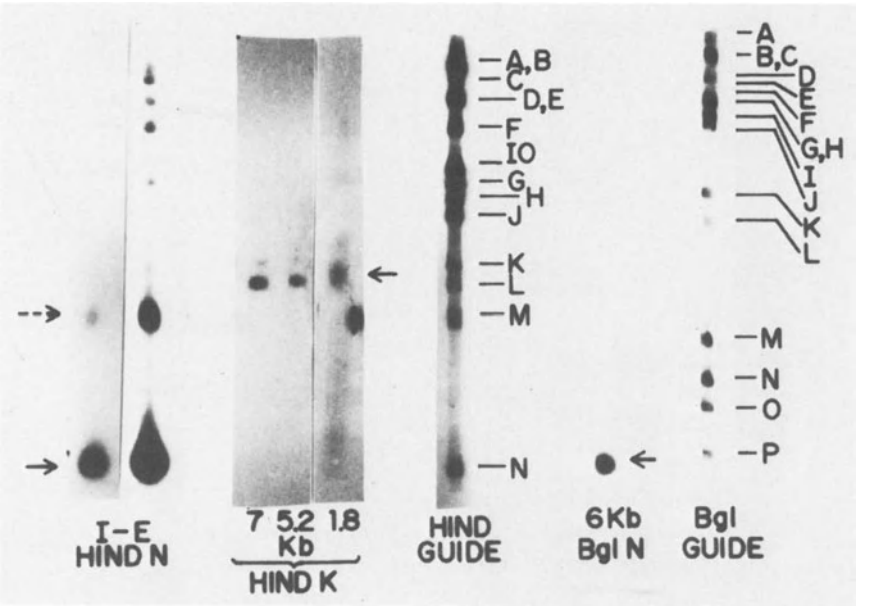

FIGURE 8. Hybridization of 3' cDNA made from specific HSV-1 mRNA species to Southern blots of restricted HSV-1 DNA. Specific HSV-1 mRNAs were partially degraded in alkali, the 3' ends isolated by chromatography through oligo-dT cellulose, and ^{32}P-labeled 3' cDNA was made using an oligo-dT primer for avian myeloblastosis virus reverse transcriptase (16, 17, 31). This 3' cDNA was hybridized to Southern blots of HSV-1 DNA to determine the locations of the RNA's 3' ends. On the left is shown the 3' cDNA made to HindIII fragment N specific immediate-early mRNA hybridized to a HindIII blot. Radioactivity is seen mainly in HindIII fragment N and some to fragment M. The middle blots are hybridization of 7, 5.2, and 1.8 kb HindIII fragment K specific mRNA. Hybridization is mainly to HindIII fragment L, which lies on the right of fragment K in the P arrangement. The HindIII guidestrip showing band resolution was made using total HSV-1 ^{32}P-labeled DNA. The blot on the right is the hybridization of 3' cDNA made to the 6 kb mRNA in BglII fragment N. Radioactivity is in BglII fragment P, which neighbors fragment N on the left in the P arrangement. A BglII guidestrip is included to show band resolution.

region encodes mainly the 140,000 d polypeptide with a minor amount of the 120,000 d one. Translation products of such mRNA are shown in Figure 7. These same polypeptides are seen when *Hind*III fragment K specific mRNA is repurified on oligo-dT cellulose prior to translation. Therefore, all are products of poly(A+) mRNA. With size-fractionated late *Hind*III fragment K specific mRNA (31), we have found that the 7 kb mRNA encodes the 54,000 d polypeptide, while the 5.2 kb mRNA encodes the 140,000 d one, as was expected from the finding of a major 5.2 kb mRNA encoding a 140,000 d polypeptide early. Since these two mRNA species are at least partially colinear by virtue of the position of their 3' ends (see below), we suggest that the 54,000 d polypeptide is encoded by the 5' end of the 7 kb mRNA and the distal 3' end is silent and its sequence similar to the 5.2 kb mRNA. The 3.8 kb mRNA encodes the 122,000 d protein and the minor 85,000 d species also is seen. The 1.8 kb mRNA encodes the minor 65,000 d doublet and, more interestingly, it also encodes the same 54,000 d polypeptide as does the 7 kb mRNA. This is not an artifact of degradation since poly(A+) 1.8 kb *Hind*III fragment K specific mRNA isolated by repurification on oligo-dT cellulose gives the same result.

As seen in Figure 8, the 3' ends of the 7, 5.2, and 1.8 kb mRNA species mapping in *Hind*III fragment K lie in the fragment to the right (*Hind*III fragment L, 0.59-0.65). From this, it is clear that the direction of transcription of these mRNA species is from left to right on the P arrangement. The situation with the 3.8 kb mRNA is not as clear since significant 3' cDNA made to this RNA maps to the left of 0.58. Our finding of a 7 and 1.8 kb mRNA with the same putative 3' ends, which encode the same polypeptide, has significant implications concerning the biogenesis of HSV-1 mRNA. We currently are examining this in detail.

Other mRNA species are being investigated as well. Two examples are briefly discussed below. The 6 kb late mRNA in *Bgl*II fragment N (0.23-0.27) encodes a 155,000 d

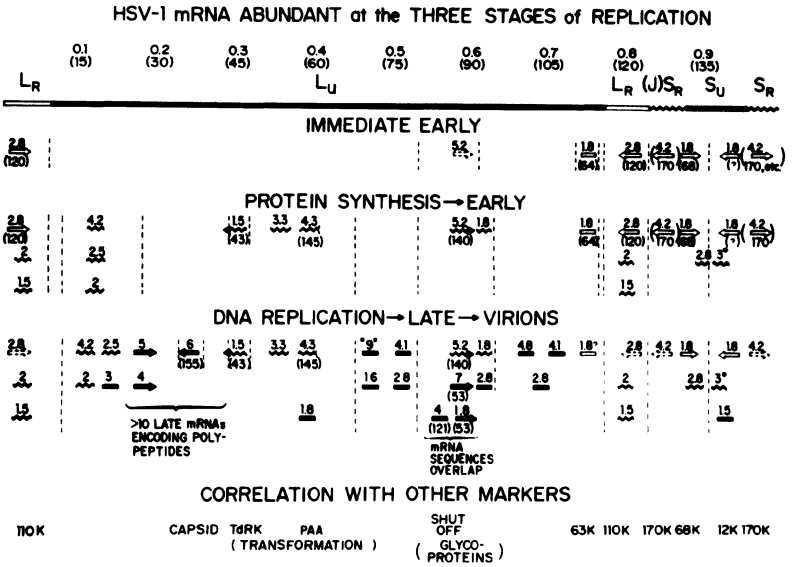

FIGURE 9. Location of HSV-1 mRNA species abundant at the three stages of replication. This figure summarizes studies described in detail elsewhere (16, 17, 29-31) and described briefly in this review. Also included are results of experiments currently in progress. Individual mRNA species are localized to the nearest restriction fragment or junction of two fragments found to have significant homology with them. The size of RNA (in kb) is indicated above the location. The direction of transcription, where known, is indicated by arrows pointing towards the 3' end in the P arrangement of HSV-1. The size of polypeptides encoded (where determined) is shown in thousands of daltons below the mRNA species in question. The locations of other markers were determined from data published by others (15, 27, 38-45).

polypeptide and maps within a region which appears to contain at least ten mRNA species encoding distinct polypeptides. The major capsid polypeptide has been located in the region where this 6 kb mRNA is found (43, 44). This

mRNA has its 3' end mapping in *Bgl*II fragment P (0.2 to 0.23; Figure 8); therefore, its direction of synthesis is from right to left. *Bgl*II fragment P also has 3' ends of mRNAs whose bulk maps to the left in *Bgl*II fragment O (0.17 to 0.2). Therefore, this region of the genome has mRNA species transcribed from both strands of the viral DNA. The 4.4 kb early mRNA homologous to *Eco*RI fragment M (0.42 to 0.45) encodes a 145,000 d polypeptide. This mRNA must be considered a candidate for the mRNA of HSV-1 DNA polymerase by virtue of its time of appearance, map location, size, and size of polypeptide it encodes.

DISCUSSION

The preparative isolation of HSV-1 mRNA, together with our rapid two-dimensional mapping techniques, has allowed us to map and begin characterization of a large number of immediate-early, early, and late viral mRNA species. These data are summarized in Figure 9. Individual mRNA species are localized to the smallest restriction fragment or fragments containing significant homology with them. Where known, the direction of synthesis and polypeptides encoded by the individual mRNA species also are shown. The correlation between our data and those of others using different techniques to map viral RNA and polypeptides is, generally, good. Thus, our data on immediate-early HSV-1 mRNA essentially confirms the recently published data of Watson et al. (15). Many of the polypeptide products for the mRNA species we have seen correlate well with map positions of similar sized polypeptides found using intertypic recombinants (43, 44). Our comparison of individual mRNA species and their *in vitro* translation products confirms that viral mRNA species can be divided into groups on the basis of their relative abundance at various times after infection. A number of the mRNA species which appear as abundant species prior to viral DNA replication continue to be

expressed as major species during viral DNA synthesis (i.e., the 5.2 kb mRNA in *Hind*III fragment K and the 4.4 kb mRNA in *Eco*RI fragment M). Their abundance is maintained or further increased upon viral DNA replication. We classify these as early mRNA species. In a second group are viral mRNA species which are characterized by a dependence on viral DNA synthesis for their becoming major mRNA species. Some of these cannot be detected at all prior to viral DNA synthesis. Others are detectable at reduced levels early (such as the 6 kb mRNA in *Bgl*II fragment N). We cannot, at this time, determine whether this difference is due to differences in the steady state level of the species prior to viral DNA replication, due to different mRNA half-lives or rates of synthesis, or whether they truly differ in whether or not they are expressed at all early. However, it is clear that only with viral DNA replication are any seen in the amounts that are normally seen late. This group, as a whole, is classified as late mRNA.

In addition to these temporal groupings of viral mRNA, there are several other patterns seen. At least one mRNA species (a 2.8 kb mRNA species in the S_U region) increases in abundance with labeling time, even in the absence of viral DNA synthesis. This could be an early viral mRNA with a very long half-life, thus causing its accumulation. Finally, there is a group of viral mRNA species which decrease in relative abundance with time of infection. These are immediate-early viral mRNAs. But not all of the immediate-early mRNAs display this decay. Further, in the case of the 2.8 kb mRNA mapping in the L_R region, it is clear that the rate of synthesis of this mRNA does not decrease with time. Only further experiments can establish those factors in viral gene expression which are responsible for the patterns described.

Finally, it should be emphasized that we have dealt only with abundant mRNA species of specific size. The correlation with the location of immediate-early and early species with earlier determinations by several labs,

including ours, using a variety of techniques, including electron microscopy, is fairly good (9, 10, 15-17, 24, 25). It is noteworthy, however, that the region between 0.18 and 0.29, where we have seen no abundant mRNA species early, hybridizes reasonably efficiently with unfractionated early mRNA, as determined by either R-loop mapping (24) or by saturation hybridization of specific restriction fragments (25). We do not, at this time, understand the significance of this finding.

In conclusion, the summary map of Figure 9 correlates well with the data of others. Naturally, there are areas to be clarified, terminology to be standardized, and minor differences to reconcile; however, it is very clear the repertory of techniques we have developed allow the isolation of biologically active mRNA. Our picture of HSV-1 gene expression, at the level of mRNA, is becoming increasingly clear. Certain regions of the genome are heavily utilized for dense packaging of information. Examples include the S_R regions, the region in *Hind*III fragment K, and there are others. As the biological function of this densely packaged information becomes clear, the significance of such highly utilized regions will emerge. Other regions of the genome are not nearly as heavily utilized for packaging abundant mRNA sequences, as least at certain times. The significance of such regions may be in the programming of appearance of the function they encode.

REFERENCES

1. Wagner, E. and B. Roizman (1969). Proc. Natl. Acad. Sci. USA *64*, 626-633.
2. Bachenheimer, S. and B. Roizman (1972). J. Virol. *10*, 875-879.
3. Silverstein, S., R. Millette, P. Jones and B. Roizman (1976). J. Virol. *18*, 977-991.
4. Stringer, J., L. Holland, R. Swanstrom, K. Pivo and E. Wagner (1977). J. Virol. *21*, 889-901.

5. Bartkoski, M. and B. Roizman (1976). J. Virol. *20*, 583-588.

6. Moss, B., A. Gershowitz, J. Stringer, L. Holland and E. Wagner (1977). J. Virol. *23*, 234-239.

7. Rakusanova, T., T. Ben-Porat, M. Himeno and A. Kaplan (1971). Virology *46*, 877-889.

8. Kozak, M. and B. Roizman (1974). Proc. Natl. Acad. Sci. USA *71*, 4322-4326.

9. Clements, J.B., R.J. Watson and N.M. Wilkie (1977). Cell *12*, 275-285.

10. Jones, P.C., G.S. Hayward and B. Roizman (1977). J. Virol. *21*, 268-276.

11. Honess, R. and B. Roizman (1974). J. Virol. *14*, 8-19.

12. Marsden, H., I. Crombie and J. Subak-Sharpe (1976). J. Gen. Virol. *31*, 347-372.

13. Preston, C.M. (1979). J. Virol. *29*, 275-284.

14. Watson, R. and J. Clements (1978). Virology *91*, 364-379.

15. Watson, R., C. Preston and J. Clements (1979). J. Virol. *31*, 42-52.

16. Holland, L., K. Anderson, J. Stringer and E. Wagner (1979). J. Virol. *31*, 447-462.

17. Anderson, K., R. Costa, L. Holland and E. Wagner (1979). Characterization and translation of HSV-1 mRNA abundant in the absence of *de novo* protein synthesis. *Submitted.*

18. Huang, H., J. Szabocsik, C. Randall and G. Gentry (1971). Virology *45*, 381-389.

19. Wagner, E. (1972). Virology *47*, 502-506.

20. Wagner, E., R. Swanstrom and M. Stafford (1972). J. Virol. *10*, 675-686.

21. Swanstrom, R. and E. Wagner (1974). Virology *60*, 522-533.

22. Murray, B., M. Benyesh-Melnick and N. Biswal (1974). Biochim. Biophys. Acta *361*, 209-220.

23. Swanstrom, R., K. Pivo and E. Wagner (1975). Virology *66*, 140-150.

24. Stringer, J., L. Holland and E. Wagner (1978). J. Virol. *27*, 56-73.

25. Jones, P. and B. Roizman (1979). J. Virol. *31*, 299-314.

26. Holland, L.E., Ph.D. Dissertation (1979). University of California, Irvine, School of Biological Sciences.

27. Powell, K., D. Purifoy and R. Courtney (1975). Biochem. Biophys. Res. Commun. *66*, 262-271.

28. Ward, R. and J. Stevens (1975). J. Virol. *15*, 71-80.

29. Holland, L., K. Anderson, C. Shipman Jr. and E. Wagner (1979). Viral DNA synthesis is required for the efficient translation of specific HSV-1 mRNA species. *Submitted*.

30. Anderson, K., J. Stringer, L. Holland and E. Wagner (1979). J. Virol. *30*, 805-820.

31. Anderson, K., L. Holland, B. Gaylord and E. Wagner (1979). Isolation and translation of mRNA encoded by a specific region of the HSV-1 genome. *Submitted*.

32. Enquist, L., M. Madden, P. Schiop-Stansly and G.F. Van de Woude (1979). Science *203*, 541-544.

33. Bailey, J. and N. Davidson (1976). Anal. Biochem. *70*, 75-85.

34. McMaster, G.K. and Carmichael, G.C. (1977). Proc. Natl. Acad. Sci. USA *74*, 4835-4838.

35. Wellauer, P.K. and Dawid, I.B. (1973). Proc. Natl. Acad. Sci. USA *70*, 2827-2831.

36. Laemmli, U.K. (1970). Nature *227*, 680-685.

37. Southern, E.M. (1975). J. Molec. Biol. *98*, 503-517.

38. Maitland, N. and J. McDougall (1977). Cell *11*, 233-241.

39. Wigler, M., S. Silverstein, L-S. Lee, A. Pellicer, Y. Cheng and R. Axel (1977). Cell *11*, 223-232.

40. Cremer, K., M. Boclemer and W. Summers (1978). Nuc. Acids Res. *5*, 2333-2344.

41. Purifoy, D., R. Lewis and K. Powell (1977). Nature *269*, 621-623.

42. Chartrand, P., N. Stow, M. Timbury and N. Wilkie (1979). J. Virol. *31*, 265-276.

43. Marsden, H., N. Stow, V. Preston, M. Timbury and N. Wilkie (1978). J. Virol. *28*, 624-642.

44. Morse, L., L. Pereira, B. Roizman and P. Schaffer (1978). J. Virol. *26*, 389-410.

45. Camacho, A. and P. Spear (1978). Cell *15*, 993-1002.

5. Properties of the Replicating HSV DNA

Ivan Hirsch

1. INTRODUCTION

The unusual structural features of herpes simplex virus (HSV) DNA have aroused vivid interest in the mechanism generating mature HSV DNA molecules. This report will deal mainly with the biochemical and biophysical properties of HSV DNA synthesized in the course of productive viral infection. The available data on the processing and topology of replication intermediates will also be discussed. Detailed aspects of the structure and function of the HSV genome are reviewed elsewhere in this book (for a better orientation in this chapter see schematic arrangement of HSV-1 DNA shown in Fig. 1).

The most relevant to the purpose of this section are the following items: (i) The replication of HSV-1 DNA is semiconservative, but its significant proportion may involve repair-type replication (26). (ii) The replication of HSV DNA proceeds *via* the formation of relatively small oligonucleotide fragments, which are mostly, but not entirely, repaired and/or ligated till maturation (5,12,18, 25,36). (iii) A combination of electron microscopy (13,17, 23,36), hydrodynamic studies (17,18,23,36) and analysis by restriction endonucleases (17,22) has revealed the presence of linear, circular, branched, lariat-type and concatemeric structures of different size, in some cases containing internal replication loops and single-stranded regions. The concatemers consist of a head-to-tail arrangement of short (S) and long (L) segments of HSV DNA (22). (iv) Defective

Y. Becker (ed), Herpesvirus DNA.

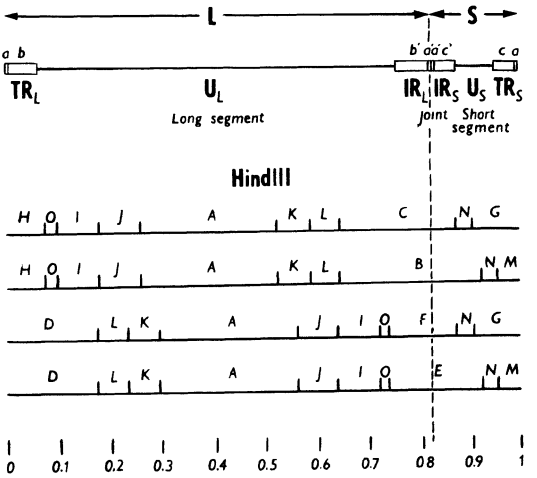

Fig. 1. Topology of the HSV-1 DNA and HindIII restriction endonuclease maps of the four arrangements of HSV-1 DNA. Long /L/ and short /S/ segments of HSV-1 DNA consist of unique sequences U_L and U_S which are bounded by inverted repetitions /TR_L and IR_L / and /TR_S and IR_S /, respectively. The L and S segments share only the sequence a.

HSV-1 DNA, consisting of repeat units which are apparently also organized in a head-to-tail tandem array (11,27), is supposed to be generated by a rolling-circle type of replication (2). At least one initiation point of HSV-1 DNA synthesis should therefore be localized in the repetitive regions of wild-type HSV-1 DNA S segment (Fig. 1) from which the defective sequences originate (11). (v) The localization of the origin of replication of wild-type HSV DNA is consistent with the hypothesis that DNA synthesis is initiated in or close to the joint region of S and L segments (17,36), although some initiation sites have also been observed at a greater distance from the DNA termini (13).

2. SINGLE-STRANDED REGIONS IN REPLICATING HSV DNA MOLECULES

The presence of single-stranded regions in replicating HSV

DNA molecules has been reported by several groups of investigators (17,23,36). Electron microscopy revealed these regions predominantly at the ends of HSV and pseudorabies virus DNAs (23,24), but also internally located (23), possibly at the sites of inverted repeats. The filling up and sealing of single-stranded gaps proceeds gradually up to HSV DNA maturation (Fig. 2a,c). The greater affinity for nitrocellulose of denatured DNA as compared with native DNA provides in this case a usefull means for monitoring the presence of single-stranded regions in the molecule. Binding to nitrocellulose reveals the presence of even a short single-stranded gap attached to long double-stranded stretches, regardless of whether it is localized in newly synthesized or template DNA. The presence of single strands in HSV DNA was highest after short pulses of ^{3}H-thymidine and decreased with prolongation of the pulse chase (Fig. 2a). The extent of retention of intracellular HSV-1 DNA by nitrocellulose never dropped below the value determined for the virion DNA. No HSV DNA was found bound to nitrocellulose if it had been treated with single-strand-specific nuclease S1 (Fig. 2a).

While no data are available on the presence and extent of single-stranded regions in template strands, the relative content of single strands in newly synthesized material has been monitored thanks to their sensitivity to single-strand-specific nuclease S1 and by hydroxylapatite chromatography (Fig. 2b). After a 30-sec pulse of ^{3}H-thymidine more than 20% of newly synthesized HSV DNA behaved as single-stranded, but this amount dropped to a few per cent after a 3-min pulse and was negligible after chasing the pulse for more than 20 min. It seems therefore that portions of the nascent HSV DNA were present in the single-stranded form without the use of any special denaturation conditions. Single-stranded regions in different replicative complexes have usually been observed in parental DNA strands (9,21,44). However, a displacement of a newly synthesized chain by the parental DNA strand,

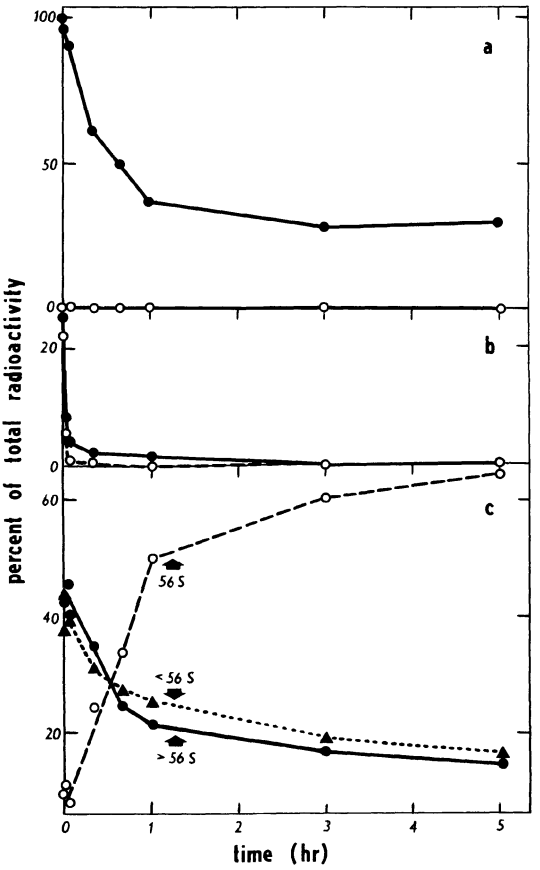

Fig. 2. The processing of replicating HSV DNA molecules in infected cells. Rabbit-embryo fibroblasts infected with HSV-1 at a MOI of 1 PFU/cell were labelled 12 hr post infection with ^{3}H-thymidine for 30 sec, 1 min, 3 min, or 3 min and chased for different periods of time. HSV-1 DNA extracted from cells by Pronase and Sarcosyl was purified on CsCl gradients. For detailed description of the individual methods see /18/. a/ Binding of purified HSV DNA molecules to nitrocellulose filters before ●—● and after ○—○ S1-nuclease treatment. b/ Proportion of single strands in newly replicated HSV DNA. Percentage of activity eluted from hydroxylapatite column by 0.21 M phosphate buffer ●—● . Percentage of trichloroacetic acid-soluble activity after S1-nuclease treatment ○---○. c/ Kinetics of changes of hydrodynamic properties of HSV DNA. Purified HSV DNA was sedimented through a 5 to 20% sucrose gradient. Each gradient was divided into three parts /see Fig. 3/: fast sedimenting DNA /fractions 1 to 13/ ●—●; virion 56 S DNA /fractions 14 to 16/ ○---○; and slowly sedimenting DNA /fractions 17 to 25/ ▲-----▲. The relative amounts of radioactivity sedimenting in each part of gradient is calculated.

which caused the daughter chain to appear single-stranded, has also been observed (9). Sometimes, this branch migration at the replication point causes newly synthesized chains to dissociate from the replication complex as single-stranded DNA (33). The behaviour of nascent HSV DNA after a very short pulse is reminiscent of the properties of newly synthesized DNA of eukaryotic (14,15,34) and prokaryotic (30,31,32) systems, where single strands in nascent DNA have also been observed.

Small RNA pieces probably acting as primers for the synthesis of nascent DNA have been described to be covalently bound to newly synthesized HSV DNA (5,29). Their total amount as well as the amount of alkali-labile sites in HSV DNA (5,29) only gradually decrease during the maturation of the molecule. A large part (over 50%) of the single-stranded gaps and nicks present in HSV DNA isolated from virions is *in vitro* repairable by DNA polymerase I and DNA ligase; consequently, a large part of the molecules become alkali resistant (20). The ribonucleotides, were also reported to be present in mature HSV-1 DNA molecules (19). If not a preparative artifact, they are probably localized at unrepairable sites or molecule ends. The possible role for uracil residues (5,19,29) in HSV DNA in the course of intramolecular recombination has been postulated by Becker (1).

3. THE PROCESSING OF HSV DNA IN INFECTED CELLS

The fate of newly-replicated DNA was followed in pulse--chase experiment. Most of the activity incorporated into HSV DNA during a very short ^{3}H-thymidine pulse (30 sec to 3 min) sedimented much faster in sucrose gradients than does mature HSV DNA (18). $s_{20,w}$ values above 200 S were found for HSV and pseudorabies virus DNAs (3,4,18,23). The percentages of the total activity sedimenting as light, virion-like (56 S) and fast HSV DNA (Fig. 3) at different

time periods after pulse labelling are shown in Fig. 2c. It is obvious that the amounts of the fast and the slowly sedimenting DNAs decrease in parallel with an increase of mature 56 S DNA molecules in the course of 1 hr after pulse.

A few tentative conclusions may be drawn on the basis of the results shown in Fig. 2. (i) At the extremely short pulse, labelled thymidine is predominantly incorporated into the rapidly sedimenting DNA, containing concatemers. (ii) The time coincidence between the decrease in the amount of single-stranded regions (Fig. 2a) and generation of 56 S DNA molecules indicates that extensive repair-type synthesis probably takes place during HSV DNA maturation. (iii) The highest proportion of single-stranded regions should be present in the rapidly sedimenting DNA.

4. TOPOLOGY OF THE REPLICATING HSV DNA MOLECULE

Restriction endonucleases have been used with success to characterize the arrangement of replicating DNA molecules of several animal viruses (4,6,8,10,17,22,30,38,43) . We have analysed intracellular CsCl-purified HSV DNA labelled for 15 min with ^{3}H-thymidine and pooled from different regions of a sucrose gradient (Fig. 3). ^{3}H-thymidine--labelled fractions were mixed with ^{32}P-labelled HSV virion DNA, cleaved with *Hin*dIII, electrophoresed in 0.4% agarose, and the normalized ratio of ^{3}H to ^{32}P was determined for each fragment (Table 1). The product of this value and the molar ratio of any particular fragment of virion DNA corresponds to the actual molar ratio of this fragment in ^{3}H-thymidine-labelled replicating HSV DNA. A normalized ratio of ^{3}H to ^{32}P equal or close to one indicates that the respective fragment in the replicating material is present in the same molar ratio as in virion DNA. This was the case for all fragments derived from continuously ^{3}H-labelled HSV DNA and for all "one molar" fragments of fast

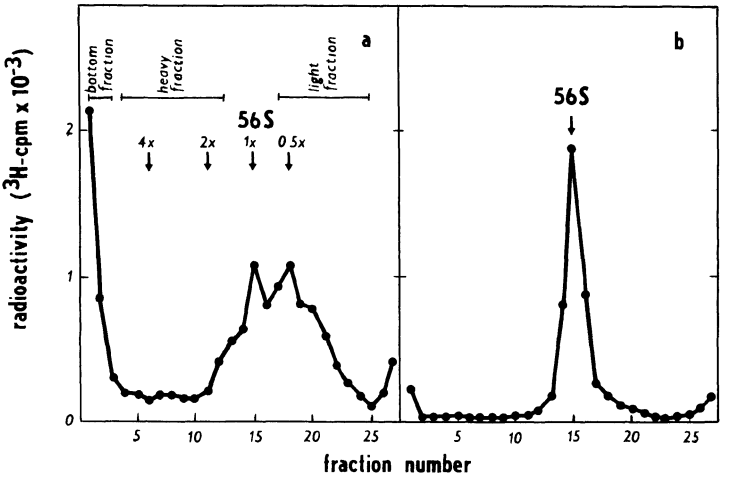

Fig.3. Neutral sucrose gradient sedimentation of pulse--labelled and continuously labelled HSV-1 DNA. HSV-1--infected rabbit kidney cells were labelled with ^{3}H-thymidine for 15 min at 12 hr p.i. /a/ or continuously for 12 hr /b/. HSV-1 DNA was isolated after centrifugation in CsCl density gradients, and purified viral DNAs were centrifuged in linear sucrose density gradients /5-20%/ overlaid on top of 0.2 ml cushions of saturated CsCl at 35,000 rpm in a Beckman SW41 rotor for 3 hr. Radioactivity of 5-µl aliquots was determined. The bottom of the tube is at the left. Arrows indicate the position of mature 56 S HSV-1 DNA /unit size/ and a hypothetical position of linear molecules having a molecular weight 0.5 x, 2 x, and 4 x that of 56 S DNA.

sedimenting pulse-labelled HSV DNA (Fig. 3, Table 1, heavy and bottom fractions).

The lowest value of normalized ratio of ^{3}H to ^{32}P in HSV DNA from bottom fraction of sucrose gradient digested by *Hin*dIII was found for the 0.5 M terminal fragments D, G, H and M. On the contrary, the highest ratio was found for the 0.25 M fragments C, E,and F originating from the junction of L and S segments of HSV-1 DNA (Fig. 1). The decrease in terminal and increase in junction fragments suggests that endless structures consisting of head-to-tail arrangement of L and S segments are present in the bottom fraction of the pulse-labelled HSV DNA. The results are consistent with the assuption that replicative HSV DNA is

in concatemeric or a circular form (4,22) . Our results are similar to those obtained by Jacob *et al.* (22) by *Bgl*II cleaveage of DNA accumulating in cell nuclei during long periods of labelling (2 to 8 hr). We assume that our arrangement using short pulses of labelling enabled us to analyse the actually replicating DNA with higher degree of reliability.

Longer-than-unit-size linear molecules were observed quite frequently by electron microscopy and many concatemers could be traced within the large tangles that resist spreading by conventional methods (3,23,36, Hirsch unpublished data). Although HSV DNA successfuly circularized *in vitro* using 5´ lambda exonuclease (39,40), unit-size circular molecules were only scarcely observed in the preparations of intracellular HSV DNA (23).

The formation of concatemers may be significant for the synthesis of 5´ ends of progeny DNA strands (42), although alternative models not requiring generation of concatemers have been proposed for DNA molecules bearing palindromes (7,16). Concatemers consisting of head-to-tail arrangement of L and S segments of HSV DNA could be generated either from unit-size molecules by some specific mechanism preventing junction of two S or two L segments together or by a rolling-circle replication. Although structures corresponding to rolling-circle replication have not been demonstrated to date, they may easily be present unrecognized in complicated tangled structures. The predominant incorporation of the short pulse of ^{3}H-thymidine into the fast sedimenting fractions of the sucrose gradient (Fig. 2c) also speaks in favour of rolling-circle replication in HSV DNA. An elegant model for HSV DNA replication *via* a rolling-circle mechanism explaining the generation of four arrangements of HSV DNA has been proposed by Jacob *et al.* (22).

Although the cleaveage pattern obtained with *Hin*dIII does not permit analysis of the molar ratio of junction fragment B, the increased molar ratio of the other junction

Table 1

Relative labelling of HindIII fragments from replicating HSV-1 DNA molecules

*Hin*dIII DNA fragments[a]	Molar ratio[b]	^{3}H-to-^{32}P normalized ratio[c]			
		Continuous labelling with ^{3}H-thymidine for 12 hr p.i.	15-min ^{3}H-thymidine pulse (12 hr p.i.)[d]		
			light fraction	heavy fraction	bottom fraction
A & B	1.0 & 0.25	1.02	0.36	0.54	0.92
C	0.25	1.10	0.98	1.12	1.31
D	0.5	1.06	0.77	0.67	0.59
E	0.25	1.13	1.46	1.33	1.47
F	0.25	1.14	2.22	1.64	1.60
G	0.5	0.85	1.01	0.64	0.63
H	0.5	0.98	1.00	0.77	0.63
I	1.0	1.09	1.15	0.92	1.02
J	1.0	0.87	1.30	0.91	1.16
K	1.0	0.95	1.25	1.03	1.14
L	1.0	0.97	1.23	1.07	1.10
M	0.5	0.99	1.08	0.82	0.61
N	1.0	1.09	1.17	1.12	1.11
O	1.0	1.02	0.96	0.95	0.91

a Nomenclature according to Skare and Summers (37). Fragments A and B comigrated. For physical mapping data see Fig. 1.

b Quarter molar junction fragments contain the joint region of L and S segments. Half molar fragments contain terminal sequences. One molar fragments are derived from unique regions U_L and U_S of L and S segments, respectively (see Fig. 1).

c Calculated according to formula:

$$\frac{\text{fragment } ^3\text{H-cpm} \times \text{total } ^{32}\text{P-cpm}}{\text{fragment } ^{32}\text{P-cpm} \times \text{total } ^3\text{H-cpm}}$$

d HSV DNA was isolated and fractionated in sucrose gradient as described in legend to Fig. 3. Light, heavy and bottom fractions correspond to fractions under the horizontal barrs. For detailed description of all methods see (17).

fragments C, E and F (Table 1) implies that at least two isomers of HSV DNA can participate in the replication process. This was even better demonstrated by Jacob *et al.* (22) with the use of restriction endonuclease *Bgl*II, which makes possible the separation of all four junction fragments. It should be remembered that the analysis of intertypic HSV-1 x HSV-2 recombinants led Morse *et al.*(28) to the assumption that only one or two arrangements of HSV DNA are able to form recombinants.

Similar values of normalized ratio ^{3}H to ^{32}P were obtained for *Hin*dIII fragments produced by the cleaveage of pulse-labelled HSV DNA pooled from heavy and bottom fractions of sucrose density gradients (Table 1). No long concatemers were observed in the heavy fraction (Fig. 3) by electron microscopy. We interpreted the results of analysis of the heavy fraction previously as consistent with the hypothesis that HSV DNA synthesis is initiated at junction fragments originating from the joint region (17). The rationale leading us to this conclusion was based on the following assumptions: A short pulse of ^{3}H-thymidine will be incorporated randomly into different regions of a replicating HSV DNA molecule in accord with the random position of replication points in a nonsynchronized population of replicating molecules. Those molecules which have succeeded to mature during the pulse will be labelled predominantly at the replication terminus. Since mature HSV DNA sediments at $s_{20,w}$ equal to 56 S and therefore is not frequently present in the "heavy fraction" of the gradient (Fig. 3), the heavy fraction should be richer for molecules labelled predominantly at the origin. When such molecules are cleaved with restriction endonucleases, one could expect a gradient of labelled fragments: the fragments nearest to the origin having maximal radioactivity and those at increasing distance from origin having less and less radioactivity.

The similarity of normalized ratios of ^{3}H to ^{32}P observed for heavy and bottom fractions of the gradient could be

alternatively explained by the presence of short oligomers (dimers and trimers) of unit-size HSV DNA or by the presence of random fragments of concatemers in the heavy fraction of the sucrose gradient. A large proportion of intracellular HSV DNA ($s_{20,w}$ < 56 S, light fraction, Fig. 3, Table 1) migrated in agarose gel heterogeneously and faster than mature HSV DNA making thus interpretation of the electrophoretic profiles after cleaveage with restriction endonucleases very difficult.

5. CONCLUDING REMARKS

A fair amount of data on the replication of HSV DNA has been accumulated within several recent years. Some of these data are reviewed in this chapter. A number of models for the basic steps in HSV DNA replication, including initiation, formation of replication intermediates, DNA chain prolongation and maturation, have been developed on the basis of the available information. The large number of assumptions involved in the play make these models rather provisional; however, the resulting predictions are invaluable for the formation of new working hypotheses and generation of alternative models.

To describe the individual steps in their time sequence, the following hypotheses may be adduced: (i) As mentioned before, at least one initiation point of HSV DNA synthesis could be localized at or near the joint region connecting the L and S segments of the mature HSV DNA molecule or in the same sequences connecting the ends of HSV DNA molecules in concatemers or circles (17,36). In addition, replication could also be initiated at other sites of HSV DNA (13).

(ii) Replication proceeds bidirectionally from the origin, forming eye-looped and branched structures (36). The formation of concatemers should follow immediately after this process. Alternatively, replication could proceed *via* a rolling-circle mechanism. The predominant incor-

poration of a short pulse of radioactive label into the fast-sedimenting DNA makes this fraction the best candidate in the search for replicative intermediates. From this point of view, the rolling-circle mechanism of HSV DNA replication is, at the moment, probably the most consistent with the known features of HSV DNA structure and synthesis.

(iii) The majority of models explaining the generation of four arrangements of HSV DNA molecules are based on intermolecular or intramolecular recombination (1,22,35,37). Alternatively, at least one type of inversion, i.e. inversion of both the L and S components, might originate as a direct result of cleavage of one portion of concatemers in the joint region occurring originally in parental HSV DNA and another portion of concatemers in the new junction of L and S component resulting from the connection of the ends of HSV DNA molecules in concatemers or circles. It is worth noting that the latter mechanism might account for heterogeneity in the joint region and the terminal fragments as observed by Wagner and Summers (41).

All the hypotheses derived from restriction endonuclease analyses of replicating DNA should be treated with some reservation. There are several reasons for this:
(i) Molecules containing single-stranded regions presumably have an abnormal restriction endonuclease cleavage pattern and the resulting fragments have an atypical electrophoretic mobility. (ii) Atypical electrophoretic mobility should also be assumed for fragments containing a replication fork. (iii) Site-specific processes (e.g. recombination) combined with repair-type DNA synthesis may cause nonuniform labeling along the molecule.

The complicated structure of the fast-sedimenting DNA containing single-stranded regions and tangled complexes, together with the possible time coincidence of replication and site-specific postreplication processes probably represent the most dangerous pitfall in the further research and interpretation of data on HSV DNA replication.

REFERENCES

1. BECKER, Y. (1978). A model for intramolecular recombination of circular, circular-linear and fragmented genomes. J. teoret. Biol. 75: 339-347.
2. BECKER, Y., ASHER, Y., WEIBERG-ZAHLERING, E., RABKIN, S., FRIEDMANN, A., and KESSLER, E. (1978). Defective herpes simplex virus DNA: Circular and circular-linear molecules resembling rolling circles. J. gen. Virol. 40: 319-335.
3. BEN-PORAT, T., KAPLAN, A. S., STEHN, B., and RUBENSTEIN, A.S. (1976). Concatemeric forms of intracellular herpesvirus DNA. Virology 69: 547-560.
4. BEN-PORAT, T., and RIXON, F. J. (1979). Replication of herpesvirus DNA. IV: Analysis of concatemers. Virology 94: 61-70.
5. BISWAL, N., MURRAY, B. K., and BENYESH-MELNICK, M.(1974) Ribonucleotides in newly synthesized DNA of herpes simplex virus. Virology 61: 87-99
6. BOURGAUX, P., DELBECCHI, L. and BOURGAUX-RAMOISY, D. (1976). Initiation of adenovirus type 2 DNA replication. Virology 72: 89-98.
7. CAVALIER-SMITH, T. (1974). Palindromic base sequences and replication of eucaryote chromosome ends. Nature 250: 467-470.
8. CRAWFORD, L. V., ROBBINS, A. K., NICKLIN, P. M., and OSBORN, K. (1974). Polvoma DNA replication. Location of the origin in different virus strains. Cold Spring Harbor Symp. Quant. Biol. 39: 219-225.
9. DELIUS, H., HOWE, C., and KOZINSKI, A. W. (1971). Structure of the replicating DNA from bacteriophage T4. Proc. natn. Acad. Sci. USA 68: 3049-3053.
10. FAREED, G.C., GARON, C. F. and SALZMAN, N. P. (1972). Origin and direction of simian virus 40 deoxyribonucleic acid replication. J Virol. 10: 484-491.
11. FRENKEL,N., LOCKER, H., BATTERSON, W., HAYWARD, G., and ROIZMAN, B. (1976). Anatomy of herpes simplex virus DNA. VI. Defective DNA originates from the S component. J. Virol. 20: 527-531.
12. FRENKEL, N., and ROIZMAN, B. (1972). Separation of the herpes deoxyribonucleic acid duplex into unique fragments and intact strand on sedimentation in alkaline gradients. J. Virol. 10: 565-572.
13. FRIEDMANN, A., SHLOMAI, J., and Becker, Y. (1977). Electron microscopy of herpes simplex virus DNA molecules isolated from infected cells by centrifugation in CsCl density gradients. J. gen. Virol. 34: 507-522
14. HABENER, J. F., BYNUM, B. S. and SHACK, J. (1970). Destabilized secondary structure of newly replicated HeLa DNA. J. molec. Biol. 49: 157-170.
15. HAYTON, G. J., PEARSON, C. K., SCAIFE, J. R., and KEIR, H. H. (1973). Synthesis of deoxyribonucleic acid in BHK-21/C13 cells. Biochem. J. 131: 499-508.
16. HEUMANN, J. M. (1976). A model for the replication of the

ends of linear chromosomes. Nucleic Acid Res. 3: 3167-3171.
17. HIRSCH, I., CABRAL, G., PATTERSON, M., and BISWAL, N. (1977). Studies of the intracellular replicating DNA of herpes simplex virus type 1. Virology 81: 48-61.
18. HIRSCH, I., ROUBAL J., and VONKA, V. (1976). Replicating DNA of herpes simplex virus type 1. Intervirology 7: 155-175.
19. HIRSCH, I., and VONKA, V. (1974). Ribonucleotides linked to DNA of herpe simplex virus type 1. J. Virol. 13: 1162-1168.
20. HYMAN, R. W., OAKES, J.E., and KUDLER, L. (1977). In vitro repair of the preexisting nicks and gaps in herpes simplex virus DNA. Virology 76: 286-294.
21. INMAN, R. B., and SCHNÖS, M. (1971). Structure of branch points in replicating DNA: Presence of single-stranded connections in lambda DNA branch points. J. molec. Biol. 56 319-325.
22. JACOB, R. J., MORSE, L. S., and ROIZMAN, B. (1979). Anatomy of herpes simplex virus DNA. XII. Accumulation of head-to-tail concatemers in nuclei of infected cells and their role in the generation of the four isomeric arrangements of viral DNA. J. Virol. 29: 448-457.
23. JACOB, R. J., and ROIZMAN, B. (1977). Anatomy of herpes simplex virus DNA. VIII. Properties of the replicating DNA. J. Virol. 23: 394-411.
24. JEAN, J.-H., and BEN-PORAT, T. (1976). Appearance in vivo of single-stranded complementary ends of parental herpesvirus DNA. Proc. natn. Acad. Sci. USA. 73: 2674-2678.
25. KIEFF, E. D., BACHENHEIMER, S. L., and ROIZMAN, B. (1971). Size, composition and structure of the deoxyribonucleic acid of herpes simplex virus subtypes 1 and 2. J. Virol. 8: 125-132.
26. KOLBER, A. R. (1975). In vitro synthesis of DNA in nuclei isolated from human lung cells infected with herpes simplex type II virus. J. Virol. 15: 322-331.
27. LOCKER, H. and FRENKEL, N. (1978). The DNA of serially passaged herpes simplex virus: Organisation, origin and homology to viral RNA. In "Oncogenesis and Herpesviruses III" (G. de Thé, W. Henle, F. Rapp, eds.), pp. 75-85. I.A.R.C., Lyon. France.
28. MORSE, L. S., BUCHMAN, T. G., ROIZMAN, B., and SCHAFFER P. A. (1977). Anatomy of herpes simplex virus DNA. IX. Apparent exclusion of some parental DNA arrangements in the generation of intertypic HSV-1 x HSV-2 recombinants. J. Virol. 24: 231-248.
29. MÜLLER, W. E. G., ZAHN, R. K., ARENDS, J., and FALKE, D. (1979). Oligoribonucleotide initiators for herpes simplex virus DNA synthesis in vivo and in vitro. Virology 98: 200-210.
30. NATHANS, D., and DANNA, K. J. (1972). Specific origin in SV 40 DNA replication. Nature New Biol. 236:

200-202.
31. OISHI, M. (1968). Studies on DNA replication in vivo. I. Isolation of the first intermediate of DNA replication in bacteria as single-stranded DNA. Proc. natn. Acad. Sci. USA. 60: 329-336.
32. OISHI, M. (1968). Studies on DNA replication in vivo. II. Evidence for the second intermediate. Proc. natn. Acad. Sci. USA. 60: 691-698.
33. OKAZAKI, R., OKAZAKI, T., SAKABE, K., SUGIMOTO, K., KAINUMA, R., SUGINO, A., and IWATSUKI, N. (1968). In vivo mechanism of DNA chain growth. Cold Spring Harbor Symp. quant. Biol. 33: 129-142.
34. PAINTER, R. B., and SCHAEFER, A. (1969). State of newly synthesized HeLa DNA. Nature 221: 1215-1217.
35. SHELDRICK, P., and BERTHELOT, N. (1974). Inverted repetitions in the chromosome of herpes simplex virus. Cold Spring Harbor Symp. quant. Biol. 39: 667-678.
36. SHLOMAI, J., FRIEDMANN, A., and BECKER, Y. (1976). Replicative intermediates of herpes simplex virus DNA. Virology 69: 647-659.
37. SKARE, J., and SUMMERS, W. C. (1977). Structure and function of herpesvirus genomes. II. EcoRI, XbaI, and HindIII endonuclease cleavage sites on herpes simplex virus type 1 DNA. Virology 76: 581-595.
38. TOLUN, A., and PETTERSSON, U. (1975). Termination sites for adenovirus type 2 DNA replication. J. Virol. 16: 759-766.
39. WADSWORTH, S., HAYWARD, G., and ROIZMAN, B. (1976). Anatomy of herpes simplex virus DNA. V. Terminally repetitive sequences. J. Virol. 17: 503-512.
40. WADSWORTH, S., JACOB, R. J., and ROIZMAN, B. (1975). Anatomy of herpes simplex virus DNA. II. Size, composition and arrangement of inverted terminal repetitions. J. Virol. 1487-1497.
41. WAGNER, M. J., and SUMMERS, W. C. (1978). Structure of the joint region and the termini of the DNA of herpes simplex virus type 1. J. Virol. 27: 374-387.
42. WATSON, J. D. (1972). Origin of concatemeric T7 DNA. Nature New Biology. 239: 197-201.
43. WINNACKER, E. L. (1974). Origins and termini of adenovirus type 2 DNA replication. Cold Spring Harbor Symp. quant. Biol. 39: 547-550.
44. WOLFSON, J., and DRESSLER, D. (1972). Regions of single stranded DNA in the growing points of replicating bacteriophage T7 chromosomes. Proc. natn. Acad. Sci. USA 69: 2682-2686.

6. Electron microscopy of branched HSV DNA molecules: Possible recombination intermediates

Adam Friedmann, Samuel Rabkin* and Yechiel Becker*

INTRODUCTION

In his review of the molecular mechanisms of DNA recombination, Hotchkiss (1) suggested that the different patterns of recombination result from the heterogeneous genetic and physiological systems involved in the process. In another communication, Meselson and Radding (2) modified and extended the Holliday model (3) for DNA recombination. Broker and Lehman (4) and Broker (5) who studied bacteriophage DNA recombination by investigating the morphology of the DNA molecules by electron microscopy, proposed that the H-shaped and branched T4 DNA molecules were recombination intermediates. Furthermore, Valenzuela and Inman (6) described a novel type of junction between the duplex strands of λ phage DNA that pointed to a crossing over of DNA from one molecule to another which could be associated with recombination. Potter and Dressler (7) used a control *in-vitro* system for studying generalized genetic recombination in *E. coli*. Their work showed a good correlation between the morphology of genomes in the recombination process and the proposed theoretical recombination stages.

In a recent paper, Wolgemuth and Hsu (8) demonstrated a number of recombination intermediates of adenovirus DNA. Since intertypic complementation and recombination between the serotypes HSV-1 and HSV-2 have been reported (9-13), we decided to investigate DNA recombination by means of electron microscopy of HSV-1. In this study, conditions leading to an abortive virus cycle were employed, with the expectation that, thus, viral DNA molecules in the process of recombination would accumulate in the cell nucleus.

Y. Becker (ed), Herpesvirus DNA.

EXPERIMENTAL

The abortive conditions used in this study included infection of BSC-1 monolayers in Dulbecco's modified Eagle's medium (Grand Island Biological Co.) with the HF strain of HSV-1 under conditions of arginine deprivation (14), or in the presence of 5×10^{-2} M hydroxyurea (HU) (15). In addition, cells were infected at a high multiplicity of infection which leads to the synthesis of defective viral DNA. Both the HF and KOS strains of HSV-1 were used for the production of defective virus (16; Chap. 10). 5-Methyl-^{3}H-thymidine (specific activity 16.3 Ci/mmol; Nuclear Research Center, Negev, Israel) was used at a final concentration of 25 μCi/ml to label the DNA. The DNA preparations from cells isolated at 4-10 hr post-infection (p.i.) depending on the specific conditions used, were centrifuged in CsCl gradients and the viral DNA was spread and examined by electron microscopy (17).

RESULTS

Under conditions leading to an abortive virus cycle, which were created by the use of HU, arginine deprivation or a high multiplicity of infection, we repeatedly encountered DNA molecules with a structure that could be interpreted as that of recombination intermediates. The three main classes of molecules observed were branched double-stranded DNA (dsDNA) molecules, dsDNA molecules with short single-stranded "whiskers", and dsDNA molecules connected by a short single-stranded bridge.

Branched dsDNA molecules

Molecules falling into this category are characterized by dsDNA filaments which branch at one or a few points along the linear molecule. Three DNA fragments with two cross-over points are shown in Fig. 1; two of the fragments have short double-stranded branches distributed randomly along the viral DNA. DNA molecules connected by double-stranded bridges are illustrated in Fig. 2.

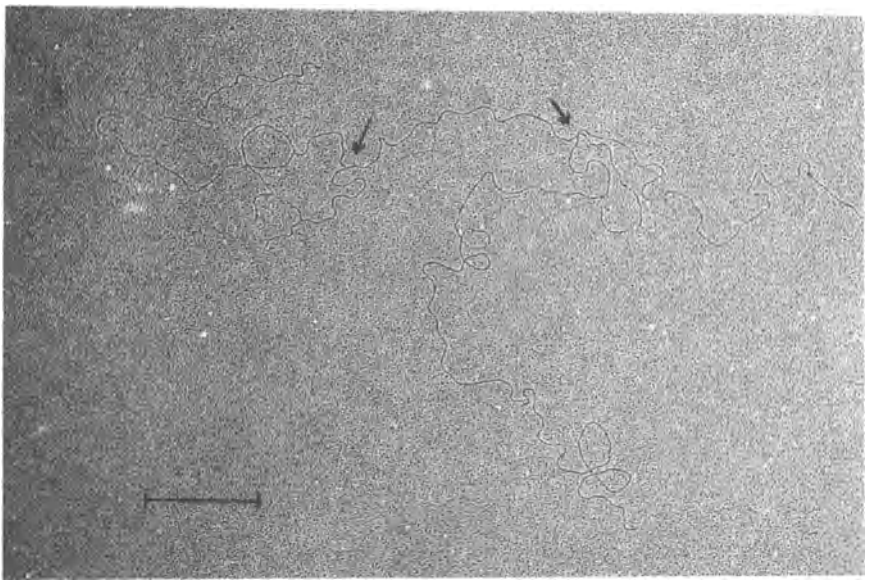

Fig. 1 *Branched linear double-stranded molecules. Three HSV-1 DNA fragments isolated from infected, arginine deprived BSC-1 cells. Arrows indicate the cross-over points. Bar represents 1 μm.*

dsDNA molecules with single-stranded "whiskers"

Such viral DNA molecules were isolated from arginine deprived cells. In the DNA molecule presented in Fig. 3, single strands are associated with the duplex DNA and look like "whiskers". DNA molecules with a similar conformation were reported in yeast DNA during recombination (18).

dsDNA molecules connected by a single-stranded component

HSV-1 DNA molecules connected by a single-stranded sequence were also seen (Figs. 4 and 5). The single-stranded branch emerges from a double-stranded region of the DNA. The two molecules in Fig. 4 which were found among defective DNA molecules, consist of a circular-linear molecule with a rolling circle configuration (16,19), joined to a linear DNA molecule. Recombination can occur between the linear components of circular-linear defective viral DNA or between two linear DNA molecules. Linear HSV molecules connected by a single-stranded filament were repeatedly found

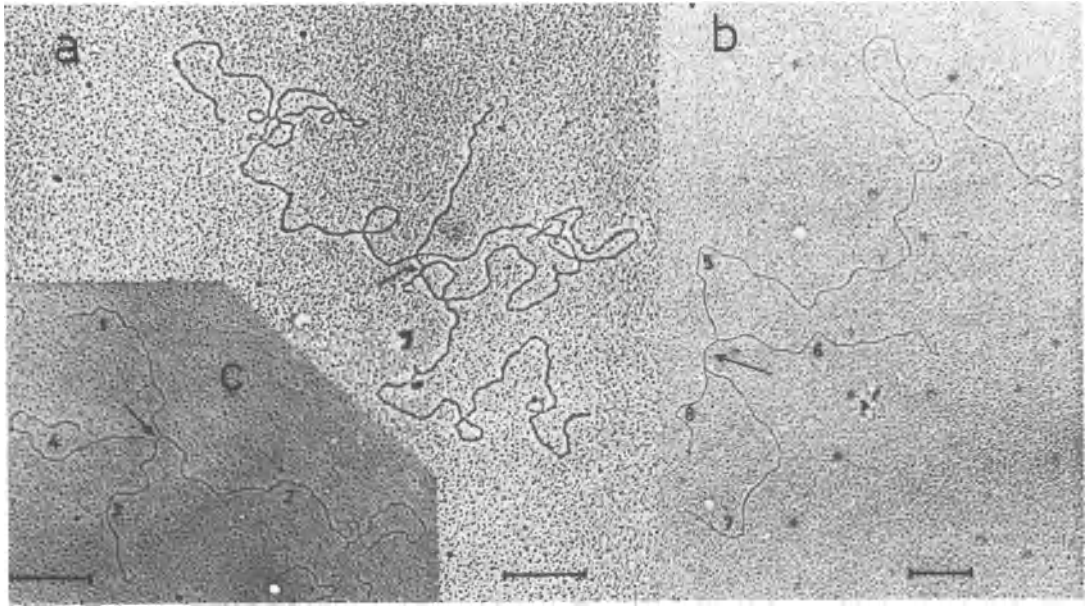

Fig. 2 *Electron micrograph of KOS strain (passage 5) presumed recombination intermediate with double-stranded DNA bridges (indicated by arrows). Two linear molecules are shown in (a), one 6.3 μm (terminus at lower right), and the other 13 μm in length (terminus at upper left). The double-stranded DNA bridge shown in (b) is 0.25 μm in length, and the various components of the molecules measure 7.5 μm (5), 2.2 μm (6), 2.2 μm (7) and 0.95 μm (8). The double-stranded DNA bridge shown in (c) is about 0.06 μm in length, with the components of the molecules measuring 1.3 μm (1), 3.0 μm (2), 1.3 μm (3) and 1.6 μm (4). The bar markers represent 0.5 μm.*

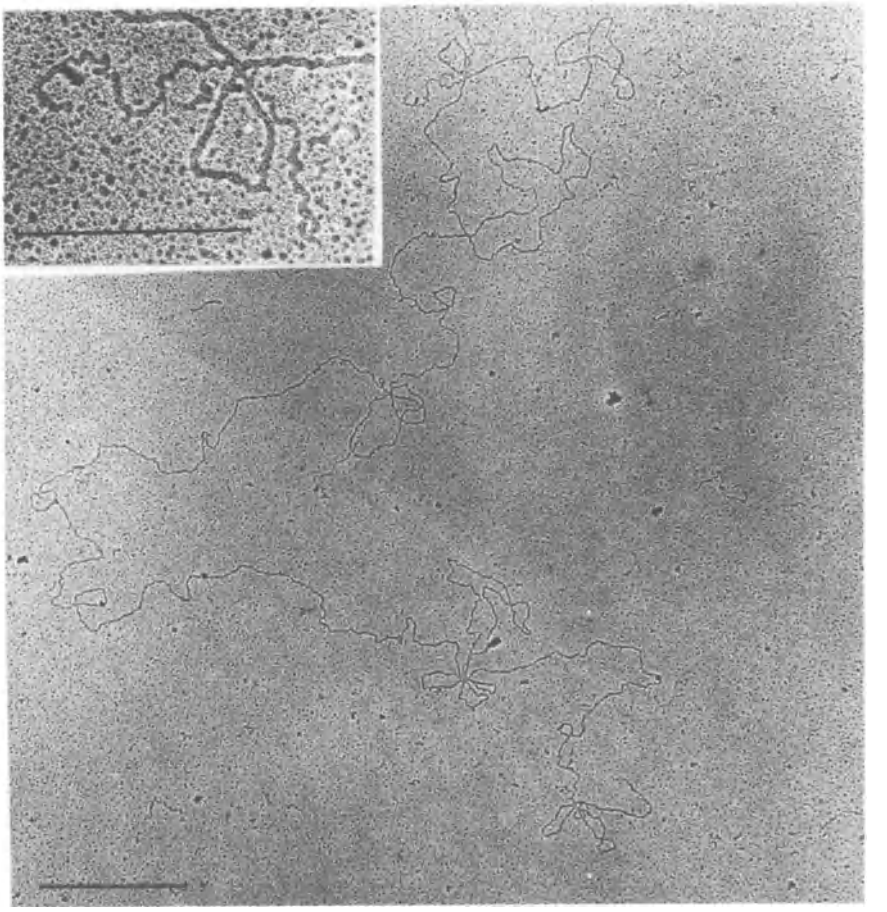

Fig. 3 *HSV-1 DNA molecules with short single-stranded "whiskers" isolated from infected, arginine deprived cells. Bar represents 1 μm.*

in the preparations of DNA grown in the presence of HU (Fig. 5). These structures, which may indicate a stage of HSV-1 DNA in recombination, were also described by Holliday (3). Also visible in Fig. 5 are what may be two cross-over points on the DNA molecules.

DISCUSSION

This study provides information for the first time on the morphology of HSV-1 DNA molecules that resemble recombination intermediates. Cells infected under nonpermissive

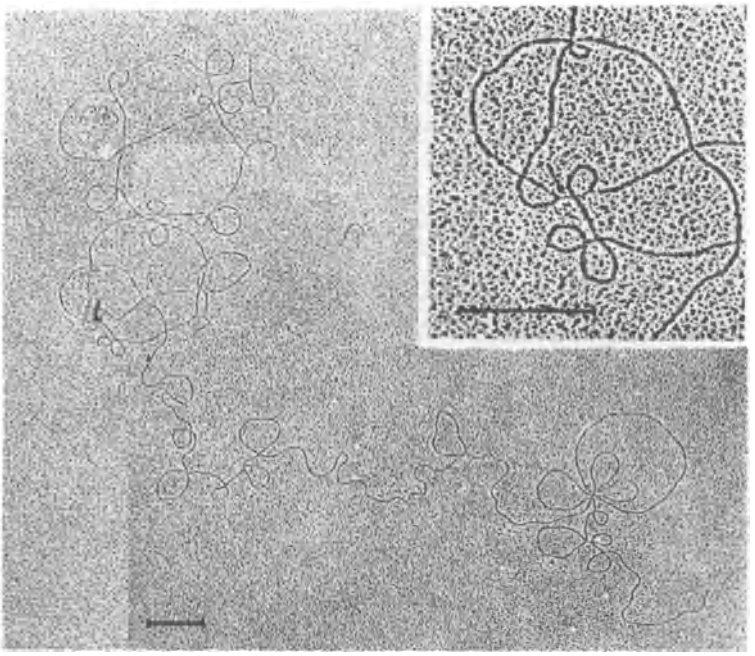

Fig. 4: Electron micrograph of KOS strain (passage 5) presumed recombination intermediate with single-stranded DNA bridge (indicated by arrow). The inset shows a 2.5 times enlargement of this region. The branch region on the left is part of a linear molecule, 31 μm in length, with one terminus in the lower right corner and the second at upper right. The second molecule is circular-linear with the circular portion 4.1 μm in length at upper left and the linear portion 8.0 μm in length, terminating in the middle right hand side of the figure. The bar represents 0.5 μm.

conditions were used, since we assumed that the rate of recombination would be enhanced under such conditions, as was reported for T4 DNA recombinants (20). The conditions used included incubation of HSV-1 infected cells in arginine deficient medium which leads to an abortive virus cycle, since the viral DNA is not encapsidated (21), infection of cells so as to produce defective HSV-1 DNA that is made up of tandem repeats of the terminal repeat of the S component (19,22), and HU treatment of HSV-1 infected cells that inhibits viral DNA replication (15) but permits some repair synthesis on the parental viral DNA templates (23). Under these conditions, DNA molecules that morpho-

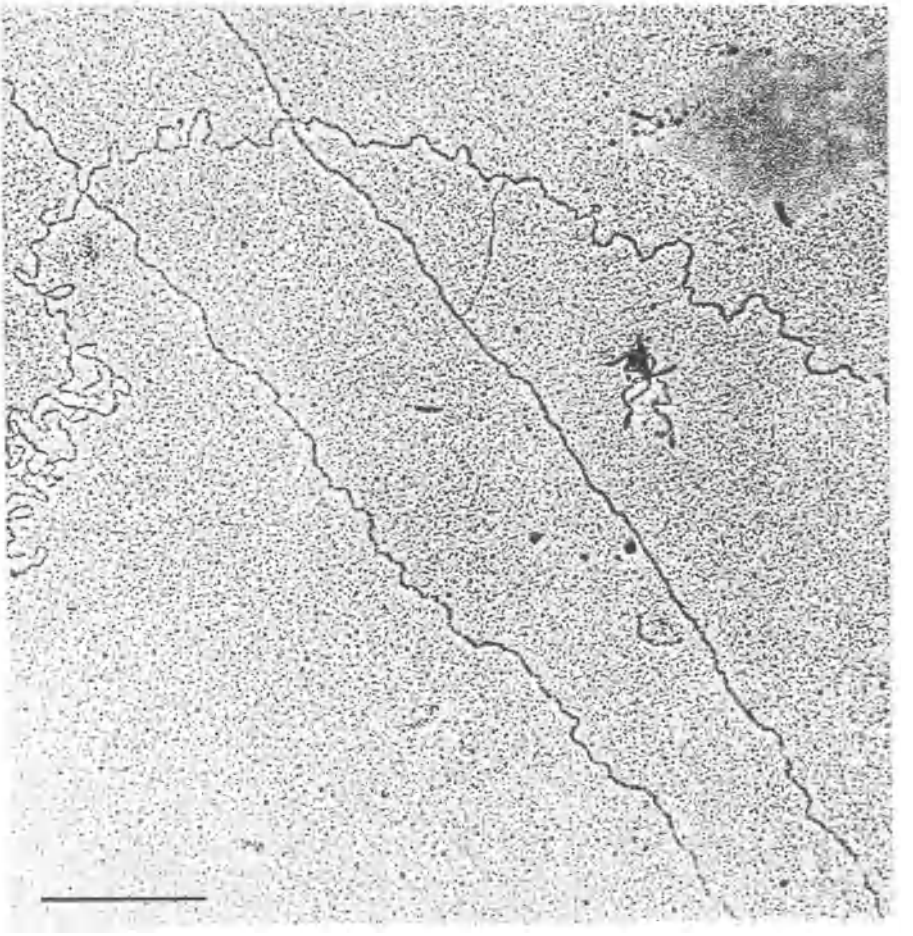

Fig. 5: Two linear HSV DNA molecules connected by a single-stranded filament, which were isolated from infected HU-treated BSC-1 cells. Bar represents 1 μm.

logically resemble recombination intermediates were observed.

One group of DNA molecules, isolated from cells infected under conditions that impair viral DNA replication, consisted of HSV-1 DNA with double-stranded branches that resemble the branched T4 DNA molecules described by Broker and Lehman (4) and Broker (5). Another group included two DNA molecules connected by a single-stranded sequence. Although the two groups of viral DNA molecules differ markedly from each other, it is possible that synthesis of

a complementary strand on the single-stranded sequence, possibly by a DNA repair type mechanism, results in the conformation of branched DNA molecules. However, the branches may not necessarily arise as a result of recombination with other DNA molecules. It is possible that displacement of one or two strands to become templates for DNA synthesis by a DNA polymerase also leads to branch formation. The presence of HSV-1 DNA molecules with single-stranded "whiskers" suggests that branch formation by this mechanism is possible. Molecules possessing "whiskers" of the type found here were described by Simchen and Friedmann (18) in recombining yeast DNA.

The observation presented in this study that two viral DNA molecules are connected by a single-stranded sequence suggests that a single-stranded sequence of one HSV DNA molecule interacts with a second, recipient viral DNA molecule. This resembles the basic concept of the model proposed by Holliday (3). These observations are also in agreement with the notion that a nick in one strand followed by strand displacement and DNA polymerization can produce a single-stranded filament that can interact with a supercoiled DNA structure (2,24).

ACKNOWLEDGMENT

This study was supported by grants to Adam Friedmann and Yechiel Becker from the Branch for Basic Research of the Israel National Academy of Sciences. The authors appreciate the editorial assistance of Julia Hadar.

REFERENCES

1. Hotchkiss, R.D. Ann. Rev. Genet. 28:445-468, 1974.
2. Meselson, M.S. and Radding, C.H. Proc. Natl. Acad. Sci. U.S.A. 72:358-361, 1975.
3. Holliday, R. Genetics 78:273-287, 1974.
4. Broker, T.R. and Lehman, I.R. J. Mol. Biol. 60:131-149, 1971.
5. Broker, T.R. J. Mol. Biol. 81:1-16, 1973.

6. Valenzuela, M.S. and Inman, R.B. Proc. Natl. Acad. Sci. U.S.A. 72:3024-3028, 1975.

7. Potter, H. and Dressler, D. Proc. Natl. Acad. Sci. U.S.A. 75:3698-3702, 1978.

8. Wolgemuth, D.J. and Hsu, M-T. Nature 287:165-171,1980

9. Esparza, J., Benyesh-Melnick, M. and Schaffer, P.A. Virology 70:372-384, 1976.

10. Halliburton, I.W., Randall, R.E., Killington, R.A. and Watson, D.H. J. gen. Virol. 36:471-484, 1977.

11. Morse, L.S., Buchman, T.G., Roizman, B. and Schaffer, P.A. J. Virol. 24:231-248, 1977.

12. Knipe, D.M., Ruyechan, W.T., Roizman, B. and Halliburton, I.W. Proc. Natl. Acad. Sci. U.S.A. 75: 3896-3900, 1978.

13. Preston, V.G., Davison, A.J., Marsden, H.S., Timbury, M.C., Subak-Sharpe, J.H. and Wilkie, N.M. J. Virol. 28:499-517, 1978.

14. Becker, Y., Asher, Y., Friedmann, A. and Kessler, E. J. gen. Virol. 41:629-633, 1978.

15. Rosenkranz, H.S. and Becker, Y. Antimicrob. Ag. Chemother. 3:325-331, 1973.

16. Becker, Y., Asher, Y., Weinberg-Zahlering, E., Rabkin, S., Friedmann, A. and Kessler, E. J. gen. Virol. 40:319-335, 1978.

17. Friedmann, A., Shlomai, J. and Becker Y. J. gen. Virol. 34:507-522, 1977.

18. Simchen, G. and Friedmann, A. Nature 257:64-66,1975.

19. Frenkel, N., Locker, H., Batterson, W., Hayward, G.S. and Roizman, B. J. Virol. 20:527-531, 1976.

20. Kozinski, A.W. and Mitchell, M. J. Virol. 4:823-836, 1969.

21. Olshevsky, U. and Becker, Y. Nature 226:851-853,1970.

22. Graham, B.J., Bengali, Z. and Vande Woude, G.F. J. Virol. 25:878-887, 1978.

23. Shlomai, J. and Becker, Y. J. gen. Virol. 37:429-433, 1977.

24. Wiegand, R.C., Beattie, K.L., Hollman, W.K. and Radding, C.M. J. Mol. Biol. 116:805-824, 1977.

7. Replication of HSV-1 DNA: Isolation of a subnuclear DNA synthesizing fraction

Samuel Rabkin, Yehuda Shtram and Yechiel Becker

SUMMARY

A subnuclear fraction able to synthesize both viral and cellular DNA in-vitro was isolated from HSV-1 infected nuclei. The degree of viral DNA synthesis in-vitro was dependent on the extraction conditions (the Mg^{++} concentration) and further fractionation of the subnuclear fraction in sucrose layers. The endogenous DNA synthesizing activity could be isolated as a complex from the nuclei and was, therefore, probably not due to random association of the free DNA polymerase and other proteins in the subnuclear fraction.

INTRODUCTION

Analyses of the replicative intermediates of HSV-1 DNA (1) revealed that the synthesis of the viral DNA can be initiated either at one of the molecular ends or internally within the viral genome. When viral DNA synthesis is initiated at the end of the molecule (most probably at the terminus of the terminal repeat of S, map position 1.0), the DNA is synthesized by strand displacement (2). When initiated internally, the synthesis of viral DNA is semiconservative, with the replication fork advancing bidirectionally. When one of the replication forks reaches the end of the DNA molecule, Y-shaped DNA molecules can be observed. The most common replicative intermediates of HSV-1 were found to be molecules with internal initiation sites (2). Since the viral DNA molecules replicate semiconservatively by means of two moving replication forks, replisomes must be present in association with the two viral DNA strands at the site of the fork. Replisomes are known to exist in replicating bacteriophage, and they contain about 10 proteins which are involved in DNA biosynthesis (3).

We attempted to develop the methodology for isolating the replicative intermediates of HSV-1 DNA with all the proteins associated with the replication forks. This would aid in studies on viral DNA replication in-vitro and in determining the contribution of the various regions of the viral DNA to this process. Complexes of viral

Y. Becker (ed), Herpesvirus DNA.

DNA and proteins were isolated from nuclei of cells infected with adenovirus or SV40 . With adenovirus it was shown that the direction and termini of replication in-vitro are essentially identical to those in-vivo (4), and that the cellular DNA polymerase is associated with the isolated replication complexes (5,6). In the SV40 system, replicating viral DNA was converted into covalently closed, superhelical DNA molecules during incubation in-vitro (7). Furthermore, 95% of the associated DNA polymerase was found to be α and the rest γ, since replication occurred in the presence of dideoxy-TTP: DNA polymerases β and γ are sensitive to dideoxy-TTP (8). A chromatin preparation isolated from the nuclei of HSV-1 infected HeLa cells synthesized both viral and cellular DNA of small size (9). The viral DNA polymerase was the predominant activity, with a small amount of host DNA polymerase γ, in contrast to chromatin from uninfected cells which contain the DNA polymerases α, β and some γ (10). Using a modification of the extraction procedure of Su and DePamphilis (7), Hirschhorn & Abrams (11) reported on a soluble nuclear extract from nuclei of HSV-1 infected cells capable of synthesizing viral DNA in-vitro.

In the present study, a subnuclear fraction capable of synthesizing viral DNA under in-vitro conditions was extracted from cells infected with wild type and defective HSV-1.

EXPERIMENTAL

Isolation of the subnuclear fraction

The KOS strain of HSV type 1 was used to infect BHK C13 cells (6×10^6 cells/milk bottle) grown in Dulbecco's modified Eagle's medium (DMEM) with 10% fetal bovine serum (Grand Island Biological Co.). Six hours after infection the cells were placed in ice and washed twice with cold RSB (0.01 M Tris-HCl, pH 7.8, 0.01 M KCl, 0.015 M $MgCl_2$) containing 10^{-3} M dithiothreitol. The cells were scraped into RSB and the suspension was Dounce homogenized with 10 strokes of a tight-fitting pestle. The lysed cells were centrifuged, and the supernatant fluid was removed. The nuclear pellet was gently resuspended in an approximately 3-fold volume of HBM buffer (10 mM HEPES, pH 7.7, 0.1 M KCl, 0.5 mM dithiothreitol, 2 mM $MgCl_2$) or HBE buffer (10 mM HEPES, pH 7.7, 0.1 M KCl, 0.5 mM dithiothreitol, 2 mM EDTA). After incubation at $37^{o}C$ for 40 min with occasional mixing, the nuclei were pelleted and were found to retain their morphology as well as being able to support

DNA synthesis in-vitro. The supernatant fluid was used at this stage or was further fractionated by centrifugation in a 5-20% (w/v) sucrose gradient in a SW41 rotor at 4°C in HB buffer (10 mM HEPES, pH 7.7, 5 mM KCl, 2 mM $MgCl_2$, 0.5 mM dithiothreitol). The complex was also isolated on a sucrose cushion made up of 1.5 ml of 30% (w/v) sucrose and 2 ml of 10% (w/v) sucrose in HBM buffer with the supernatant fluid layered gently on top and centrifuged in an SW50.1 rotor at 42,000 rpm for 45 min at 4°C in a Beckman ultracentrifuge.

Assays:

HSV DNA polymerase (endogenous) activity: The sample in 10 µl was mixed with an equal amount of the endogenous mixture to a final concentration of 0.5 mg/ml bovine serum albumin, 75 mM KCl, 100 mM Tris-HCl, pH 7.7, 2.5 mM $MgCl_2$ (or 6 mM in some experiments), 2.5 mM dithiothreitol, 0.3 mM each of dGTP, dATP, dCTP, 2 µM of ^{3}H-TTP or 20 µM ^{32}P-dGTP, and incubated for 30 min at 37°C. The reaction was stopped by the addition of ice cold 10% (v/v) TCA.

HSV DNA polymerase (exogenous) activity: The sample in 5 µl was mixed with an equal amount of the exogenous mixture to a final concentration of 0.5 µg/ml bovine serum albumin, 250 mM KCl, 100 mM Tris-HCl, pH 7.7, 2.5 mM $MgCl_2$, 2.5 mM dithiothreitol, 0.3 mM each of dGTP, dATP, dCTP, 2 µm of ^{3}H-TTP, 300 µg/ml of activated calf thymus DNA and incubated for 30 min at 37°C. The reaction was stopped by the addition of ice cold 10% (v/v) TCA.

Thymidine kinase: A sample of 10 µl was added to the reaction mixture containing 150 mM Tris-HCl, pH 7.7, 16 mM $MgCl_2$, 16 mM ATP, 25 mM NaF, 1 unit/ml of creatine kinase, 8 mM creatine phosphate, 0.75 µCi of ^{3}H-thymidine (specific activity 5 Ci/mmol) and incubated overnight at 37°C. The reaction was stopped by boiling for 2 min. Twenty µl was added to a DEAE filter (Whatman DE81) and placed in 3 mM ammonium formate at 37°C, washed twice with 3 mM ammonium formate and then ethanol. The filters were dried and the radioactivity determined.

RESULTS

Isolation of a subnuclear fraction from HSV-1 infected nuclei

Six hr post-infection (p.i.) was chosen as the optimal time for extraction of the DNA synthesizing fraction from KOS strain infected BHK C13 cells, since by 9 hr p.i. infectious virus progeny was being produced in the cells, and viral DNA labeled with ^{3}H-thymidine could be isolated in CsCl density gradients from 5 hr onwards.

The supernatant fluid in HBE buffer which constituted the subnuclear fraction was prepared at different times after infection and assayed for exogenous and endogenous DNA synthesizing activities. The endogenous HSV-1 DNA polymerase activity, assayed with 75 mM KCl (Fig. 1a), did not require any added template, indicating that activated DNA templates present in the supernatant fluid were utilized for DNA synthesis. This activity increased and had a time course similar to that seen in whole infected cells. The endogenous activity was partially resistant to PAA (150 µg/ml).

The HSV-1 DNA polymerase activity which was assayed at high salt concentration (250 mM KCl) with activated calf thymus as added template (exogenous activity) was demonstrable in the supernatant fluid at 4 hr p.i., reaching maximal activity at 6 hr p.i. (Fig. 1b). The HSV-1 coded thymidine kinase (TK), which was also assayed in the supernatant fluid (Fig. 1c) gradually increased to a maximum at 8 hr p.i., as was found with total nuclei (12). The exogenous HSV-1 DNA polymerase activity in unfractionated infected nuclei (Fig. 1d) reached a maximum at 10 hr p.i. The DNA polymerase activity was sensitive to PAA.

The parameters for DNA synthesis in the subnuclear fraction are shown in Table 1. DNA synthesis depends on the presence of the four nucleoside triphosphates, ATP and KCl. At concentrations of KCl higher than 100 mM, the reaction was inhibited. The purified HSV-1 DNA polymerase requires 250 mM KCl for activity (13).

The DNA synthesized in the subnuclear fraction was characterized by centrifugation in CsCl density gradients. In the presence of 2mM EDTA, most of the in-vitro synthesized DNA banded at the density of cellular DNA. Some viral DNA was detected when Mg^{++} (2 mM) was added to the reaction instead of EDTA. When studied by neutral sucrose gradient centrifugation, the DNA was found to be small in size, about 8×10^{6} daltons (not shown).

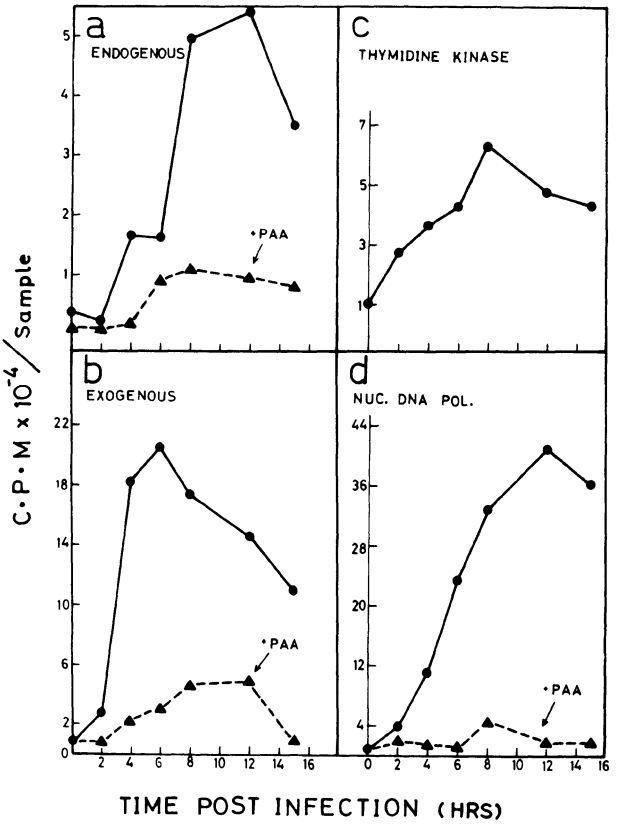

Fig. 1: Enzyme activity in subnuclear fraction. Nuclei isolated from HSV-1 infected cells at different times p.i. were resuspended in HBE buffer (2 mM EDTA) and incubated at 37°C for 40 min. Uninfected cells constituted the zero time point. Assays were done in duplicate using about 1.2 x 10^5 nuclei for each. The DNA polymerase activity (●——●) was assayed under endogenous (a) and exogenous (b) conditions in the absence of and presence of PAA (▲---▲), concentrations of 150 (a) and 100(b) µg/ml. The TK activity was assayed using an extract from about 5 x 10^5 nuclei (c). Whole infected nuclei were sonicated and the exogenous HSV-1 DNA polymerase activity was determined (13) using about 3.6 x 10^4 resuspended nuclei per sample (d).

Table 1 *Parameters for in-vitro DNA synthesis*

	Activity %
Complete	100
-dATP, dCTP, dGTP	10
-mix (only ^{3}H-TTP)	6
KCl 100 mM	61
200 mM	32
250 mM	16
300 mM	9
ATP (5 mM)	61
ATP, CTP, GTP, UTP (0.1 mM)	76

The subnuclear fraction was assayed for endogenous activity and the incorporation of radioactivity was designated complete (100% activity). Further assays were done in the presence of only ^{3}H-TTP, without the other three dNTP's (-dATP, dCTP, dGTP), without the salt mixture, and the three dNTP's (-mix, only ^{3}H-TTP), and in the presence of different concentrations of KCl, with ATP and with all four rXTP's.

The optimal conditions for synthesis of DNA by the subnuclear fraction are shown in Fig. 2. KCl which inhibited the endogenous activity at a concentration of 250 mM was optimal between 75-100 mM (Fig. 2a); dithiothreitol (DTT) was optimal at 2 mM (Fig. 2b), ^{3}H-TTP at 2 µM (Fig. 2c) and Mg^{++} at 2.5 mM (Fig. 2d). Zn^{++} inhibited all activity.

Isolation of DNA synthesizing subnuclear fraction in sucrose layers

The DNA synthesizing subnuclear fraction extracted from cells infected in the presence and absence of arginine (14) was further characterized by centrifugation through sucrose layers. The endogenous DNA synthesizing activity (presumably DNA polymerase bound to DNA template) banded mainly in the 10% (w/v) layer of sucrose (Fig. 3), whereas the DNA polymerase activity which required exogenous DNA template was distributed throughout the sucrose layers.

Properties of the subnuclear fraction from nuclei synthesizing defective HSV

Nuclei were isolated from cells synthesizing defective KOS strain HSV-1 at passage 5 (Chap.10 and ref. 12) and the subnuclear fraction was centrifuged through sucrose layers (Fig. 4a). The endogenous DNA synthesizing activity banded in the 10% (w/v) sucrose layer, as shown in

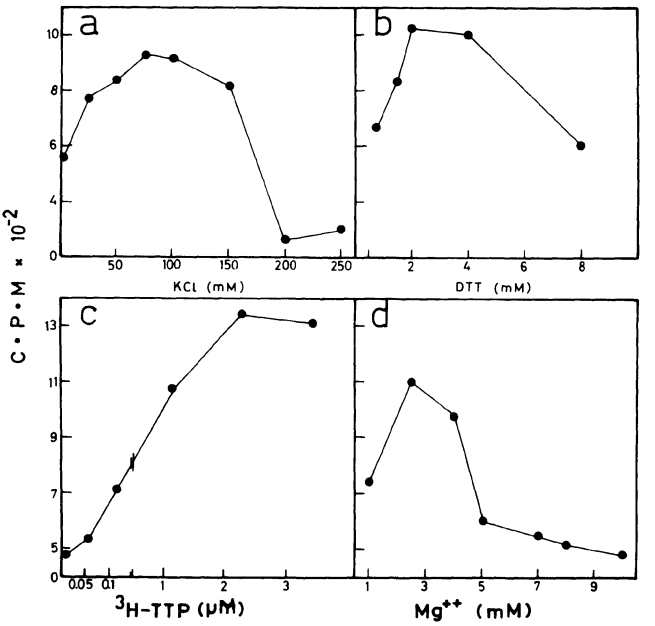

Fig. 2: Assay conditions. The endogenous activity was assayed in duplicate with varying concentrations of KCl (a), dithiothreitol (DTT) (b), and ^{3}H-TTP (c). Five µl from pooled fractions 11, 12 and 13 from the sucrose layer illustrated in Fig. 3 were used in the assay. Ten µl from pooled fractions 14 and 15 from the sucrose layer illustrated in Fig. 4a were assayed with varying concentrations of $MgCl_2$ (d).

Fig. 3. The peak fractions designated b and C in Fig. 4a were pooled and used for DNA synthesis in-vitro. Analysis of the in-vitro synthesized DNA in CsCl gradients with ^{14}C-HSV DNA as marker showed that mainly viral DNA was synthesized in fraction b (Fig. 4b). In fraction c, mainly defective DNA and some viral DNA were produced. Thus, a subnuclear fraction isolated from cells producing defective virus can synthesize defective HSV DNA endogenously in-vitro.

A subnuclear fraction from nuclei of uninfected cells showed no endogenous DNA synthesizing activity after centrifugation through sucrose layers.

Fraction c from Fig. 4a was fixed with glutaraldehyde, and the DNA spread for viewing in the electron microscope (2). A branched DNA molecule partially covered with protein (probably a DNA-protein complex) is presented in Fig. 5.

Centrifugation of the subnuclear fraction from cells synthesizing

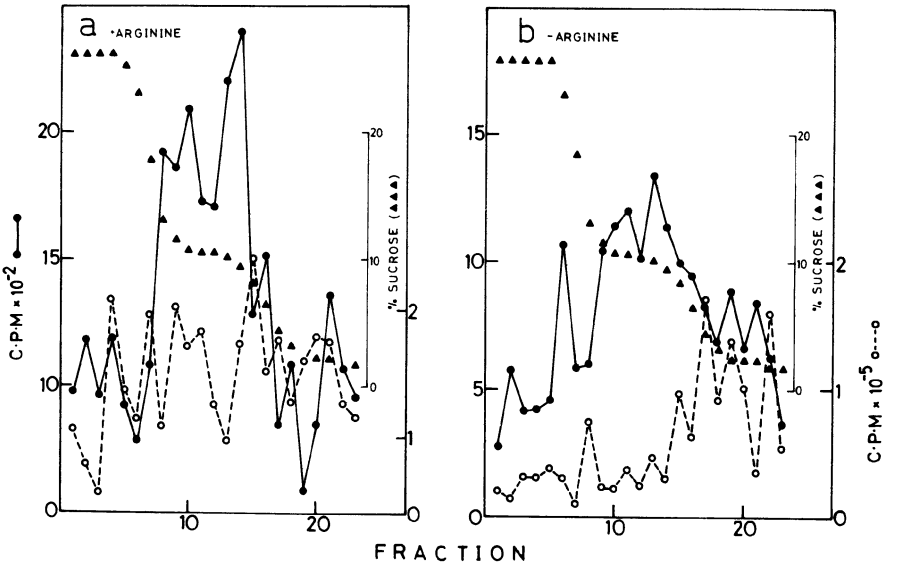

Fig. 3: Isolation of DNA synthesizing complexes. BHK C13 cells were infected with HSV(KOS) in the presence of arginine (a); at 7hr p.i. the nuclei were isolated, resuspended in HBM buffer and incubated for 40 min. The supernatant fluid was further centrifuged for 5 min in an Eppendorf centrifuge and then added to a layer of 10% (w/v) sucrose in HB layered onto 30% (w/v) sucrose in HB and centrifuged at 42,000 rpm for 45 min in an SW 50.1 rotor. Ten µl from each fraction (225 µl) were assayed for endogenous activity (●—●) and 5 µl for exogenous activity (o--o). The sucrose concentration (▲) was determined using a Bausch and Lomb refractometer. BHK cells infected with HSV-1 and incubated in RPMI medium without arginine were similarly treated (b).

defective virus in a linear sucrose gradient yielded three peaks of endogenous activity. The exogenous activity was concentrated at the very top of the gradient. Centrifugation of the in-vitro synthesized DNA from the three peaks in CsCl gradients showed that the bottom peak contained about 20% of DNA with the density of cellular DNA. In contrast, the middle and upper peaks contained DNA which banded exclusively at the density of viral DNA. Thus it was relatively easy to isolate homogenous in-vitro synthesized DNA of viral density from cells producing defective virus, as opposed to cells producing only wild type virus.

Electrophoresis of fractions from Fig. 4a in 9% SDS-polyacrylamide showed that fractions b and c which synthesize viral DNA in-vitro contain proteins which differ from those present in a fraction at the top

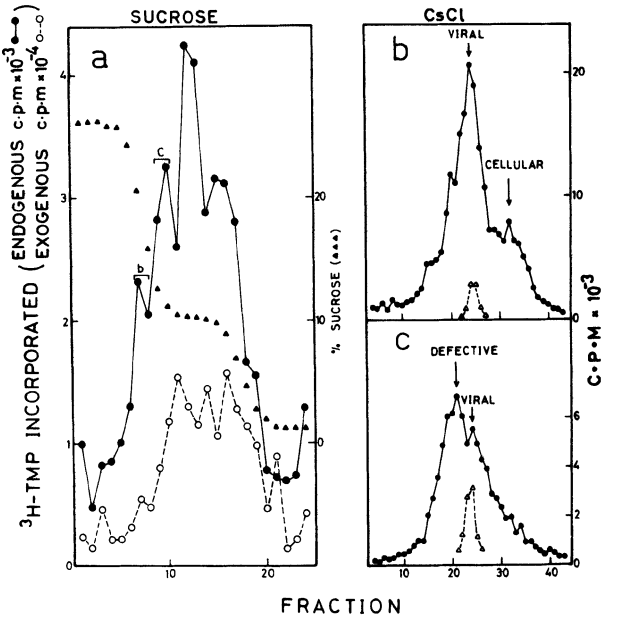

Fig. 4: Isolation of DNA synthesizing complex from defective (passage 5) virus. BHK C13 cells were infected with KOS strain virus (passage 4). At 8.5 hr p.i. the nuclei were isolated, resuspended in HBM buffer and incubated at 37°C for 45 min. The supernatant fluid (90%) was placed on a layer of 10% (w/v) sucrose in HB, layered on 30% (w/v) sucrose in HB and centrifuged at 42,000 rpm for 50 min in a SW 50.1 rotor. Ten µl from each fraction (200 µl) were assayed for endogenous activity (●—●) and 5 µl for exogenous (o--o) activity (a). DNA was synthesized in-vitro with ^{3}H-TTP using 125 µl from pooled fractions 12 and 13, marked b on the curve in (a). After SDS-pronase treatment, this DNA with ^{14}C-HSV DNA (Δ--Δ) as marker was centrifuged in CsCl density gradients for 60 hr at 37,000 rpm in the 50 Ti rotor (b). DNA was synthesized in-vitro with ^{32}P-dGTP using 50 µl from pooled fractions marked c on curve in (a) and centrifuged in CsCl gradients as above (c).

of the sucrose layer or in the complete subnuclear fraction. In fractions b and c, polypeptides with molecular weights of 125, 102, 90, 67, 60, 55, 51, 33 and 29 x 10^{-3} were identified.

DISCUSSION

A particulate subnuclear fraction which synthesizes mostly viral DNA under in-vitro conditions has been isolated from cells infected with HSV under regular conditions, under conditions of arginine deprivation when the structural viral proteins do not reach the nucleus (14), and at the time of defective virus synthesis (12).

Fig. 5: Electron microscopy of a DNA molecule partially covered with protein from fraction c (Fig. 4a) (Magnif. x 30,000).

The use of sucrose layers to further fractionate the subnuclear fraction greatly increased the proportion of viral DNA synthesized in-vitro, as opposed to cellular DNA. The particulate matter which can be seen in the subnuclear fraction may be membrane-chromatin fragments of the nuclear envelope. In some of the sucrose gradients, a very small pellet was visible. If the subnuclear fraction was centrifuged prior to centrifugation in sucrose layers, and the particulate material which sedimented to the bottom was resuspended and used to synthesize DNA in-vitro, almost none of the DNA hybridized to the HSV DNA probe.

The activity in the subnuclear fraction was characterized to determine whether a viral DNA polymerase was involved. The endogenous activity was sensitive to both PAA and Zn^{++}, as is the HSV-1 coded DNA polymerase (13, 15). Even fractions that were synthesizing cellular DNA were sensitive, indicating that the viral polymerase was synthesizing DNA on host DNA templates. This was also found to be the case in the chromatin-system of Yamada et al. (9). The data indicate that what we are studying is a DNA-protein complex and not an association between free DNA polymerase and activated templates. When centrifuged in sucrose gradients, the endogenous activity traveled much further in the

gradient than free DNA polymerase. When the supernatant fluid was incubated at 37°C without nuclei, there was no increase in the endogenous activity. In addition, K^+ optimum differed from that required by the free HSV DNA polymerase.

The basic problem with DNA synthesis under in-vitro conditions is the small size of the molecules synthesized (16, 17). It was thought that under conditions of extraction of the subnuclear fraction with EDTA, degradation of DNA would be kept to a minimum (16), but this was not the case. Neutral sucrose gradients indicated that the DNA synthesized in-vitro was in the $8x10^6$ dalton size range. Electron microscopic examination of DNA isolated from the sucrose layer in the position of endogenous activity revealed molecules ranging in size from 3-46 μm, with over half the molecules less than 7 μm in length. A few contained regions that may correspond to areas of DNA synthesis, namely branches, loops, collapsed regions, and regions to which protein molecules were attached.

The soluble nature of the subnuclear fraction allows one to add any desired compounds to the reaction mixture (e.g. antiviral drugs) and to isolate the DNA and proteins. The results indicate that selected proteins can be found in the fractions which synthesize HSV-1 DNA in-vitro. The development of in-vitro systems therefore open the way to a better understanding of the molecular processes involved in the replication of herpesvirus DNA.

ACKNOWLEDGMENTS

The technical assistance of Yael Asher and Eynat Tabor is greatly appreciated, as is the help of Dr. Julia Hadar with the preparation of the manuscript.

The study was supported by a grant from the Basic Sciences Branch of the Israel National Academy of Sciences.

REFERENCES

1. Shlomai, J., Friedmann, A. and Becker, Y. Virology 69:647-659, 1976.

2. Friedmann, A., Shlomai, J. and Becker, Y. J. gen. Virol. 34: 507-522, 1977.

3. Kornberg, A. Aspects of DNA replication. Cold Spring Harbor Symp. Quant. Biol. 43:1-9, 1978.

4. Kaplan, L.M., Kleinman, R.E. and Horwitz, M.S. Proc. Natl. Acad. Sci. U.S.A. 74:4425-4429, 1977.

5. Brison, O., Kedinger, C. and Wilhelm, J. J. Virol. 24:423-435,1977.

6. Ito, K., Arens, M. and Green, M. J. Virol. 15:1507-1510, 1977.

7. Su, R.T. and DePamphilis, M.L. Proc. Natl. Acad. Sci. U.S.A. 73:3466-3470, 1976.

8. Edenberg, H.J., Anderson, S. and DePamphilis, M.C. J. Biol. Chem. 253:3273-3280, 1978.

9. Yamada, M., Brun, G. and Weissbach, A. J. Virol. 26:281-290,1978.

10. Knopf, K.W. and Weissbach, A. Biochemistry 16:3190-3194, 1977.

11. Hirschhorn, R.R. and Abrams, R. Biochem. Biophys. Res. Commun. 84:1129-1135, 1978.

12. Becker, Y., Gutter, B., Cohen, Y., Chejanovsky, N., Rabkin, S. and Fridlender, B. Arch. Virol. 62:163-174, 1979.

13. Fridlender, B., Chejanovsky, N. and Becker, Y. Antimicrob. Ag. Chemother. 13:124-127, 1978.

14. Olshevsky, U. and Becker, Y. Nature 226:851-853, 1970.

15. Fridlender, B., Chejanovsky, N. and Becker Y. Virology 84:551-554, 1978.

16. Franke, B. Biochemistry 16:5664-5670, 1977.

17. Shlomai, J., Asher, Y. and Becker, Y. J. gen. Virol. 34:223-234, 1977.

8. Tandem repeat defective DNA from the L segment of the HSV genome

Dolores M. Cuifo and Gary S. Hayward

SUMMARY

Restriction enzyme analysis of the DNA from a collection of defective populations of herpes simplex virus generated by serial undiluted passage in HEp-2 or Vero cells indicates that the amount and sequence complexity of the accumulated tandem repeat DNA species varies considerably in different strains and passaging series. One particular reiterated DNA species accounting for between 50% and 90% of the viral DNA of the 14th to 20th passage of HSV-1(MP) virus has been studied in some detail. It differs from previously well characterized species by not having a higher buoyant density and (G + C)- content than the complete parent genomes and being derived from the centre of the L-segment of the genome rather than the right-hand end of the S-segment. The repeat unit of this new defective DNA has a molecular size of 5.2×10^6 daltons or approximately 7800 base pairs and has homology with sequences from coordinates 0.385 to 0.437 in the standard HSV-1 physical map. This sequence overlaps with part or all of the DNA polymerase gene and we presume that it also possesses an origin for the initiation of DNA synthesis. Each repeat unit also retains approximately 200 base pairs from near the right-hand terminus of the parental S segment that are apparently necessary for site-specific cleavage events during the packaging of mature virion DNA. An exactly integral number of copies of adjacent tandem repeat units totalling close to 100×10^6 daltons are encapsidated to form the completed defective DNA molecules

Y. Becker (ed), Herpesvirus DNA.

from a pool of much larger replicating molecules in the nucleus.

INTRODUCTION

Like many other animal viruses the herpes simplex group accumulates defective interfering particles in a cyclical manner when virus stocks are passsaged in either cultured cells or experimental animals (1-3). Defective virions contain incomplete DNA genomes that are non-viable by themselves and only able to produce progency virions by co-infection with complete "helper virus" genomes. Most of the defective populations of herpes simplex virus that have been described in detail are characterized by the presence of DNA molecules of normal length but greater than normal buoyant density (1,4,5). This is accomplished by packaging tandemly reiterated portions of (G + C)-rich sequences from the extreme right-hand end of the viral genome (5-7). The tandem repeat nature of this DNA is best demonstrated by the appearance of a small number of new relatively intense bands in the DNA fragment profile displayed on agarose gels after cleavage with restriction enzymes (8) or by the observation of repetitive partial denaturation patterns by electron microscopy (5,9). The interference properties and ratio of plaque forming units to particles in HSV defective populations do not always correlate well with the proportion of tandem repeat DNA present (5) and the possibility remains that other kinds of noninfectious molecules with genomes of relatively normal structure contribute to the biological properties of these virus populations.

Amongst other herpes viruses, defective pseudorabies DNA molecules of normal size have been described in which portions of the genome have been substituted by small, relatively (A + T)-rich tandem repeats (10). Similarly, the HR-1 lymphoblast cell line releases Epstein-Barr virus particles containing a mixture of normal complete genomes

and defective reiterated DNA molecules (11,12) and new tandem repeat species of lower sequence complexity can be generated after superinfection of Raji cells with this strain of EBV (G.S. Hayward, unpublished observations). In contrast, human cytomegalovirus populations containing defective virions encapsidate shortened DNA molecules of only 100 x 10^6 molecular weight in place of the normal full-sized infectious genomes of 150 x 10^6 (13,14). These populations show only minor changes in cleavage patterns and do not appear to contain tandemly repeated sequences (G.S. Hayward, unpublished observations).

In the present study we set out to examine the extent of genetic variability in a number of different HSV populations containing defective DNA and report the finding of a new class of HSV-1 tandem repeat DNA arising from the L component. Earlier discoveries about the structure of the HSV-1 (Justin) defective DNA molecules enabled us to predict that both wild-type and defective HSV DNA molecules replicated through concatemeric forms possibly arising by a unidirectional rolling circle mechanism as described for the late phase of phage lambda replication (15,16). Similarly, from the further studies reported here we suggest firstly, that the two classes of tandem repeat DNA may indicate the presence of two origins of replication in the HSV genome, one in the L segment and one in the S segment, and secondly, that the mechanism for packaging linear monomer genomes involves a combination of the "head-full" and "sequence-specific" cleavage events described earlier in phage systems.

RESULTS

Serial Passaging to Generate Defective Virus

A number of different sets of defective HSV populations were obtained by serially passaging the virus from

infected plaque dish cultures (2 x 10^6 cells/dish) at high multiplicities of infection. At each passage the infected dish was freeze-thawed three times and one-fifth of the culture was used as inoculum for the next infection.

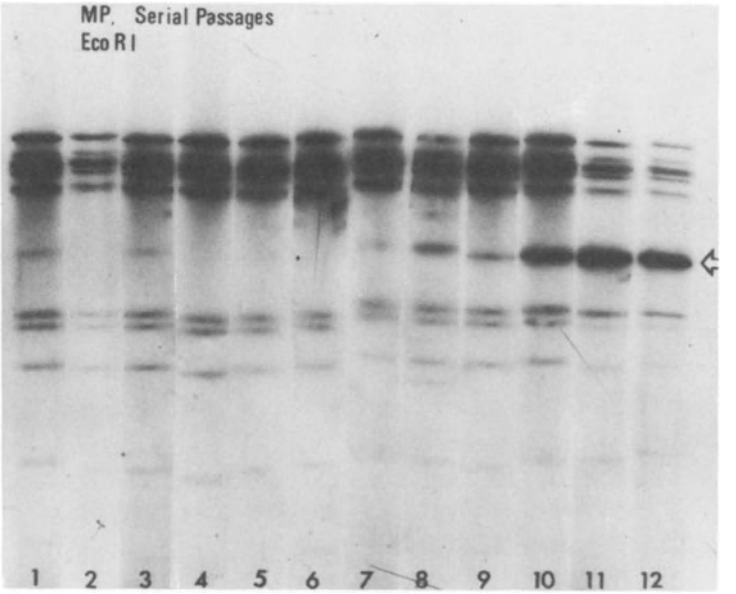

Figure 1: The accumulation of tandem repeat defective DNA in virions from successive passages of undiluted HSV-1(MP) series "b" in HEp-2 cells. The DNA was extracted from PEG-precipitated supernatant virus released 48 hours after infection in low phosphate medium containing ^{32}P-phosphate. The figure shows an autoradiograph of EcoRI cleaved DNA after electrophoresis through 0.6% agarose gels. The major new band (arrowed) contains the 5.2 x 10^6 molecular weight EcoRI fragment from the tandem repeat DNA molecules.

The initial series were grown in HEp-2 cells but in later stages of the work we used Vero cells and added a sonication step after the freeze-thawing. The advantages of using small scale cultures instead of the 100-fold larger scale used in the original passaging series of Frenkel et al (5) were made possible by our development of a rapid procedure for analysis of small quantities of ^{32}P-labeled viral DNA from plaque dishes. The virus preparations were screened at least once every three passages and considered positive when a new band was seen

consistently for three consecutive passages and had reached at least 5% of the total DNA. The defectives appeared to develop much faster in Vero cells than in HEp-2 cells (sometimes within three passages) and also reached much higher proportions of the total DNA in these cells (often greater than 90%). It should be noted that our definition of tandem-repeat DNA for these purposes depends on the appearance of new low sequence complexity DNA bands in restriction enzyme patterns of cleaved DNA and an increase in the proportion of this DNA relative to the parent wild-type bands on subsequent undiluted passaging of the virus. The suggestion that these represent tandem-repeat DNA is a reasonable assumption based on previous experience but the question of whether or not particles containing this DNA has defective interfering properties has not been investigated in this work.

A summary of the appearance and characteristics of new "tandem-repeat" defective DNA from eleven different passaging series with HSV-1(MP), HSV-1(STH2) and HSV-2(333) virus stocks is presented in Table I for comparison with the original HSV-1 (Justin) series of Frenkel et al (5). Only the HSV-1(MP) passaging series will be described here. Four sets of experiments were performed in parallel: two series were initiated with non-plaque purified virus from a single stock virus pool and two with virus from a freshly plaque purified virus stock called HSV-1(MPc1-5). All four were examined at regular intervals during serial passage in HEp-2 cells. Only the first two series ("a" and "b") using non-plaque purified virus yielded defective DNA within the twelve passages examined and in both of these the repeat unit appeared to be identical. Samples of the progeny viral DNA from each of the passages in series "b" are shown in Figure 1 after cleavage with EcoRI and electrophoresis through agarose gels. A new 5.2 x 10^6 molecular weight species was first detected at the seventh passage and it increased in amount at the expense of all the original wild-type DNA bands to greater than

25% by twelfth passage.

From these results one suspects that the defective DNA may have been present in very low quantities in the original stock virus preparation and may have been eliminated in the plaque-purified series.

Characterization of the MPal8 Repeat Unit

The 5.2 x 10^6 dalton or 7.8 kb repeat unit from HSV-1(MP) defective DNA was chosen for further extensive study. Twelfth passage virus from the HSV-1(MP) series "a" was grown up into large scale stocks in roller bottle cultures of HEp-2 cells (MPal4) and later in Vero cells (MPal8 and MPa20). The proportion of tandem repeat DNA varied between 50% and 95% in different preparations grown from these virus pools. At first sight the HSV-1(MPal4) repeat unit appears very similar to those described earlier from the HSV-1(Justin) and HSV-1(Patton) series: it has essentially the same molecular weight (5.2 x 10^6), contains a single site for EcoRI and is resistent to cleavage with the HindIII enzyme. However, it also differs from both of the other species in having a BglII cleavage site and in giving an extremely homogeneous band in the gels. In contrast, cleavage of HSV-1(Justin) p14 DNA with SalI reveals at least three closely related species of repeat units (21) and the repeat unit in the HSV-1(Patton) defective population varied in size from 5.4-5.7 x 10^6 (7). The population described by Wagner et al (4) was also extremely heterogeneous in the size of the EcoRI repeat units displayed on gels.

With a single exception (17) all of the HSV defective DNA species described previously have been characterized by having an unusually high buoyant density. Indeed, the high (G + C) - content of the repeat unit DNA has been suggested as a diagnostic test for the presence of

Table I: Characteristics of Different Tandem Repeat DNA Populations

Defective DNA Series	Estimated Maximum Amount		Repeat Unit Molecular Weight	Buoyant Density	Restriction Enzymes Number of Cleavages				
	% of Total	Passage Level[a]			EcoRI	BglII	HindIII	XbaI	BamHI
HSV-1(Justin)	50%	H14	5.5×10^6 het[b]	High	1	0	0	0	3
HSV-1(MP)a	90%	H12+V8	5.2×10^6	Standard	1	1	0	0	3
HSV-1(MP)b	25%	H12	5.2×10^6	ND	1	1	0	0	3
HSV-2(333)a	7%	H12	6.5×10^6 het	ND	1	0	0	1	ND
HSV-2(333)b	15%	H12	6.5×10^6 het	ND	1	0	0	1	ND
HSV-2(STH2)a	15%	V9	a) 2.3×10^6	ND	1	1	0	0	1
			b) 3.0×10^6		1	1	0	0	2
HSV-1(STH2)b	20%	V3	5.4×10^6	ND	1	1	0	0	ND
HSV-1(STH2)c	90%	V12	17×10^6[c]	ND	3	2	0	ND	ND
HSV-1(STH2)d	80%	V9	Complex	Standard	2[d]	5[d]	ND	0	3[d]
HSV-2(333cl-5)c	90%	V12	6.5×10^6 het	High	1	0	0	1	ND
HSV-2(333cl-5)d	80%	V8	6.5×10^6 het	ND	1	0	0	1	ND
HSV-2(333cl-7)g	5%	V7	6.5×10^6 het	ND	1	0	0	1	ND

(a) H = HEp-2 cells, V = Vero cells
(b) Consisting of multiple related components with similar molecular weights
(c) Assuming a single defective population only
(d) Major components only

defective DNA. However, the HSV-1(MPal8) DNA that we have described here does not have a high (G + C)-content: its buoyant density is undistinguishable from that of the

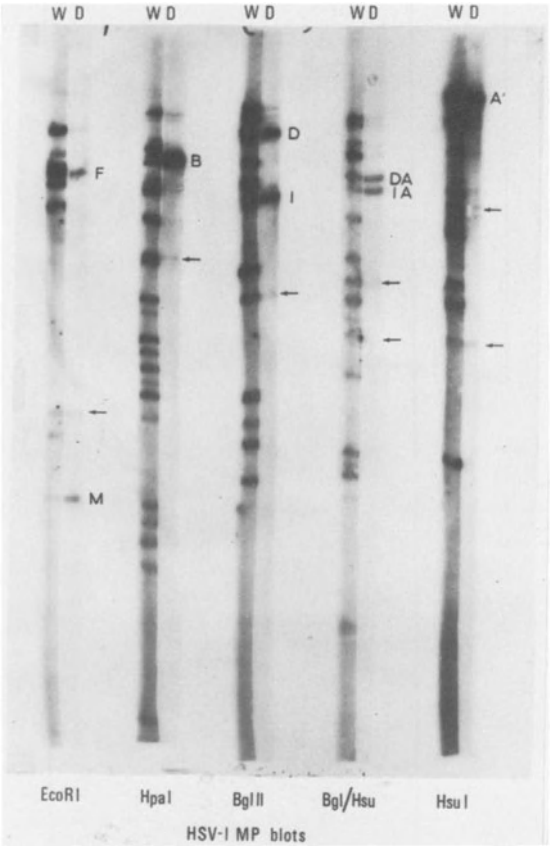

Figure 2: Blot hybridization of the purified EcoRI repeat unit probe from HSV-1(MPa18) to the cleaved DNA from parental plaque-purified HSV-1(MPc1-10) virus. The probe was isolated as the 5.2 x 10^6 molecular weight EcoRI species from preparative agarose gels then eluted by the saturated KI procedure (G.S. Hayward, Ph.D. Thesis, 1972) and labeled in vitro with ^{32}P-TTP and ^{32}P-dCTP by the nick translation reaction of E. coli DNA polymerase I. Unlabeled HSV-1 (MPc1-10) DNA was cleaved with the restriction enzymes indicated, then fractionated by agarose gel electrophoresis in long 0.5% cylinders before being denatured in situ and transferred onto nitrocellulose filter strips by the Southern blotting procedure. Hybridization was carried out for 36 hr at 68°C in 1 M NaCl, 0.2 M Tris, 0.02 M EDTA (pH 8) buffer with 10% formamide and 0.2% SDS. Those L-segment fragments showing strong hybridization are identified by the appropriate standard letter designation. The much fainter hybridization to 1/2 molar terminal fragments from the S-segment is indicated by arrows.

average density for intact HSV-1 DNA, i.e. 1.726 g/cm^3 (not shown).

The MPa18 Repeat Unit Originates from the L Component of the Parent Genome

An explanation for the high (G + C) content of the HSV-1 (Justin) p14 DNA was first suggested on the basis of the similarity of cleavage sites within the repeat unit and those from the extreme right-hand 5% of HSV-1 DNA, which includes the (G + C)-rich *ac* inverted repeat sequence from the S segment of the molecule. This model was confirmed by partial denaturation mapping (5) and blot hybridization studies (6). To examine the nature of the repeat unit in our HSV-1(MPa18) DNA we performed blot hybridization

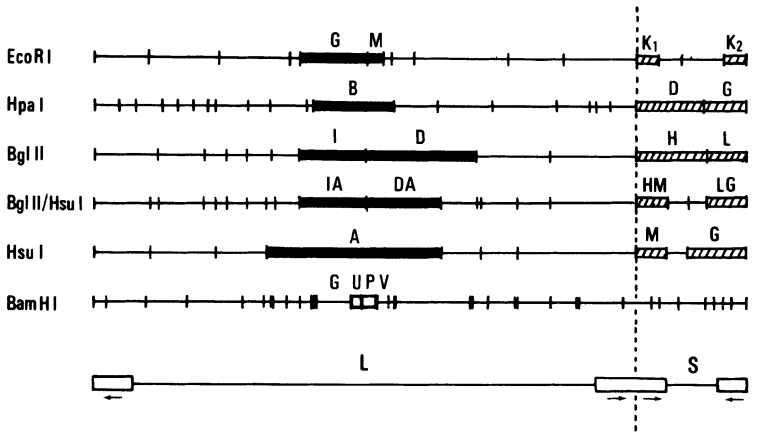

Figure 3: Location of sequences in the standard physical map of the HSV-1(MPc1-10) genome that hybridize with the HSV-1(MPa18) defective repeat unit DNA. The diagram summarizes results from the experiment shown in Figure 2 and also gives the location of the BamHI-P and -U fragments that are amplified intact in the defective DNA (see Figure 4). Solid areas indicate fragments with strong homology and hatched areas indicate the weak homology to the S-segment 1/2 and 1/4 molar fragments. The cleavage maps for EcoRI, HpaI, BglII and HsuI are drawn in the P orientation and are derived from the work of G.S. Hayward, T.G. Buchman and B. Roizman as cited in Morse et al (24). The BamHI map for HSV-1(MP) was constructed by G.S. Hayward (unpublished data).

studies using the isolated EcoRI 5.2 x 10^6 species as probe. Figure 2 shows the pattern of hybridization to the EcoRI, HpaI, BglII, BglII/HsuI double cut and HsuI profiles of wild-type HSV-1(MPcl-10) DNA. By reference to the cleavage maps of HSV-1(MP) DNA we conclude that the HSV-1 (MPa18) repeat unit originated predominantly from within the central unique portion of the L-segment and not from the S repeats (see Figure 3).

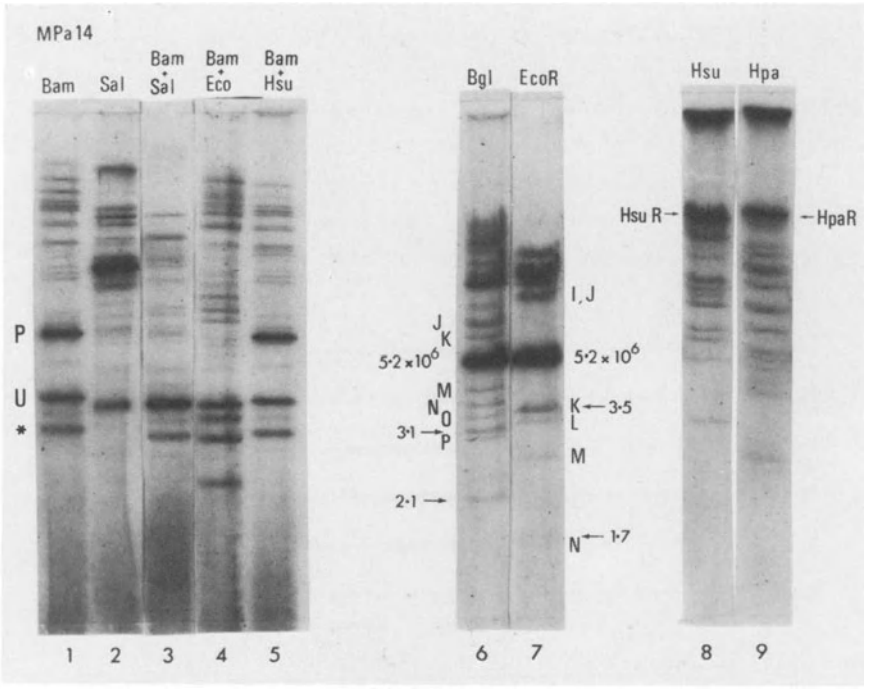

Figure 4: Illustrative cleavage patterns of the intact repeat units and terminal fragments from HSV-1(MPa18) defective DNA. The figure shows autoradiographs of ^{32}P-labeled virion DNA after electrophoresis through agarose gels of 1.0% (#1-5), 0.6% (#6 and 7) or 0.45% (#8 and 9). DNA fragment species derived from the tandem repeat units are easily recognized by their greatly increased abundance. The first two defective bands in the BamHI profile correspond to the BamHI-P and -U species from plaque-purified HSV-1 (MP) DNA but the third band represents a novel fusion between portions of the BamHI-G and -V sequences at the ends of the repeat unit. The arrows by gels 6 & 7 indicate the terminal BglII and EcoRI fragments derived from the left and right ends of the defective molecules. Gels 8 & 9 show the complete resistance of HSV-1 (MPa18) defective DNA to cleavage with the HsuI or HpaI enzymes.

Cleavage Maps of the MPa18 Repeat Unit

Figure 4 illustrates the patterns of cleavage of total HSV-1(MPa14) DNA with BglII, EcoRI, HsuI, HpaI, BamHI, SalI and several double digests with the BamHI enzyme. Numerous other single, double and triple digests have also

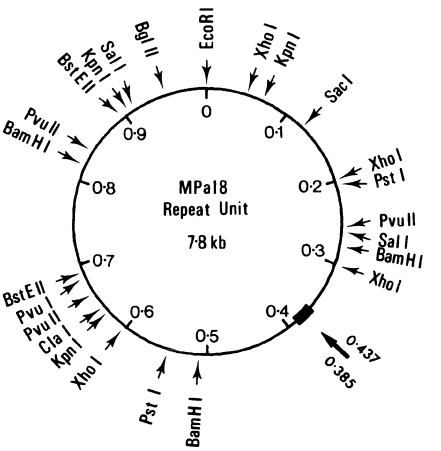

Figure 5: Circular cleavage map of the HSV-1(MPa18) tandem repeat unit DNA. The zero reference point is arbitrarily defined by the EcoRI site at 0.418 in the parent genome. BamHI-U occupies a position from 0.51 to 0.82 on the circular map and BamHI-P encompasses co-ordinates 0.82 to 0.28. The third BamHI fragment, between 0.28 and 0.51, contains the novel joint between sequences close to 0.385 and 0.437 from the parent genome and the sequences homologous with the S-repeats are presumed to be located at this site (arrowed).

been carried out. The repeat unit is resistant to cleavage with HsuI (HindIII), HpaI, XbaI and BclI and contains one cleavage site each for BglII, EcoRI, PvuI, SacI and ClaI. There are two sites for KpnI, BstEII, PstI and SalI, at least three sites for BamHI and PvuII and four sites for XhoI. Figure 5 presents our current cleavage map for the entire repeat unit in a circular format. Since the exact physical ends of the repeat unit are not known we have chosen the EcoRI cleavage site at 0.418 in the parent genome as the origin or zero reference point for the

repeat unit map. From these experiments and the blot hybridization data we know that the repeat unit contains sequences from portions of the adjacent BglII-I and -D fragments and the EcoRI-F and -M species. It also contains the entire BamHI-P and -U fragments and must therefore consist of at least those sequences from 0.391 to 0.432 in the wild-type HSV-1(MP) genome (Figure 3).

Packaged Defective DNA Contains an Exactly Integral Number of Repeat Units

Inspection of the EcoRI and BglII gel profiles in Figure 4 (and also Figure 1) reveals the presence of two other new DNA species in addition to the predominant 5.2 x 10^6 molecular weight repeat unit. These minor components have sizes of 3.5 and 1.7 x 10^6 for EcoRl and 3.1 and 2.1 x 10^6 for BglII i.e. exactly equal to the size of the major repeat unit. In all preparations of HSV-1(MPa) and HSV-1(MPb) series defective DNA these bands invariably represented close to 5% of the total tandem repeat DNA. Blot hybridization experiments (not shown) have indicated that sequences present within the isolated 5.2 x 10^6 repeat unit DNA are also present in both minor components. These findings favor the interpretation that the minor components represent terminal fragments from the same molecules that give rise to the intact 5.2 x 10^6 repeat units. However, it is also formally possible that they come from a subpopulation of distinct DNA molecules containing shorter repeat units than those of the major species. A prediction of the former but not the latter hypothesis is that the terminal fragments would not be seen in replicating intracellular DNA preparations. The experiment presented in Figure 6 shows that this is indeed the case. Both of the minor components from the defective DNA and the known terminal l/2M fragments from wild-type DNA are completely absent in ^{32}P-labeled DNA extracted

from the nucleus 20-hours after infection, presumably because in both cases genome-sized lengths of viral DNA are linked end-to-end as concatemers or in circular forms in the replicating pool (18-20).

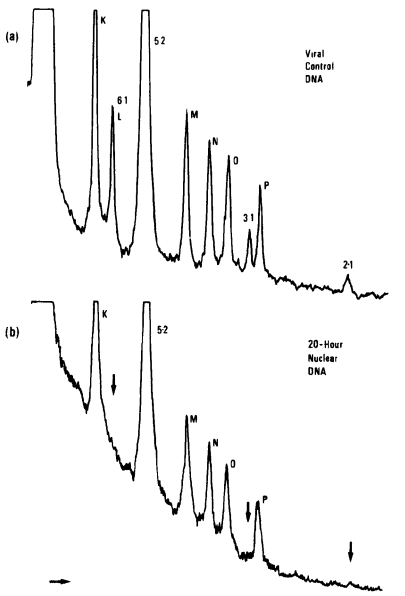

Figure 6: Absence of terminal fragments from both wild-type and defective DNA in replicating molecules isolated from the nucleus. HSV-1(MPa18) infected Vero cells were labeled continuously with ^{32}P-phosphate added to low phosphate medium at 0 hr. One portion of the culture (B) was lysed after 20 hr at 37°C and viral DNA extracted from the nuclear fraction was purified on a CsCl buoyant density gradient. Supernatant virus particles were collected from the other portion (A) at 40 hr after infection. DNA from both portions was cleaved with BglII and subjected to electrophoresis through 0.6% agarose gels. Microdensitometer tracings of relevant portions of the autoradiographs are shown. Arrows in panel B indicate the positions of the missing end fragments in replicating DNA forms compared with the DNA from virus particles: i.e. the 6.2 x 10^6 BglII-L species from standard genomes and the 3.1 x 10^6 and 2.1 x 10^6 minor species from the tandem repeat defective molecules. The total proportion of defective 5.2 x 10^6 repeat unit DNA to standard (approximately 30%) remains roughly equal in the two samples.

We conclude that most defective DNA molecules must therefore consist of approximately 15-17 complete BglII repeat units of 5.2 x 10^6 plus left and right end

fragments that together comprise one additional complete repeat unit. In other words, each packaged defective DNA molecule contains an exactly integral number of copies of adjacent tandem repeat units. Furthermore, since the BglII cleavage at 0.415 in the parent genome lies approximately 500bp to the left of the EcoRl site at 0.418 we can tentatively assume that the BglII species of 3.1×10^6 and the EcoRI species of 3.5×10^6 represent the left terminal fragments and that the other two minor species are the right hand side terminal portions of the defective DNA molecules. Therefore, provided that there are no sequence rearrangements, the physical limits of each complete repeat unit would lie between coordinates 0.385 to 0.437 in the parent genome with a novel joint occurring between sequences at these two coordinates at the junctions of each pair of adjacent repeat units. This interpretation as shown in Figure 7 is completely consistent with all of the available mapping data.

Homology Between the L Segment Repeat Unit and Sequences in the S Segment of the Parent Genome

The structure described above for the HSV-1(MPa) series defective DNA molecules raises the question of whether or not the same specific DNA sequences exist at the termini in linear genome-sized defective DNA as in the wild-type parental genomes. The experiment described earlier in Figure 2 gives positive information on this point. In addition to strong hybridization to fragments around 0.4 in the L-segment, the 5.2×10^6 repeat unit probe also hybridized faintly to some fragments in the plaque-purified HSV-1(MPcl-10) DNA that contained terminal sequences. For example, the following fragments (arrowed in Figure 2) showed up distinctly in the autoradiograph: EcoRI-K, BglII-H and -L, HsuI-M and -G, HpaI-D and -H and all 1/4M fragments. On the other hand the Hpa-M complex exhibited

barely detectable cross homology and EcoRl-G, BglII-J and -F and HsuI-I did not show up at all. These results indicate that the common sequence lies within both copies

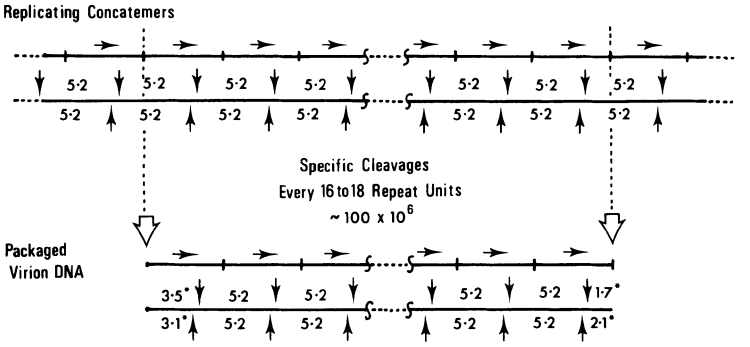

Figure 7: Diagram illustrating the generation of mature defective DNA molecules from replicating concatemeric forms and the origin of the terminal fragments in packaged defective DNA. Horizontal arrows indicate individual repeat units and small vertical arrows denote cleavage sites.

of the S inverted repeats but not in the S unique region and that there is much less homology to the L segment repeats. M. Denniston-Thompson (personal communication) has shown further that the HSV-1(MPal8) repeat unit cloned in phage lambda has homology with the S-segment repeat unit from HSV-1(Patton) defective DNA. In each case this homology resides entirely within the BamHI fragment containing the novel joint, which in the HSV-1(Patton) repeat unit means within the sequence from parental coordinates 0.977 to 1.000 and in the HSV-1(MPal8) repeat unit means to the left of 0.392 and to the right of 0.432 (i.e. between 0.27 and 0.47 on the circular map given in Figure 5).

DISCUSSION

By examining several new passaging series of undiluted HSV

populations we have demonstrated that: (1) Tandem repeat units in HSV defective DNA can arise from the L segment as well as from the terminal portions of the S segment of the parent genome; (2) The size and sequence complexity of tandem repeat units can vary enormously and (3) Some tandem repeat species do not exhibit the relatively high buoyant density previously thought to be characteristic of HSV defective DNA.

The particular species of HSV-1 tandem repeat defective DNA that we have examined in detail here differs markedly from the two other populations studied in greatest detail previously (Figure 8). The repeat units of HSV-1(MPal8) DNA consist predominantly of an intact block of sequences from 0.385-0.437 in the parent genome arranged in tandem and packaged as genome-sized pieces of approximately 16 to 18 adjacent copies totalling close to 100 x 10^6 molecular weight. The other two species, HSV-1(Justin pl4) and HSV-1 (Patton pl6) have the same general structure but consist exclusively of sequences from coordinates 0.945-1.000. A species of defective DNA that has normal buoyant density and contains sequences from both the L and S segments was found earlier in laboratory stocks of HSV-1(ANG) strain but has not been mapped in any detail (17) and another similar species has also been mentioned recently by Locker and Frenkel (21).

We anticipate that there are at least two *cis*-acting functions that must always be retained in HSV defective DNA populations that are capable of being propagated in virions. Firstly, virtually by definition, they must contain an origin of replication, and secondly they must retain the sequence-specific recognition site necessary for cutting out and packaging genome-size pieces from concatemeric replicative forms. All functions acting in *trans* could presumably be supplied by the wild-type helper virus genomes.

In this regard, there are several alternative explanations for the homology between the HSV-1(MPal8) repeat unit and sequences within the EcoRl-K fragment from the

S repeats of wild-type DNA. For example there may simply be cross-homology between these two portions of the genome, possibly because both contain origins of replication. More likely, however, the HSV-1(MPa18) repeat unit retains certain sequences derived from the S end of the molecule that are necessary for successful propagation of the defective DNA molecules. These sequences might either provide the recognition site for termination/packaging events or provide an origin for replication or possibly both. Although we have not looked for it specifically, we are not aware of any evidence for cross-homology between

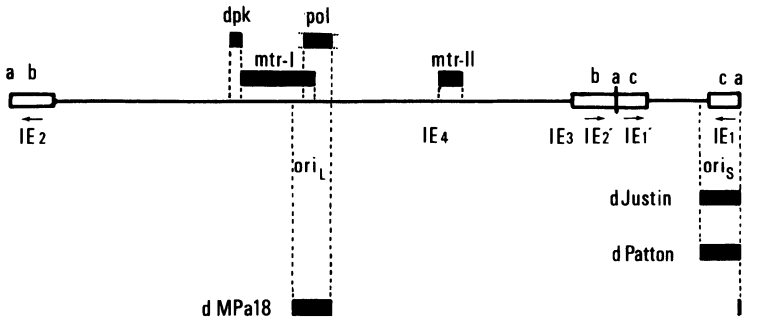

Figure 8: Comparison of the map locations of the three well characterized species of HSV-1 defective DNA (ref. 5 and 7) and correlation with major features of the HSV-1 genome IE-1 to IE-4 indicate the four currently recognized regions for immediate-early transcription and the notations dpk, pol, mtr-I and mtr-II refer to the minimal defined map locations of the loci for the viral thymidine kinase and DNA polymerase enzymes and the morphological transforming regions (G.R. Reyes, R. LaFemina, S.D. Hayward and G.S. Hayward Cold Spring Harbor Symp. Quant. Biol. 44, 1979, in press).

these two regions within the parental genomes. However, the location of the homology within the S-sequences from 0.977-1.000 in the HSV-1(Patton) tandem repeat and at the novel junction within the HSV-1(MPa18) repeat supports the notion that these sequences come from a recombination

event with terminal S region sequences. Until the homology has been precisely mapped we cannot distinguish between the alternatives that these sequences provide only the normal packaging signals or that they provide both the necessary packaging signals and the replication origin. Although the size of the homologous region is very small (estimated to be a maximum of 200 base pairs) the homology cannot reside entirely within the terminally redundant *a* sequence as might be expected, because otherwise we should have found equal hybridization to the L-segment repeats.

The finding of an exactly integral number of copies of the 5.2×10^6 repeat units in all packaged defective DNA molecules, together with a precisely defined site for termination at 3.1×10^6 daltons to the left of the first BglII site at one end of all molecules and 2.1×10^6 daltons to the right of the first BglII site at the other end, clearly implies the existence of a sequence-specific cleavage event during packaging from concatemeric replicative forms. Further, since the left and right terminal fragments exactly comprise a single repeat unit and the homology with the S terminal fragments of wild-type DNA resides within the intact 5.2×10^6 repeat units as well as in the terminal fragments, we conclude that the potential packaging site must be present in every repeat unit rather than located only at the ends of the defective molecules. Consequently, a "head-full" packaging mechanism must also be operating such that only those termination sites spaced a full genome length apart (i.e approximately 100×10^6 daltons) are actually cleaved (see Figure 7).

Two other constraints (in addition to the presence of an origin and the packaging signals) are probably also necessary before defective genomes can accumulate: firstly, the new DNA species should be capable in some way of replicating faster or more efficiently than the parent genomes and secondly, the basic repeat unit size should be such that an exactly integral number of adjacent copies

fulfills the requirements of the "head-full" part of the packaging mechanism. We presume that initially a large and very heterogeneous mixture of deleted or aberrant molecules are constantly arising in HSV DNA populations but that these are usually lost as obviously lethal events unless a sufficiently high multiplicity of infection permits those that satisfy the criteria stated above to be propagated. After a series of undiluted passages the small number of specific units that we see evolve are likely to have had the selective advantage of being able to replicate and/or be packaged more efficiently than the others. The defective DNA population shown in Figure 3 of Wagner et al (4) would represent an early stage in this process.

In the case of the S-segment repeats it is easy to envisage that simple single deletions which leave the origin and termination signals on the same short stretch of DNA from the right hand end of the molecule would be likely to occur at relatively high abundance and quickly predominate. Probably the smallest repeat units containing both of these functions would be the most efficiently replicated, because they have more initiation sites per genome-sized molecule, although since very slight size differences would be unlikely to have a selective advantage the populations might also be expected to retain the heterogeneity that we observe. The long-term stability of S region repeats of between 5.2×10^6 (HSV-1) and 6.5×10^6 (HSV-2) also suggests that the two necessary functions may be that far apart on the genome: i.e. we might guess that the replication origin is actually within the unique portion of the S segment at approximately 0.945-0.955 on the physical map of HSV-1 DNA. Smaller repeat units can be derived from abundant S repeat unit species at low frequency (21) but these tend to be deleted only in the central portions of the sequence supporting the idea that both ends are necessary components.

On the other hand, the L segment repeat seemingly must

have additional selective advantages over the S repeats, since the chances of its initial appearance must be much lower and require at least two appropriately located deletions to fuse the terminal packaging sequence with an origin from the center of the L-segment. Interestingly, the results of Chartrand et al (22) indicate that the map location of the bulk of the L repeat unit sequence (0.385-0.437) coincides almost exactly with that of the genetic locus for both ts and PAA^r mutations in the viral DNA polymerase at approximately 0.400-0.437 (our coordinates). Although we do not yet know for sure that the repeat unit can encode an active DNA polymerase enzyme, the ability to do so would probably supply the additional selective advantage needed. Furthermore, if as we suspect, this repeat unit had been present already in the original HSV-1(MP) virus pool, it would have had a much longer opportunity to express its selective advantage and this might also explain the extreme homogenity of this repeat unit in contrast to all of the presumably younger S-segment defective populations that have been studied.

On balance the evidence allows us to tentatively conclude that the HSV-1(MPal8) repeat unit defines a second origin of replication within the L-segment of HSV DNA, one directly adjacent to or within the DNA polymerase gene itself. We suggest that all tandem repeat defective DNAs will fall into one or other of two classes containing either the ori_S or the ori_L sequence plus the terminal packaging signals. More complicated defective species presumably have picked up or retained additional portions of the genome and amplified them as tandem repeats along with the ori_S or ori_L sequences.

Preliminary electron microscopic evidence from both HSV and pseudorabies virus intracellular DNA supports the idea of replication origins in both the L- and S-components of the wild-type genomes (23; A. Kaplan and T. Ben-Porat, personal communication). We would further speculate that an origin within the unique L-segment could operate in a

late undirectional rolling circle mode of replication to produce replicative pools in which most or all of the L segments would have the same orientation relative to one another and thus perhaps account for the observations that heterotypic recombinants are formed between genomes with their L segments predominantly in the P or prototype orientation (24,25) whereas packaged virion DNA has both P and I_L (inverted) orientations in equal abundance (26,27)

ACKNOWLEDGEMENTS

This investigation was supported by Grant Number R01 CA22130 awarded by the National Cancer Institute, DHEW. One of us (G.S.H.) was a Special Fellow of The Leukemia Society of America during the initial stages of the work.

REFERENCES

1. Bronson, D.L., Dreesman, G.R., Biswal, N. and Benyesh-Melnick, M. (1973). Intervirology 1, 141-153.
2. Ben-Porat, T., DeMarchi, J.M. and Kaplan, A.S. (1974). Virology 60, 29-37.
3. Campbell, D.E., Kemp, M.C., Perdue, M.L., Randall, C.C. and Gentry, G.A. (1976). Virology 69, 737-750.
4. Wagner, M., Skare, J. and Summers, W.C. (1974). Cold Spring Harbor Symp. Quant. Biol. 39, 683-686.
5. Frenkel, N., Jacob, R.J., Honess, R.W., G.S. Hayward, Locker, H. and Roizman, B. (1975). J. Virol. 16, 153-167.
6. Frenkel, N., Locker, H., Batterson, W., Hayward, G.S. and Roizman, B. (1976). J. Virol. 20. 527-531.
7. Graham, B.J., Bengali, Z. and Vande Woude, G.F. (1978). J. Virol. 25, 878-887.
8. Hayward, G.S., Frenkel, N. and Roizman, B. (1975). Proc. Nat. Acad. Sci. U.S.A. 72, 1768-1772.
9. Murray, B.K., Biswal, N., Bookout, J.B., Canford, R.E., Courtney, R.J. and Melnick, J.L. (1975). Intervirology 5, 173-184.
10. Rubenstein, A.S. and Kaplan, A.S. (1975). Virology 66, 385-392.
11. Fresen, K.-O., Merkt, B., Bornkamm, G.W. and zur Hausen, H. (1977). Int. J. Cancer 19, 317-323.
12. Delius, H. and Bornkamm, G.W. (1978). J. Virol. 27, 81-89.
13. Kilpatrick, B.A. and Huang, E.-S. (1977). J. Virol.

24, 261-276.
14. Stinski, M.F., Mocarski, E.S. and Thomsen, D.R. (1979). J. Virol. 31, 231-239.
15. Carter, B.J., Shaw, B.D. and Smith, M.G. (1969). Biochem. Biophys. Acta. 195, 494-505.
16. Skalka, A., Poonian, M. and Bartl, P. (1972). J. Mol. Biol. 64, 541-550.
17. Schroeder, C.H., Stegman, B., Lauppe, H.F. and Kaerner, H.C. (1975). Intervirology 6, 270-284.
18. Ben-Porat, T., Kaplan, A., Stehn, B., Rubenstein, A.S. (1975). Virology 69, 547-560.
19. Becker, Y., Asher, Y., Weinberg-Zahlering, E. and Rabkin, S. (1978) J. gen. Virol. 40, 319-335.
20. Jacob, R.J., Morse, L.S. and Roizman, B. (1979). J. Virol. 29, 448-457.
21. Locker, H. and Frenkel, N. (1979). J. Virol. 29, 1065-1077.
22. Chartrand, P., Stow, N.D., Timbury, M.C. and Wilkie, N.M. (1979). J. Virol. 31, 265-276.
23. Freidmann, A., Schlomai, J. and Becker, Y. (1977). J. gen. Virol. 34, 507-522.
24. Morse, L.S., Buchman, T.G., Roizman, B. and Schaffer, P.A. (1977). J. Virol. 24, 231-248.
25. Wilkie, N.M., Davison, A., Chartrand, P., Stow, N.D., Preston, V.G. and Timbury, M.C. (1978). Cold Spring Harbor Symp. Quant. Biol. 43, 827-840.
26. Hayward, G.S., Jacob, R.J., Wadsworth, S.C. and Roizman, B. (1975). Proc. Nat. Acad. Sci. U.S.A. 72, 4243-4247.
27. Delius, H. and Clements, J.B. (1976). J. gen. Virol. 33, 125-133.

9. Structure and physical mapping of different classes of defective HSV-1 ANG DNA

H.C. Kaerner

SUMMARY

Two major classes of defective herpes simplex virus type 1 ANG (HSV-1 ANG) DNA have been shown to accumulate in independent serial virus passages at high multiplicity of infection. Both types of the DNA's consist of tandem repeats of small portions of the viral genome and are resistant to Hind III and Hpa I restriction enzyme cleavage. One species of defective DNA - dDNA1 - is not cleaved by Eco RI, whereas the other species has one Eco RI cleavage site in its repeats.

The Eco RI-resistant dDNA1 has a repeat sequence of approximately 6 x 10^6 dalton MW and originates from non-contiguous sites of the viral genome, located between 0.368 - 0.413 and between 0.95 - 1.0 map units on the prototype isomer of HSV-1 ANG DNA.

The Eco RI-sensitive defective HSV-1 ANG DNA consists of at least two subclasses of molecules dDNA2 and dDNA2* which have different repeat sequences of 3.4 and 4.0 x 10^6 daltons, respectively, mapping between the positions 0.90 and 1.0 of the viral genome.

All classes of the defective DNA contain multiple insertions of a 550 base pairs' sequence, which is also present in several copies in the S-redundant regions TR_S and IR_S of the parental HSV-1 ANG DNA.

Y. Becker (ed), Herpesvirus DNA.

1. INTRODUCTION

Virions containing defective viral DNA accumulate in the virus progeny during serial passages of herpesviruses at high multiplicity of infection (MOI) (1-14). The defective DNA has approximately the same molecular weight as the respective parental viral genome and is made up by repetition of restricted portions of the viral standard DNA. The present communication is concerned with two different classes of defective DNA, derived from HSV-1 ANG, which developed in independent series of high MOI virus passages (7, 10, 13). dDNA1 has the same buoyant density as the parental viral DNA, whereas the Eco RI-sensitive DNA species dDNA2 and dDNA2* are heavier than HSV-1 ANG standard DNA. dDNA1, -2 and -2* are insensitive to the restriction endonucleases Hind III and Hpa I, both of which cleave the parental viral standard DNA. dDNA1 and dDNA2 furthermore are cleaved by Kpn I, whereas dDNA2* is resistant to this enzyme. The defective HSV-1 ANG DNA's have been studied with respect to their structural organization, sequence complexity, and the localization of their repeat units on the parental genome.

2. EXPERIMENTAL APPROACH

2.1. Development of defective HSV-1 ANG DNA during high MOI virus passages

Plaque-purified HSV-1 ANG was passaged 5 times at an MOI of 0.01 PfU/cell (low passages LP1-LP5). LP3 and LP5 were separately passaged serially at an MOI of 10 (high passages HP3/1 - HP3/n and HP5/1 - HP5/n, respectively). In the HP3/1 - HP3/n series increasing fractions of virions accumulated, which contained dDNA1 as judged by its resistance to Eco RI, Hind III and Hpa I and its Kpn I restriction

pattern. Whereas HP3/7 contained as much as 50% of dDNA1, Eco RI-sensitive DNA was not present in detectable amounts (7). In the HP5/1-n series, in addition to dDNA1, Eco RI-sensitive defective DNA appeared, being first detected in HP5/3 and 4 (3-5%) and reaching about 15% of the total DNA in HP5/11. It is noteworthy that in this series of high MOI passages defective DNA accumulated much slower and did not exceed 30% (15% dDNA1 and 15% dDNA2 + -2*) of the total DNA isolated from mature virions (10). Analyses of the intracellular viral DNA in all cases revealed identical ratios of defective/standard DNA as determined in mature virions.

2.2. Preparation of defective HSV-1 ANG DNA's

dDNA1 was isolated from the total DNA of HP3/7 virions by 1) digestion with Eco RI and 2) separating the restriction fragments of standard DNA from the undegraded dDNA1 by repeated sucrose gradient centrifugation. The Eco RI-sensitive dDNA2 and -2* were prepared in two steps from HP5/11 virions containing 15% each of Eco RI-resistant dDNA1 and Eco RI-sensitive DNA, and 70% standard DNA. First Hind III-resistant DNA was isolated which was then treated with Eco RI. The resulting Eco RI fragments of dDNA2 and -2* were separated from uncleaved dDNA1 by sedimentation in sucrose gradients. It has not yet been possible to separate dDNA2 from dDNA2*.

The Kpn I-resistant dDNA2* was isolated in one step by digestion of the original DNA mixture with Kpn I and subsequent separation of undegraded dDNA2* from the Kpn I restriction fragments of standard DNA and dDNA1 and of the Kpn I-sensitive fraction of dDNA2, by velocity sedimentation. The amount of dDNA2* accounted for about 20-30% of the total of Eco RI-sensitive DNA i.e. about 3-5% of the total DNA mixture.

3. RESULTS

3.1. The DNA of the parental virus strain HSV-1 ANG

The genome of HSV-1 consists of a linear double-stranded DNA molecule of about 100 x 10^6 dalton MW (15-17), which is composed of a large segment L and a small segment S accounting for 82% and 18%, respectively, of the total genome length. Both, L and S are bracketed by short inverted redundant sequences designated as TR_L and IR_L (6 x 10^6 dalton) and as TR_S and IR_S (4.3 x 10^6 dalton), respectively. The L- and the S-segment are joined in all of the four possible orientations to each other giving rise to four genome isomers P, I_S, I_L and I_{SL}, which have been demonstrated to be present in standard DNA populations at equimolar ratios (18-26, for Review see 27). Fig. 1 shows the physical maps of the four isomers of HSV-1 ANG DNA for the restriction endonucleases Hind III and Hpa I (13), which are consistent with corresponding maps established by several investigators (15,27,28,29,30). A specific feature of HSV-1 ANG DNA, relevant for the present study, is the stepwise insertion of 1 to at least 6 copies of a 550 base pairs' sequence in the S-terminal redundancy TR_S. Consequently, the S-terminal fragments Eco RI K (29), Hind III G and M, and Hpa I G migrate in agarose gels as series of bands equidistant in molecular weight by approximately 0.35 x 10^6 dalton (Fig. 2). The second S-terminal fragment Hpa I C appears as a broad smeary DNA band which is due to the limited resolution of the gel in the higher MW range. From the finding that also the L-S joint fragments are in a similar way heterogeneous in size it can be concluded that the 550 base pairs sequence is also multiply inserted in the internal S-redundancy IR_S of the HSV-1 ANG genome. This heterogeneity could be resolved in the cases of the fragments Hind III F (Fig. 2), and Kpn I D (Fig. 6).

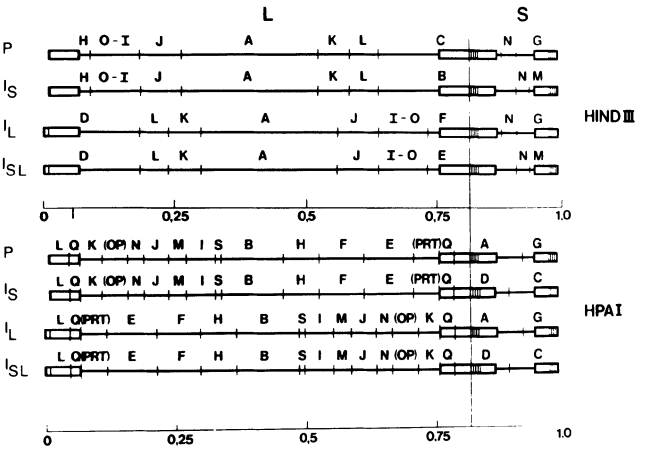

Figure 1

Scale maps of Hind III and Hpa I cleavage sites on HSV-1 ANG DNA. The designation of the DNA fragments is according to Wilkie (28) and to Buchman et al. (31, Hpa I map) and to Skare and Summers (29, Hind III map). The joint of the L- and S-segment is marked by a vertical line. The inverted redundant sequences bracketing the unique sequences of the L- and the S-segment are indicated as rectangles. The four isomers are designated as P (prototype), I_S (inverted S-segment), I_L (inverted L-segment) and I_{SL} (inverted L- and S-segment).

3.2. Localization of the nucleotide sequences of defective HSV-1 ANG DNA on the parental viral genome

3.2.1. Map coordinates of dDNA1 and dDNA2*

Purified dDNA1 and dDNA2* were ^{32}P-labeled by nick translation (32) and blot hybridized to Hpa I restriction fragment patterns on nitrocellulose filters (33). The filter strips were monitored by autoradiography. The obtained hybridization patterns are shown in Fig. 3b and c, respectively. The results suggest, that both, dDNA1 and dDNA2*, contain nucleotide sequences stemming from the S-segment

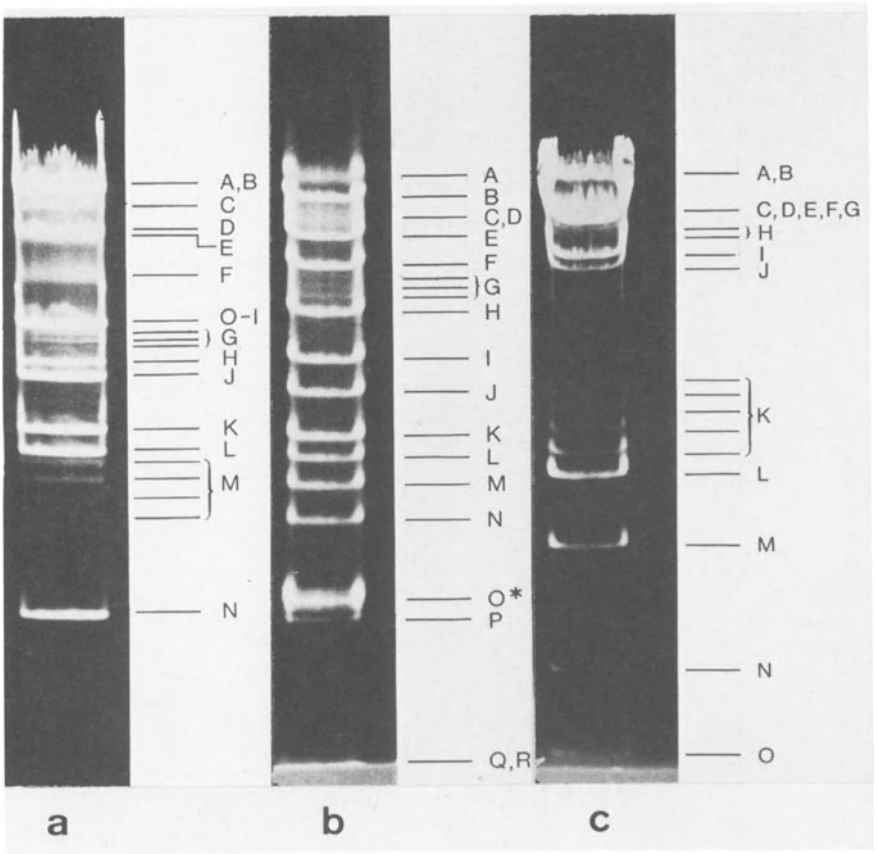

Figure 2

Ethidium bromide-stained Hind III (a), Hpa I (b) and Eco RI (c) restriction fragments of HSV-1 ANG DNA separated by electrophoresis in 0.5% agarose gels. The gel tracks (1 cm in width) were loaded with as much as 4 ug DNA each in order to display the series of bands representing the S-terminal fragments Hind III G and M, Hpa I G and Eco RI K.

of the parental genome, in that they hybridize to the S-terminal fragments Hpa I C and G. To a minor degree, both classes of defective DNA also hybridize to the L-terminal fragment Hpa I L. The latter finding could be explained by the fact, that the L- and S-terminus of HSV-1 DNA have a small sequence ("a") in common (34-36).

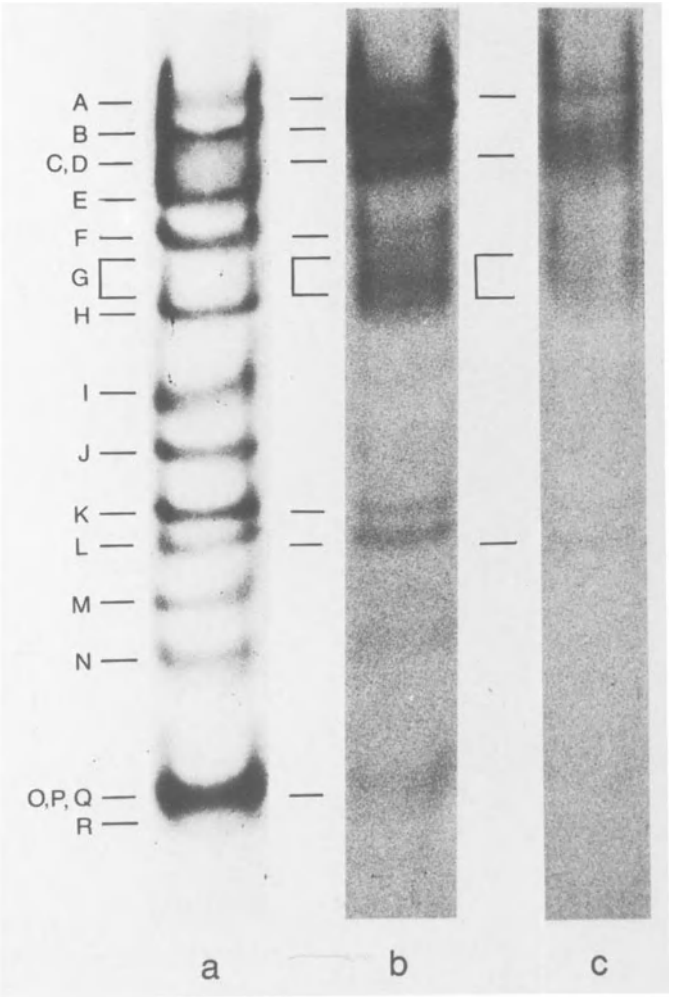

Figure 3

Blot hybridization of ^{32}P-labeled dDNA1 (b), dDNA2* (c) to unlabeled Hpa I restriction fragments of HSV-1 ANG standard DNA on nitrocellulose filter strips. The filters were monitored by autoradiography. The complete Hpa I restriction pattern of standard DNA was displayed by hybridization with ^{32}P-labeled standard DNA (a).

In contrast to dDNA2*, which apparently maps in the S-segment exclusively (map coordinates 0.90 - 1.0, Hpa I C), dDNA1 displays pronounced sequence homology to the frag-

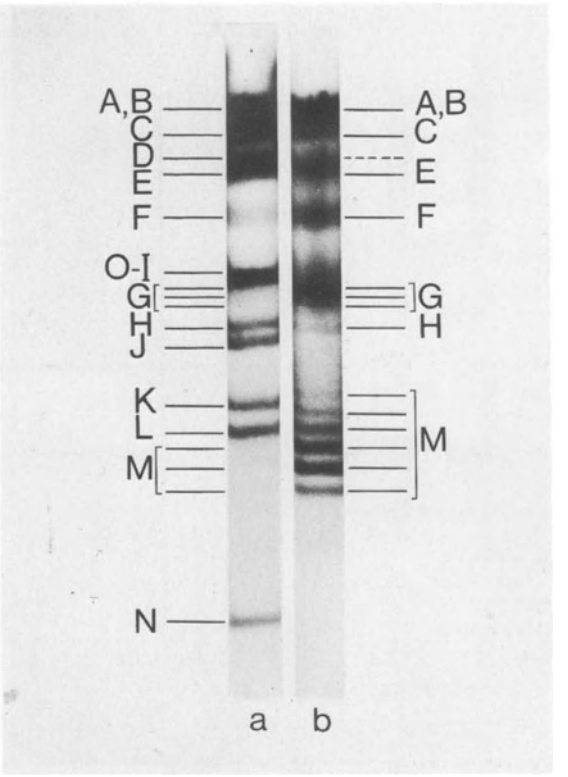

Figure 4

Blot hybridization of ^{32}P-labeled dDNA1 to unlabeled Hind III restriction fragments of HSV-1 ANG standard DNA monitored by autoradiography (b). The positions of the unlabeled standard DNA fragments were localized by hybridization of ^{32}P-labeled standard DNA to a parallel Hind III restriction fragment pattern (a).

ment Hpa I B mapping in the unique part of the L-segment (U_L-sequences) from 0.34 to 0.45 units in the prototype DNA isomer shown in Fig. 1. The latter finding suggests that the repeat unit of dDNA1 originated from non-contiguous sites of the parental viral genome. There is also some weak hybridization of dDNA1 to the standard DNA fragments Hpa I K and the (O,P,Q,R)-cluster which rather reflects minor contaminations of dDNA1 with other standard DNA fragments than true sequence homology of dDNA1 to these regions of the standard genome.

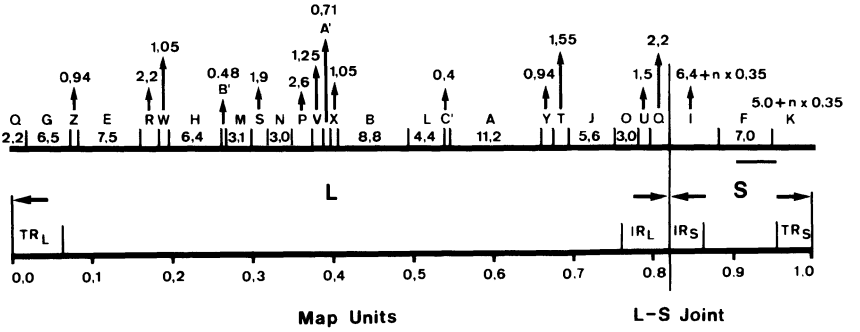

Figure 5

Scale map of Kpn I cleavage sites on HSV-1 ANG standard DNA. The map represents the prototype arrangement of the DNA molecule. The nomenclature of the fragments is according to Locker and Frenkel (37) despite the fact that some of the HSV-1 ANG DNA fragments differ in size from the corresponding fragments of HSV-1 strains Justin and F.

Similar conclusions can be drawn from blot hybridization of dDNA1 to Hind III restriction fragments of viral standard DNA which is illustrated in Fig. 4. Homology of dDNA1 is observed to the S-terminal Hind III fragments G and M and, as expected, to the L-S joint fragments B, C, E and F (Fig. 1). The homology of dDNA1 to the 0.34 -0.45 map units region cannot be distinguished in the Hind III fragment pattern since Hind III A (0.258 - 0.523 map units) comigrates with Hind III B.

It is noteworthy, that blot hybridization of dDNA1 to the Hind III standard DNA fragment pattern clearly resolves the multiple insertions of the 550 base pairs sequence unit in the S-terminal fragments Hind III G and M (Fig. 4b) as mentioned above. This finding strongly suggests that dDNA1 contained sequences of the S-redundant region TR_S (Fig. 2).

More refined mapping of dDNA1 on the standard genome was achieved by blot hybridization to Kpn I restriction

L-S joint fragments C and D, to the S-terminal fragments Kpn I K and I, and to the U_L-fragments P, V, and A'. In the Kpn I fragment pattern not only the S-terminal fragment K but also the L-S joint fragment D are resolved by blot hybridization with dDNA1 as "step ladders" of equidistant bands suggesting that the 550 base pairs' sequence mentioned above is also multiply inserted in the internal S-redundant region IR_S.

From the fact that dDNA1 does not display homology to the standard DNA fragments Hind III N (Fig. 4) and Kpn I F (Fig. 6) it must be concluded that dDNA1 does not contain U_S-sequences mapping between the positions 0.88 and 0.957 (Fig.'s 1 and 5).

The above results can be summarized as follows. The repeat sequence unit of dDNA1 consists of sequences mapping between the coordinates 0.368 and 0.413 in U_L and between 0.95 and 1.0 in U_S of the HSV-1 ANG standard DNA. The repeat of dDNA2* does not contain any U_L-sequences and maps between 0.90 and 1.0 units in the prototype arrangement of the S-segment of the HSV-1 ANG genome. From the provided data we cannot say, whether or not the repeats of dDNA1 and dDNA2* contain any unique sequences of the S-segment (U_S-sequences). In the case of dDNA1, eventual U_S-sequences could map only between 0.950 (Kpn I K cleavage site, Fig. 5) and 0.957 (left hand boundary of TR_S) units.

3.2.2. Map coordinates of dDNA2

As described in Methods, the Kpn I-sensitive fraction of Eco RI-sensitive, defective DNA (dDNA2) cannot be separated from the Kpn I-resistant fraction dDNA2*. Digestion with Hind III and subsequent Eco RI digestion of the isolated Hind III-resistant total fraction of defective DNA from a mixture of standard DNA, dDNA1, -2 and -2* yielded a mixture of Eco RI fragments of dDNA2 and -2* which accounted for 10-15% of the original amount of total DNA. Fig. 7

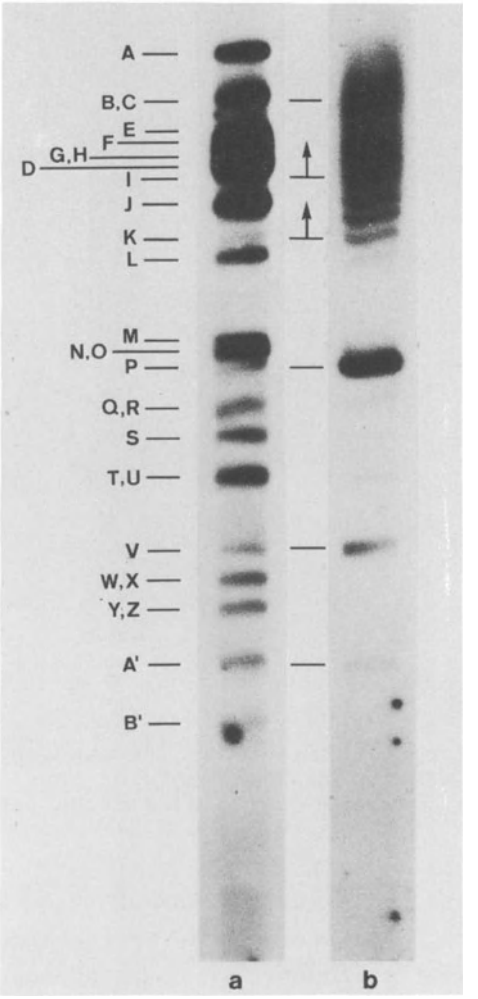

Figure 6

Blot hybridization of dDNA1, ^{32}P-labeled by nick-translation, to unlabeled Kpn I restriction fragments of HSV-1 standard DNA (a). The complete Kpn I restriction fragment pattern (b) was obtained by blot hybridization of ^{32}P-labeled standard DNA.

fragments of standard DNA. Fig. 5 shows the Kpn I cleavage site map of HSV-1 ANG which was established in our laboratory, and which is very similar to the Kpn I maps of HSV-1 strains Justin and F reported by Locker and Frenkel (37). As demonstrated in Fig. 6, dDNA1 hybridizes to the Kpn I

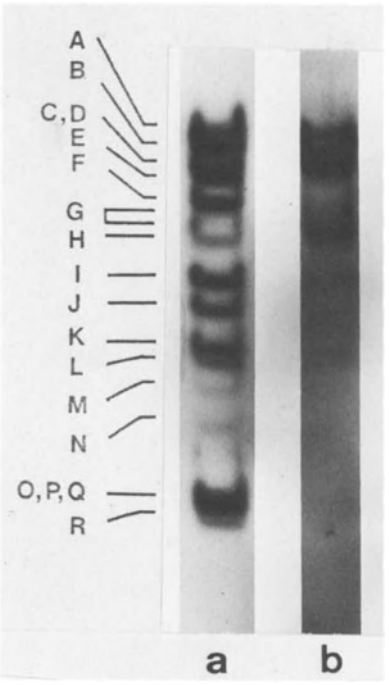

Figure 7
Blot hybridization of a mixture of ^{32}P-labeled dDNA2 and dDNA2* to Hpa I restriction fragments of HSV-1 ANG standard DNA (b). The complete Hpa I restriction pattern of the standard DNA is shown in a.

shows the blot hybridization pattern of these fragments to Hpa I standard DNA fragments. As in the case of dDNA2* (Fig. 3) hybridization occured to Hpa I standard DNA fragments A, C, D, G. In contrast to dDNA2*, however, the probe displayed homology to Hpa I B. This finding supports the assumption that the Eco RI-sensitive defective HSV ANG DNA in addition to the Kpn I-resistant dDNA2* contains another class of molecules, which evidently are Kpn I-sensitive and comprize sequences homologous to Hpa I B being absent in dDNA2*. The latter sequences have not yet been precisely mapped. Possibly the observed hybridization to Hpa I B could be due to sequence homology between TR_S and part of Hpa I B sequences (12). Taking into account the results

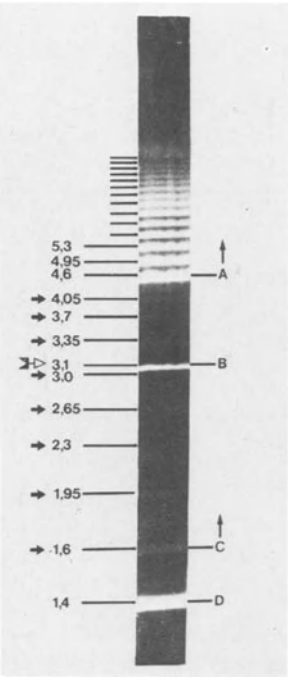

Figure 8

Ethidium bromide stained Kpn I restriction fragments of dDNA1 electrophoretically separated in an 0.5% agarose gel. The numbers represent the molecular weights x 10^6 which were estimated by calibration of the gel with Hind III restriction fragments of λ DNA (38) and SV40 DNA (39) and Hae III restriction fragments of ØX RF DNA (40) as markers. The open and filled arrows at the left side mark the left hand terminal fragment and the series of right hand terminal fragments, respectively.

of restriction enzyme analyses described below, it can be assumed that the repeats of dDNA2 and dDNA2* are closely related to each other and that they map in similar regions of the parental viral genome.

3.3 The structural organization of defective HSV-1 ANG DNA

The Kpn I restriction fragment pattern of dDNA1 is shown in Fig. 8. Besides DNA band D (about 15 molar) of 1.4 x 10^6

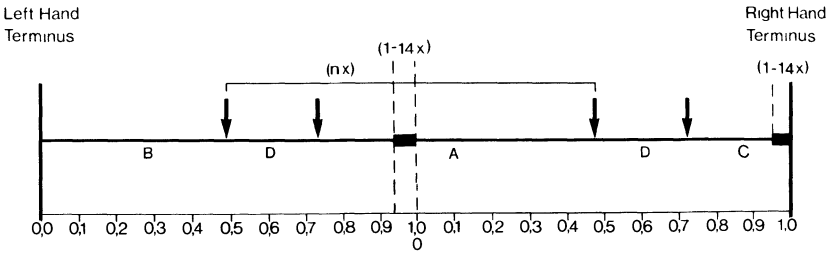

Figure 9

Scale maps of Kpn I cleavage sites on the repeat sequence of HSV-1 ANG dDNA1. The black bars indicate the multiple insertions of the 550 base pairs sequence in the repeats, n, number of complete repeats.

daltons and band B (1 molar) of 3.1 x 10^6 daltons, the pattern displays a major "step ladder" of at least 14 DNA fragment bands A, equidistant in molecular weight by 0.35 x 10^6 daltons. This suggests that the repeat sequence unit of dDNA1 contains multiple insertions of a 550 base pairs' sequence. The smallest fragment of the step ladder has a MW of 4.6 x 10^6 daltons. This step ladder appears to be analoguous to the series of fragment bands representing the S-terminal HSV-1 DNA fragments Eco RI K, Hpa I G, Hind III G and M (Fig. 2), and we assume that the 550 base pairs interspersed in dDNA1 is identical with that found in the S-terminal redundancy of the viral standard genome.

In addition, the fragment pattern in Fig. 8 displays a second minor step ladder of submolar fragments C, which are also equidistant by 0.35 x 10^6 daltons and the molarities of which sum up to approximately 1 M. The molarities of the fragment bands were roughly estimated from their molecular weights and by optical scanning of the stained gel. It was assumed that the fragment B and the C fragment series represent the Kpn I left and right hand terminal fragments of the complete dDNA1 molecules. This assumption would imply that one of the termini does contain the 550

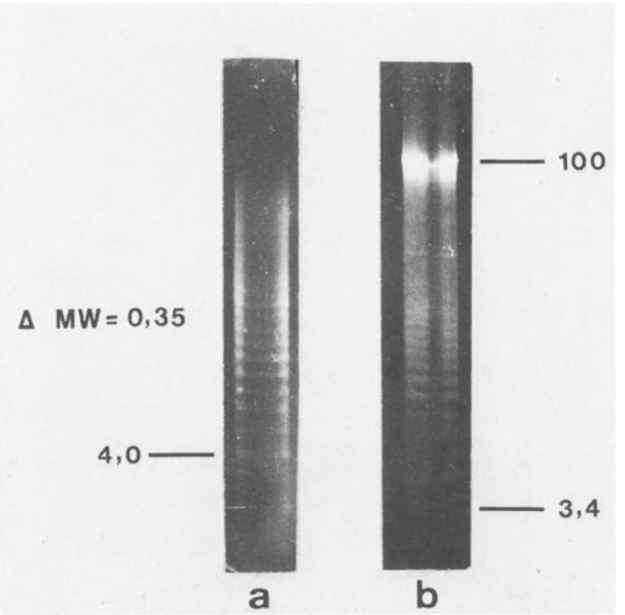

Figure 10

Ethidium bromide-stained Eco RI restriction fragment pattern of dDNA2* (a) and dDNA1 + dDNA2* (b) in a 0.7% agarose gel. The MW's x 10^{-6} of individual fragments are indicated by numbers and were determined by calibration of the gels with Eco RI restriction fragments of λ DNA.

base pair inserts, whereas the other does not. A tentative model of the arrangement of the Kpn I dDNA1 fragments is shown in Fig. 9. The fact that Kpn I creates obviously only two internal fragments (A series and D), suggests a tandem array of the repeat sequence of dDNA1. From the molecular weights of the fragments A and D a value of 6 x 10^6 daltons is calculated for the sequence complexity of the dDNA1 repeats. The precise position of the 550 base pair inserts within the repeats is not yet known. In the map of Fig. 9 they are tentatively placed at the right hand end of the molecules and at the corresponding internal sites.

For structural analysis dDNA2* and a mixture of dDNA1, dDNA2 and dDNA2* were separately digested with Eco RI. The

ethidium bromide stained fragment patterns of the digest obtained by agarose gel electrophoresis are shown in Fig. 10. Both patterns display very similar step ladders of fragment bands which differ in MW by 0.35 x 10^6 daltons suggesting that dDNA2 also contains multiple insertions of the 550 base pair sequence found in the S-redundancy of HSV-1 ANG DNA. No other fragments could be detected in the gels. Whereas the base fragment of the dDNA2* fragment series (Fig. 10a) has a MW of 4 x 10^6, the fragment series obtained from the dDNA2 and dDNA2* mixture starts with a molecular weight of 3.4 x 10^6 daltons (Fig. 10b). The fragment bands of Fig. 10b appear more diffuse as compared to those of Fig. 10a suggesting that they contain DNA fragments of slightly different molecular weights. These phenomena confirm the existence of the two classes of dDNA2 and -2*, the repeat units of which differ by about 900 base pairs. From the above data follow a sequence complexity of 3.4 x 10^6 daltons for dDNA2 and 4.0 x 10^6 daltons for dDNA2*. The band of 100 x 10^6 dalton MW DNA in the pattern of Fig. 10b represents undegraded dDNA1, which was identified by Kpn I digestion (not shown).

Since both, dDNA2 and -2* yield only one type of Eco RI fragment each it is supposed that their repeats contain only Eco RI cleavage site and that the repeats are arranged in tandem arrays.

4. DISCUSSION

HSV-1 ANG is capable of developing defective DNA in independent series of high MOI virus passages. The present study is concerned with two major classes of defective DNA1, both of which consist of tandem repeats of restricted portions of the parental genome. According to the reported data, a minor part of the 6 x 10^6 dalton repeat unit of the Eco RI-resistant dDNA1 consists of sequences stemming

from the S-redundancy TR_S of the standard DNA and mapping right hand of the Eco RI K cleavage site (0.957 units (30)). The bulk of the dDNA1 repeat originated from U_L-sequences and maps between the coordinates 0.368 and 0.413 in the prototype arrangement of the parental genome. Whether or not dDNA1 contains any U_S-sequences is still unknown.

The Kpn I cleavage pattern shown in Fig. 8 suggests that dDNA1 has 2 Kpn I cleavage sites and that the complete dDNA1 molecules have two defined ends. The presented data further suggest that the dDNA1 repeats contain various copy numbers of a 550 base pair sequence which is also multiply inserted in the fragment Eco RI K, i.e. in the terminal redundancy TR_S of standard DNA (13) (Fig. 2).

At the moment we cannot answer the question whether the step ladder of Kpn I A fragments of dDNA1 reflects the existence of 14 different classes of dDNA1 molecules or whether the inserts are distributed at random in all of the dDNA1 molecules. Assuming a rolling circle mechanism involved in the generation of 100 x 10^6 dalton defective DNA molecules from the individual repeat units the latter possibility appears unlikely.

A second major class of defective HSV-1 ANG DNA, in contrast to dDNA1, is Eco RI-sensitive and has a higher buoyant density than standard DNA (13). Similar properties have been reported by Locker and Frenkel (14) and by Graham et al. (11) of defective HSV-1 Justin and Patton DNA. The Eco RI-sensitive HSV-1 ANG dDNA turned out to be heterogeneous with respect to its repeat unit. A 30% fraction (dDNA2*) has no Kpn I cleavage site, whereas about 70% (dDNA2) is sensitive to Kpn I. The Eco RI cleavage patterns of dDNA2 and -2* (Fig. 10) confirmed the heterogeneity of the Eco RI-sensitive dDNA suggesting sequence complexities of 4.0 and 3.4 x 10^6 daltons for dDNA2 and dDNA2*, respectively. Similar heterogeneities have been reported for defective HSV-1 Justin DNA by Locker and Frenkel (11). Similarly to dDNA1 both, dDNA2 and -2*

contain multiple 550 base pair inserts. It is notable that this insert is amplified in the defective HSV-1 ANG DNA to much higher copy numbers than in the S-redundancy of the parental viral genome. No terminal and only one internal fragment could be detected in Eco RI digests of dDNA2 and -2*. This phenomenon could mean that both DNA's have only one Eco RI cleavage site and no defined ends. Cleavage with Eco RI then would create terminal fragments of random size which could not be identified in the patterns.

Both, dDNA2 and -2* evidently do not comprize the complete S-redundancy TR_S (4.3×10^6 daltons). Tentatively, one could assume that its Eco RI cleavage site is identical with the Eco RI K site on the viral standard DNA (map position 0.957). Furthermore the Kpn I cleavage site of dDNA2 could be identical with the Kpn I K site of the parental genome (0.95 map units; 37). It must be concluded that the majority of TR_S-sequences being deleted in dDNA2 and -2* map right hand of the Eco RI cleavage site, i.e. between 0.965 and 1.0 map units of the viral genome. The observed homology of dDNA2 to part of the Hpa I standard DNA fragment B remains to be explained. We tend to assume that there is homology between TR_S-sequences and part of Hpa I B (13) which could be responsible for this finding.

Further investigations including molecular cloning are now in progress in order to accomplish fine mapping and to identify the recombination sites of the repeats of defective HSV-1 ANG DNA. Interesting questions in this connection are the location and the nature of the 550 base pair sequence which with some respect resembles insertion sequences found in prokaryotic DNA.

5. REFERENCES

1. Bronson, D.L., Dressman, G.R., Biswal, N. and Benyesh-Melnick. (1973) Intervirology 1, 141-153.

2. Ben-Porat, T., Demarchi, D.M. and Kaplan, A.S. (1974) Virology 60, 29-37.
3. Wagner, M., Skare, J. and Summers, W.C. (1974) Cold Spring Harbor Symp. Quant. Biol. 39 683-686.
4. Fleckenstein, B., Bornkamm, G.W. and Ludwig, H. (1975) J. Virol. 15, 398-406.
5. Frenkel, N., Jacob, R.J., Honess, R.W., Hayward, G.S., Locker, H. and Roizman, B. (1975) J. Virol. 16, 153-167.
6. Murray, B.K., Biswal, N., Bookout, J.B., Lanford, R.E., Courtney, R.J. and Melnick, J.L. (1975). Intervirology 5, 173-184.
7. Schröder, C.H., Stegmann, B., Lauppe, H.F. and Kaerner, H.C. (1975/76) Intervirology 6, 270-284.
8. Campbell, D.E., Kemp, M.C., Perdue, M.L., Randall, C.C. and Gentry, G.A. (1976). Virology 69, 737-750.
9. Frenkel, N., Locker, H., Batterson, W., Hayward, G.S. and Roizman, B. (1976) J. Virol. 20, 527-531.
10. Stegmann, B., Zentgraf, H., Ott, A. and Schröder, C.H. (1978), Intervirology 10, 228-240.
11. Graham, B.J., Bengali, Z. and Vande Woude, G.F. (1978) J. Virol. 25, 878-887.
12. Ott, A., Föhring, B. and Kaerner, H.C. (1979) J. Virol. 29, 423-430.
13. Kaerner, H.C., Maichle, I.B. and Schröder, C.H. (1979) Nucleic Acids Res 6, 1467-1478.
14. Locker, H. and Frenkel, N. (1979) J. Virol. 29, 1065-1077.
15. Becker, Y., Dym, H. and Sarov, I. (1968). Virology 36, 184-192.
16. Kieff, E.D., Bachenheimer, S.L. and Roizman, B. (1971) J. Virol. 8, 125-132.
17. Wagner, E.K., Tewar, K.K., Kolodner, R. and Warner, R.C. (1974). Virology 57, 436-447.
18. Sheldrick, P. and Berthelot, N. (1974) Cold Spring Harbor Symp. Quant. Biol. 39, 667-678.
19. Grafstrom, R.H., Alwine, J.G., Steinhart, W.L. and Hill, C.W. (1974). Cold Spring Harbor Symp. Quant. Biol. 39, 679-681.
20. Hayward, G.S., Frenkel, N. and Roizman, B. (1975) Proc. Nat. Acad. Sci. USA 72, 1768-1772.
21. Hayward, G.S., Jacob, R.J., Wadsworth, S.C. and Roizman, B. (1975) Proc. Nat. Acad. Sci. USA 72, 4243-4247.
22. Wadsworth, S., Jacob, R.J. and Roizman, B. (1975) J. Virol. 15, 1487-1497.
23. Roizman, B., Hayward, G., Jacob, R., Wadsworth, S., Frenkel, N., Honess, R.W. and Kozak, M. (1975) Oncogenesis and Herpesviruses II, International Agency for Research on Cancer 1, 3-38.
24. Delius, H. and Clements, J.B. (1976). J. Gen. Virol. 33, 125-133.
25. Clements, J.B., Cortini, R. and Wilkie, N.M. (1976) J. Gen. Virol. 30, 243-256.

26. Wilkie, N.M. and Cortini, R. (1976) J. Virol. 20, 211-221.
27. Review: Roizman, B. (1979) Cell 16, 481-494.
28. Wilkie, N.M. (1976) J. Virol. 20, 222-223.
29. Skare, J. and Summers, W.C. (1977) Virology 76, 581-595.
30. Wilkie, N.M., Cortini, R. and Clements, J.B. (1977) J. of Antimicrobiol. Chemotherapy 3 (Suppl. A) 47-62.
31. Buchman, T.G., Roizman, B., Adams, G. and Stover, B.H. (1978) J. Infect. Dis. 138, 488-498.
32. Rigby, P.W.J., Pieckmann, M., Rhodes, C. and Berg, P. (1977). J. Mol. Biol. 113, 237-251.
33. Southern, E.M. (1975). J. Mol. Biol. 93, 503-517.
34. Grafstrom, R.H., Alwine, J.C., Steinhart, J.C., Hill, C.W. and Hyman, R.W. (1975) Virology 67, 144-157.
35. Hyman, R.W., Burke, S. and Kudler, L. (1976) Biochem. Biophys. Res. Comm. 68, 609-615.
36. Wadsworth, S., Hayward, G.S. and Roizman, B. (1976) J. Virol. 17, 503-512.
37. Locker, H. and Frenkel, N. (1979) J. Virol. 32, 429-441.
38. Thomas, M. and Davis, R.W. (1975) J. Mol. Biol. 91, 315-328.
39. Reddy, V.B., Thimappaya, B., Dhar, R., Subramanian, K.N., Zain, B.S., Pan, J., Ghosh, P.K., Celma, M.L. and Weissman, S.M. (1978) Science 200, 454-502.
40. Lee, A.S. and Sinsheimer, R.L. (1974) Proc. Nat. Acad. Sci. USA 71, 2882-2886.

10. Structure and expression of class I and II defective interfering HSV genomes

Niza Frenkel*, Hilla Locker and Don Vlazny

INTRODUCTION

The serial undiluted propagation of herpes simplex viruses results in the accumulation of defective virus particles containing altered viral genomes. Previous analyses of the structure of such defective HSV genomes have shown that they consist of multiple reiterations of sequences corresponding to limited subsets of the parental non-defective HSV DNA (3, 9, 10, 12, 18, 22, 25, 32, and 39). Furthermore, certain passages of the virus populations that were propagated undiluted have been shown to interfere with the replication of non-defective virus, and to exhibit characteristic changes in the pattern of viral polypeptide synthesis in the infected cells (2, 3, 9, 18, 25, 33, and 36).

In the present communication, we have attempted to review our previous and ongoing studies concerning several HSV populations that were propagated undiluted. The objectives of these studies were several. Firstly, by characterizing the structure of defective genomes present in a number of independently derived serially propagated virus populations we wished to identify the basic structural features which are common to defective HSV genomes. Secondly, by studying aspects of defective genome replication, we hoped to define specific determinants which operate in the selection of those HSV variants which become abundant in the course of undiluted virus propagation. Thirdly, by studying the pattern of polypeptide synthesis in serially passaged virus infected cells, we wished to determine the effect of viral gene reiteration on viral gene expression. Finally, by correlating the extent of interference exhibited by various defective virus populations with other

Y. Becker (ed), Herpesvirus DNA.

changes in viral gene expression, we wished to characterize the mechanism(s) underlying the capacity of the defective genomes to interfere with the replication of their non-defective counterparts.

Derivation of the Serially Passaged Virus Stocks

Virus stocks of HSV-1 (Justin) and HSV-2 (G), both representing wild type genital isolates, and of the temperature sensitive mutant LB2 (tsLB2), derived by I. Halliburton from the HFEM strain of HSV-1 (13), were continuously propagated in 1:4 dilution (starting from plaque purified virus stocks), to generate the three series shown in Figure 1. As seen in the figure, the yields of infectious virus in the three series followed a characteristic cyclic pattern, reflecting the dynamic competitive balance between defective interfering particles and the wild type helper virus. Additional defective genomes contained in virus populations of HSV-1 (KOS) have been only partly characterized, and consisted of separate virus stocks propagated from different plaque isolates of that HSV strain.

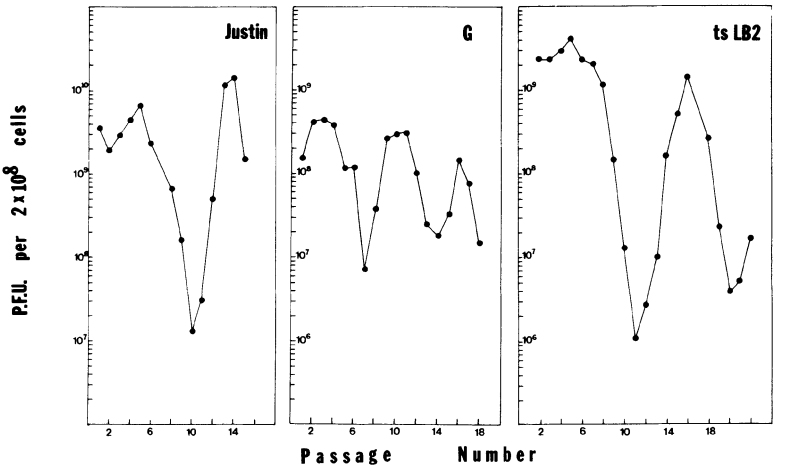

Figure 1--Yields of infectious virus produced in the course of serial propagation of undiluted stocks of HSV-1 (Justin), HSV-2 (G) and tsLB2 of HSV-1 (HFEM) (13). Initial stocks of each virus were prepared following three sequential plaque purifications. Each of the passages was derived by 24-hour infection (at 34°C) with 1/4 of the virus yield from the former passage (9). The total yields of infectious virus are shown per cultures containing 2x10^8 cells.

The Structure of the Variant Genomes

Restriction enzyme analyses of DNA prepared from various passages of the Justin, G and tsLB2 series revealed the presence of variant DNA molecules with altered cleavage patterns. In each case, the variant DNA could be separated from the helper virus non-defective DNA by its resistance to a number of restriction endonucleases. Examples of our analyses of the structure of the purified variant DNA molecules are shown in Figure 2 for the HSV-1 (Justin)

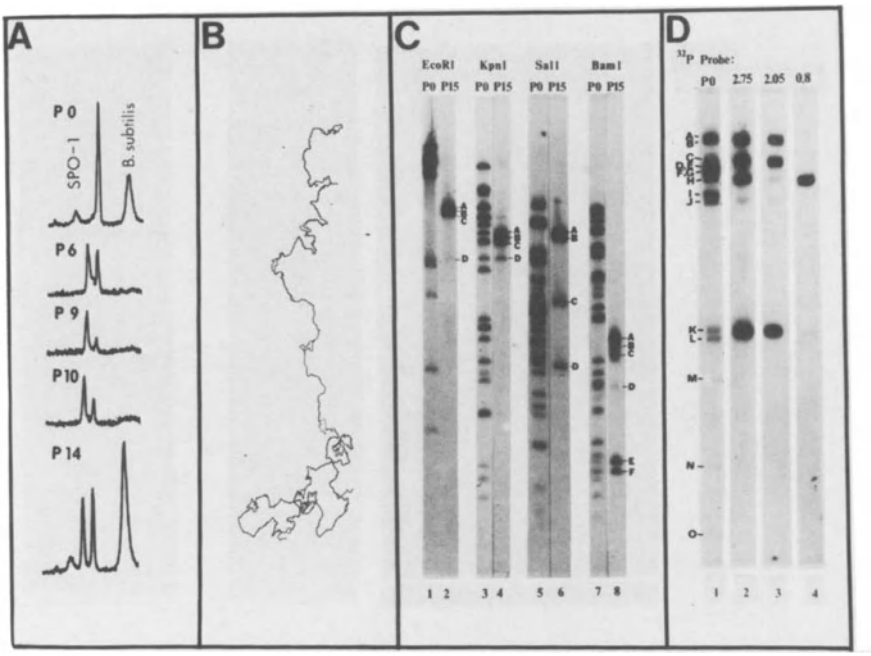

Figure 2--Examples of the analyses employed in the characterization of the structure and origin of defective virus genomes. A. CsCl equilibrium density centrifugations of viral DNA prepared from cells infected with different Justin passages (R. Jacob, reference 9). Note the appearance of the heavy density defective DNA species (1.732 gr/cm^3 as compared to 1.726 gr/cm^3 of P0 DNA). B. Partial denaturation mapping of HindIII resistant defective virus DNA (R. Jacob, see reference 9). Note the regular organization of repeat units defined by a small AT rich bubble and an undenatured segment of G+C rich DNA sequences. C. Restriction enzyme patterns of heavy density, HindIII resistant DNA (P15) as compared to digests of plaque purified DNA (P0). Data from reference 22. D. Hybridizations of restriction enzyme probes (in this example BamI/SalI fragments) from purified defective Justin DNA to Southern blots (35) containing fragments (EcoRI) of P0 DNA. Data from reference 22.

defective genomes. These analyses included equilibrium density centrifugations, partial denaturation mapping, restriction enzyme cleavages and Southern blot (15) hybridizations. Figures 3-5 summarize the information obtained from these analyses, concerning the structural organization of the most abundant species of defective virus genomes present in the Justin, G and tsLB2 series (9, 22 and H. Locker, N. Frenkel and I. Halliburton, manuscript in preparation). The salient features of these results are the following:

(i) The defective genomes in the Justin, G and tsLB2 series are all composed of multiple head-to-tail reiterations of DNA sequences of relatively low complexity. This head-to-tail repeat organization is characteristic also of defective HSV genomes studied by other investigators and generated from different HSV strains (12 and 18).

(ii) The serially passaged virus stocks of the Justin, G and tsLB2 series each contains a mixture of variant DNA molecules composed of different sized repeat units. The heterogeneity in repeat unit size reflects mostly the fact that the larger repeat units contain sequences in addition to those present in the smaller repeat units. These additional sequences of the larger repeat units are in all cases directly contiguous with the wild type viral DNA sequences contained in the smaller repeat units.

(iii) Comparisons of defective genome composition in various passages of the Justin, G and tsLB2 series have shown that the different size repeat units (displayed in Figures 3-5) are present even in early passages of the series and remain stable throughout the passaging, although their relative proportions fluctuate during the serial undiluted propagation.

(iv) On the basis of the origin of DNA sequences contained within their repeat units, the defective HSV genomes can be generally divided into two classes. Class I defective genomes contain reiterations of sequences arising either exclusively from or in direct continuity with either end of the S component of the parental DNA. Because these regions of the HSV DNA are of relatively high G+C content

(14), defective genomes of this type display a buoyant density which is higher than that of the standard helper virus DNA. In the class I category are those defective genomes of the Justin and G series, whose structure and origin are shown in Figures 3 and 4. Specifically, the majority of the defective genomes contained in the Justin

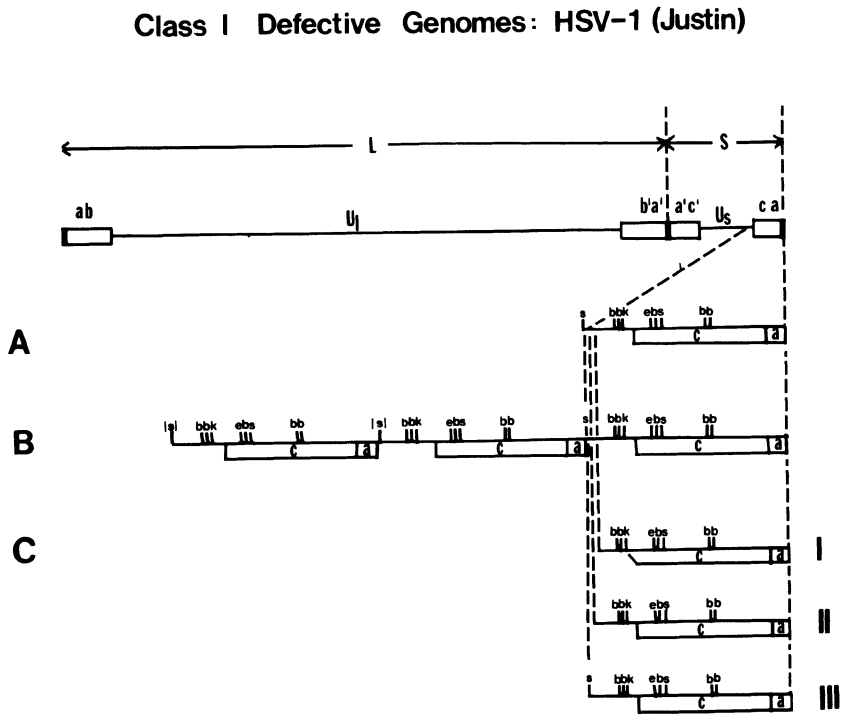

Figure 3--The structure of defective Justin genomes. Top: schematic representation of standard HSV DNA. A. Arrangement of the BamI (b), EcoRI (e), SalI (s) and KpnI (k) sites within map coordinates 0.94-1.00 of standard HSV-1 (Justin) DNA. B. The repeat units are reiterated in head to tail fashion within the defective genomes. Repeat unit DNA sequences are derived from the end of S of the parental HSV DNA as judged by colinearity of restriction enzyme sites and by hybridization experiments. I, II and III represent three types of repeat units (sizes 5.38, 5.48 and 5.58x10^6, respectively), differing only with respect to the amount of U_S sequences which they contain. The SalI site at map coordinate 0.944 is present only in the repeat unit III. Data from reference 22.

series consist of three types of repeat units of molecular weights 5.38, 5.48 or 5.58x10^6 (a minority of the variant DNA molecules consist of repeat units of intermediate sizes between 5.3 and 5.8x10^6). These different sized repeat units appear to be segregated into separate DNA molecules, with only limited degree of intermixing between different repeat units within the same DNA molecule. All three major repeat units contain sequences derived from the right hand end of the S component, within map coordinates 0.94-1.00 of

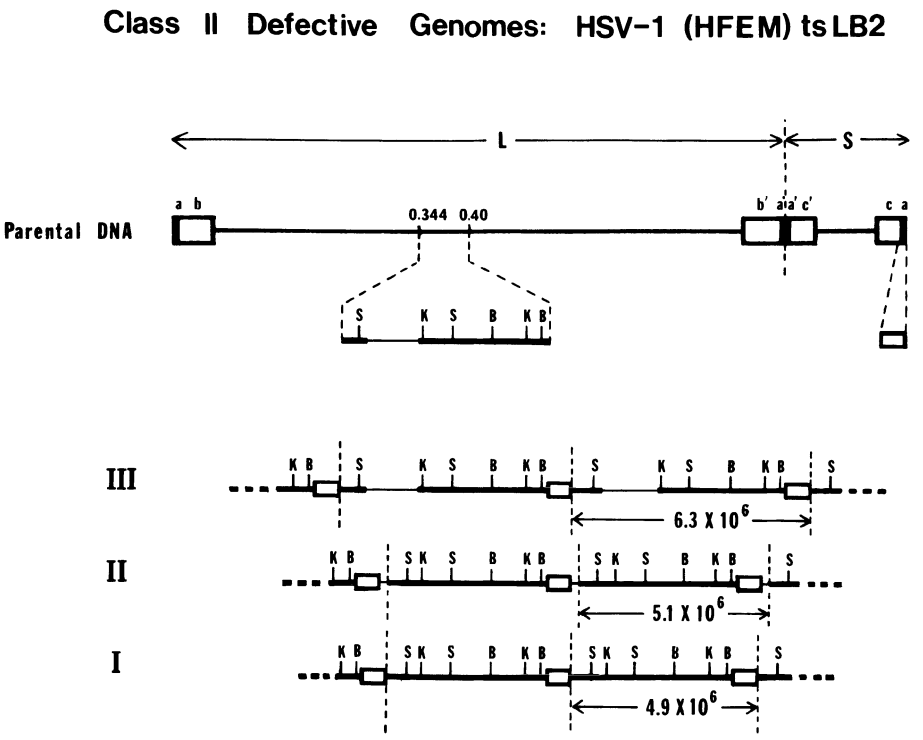

Figure 5--The structure of defective genomes in the tsLB2 series. Top: schematic representation of the parental DNA, showing the arrangement of the BamI (B), KpnI (K) and SalI (S) restriction enzyme sites within the U_L sequences bounded by map coordinates 0.34 to 0.40. I, II and III represent different sized repeat units. The majority of molecules contain the 4.9x10^6 repeats. The U_L sequences represented by thinner lines in repeat units II and III are deleted in repeat unit I and II. The portion of ac sequences, which is present in the defective genomes is estimated to be of 0.5x10^6 complexity as evidenced by blot hybridization experiments. Data from H. Locker, N. Frenkel and I. Halliburton, manuscript in preparation.

the parental HSV DNA. Thus, repeat units of HSV-1 (Justin) contain the entire S inverted repeat ac (29, 34 and 38) region and variable proportions of the U_S sequences directly adjacent to the inverted repeat sequences. The defective genomes which are contained in cytoplasmic or purified virion DNA preparations actually terminate at one end with the S terminus of the parental DNA, while at their other end they seem to terminate at random locations within

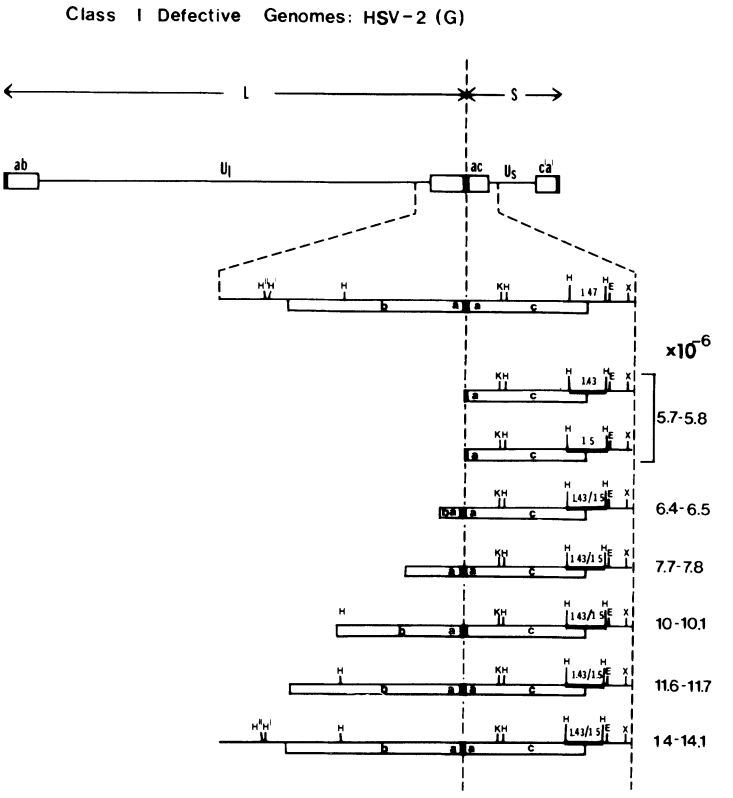

Figure 4--The structure of HSV-2 (G) defective genomes. Top: schematic representation of the standard HSV DNA, showing arrangement of the XbaI (X), EcoRI (E), HincII (H), KpnI (K), HpaI (H') and HindIII (H") restriction enzyme sites within the S-L junction region of HSV-2 (G) DNA displayed in the I_S orientation. Bottom: the repeat units of HSV-2 (G) defective genomes, ranging in size from 5.7 to 14.1x10^6, and containing DNA sequences, the majority of which are colinear with the S-L junction region of the standard HSV-2 (G) DNA (in either the I_S or the I_{SL} orientations). Repeat units of all size classes contain either a HincII fragment of size 1.43x10^6, or a HincII fragment of 1.5x10^6 in place of the original 1.47x10^6 HincII fragment of the standard DNA. Data from N. Frenkel and H. Locker (unpublished results).

their last repeat units, yielding a total size which is indistinguishable from that of parental non-defective viral DNA.

The majority of the serially passaged HSV-2 (G) defective genomes consist of at least 6 different classes of repeat units ranging in size from 5.7 to 14.1×10^6. These repeat units differ from those in the Justin series in three respects. First, whereas the smallest (and most abundant) repeat units of the G defective genomes (m.w. 5.7×10^6) resemble the HSV-1 (Justin) repeat units in that they contain predominantly sequences from the right end of the S component, all larger repeat units in the HSV-2 (G) populations contain additional sequences derived from the S-L junctions when displayed in either the I_S or I_{SL} (6, 14 and 29) orientations. Thus, in addition to ac and U_S sequences, these larger repeat units contain increasing segments of the L inverted repeat-ab-region and the U_L sequences adjacent to the L inverted repeat. Second, the sequences contained within each of the different sized repeat units are not entirely colinear with the corresponding sequences of the parental DNA, but rather contain small and discrete deletions or deletion/substitutions in a single defined location within the S inverted repeat portions shared by all the repeat units. Thus, repeat units of each size class contain either a HincII fragment of molecular weight 1.50×10^6, or a fragment of molecular weight 1.43×10^6, in place of the parental HincII fragment of size 1.47×10^6, spanning map coordinates 0.951 to 0.965 (see Figure 4). Finally, each of the classes of repeat units larger than 5.7×10^6 contains several subspecies differing in the number of the terminal reiteration-a sequences which they contain. In this respect, the defective genome repeat units of HSV-2 (G) which span the S-L junctions possess the same type of variability described previously for the S-L junctions of the non-defective HSV DNA (21 and 40).

In addition to the class I defective genomes present in the Justin and G series, our recent analyses of an additional series derived from HSV-1 (KOS) have revealed the presence of defective genomes arising from the left end of

S in the P/I_S orientations (A. Kwong and N. Frenkel, unpublished results). It is noteworthy that the defective genomes of HSV-1 (Patton) studied by Graham et al.(12) are also of the class I type. Furthermore, the appearance of high density variant DNA molecules characteristic of class I defective genomes has been reported for eight additional strains of HSV-1 and HSV-2 (KOS, 13, HF, SA, ANG, 307, 333 and 186, references 1, 3, 18, 25 and 39).

The class II defective genomes contain DNA sequences derived from two non-contiguous regions of the parental DNA, within the S and L components. Such class II defective genomes are shown in Figure 5 for the tsLB2 series (H. Locker, N. Frenkel and I Halliburton, manuscript in preparation). As seen in the figure, the serially passaged tsLB2 populations contain defective virus DNA molecules consisting of three major types of repeat units of sizes 4.9, 5.1 and 6.3×10^6. Unlike their Justin or G counterparts, each of these three types of tsLB2 repeat units contain DNA sequences approximately 0.5×10^6 in molecular weight from the end of S (within map coordinates 0.99 to 1.00) covalently linked to DNA sequences from U_L within map coordinates 0.34-0.40. Whereas the 6.3×10^6 repeat units consist of sequences which are entirely colinear with the corresponding U_L region of the parental DNA, the two smaller major repeat units contain one (in the 5.1×10^6 repeat units) or two (in the 4.9×10^6 repeat units) discrete deletions within the U_L sequences of the repeat units. Similar defective genomes consisting of covalently linked U_L and S sequences also occur in several HSV-1 (KOS) populations which we have studied (A. Kwong and N. Frenkel, unpublished results), and in several HSV-1 (Patton) series derived by Murray et al. (25) and recently analyzed by us (L.P. Deiss, N. Frenkel and B.K. Murray, unpublished results) for their content of defective viral DNA. Defective genomes of the class II structure have been previously shown to occur in the HSV-1 (ANG) series derived by Kaerner and coworkers (18 and 32), and in HSV-1 (MP) series derived by Hayward and coworkers (G.S. Hayward, personal communication).

It is noteworthy that both classes (I and II) of defective genomes can be generated upon parallel propagation of separate series from a given HSV strain. Thus, the parallel passaging of separate series from the HSV-1 strain ANG by Kaerner and coworkers (18) and from the HSV-1 strain KOS (A. Kwong and N. Frenkel, unpublished observations) resulted in each case in the generation of separate series containing either class I or class II defective genomes.

Studies of Defective Genome Replication

This section describes our ongoing studies concerning the replication of defective HSV genomes. These studies are of interest for two reasons. First, it is possible that the specific pattern of development of any given series, as regards the types of defective genomes which it contains could be explained in terms of the relative ability of the defective genomes which become abundant in the population to replicate and become and become propagated in cells which are coinfected with standard helper virus. Second, by analogy with other virus systems (reviewed in 7, 17 and 19) we expect that the replication and packaging of defective genomes would involve at least a subset of the same trans (enzymes and factors) and cis (recognition sites such as origins) functions operating in the replication and packaging of the wild type HSV genomes. Thus, the studies of the localization and nature of replication functions within the defective genomes are of potential interest, especially in view of the fact that studies designed to identify replication origin(s) within the standard HSV DNA, and to elucidate the structure of HSV DNA replicative intermediates, have been complicated by the complex structural organization of the wild type standard virus DNA (for review, see reference 29).

One can envision two distinct routes for the replication and propagation of defective viral genomes in serially passaged HSV populations containing mixtures of defective and non-defective particles. First, they could be replicated as autonomous units without physical association with the non-defective helper virus DNA, albeit using the trans-replication/propagation functions (enzymes, structural polypeptides) encoded by the standard helper HSV DNA.

Alternatively, defective HSV genomes could become covalently associated with helper virus non-defective DNA, yielding defective virus-helper recombinant DNA molecules which are replicated and matured using cis recognition signals located within the helper virus DNA sequences. Such a mechanism might operate in the replication of pseudorabies defective genomes (T. Ben-Porat, personal communication).

Our recent studies of the replication of the Justin defective virus genomes strongly support the hypothesis that at least the class I defective genomes can be autono-

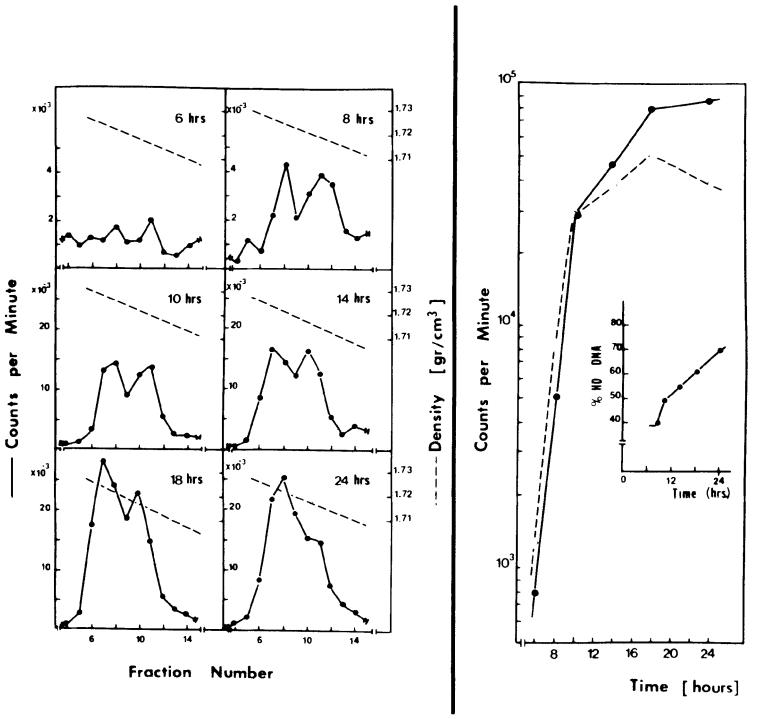

Figure 6--Time course of replication of defective HSV-1 (Justin) genomes. Replicate cultures were infected with Justin P15, labeled from 2 hours post infection with H^3-thymidine and harvested at the times shown. Following lysis and proteinase K digestion the cell lysates were centrifuged to equilibrium in CsCl. The portions of the gradients shown at the left represent the regions of the gradients containing HSV DNA. The buoyant densities were estimated from the refractive indices, and are in slight error due to the presence of SDS in the gradients. The left and right peaks in each gradient represent heavy (defective) and light (helper) virus DNA as judged by restriction enzymes. On the right, distribution of counts in heavy (—•—) and light ( ) viral DNA as determined from the corresponding gradients shown on the left. Data from D. Vlazny and N. Frenkel, manuscript in preparation.

mously replicated and propagated in cells infected with non-defective helper HSV. These conclusions rest on three lines of evidence. First, analyses of the time course of defective genome replication in cells infected with passage 15 (P15) Justin virus (Figure 6) have shown that the initial rate of variant DNA synthesis paralleled that of the helper virus DNA. However, variant DNA molecules continued to replicate at later time intervals in which the replication of the non-defective standard virus DNA had already been completed (R. Jacob, unpublished results, and D. Vlazny and N. Frenkel, manuscript in preparation). Thus, the defective Justin genomes seem to replicate as autonomous units, without linear dependence on the replication of helper virus genomes.

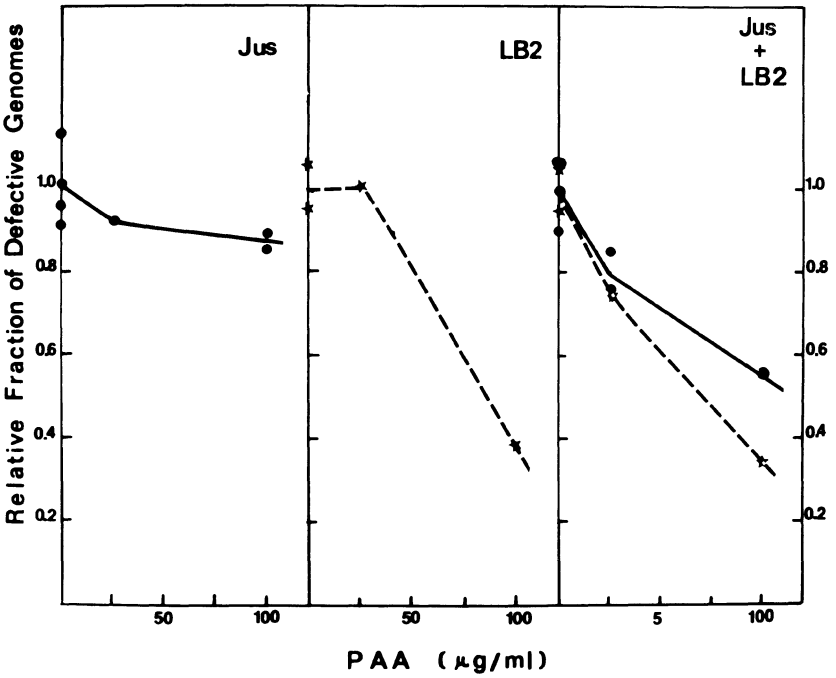

Figure 7--Effect of phosphonoacetate on replication of Justin and tsLB2 defective genomes. Replicate cultures were infected with 1 PFU/cell of P15 Justin (‹), 1 PFU/cell of P17 tsLB2 (‹) or a mixture of both, in the presence of 0, 25 or 100 µg of PAA per ml (23). The fractions of defective DNA of the Justin and tsLB2 types were estimated by restriction enzyme analyses and are shown relative to the fractions of the corresponding defective genomes in the absence of the drug. These plots represent one of two independent experiments, both of which yielded similar results. Data from D. Vlazny and N. Frenkel (unpublished).

Second, the replication of the defective Justin and tsLB2 variant DNA molecules is sensitive to phosphonoacetate (PAA) at concentrations which have been shown (23) to selectively inhibit the HSV specified DNA polymerase (Figure 7, D. Vlazny and N. Frenkel, unpublished observations). Thus, the replication of both class I and class II defective HSV genomes seems to involve the viral specified DNA polymerase. It is noteworthy that the PAA dose dependence curve (see Figure 7) for the Justin defective genome replication was found to be indistinguishable from that of the non-defective helper virus DNA replication (i.e., the ratio of defective to helper virus DNA was unaffected by increasing concentrations of the drug). However, the drug preferentially inhibited the replication of tsLB2 defective genomes (i.e., the ratio between defective to helper tsLB2 virus was greatly diminished at increasing PAA concentrations, between 20-100 μg/ml).

Thirdly, individual Justin defective repeat units (size $5.3\text{-}5.6\times10^6$) can give rise to multimeric DNA molecules (size 100×10^6) which are successfully propagated in serially passaged virus populations. This conclusion is based on the results of a series of experiments (D. Vlazny and N. Frenkel, manuscript in preparation) involving transfection of cells with mixtures of helper virus DNA and individual defective Justin genome repeat units which were prepared by EcoRI cleavage of purified defective virus DNA. Analyses of the viral DNA present in derivative stocks from these transfections (Figure 8) have revealed that:

(i) The EcoRI cleaved individual repeat units, as well as slightly shortened repeat units trimmed at both EcoRI cleaved ends, were capable of autonomous replication, generating progeny defective genomes which were either indistinguishable from the defective genomes in the original Justin series or contained small discrete deletions in the region of the repeat units flanking the EcoRI site.

(ii) The repeat units within the progeny defective genomes were organized in a head-to-tail fashion similar to the defective genomes in the original Justin series.

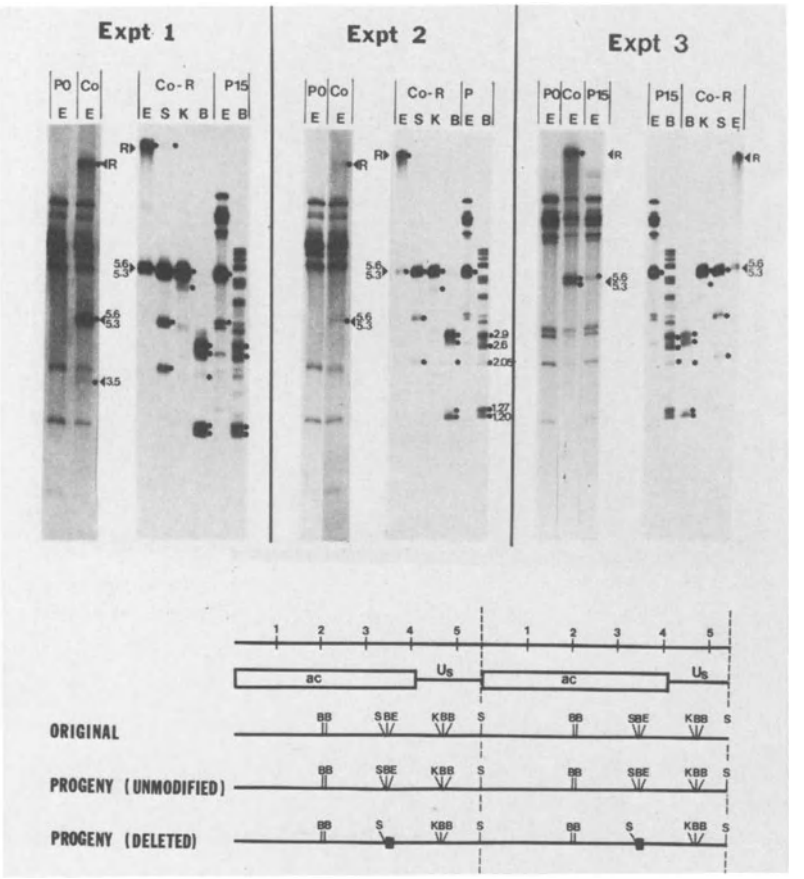

Figure 8--Cis replication functions within the Justin defective genomes. Cells were cotransfected with mixtures of helper virus DNA and EcoRI cleaved defective Justin repeat units (Co) or with helper virus DNA alone (P0). Viral DNA extracted from derivative stocks was analyzed by cleavage with EcoRI (E), SalI (S), KpnI (K) or BamI (B) enzymes. In experiments 1 and 2 the helper virus DNA was from HSV-1 (F). In experiment 3, the helper virus DNA was from HSV-1 (Justin). Co-R represents purified (BglII resistant) defective virus DNA prepared from the cotransfected stock. P15 represents DNA from the original Justin series. The minor fragments EcoRI 3.5, BamI 2.05 and KpnI 4.7x10^6 represent the ends (as judged by exoIII digestion) of progeny defective DNA molecules and correspond to S end fragments of P0 Justin DNA. Bottom: the structure of unmodified (EcoRI sensitive) and deleted (EcoRI resistant) progeny DNA repeat units. The majority of the progeny defective DNA molecules (of size 100x10^6) are either entirely EcoRI resistant or are cleaved by EcoRI to monomeric repeat units (5.3-5.6x10^6), indicating that the bulk of the EcoRI resistant and EcoRI sensitive repeat units are segregated in separate DNA molecules. Data from D. Vlazny and N. Frenkel, manuscript in preparation.

Furthermore, the various types of repeat units were clearly segregated in separate $100x10^6$ molecules with only a minimal degree of intermixing of different type repeat units within individual defective virus DNA molecules. This observation showed that the elongation of the input repeat units into concatemeric structures occurred by amplification of single monomeric repeat units, rather than by recombinations between separate repeat units.

(iii) Comparison of the size distribution of the variant DNA molecules in the cytoplasmic and nuclear fractions of the infected cells (data not shown) revealed that molecules approximating $100x10^6$ daltons in overall size were preferentially selected for (or by) encapsidation among a wide range of sizes of nucleus-associated defective viral DNA molecules. Furthermore, the progeny defective virus DNA resembled the original serially passaged Justin defective genomes in that they uniformly terminated at one end with the original S terminus of the parental Justin DNA.

Models for the Replication of Defective HSV Genomes

The observations reported above have several implications with regard to the replication of both defective and non-defective HSV DNA. First, our results strongly support the hypothesis that defective HSV genomes are replicated by a rolling circle mechanism and therefore that HSV infected cells must contain the enzymatic and structural functions necessary to support this type of replication. In support of a rolling circle replication mode are: (i) the uniform head-to-tail reiterated structure of the defective HSV genomes and (ii) the observation that individual repeat units are capable of replicating into long head-to-tail concatemers. In this light it is noteworthy that Becker et al. (1) have proposed on the basis of electron microscopy studies that defective HSV-1 (HF) genomes are replicated by a rolling circle mechanism. Second, our results suggest that the replicating units of the defective genomes (i.e. the rolling circles) correspond at least predominantly to monomeric repeat units. Evidence for this hypothesis comes from the observation that various

types of repeat units within given virus populations are segregated into separate molecules even following prolonged serial passaging. If the defective genomes were replicated as multimers (i.e. several repeat units forming the replicating circle), one would expect that ongoing recombinations between DNA molecules composed of different sized repeat units would result in the accumulation of progeny DNA molecules, containing tandem arrays of different sized repeat units. However, if the replicative circles consist of single repeat units, recombinants consisting of mixtures of repeat units will be dissociated into individual repeat units in each round of replication and will not be amplified. The nature of the intramolecular recombinational event leading to the regeneration of circular single repeat units is unclear. However, it might involve the regions which are variable between the various repeat units (e.g. the U_S sequences located at the ends of the Justin repeat units I, II and III, Figure 3), thus providing a possible explanation to the variability in repeat unit sizes. Thirdly, our data reveal the operation of two specific mechanisms in the maturation and/or packaging of the progeny defective DNA molecules. The first involves the recognition of the S end sequences either for processing or for packaging of large concatemeric structures of viral DNA. The second involves a size requirement resulting in the preferential packaging of unit length (100×10^6 in size) progeny viral DNA. In this regard, it is noteworthy that a model proposed by Roizman et al. (29 and 30) for wild type HSV DNA replication involved a rolling circle replicative intermediate and the processing of the resultant concatemers via differential cutting at specific recognition sites.

Models for the Evolution of Defective Genomes

One can envision two mechanisms underlying the selective pattern of sequence incorporation into the serially passaged HSV defective genomes. First, it is possible that the intramolecular recombinational events leading to the formation of both the class I and class II defective genomes are of higher probability than recombinational events leading

to other types of rearrangements. Support for this hypothesis comes from the finding that a separate series derived from HSV-1 (KOS) (A. Kwong and N. Frenkel, unpublished results), contains class II defective genomes which resemble those present in the tsLB2 series, despite the fact that the generation of the tsLB2 repeat units had to involve intramolecular recombinational events (see Figure 5). Second, the limited diversity of the defective HSV genomes most likely reflects the selection of those variant DNA molecules which possess preferential advantage in replication. This last hypothesis is supported by: (i) the rapid accumulation of defective genomes in the course of the serial passaging, (ii) the observation that defective genomes continue to replicate at late intervals post-infection, in which the replication of wild type helper virus DNA has already slowed down, and (iii) the experiments showing that defective HSV-1 (Justin) repeat units contain a sufficient set of cis replication functions.

Because class I and class II defective genomes share the DNA sequences originating from the very end of S (within map coordinates 0.995-1.00) it is possible that both the replication origin and the processing/packaging signal are located within these common DNA sequences. Such a model, however, would fail to explain the selective forces operating in the incorporation of the U_L sequences (map coordinates 0.344-0.40) within class II defective genomes. Furthermore, the experiments discussed above have revealed differences in the sensitivity of class I and class II defective genome replication to PAA. Thus, it is possible that the U_L sequences of class II defective genomes contain a separate origin for replication and that the covalent interaction between the U_L sequences containing this second origin and the DNA sequences at the end of S which are required for processing and/or packaging, could result in a "viable" repeat unit which could be replicated and successfully propagated in the presence of helper virus genomes. In this respect it is noteworthy that electron microscopy studies by Friedmann et al. (11), of unit length linear replicating HSV DNA

have indicated the presence of three possible replication origins, located at approximately 0, 10 and 18 μm away from either end of the molecule. If the two sites at 0 and 10 μm are located in the S end of the DNA, they would map within the inverted repeat of S and could thus correspond to the replication origin within the class I defective genomes. Furthermore, if the third site is located 18 μm away from the left end of the P/I_S orientations, it would correspond to the putative initiation site located within the U_L sequences of the tsLB2 defective genomes.

A final point in this discussion concerns the evolutionary pattern of the serially passaged virus populations with respect to the types of defective genomes which they contain. As noted above, the parallel passaging of different series from the ANG (18) and KOS (A. Kwong and N. Frenkel, unpublished observations) strains resulted in the evolution of both classes of defective genomes. If additional HSV strains are capable of generating both classes of defective genomes the limited span as well as the notable lack of drift in the composition of defective genomes in a given series must necessarily reflect an imbalance between low rates of de novo generation as compared to high rates of defective genome replication and propagation. Thus, if the generation (from parental helper virus DNA) of replicatable monomers is a relatively (rate-limiting) event, one could predict that the progeny of the "first" generated repeat unit (as well as deleted versions derived from it), will reach substantial proportions in the population prior to the de novo generation of "secondary" types of monomeric repeat units. In contrast, the proportion of these later independently evolving species of defective genomes is expected to remain low in the population due to the competition for limited factors in the replication machinery exerted by multiple copies of the previously formed defective genomes, each containing a battery of approximately twenty origins for replication. Thus, whether a series will contain class I, class II, or both classes of the defective genomes would depend solely on the exact nature of the first recombinational event(s) leading to the formation of a "viable" (containing replication cis functions) repeat unit.

The Expression of Defective HSV Genomes

The presence of defective HSV particles in serially passaged virus populations has been shown to result in significant alterations in the pattern of viral gene expression in the infected cells and in concomitant interference with the replication of non-defective virus (2, 3, 9, 18, 25, 33 and 36). Interest in the studies concerning the biologic expression of the serially passaged HSV populations is two-fold. First, because the defective genomes which are present in the serially passaged virus populations consist of reiterated sequences of low complexity, the comparative analyses of viral gene expression in cells infected with different virus populations containing variable ratios of defective to standard viral genomes could shed light on the effect(s) of alterations in the dosage of specific viral genes on the overall pattern of viral gene expression. Second, despite the fact that the occurrence of defective herpes simplex viruses in natural human infections has not yet been studied, defective genomes of other viruses have been implicated in the modulation of virus production in the course of persistent animal infections (16 and 17). Furthermore, studies with other herpesviruses have clearly shown that defective genomic variants of herpesviruses could indeed evolve in the course of in vivo passaging (4 and 8) and that infections of cell cultures with defective virus stocks could lead under certain conditions to higher cell survival (26, 31 and 33) and the establishment of tissue culture persistent infections coupled with cell transformation (26). In addition, recent studies involving innoculation of laboratory animals with HSV stocks containing defective particles have revealed significant changes in the pattern of these animal infections, including changes in the killing doses (S.S. Zenda and B.K. Murray, manuscript submitted). It is therefore of great interest to assess the dependence of the interference phenomenon, exhibited in tissue culture infected cells, on particular structural features of viral DNA contained in serially passaged virus populations. The results of our studies concerning the biologic properties of serially passaged HSV populations are summarized below. For the sake of simplicity, we shall

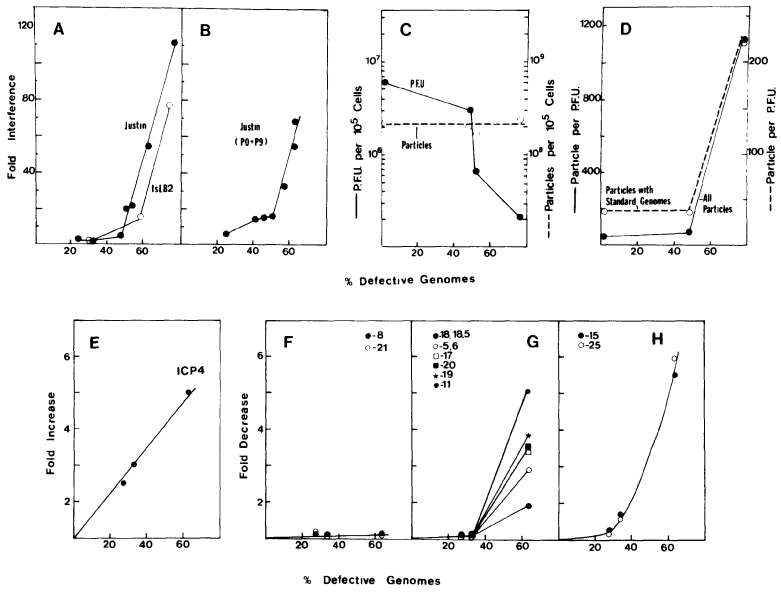

Figure 9--Dependence of viral gene expression on the fraction of defective genomes. A: Fold interference represents fold reduction in infectious virus produced in the course of 24 hr. infection with various passages as compared to virus yield in P0 infected cells. Interference is plotted against the fraction of defective genomes in viral DNA extracted from cells following 24 hours infection with the corresponding passages. B: same as in A above, except that various mixtures of P0 and P9 Justin were used as virus innoculum. C: infectious virus (PFU) and particles produced per culture during infections with 10 PFU/cell of Justin passages. The number of particles was calculated by multiplying the yield (PFU) per culture by the particle to PFU ratio characteristic of that passage. D: particle to PFU ratios for "all particles" (—●—) were obtained by parallel titration and EM particle counts performed on purified virion preparations. The ratios of particle to PFU for particles with standard genomes (-○-) were calculated by multiplying the particle to PFU by the fraction of standard virus DNA in that passage. E-H: change in specific ICP synthesis in cells infected with various Justin passages as compared to ICP synthesis in cells infected with P0 Justin (all at 2 PFU/cell). Infected cells were labeled with C^{14} amino acids during four intervals (1-3, 5-7, 9-11, 13-15 hours) and the ICPs were resolved in SDS polyacrylamide gels. The cumulative radioactivity for each ICP during the four labeling intervals in cells infected with the Justin passages was compared to that of the corresponding ICPs in P0 infected cells. Data from reference 9 and H. Locker and N. Frenkel, manuscript in preparation.

first review our studies related to viral gene expression in cells infected with class I defective virus populations. These results will be contrasted with data obtained from similar studies of class II defective HSV populations. Finally, we shall discuss more general aspects of viral gene expression in the serially passaged virus infected cells.

Biologic Properties of Virus Populations Containing Class I Defective Virus Genomes

Our studies concerning the biologic properties of class I defective virus populations were performed with several passages of the main Justin series as well as "side" passages derived from the original "backbone" of the series by three additional passages (in order to produce sufficiently large virus stocks for the studies below). Infections of cells with these various virus populations resulted in the production of characteristic but variable proportions of defective genomes (ranging from 27% in the lowest case to 78% in the highest case), all possessing the structural features shown in Figure 3. The results of these comparative analyses (9, 20 and H. Locker and N. Frenkel, manuscript in preparation) can be summarized as follows:

(i) We have analyzed the capacity of the various Justin passages to interfere with wild type virus replication, by determining the yields of infectious virus produced in the course of infections with equal PFU/cell (5-10) of the various passages. Figure 9, panel A shows a plot of the extent of interference exhibited by the various passages as a function of the fraction of defective genomes produced in the course of infections with these passages. As seen in the figure, the resultant curves show a biphasic dependence of interference on the proportion of defective virus genomes. Thus, in the first portion of the curve (e.g. below the threshold level of 50% defective Justin genomes) changes in the fraction of defective genomes resulted in relatively limited changes in the capacity to interfere with infectious virus production.

However, in the second part of the curve (above 50% defective genomes) even a small increase in the proportion of defective virus DNA resulted in a dramatic rise in the interference capacity.

(ii) A similar biphasic pattern of interference could be produced using artificial mixtures of the Justin P0 and P9 stocks, containing variable ratios of defective to standard virus DNA (Figure 9, panel B).

(iii) Analyses of purified virion preparations obtained from cells infected with various Justin passages revealed large fluctuations in the ratios of particle to PFU. Once again the change in the particle/PFU ratio as a function of the fraction of defective genomes in the population followed a threshold pattern (Figure 9, panel D). Furthermore, estimation of the particle/PFU ratios for particles containing standard non-defective genomes (as judged by restriction enzymes, see legend to Figure 9) yielded a curve (panel D) which was similar to the threshold interference curve (panel A). Thus, in cells infected with passages containing defective genomes in excess of 50%, increasing proportions of the non-defective helper virus genomes were packaged into defective virions.

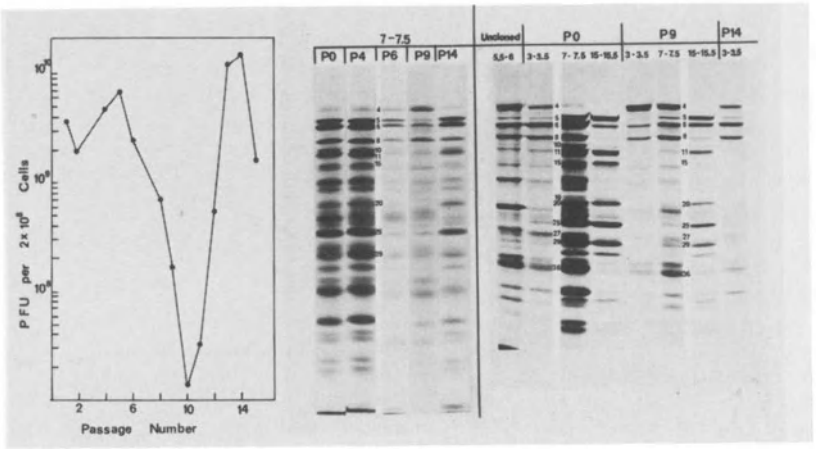

Figure 10--Example to analyses of ICP synthesis in cells infected with Justin passages. Left: plot of the infectious yield curve for the Justin series. Right: electrophoretic patterns of ICPs from cells infected with 20 PFU/cell of the passages shown and pulse labeled at times shown. Data by R. Honess, from reference 9.

(iv) The number of physical particles produced in cells infected with various passages of the Justin series was calculated using the particle/PFU ratios and data concerning the total yield of infectious virus produced per cell in the course of infections with equal PFU/cell of the various passages. As seen in Figure 9, panel C these analyses revealed no significant changes in the total number of physical particles produced per infected cell. Thus, the presence of class I defective genomes did not significantly impair the capacity of the infected cells to produce virus particles.

(v) Analyses of the polypeptides produced in cells infected with various passages of the Justin series (e.g. Figure 10) have revealed deviations from the normal pattern of infected cell polypeptide (ICP) synthesis. The ICPs analyzed could be grouped into three categories on the basis of their dependence on the fraction of defective genomes in the population. The first group included ICP8 and 21, the synthesis of which was unaffected by the presence of defective genomes (Figure 9, panel F). The second group included ICP4 which was overproduced in cells infected with the serially passaged virus. The extent of overproduction was linearly related to the fraction of defective genomes (Figure 9, panel E). The third group of ICPs including 5, 6, 11, 15, 17, 18, 18.5, 20 and 25 were underproduced in serially passaged Justin infections. The extent of reduction in the synthesis of most of these polypeptides (Figure 9, panels G and H), resembled the threshold pattern of interference, with respect to its dependence on the fraction of defective genomes. It is noteworthy that cells infected with serially passaged HSV populations characterized by Murray et al. (25) have also been shown by these authors to overproduce ICP4 (VP175).

(vi) Analyses of viral transcription in cells infected with P9' and P11' of the Justin series (containing defective virus genomes in excess of 63%) revealed gross deviations from the normal pattern of virus transcription in cells infected with plaque purified virus stocks. Specifically,

as exemplified in Figure 11, the cells infected with these serially passaged virus stocks synthesized abundant RNA from the regions which are represented in the Justin defective genome repeat units, whereas the transcription of the bulk of the L sequences was greatly reduced. Thus, the presence of defective genomes in sufficient proportions resulted in reduced transcription of large sets of the DNA sequences of the helper virus genomes.

Biologic Properties of Serially Passaged Virus Populations Containing Class II Defective Genomes

Our studies concerning the biologic properties of serially passaged HSV populations containing class II defective genomes (H. Locker, N. Frenkel and I. Halliburton, manuscript in preparation) were performed with various passages of the tsLB2 series, containing variable proportions of defective genomes of the type shown in Figure 5. Unlike the Justin series in the case of the tsLB2 series, the fraction of defective genomes does not closely follow the pattern of infectious virus yield production depicted in Figure 1. Thus, highest proportions of defective genomes are produced in cells infected with passages 8-10 and 18, 19, i.e. passages which fall on the descending slopes of the cyclic infectious virus yield curve, whereas cells infected with passages 11, 12 and 21, which are located at the very bottom of the infectious virus yield curve of the series, produce lower proportions of defective genomes.

As seen in Figure 9 (panel E) passages of the tsLB2 series exhibited an interference pattern which in similarity to the interference exhibited by the Justin passages, followed a biphasic dependence on the fraction of defective viral genomes in the population. However, unlike the case with the Justin series, cells infected with the tsLB2 defective virus populations produced significantly lower numbers of particles per cell, as shown by electron microscopic examinations of thin sections of the infected cells (D.K. Furlong and N. Frenkel, unpublished results).

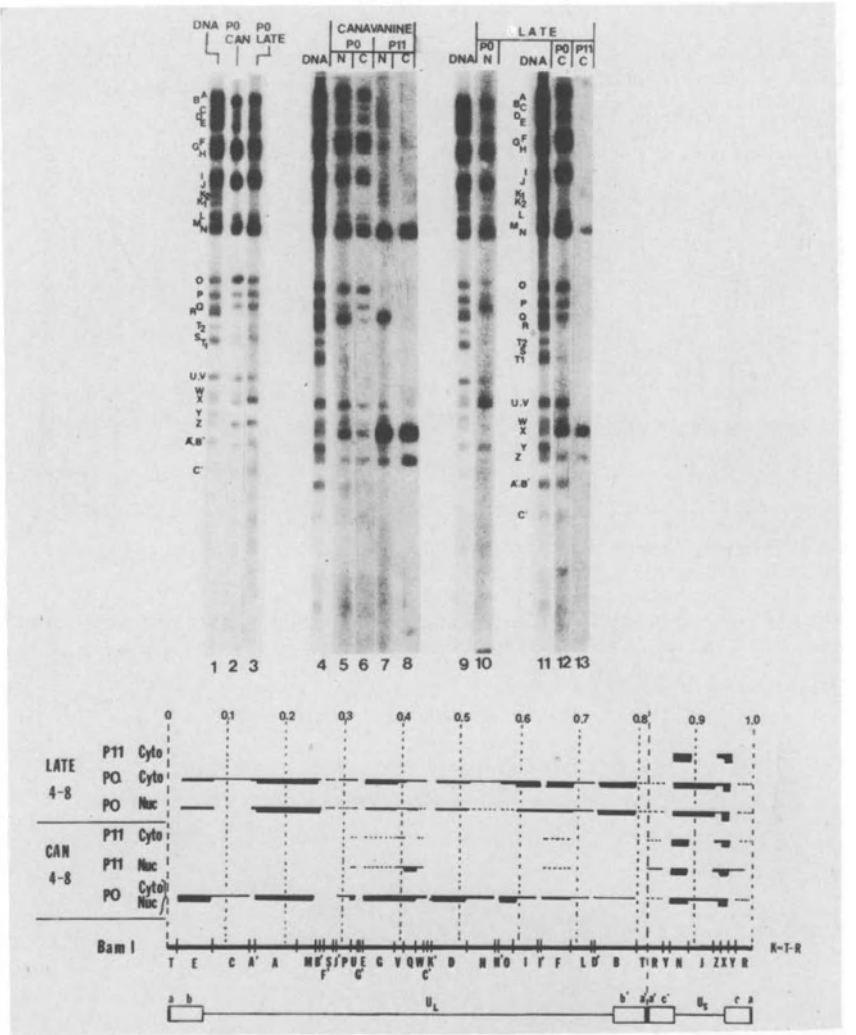

Figure 11--Viral transcription in P11' Justin infected cells. Shown here are blot (BamI) hybridizations with P^{32}labeled cytoplasmic (C) and nuclear (N) RNA extracted from cells infected with 10 PFU/cell of either P0 or P11' Justin in the presence ("canavanine") or absence ("late") of 500 μg/ml canavanine and labeled from 4-8 hours post infection with P^{32} phosphate. Also shown are control blots hybridized with P^{32} labeled HSV DNA, and total cell RNA from cells infected with P0 virus in the presence (P0 can) or absence (P0 late) of canavanine. Additional blot hybridizations (not shown) performed with "early" RNA (synthesized in the presence of cycloheximide) revealed abundant hybridizations to the early portions of the repeat unit sequences (fragments Y, R and the S-L junction fragments). Data from H. Locker and N. Frenkel, manuscript in preparation.

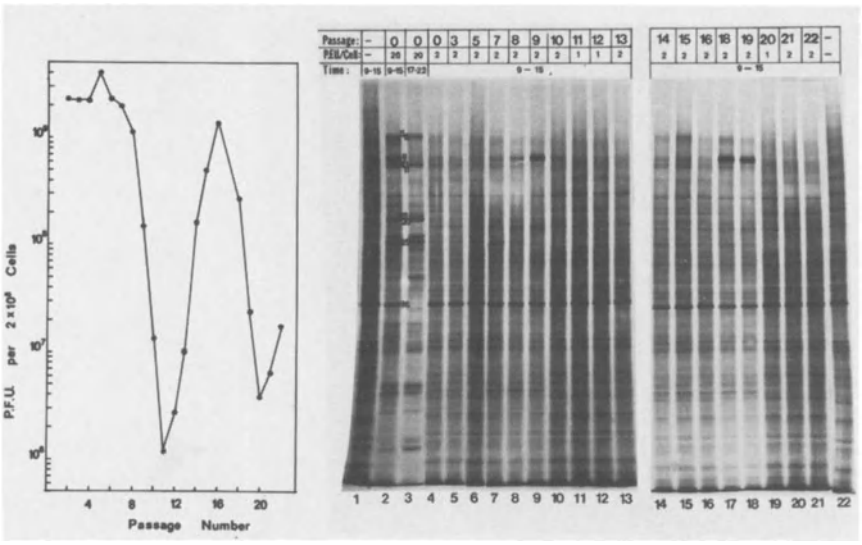

Figure 12--ICP synthesis in cells infected with the tsLB2 passages. Cells infected at 34°C with the various passages at input PFU/cell as shown were pulse labeled with C14 amino acids at the times shown.

Analyses of the electrophoretic patterns of polypeptides produced in cells infected with various passages of the tsLB2 series (e.g. Figures 12 and 13) revealed gross deviations from the normal pattern of ICP synthesis in standard virus infected cells. Although quantitations of the amounts of various polypeptides synthesized have not yet been done, it is apparent from the gel profiles

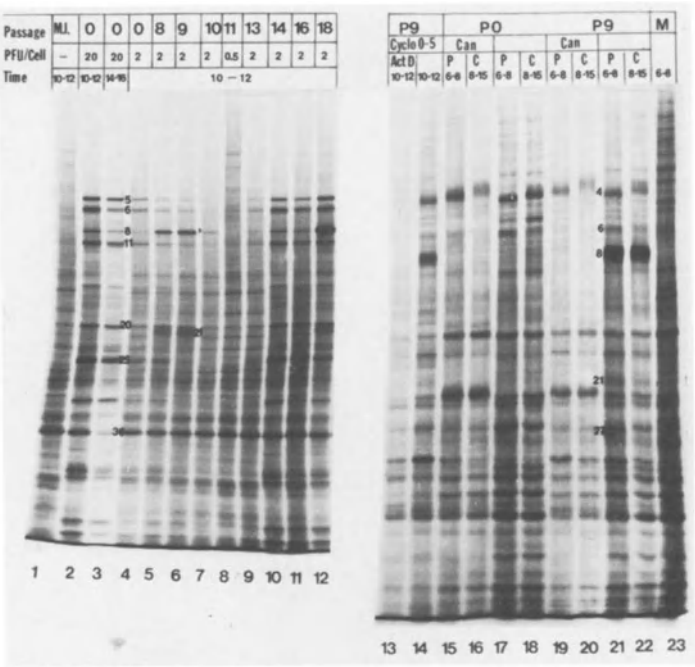

Figure 13--ICP synthesis in cells infected with tsLB2 passages. Left: infection at 34°C. M.I.=mock infected. Right: infection at 39°C with either P0 or P9 of tsLB2. Slots 13 and 14: infection was done in the presence of 50 µg/ml of cycloheximide from 0 to 5 hours followed by cycloheximide reversal (at 5 hours) in the presence (slot 13) or absence (slot 14) of 10 µg/ml of actinomycin D. Cells were labeled from 10 to 12 hours and were harvested thereafter; slots 15-23--the infections were in the presence or absence of 500 µg/ml of canavanine. Labeling was done from 6-8 hours, and cultures were either harvested (P=pulse, slots 15, 17, 19 and 21) or incubated in the presence of unlabeled amino acids (C=chase) from 8-15 hours (slots 16, 18, 20 and 22). The protocols for these experiments follow those of Honess and Roizman (15). Note that the synthesis of ICP8 and 21 is inhibited by canavanine, and that throughout the chase, ICP8 remains stable, whereas ICP21 is greatly reduced. Data from H. Locker, N. Frenkel and I. Halliburton, manuscript in preparation.

that in cells infected with passages located at the bottoms of the infectious virus yield curve (P10-13, P20 and P21) the synthesis of the majority of ICPs was greatly reduced. In similarity with the Justin series, infections of cells with certain passages of the tsLB2 series also resulted in the overproduction of certain ICPs. This overproduction, however, differed from the observed ICP4 overproduc-

tion in the Justin series in two respects. First, cells infected with certain passages overproduced the infected cell polypeptides 8 and 21 (which as discussed above were unaffected by the presence of Justin defective genomes), and second, the overproduction did not coincide with the infectious virus yield curve of the series. Rather, the most pronounced overproduction of ICP8 and 21 was observed in cells infected with passages located at the descending slopes of the infectious virus yield curve (i.e. P9, P18 and P19). As described above, these passages have also been shown to contain the highest proportions of defective genomes.

General Aspects of the Biologic Properties of Serially Passaged HSV Populations

The studies summarized thus far provide some insight into the events related to the presence of defective HSV genomes in serially passaged virus infected cells. Specifically, the defective genome-induced deviations from the normal pattern of viral gene expression can be grouped into two separate categories on the basis of their dependence on the relative proportion of defective viral genomes. The first group of alterations is characterized by the biphasic dependence on defective genome presence and includes the capacity to interfere with wild type virus replication (= reduced infectious virus yields), the production of defective physical particles (containing both standard and defective virus DNA in the case of the Justin series) or altogether reduced production of physical particles (in the case of the tsLB2 series), reduced synthesis of certain ICPs, and possibly reduced transcription from helper virus genomes. Alterations in this category are most apparent in cells infected with serially passaged virus stocks containing fractions of defective genomes in excess of the threshold level. The second group of alterations includes the overproduction of polypeptides by certain passages of the series. Alterations in this category do not show the biphasic dependence on defective genome presence. These two groups of alterations will be discussed separately below.

Figure 14--Electrophoretic patterns of ICPs synthesized in cells infected with standard HSV-1 (Justin) and HSV-2 (G) and the virus stock (G+P6). G+P6 was prepared from cultures cotransfected with purified heavy density defective Justin P6 DNA and standard HSV-2 (G) DNA. The G+P6 stock contained a mixture of defective Justin and standard helper G genomes, as judged by restriction enzyme analyses. Note that the ICP4 which is overproduced is of the HSV-1 type. Data from H. Locker and N. Frenkel, manuscript in preparation.

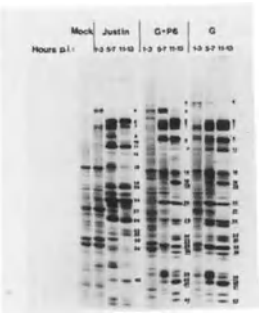

Aspects of ICP Overproduction

Examination of the pattern of polypeptide synthesis in serially passaged virus infected cells reveals two necessary requirements for the overproduction of specific ICPs by defective virus populations. The first is the presence of intact gene templates for the overproduced ICPs within the repeat units of the defective genomes, resulting in increased gene dosage for these polypeptides in the infected cells. The second, is that the normal regulatory substances required for the turning on of the synthesis of these ICPs will be present in sufficient quantities.

There are several lines of evidence for the hypothesis that the overproduced ICPs are indeed expressed from defective genome templates. First, ICP4 and ICP8 genes have been previously mapped to the ac and U_L regions contained within the Justin and tsLB2 defective genomes respectively (5, 24 and 28) (ICP21 has not yet been mapped). Second, as already discussed above, the DNA sequences which are represented within the Justin defective genome repeat units are abundantly transcribed in the serially passaged virus infected cells. Thirdly, we have analyzed (H. Locker and N. Frenkel, unpublished results) the pattern of ICP synthesis in cells infected with new virus stocks containing defective HSV-1 (Justin) and helper HSV-2 (G) genomes. As seen in Figure 14, these infections resulted in pronounced overproduction of the ICP4 characteristic

of HSV-1 infections (27), whereas the ICP4 characteristic of HSV-2 infections (and expressed from the helper virus genomes) was produced in normal quantities.

Evidence for the hypothesis that gene templates located within the defective genomes retain (in the case of ICP4, 8 and 21 overproduction) the dependence for their expression on the sequential regulatory scheme operating in standard HSV infections comes from experiments designed to classify the overproduced ICPs into the known α, β and γ regulatory classes (15) of HSV infected cell polypeptides. These analyses have revealed that the Justin overproduced ICP4 falls into the α class of viral polypeptides, in that its overproduction does not require prior synthes is of infected cell polypeptides (R. Honess, unpublished observations) in similarity with ICP4 production in standard virus infected cells (15). In line with these findings is the observation that the extent of ICP4 overproduction is determined solely by defective genome concentration. In contrast, as shown in Figure 13, the overproduced tsLB2 ICP8 and 21 exhibit all the "classical" properties of β polypeptides in that their synthesis requires the presence of functional early (α) viral polypeptides in similarity with their counterparts produced in standard virus infected cells (15). Thus, the tsLB2 induced overproduction of ICP8 and 21 is expected to depend on defective genomes concentration as well as on sufficient prior synthesis of the α gene product(s) required for the turning-on of β polypeptide synthesis.

The Mechanism of Interference

The biphasic dependence pattern of interference on the fraction of defective genomes could reflect the composite effect of two separate processes. The first (operating throughout the entire range of defective to wild type genome ratios) could simply result from stoichiometric decrease in the proportion of wild type DNA in a given number of progeny physical particles produced per infected cell. The second process (which becomes most apparent

at defective genome concentrations which are above threshold level) could involve the titration by the defective genomes of one or more catalytic substances which operate in synthetic pathways of the virally infected cell. In the case of the Justin series, we have completed the detailed quantitative analyses of the dependence of the various aspects of interference on the fraction of defective genomes contained in the different passages. Based on the types of defective genome-mediated alterations occurring at defective genome fractions in excess of the threshold level, the "catalytic" interference mediated by the Justin defective genomes seems to involve (i) competition between defective and wild type genomes on limited amounts of synthetic machinery, resulting in reduced synthesis of the bulk of viral polypeptides; (ii) production of aberrant virions, containing perhaps insufficient numbers of some of the structural viral polypeptides; (iii) packaging of wild type (as well as defective) genomes into the aberrant structural virions, and a concomitant reduction in the infectivity of particles containing otherwise non-defective viral DNA, and (iv) the observed reduction in infectious virus yields. As already noted above in the case of tsLB2 defective virus infections, the observed reduction in viral polypeptide synthesis is even more dramatic than that observed in the course of serially passaged Justin infections, resulting in significant reduction in the actual number of physical virus particles produced per infected cell.

The exact nature of the competitions event(s) resulting in reduced synthesis of viral polypeptides is not entirely clear. However, as discussed above in the case of the Justin series, the presence of high proportions of defective genomes is accompanied by preferential transcription of defective genome DNA sequences and reduced transcription of the vast majority of the helper virus DNA sequences. Thus, it seems reasonable to suggest that the presence of sufficient numbers of defective genomes, each

containing multiple sets of transcriptional promoters (or other binding sites) will reduce the expression of helper virus genes by competing for limited substances of transcriptional machinery. A central prediction of this transcriptional-competition model relates to the complexity of the defective genome DNA sequences directly responsible for interference. Specifically, if indeed the transcriptional competition is the first step in the chain of interference events, it can be predicted that the capacity to interfere should be associated with only small subsets of the defective genome DNA sequences (promoter or other binding sites). Furthermore, it can also be predicted that the probability of selection of "catalytically inert" defective genomes (i.e. defective genomes which have lost their second phase of interference above the threshold levels) would be directly dependent on the physical distance between the putative competing (promoter or binding) site and the cis replication functions involved in the replication and propagation of the defective genomes. It remains to be seen whether the evolutionary stability of the interfering forms of the defective HSV genome could indeed be explained in terms of proximity of transcriptional binding sequences to the cis replication functions of the defective viral genomes.

Whereas the transcriptional competition model is supported by the data concerning the alterations of viral transcription in the serially passaged Justin infected cells, it cannot by itself explain the pattern of interference observed in the tsLB2 series. Specifically, as discussed above, the overproduction of ICP8/21 and therefore most likely enhanced transcription of the tsLB2 defective genomes is not coincident with reduced synthesis of the bulk of the viral polypeptides specified by helper virus genomes (e.g. see passage 18, Figure 12). Furthermore, the fraction of defective genomes does not seem to correspond to the pattern of infectious virus yield shown

in Figure 1, in that passages 12-13 contain a smaller fraction of defective genomes than passages 8 or 9, which are located on the descending slopes of the infectious yield curve. Further detailed analyses of these tsLB2 passages will therefore be required, in order to establish all facets of interference exhibited by the tsLB2 defective viruses. These analyses are currently in progress.

ACKNOWLEDGMENTS

The studies described in this paper were supported by U.S. Public Health Service research grants AI-15488 and CA-19264, from the National Cancer Institute, and by National Science Foundation grant PCM78-16298.

REFERENCES

1. Becker, Y., Y. Asher, E. Weinberg-Zahlering, and S. Rabkin. 1978. Defective herpes simplex virus DNA: Circular and circular-linear molecules resembling rolling circles. J. Gen. Virol. 40: 319-335.

2. Becker, Y., B. Gutter, Y. Cohen, N. Chejanovsky, S. Rabkin, and B. Fridlender. 1979. Herpes simplex virus DNA polymerase, thymidine kinase and deoxyribonuclease activities in cells infected with wild type, ultraviolet-irradiated and defective virus. Arch. Virol. 62: 163-174.

3. Bronson, D.L., G.R. Dreesman, N. Biswal, and M. Benyesh-Melnick. 1973. Defective virions of herpes simplex viruses. Intervirol. 1: 141-153.

4. Campbell, D.E., M.C. Kemp, M.L. Perdue, C.C. Randall, and G.A. Gentry. 1976. Equine herpesvirus in vivo: Cyclic production of a DNA density variant with repetitive sequences. Virol. 69: 737-750.

5. Clements, J.B., R.J. Watson, and N.M. Wilkie. 1977. Temporal regulation of herpes simplex virus type 1 transcription: location of transcripts on the viral genome. Cell 12: 275-285.

6. Delius, H. and J.B. Clements. 1976. A partial denaturation map of herpes simplex virus type 1 DNA: Evidence for inversions of the unique DNA regions. J.Gen. Virol. 33: 125-133.

7. Fareed, G.C. and D. Davoli. 1977. Molecular biology of papovaviruses. Annu. Rev. Biochem. 46: 471-522.

8. Fleckenstein, B., G.S. Bornkamm, and H. Ludwig. 1975. Repetitive sequences in complete and defective genomes of herpesvirus saimiri. J. Virol. 15: 398-406.

9. Frenkel, N., R.J. Jacob, R.W. Honess, G.S. Hayward, H. Locker, and B. Roizman. 1975. Anatomy of herpes simplex virus DNA. III. Characterization of defective DNA molecules and biological properties of virus populations containing them. J. Virol. 16: 153-167.

10. Frenkel, N., H. Locker, W. Batterson, G.S. Hayward, and B. Roizman. 1976. Anatomy of herpes simplex virus DNA. VI. Defective DNA originates from the S component. J. Virol. 20: 527-531.

11. Friedmann, A., J. Shlomai, and Y. Becker. 1977. Electron microscopy of herpes simplex virus DNA molecules isolated from infected cells by centrifugation in CsCl density gradients. J. Gen. Virol. 34: 507-522.

12. Graham, B.J., Z. Bengali, and G.F. Vande Woude. 1978. Physical map of the origin of defective DNA in herpes simplex virus type 1 DNA. J. Virol. 25: 878-887.

13. Halliburton, I.W., R.E. Randall, R.A. Killington, and D.H. Watson. 1977. Some properties of recombinants between type 1 and type 2 herpes simplex viruses. J. Gen. Virol. 35: 471-484.

14. Hayward, G.S., R.J. Jacob, S.C. Wadsworth, and B. Roizman. 1975. Anatomy of herpes simplex virus DNA: Evidence for four populations of molecules that differ in the relative orientation of their long and short components. Proc. Natl. Acad. Sci. U.S.A. 72: 4243-4247.

15. Honess, R.W. and B. Roizman. 1975. Regulation of herpesvirus macromolecular synthesis: Sequential transition of polypeptide synthesis requires functional viral polypeptides. Proc. Natl. Acad. Sci. U.S.A. 72: 1276-1295.

16. Huang, A.S. 1973. Defective interfering viruses. Annu. Rev. Microbiol. 27: 101-117.

17. Huang, A.S. and D. Baltimore. 1977. Defective interfering animal viruses. In Comprehensive Virology. H. Fraenkel-Conrat and R.R. Wagner, eds. Vol. 10: 73-116.

18. Kaerner, H.C., I.B. Maickle, A. Ott, and C.H. Schroder. 1979. Origin of two different classes of defective HSV-1 Angelotti DNA. Nucleic Acid Research 6: 1467-1478.

19. Kelly, T.J. and D. Nathans. 1977. The genome of simian virus 40. Adv. Virus Res. 21: 85-113.

20. Locker, H. and N. Frenkel. 1978. The DNA of serially passaged herpes simplex virus: Organization, origin and homology to viral RNA. In Oncogenesis and Herpesviruses III/Part I: 75-85. G. de The, W. Henle and F. Rapp, eds.

21. Locker, H. and N. Frenkel. 1979. The BamI, KpnI and SalI restriction enzyme maps of the DNAs of herpes simplex virus strains Justin and F: Occurrence of heterogeneities in defined regions of the viral DNA. J. Virol. 32: 429-441.

22. Locker, H. and N. Frenkel. 1979. Structure and origin of defective genomes contained in serially passaged herpes simplex virus type 1 (Justin). J. Virol. 29: 1065-1077.

23. Mao, J.C.H., E.E. Robishaw, and L.R. Overby. 1975. Inhibition of DNA polymerase from herpes simplex virus infected WI-38 cells by phosphonoacetic acid. J. Virol. 15: 1281-1283.

24. Morse, L.S., L. Pereira, B. Roizman, and P.A. Schaffer. 1978. Anatomy of HSV DNA. X. Mapping of viral genes by analysis of polypeptides and functions specified by HSV-1x HSV-2 recombinants. J. Virol. 26: 389-410.

25. Murray, B.K., N. Biswal, J.B. Bookout, R.E. Lanfore, R.J. Courtney, and J.C. Melnick. 1975. Cyclic appearance of defective interfering particles of herpes simplex virus and the concomitant accumulation of early polypeptide VP175. Intervirol. 5: 173-184.

26. O'Callaghan, D., B.E. Henry, J.H. Wharton, S.A. Dauenhauer, R.B. Vance, J. Staczek, and R.A. Robinson. 1980. Equine herpesviruses: Biochemical studies on genomic structure, DI particles, oncogenic transformation and persistent infection. This volume (Chap. 19).

27. Pereira, L., H.M. Wolff, M. Fenwick, and B. Roizman. 1977. Regulation of herpesvirus macromolecular synthesis. V. Properties of α polypeptides made in HSV-1 and HSV-2 infected cells. Virol. 77: 733-749.

28. Preston, V.G., A.J. Davison, H.S. Marsden, M.S. Timbury, J.H. Subak-Sharpe, and J.M. Wilkie. 1978. Recombinants between herpes simplex virus type 1 and 2: Analysis of genome structures and expression of immediate early polypeptides. J. Virol. 28: 499-517.

29. Roizman, B. 1979. The structure and isomerization of herpes simplex virus genomes. Cell 16: 481-494.

30. Roizman, B., R.J. Jacob, D.M. Knipe, L.S. Morse, and W.T. Buchman. 1978. On the structure, functional equivalence and replication of the four arrangements of herpes simplex virus DNA. Cold Spring Harbor Symp. Quant. Biol. 38: 809-826.

31. Schroder, C.H., H.C. Kaerner, K. Munk, and G. Darai. 1977. Morphological transformation of rat embryonic fibroblasts by abortive herpes simplex virus infection: Increased transformation rate correlated to a defective viral genotype. Intervirol. 8: 164-171.

32. Schroder, C.H., B. Stegmann, H.F. Lauppe, and H.C. Kaerner. 1975/76. An unusual defective genotype derived from herpes simplex virus strain ANG. Intervirol. 6: 270-284.

33. Schroder, C.H. and G. Urbaczka. 1978. Excess of interfering over infectious particles in herpes simplex virus passaged at high m.o.i. and their effect on single cell survival. J. Gen. Virol. 41: 493-501.

34. Sheldrick, P. and N. Berthelot. 1974. Inverted repetitions in the chromosome of herpes simplex virus. Cold Spring Harbor Symp. Quant. Biol. 39: 667-678.

35. Southern, E.M. 1975. Detection of specific sequences among DNA fragments separated by gel electrophoresis. J. Mol. Biol. 98: 503-517.

36. Stegmann, B., H. Zentgraf, A. Ott, and C.H. Schroder. 1978. Synthesis and packaging of herpes simplex virus DNA in the course of virus passages at high multiplicity. Intervirol. 10: 228-240.

37. Von Magnus, P. 1954. Incomplete forms of influenza virus. Adv. Virus Res. 2: 59-78.

38. Wadsworth, S., R.J. Jacob, and B. Roizman. 1975. Anatomy of herpes simplex virus DNA. II. Size, composition and arrangement of inverted terminal repetitions. J. Virol. 15: 1487-1497.

39. Wagner, M., J. Skare, and W.C. Summers. 1974. Analysis of DNA of defective herpes simplex virus type 1 by restric-endonuclease cleavage and nucleic acid hybridization. Cold Spring Harbor Symp. Quant. Biol. 39: 683-686.

40. Wagner, M.J. and W.C. Summers. 1978. Structure of the joint region and the termini of the DNA of herpes simplex virus type 1. J. Virol. 27: 374-387.

11. Biosynthesis of defective HSV DNA

Yechiel Becker and Samuel Rabkin

SUMMARY

Circular-linear molecules are produced during the synthesis of defective HSV-1 DNA in infected cells. The circular component of these DNA molecules is most probably derived from parental viral DNA and serves as a template for DNA synthesis by a mechanism resembling rolling circles. The linear DNA molecules which are formed on the rolling circles are reiterations of the DNA sequence of the circular component.

INTRODUCTION

In our previous study on defective HSV-1 (HF strain), circular and circular-linear DNA molecules were found to band together with the linear viral DNA in CsCl gradients (1,2). The circular DNA molecules have a density similar to that of the repeat sequences of the S component (3). It was proposed (1,4) that the repeat sequence is released from wild type (wt) DNA and becomes a circular DNA fragment to serve as template for synthesizing linear defective DNA molecules by a mechanism resembling the rolling circle model (5). The finding (6,7) that linear defective viral DNA is made up of tandem repeats of the terminal repeat sequence of the S component may be explained by a rolling circle type of DNA synthesis.

To gain further insight into the mechanism of defective DNA synthesis, we used the KOS and Patton strains of HSV-1, in addition to the HF strain, to investigate the generation of circular DNA molecules.

EXPERIMENTAL

Cells and virus

BHK (C13) cells (obtained from Prof. J. Subak-Sharpe, Institute of Virology, Glasgow, Scotland), were grown in Dulbecco's modified Eagle's medium (DMEM; Grand Island Biological Co.) containing 10% tryptose phosphate and 5% calf serum (Biolab, Israel). Forty-eight hr after

Y. Becker (ed), Herpesvirus DNA.

seeding, the cells (about 6 x 10^6) were infected with the KOS strain of HSV-1 (obtained from Prof. F. Rapp, The Pennsylvania State University, Hershey, Penn.) at a multiplicity of infection of 10 pfu per cell. Vero cells (10^8 cells/roller bottle) grown in Eagle's medium with 10% fetal calf serum, 25 mM HEPES buffer and 2 mM glutamine were infected with the Patton strain of HSV type 1 (obtained from Dr. G. Vander Woude, National Cancer Institute, Bethesda, Maryland) and BSC-1 cells (2 x 10^6 cells/milk bottle) grown in DMEM with 10% fatal bovine serum (Grand Island Biological Co.) were infected with the HF strain of HSV type 1. Cells were infected at a multiplicity of infection of 0.1 pfu/cell to prepare stock virus, whereas for regular experimental procedures, the cells were infected with 10 pfu/cell.

Defective virus preparations were obtained by infecting the cells at 100 pfu/cell, followed by successive transfer of undiluted virus up to passage level 7. Production of defective virus was established by reduction in infectivity titer, as determined by the plaque assay and by density determination of defective virus DNA in CsCl gradients (1).

Isolation of DNA

At 1.5 hr postinfection (p.i.), non-absorbed virus was removed and fresh medium was added to the cultures. The infected cells were labeled with methyl ^{3}H-thymidine (10-25 µCi/culture; specific activity 40 Ci/mM, Nuclear Research Centre, Negev, Israel) or 45 µCi/culture of ^{32}P-orthophosphate (specific activity 10 mCi/ml, Nuclear Research Centre, Negev, Israel). After labeling, the DNA was obtained by digestion of the cells with sodium dodecyl sulfate and pronase, and by centrifugation of the cell lysates in CsCl, as previously described (8). The buoyant densities of the various fractions were determined by measuring the refractive indices in a Bausch & Lomb refractometer. Ethidium bromide-CsCl gradients were prepared by the addition of 5.8 gm of solid CsCl to 6.24 ml of DNA solution which then had an isodensity of 1.58 gm/cm^3. To this was added 0.2 ml of ethidium bromide (12 mg/ml) in the dark. All subsequent steps were identical to those described for the CsCl density gradients.

Electron microscopy

The DNA preparations were spread and examined by electron microscopy, as previously described (9).

RESULTS

Defective viral DNA

The densities of KOS strain HSV-1 DNA at different passage levels were determined. The density of wt virion DNA was found to be 1.725 g/ml and that of defective DNA 1.733 g/ml. At passage levels 4 and 5, most of the labeled DNA had a density of defective viral DNA, although labeled defective DNA was synthesized to a lesser extent at passage 5 than at passage 4 (Fig. 1).

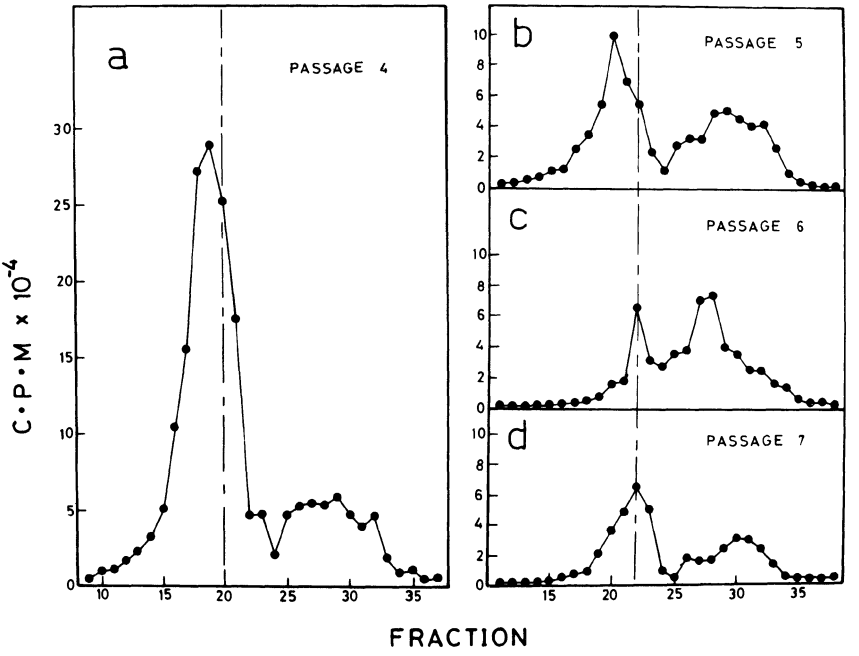

Fig. 1: Synthesis of defective KOS DNA. Cells were labeled with ^{3}H-thymidine at 2 hr p.i. for 20 hr at passage levels 4(a), 5(b), 6(c) and 7(d). The DNA was isolated by centrifugation in CsCl density gradients, fractions were collected, and the radioactivity determined. Position of wt HSV DNA is indicated by the dashed line.

Hardly any defective DNA appeared to be synthesized at subsequent passage levels. The virus titer at passage level 3 was 3 x 10^{7} pfu/ml; With the increase in defective virus synthesis at passage levels 4 and 5 the virus titer dropped to 1.5 x 10^{6} and 5 x 10^{5} pfu/ml respectively. At passage levels 6 and 7 the virus titers rose to 3 x 10^{6} and 4.5 x

10^6 pfu/ml respectively with the increased synthesis of wt virus. The synthesis of defective viral DNA at passage 5 was further investigated.

The amount of defective DNA synthesized at passage level 5 was determined by labeling infected cells with ^{3}H-thymidine and centrifugation of the DNA in CsCl density gradients. The ratios of defective to wt DNA obtained at various times after infection were determined (Fig. 2). A ratio close to 2 was reached at 9 hr p.i., indicating the degree to which defective DNA is synthesized in excess of wt virus DNA.

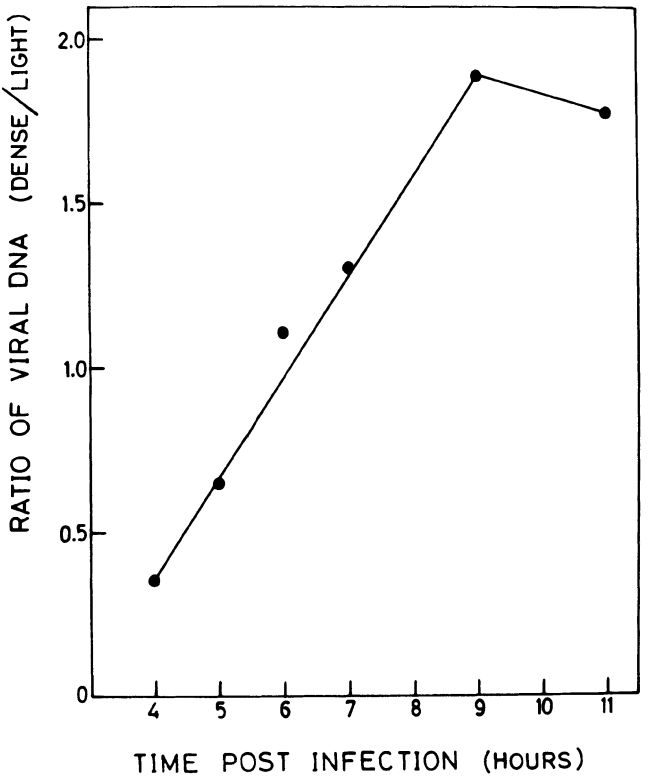

Fig. 2: Time course of DNA synthesis. Cells infected at passage level 5 were labeled with ^{3}H-thymidine from 2 hr p.i. for 2, 3, 4, 5, 7 and 9 hr. The DNA was isolated in CsCl gradients and the amount of defective and wt DNA determined at each time interval. The ratios of more dense (defective) to less dense (wt) DNA were plotted.

Electron microscopy of defective DNA

Circular defective DNA. Circular DNA molecules with contour lengths from 2.5-5.0 μm were described for defective HF strain HSV-1 DNA (2). Similar circular DNA molecules were found in preparations of defective KOS strain viral DNA, but most of these molecules had a contour length of 2-2.25 μm, with some ranging from 4.0-5.0 μm (Fig. 3). It is of interest that the circular defective DNA molecules of the Patton strain had a contour length of about 3.0 μm, whereas the HF strain DNA ranged from 2.5-5.0 μm (Fig. 3).

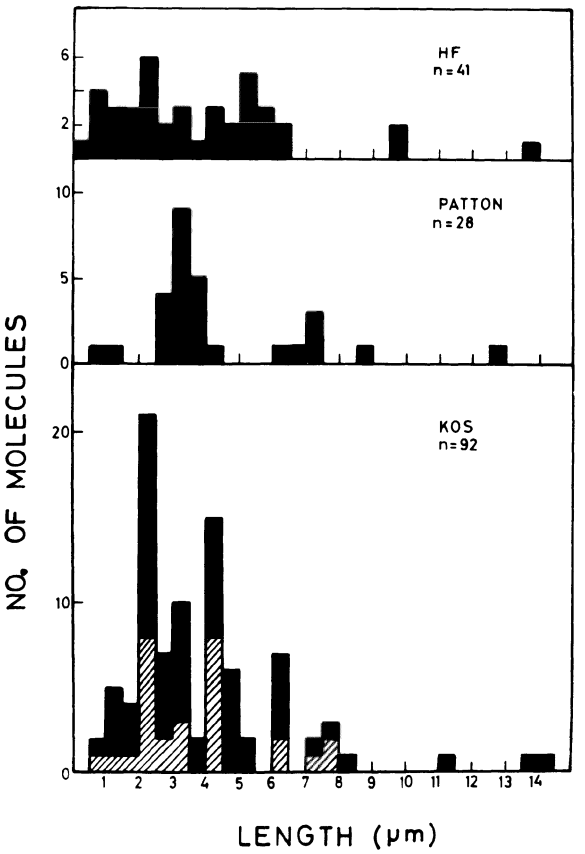

Fig. 3: Histogram of contour lengths of circular DNA molecules including the circular portion of circular-linear DNA molecules. Defective HSV-1 DNA from the HF strain passage 6, Patton strain passage 8, and KOS strain passage 5 were compared. The hatched area shown for the KOS strain represents the number of molecules isolated one year earlier.

Circular DNA molecules from wt DNA. A few circular DNA molecules were seen among the linear wt DNA molecules of the KOS strain. One of the molecules appeared in a supercoiled form with a contour length about 12-19 μm. Circular-linear molecules were not seen.

Circular-linear defective DNA molecules of the rolling circle type. The circular-linear DNA molecules shown in Fig. 4 were isolated in CsCl density gradients from defective passage 5 KOS strain virus. There are distinct junctions between the linear and circular components. It is of interest that the circular components also display a loop or loops.

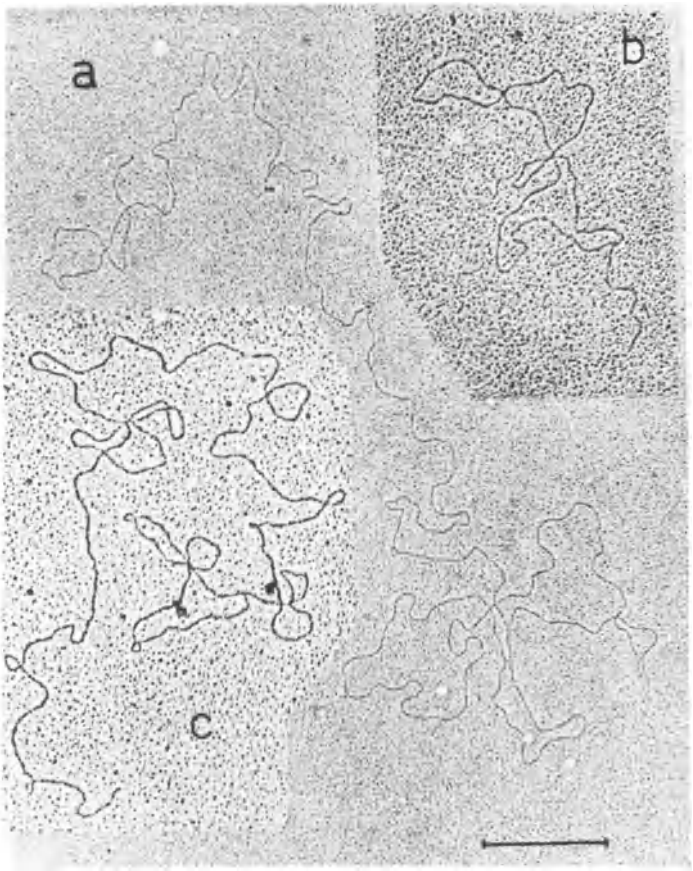

Fig. 4: Electron micrograph of circular-linear DNA molecules from defective (passage 5) KOS strain DNA. The contour lengths of the circular and linear components respectively are a) 13.7 and 15.6, b) 6.2 and 0.95, c) 3.6 and 11.8 μm. Bar marker represents 1.0 μm.

The histogram in Fig. 5 shows that the circular components of the circular-linear defective DNA molecules range in length from 2.2-14 μm, half of them with circular components of 2-3 μm. The linear components vary in length from a fraction of 1 μm to longer than 16 μm.

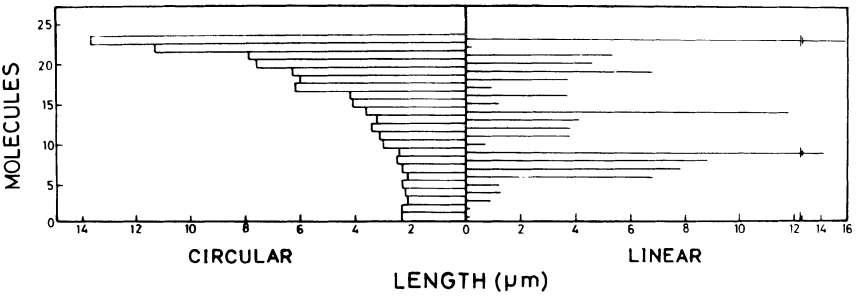

Fig. 5: Histogram of the contour lengths of circular-linear DNA molecules seen with defective (passage 5) KOS strain DNA.

Fate of prelabeled viral DNA during defective DNA biosynthesis

To obtain information on the generation of circular DNA molecules, BHK cells were infected with KOS strain virus at passage 4 and incubated in the presence of ^{32}P-orthophosphate from 2-18 hr p.i. After washing the cells and changing to unlabeled medium plus phosphate, the cells were reincubated for 4 hr. The virus from the cells was passaged undiluted in unlabeled medium and the passage 5 infected cells were harvested at 2 and 6 hr p.i. The nuclei were isolated and treated with SDS-pronase and the DNA was centrifuged in CsCl density gradients. To isolate the circular DNA molecules, viral DNA from the more and less dense regions of the CsCl gradients was further centrifuged in ethidium bromide-CsCl density gradients with ^{3}H-SV40 DNA as a marker (10). The ^{32}P-labeled, more dense DNA molecules isolated in CsCl gradients are the parental defective DNA molecules that enter the nuclei of infected cells. On further centrifugation in ethidium bromide CsCl density gradients, some radioactivity was found at the same position as circular SV40 DNA at 2 hr p.i. (Fig. 6a) and this increased in amount at 6 hr p.i. (Fig. 6b).

Analysis of the wt (less dense) DNA in ethidium bromide-CsCl density gradients revealed only linear DNA molecules at 2 hr p.i. (Fig. 6c), although at 6 hr p.i. some circular labeled DNA molecules were also present (Fig. 6d). Since the separation between defective and wt DNA is not absolute, the nature of the circular labeled wt DNA

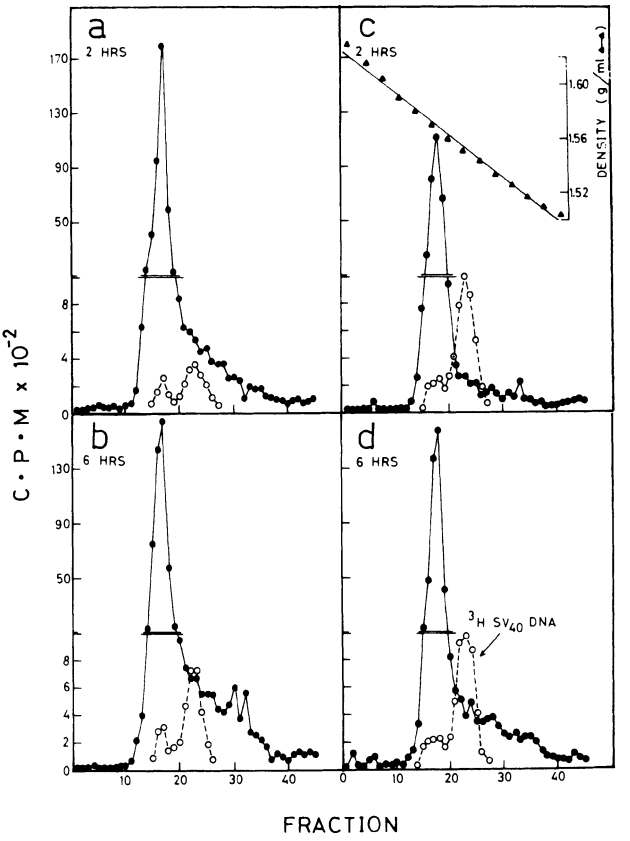

Fig. 6: Cells were infected with ^{32}P-prelabeled passage 4 virus. At 2 and 6 hr p.i., the DNA was isolated and centrifuged in CsCl density gradients. The DNA from the more dense (a,b) and less dense (c,d) viral peaks was then centrifuged in CsCl-ethidium bromide density gradients at 37,000 rpm at 20°C in a 50Ti rotor for 60 hr with ^{3}H-SV40 DNA as a marker. Fractions were collected from the bottom of the tube and the radioactivity determined after TCA precipitation.

is not known. It is possible that wt (less dense) circular DNA molecules also arise during the synthesis of defective DNA. Cuifo and Hayward (Chap. 7) have indeed shown that defective HSV DNA arises from the center of the L component which has a lower density in CsCl gradients than the repeat sequences of S. Circular DNA molecules were also observed when the viral DNA isolated from the less dense region of the gradient was examined by electron microscopy.

It should be noted that when the DNA was labeled after infection at passage 5, and similarly centrifuged in ethidium bromide-CsCl gra-

dients, all the DNA banded at the position of linear DNA. These results indicate that the circular DNA molecules present in defective virus DNA at passage level 5 are generated from parental DNA and are not synthesized as progeny DNA.

The labeled circular DNA molecules which arise from parental linear viral DNA probably differ from the circular twisted SV40 DNA molecules. It may be assumed that the circular defective HSV DNA molecules are relaxed circles with a nick or a single-stranded sequence. If changes occur in the circular defective and wt DNA molecules during generation from parental viral DNA, there should be a change in the sedimentation properties of the DNA. This was indeed found to be the case when ^{32}P-labeled defective and wt viral DNA molecules, isolated in CsCl gradients, were centrifuged in sucrose gradients using wt virion linear DNA as a marker. At 2 hr p.i., the defective parental (more dense) ^{32}P-labeled DNA had a sedimentation constant similar to that of wt DNA, but at 6 hr the defective DNA sedimented more slowly than the marker DNA. Similar results were obtained with the wt DNA (not shown).

It should also be pointed out that in our studies on the HF strain of HSV-1 grown in BSC-1 cells, the passage level at which circular DNA molecules are formed was determined. Infected cells were labeled with ^{3}H-thymidine, and the DNA was extracted and centrifuged in CsCl-ethidium bromide density gradients. Radioactive circular DNA molecules which banded at a lower density than linear viral DNA appeared at passage levels 3 and 4. Circular SV40 DNA bands at the same position in CsCl-ethidium bromide density gradients (10).

DISCUSSION

This is an extension of our previous studies on HSV-1 (HF strain) defective DNA (1). Infection of cells under conditions of defective virus synthesis with two additional strains of HSV-1 (KOS and Patton) also leads to the generation of circular and circular-linear DNA molecules with the density of defective linear viral DNA. Circular DNA molecules were also observed among the linear DNA of wt density obtained at passage 5, but circular-linear DNA molecules were never observed among the DNA molecules of wt density.

The circular-linear DNA molecules found only at the density of

defective viral DNA in CsCl gradients may be the replicative intermediates active in the synthesis of defective linear DNA; replication is probably by the rolling circle mechanism (5).

A model for the generation and synthesis of defective HSV DNA from the terminal repeat of the S unique sequence is presented in Fig.7.

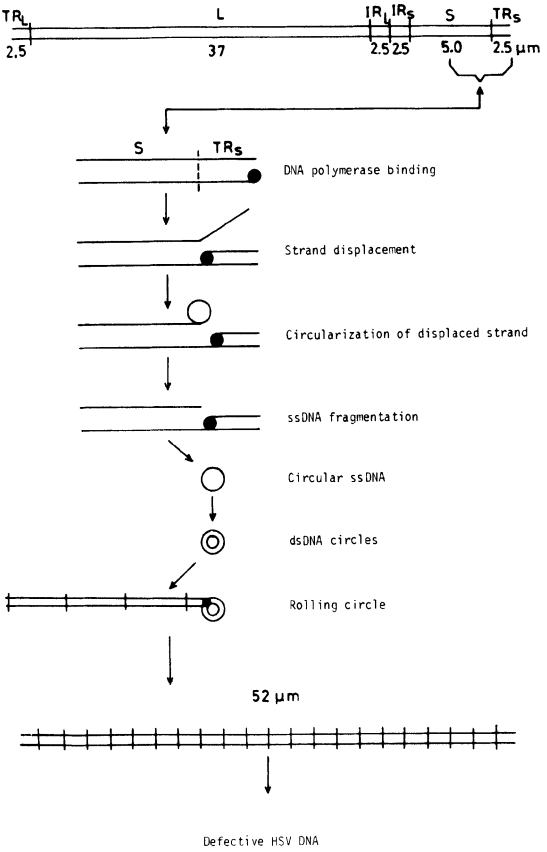

Fig. 7: Model for synthesis of defective HSV-1 DNA by the rolling circle mechanism.

It is assumed that due to an error the viral DNA polymerase initiates DNA synthesis on one of the two viral DNA strands at the terminal repeat of S. As a result, the second strand that does not serve as a template is displaced, becomes circularized, and is cut off. The circular single-stranded DNA molecule serves as a template for the

synthesis of double-stranded DNA which is the template for the reiterated linear DNA molecule. The studies by Frenkel et al. (6) and Cuifo and Hayward (Chap. 7) on the structure of linear defective DNA revealed reiterated DNA compatible with the rolling circle mechanism of biosynthesis. Cuifo and Hayward (Chap. 7) show that defective DNA molecules are generated from the center of the unique L sequence of the viral DNA genome. The mechanism that determines whether defective viral DNA will arise from the center of the L sequence or from the repeat sequence is not yet known.

ACKNOWLEDGMENTS

Our thanks to Dr. Julia Hadar for assistance with the manuscript. This work was supported by a grant from the Basic Research Branch of the Israel National Academy of Sciences.

REFERENCES

1. Becker, Y., Asher, Y., Weinberg-Zahlering, E., Rabkin, S., Friedmann, A. and Kessler, E. J. gen. Virol. 40:319-335, 1978.

2. Becker, Y., Asher, Y., Friedmann, A. and Kessler, E. J. gen. Virol. 41:629-633, 1978.

3. Friedmann, A., Broit, M. and Becker, Y. In: Oncogenesis and Herpesviruses III (Eds. G. de-The, W. Henle and F. Rapp), IARC Scientific Publications No. 24, Lyon. pp. 137-148 (1978).

4. Becker Y. J. Theor. Biol. 75:339-347, 1978.

5. Gilbert, W. and Dressler, D. Cold Spring Harbor Symp. Quant.Biol. 33:473-484, 1968.

6. Frenkel, N., Locker, H., Batterson, W., Hayward, G.S. and Roizman, B. J. Virol. 20:527-531, 1976.

7. Graham, B.J., Bengali, Z. and Vande Woude, G.F. J. Virol. 25:878-887, 1978.

8. Shlomai, J., Friedmann, A. and Becker, Y. Virology 69:647-659,1976.

9. Friedmann, A., Shlomai, J. and Becker, Y. J. gen. Virol. 34:507-522, 1977.

10. Su, R.T. and DePamphilis, M.L. Proc. Natl. Acad. Sci. U.S.A. 73:3466-3470, 1976.

12. Mapping of the HSV sequences in transformed cells

Jeffrey M. Leiden and Niza Frenkel

INTRODUCTION

Following infection with inactivated herpes simplex viruses or transfection with fragmented HSV DNA, a small proportion of cultured cells from a variety of hosts can be shown to exhibit altered growth properties, i.e. to have acquired the capacity to proliferate under restrictive growth conditions (1, 5, 7, 8, 10, 21, 25, 26, 28, 30, 32 and 46). Such "HSV transformed cells" have been selected in two ways. First, cells exhibiting altered growth properties have been selected by their ability to grow continuously in culture, to grow in medium containing low concentrations of serum, to form foci in culture or to grow in semi-solid medium (5, 7, 10, 21, 25 and 32). Cell lines selected in these ways exhibit one or more of the altered growth properties which have been shown to be characteristic of cells transformed by other oncogenic viruses (41). However, the relationship between these altered growth phenotypes and oncogenic transformation remains unclear, because these morphologic transformants have been reported to exhibit variable degrees of tumorigenecity (11).

Several recent reports have attempted to localize the HSV gene(s) which are responsible for HSV mediated morphologic transformation. Specifically, Camacho and Spear have reported that the viral DNA sequences contained in the XbaI F fragment of HSV-1 (F) DNA (spanning map coordinates 0.30-0.45) are sufficient to cause morphologic transformation of primary hamster cells as assayed by the ability of the transformed cells to grow in low concentrations of serum (5). In agreement with these results, Reyes et al. (G.R. Reyes, R. LaFemina, S.D. Hayward and

Y. Becker (ed), Herpesvirus DNA.

G.S. Hayward, 1979, Cold Spring Harbor Symp. Quant. Biol., 44, 629-641), have reported that transfection with fragments of HSV-1 DNA spanning map coordinates 0.31-0.41 resulted in the morphologic transformation of Balb/3T3 and hamster embryo cells as defined by focus formation. However, these authors have also reported that fragments derived from the corresponding region of the HSV-2 genome fail to transform cells. On the other hand, they have shown that the focus inducing function of HSV-2 DNA can be localized to the BglII N fragment spanning map coordinates 0.58-0.63. Finally, Jariwalla and Aurelian (personal communication) have shown that transfection with the BglII/HpaI fragment CD (map coordinates 0.42-0.57, i.e. mapping to the left of the sequences reported by Hayward et al. to contain the HSV-2 transforming gene(s)) results in morphologic transformation of hamster cells as assayed by colony formation in agar. From these results, it is apparent that the location of both the HSV-1 and HSV-2 transforming gene(s) remains unclear.

The second type of HSV mediated cell conversion involves the transfer of the HSV encoded thymidine kinase (tk) gene to mouse cells previously lacking this enzyme (1, 8, 26, 28, 30 and 46). Such HSV mediated biochemical (tk) transformation was first demonstrated by Munyon et al. (30), who showed that following infection with UV irradiated HSV, a small proportion of thymidine kinase negative (tk^-) mouse cells survive selection in HAT containing medium and can be shown to have acquired and to express the viral tk gene. More recently, tk^- mouse cells have been converted to the tk positive (tk^+) phenotype following transfection with either sheared HSV DNA or purified restriction enzyme fragments thereof (1, 26, 28 and 46). Using this approach, Wigler et al. have shown that a 3.4 kilobase fragment of HSV-1 (F) DNA is sufficient to convert tk^- cells to the HSV tk positive ($HSVtk^+$) phenotype (46). Furthermore, Maitland and McDougall have re-

ported that the purified restriction enzyme fragments of HSV-2 (333) DNA which contain the viral DNA sequences between map coordinates 0.53 and 0.65 are sufficient to convert tk^- mouse cells to the $HSVtk^+$ phenotype (26). This map location for the HSV-2 tk gene was surprising, in light of recent studies of HSV-1xHSV-2 recombinants which have revealed that most, if not all of the genes of these viruses are colinear and which have mapped the HSV-1 tk gene between coordinates 0.27 and 0.35 (29).

The $HSVtk^+$ cell has also been used as a model system for studies of the regulation of a cell associated viral gene. Thus, it has been shown that when $HSVtk^+$ cells are continuously propagated in HAT containing selective medium, they continue to stably express the viral tk gene (8 and 30). However, propagation of these cells in non-selective medium has allowed the definition of two groups of transformants differing with respect to the stability of their tk gene expression (8). Specifically, the first group of $HSVtk^+$ cells are stable transformants which continue to express the viral gene even following prolonged passaging under non-selective conditions. In contrast, the second group of biochemical transformants has been shown to display an unstable expression of the viral tk gene, exponentially reverting to the tk^- phenotype during passaging under non-selective conditions (in the absence of HAT). Furthermore, it has been shown that the tk^- revertants resulting from such propagation in non-selective medium display low rates of rereversion to the $HSVtk^+$ phenotype upon reselection in HAT containing medium (8).

Several previous reports have demonstrated the presence of HSV DNA sequences in both HSV morphologic transformants and $HSVtk^+$ cells (9, 12, 20, 27 and reviewed in 13). However, in no case have these cell associated viral DNA sequences been physically mapped. The present communication reviews our attempts to map the HSV DNA sequences which are present in several HSV-1 morphologic trans-

formants as well as a number of HSVtk$^+$ and related derivative cell lines.

The specific objectives of these studies can be summarized as follows:

(i) By identifying those HSV DNA sequences common to all HSV-1tk$^+$ and HSV-2tk$^+$ transformed cells we hoped to unambiguously map both the HSV-1 and HSV-2 tk genes.

(ii) By mapping the HSV DNA sequences which are present in several stable and unstable HSV-1tk$^+$ transformants, we hoped to ascertain whether specific HSV DNA sequences are responsible for determining the stability of tk gene expression in these cells.

(iii) By mapping the HSV DNA sequences present in one unstable HSVtk$^+$ cell line as well as those present in tk$^-$ revertant and tk$^+$ rerevertant derivative cell lines, we hoped to determine whether reversion was accompanied by the loss of either tk gene or non-tk gene viral DNA sequences.

(iv) By identifying those viral DNA sequences which are present in cells morphologically transformed by HSV, we hoped to identify the regions of the HSV genome which are involved in morphologic transformation. Specifically, in our initial experiments which are reported below, we have attempted to map the viral DNA sequences which are present in several of the morphologic transformants produced by Camacho and Spear following transfection of hamster embryo cells with the XbaI F fragment of HSV-1 (F) DNA (map coordinates 0.30-0.45).

RESULTS

Characterization of the Mapping Approach

Two different hybridization approaches have been

successfully employed in mapping the viral DNA sequences which are present in adenovirus and SV40 transformed cells (2, 3, 4, 35 and 40). These are liquid reassociation kinetics and the blot hybridization approach originally described by Botchan et al. (2 and 4). However, due to the complexity of the HSV genome, neither of these methods is ideally suited to the mapping of transformed cell associated HSV DNA sequences. Specifically, liquid reassociation kinetics using isolated restriction enzyme fragment probes require large numbers of hybridizations (due to the large size of the HSV genome) and consequently very large amounts of transformed cell DNA. Similarly, blot hybridizations using whole HSV DNA probes possess limited sensitivities (in our hands this approach did not allow detection of 5 copies per cell of a $2x10^6$ m.w. fragment of HSV DNA), whereas the use of isolated restriction enzyme fragment probes in such blot hybridizations is too tedious for the analysis of multiple cell lines. Consequently, we have developed a hybridization approach which combines the sensitivity needed to detect a small fraction of the HSV genome present in one copy per cell abundance with the ability to simultaneously map the viral sequences present in multiple cell lines(22).

This mapping approach, which has been described and characterized in a previous report (22), is shown in schematic form in Figure 1 and involves three sequential steps. In the first step, transformed cell DNA is randomly sheared to fragments of molecular weight $5-7x10^6$ and subjected to CsCl equilibrium density gradient centrifugation. Because HSV and cellular DNAs display widely different buoyant densities (1.726 and 1.729 gm/cm^3 for HSV-1 and HSV-2 DNAs, respectively (18), and 1.69-1.70 gm/cm^3 for cellular DNA), this step results in the partial purification of any viral DNA sequences which are present in the transformed cells. In the second step, the DNA banding at densities greater than or equal to 1.710 gm/cm^3 is labeled in vitro with

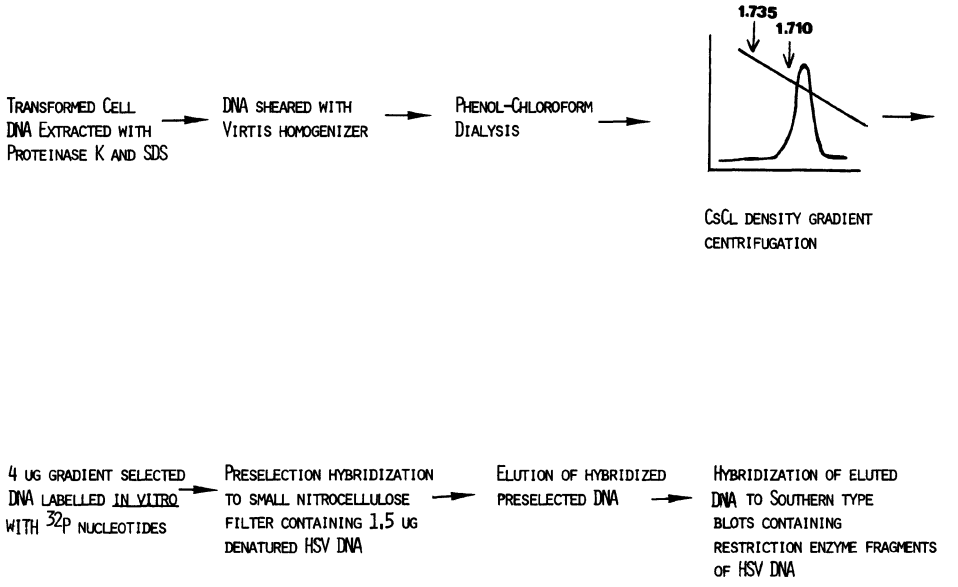

Figure 1--Diagrammatic representation of the hybridization approach. The individual steps of this approach have been described in detail elsewhere (22) and are summarized in the text.

α-32P nucleotides, and further enriched for viral DNA sequences by hybridization to a small nitrocellulose filter containing denatured unlabeled HSV DNA. Finally, the hybridized, labeled transformed cell DNA is eluted from the filters and rehybridized to Southern type blots containing unlabeled restriction enzyme fragments of HSV DNA (42). The resulting bands are visualized by autoradiography, and are identified by comparison to autoradiograms of replicate control blots which were hybridized to purified, in vitro labeled HSV DNA. In order to unambiguously map the HSV DNA sequences which were present in a given HSVtk$^+$ cell line, at least two different restriction enzyme cleavage patterns were used in the analysis of each cell line.

Previous reconstruction experiments have shown that this mapping approach possesses sufficient sensitivity to detect a piece of unintegrated viral DNA of molecular weight greater than or equal to $1x10^6$ which is present in an average abundance of one copy per cell (22). Because the mapping approach includes an initial CsCl density gradient fractionation it is possible that small pieces of integrated viral DNA would not be detected using this hybridization approach. However, theoretical considerations, assuming average buoyant densities for both the integrated viral DNA and the surrounding cellular DNA sequences (18), have shown that this procedure should allow the detection of integrated viral DNA sequences of molecular weight greater than $3.0x10^6$ which are present in an average abundance of one copy per cell (22).

Mapping of the HSV-1 and HSV-2 tk Genes

In order to map the HSV-1 and HSV-2 tk genes we have mapped the HSV DNA sequences which are present in a number of HSV-1tk$^+$ and HSV-2tk$^+$ transformed cell lines (8 and 32). These studies have been described in detail elsewhere (22; J. Leiden, N. Frenkel, D. Sabourin and R.

Davidson, manuscript submitted), and will be reviewed below. Briefly, DNA extracted from various passages of these cell lines was preselected and hybridized as described above to blots containing either the KpnI or EcoRI/HpaI restriction enzyme fragments of HSV-2 (G) DNA (in the case of HSV-2tk$^+$ cells), or the KpnI, BamHI and BglII/HindIII restriction enzyme fragments of HSV-1 strains Justin (Jus) or macroplaque (MP) DNAs (in the case of HSV-1tk$^+$ cells). An example of these hybridizations is seen in Figure 2, which shows the mapping data of cell line 33A$^+$, an HSV-2tk$^+$ cell line produced by Rapp and Turner (32) following infection of tk$^-$ NclA Cl10 mouse cells with UV light irradiated HSV-2 (333), and subsequent HAT selection (23). The results of this experiment (Figure 2) can be summarized as follows: (i) The maps generated from the two different restriction enzyme cleavages used in this experiment were in agreement, and indicated that this cell line contains a contiguous set of HSV-2 DNA sequences located between map coordinates 0.14 and 0.57. (ii) As seen in Figure 2, a comparison of the intensities of the bands produced by 33A$^+$ DNA with those produced by the 1 copy per cell reconstruction mixture, which was hybridized to replicate nitrocellulose blots, revealed that 33A$^+$ cells contain between 1 and 5 copies per cell of these HSV-2 DNA sequences. (iii) In order to assess the reproducibility of the mapping approach, two additional preparations of 33A$^+$ DNA (passages 60-70) were separately preselected and hybridized to different sets of filters and blots containing HSV-2 DNA. As can be seen in Figure 2, the three preparations of transformed cell DNA yielded identical hybridization patterns. Similar mapping analyses were performed on the DNA from three additional HSV-2tk$^+$ cell lines produced by Rapp and Turner (32) following infection of tk$^-$ mouse cells with UV light irradiated HSV-2 strains Silow, 333 and 324 (cell lines Silow, 39A$^+$ and 59D$^+$, respectively). In addition, we have mapped the HSV DNA sequences present in

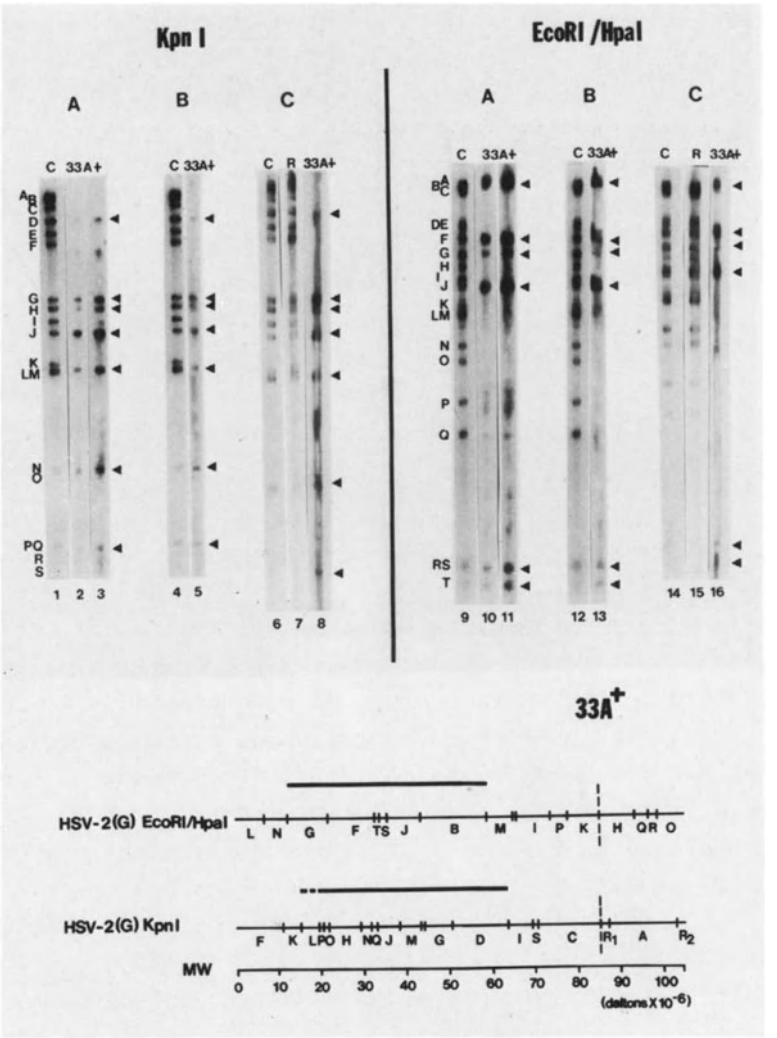

Figure 2--Mapping of the HSV-2 DNA sequences present in the HSV-2tk$^+$ cell line 33A$^+$. Top: Control DNA (purified in vitro labeled HSV-2 (G) DNA) (C) or in vitro labeled 33A$^+$ DNA (33A$^+$) was hybridized to nitrocellulose strips containing either the KpnI, or the EcoRI/HpaI restriction enzyme fragments of HSV-2 (G) DNA. A, B, and C show the autoradiograms from three separate hybridization experiments. (R) represents a 1 copy per cell reconstruction mixture produced by adding 3x10^{-2} μg of purified viral DNA to a lysate of 2x10^8 Cl1D tk$^-$ cells. Bottom: Schematic representation of the regions of homology between 33A$^+$ DNA and the KpnI, or EcoRI/HpaI restriction enzyme fragments of HSV-2 (G) DNA. The dotted line represents a region of uncertain homology, due to the ***comigration of the KpnI fragments L and M.***

two HSV-1tk$^+$ cell lines (8N and 5A) produced by Polacek and Roizman (unpublished results) following transfection of tk$^-$ mouse cells with randomly sheared HSV-1 (1023) DNA, as well as three HSV-1tk$^+$ cell lines (LH1, LH2 and LH3) produced by Davidson and coworkers following infection of tk$^-$ mouse cells with UV light irradiated HSV-1 (VR3) (8). The results of these studies are summarized in schematic form in Figures 3 and 4. As seen in these figures, the only HSV DNA sequences which are common to all HSVtk$^+$ transformants are those located between map coordinates 0.28 and 0.32. Thus, the HSV-1 and HSV-2 tk genes are colinear and the location of the HSV tk gene does not appear to vary between different strains of HSV.

Comparison of the HSV DNA Sequences Present in Stable and Unstable HSV-1tk$^+$ Cells

In order to ascertain whether specific viral DNA sequences are involved in determining the stability of tk gene expression in HSVtk$^+$ cells, we have mapped (J. Leiden, N. Frenkel, D. Sabourin and R. Davidson, manuscript submitted) the viral DNA sequences which are present in two unstable (LH1 and LH2) and one stable (LH3) HSV-1tk$^+$ cell lines produced by infection of tk$^-$ C1ID mouse cells with UV light irradiated HSV-1 (VR3) (8). An example of these mapping analyses is shown in Figure 5. The mapping data is summarized in Figure 4 and revealed the following: (i) The LH1 cells which display an unstable HSVtk$^+$ phenotype contain a single contiguous set of viral DNA sequences located between map coordinates 0.23 and 0.31. (ii) The LH2 cells which also display an unstable HSVtk$^+$ phenotype contain two sets of non-contiguous viral DNA sequences located between map coordinates 0.08-0.52 and 0.82-1.00. (iii) LH3 cells which stably express the viral gene contain a single contiguous set of viral DNA sequences located between map coordinates 0.11 and 0.42.

Thus, the stable LH3 cells contain all of the viral DNA sequences which were present in the unstable LH1 cells,

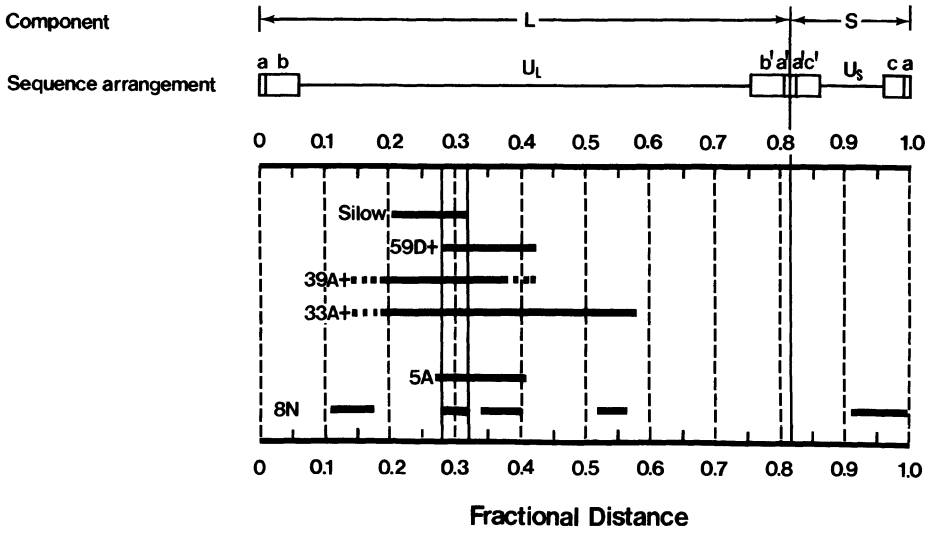

Figure 3--Summary of the mapping data of the HSV DNA sequences present in four HSV-2tk$^+$ cell lines (Silow, 59D$^+$, 39A$^+$, and 33A$^+$) produced by Rapp and Turner (32) following infection of tk$^-$ mouse cells with UV light irradiated HSV-2 and 2 HSV-1tk$^+$ transformed cell lines (8N and 5A) produced by Polacek and Roizman (unpublished results) following transfection of tk$^-$ mouse cells with randomly sheared HSV-1 (1023) DNA. The dotted lines represent a region of uncertain homology (see legend to figure 2). Data taken from Leiden et al. (22).

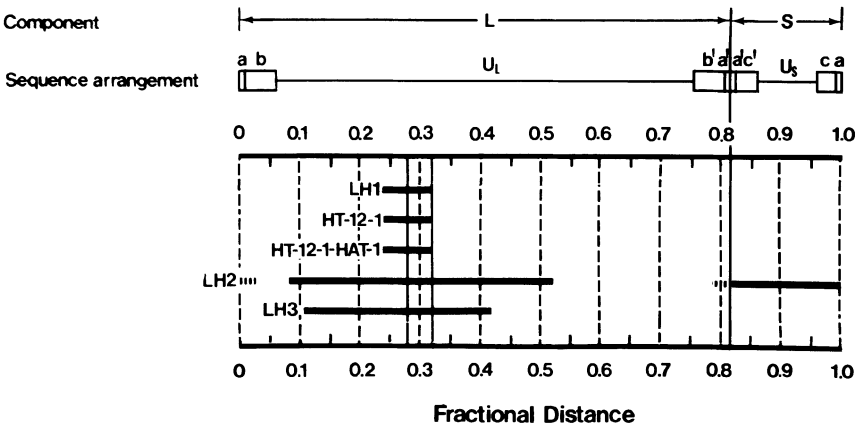

Figure 4--Summary of the mapping data of the HSV DNA sequences present in three HSV-1tk$^+$ cell lines (LH1, LH2 and LH3) produced by Davidson and coworkers (8) following infection of tk$^-$ mouse cells with UV light irradiated HSV-1 (VR3), as well as the HT-12-1 cell line, a revertant of LH1 cells, and the HT-12-1-HAT-1 cell line, a tk revertant of HT-12-1 cells (see Figure 6). Data taken from J. Leiden, N. Frenkel, D. Sabourin and R. Davidson, manuscript submitted for publication.

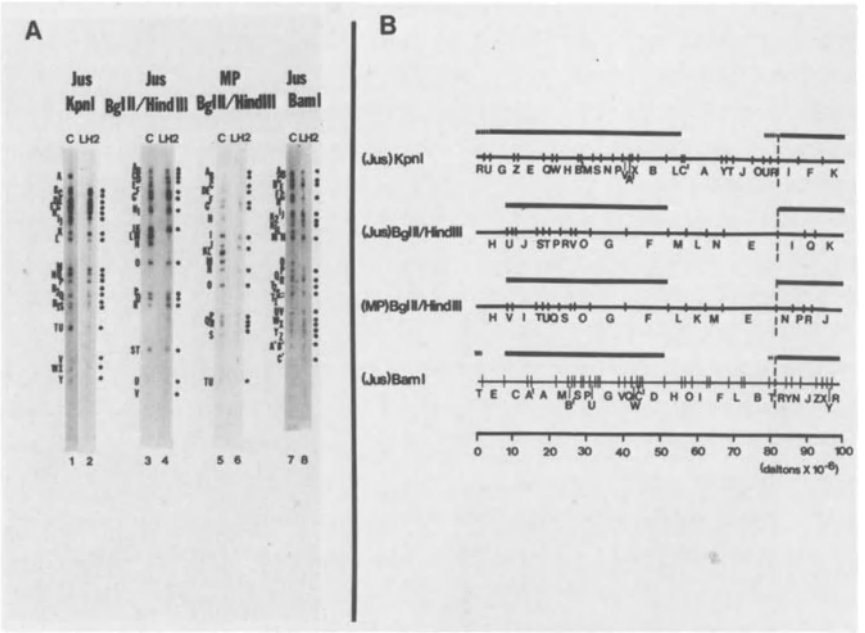

Figure 5--Mapping of the HSV-1 DNA sequences present in the unstable HSV-1tk$^+$ cell line LH2. A: Control (purified in vitro labeled HSV-1 DNA) (C) or in vitro labeled LH2 DNA which was pre-selected to enrich for viral DNA sequences, was hybridized to nitro-cellulose blots containing various restriction enzyme fragments of HSV-1 (MP) or HSV-1 (Jus) DNAs. KpnI fragments R_1 and R_2 and BamI fragments T_1 and T_2 are all derived from the ends of the L region and reflect the heterogeneity of the viral DNA sequences in this region of the HSV-1 genome (24 and 45). B: Schematic representation of the regions of homology between LH2 DNA and various restriction enzyme fragments of HSV-1 DNA. The BglII/HindIII restriction enzyme maps were taken from G.S. Hayward, T.G. Buchman and B. Roizman (unpublished results). The BamI and KpnI restriction maps were taken from reference 24.

while the unstable LH2 cells contain all of the viral sequences which were contained in the stable LH3 cells. Therefore the presence or absence of a specific set of viral DNA sequences does not appear sufficient, in itself, to determine the stability of the tk phenotype of an HSVtk$^+$ transformant.

Comparison of the HSV DNA Sequences Present in an Unstable HSV-1tk$^+$ Cell Line with those Present in tk$^-$ Revertant and tk$^+$ Rerevertant Derivative Cell Lines

In order to determine whether the reversion of HSVtk$^+$ cells to the tk$^-$ phenotype during propagation in non-selective medium was accompanied by the loss of either the tk gene or of specific non-tk gene viral DNA sequences, we have mapped (J. Leiden, N. Frenkel, D. Sabourin and R. Davidson, manuscript submitted) the viral DNA sequences which are present in one HSV-1tk$^+$ transformed cell line (LH1) as well as those present in tk$^-$ revertant (HT-12-1) and tk$^+$ rerevertant (HT-12-1-HAT-1) cells which were sequentially derived from the original LH1 HSVtk$^+$ cells as shown in Figure 6 (8). The results of these mapping analyses are summarized in Figure 4 and reveal that these three cell lines contain an identical set of viral DNA sequences located between map coordinates 0.23 and 0.31. Thus reversion and rereversion of the HSV-1tk$^+$ phenotype does not appear to involve changes in viral DNA content.

Mapping of the Viral DNA Sequences Present in Hamster Cells Morphologically Transformed with the XbaI F Fragment of HSV-1 DNA

As described above, Camacho and Spear (5) have recently found that transformed colonies could be reproducibly obtained from hamster embryo cells following transfection with the XbaI F fragment of HSV-1 (F) DNA, while few, if any, colonies were produced following transfection with the other XbaI fragments. In our efforts to identify

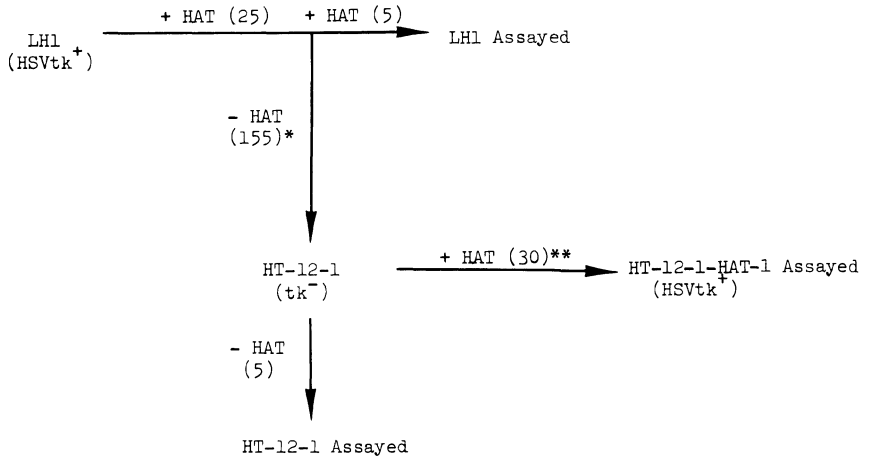

*Figure 6--Passage histories of cell lines LH1, HT-12-1 and HT-12-1-HAT-1. Numbers in parentheses represent numbers of population doublings in medium either containing or lacking HAT (23). *Following 25 cell doublings in HAT containing medium, LH1 cells were transferred to non-selective medium. HT-12-1 cells were derived from this culture by further propagation and two sequential cloning steps in non-selective medium. **Following 155 cell doublings in non-selective medium, HT-12-1 cells were transferred to HAT containing medium. HT-12-1-HAT-1 cells were derived from this culture by cloning and further propagation of the clone in HAT containing medium.*

those regions of the HSV genome which are involved in virally mediated morphologic transformation, we have attempted to map the HSV DNA sequences present in early passages (<15) of four of these cell lines. However, in no case have we been able to detect HSV DNA sequences in these cells (J.M. Leiden, N. Frenkel, A. Camacho and P.G. Spear, unpublished results). It should be noted that a 1 copy/cell reconstruction mixture analyzed side by side with the transformed cell DNA revealed that these experiments possessed sufficient sensitivity to detect a small fragment ($1x10^6$ m.w.) of unintegrated DNA which was present in an abundance of 1 copy/cell. However, as described above, the hybridization approach used in these studies might fail to detect small pieces of integrated viral DNA (<$3x10^6$ m.w. from previous theoretical calculations (22)).

DISCUSSION

Mapping of the HSV tk Gene

In the studies reported in this paper, we have employed a hybridization mapping approach which has allowed the simultaneous detection and identification of the HSV DNA sequences which are present in a number of $HSVtk^+$ transformed cell lines. The maps shown in Figures 3 and 4 indicate that the viral DNA sequences located between map coordinates 0.28 and 0.32 are the only viral sequences which are common to all $HSVtk^+$ transformed cells. Therefore, both the HSV-1 and HSV-2 tk genes are located between map coordinates 0.28 and 0.32 and this location does not vary between viral strains. These results are in accord with the findings of Morse et al. (29). However they are in disagreement with the results of Maitland and McDougall (26).

Patterns of Incorporation of HSV DNA Sequences into HSVtk$^+$ Cells

In addition to the viral DNA sequences located between map coordinates 0.28 and 0.32, all of the HSVtk$^+$ transformed cell lines which we have tested contain substantial, but variable amounts of non-tk gene viral DNA sequences located between map coordinates 0.06-0.58 and 0.82-1.00. Therefore it would appear that incorporation of these non-tk gene viral DNA sequences into HSVtk$^+$ cells is a relatively random event. The results shown in Figures 3 and 4 have also revealed that there are two regions of the viral genome which are uniformly absent from all of the HSVtk$^+$ transformed cell lines which we have studied. These regions are located between map coordinates 0-0.06 and 0.58-0.82. One can envision at least two alternative explanations for the uniform absence of these viral DNA sequences. First, these sequences may contain non-suppressible viral lytic functions. Thus, any cell originally containing them would be unable to survive. In this light it is interesting to note that Morse et al. (29) have mapped a host shut-off function between coordinates 0.52 and 0.59 on the HSV-2 genome. Alternatively, the sequences which are uniformly deleted from the transformed cells could contain early (α) viral functions which are needed to turn on the expression of lytic viral functions located elsewhere on the genome (15). Thus the absence of these regions could assure the lack of expression of late viral lytic functions. This possibility is especially attractive in view of recent studies which have indicated that some of the early viral genes are located within the inverted repeat regions of the L component of HSV DNA as well as between map coordinates 0.56 and 0.79 (6, 16, 29, 31 and L. Morse and B. Roizman, unpublished observations).

Finally, it should also be noted that most, if not all, of the UV light irradiated HSV produced cell lines appear to contain a single contiguous sequence of HSV DNA,

whereas 8N cells which were produced by transfection of tk^- cells with sheared HSV DNA, clearly contain a large number of non-contiguous HSV DNA sequences. This difference might reflect the fact that DNA transfections result in the incorporation of multiple DNA fragments into the same cell. Moreover, the finding of the multiple non-contiguous sets of HSV DNA sequences in 8N cells indicates that the incorporation of viral DNA fragments during HSV mediated tk transformation is a relatively random process, i.e. that any piece of viral DNA which does not encode non-suppressible lytic HSV functions could be incorporated into the cells during HSV mediated tk transformation.

Regulation of the Cell Associated HSV tk Gene

Our analyses of several $HSVtk^+$ cell lines, differing with respect to the stability of their tk phenotypes, have a number of implications as regards the regulation of viral tk gene expression in these cells. First, our findings indicate that both the expression of the viral tk gene during passaging of $HSVtk^+$ cells in selective HAT containing medium and the stability of this expression during propagation of the cells in non-selective medium are most likely under cellular rather than viral control. Specifically, our finding that the stable and unstable $HSVtk^+$ transformed cells contain the same or overlapping sets of viral DNA sequences surrounding their tk genes suggests that cellular rather than viral DNA sequences determine the stability of viral tk gene expression during propagation of $HSVtk^+$ cells in non-selective medium. Furthermore, as discussed above, our studies have revealed that most of these $HSVtk^+$ cell lines do not contain the HSV DNA sequences which have thus far been shown to encode the early (α) viral regulatory genes. Therefore, the regulation of tk gene expression in these $HSVtk^+$ cells would appear to be different from that known to occur during lytic HSV infections, in which viral tk gene expression has been

shown to be dependent upon the presence of functional early (α) viral polypeptides (14, 15 and R. Honess and B. Roizman, unpublished results). This hypothesis is in agreement with the findings of Wigler et al. (46), who have shown that a single 3.4 kilobase fragment of HSV DNA is sufficient to transform tk^- mouse cells to the $HSVtk^+$ phenotype.

Our observation that reversion and rereversion of the $HSVtk^+$ phenotype are not accompanied by changes in the complexity of the cell associated viral DNA sequences confirms previous genetic data which suggested that most, if not all, of the tk^- revertant cells produced upon propagation of unstable $HSVtk^+$ cells in non-selective medium retained the viral tk gene (8). In this light, it is interesting to note that Kraiselburd et al. (20) have previously reported that a tk^- revertant of an $HSVtk^+$ cell line, which was selected by growth of the $HSVtk^+$ cells in BudR containing medium (as opposed to the more gradual reversion seen upon propagation in non-selective medium), had lost all detectable HSV DNA sequences. Thus, it appears that different mechanisms may be responsible for reversion of the $HSVtk^+$ phenotype, and that these different mechanisms may depend upon the type of selection employed in obtaining the revertants.

Given that reversion of $HSVtk^+$ cells to the tk^- phenotype during propagation of the cells in non-selective medium does not involve changes in the complexity of the cell associated viral DNA sequences, one can envision at least three alternative models which could explain this reversion phenomenon. First, reversion could involve the elaboration of a repressor substance of either cellular or viral origin, which acts upon a specific viral or cellular promoter to prevent expression of the viral tk gene. However, evidence has been reported which makes this model unlikely. Specifically, it has been shown that the fusion of tk^- revertant HT-12-1 cells with parental $HSVtk^+$ LH1 cells

did not result in the inhibition of viral tk gene expression in the hybrid cells (17). Second, reversion could involve small changes in the number of copies per cell of the viral tk gene. Such changes would not be detected by our hybridization assay. Finally, reversion could involve a structural change either in the viral tk gene or in the cellular DNA sequences surrounding an integrated viral gene. For example, high rate mutation, changes in the viral integration site, the insertion of a foreign piece of DNA either into the tk gene or into surrounding cellular DNA sequences, or base modification of the viral gene, could all result in alterations in viral tk gene expression.

Lack of Detectable HSV DNA Sequences in Morphologic Transformants

There are at least two possible explanations for our failure to detect HSV DNA sequences in the morphologically transformed hamster cells produced by Camacho and Spear following transfection of primary hamster cells with the XbaI F fragment of HSV-1 DNA (5). First, it is possible that the morphologic transformants do contain HSV DNA sequences, but that these sequences are incorporated into the transformed cells in pieces which are too small to be detected by the hybridization approach which we have used in these studies. If this were the case for all of the morphologic transformants tested, it would indicate a fundamental difference in the way these morphologic transformants and $HSVtk^+$ cells incorporate viral DNA. One can envision at least three such differences. First, the morphologic transformants were all produced by transfection with a DNA fragment of m.w.=$15x10^6$, whereas the $HSVtk^+$ cells which we have analyzed were transformed either with UV light irradiated virus or with HSV DNA sheared to m.w.=$20-30x10^6$. Second, all of the $HSVtk^+$ transformants were mouse cell lines while the morphologic transformants were all derived from primary hamster cells. Thus, it is possible that ham-

ster cells incorporate smaller pieces of viral DNA than their mouse cell counterparts. Finally, the viral genes surrounding the HSV transforming gene may be selected against during HSV mediated transformation, resulting in the survival of those cells containing only the transforming gene with little or no surrounding viral DNA sequences. This would be the case, for example, if the sequences surrounding the transforming gene encode non-suppressible lytic functions. However, as seen in Figures 3 and 4, several of the HSVtk$^+$ cells contain the viral sequences corresponding to the entire HSV-1 XbaI F fragment, making it unlikely that these sequences are selected against during HSV mediated morphologic transformation.

An alternative explanation for our failure to detect HSV DNA sequences in the HSV-1 morphologically transformed cells is that these cells are indeed, devoid of viral DNA. Thus, it is possible that HSV-1 DNA sequences are needed for the initiation of transformation, but are subsequently lost from the transformed cells, with or without the loss of the transformed phenotype. If the transformed phenotype remains even after the viral DNA sequences have been lost, this would represent a novel type of "hit and run" transformation in which continued viral gene expression is not required for the maintenance of the transformed phenotype. Due to the lack of temperature sensitive mutants in the putative HSV-1 transforming gene, it has thus far been impossible to assess the importance of continued viral gene expression in maintaining the transformed phenotype. However, recent studies of papovavirus transformed cells have revealed that the requirements for continued expression of viral transforming genes for the maintenance of the transformed phenotype vary with the type of selective conditions employed in the initial transformation assay (37-39). In this light, it should also be noted that the hamster transformed cell lines produced by Duff and Rapp (10) using UV light irradiated HSV in focus

formation assays, have been shown to retain their transformed phenotypes, even following prolonged propagation in culture, and have also been found to retain HSV-2 DNA sequences (12 and reviewed in 13).

If both the viral DNA sequences and the transformed phenotype are simultaneously lost from the HSV-1 morphologically transformed cells, this would represent an abortive type of transformation similar to that previously reported for papovaviruses (36, 43 and 44). One can envision several possible factors which could predispose to such abortive transformation. First, the morphologic transformants which we have analyzed were maintained in low serum only during the initial colony formation and were thereafter propagated in medium containing 10% serum. In this respect, they are different from the HSVtk$^+$ cells which were continuously propagated under selective conditions for at least 25 passages prior to transfer to non-selective medium. Therefore, it is possible that a longer selection period may be required for stabilization of the transformed phenotype. Alternatively, the function contained in the XbaI F fragment as assayed by Camacho and Spear (5) may only be one of several functions required for stable HSV mediated transformation. Thus, one could envision a stabilizing and/or a synergistic transformation gene located elsewhere on the genome which would be lacking in cells transformed with the XbaI F fragment alone. Finally, the function assayed by Camacho and Spear in their low serum assay may be a cell proliferation inducing function which allows the primary cells to grow in low serum but is unrelated to the putative HSV transforming gene.

ACKNOWLEDGMENTS

We thank Drs. Rapp, Davidson, Roizman, Camacho and Spear for supplying the cell lines used in these studies, and Drs. Roizman and Spear for useful comments on this manuscript.

This work was supported by U.S. Public Health Service research grants AI-15488 and CA-19264, from the National Cancer Institute, and by National Science Foundation grant PCM78-16298. JML was a predoctoral fellow supported by USPHS grant 5-T32 HD-07009-03.

REFERENCES

1. Bacchetti, S. and Graham, F. Proc. Natl. Acad. Sci USA 74:1590-1594, 1977.
2. Botchan, M.R. and McKenna, G. Cold Spring Harbor Symp. Quant. Biol. 38:383-395, 1973.
3. Botchan, M.R., Ozanne, B., Sugden, B., Sharp, P.A. and Sambrook, J. Proc. Natl. Acad. Sci. USA 71:4183-4187, 1974.
4. Botchan, M., Topp, W. and Sambrook, J. Cell 9:269-287, 1976.
5. Camacho, A. and Spear, P.G. Cell 15:993-1002, 1978.
6. Clements, J.B., Watson, R.J. and Wilkie, N.M. Cell 12:275-285, 1977.
7. Darai, G. and Munk, K. Nature New Biol. 241:268-269, 1973.
8. Davidson, R., Adelstein, S. and Oxman, M. Proc. Natl. Acad. Sci. USA 70:1912-1916, 1973.
9. Davis, D.B. and Kingsbury, D.T. J. Virol. 17:788-793, 1976.
10. Duff, R. and Rapp, F. J. Virol. 8:469-477, 1971.
11. Duff, R., Kreider, J.W., Levy, B.M., Katz, M. and Rapp, F. J. Nat. Cancer Inst. 53:1159-1164, 1974.
12. Frenkel, N., Locker, H., Cox, B., Roizman, B. and Rapp, F. J. Virol. 18:885-893, 1976.
13. Frenkel, N. and Leiden, J. In: Integration and Excision of DNA Molecules (Eds. P. Hofschneider and P. Starlinger), Heidelberg, Germany, Springer-Verlag Press, pp. 71-77, 1978.
14. Garfinkle, B. and McAuslan, B. Biochem. Biophys. Res. Comm. 58:822-829, 1974.
15. Honess, R.W. and Roizman, B. Proc. Natl. Acad. Sci. USA 72:1276-1295, 1975.
16. Jones, P.C., Hayward, G.S. and Roizman, B. J. Virol. 21:268-276, 1977.
17. Kaufman, E.R. and Davidson, R.L. Somatic Cell Genet. 1:153-164, 1975.
18. Kieff, E.D., Bachenheimer, S. and Roizman, B. J. Virol. 8:125-132, 1971.

19. Kimura, S., Flannery, V.L., Levy, B. and Schaffer, P.A. Int. J. Cancer 15:786-798, 1975.

20. Kraiselburd, E., Gage, L.P. and Weissbach, A. J. Mol. Biol. 97:533-542, 1975.

21. Kucera, L.S. and Gudson, J.P. J. gen. Virol. 30: 257-261, 1976.

22. Leiden, J.M., Frenkel, N. and Rapp, F. J. Virol. 33:272-285, 1980.

23. Littlefield, J. Science 145:709-710, 1964.

24. Locker, H. and Frenkel, N. J. Virol. 32:429-441, 1979.

25. MacNab, J.C.M. J. gen. Virol. 24:143-153, 1974.

26. Maitland, N.J. and McDougall, J.K. Cell 11:233-241, 1977.

27. Minson, A.C., Thouless, M.E., Eglin, R.P. and Darby, G. Cancer 17:493-500, 1976.

28. Minson, A.C., Wildy, P., Buchan, A. and Darby, G. Cell 13:581-587, 1978.

29. Morse, L.S., Pereira, L., Roizman, B. and Schaffer, P.A. J. Virol. 26:389-410, 1978.

30. Munyon, W., Kraiselburd, W., Davis, D. and Mann, J. J. Virol. 7:813-820, 1971.

31. Preston, V.G., Davison, A.J., Marsden, H.S., Timbury, M.C., Subak-Sharpe, J.H. and Wilkie, N.M. J. Virol. 28:499-517, 1978.

32. Rapp, F. and Turner, N. Arch. Virol. 56:77-87,1978.

33. Rassoulzadegan, M., Seif, R. and Cuzin, F. J. Virol. 28:421-426, 1978.

34. Roizman, B. Cell 16:481-494, 1979.

35. Sambrook, J., Botchan, M., Gallimore, P., Ozanne, B., Pettersson, U., Williams, J. and Sharp, P.A. Cold Spring Harbor Symp. Quant. Biol. 39:615-632, 1974.

36. Schlegel, R. and Benjamin, T.L. Cell 14:587-599,1978.

37. Seif, R. and Cuzin, F. J. Virol. 24:721-728, 1977.

38. Seif, R. and Martin, R.G. J. Virol. 31:350-359, 1979.

39. Seif, R. and Martin, R.G. J. Virol. 32:979-988, 1979.

40. Sharp, P.A., Pettersson, U. and Sambrook, J. J. Mol. Biol. 86:709-726, 1974.

41. Shin, S.-I., Freedman, V.H., Risser, R. and Pollacek, R. Proc. Natl. Acad. Sci. USA 72:4435-4439, 1975.

42. Southern, E.M. J. Mol. Biol. 98:503-517, 1975.

43. Stocker, M. Nature 218:234-238, 1968.

44. Stocker, M. and Dulbecoo, R. Nature 223:397-398,1969.

45. Wagner, M.J. and Summers, W.C. J. Virol. 27:374-387, 1978.

46. Wigler, M., Silverstein, S., Lee, L., Pellicer, A., Cheng, Y. and Axel, R. Cell 11:223-232, 1977.

13. Transfection with HSV DNA fragments and DNA from HSV transformed cells

G. Darby, K.F. Bastow and A.C. Minson

1. GENERAL INTRODUCTION

1.1. The thymidine kinase gene of herpes simplex virus

Herpes simplex (HSV) possesses a gene coding for the enzyme thymidine kinase (TK). The primary role of this enzyme in the infected cell is the phosphorylation of thymidine to the monophosphate, although it has recently become apparent that the same enzyme is involved in the phosphorylation of TMP to TDP (1). Although experiments in tissue culture have suggested that possession of this enzyme by the virus is a luxury which it can do without (2), more recent studies on the pathogenicity of the virus and TK^- mutants have pointed to an important role for the enzyme in animal infections (3,4,5).

The location of the TK gene has been mapped for HSV types 1 and 2 and in each case it lies about 0.3 map units from the left hand end in the long unique region of the DNA (6,7,8). The gene product responsible for the enzyme activity has also been identified in both type 1 and type 2 infected cells and it is a polypeptide of approximately 40,000 molecular weight (9,10).

Expression of the virus TK gene in the infected cell is regulated by other virus functions and transcription of the gene is initiated only after 'immediate early' or α-proteins have been produced (11). For type 1 virus it has been shown that the gene product VP 175 (12) must be present for expression of TK and a similar situation probably pertains in cells infected with type 2.

Y. Becker (ed), Herpesvirus DNA.

1.2. Cellular synthesis of TMP

The TK gene of HSV may be introduced into eukaryotic cells which lack the ability to induce their own thymidine kinase. This process relies on our ability to manipulate the cellular machinery for the synthesis of TMP. The normal eukaryotic cell has available two pathways which lead to the synthesis of this mononucleotide (Figure 1).

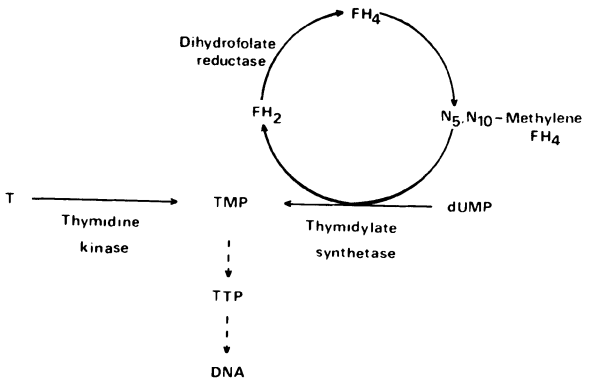

Figure 1 Pathways for the synthesis of TMP

Exogenous thymidine may be phosphorylated directly by the cellular thymidine kinase or alternatively dUMP may be methylated by the enzyme thymidylate synthetase. It is essential for a dividing cell to have available one or other of these pathways or it will be deprived of an essential ingredient required for DNA synthesis. However, both pathways can be manipulated by the use of appropriate drugs and it is this which forms the basis of 'biochemical' transformation.

1.3. Principles of 'biochemical' transformation

The term 'biochemical' transformation implies the incorporation into a cell of foreign DNA sequences which encode specific biochemical functions required for the survival of the cell in a particular selection system. To introduce the HSV TK gene the first requirement is a cell which has a TK^- phenotype. Such cells may be derived from normal cells by passage in the presence of the thymidine analogue, 5-bromo-2'-deoxyuridine (BUdR) (13). The drug is phosphorylated by the cellular TK and ultimately incorporated into DNA. This is lethal and the cell dies. However if the cell fails to synthesise TK the drug cannot be phosphorylated and the cell survives. Such a system permits the selection of phenotypically TK^- cells which must rely solely on the thymidylate synthetase pathway for the provision of TMP and indirectly for their ability to synthesise DNA and undergo division.

Cells which cannot phosphorylate thymidine are extremely sensitive to dihydrofolate analogues such as methotrexate, since these block the function of dihydrofolate reductase and therefore the methylation of dUMP (Figure 1). It was Munyon and his co-workers who recognized several years ago that if TK^- cells could be provided with a replacement TK gene they might survive in the presence of dihydrofolate analogues. This led them to perform the first 'biochemical' transformations, using ultraviolet-irradiated HSV as the gene donor and LTK^- cells as the recipients (14).

Subsequently several groups demonstrated that the same transformation could be accomplished using fragments of the virus genome as gene donor by exploiting techniques developed for infecting cells with naked DNA (15) to introduce the virus sequences into the cells. It could be done with specific restriction fragments derived from the virus DNA (7) or with those produced by random shearing of the genome (16,17). Transformed cell DNA (17) and more recently normal cellular DNA have also been used as a source of a TK gene (18).

1.4. Summary

In this chapter we review the properties of several 'biochemically' transformed cell lines generated in this laboratory using both randomly sheared HSV-2 DNA and Hind III restriction fragments as the gene source. Evidence will be presented which shows that the DNA is integrated into the host cell chromosome, that non-selected virus genes may also be incorporated and expressed under appropriate conditions, and also that the virus TK gene in the transformed cell is likely to be under the control of host cell promoters.

The isolation of phenotypically TK^- revertants using selection in either BUdR or acyclovir (9-(2-hydroxyethoxymethyl)guanine) is described and possible mechanisms to explain the generation of these revertants are discussed.

Finally we describe the transformation of $LMTK^-$ cells to TK^+ phenotype using transformed cell DNA as the gene source and we discuss the properties of the cell lines derived.

2. THE GENERATION OF 'BIOCHEMICALLY' TRANSFORMED CELLS

The method used to transform cells (17) involved co-precipitation of HSV DNA fragments and carrier DNA with calcium phosphate, followed by treatment of $LMTK^-$ cells with the precipitate. Two days after exposure to DNA, cells were transferred into selective medium containing methotrexate and maintained subsequently in that medium. Visible colonies appeared after about 2 weeks and cell lines were generated from selected clones.

A series of clonally unrelated lines were produced using as gene donor sheared HSV-2 DNA (approximately $10 - 20 \times 10^6$ daltons molecular weight). The 9 cell lines produced in this way all expressed HSV-specific TK since the enzyme activities in cell extracts could be inactivated by incubation with hyperimmune rabbit serum prepared against

HSV-2 infected rabbit kidney cells (17). Furthermore, in three lines examined in detail, expression of the virus gene appeared to be a stable character which was not affected significantly by extensive passage in either selective or non-selective medium (19). It was also noticeable that although the enzyme levels in lines varied over a four-fold range the level in a particular line appeared to be fairly constant and characteristic of that line (19).

A further series of four cell lines were isolated following transformation of LMTK$^-$ cells with Hind III-digested HSV-2 DNA as gene donor. These lines also expressed the virus coded enzyme.

The cell lines of the D2 series ($D2_1$, $D2_2$ etc.) were transformed with sheared fragments of HSV-2 DNA and those of the H2 series with Hin restriction endonuclease fragments.

3. PROPERTIES OF 'BIOCHEMICALLY' TRANSFORMED CELLS

Although it was relatively straightforward to demonstrate that transformed cells expressed virus specific TK and it was undoubtedly this character which permitted their survival in methotrexate, further characterization of the virus-specific sequences in the cells proved more difficult. We approached this problem in two ways, firstly using molecular hybridization techniques to define virus DNA sequences present and secondly using genetic complementation to reveal non-selected virus genes.

3.1. Virus DNA content of transformed cells

To define the DNA sequences of virus origin carried in our cell lines a prerequisite was a detailed physical map of the virus genome. This is illustrated in Figure 2 which shows the Eco Rl and Bam Hl sites for the entire genome

(20,21) and the fine structure map of the Sal 1 g fragment which encodes the TK gene (provided by Dr. Gary Hayward). Work of Reyes, McNight and Hayward (personal communication) has shown that the smallest sequence derived from the Sal g fragment which can be used to transform cells is that bordered by a Pvu II site at 0.300 and the Bgl II site at 0.314 map units. We therefore assume that the structural gene for TK lies between these co-ordinates and the cells which express virus TK must possess sequences derived from this region. It should also be noted that there are Bam and Eco restriction sites within the structural gene and digestion with either of these enzymes destroys the transforming capacity of the virus DNA.

We have used three approaches to define virus sequences in our transformed cells; kinetic hybridization (Cot analysis) using ^{125}I-labelled Eco fragments of HSV-2 DNA as probes, Southern blot hybridization (22) using Bam restricted transformed cell DNA and ^{125}I-labelled HSV-2 DNA as probe, and finally blot hybridization using cell DNA cut with a variety of restriction enzymes or combinations of enzymes and ^{32}P-labelled Sal g fragment as probe (a clone of this fragment in PBR322 was provided by Dr. Gary Hayward).

3.1.1. Kinetic hybridization

Solution hybridization has a number of severe disadvantages when compared with blotting methods. The experiments are tedious and large quantities of valuable materials are required. Nevertheless they have the advantage that in theory the data generated are quantitative. We have used this approach to look at the sequences in two of our cell lines, $D2_1$ and $D2_5$ (8).

Initially HSV-2 DNA was digested with Eco and the fragments separated by agarose gel electrophoresis. The individual fragments were labelled in vitro with ^{125}I to high specific activity and each was then used in kinetic hybridization experiments. Fragments were denatured and their reannealing rates measured in the presence of high

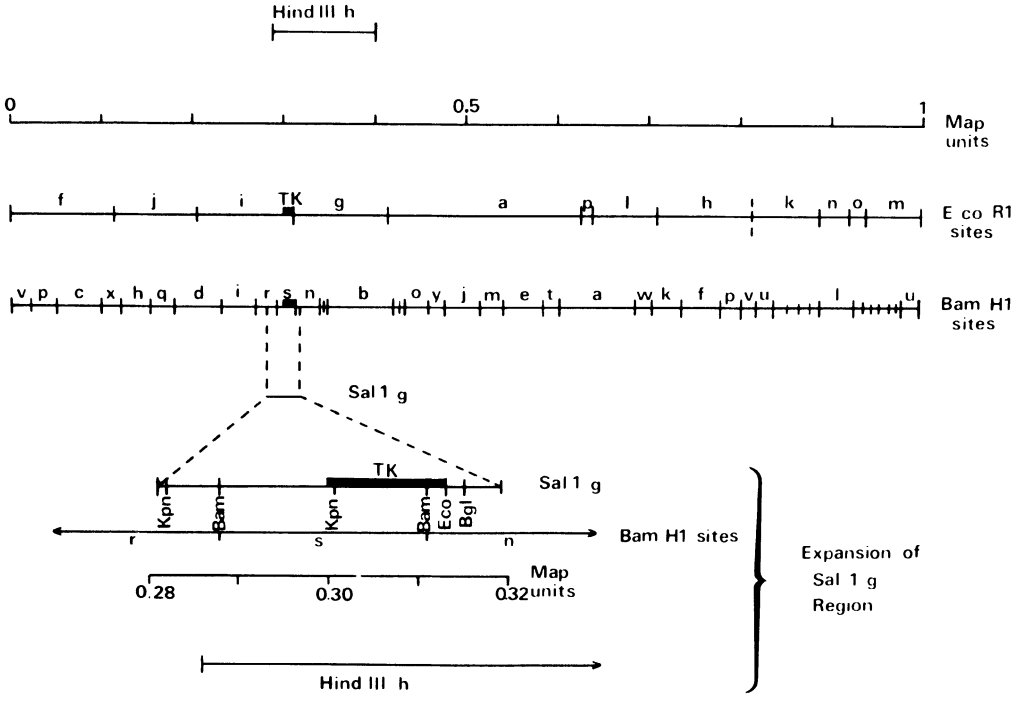

Figure 2 Physical maps of the HSV-2 genome

concentrations of transformed cell DNAs or control DNAs at similar concentrations. Higher annealing rates in the presence of transformed cell DNA compared to control indicated the presence of complementary sequences. Reconstruction experiments (where 1 genome of virus DNA per haploid cell DNA equivalent was added to each fragment) were also carried out.

The results of these experiments (summarized in Figure 3) showed that $D2_1$ contained sequences represented in Eco fragments i, g and possibly j and that $D2_5$ had sequences

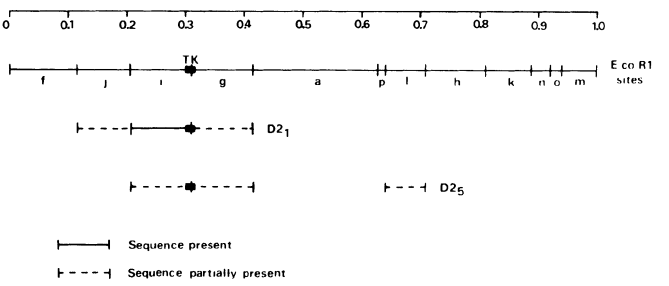

Figure 3

Virus sequences in $D2_1$ and $D2_5$ defined by Cot analysis

from fragments i, g and l. The Eco cut in the TK gene separates the i and g fragments and so it was anticipated that all lines would contain some sequences derived from these. The sequence concentrations were of the order of 1 genome per cell and so in interpreting the data we have assumed that there is no duplication of virus information. It is worth noting that $D2_5$ appears to have two virus DNA inserts which are non-contiguous and it is likely that these represent independent integration events.

3.1.2. Southern blot hybridization using ^{125}I-labelled HSV DNA as probe

A more detailed analysis of the virus DNA sequences present was possible using blotting techniques. Transformed cell DNA was digested with Bam and the fragments separated by agarose gel electrophoresis. They were then transferred to nitrocellulose paper by blotting and hybridized with high specific activity ^{125}I-labelled HSV-2 DNA. This approach is illustrated in Figure 4 where the line $D2_5$ has been analysed.

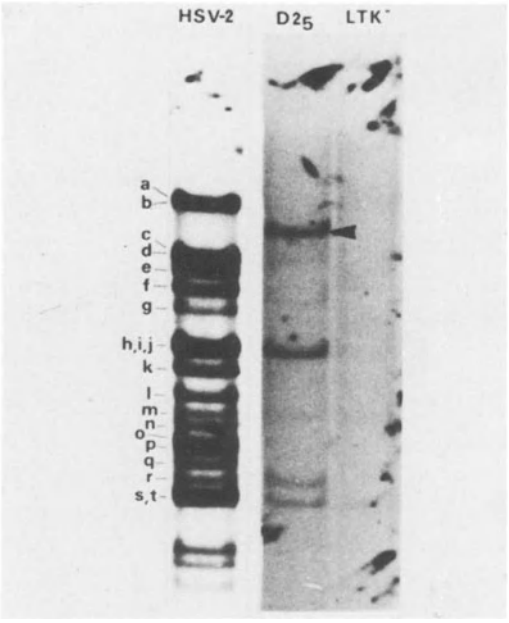

Figure 4 $D2_5$ Bam digests analysed with HSV probe ^{125}I-labelled HSV-2 DNA used to detect fragments containing virus DNA generated by Bam digestion of $D2_5$ DNA. The controls were LMTK$^-$ DNA and HSV-2 DNA digested with Bam. The arrow indicates a band derived from $D2_5$ which did not migrate with any of the fragments from HSV-2 DNA.

The interpretation of the data is complicated by the co-migration of several fragments derived from virus DNA. A fragment was derived from $D2_5$ which co-migrated with Bam r. A second co-ran with the Bam s and Bam t fragments

from virus DNA, but since we know from Cot analysis that Bam t is not present in $D2_5$ DNA this fragment almost certainly corresponds with Bam s. Such an interpretation appears reasonable in view of the fact that the TK structural gene is known to include sequences in Bam s. A band co-migrated with the three virus-derived fragments Bam h, i & j. Since we know from Cot analysis that Bam h and Bam j are not represented in $D2_5$, this fragment is likely to correspond with Bam i. A fourth band did not co-run with any virus-derived fragment and assignment of the origin of this sequence required more detailed analysis with the Sal g probe (see below).

3.1.3. Southern blot hybridization using ^{32}P-labelled Sal g probe

The sequences around the TK gene was mapped in finer detail using the Sal g fragment of HSV 2 DNA as a probe. This fragment overlaps the Bam fragments r, s and n (Figure 2). The cloned fragment was labelled in vitro by nick translation, with ^{32}P and hybridized to blots of restricted transformed cell DNAs (Figure 5).

The Bam fragments r and s were detected in the Bam digest of $D2_5$ DNA using this probe, but as expected the i fragment was not. The high molecular weight fragment was also detected and this implies that this fragment must contain virus sequences from Bam n. Since the fragment is considerably larger than n it must also contain flanking host sequences and this is an indication that the virus fragment was integrated into the host chromosome.

An analysis of $D2_3$ DNA is also shown. This is of interest since we were unable to detect any virus specific bands in $D2_3$ using total DNA probe. Using the Sal g probe we detected 2 virus-specific bands in the Bam digest (Figure 5). Neither co-migrated with fragments detected in a Bam digest of virus DNA (Bam r, s or n). Since the TK gene spans the junction between Bam s and n it is likely that the fragments derived from $D2_3$ were generated by a Bam cut at this site and two additional cuts in flanking

host sequences. Such a model explains the generation of large fragments which have sequences in common with the Sal g probe.

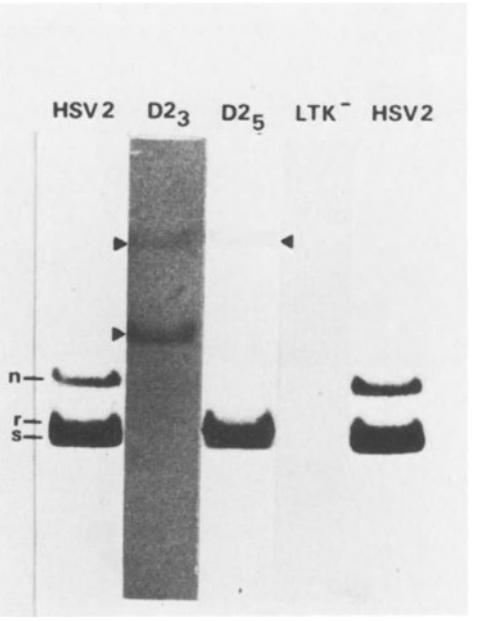

Figure 5 D2$_5$ & D2$_3$ Bam digests analysed with Sal g probe

^{32}P-Labelled Sal g was used to detect bands containing virus sequences derived from the Sal g region generated by Bam digestion of D2$_3$ and D2$_5$ DNAs. No bands were detected in the LMTK$^-$ DNA control and as expected (see Figure 2) 3 bands (n, r & s) were detected in the control digest of HSV-2 DNA. The arrows indicate bands from transformed cell DNAs which failed to migrate with any of those derived from virus DNA.

D2$_5$ and D2$_3$ DNAs were further analysed using four restriction enzymes (Eco, Sal, Bgl and Kpn I). The arguments used in interpretation of the data are similar to those above and allow us to define the restriction sites present in the inserted fragments. In the case of D2$_5$ the analysis did not alter the assignment of sequences at the left hand end of the integrated virus sequences. Extra information was, however, generated concerning the right hand end of the fragment. This is illustrated by

the Kpn/Bgl double digest (Figure 6). Three bands were detected in the digest of virus DNA. The larger band was

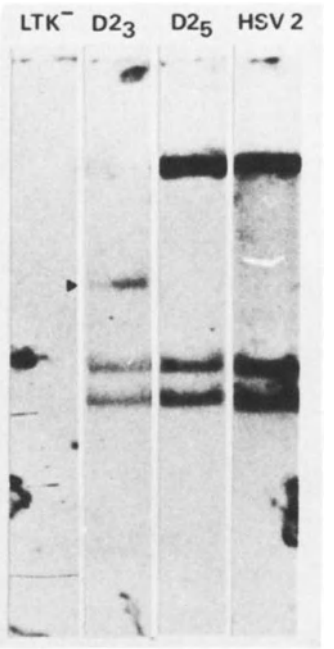

Figure 6

$D2_5$ & $D2_3$ Kpn/Bgl double digests analysed with Sal g probe

^{32}P-Labelled Sal g was used to detect virus sequences derived from this region in bands generated by Kpn/Bgl digestion of $D2_3$ and $D2_5$ DNAs. No bands were detected in the LMTK⁻ DNA control. As predicted, (Figure 7), 3 bands were detected in the HSV-2 digest. The arrow indicates a band which failed to migrate with any of those derived from virus DNA.

the Kpn/Kpn fragment which spans the junction between Bam r and s (Figure 7). The smaller bands were the Kpn/Bgl fragment spanning Bam s and n and the Bgl/Kpn fragment contained within Bam n. All three were detected in digests of $D2_5$ DNA. These results therefore show that the virus DNA insert in $D2_5$ DNA extends rightwards further than the Kpn site in Bam n. Only the two smaller bands were present in $D2_3$ DNA showing that the virus insert in these cells extends rightwards past the Kpn site in Bam n and leftwards

past the Kpn site in Bam s. Other digests were consistent with these interpretations.

These experiments have been repeated with a number of cell lines and the data are summarized in Figure 7. The situation with $D2_1$ is complex but can best be explained by the presence of two virus DNA sequences both containing the TK gene.

3.2. Topography of integrated virus sequences

Several interesting features emerge from an examination of sequences represented in transformed lines.

Our results so far are consistent with those of Reyes et al. (personal communication) in that all cell lines contain the minimum virus sequence required for TK transformation.

The Hin fragment which contains the TK gene is Hin h. This is a large fragment of 12 x 10^6 molecular weight which spans the region from 0.28 to 0.40 map units (Figure 6). However it is clear from data in Figure 7 that only a subset of these sequences are present in the H2 lines. None of the lines analysed contained sequences derived from the right hand half of the fragment (0.33 - 0.4 map units). One line contained essentially all sequences from the left hand end ($H2_3$). It is difficult to know whether any special significance should be attached to the loss of right hand sequences since the TK gene itself is towards the left hand end of the fragment and there will only be positive selection operating for this region. However it is apparent from data on lines transformed with sheared DNA that large virus sequences may be incorporated. $D2_1$ appears to have a contiguous insertion of a virus DNA fragment 20 - 25 x 10^6 molecular weight, the fragment in $D2_5$ is 9 - 14 x 10^6 and that in $D2_6$ is 5 - 8 x 10^6. Hence there is no obvious reason why the Hin transforming fragment should have been trimmed in size. Nevertheless, a common feature of the lines, both of the D2 and H2 series, with the single possible

exception of $D2_1$, is that virus sequences to the right of the TK gene are relatively short, 1 - 2.5 x 10^6 molecular weight. It is known (23) that the direction of transcription of the TK gene is from right to left and so the sequences trimmed are upstream from the gene. The possible significance of such deletions is discussed later.

Deletion of sequence from the transforming fragment is not restricted to the right hand end since $H2_4$ and $H2_1$ have both lost sequences from the left hand end of Hin h. This observation suggests a very simple model for integration in which two recombination events occur.

Finally, since quite large virus sequences are incorporated into some transformed cells it is inevitable that non-selected genes must also be present. In the following section we describe the quest for expression of these genes.

3.3. Expression of non-selected genes in transformed cells

The method chosen to test for expression of non-selected genes was to look for the ability of cells to complement defects in temperature sensitive (ts) mutants grown at the non-permissive temperature. In all we tested 15 mutants in 9 cell lines[1]. The results were somewhat disappointing in that non-selected genes were revealed in only two lines, $D2_1$ and $D2_5$. In the case of $D2_1$ two mutants were able to grow at the non-permissive temperature. These were the type 1 mutant ts N1O2 and the type 2 mutant ts 2O8. Only ts 2O8 grew in $D2_5$ (Table 1).

Perhaps the most surprising observation in this context was that ts 5 which maps very close to TK (21) and must certainly be present in $D2_1$, was unable to grow in these cells at the non-permissive temperature. This suggests that not all genes present will be revealed by

[1]We are grateful to Drs. Ian Halliburton, Sandy Buchan, Dorothy Purifoy and Morag Timbury all of whom provided us with ts mutants.

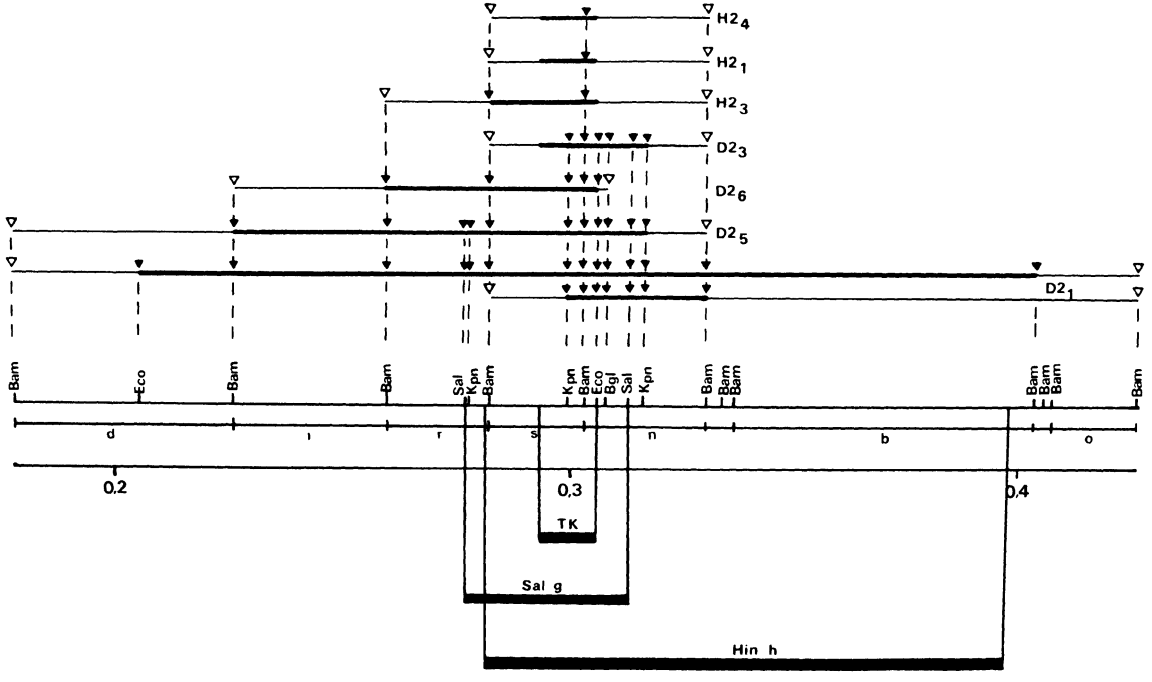

Figure 7 Topography of virus DNA sequences in transformed cells

Restriction sites present in transformed cells are marked with filled triangles (▼) and those known to be absent are indicated with open triangles (▽).

complementation experiments and caution must be applied when interpreting negative results.

Whether a non-selected gene in the transformed cell will be effective in complementation must depend upon many factors. It is possible that non-selected genes are switched on by the superinfecting mutant. If this is the case then the quality of product which accumulates will be controlled to some extent by the rapidity with which the virus closes down host expression and this in turn may depend upon the integration site of the virus sequence. It is also likely that the quantity of gene product required for effective complementation will vary widely according to the function of the defective gene.

3.4. Regulation of expression of TK

The situation concerning regulation of the integrated TK is clearer than that for the non-selected genes since we know that this function is expressed continually in transformed cells. It is known that the 'immediate early' gene product, VP 175, is required for expression of TK in infected cells (12) and since this gene maps in the short repeat regions of the DNA it is not present in our transformed lines. There would appear to be two possible mechanisms to explain the expression of TK; either the normal virus promoter sequence is present and recognized by cell functions or alternatively expression is from an upstream host cell promoter. Information on the topography of integrated virus sequences in our lines suggested that virus sequences upstream from TK tend to be eliminated upon integration (see below) and this may favour a model in which the TK gene is integrated close to a host promoter.

In has been shown (24) that the normal virus promoter may be integrated along with the TK gene. Superinfection with a TK^- virus mutant then induces enhanced expression of the resident gene presumably by interaction of an 'immediate early' product with the virus promoter. If,

Table 1 Growth of ts mutants at non-permissive temperature in transformed cells

Cell Line	Yield of mutant at non-permissive temperature (% wt)														
	Type 2 mutants[a]								Type 2 mutants[b]				Type 1 mutants[c]		
	1	2	4	5	6	7	8	9	776	208	19	50	B5	B9	N102
LMTK$^-$	0.50	0.01	0.10	0.10	0.07	0.01	0.16	0.01	1.0	1.2	0.70	0.10	0.03	0.03	2.0
$D2_1$	0.30	0.01	0.43	0.10	0.57	0.01	0.02	0.02	2.8	77	2.6	0.30	0.06	0.01	140
$D2_2$	0.80	0.02	0.03	0.07	0.13	0.07	0.04	0.04	0.50	0.40	1.1	0.10	0.04	0.01	2.0
$D2_3$	0.50	0.01	0.15	0.03	0.12	0.02	0.03	0.16	6.8	3.4	0.60	0.20	0.07	0.01	0.70
$D2_4$	0.20	0.02	0.12	ND[d]	0.33	0.06	0.03	0.01	2.3	0.80	0.70	0.10	0.02	0.01	0.80
$D2_5$	0.10	0.01	0.42	0.12	0.68	0.05	0.04	0.02	1.1	84	1.0	0.20	0.03	0.01	1.2
$D2_6$	0.10	0.01	0.01	0.06	0.07	0.02	0.02	0.01	2.0	0.50	0.90	0.30	0.03	0.01	0.90
$D2_7$	0.40	0.01	0.03	0.01	1.9	0.03	0.75	0.01	0.70	0.20	2.0	0.70	ND	0.01	5.0
$D2_8$	0.40	0.01	0.08	0.20	1.7	0.01	0.06	0.01	3.6	0.60	1.5	1.0	0.03	0.02	ND
$D2_9$	0.50	0.01	0.07	0.20	1.3	0.10	0.06	0.01	1.3	ND	ND	ND	ND	0.01	1.0

a. mutants isolated by Dr. M. Timbury
b. mutants isolated by Dr. D. Purifoy
c. mutants isolated by Dr. A. Buchan
d. ND = not done

as we propose above, expression of the resident TK gene is normally under control of a host cell promoter then co-integration of the virus promoter must be accidental. If however expression of TK relies on recognition of the virus promoter by host cell functions then all transformed cells would carry the promoter sequence. In an attempt to distinguish between these possibilities we have used superinfection with a TK^- mutant (B2006) (2) to probe for virus promoters in our cells. The results of these experiments (Table 2) showed that while the TK in $D2_1$ and $D2_5$ was considerably enhanced upon superinfection, there was little effect on the levels present in other cell lines. It would

Table 2 Induction of TK by superinfection

Cell Line	Thymidine kinase activity induced by superinfection[a]
LTK^-	<0.05
$D2_1$	1.8
$D2_3$	0.07
$D2_4$	0.10
$D2_5$	2.10
$D2_6$	0.06
$D2_8$	0.07
$D2_9$	<0.05
$H2_1$	<0.05
$H2_2$	0.06
$H2_3$	0.09
$H2_4$	<0.05

[a]Results are activity in cells, 8h after infection with B2006, above that in mock infected controls (p moles thymidine phosphorylated/10^4 cells/min).

therefore appear from these observations that regulation of the resident virus TK gene is most likely to be mediated via a host cell promoter.

4. ISOLATION OF REVERTANT CELLS WITH TK$^-$ PHENOTYPE

The original isolation of LMTK$^-$ cells involved the serial passage of L cells in the presence of BUdR. This procedure selected against cells which expressed TK and permitted the isolation of cells with TK$^-$ phenotype. The same procedure may be used with 'biochemically' transformed cells to select out cells which can no longer express virus TK. As the virus DNA sequences in the lines are defined we can ask about the events which lead to acquisition of the TK$^-$ phenotype. The two cell lines chosen for these investigations were those which carry the non-selected markers and the virus promoter sequence, $D2_1$ and $D2_5$.

Revertants were isolated by plating either in 50 µg/ml BUdR or alternatively in the presence of 10 µg/ml acyclovir. Acyclovir is a nucleoside analogue which is phosphorylated specifically by the virus TK and the phosphorylated drug is toxic for the cells (25). This compound can therefore be used to select TK$^-$ revertants of transformed cells. Revertants isolated using selection in one drug always acquired resistance to the other compound. The reversion frequency in each case was in the range 10^{-3} and 10^{-4}.

4.1. Phenotypic characterization of revertants

A series of mutants were isolated from each cell type and these were then characterised phenotypically. They were tested for ability to support the growth of ts mutants known to grow in the parent cells at the non-permissive temperature. They were also superinfected with the TK$^-$ mutant B2006 to ask whether the TK gene and its associated virus promoter were still operational.

The results of these experiments showed that revertants fell into 3 distinct classes:

Class I: These revertants were no longer able to complement ts mutants and TK could not be induced by

superinfection.

Class II: Representatives of this class were derived only from $D2_1$. They complemented ts N102 but not ts 208 and were non-inducible.

Class III: Revertants of this type complemented the growth of mutants which would grow in the parent cells and furthermore TK synthesis could be induced by superinfection. This latter observation shows that there has been no lethal mutation in the TK structural gene.

The phenotypic properties of representatives of each class are shown in Table 3.

Table 3 Phenotypic properties of TK⁻ revertants

Cell Line	Class	Mutant yield[a]		Thymidine kinase activity induced by superinfection[b]
		ts N102	ts 208	
LTK^-	Control	0.4	0.6	<0.05
$D2_1$	Control	5.4	95	2.9
$D2_5$	Control	1.2	65	1.8
$D2_1R1$	I	0.1	2.1	<0.05
$D2_5A2$	I	ND[c]	0.8	<0.05
$D2_1A1$	II	112	4.4	0.05
$D2_1R4$	III	37	146	1.9
$D2_5A1$	III	ND	126	1.7

[a]Mutant yields are expressed as % wt yield in the same line at the non-permissive temperature

[b]Results are activity in cells, 8h after infection with B2006, above that in mock infected control (p moles thymidine phosphorylated/10^4 cells/min)

[c]ND = not done

4.2. Virus DNA sequences in revertant cells

Representatives of each revertant class were analysed by

the Southern blot technique to define the virus DNA sequences present (Figure 8). No virus DNA sequences were detected in the Class I revertants ($D2_1R1$ and $D25_A2$) (the suffix 'R' refers to mutants isolated in BUdR, 'A' to revertants isolated in acyclovir). Thus it appears that all virus sequences have been eliminated from these cells, either by deletion of a large DNA fragment or by complete loss of the chromosome.

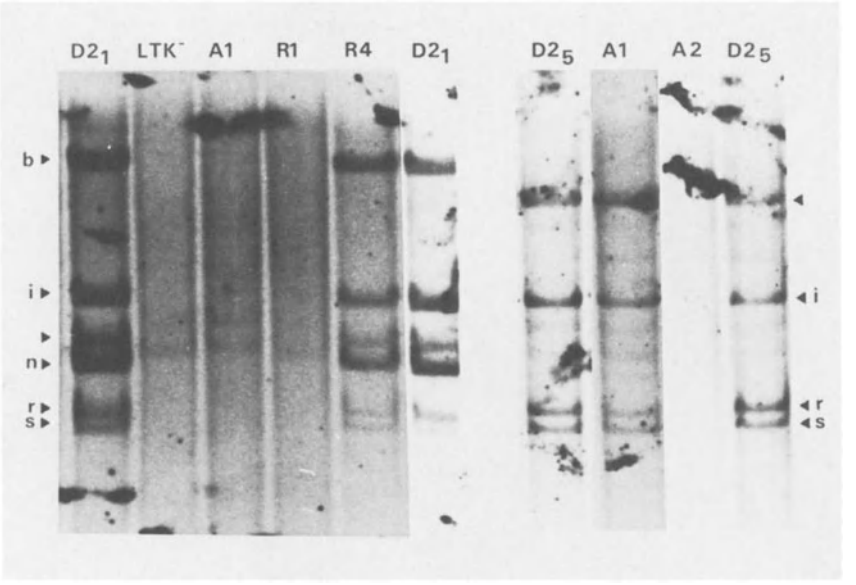

Figure 8

Bam digests of revertant cell DNAs analysed with HSV-2 probe ^{125}I-Labelled HSV-2 DNA was used to detect fragments containing virus DNA derived from revertant cells by Bam digestion. LTK⁻ and parent cell lines are included as controls.

The situation with Class II revertants ($D2_1A1$) is unsatisfactory. We have been unable to detect virus sequences in these cells by blot hybridization using total ^{125}I-labelled HSV DNA as probe. However, the gene which complements ts N1O2 must be present and so we assume that

the cells contain only a very small virus sequence which is beyond the limits of detection in the experiment. This idea is reasonable as it was not possible to detect virus sequences known to be present in $D2_3$ using whole probe and it required the greater sensitivity of the Sal 1 g cloned probe.

4.3. Mechanisms of reversion

Since all three classes of mutants arise with a similar frequency (10^{-3} - 10^{-4}) it is tempting to argue that they arise by a similar mechanism. In view of the high frequency of reversion and the failure to detect lethal mutations in the structural gene it would seem unlikely that reversion could be explained by base-pair substitutions. It is possible to explain the three classes if we assume that they all arise by a deletion of DNA sequences from the host cell chromosome. Such a model is outlined in Figure 9.

In this model we assume that the TK gene in the transformed cell is transcribed from a host promoter (P_h). The virus promoter for TK (P_{tk}), if present, is assumed to be upstream from TK but transcription is initiated at this site only upon superinfection. Non-selected genes (X) may also be present but these are likely to be downstream from TK and these also may only be switched on upon superinfection and may require a second virus promoter (P_x).

Class I revertants would arise by deletion of the whole virus sequence along with flanking host sequences.

Class II would require a deletion in at least TK or both P_{tk} and P_h. Clearly in $D2_1A_1$ the deletion must be fairly large and it is quite possible that host as well as virus sequences have been eliminated. All that is required is that the non-selected gene (X) and its postulated virus promoter (P_x) remain.

To explain Class III mutants which appear to have identical virus sequences to the parent lines with the same

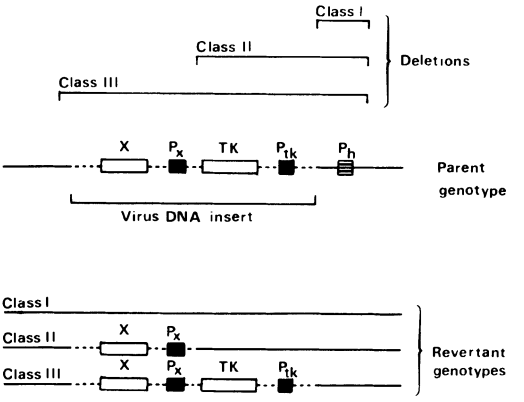

Figure 9

Model for the generation of revertants by deletions of DNA sequences

P_h is the postulated host promoter for virus TK. TK is the structural gene and P_{tk} is the virus promoter. X is a non-selected virus gene with its promoter P_x.

flanking host sequences we have to postulate a deletion of host sequences some distance from the virus DNA insert (at least beyond the closest host Bam site). The simplest explanation is deletion of the host promoter.

A further possible explanation for Class III revertants is the excision of the virus sequence along with flanking host sequences and its insertion in a transcriptionally silent region of the host chromosome.

Clearly information about the TK mRNA and its precursors in the transformed cell and in the superinfected cell would help to sort out some of these possibilities.

5. TRANSFORMED CELL DNA AS A TK GENE DONOR

We were able to show that the DNA isolated from a transformed cell can be used as a TK gene donor to transfect LMTK$^-$ cells (17). The most remarkable feature of this transfer was the efficiency. Although it is not an easy parameter to measure it appeared that the gene dose required to transfect using transformed cell DNA was at least 100 fold lower than that required using virus DNA.

5.1. Properties of transfectants

Several lines were generated using $D2_1$ DNA as donor and their phenotypic properties are summarized in Table 4. In contrast to the parent line, the derived cells were unable to complement ts N102 or ts 208. Furthermore the virus promoter appeared to be absent since there was no enhancement of TK activity upon superinfection with B2006.

Analysis of the virus DNA content of these cells is incomplete. However, it is clear that none of the five $D2_1$ tranfectants examined so far contain the entire Bam s or n fragments known to be present in the parent line. The conclusion must be, therefore, that in these cases only a small segment of virus DNA was transferred and that this sequence was integrated into a new site in the host cell chromosome.

Several lines have also been generated using $D2_5$ and $D2_3$ DNAs as gene donors and efficiency of transfection was similar to that seen with $D2_1$ DNA. These lines are less well-characterized but it is interesting that the majority of those derived using $D2_5$ DNA are unlike those from $D2_1$ in that they are able to complement ts 208 at the non-permissive temperature, but they may resemble $D2_1$ derived lines in that the virus promoter appeared to be absent in the two lines examined (Table 4).

Table 4 Phenotypic properties of transfectants

Cell Line	Mutant yield (% wt)		TK activity induced by superinfection[a]
	ts 208	ts N102	
LTK$^-$	1.0	0.3	<0.05
$D2_1$	75	48	0.9
$D2_1$T1	0.2	0.3	0.06
T2	0.6	0.01	ND[b]
T3	2.6	0.40	ND
T4	0.9	0.20	ND
T5	4.1	0.06	ND
T6	2.1	ND	ND
T7	1.3	ND	ND
T8	2.1	ND	ND
T9	1.3	ND	ND
T10	1.0	0.3	0.07
$D2_5$	145		1.1
$D2_5$T1	93		ND
T2	94		ND
T3	27		<0.05
T4	50		ND
T5	90		ND
T6	82		ND
T7	51		ND
T8	66		0.07
T9	111		ND

[a]Results are activity in cells, 8h after infection with B2006, above that in mock infected controls (p moles thymidine phosphorylated/10^4 cells/min

[b]ND = not done

5.2. Models of transfection

Perhaps the simplest models to explain high efficiency

transformation are that flanking host sequences provide recognition signals for integration, or that co-transfer of the host promoter ensures expression of the integrated gene. Neither explanation appears tenable in the face of the observations above which show that virus sequences are trimmed from both ends of the fragment from the parent line, since we must therefore assume that flanking host sequences are also deleted. However there are several other possibilities which should be considered.

5.2.1. Absence of lethal virus genes

It is well known that there are virus-specific products in infected cells which interfere with host cell metabolism. It is possible that the products of these genes usually kill the cells which acquire them and it is only rarely that a cell acquires the TK gene in their absence. Only this latter situation would lead to successful transformation. One prediction of this model is that the transformation frequency with small isolated restriction fragments would be significantly higher than with mixed fragments. There is a report which suggests that this may be the case (7) but data obtained in this laboratory (M. Inglis, personal communication) have shown no significant differences in relative efficiencies.

5.2.2. Gene modification

The second possibility is that the gene present in the cell chromosome is modified chemically, perhaps by methylation. There is certainly some evidence for modification of virus DNA sequences in transformed cells (26,27). This modification might then increase the efficiency of gene transfer by improving the probability of recombination between donor and recipient, or by increasing the likelihood of expression of the gene in the recipient cell.

5.2.3. Expression of episomal genes

A third possibility is that the increased efficiency is due

to the presence of the cellular promoter associated with the virus TK gene. Such a combination might permit expression of the gene in an episomal state, prolonging life of the cell and making possible the inheritance of a functional TK gene by daughter cells following division. Integration would be required to generate a stable transformed cell and ensure inheritance of the gene by its progeny. The situation with virus DNA as gene donor would differ in that expression of the episomal gene would not be feasible as no suitable cell promoter would be available. Therefore acquisition of the TK gene by a cell would have to be followed immediately by integration of the gene into an appropriate site in the chromosome to enable its expression and the survival of the cell. According to this model a cellular promoter associated with the virus TK provides 'breathing space' for the cell and increases the probability of integration.

6. SUMMARY AND CONCLUSIONS

The 'biochemical' transformation system exploiting the HSV TK gene has the potential to provide considerable useful information about gene expression and regulation in eukaryotic cells. Perhaps one of the most important features of the system is that the genetic information introduced is of virus origin. This means that the gene itself and its transcripts may be detected by sensitive hybridization techniques and furthermore the gene product may also be identified. This taken in conjunction with effective selection systems both for and against TK offers a unique opportunity to follow the fate of a foreign gene incorporated into the chromosome of a eukaryotic cell.

It has become clear that non-selected genes may also be acquired by recipient cells. In our experiments these genes were of virus origin. However other groups have now

shown that genes of cellular origin may be physically linked to TK in vitro and such genes may be introduced into cells and expressed (28,29). The system therefore provides us with the technology to alter the genetic make-up of cells in a controlled way.

It is difficult to make any firm pronouncements about the mechanisms by which cells acquire and express these new genes although the investigations described in this chapter do provide some clues. Firstly it is clear that the new DNA becomes integrated into the cellular chromosome and is flanked by host sequences. It is also clear from our data on the topography of the integrated DNA that sequences may be trimmed from either end of the transforming fragment. There is a suggestion that sequences upstream from the selected gene are preferentially deleted and this may be necessary in order to integrate TK close to an upstream cellular promoter. Certainly our evidence shows that it is not necessary for the virus promoter to be integrated along with the gene.

Revertants of transformed cells may be isolated relatively easily using selection in either BUdR or acyclovir. The revertants are of three types. They may be regulatory variants which retain all virus DNA sequences, or deletion mutants which have lost some or all virus sequences. Interestingly we could obtain no evidence for revertants with point mutations in the TK structural gene since all which retained the gene were inducible upon superinfection with TK^- virus. As mutants of the three classes arise with similar frequency it is tempting to ascribe a common mechanism to their generation. The most likely would seem to be deletion of DNA sequences since we already know that this is the mechanism by which two of the classes arise. The third class of revertants would then be explained by deletion of the host promoter.

Finally, experiments on the DNA mediated transfer of the integrated TK gene from cell to cell indicated a fundamental difference in the gene isolated from this source and

that from virion DNA. This difference was manifested in a far higher transforming efficiency for DNA isolated from transformed cells. Although the reasons for this are not clear, one attractive idea is that it is due to the presence of a host promoter associated with the virus gene in the transformed cell. Upon transfection this could lead to an unstable situation where cells are capable of growth and division, the cellular promoter permitting expression of the TK gene without integration. A more stable situation would result if the gene subsequently became integrated in a suitable site. Such an unstable phase, which in effect permits amplification of the cellular population expressing TK, is precluded if the gene donor is virus DNA since we assume that this DNA carries no host promoters.

We would like to acknowledge the Cancer Research Campaign for support of this work and also the Medical Research Council for provision of a research studentship for one of us (K.F.B.).

REFERENCES

1. Chen MS, Prusoff WH: Association of thymidylate kinase activity with pyrimidine deoxyribonucleoside kinase induced by herpes simplex virus. J Biol Chem 253: 1325-1327, 1978.

2. Dubbs DR, Kit S: Mutant strains of herpes simplex virus deficient in thymidine kinase activity. Virology 22: 493-502, 1964.

3. Field HJ, Wildy P: The pathogenicity of thymidine kinase-deficient mutants of herpes simplex virus in mice. J Hygiene (Cambridge) 81: 267-277, 1978.

4. Field HJ, Darby G: Pathogenicity in mice of strains of herpes simplex virus which are resistant to acyclovir *in vitro* and *in vivo*. Antimicrobial Agents and Chemotherapy 17: 209-216, 1980.

5. Tenser RB, Miller RL, Rapp F: Trigeminal ganglion infection by thymidine kinase-negative mutants of herpes simplex virus. Science 205: 915-917, 1979.

6. Morse LS, Pereira L, Roizman B, Schaffer PA: Anatomy of herpes simplex virus (HSV) DNA. X Mapping of viral genes by analysis of polypeptides and functions specified by HSV-1 x HSV-2 recombinants. J Virol 26: 389-410, 1978.

7. Wigler M, Silverstein S, Lee L-S, Pellicer A, Cheng Y-C, Axel R: Transfer of purified herpes virus thymidine kinase gene to cultured mouse cells. Cell 11: 223-232, 1977.

8. Minson AC, Darby G, Wildy P: Virus specific DNA seqeuences present in cells which carry the herpes simplex virus thymidine kinase gene. J Gen Virol 45: 489-496, 1979.

9. Honess RW, Watson DH: Herpes simplex virus specific polypeptides studied by polyacrylamide gel electrophoresis of immune precipitates. J Gen Virol 22: 171-185, 1974.

10. Thouless ME, Wildy P: Deoxypyrimidine kinases of herpes simplex viruses types 1 and 2: comparison of serological and structural properties. J Gen Virol 26: 159-170, 1975.

11. Honess RW, Roizman B: Regulation of herpesvirus macromolecular synthesis. Sequential transition of polypeptide synthesis requires functional viral polypeptides. Proc Natl Acad Sci USA 72: 1276-1295, 1975.

12. Watson RJ, Clements JB: A herpes simplex virus type 1 function continuously required for early and late virus RNA synthesis. Nature 285: 329-330, 1980.

13. Littlefield J: Selection of hybrids from matings by fibroblasts *in vitro* and their presumed recombinants. Science 145: 709-710, 1964.

14. Munyon W, Kraiselburd E, Davis S, Mann J: Transfer of thymidine kinase to thymidine kinaseless L-cells by infection with ultraviolet irradiated herpes simplex virus. J Virol 7: 813-820, 1971.

15. Graham FL, Van der Eb AJ: A new technique for the assay of infectivity of human adenovirus 5 DNA. Virology 52: 456-467, 1973.

16. Bacchetti S, Graham FL: Transfer of the gene for thymidine kinase deficient human cells by purified herpes simplex viral DNA. Proc Natl Acad Sci USA 74: 1590-1594, 1977.

17. Minson AC, Wildy P, Buchan A, Darby G: Introduction of the herpes simplex virus thymidine kinase gene into mouse cells using virus DNA or transformed cell DNA. Cell 13: 581-587, 1978.

18. Wigler M, Pellicer A, Silverstein S, Axel R: Biochemical transfer of single copy eucaryotic genes using total cellular DNA as donor. Cell 14: 725-731, 1978.

19. Minson AC, Bastow K, Darby G: The herpes simplex thymidine kinase gene as a transmissible genetic element in mammalian cells. In: *Antiviral Mechanisms in the Control of Neoplasia*, Chandra P(ed) New York and London, Plenum Press, 1979, p7-16.

20. Cortini R, Wilkie NM: Physical maps for HSV-2 DNA with five restriction endonucleases. J Gen Virol 39: 259-280, 1978.

21. Wilkie NM, Davison A, Chartrand P, Stow ND, Preston VG, Timbury MC: Recombination in herpes simplex virus: mapping of mutations and analysis of intertypic recombinants. Cold Spr Harb Symp Quart Biol XLIII: 827-840, 1978.

22. Southern EM: Detection of specific sequences among DNA fragments separated by gel electrophoresis. J Mol Biol 98: 503-517, 1975.

23. Smiley JR, Wagner MJ, Summers WP, Summers WC: Genetic and physical evidence for the polarity of transcription of the thymidine kinase gene of herpes simplex virus. Virology 102: 83-93, 1980.

24. Leiden JM, Bullyan R, Spear PG: Herpes simplex virus gene expression in transformed cells. Regulation of the viral thymidine kinase gene in transformed L cells by products of superinfecting virus. J Virol 20: 413-424, 1976.

25. Nishiyama Y, Rapp F: Anticellular effects of 9-(2-hydroxyethoxy-methyl)guanine against herpes simplex virus transformed cells. J Gen Virol 45: 227-230, 1979.

26. Desrosiers RC, Mulder C, Fleckenstein B: Methylation of herpesvirus saimiri DNA in lymphoid tumour cell lines. Proc Natl Acad Sci USA 76: 3839-3843, 1979.

27. Sutter D, Doerfler W: Methylation of integrated adenovirus type 12 DNA sequences in transformed cells is inversely correlated with viral gene expression. Proc Natl Acad Sci USA 77: 253-256, 1980.

28. Lai EC, Woo SLC, Bordelon-Riser ME, Fraser TH, O'Malley BW: Ovalbumin is synthesised in mouse cells transformed with the natural chicken ovalbumin gene. Proc Natl Acad Sci USA 77: 244-248, 1980.

29. Mantei N, Boll W, Weissman C: Rabbit β-globin mRNA production in mouse L cells transformed with cloned rabbit β-globin chromosomal DNA. Nature 281: 40-46, 1979.

14. Viral genes in HSV transformed cells as detected genetically

Joan C.M. Macnab

SUMMARY AND INTRODUCTION

One method of detecting HSV sequences in herpes simplex virus (HSV) transformed cells is by using classical genetics to generate recombinant virus the restriction enzyme pattern of which can unambiguously identify gene sequences which can only arise from the HSV transformed cell line.

To generate recombinants for analysis, lines of HSV transformed cells are superinfected by temperature sensitive (ts) mutants of HSV and the yields of virus obtained after infection for 24 hours at the non-permissive temperature (NPT) of 38.5°C or the permissive temperature (PT) of 31°C are titrated at the NPT of 38.5°C and compared with the yield from a similar infection of an equal number of control cells. An increased yield of virus at 38.5°C after superinfection of transformed cells indicates that the transformed cells contain HSV information, that the increased plaque yield represents putative recombination events and further analysis of these plaques, by analyses of series of restriction enzyme digests, will define those regions of the recombinant which arose from HSV DNA sequences contained in the transformed cell.

Titration at 31°C of the yields of superinfection at 38.5°C of HSV transformed cell lines by ts mutants where an increase in virus seen at 31°C from superinfection of transformed compared with control cells indicates complementation between the virus information in the transformed cell line and the particular ts lesion of the mutant which it can complement.

However, titration at 31°C of the yields of superinfection at 31°C of HSV transformed lines by mutants where

Y. Becker (ed), Herpesvirus DNA.

markers other than ts eg the plaque morphology marker syn, are used, could indicate a recombination event (see "Diagrammatic representation of recombinant progeny virus".... later in this text). In such experiments increased yields from transformed cells at 31°C and also the appearance of a plaque morphology marker (originally present in the HSV used to transform the cell line) indicates possible recombination events.

Here specific studies are reported in which HSV information in transformed cell lines has been analysed using the techniques of superinfection both to study expression of information by complementation and also to study viral DNA sequences in transformed cells by the construction of recombinants.

EXPERIMENTAL APPROACH AND RESULTS

Complementation studies to detect HSV information in rat embryo cells transformed by HSV-2 HG 52 ts 1 - RE1 cells (1, 2, 3, 4) - were carried out by Macnab and Timbury (5). In these experiments rat embryo control cells -RE- or Hood (continuous line of RE) (4) and rat embryo cells transformed by HSV-2 HG52 ts 1 (RE 1) (5) were superinfected with 5 ts mutants of HSV-2 HG 52 and titrated on BHK C13 cells (Figure 1). Increased titres from superinfection of the transformed cells (a greater than twofold increase over control RE cells) indicated complementation of the resident HSV information in the transformed cell with the superinfecting ts mutant. Information from these tests indicated that the HSV transformed rat embryo cell line RE 1 could be complemented by 3 out of 10 different superinfecting ts mutants, 2 of these mutants having DNA positive phenotypes at 38°C, ts 3 and ts 4, and one, ts 10, having a DNA negative phenotype at 38°C.

The results of Macnab and Timbury were highly suggestive that HSV specific genes capable of complementing the ts lesion in ts mutants were being expressed in the transformed cells. However, it was not possible to exclude from these experiments the possibility that transformation was able to switch on host genes whose expression activated

the growth of HSV in the transformed cells. Nor was it possible by complementation to exclude the possibility that HSV DNA capable of complementing the lesion in other ts mutants was indeed contained in the transformed cells but was not being transcribed.

Table 1 Yield of virus from transformed and control cells infected with three complementing ts mutants of HSV-2.

Mutant	No of PFU in yield* after infection of cells for 24 h at 38.5°C	
	Control rat embryo cells	RE 1-transformed cells
ts 10	9	432
ts 10	2	298
ts 10	0	14
ts 3	3	210
ts 3	45	416
ts 3	272	578
ts 4	10	300+
ts 4	0	4+
ts 4	2	30+
ts 1‡	0	0
ts 1	2	4
ts 1	404	309
ts 1	0	0
ts 1	0	0

* Plaques obtained on titration at 31°C: no plaques were found on titration at 38.5°C.

\+ Plaques obtained by infection of RE 1 cells by ts 4 were consistently larger than those on control plates.

‡ Infection of transformed and control cells by ts 1, the mutant used for the original transformation of RE 1 was included as a control of the specificity of the complementation.

At the time of these studies it was possible to isolate virus after superinfection of transformed cell lines by ts mutants which grew at the NPT of 38.5°C. However, in early studies it was impossible to unambiguously identify this virus as recombinant virus and not revertant virus. Thus

early studies do not mention the possible generation of recombinant virus.

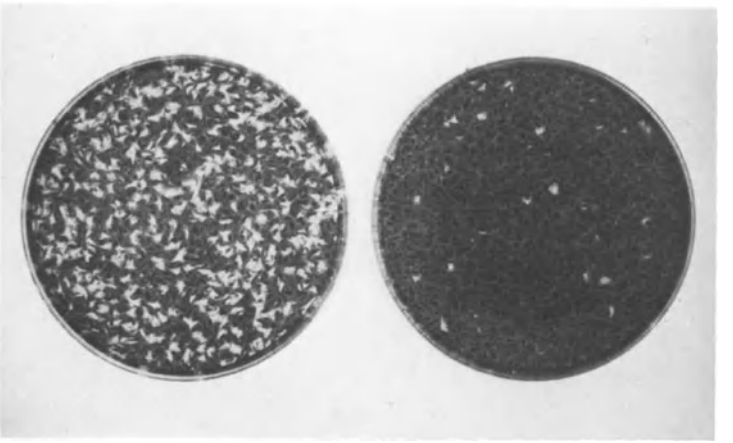

Figure 1 1a ⟷ 1b

Monolayers of equal quantities of rat embryo control cells -RE or Hood control cells (a continuous line of RE) (4) and rat embryo cells transformed by HSV-2 HG52 ts 1 - RE1 - (5) were superinfected with 5 pfu/cell of ts mutants of HSV-2 HG 52. After incubation for 24 hrs at 38.5°C the cells were scraped into 1 ml of the medium overlay and sonicated. Samples - 0.2 ml - of this cell sonicate were titrated on BHK C13 cells at 31°C. Increased titres at 31°C from superinfection of the transformed cell line figure 1a compared with superinfection of the control cells figure 1b indicated complementation of the resident HSV information in the transformed cell with the superinfecting ts mutant.

Such complementation studies confirmed the results of Kimura et al (6) who described significant enhancement of the titre of two HSV-1 mutants ts G4 and ts D6 (both phenotypically DNA positive) when grown in the HSV transformed hamster embryo cell line MS-4 and in the tumour cell line 333-8-9.

Similar complementation studies were later extended to include both intertypic and intratypic studies with the rat embryo cell line transformed by HSV-1 ∝ -RE∝- (7) and the rat embryo cell line transformed by HSV-2 HG 52 ts 1 -RE1. These complementation studies are seen in table 2. The indices range from 3.4 up to 39 (8)

Table 2 Complementation of ts mutants by transformed cell lines

Transformed cell line	Superinfecting ts mutant	Complementation index
REα	HSV-1 tsG	39
	tsl	3.4
	tsA	13
	tsD	3.7
	HSV-2 tsl	7.7
REl	HSV-1 tsJ	31
	tsl	15
	tsF	6.5
	tsA	6

A complementation index > 3 on titration of yields of ts superinfecting virus obtained at 38.5°C from the transformed cell line compared to the control cell line is regarded as evidence for complementation of the mutant virus by the transformed cell line.

The ultimate genetic test to detect resident HSV sequences present in HSV transformed cells was to be resolved as a consequence of the everyday use of restriction enzyme analyses (8), where it was possible to use superinfection techniques to generate recombinant viruses, the DNA of which could be analysed by resolution on agarose gels after treatment with restriction endonucleases. In these experiments both HSV transformed and control rat embryo cells were superinfected with ts mutants at the temperatures of 31°C and 38.5°C for 24 hours. Yields were titrated in BHK C13 cells at 38.5°C (NPT) to test for recombination or wild-type virus. A considerable increase in yield at NPT from superinfection of the transformed cells as compared with the control cells indicates recombination. Ideally superinfecting ts virus should be of the alternative serotype in order to generate intratypic recombinants whose resolution is unambiguous in restriction enzyme analysis (Figure 2).

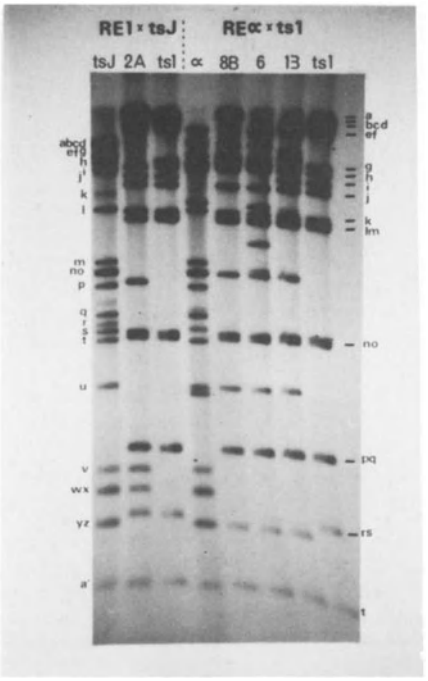

Figure 2

Autoradiograph of ^{32}p-labelled DNAs of HSV-1 tsJ, HFEM, HSV-2 tsl and recombinants 2A, 6, 8B, 13 which were digested with restriction endonuclease Kpnl and subjected to electrophoresis on an 0.8% agarose gel. DNA fragments are lettered in accordance with the HSV-1 17 Kpnl restriction endonuclease map and HSV-2 HG 52 Kpnl restriction endonuclease map. Isolates 6, 8B, 13 are characteristic of recombinants analysed and resemble one another, due to the HSV-2 ts 1. The site of the ts 1 mutation is known to map at position 0.7 from marker rescue studies and all recombinants produced after superinfection with ts 1 have a substitution of DNA in this region, although each recombinant contains differing amounts of rescued information. Recombinant 2A isolated after superinfection of RE1 cell line with HSV-1 tsJ has a characteristic DNA profile of HSV-2 with an HSV-1 insertion between 0.38 and 0.50 map units. The restriction endonuclease profiles of these intertypic recombinants can clearly be related to bands originating from either the superinfecting virus of the original transforming virus. Bands which are not represented in either the superinfecting or the transforming virus are evidently intermediate bands formed as a result of the recombination event and could be identified by analysis of bands flanking the crossover region(s).

Intratypic recombinants were also generated and were more easily detected where a plaque morphology marker eg syn was used. This can be seen where RE ∝ (rat embryo transformed by HSV-1 ∝) cells are superinfected by HSV-1, 17 ts G syn+. Virus rescued from superinfection of RE ∝ cells and titrated at 31°C may be syn and ts indicating recombination between the plaque morphology marker of the transformed cells (syn) and the superinfecting virus (syn+). Such virus may also of course, be ts+ if the recombination event also includes that portion of the DNA coding for the ts lesion (Park and Macnab, unpublished observations).

Diagrammatic representation of recombinant progeny virus when RE ∝ cells are superinfected at NPT or PT with HSV-1, 17 ts G syn+.

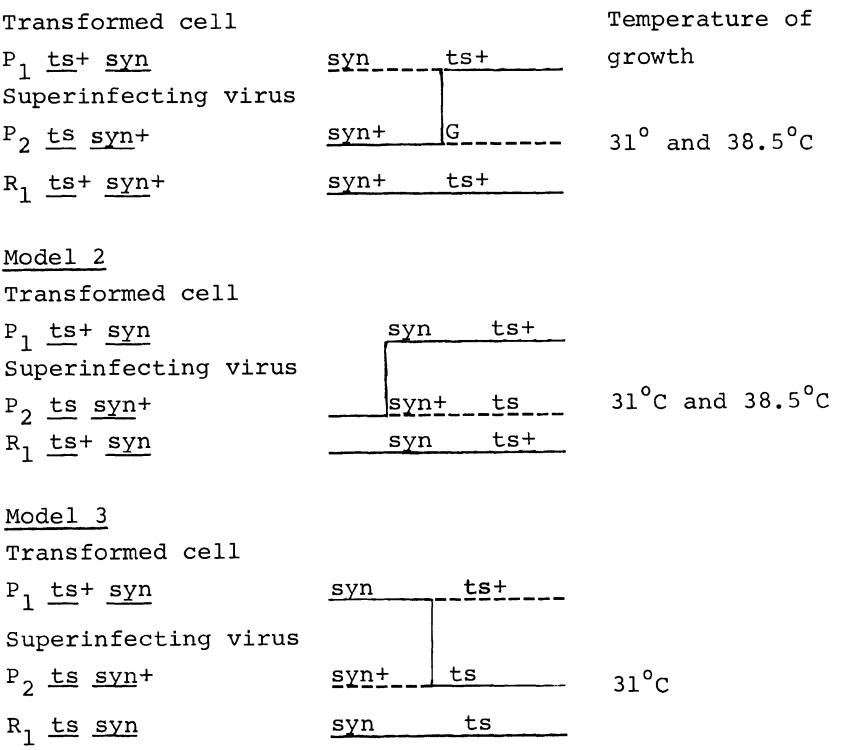

The plaque morphologies of this cross distinguishable in BHK C13 cells are Figures 3a, 3b and 3c. In addition, restriction enzyme analyses differentiates HSV-1∝ (HFEM) from HSV-1 17 as all HSV-1 isolates have different restriction enzyme patterns(9). This differentiation has been used to identify intratypic recombinants after superinfection of RE∝ cells with ts G syn+ (Figure 4).

Superinfection of rat embryo cells transformed by HSV-2 HG 52 ts 1 -RE1- with HSV-1 tsJ syn yielded recombinant virus whose plaque morphology was syn^{+}. This virus could be unambiguously identified by restriction as enzyme analysis as recombinant (Figure 3). The plaque morphologies of HSV-1 and HSV-2 are distinct on BHK C13 cells and can be

easily identified.

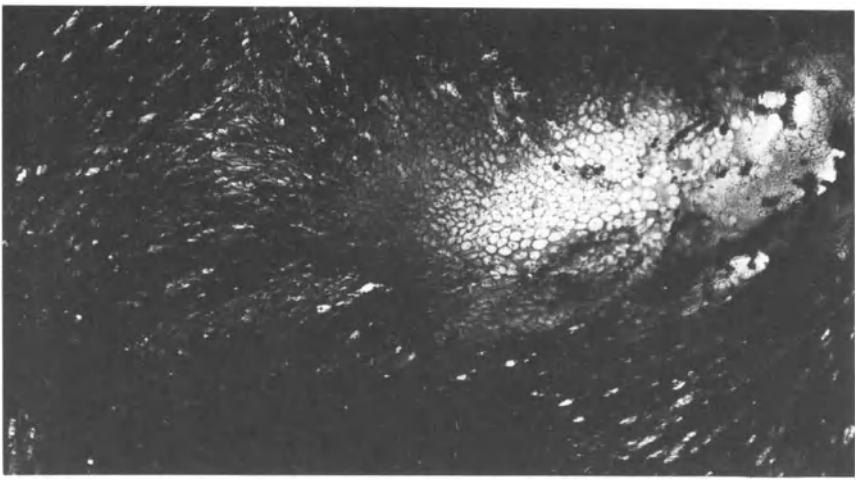

Figure 3a. HSV-1 ∝ (HFEM).

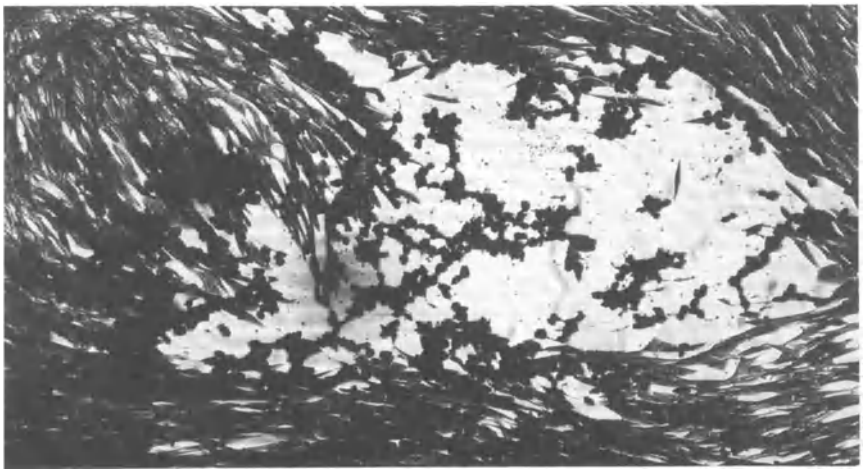

Figure 3b. HSV-1 17 G syn+ plaque.

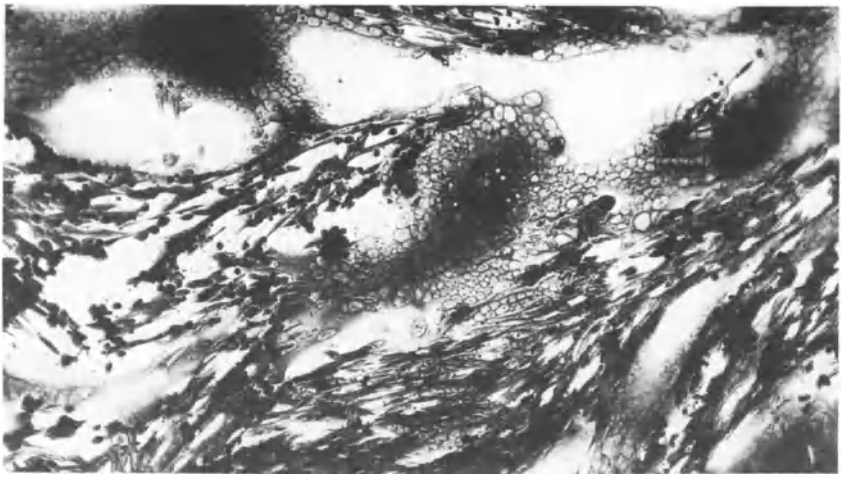

Figure 3c.

Titration of the yield of superinfection by HSV-1, 17, G syn+ of the rat embryo cell line transformed by sheared DNA of HSV-1 ∝ (HFEM) shows syn plaques resulting from the original ∝ virus used to transform. Syn+ plaques arising from the G syn+ superinfecting virus are also seen.

In all recombination studies equal quantities of transformed and control rat embryo cells were superinfected at 31°C or 38.5°C with 5pfu/cell of a ts mutant. After 24 hours incubation the cell sheet was scraped into 1 ml of medium and sonicated. Samples of 0.2 ml were then titrated on BHK C13 cells where ts recombinant virus could be shown at 38.5°C and at 31°C where recombinants of plaque morphology only could be demonstrated (Figure 3c).

In addition to the recombinants, virus was isolated whose restriction enzyme pattern did not show it to differ from the original virus used to transform the cells. This was surprising particularly as the RE∝ and RE1 cell lines had been established for 6 and 7 years respectively. These cell lines had both been stored frozen (-70°C) one to 4 times during their history and were in culture for up to 40 passages when experiments were carried out. A diagram of the recombinant DNA rescued from virus generated from superinfection studies is seen in Figure 5. Rescue of the transforming virus suggests that recombination may have followed initiation of replication of the original transforming virus upon superinfection.

Although studies on recombinant DNA can unambiguously define portions of the HSV genome present in the transformed

cell it cannot answer the question as to what is the state of viral DNA in the transformed cell. The viral DNA may be present as different fragments in different cells of the transformed line or the viral DNA may be totally present in one or a small number of the transformed cells, presumably, in that case, in a latent state.

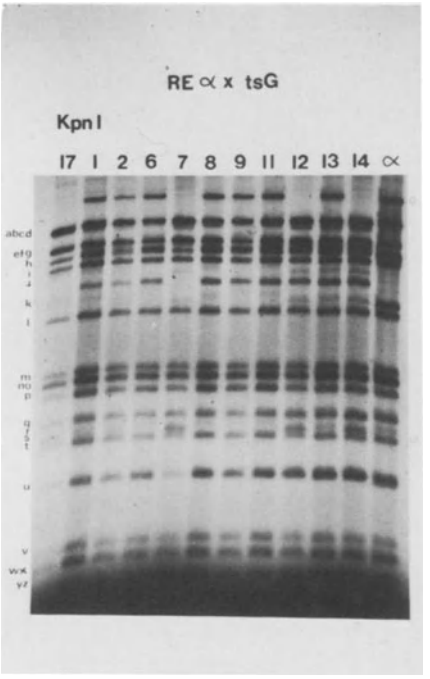

Figure 4

Autoradiograph of ^{32}p-labelled DNA of HSV-1 HFEM ∝ and 7 representative recombinants (nos. 1, 2, 6, 8, 9, 11, 13) which were digested with restriction endonuclease Kpn1 and subjected to electrophoreses on a 0.5% agarose gel, DNA fragments are lettered in accordance with HSV-1 strain 17 Kpn1⁻ restriction endonuclease map. Those sequences characteristic of HSV-1 ∝ at 0.54-0.65 map co-ordinates are detected by a Kpn1⁻ digest shown by the separate bands d and s of HSV-1 17 which are fused to give a new (d+s) larger molecular band characteristic of HSV-1 ∝. The d+s fusion of HSV-1 HFEM ∝ is marked ds, the molar band presentation the recombinant which corresponds to neither HSV-1 strain 17 or HSV-1 HFEM ∝ represents an intermediate band resulting from the crossover event. The restriction enzyme profiles of the live recombinants analysed resemble one another due to the similarities between the genome structures of HSV-1 HFEM ∝ and HSV-1 17 analysis and definition of the crossover regions in these recombinants is not possible. (Gel copy by courtesy of M. Park)

Difficulty in defining a set of conditions under which recombinant virus may consistently be rescued on superinfection has hindered progress in examining different clones of a single transformed line to define whether each clone contains the same amount of HSV DNA.

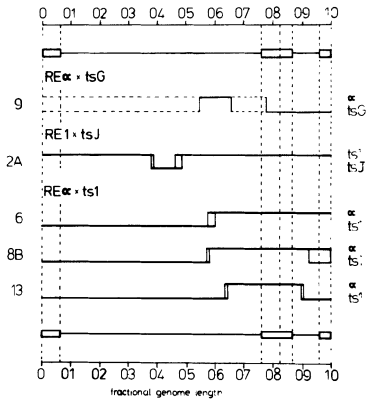

Figure 5.

Molecular model for the HSV genome and analysis of crossover points in recombinants 9, 2A, 6, 8B, 13. The DNA sequences rescued from the transformed cell line form the uppermost line in each recombinant, whereas those present from the superinfecting virus compose the lower line of each structure. The box areas are those regions of uncertainty where a crossover event has occured. The dotted lines in recombinant 9 indicate regions of uncertainty; due to similarities in restriction endonuclease profiles, HSV-1 tsG and HFEM cannot be distinguished in these regions. The solid lines in this recombinant represent regions of the genome which can be identified as originating from either the superinfecting virus of the original transforming virus. Several restriction digests have revealed substantial differences between HFEM and HSV-1 17 which show that the sort unique of these recombinants arises from the superinfecting virus HSV-1 tsG. Furthermore, HFEM has a 2 x 10^6 dalton deletion in the internal long repeat compared to HSV-1 17: this is not represented in any of the recombinants allowing characterization of these sequences as arising from HSV-1 tsG.

Recombination studies (Nimmo and Macnab, personal communication) as a means of analysing the function of the thymidine kinase (TK) gene involved in biochemical transformation of TK negative cells transformed by the Bam HI p fragment of HSV-1 17 (10) have been applied using superinfection studies with the TK negative mutant HSV-1 17 ts G syn both PT and NPT. Yields from control and transformed cells after superinfection at 38.5°C were plated in HAT (hypoxanthine, aminopterin, thymidine) selective medium on to $LMTK^-$ cells. After 4-5 days the $LMTK^-$ cells were scraped into 1 ml medium, sonicated and surviving virus plated on to BHK C13 cells from which plaques were picked and analysed using a modification of the TK assay of

Jamieson and Subak-Sharpe (11).

In the superinfection studies of TK transformed LMTK$^-$ cells it has been possible to demonstrate putative recombinant virus with a TK activity intermediate between the wild-type values and the TK negative mutant used to superinfect.

Table 3 Thymidine Kinase Values of Potential recombinant plaques which show HSV TK activity picked from Cl3 cells

	Counts per minute of ^{3}H-thymidine incorporated		
Virus	a	b	c
HSV-1, 17 syn+ (TK+)	84,943	39,628	52,981
HSV-1, 17 ts G syn	10,993	7,845	4,356
Plaque 3	33,396	3,600	40,132
Plaque 5	35,065	4,348	29,133

a saline used in incubation reaction

b HSV-1 specific anti HSV-1 thymidine kinase antiserum used in reaction

c normal control rabbit antiserum used in reaction

Plaques 3 and 5 show 89% and 88% knockdown of HSV specific TK activity (counts from b compared with a)

However, incorporation - counts in a - are not as high as wild-type virus HSV-1. 17 syn+ so indicating that the potential recombinant has not the same level of HSV TK activity as the wild type used originally to transform.

The specificity of the rabbit antiserum was verified by a five fold knockdown in ^{3}H thymidine incorporated by WT HSV-1 TK positive virus.

Thirteen other plaques examined in this assay did not give a level of incorporation of ^{3}H-thymidine significantly above control cells whose incorporation in these experiments is a mean of 2,000 cpm.

The ts mutant HSV-1, 17 ts G syn is a multiple mutant having lesions in syn ts and TK at 31° and 38.5°C. It has never been possible to isolate revertants of this mutant and it is possible that there are other non-lethal mutations which have not been identified. Certainly the intermediate value of the TK activity found in plaques 3 and 5 would appear to represent some type of recombination but obviously not in the total TK gene necessary for wild-type expression. In these studies the transforming virus fragment was cloned from HSV-1, 17 the parent virus of ts G syn so it was not possible to identify a recombinant virus by restriction

enzyme analysis.

DISCUSSION

What is the attraction of studying the amount of HSV information in HSV morphologically transformed cells by genetic means, namely the detection of recombinant DNA?

Southern (12) blotting technique, which is so successfully used to demonstrate integrated viral sequences in rodent cells transformed by the smaller DNA viruses polyoma, SV40 and adenoviruses has not so far been very easily useful in detecting HSV sequences present in HSV transformed cells. Although its use has been reported (14, 15, 16). The exact reason for this is not known but may be attributed to the size and complexity of the HSV genome, the fact that the genome of HSV cross hybridizes to some regions of rat embryo, monkey and other tissue culture cells or that the correct hybridization techniques using cloned defined fragments have not yet been clearly resolved.

In the hamster system it has been shown by liquid hybridization that continued passage and cloning of HSV transformed cells results in loss of HSV DNA (13). These results may indicate that transformation by HSV results in cells whose HSV is not stably integrated in the host cell DNA; but the results do not exclude the possibility that the total DNA is present but is only maintained in a small number of cells. It is also possible that the HSV may be present in plasmid form in the HSV transformed cells and the state of molecular studies at the present time is not able to answer these different possibilities.

The technique of superinfection can be used with clinical material and the detection by complementation of defective or uninducible virus genome latent in human

ganglia (17) shows the usefulness of this technique. Similar studies on superinfection by cytomegalovirus (CMV) of human embryo lung cells latently infected with HSV-1 has resulted in the rescue of reactivated HSV-1 virus whose growth properties resemble the latent HSV-1 and not the superinfecting CMV (18). Restriction enzyme analysis of putative recombinant DNA might, however, reveal some DNA sequences of CMV present in the reactivated virus. One unresolved problem of superinfection has been the isolation of revertant virus (restriction enzyme pattern of super-infecting virus) after superinfection of transformed cells by ts mutants. This revertant virus, phenotypically ts+, is not seen in superinfection of control cells. In addition to the consistent way in which it has been isolated from transformed cells Dr S.M.Brown of this Institute confirms that a similar problem is seen when nervous tissue is super-infected by ts mutants to probe for HSV DNA. It is possible that such virus represents recombination event where the units of resolution of restriction enzyme analyses do not allow identification of the DNA sequences incorporated from the transformed cells. Halliburton (19) cites examples, in his review of recombination events between herpesviruses, where recombinants RSl_0 and $RB7_4$ can be identified in protein analyses by polyacrylamide gel electrophoresis in cases where restriction enzyme analysis has not succeeded in detecting recombinant DNA sequences. However, at present, the consistent finding of revertant virus present after superinfection of transformed, tumour or nervous tissue and not present from superinfection of similar control tissue has no clear explanation.

Genetic probing by superinfection will continue to be a useful tool in the study of human disease whose aetiology is associated with viral infection eg cancer of the cervix.

REFERENCES

1. Macnab, J. C. M. (1974). J. Gen. Virol 24, 143-153.

2. Macnab, J. C. M. (1975). Second International Symposium on Oncogenesis and Herpesviruese 1, 227-236 International Agency for Research on Cancer, Lyon.

3. Macnab, J. C. M. (1976). PhD thesis, University of Glasgow.

4. Macnab, J. C. M. (1979). J. Gen. Virol. 43, 39-56.

5. Macnab, J. C. M. and Timbury, M. C. (1976). Nature 261, 233-235.

6. Kimura, S., Esparza, J., Beynish-Melnick, M. and Schaffer, P. A. (1974). Intervirology 3, 162-169.

7. Wilkie, N. M., Clements, J. B., Macnab, J. C. M. and Subak-Sharpe, J. H. (1974). Cold Spring Harbor Symp. Quant. Biol. 39, 657-666.

8. Park, M., Lonsdale, D. M., Timbury, M. C., Subak-Sharpe, J. H. and Macnab, J. C. M. (1980). Nature 285, 412-415.

9. Lonsdale, D. M. (1979). Lancet 1, 849-851.

10. Wilkie, N. M., Clements, J. B., Boll, W., Mantei, N., and Lonsdale, D. M. and Weissman, C. (1979). Nucleic Acids Res. 7, 859-877.

11. Jamieson, A. J. and Subak-Sharpe, J. H. (1974). J. Gen. Virol 24, 481-492.

12. Southern, E. M. (1975). J. Mol. Biol. 98, 503-517.

13. Minson, A. C., Thouless, M. E., Eglin, R. P. and Darby, G. (1976). Int. J. Cancer 17, 493-500.

14. Reyes, G. R., La Femina R., Hayward, S. D. and Hayward, G. S. (1979). Cold Spring Harbor Symp. on Quant Biol. 44, In press.

15. Galloway, D. (1980). Transformation Workshop Communication at the International Conference on Human Herpesviruses, Atlanta March 17-21. In press.

16. Hayward, G. S. (1980). DNA Workshop Communication at the International Conference on Human Herpesviruses, Atlanta March 17-21. In press.

17. Brown, S. M., Subak-Sharpe, J. h., Warren, K. G., Wroblenska, Z. and Koprowski, H. (1979). Proc. Natl. Acad. Sci. 76, 2364-2368.

18. Colberg-Poley, A. M., Isom, H. C. and Rapp, F. (1979).

Proc. Natl. Acad. Sci. 76, 5948-5951.

19. Halliburton, I. W. (1980). J. Gen. Virol. 48, 1-23.

ACKNOWLEDGMENTS

I acknowledge with thanks the courtesy of Mrs. M. Park in allowing me to print her as yet unpublished Figure 4. Table 1 was reprinted by permission from Nature, Vol. 261, No. 5557, pp. 233-235, copyright (c) 1976, Macmillan Journals Ltd. Figures 2 and 5 were reprinted by permission from Nature, Vol. 285, No. 5764, pp. 412-415, copyright (c) 1980, Macmillan Journals Ltd.

15. Identification, cloning and sequencing of the HSV thymidine kinase genes

G.S. Hayward*, G.R. Reyes*, E.R. Gavis† and S.L. McKnight†

SUMMARY

We have identified the map locations of the thymidine kinase genes from HSV-1 and HSV-2 by transfecting Ltk^- cells with isolated DNA fragments and selecting for TK^+ colonies in HAT medium. For HSV-1(MP), the XbaI-D, XhoI-E, and BamHI-O restriction fragments transferred TK activity whilst for HSV-2(333) the BglII-G, HindIII-H, SalI-G and BstEII-H fragments were positive. The BamHI-O fragment of HSV-1 (map coordinates 0.291-0.316) and the SalI-G fragment of HSV-2 (0.281-0.319) were then cloned in the prokaryotic plasmid pBR322 by recombinant DNA techniques. In addition, a series of defined deletion mutants of the HSV-1 TK gene were constructed *in vitro*. Assays of the ability of deleted DNAs or restriction enzyme cleaved plasmid DNA to rescue Ltk^- cells defined the functionally active gene sequence to lie between map coordinates 0.304-0.313 in both genomes. The same deletion mutants that were positive in transfection experiments also expressed viral thymidine kinase activity when injected into *Xenopus* oocytes. A contiguous 1800bp segment of the BamHI-O fragment of HSV-1 has been sequenced on both strands by chemical methods. This sequence contains a single open reading frame on the *r*-strand consistent with the known polarity of TK mRNA synthesis and between recognizable transcription initiation (TATTAA) and poly A (AATAAAA) signals. Hybridization and S1 nuclease mapping of poly A-containing RNA (synthesized at early times after

Y. Becker (ed), Herpesvirus DNA.

infection) to an appropriate section of single stranded TK DNA cloned in bacteriophage M13 confirms that the predominant TK mRNA is unspliced and roughly 1310 nucleotides in length. The putative 5' initiator nucleotide occurs 77 bp downstream from the EcoRI site at map coordinate 0.3125. The location of probable translation initiator and terminator codons suggest that the TK protein consists of 376 amino acids. Closely spaced deletions across the promotor region at the 5' end indicate that at least 95 nucleotides of 5' flanking DNA upstream from the TATTAA transcription signal are required for quantitive synthesis of TK mRNA in Xenopus oocytes.

INTRODUCTION

The synthesis in HSV-infected cells of a virus-coded TK enzyme that has quite distinct biochemical properties from those of host enzyme(s)(1, 2) has elicited a great deal of interest and research in recent years. Initially, the system offered a unique model for studying biochemical transformation of mammalian cells and the associated integration and retention of herpesvirus- specific genetic information in the cellular genome (3-7). Secondly, because the viral TK enzyme has a much wider substrate specificity than the cellular enzyme, it provides the primary target of action for a group of new and effective antiviral agents that are analogues of thymidine and are phosphorylated in viral infected cells but not in uninfected cells (8). Thirdly, following the work of Wigler et al. (9) there has been widespread realization that the HSV TK transformation assay provides a very powerful co-selection mechanism for inserting other foreign genes into eukaryotic cells (10, 11). Fourthly, the fact that the biological activity of the gene can easily be assayed, plus the observation that during infection the

viral tk gene is apparently not activated until after the immediate early genes are expressed, offers an exciting model system for studying eukaryotic gene regulation (12).

A number of researchers have been studying various aspects of the molecular biology of the HSV thymidine kinase for several years, especially the groups of Kit at Baylor; Summers and Summers at Yale; Jamieson, Preston and Subak-Sharpe in Glasgow; and Silverstein and Axel at Columbia. More recently, following the introduction of restriction enzyme mapping and recombinant DNA cloning, several groups including ourselves have simultaneously embarked on a detailed characterization of the isolated tk genes from different strains of herpes simplex virus.

This report contains a brief description of the results obtained from a collaboration between the laboratory of G. Hayward at Johns Hopkins and that of S. McKnight at the Carnegie Institution in Baltimore and includes the complete nucleotide sequence of the HSV-1(MP) TK gene (12a).

RESULTS AND DISCUSSION

Biochemical Transformation with Isolated Fragments of HSV-1 and HSV-2 DNA

We initially became involved in this work because of questions raised during our attempts to obtain focus formation (morphological transformation) in Balb/3T3 cells with isolated fragments of HSV DNA (13). Surprisingly the map locations of "transforming" fragments from HSV-1 differed widely from those of HSV-2 but correlated well with a similar difference in the published map locations of fragments that transferred TK activity in the two genomes (9, 14). Since biochemical and morphological transformation have often been discussed and assayed synonymously in HSV in the past

these results tended to imply a very close association between the two functions and possibly also a translocation in their map locations between the HSV-1 and HSV-2 genomes. However, our attempts by blot hybridization to detect cross-homology between DNA sequences at 0.31-0.415 in HSV-1 and 0.58-0.63 in HSV-2 proved negative, and Balb/3T3 cells transformed with these fragments did not synthesize detectable levels of viral TK enzyme (13). We therefore decided to test the morphologically transforming fragments directly for the ability to transfer viral TK activity. The number of TK^+ colonies developing in experiments with sets of XbaI, BglII and BamHI fragments from HSV-1(MP) DNA, and EcoRI, BglII and HindIII fragments from HSV-2(333) DNA are listed in Table 1. The map locations of all positive fragments and the presumed inactivating cleavages by BglII for HSV-1 and EcoRI and BamHI for HSV-2 are illustrated in Figure 1. These results are consistent with the conclusions of Wigler et al. (9) for HSV-1 but differ from those of Maitland and McDougall (14) for HSV-2. Wigler, et al. (9) identified the HpaI-I and BamHI-P fragments from HSV-1(F) as being positive in similar assays, although only the map location of HpaI-I (0.266-0.322) was known at the time. They also concluded that one of the two EcoRI sites within BamHI-P inactivated transfer of TK activity. These sites map at 0.296 and 0.3125. In our experiments the 29kb XbaI-F and 3.5kb BamHI-O fragments of HSV-1(MP) were positive. Although the BamHI fragment patterns of HSV-1(MP) and HSV-1(F) differ in several ways our BamHI-O fragment is clearly equivalent to the positive BamHI fragment in the experiments of Wigler et al. (9). It maps at 0.292-0.316 in HSV-1(MP) DNA (G.S. Hayward, unpublished experiments) and lies entirely within the large Xba-F fragment at coordinates 0.291-0.451. Other fragments from HSV-1(MP) DNA that we have identified as being capable of producing stable TK^+ transformants of Ltk^- cells are the 8.2kb XhoI-E species, and the 5.7kb BstEII-H species. Blot

hybridization experiments indicate that XhoI-E and BstEII-H map at 0.278-0.333 and 0.299-0.337 (Figure 1). Therefore, the inactivation by BglII and EcoRI must occur at the sites at 0.311 and 0.3125 map units.

Remapping of the HSV-2 Thymidine Kinase Gene

In our experiments the BglII-G and HindIII-H fragments of HSV-2(333) DNA rescued Ltk$^-$ cells at high efficiency

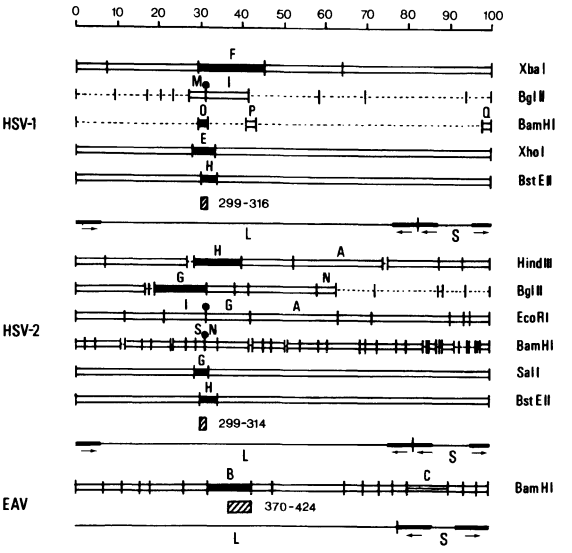

Figure 1: Physical locations in the genomes of HSV-1(MP), HSV-2(333) and EHV-1 of isolated DNA fragments that proved capable of transferring viral thymidine kinase activity to Ltk$^-$ cells in transfection experiments. Solid bars represent positive fragments and open bars record all negative fragments whose map coordinates are known. Hatched bars illustrate for HSV-1 and HSV-2 the minimum areas common to all positive fragments and for EHV-1 the sequences which exhibit cross-homology with the HSV-1 BamHI-O fragment. Horizontal arrows indicate the inverted repeat segments of each genome. Mapping data for HSV-1 and HSV-2 DNA are derived from Hayward, G., Buchman, T. and Roizman, B. (unpublished experiments) as cited in Morse, et al (35) and for EHV-1 DNA from B. Henry, R. Robinson, G. Hayward and D. O'Callaghan (manuscript in preparation).

Table 1. Remapping HSV-2 Thymidine Kinase by Biochemical Transformation of Ltk⁻ Cells

HSV-2 DNA Fragment		No. of Colonies/ No. of Dishes			HSV-1 DNA Fragment		Colonies/Dishes	
BglII	C	-	-	0/2	BglII	I	0/6	0/2
"	G	34/6	49/2	18/2	"	M	0/2	0/2
"	J	-	-	1/2				
"	N	-	-	0/2	BamHI	O	3/2	11/2
"	O	0/2	1/2	0/2	"	P	0/2	0/2
EcoRI	B-J	0/2	0/2	-	XbaI	DS	0/2	0/2
"	C-J	0/2	0/2	-	"	GS	0/2	0/2
"	A,F-J	0/2	0/2	-	"	C	0/2	0/2
"	D	0/2	0/2	-	"	D,E	0/2	0/2
"	E	0/2	0/2	-	"	F	5/2	4/2
"	G,H	0/2	0/2	-	"	G	0/2	0/2
"	I	0/2	0/2	-				
"	J	0/2	0/2	-	No DNA		0/4	0/5
"	K	0/2	0/2	-	Carrier Only		0/2	0/4
"	L	0/2	0/2	-	No DMSO		0/3	0/4
"	M	0/2	0/2	-				
HindIII	A	1/2	0/2	0/2				
"	B	-	0/2	0/2				
"	C,D	-	0/2	0/2				
"	E,F,G,	-	0/2	0/2				
"	H	14/2	34/2	10/2				
"	I	-	0/2	0/2				
"	J	-	0/2	0/2				
"	K	-	0/2	0/2				
"	L	-	(5)+/2	0/2				
"	M	-	0/2	0/2				
No DNA		0/5	0/5	0/2				
Carrier Only		0/6	0/2	0/2				
No DMSO		0/4	0/2	0/2				

+ Transient Colonies Only

whereas all other BglII or HindIII species and all EcoRI fragments were negative (Table 1). The map coordinates of these two fragments overlap by 4.6kb at 0.286-0.315 (Figure 1) an exactly equivalent position to that of the BamHI-O fragment in HSV-1 DNA and quite different from that described by Maitland and McDougall (14). More recently, McDougall et al (15) have revised their interpretation of the location of the HSV-2 gene and reported results similar to ours. In additional

experiments we found that the 5.6kb SalI-G fragment of HSV-2(333) from map position 0.281-0.319 and also the BstEII-H fragment were positive in biochemical transfection experiments, but that no BamHI fragments transferred TK activity. We conclude that the EcoRI site at 0.313, and a BamHI site close to it, must render the HSV-2 TK gene inactive whereas the BglII site at 0.315 does not.

Cloning of the HSV-1 and HSV-2 TK Fragments in pBR322

We have inserted a number of HSV DNA fragments that carry an intact TK gene into the E. coli K12 plasmid pBR322. The 3.5kb HSV-1(MP) BamHI-O fragment was ligated into the BamHI site within the tetracycline resistance gene of pBR322 and a recombinant plasmid referred to as pHSV106 was selected for use in the functional mapping and sequencing work described below. Similar clones have been described by others (16-18). For HSV-2(333), several pBR322 derived plasmids containing the TK gene have been constructed: pGR1 contains the 5.6kb SalI-G fragment in the leftward orientation, pGR3 contains the SalI-G fragment in the rightward orientation, pGR28 contains the 17kb BglII-G fragment inserted into the pBR322 BamHI site and pGR93 contains the 17.5kb HindIII-H fragment.

Cleavage Maps and Biological Activity of the Cloned TK DNA Fragments:

Detailed restriction enzyme cleavage maps of the cloned BamHI-O and SalI-G fragments in the pHSV106, pGR1 and pGR3 plasmid DNAs were constructed by standard double digest and blot hybridization procedures. The results of these experiments proved to be consistent with what we knew from mapping the viral DNA directly. The efficiency

Table 2. Thymidine Kinase Transfer with Cleaved and Deleted pHSV106 Plasmid DNAs

Treatment	Colonies/ Dishes	Treatment	Colonies/ Dishes
pHSV106 (100ng)		pHSV106 Deletions (200ng)	
Uncleaved	41/3	Parent (3500bp)	105/2
BamHI	32/2	Δ5'(a) (-200bp)	75/2
BglII	0/4	Δ5'(b) (-670bp)	0/2
EcoRI	0/4	Δ5'(c) (-720bp)	0/2
HincII	0/2	Δ5'(d) (-1010bp)	0/2
BamHI/AluI	1/2	Δ5'(e) (-1090bp)	0/2
BamHI/BstEII	36/2	Δ5'(f) (-1190bp)	0/2
BamHI/EcoRI	1/2	Δ5'(g) (-1240bp)	0/2
BamHI/HincII	0/2	Δ5'(h) (-1340bp)	0/2
BamHI/PvuII	20/2		
BamHI/PstI	0/2	Δ3'(i) (-210bp)	121/2
		Δ3'(j) (-570bp)	79/2
DMSO Only	0/2	Δ3'(k) (-770bp)	47/2
Carrier Only	0/2	Δ3'(l) (-1130bp)	27/2
Carrier and DMSO Only	0/2	Δ3'(m) (-1320bp)	37/2
		Δ3'(n) (-1600bp)	0/2
		Δ3'(o) (-1940bp)	0/2
		No DNA	0/5
		Carrier Only	0/2

of biochemical transfection of Ltk^- cells in HAT selection media with either BamHI and SalI cleaved plasmid DNA or supercoiled plasmids was also found to be essentially equivalent to that with isolated viral DNA fragments (100-300 colonies/μg DNA/10^6 cells). Using this assay system we attempted to further delimit the location of the smallest active TK gene fragments by measuring colony formation after cleavage with various restriction enzymes in addition to BamHI. The results are listed in Tables 2 and 3 and summarized in Figure 2. The single cleavage sites in BamHI-O for HincII (0.3115), BglII (0.311), SacI (0.308) and KpnI (0.3075) inactivated transfer of TK activity whereas the BstEII site at 0.299 and neither of the PvuII sites at 0.300 or 0.313 did so. Presumably the EcoRI site at 0.3125 and

not that at 0.296 was responsible for the at least 50-fold reduction in numbers of colonies formed after cleavage with that enzyme.

Comparison of the cleavage maps of the HSV-2 SalI-G fragment and the HSV-1 BamHI-O fragment indicates that several sites may be common to both, namely PvuII at 0.3135/0.313, EcoRI at 0.313/0.3125, KpnI at 0.308/0.3075, PvuII at 0.300/0.300 and BstEII at 0.299/0.299. From our original mapping of viral DNA, the single BglII sites at approximately 0.311 in both genomes were assumed to be identical; however, the differences in effect on TK transfer by BglII cleavage of the two genomes necessitated a re-evaluation which showed that this site lies to the left of the inactivating EcoRI site in HSV-1 but to the right of it (at 0.315) in HSV-2. Since the right hand end of the HSV-2 TK gene in pGR3 lies between 0.313 (EcoRI) and 0.315 (BglII) at virtually

Table 3. Thymidine Kinase Transfer with pGR1 and pGR3 Plasmid DNAs

Treatment	Colonies/ Dishes	Treatment	Colonies/ Dishes	Treatment	Colonies/ Dishes
pGR1 (100ng)		pGR1 (70ng)		pGR3 (70ng)	
Uncleaved	54/2	EcoRI	0/2	ClaI	0/2
Uncleaved	44/2	HindIII	11/2	EcoRI	0/2
		HindIII/BamHI	0/2	HindIII	20/2
pGR3 (100ng)		HindIII/BglI	0/2	SacI	9/2
		HindIII/BglII	27/2	SalI	19/2
Uncleaved	44/2	HindIII/HincII	27/1	HindIII/AvaI	0/2
Uncleaved	15/1	HindIII/KpnI	0/2	HindIII/BamHI	0/2
Uncleaved	52/2	HindIII/MboII	0/2	HindIII/BglI	0/2
		HindIII/PvuII	1/2	HindIII/BglII	10/2
pGR1		HindIII/XhoI	28/1	HindIII/HincII	24/2
				HindIII/KpnI	0/2
BamHI (1μg)	0/2	No DNA	0/2	HindIII/MboII	0/2
BamHI (2μg)	0/2	Carrier Only	0/3	HindIII/PvuII	0/2
BamHI (4μg)	0/2			HindIII/XhoI	10/2
EcoRI (1μg)	1/2			No DNA	0/2
EcoRI (2μg)	0/2			Carrier Only	0/2
EcoRI (4μg)	0/2				

the identical map location as the right hand end of the gene in pHSV106 (between EcoRI at 0.3125 and PvuII at 0.313) we can be reasonably confident that other sites that inactivate HSV-2 TK should lie to the immediate left of 0.313. Accordingly, we presume that it is the PvuII site at 0.310 not that at 0.3135, the BamHI site at 0.311 not that 0.288 and the KpnI sites at 0.306 and

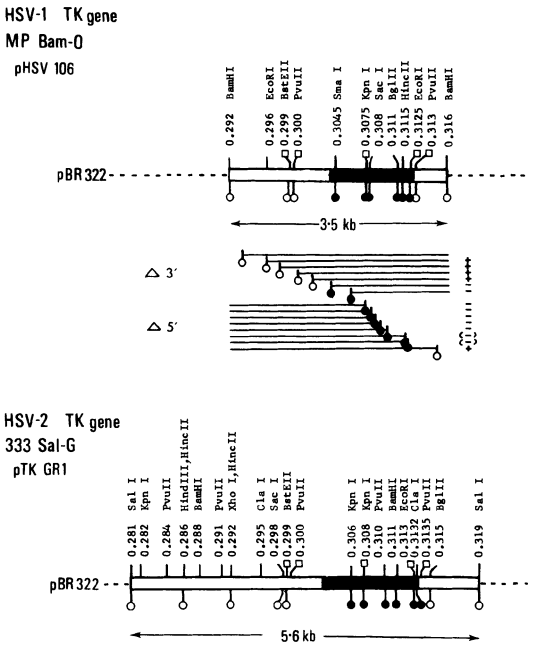

Figure 2: Structure of the cloned HSV-1 BamHI-O and HSV-2 SalI-G fragments illustrating the approximate map location of the TK gene and relevant restriction enzyme cleavage sites. Cleavage at coordinates marked with closed circles (●) inactivates transfer of TK activity to Ltk⁻ cells whereas the transfer is unaffected by cleavage at the open circles (o). The lengths and positions of remaining viral sequences in the 3' and 5' deletion plasmids derived from pHSV106 are also indicated. The retention of or loss of ability of each deletion plasmid to synthesize TK enzyme in oocytes is denoted with (+) or (-) symbols.

0.308 not that at 0.282 that inactivate TK transfer from this plasmid. Consistent with this interpretation we found that cleavage at several unambiguous sites to the left of 0.299 did not affect TK activity: namely, HindIII at 0.286, XhoI at 0.292 or SacI at 0.298. As expected, cleavage with HincII (sites at 0.281, 0.286, 0.292 and 0.319) did not inactivate TK transfer either but a subseqently identified ClaI site approximately 20bp to the right of EcoRI at 0.313 does eliminate transfer of TK activity. Therefore, the TK genes in HSV-1 and HSV-2 occupy identical positions between co-ordinates that do not extend beyond 0.300 or 0.3135 (2.0kb). Taking into account the finding by Colbere-Garapin et al. (16) that the SmaI site, which we map at 0.3045, inactivates HSV-1 TK the dimensions for the HSV-1(MP) gene location are reduced to no more than 1.6kb.

Further Definition of the Left-Hand End of the HSV-1 TK Gene Using Deletion Plasmids

The results described above gave fairly precise definition of the right hand or 5' ends of both TK genes (ie. within 100bp and 300bp of 0.313 map units) but none of the enzymes used in our experiments gave any useful cleavage sites in the 1200bp region between map units 0.300 and 0.308 at the left hand or 3' ends of either gene. The problem was overcome by using two series of plasmids derived from pHSV106 which contained defined deletions extending inwards from the BamHI sites on either side. Construction of these deletions is described elsewhere by McKnight and Gavis (18a). Figure 3 illustrates the size range of the deletion plasmids selected for use and Table 2 shows the number of colonies obtained in biochemical transfection experiments. The plasmids deleted by 1940bp and 1600bp from the 3' end or greater than 670bp from the 5'end are inactive in the assay whereas those with deletions

extending only 210bp, 570bp, 770bp, 1130bp and 1320bp from the 3' end or 200bp from the 5' end retain the ability to biochemically transform Ltk^- cells. These results place the left hand or 3' boundary within a 280bp region between 0.302 and 0.304 in the viral genome.

Viral Thymidine Kinase Activity in Xenopus Oocytes

Microinjection of 10 nanogram quantities of supercoiled pHSV106 plasmid DNA into Xenopus oocytes (50 per assay)

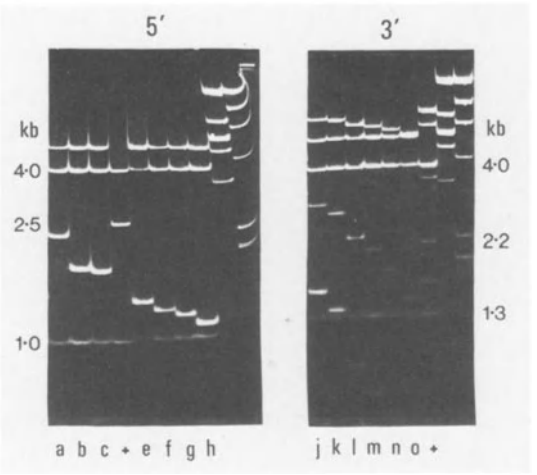

Figure 3: Agarose gel electrophoresis of cleaved DNA from thirteen of the deletion plasmids used in these experiments. The photograph allows comparison of the relative sizes and locations of the deletions from each plasmid within the 5'-set (left hand panel) or within the 3'-set (right hand panel). The DNAs from the 5' deleted plasmids were cleaved with BstEII, BamHI and HindIII whereas those from the 3'-set were digested with BamHI, KpnI and HindIII. Partial cleavage with KpnI permitted accurate size measurements of both large and small deletions in the 3'-set on a single gel: however, since the BamHI digestions were also incomplete some additional high molecular weight bands are apparent in both DNA sets. The sizes and locations of limit digest fragments in the parental pHSV106 channels (+) are given alongside each gel. EcoRI and HindIII cleaved phage lambda DNA samples are included in the last two channels in both gels. The number of base pairs of viral DNA deleted in plasmids (a) to (h) and (i) to (o) are listed in Table II. The structures of two of the deletion plasmids (a=H24, and m-S29) are drawn in Figure 7.

resulted in a 100 to 200-fold stimulation of TK activity. Enzyme activity was measured by phosphorylation of ^{3}H-thymidine in extracts prepared 24 hr after microinjection. All of the same deletion plasmids that were active in biochemical transfection assays were also strongly positive in the oocyte assay (60 to 200 fold stimulation) but two other plasmids that were deleted by 670bp and 720bp from the 5'end including the EcoRI site at 0.3125, exhibited low but detectable levels of TK activity in oocytes (3 to 12-fold stimulation). Control experiments showed that pBR322 DNA did not increase thymidine phosphorylation in oocytes at all and that the presence of anti-TK antibody but not non-immune IgG reduced the activity with pHSV106 by 85%. When ^{125}I-iododeoxycytidine, which can be phosphorylated only by the HSV TK and not cellular enzymes (19), was used in the assay, micro-injection of pHSV106 DNA again stimulated TK enzymatic activity in oocytes 200-fold: in comparison, infection with HSV-1 virus yielded a 600-fold stimulation in cultured mouse Ltk^{-} cells. Similarly, oocytes injected with pHSV106 (but not those injected with pBR322) synthesized an immunoprecipitable polypeptide of 40,000 daltons which comigrates with a polypeptide precipitated with anti-TK antibody from HSV-1 infected Vero cells. Finally, we found that induction of TK activity is inhibited by α-amanatin at 0.1 to 1 μg/ml, a concentration known to specifically inhibit form II RNA polymerase. These studies are reported in greater detail elsewhere (18a).

TK^{+} Cell Lines

A panel of more than forty mouse tk^{+} cell lines derived by calcium transfection of Ltk^{-} or Swiss(4E)tk^{-} cells with isolated fragments of HSV-1, HSV-2 and equine abortion virus DNA or with cleaved TK plasmid DNA have

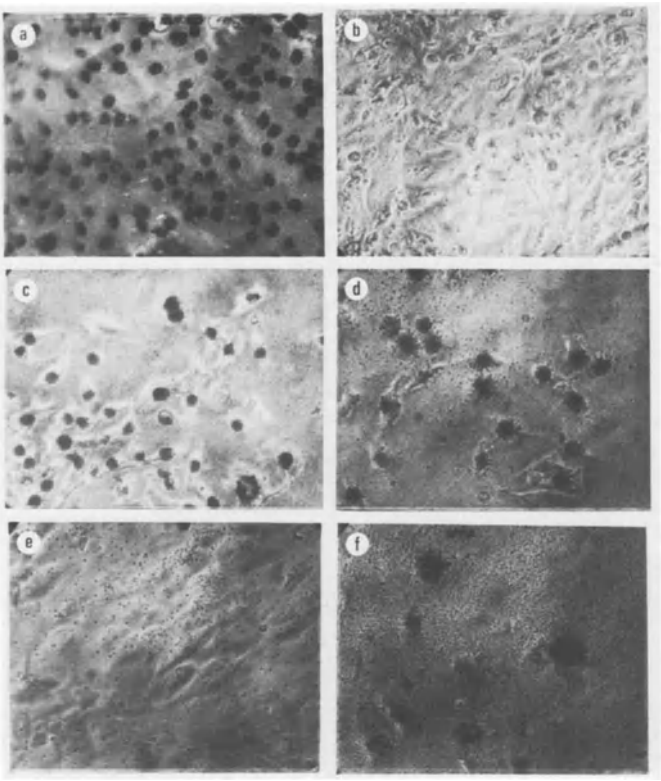

Figure 4: Demonstration by autoradiography of the specific incorporation of ^{125}I-iododeoxycytidine into nuclei of cells expressing HSV TK. Monolayer cultures were prepared in 8-well LabTek slides and grown for 12 hr in the presence of either 10 Ci/µl of ^{3}H-thymidine or 10 Ci/µl of ^{125}I-iododeoxycytidine and 50µg/ml of tetrahydrouridine. After washing, and fixing in methanol, the slides were dipped in Kodak NTB-2 emulsion and exposed in the dark for 24 hr. Panel (a) Vero cells, ^{3}H-TdR; (b) Vero cells, ^{125}ICdR; (c) LH1B2 cells, ^{3}H-TdR; (d) LH1B2 cells (at 30th passage), ^{125}ICdR; (e) LMtk- cells, ^{125}ICdR; (f) LH1X2 cells (at 30th passage), ^{125}ICdR.

been established (G. Reyes and G. Hayward, manuscript in preparation). Note that we used Ltk^{-} cell DNA as carrier in all of these experiments, rather than the more commonly used salmon sperm DNA, to minimize alterations in the genetic content of the resulting Ltk^{+} lines. We hoped that some of these cells might contain and express various portions of additional viral DNA sequences adjacent to the TK genes. The Ltk^{+} cells

have stably retained the ability to express the viral TK genetic information for at least 30 passages in some cases (eg. LH1-B2 and LH1-X2) provided they were maintained and passaged in HAT selective medium. As a convenient and specific assay for viral TK activity we screened for incorporation of ^{125}I-iododeoxycytidine into cell nuclei by autoradiography (Figure 4).

Integration and Amplification of Viral DNA Fragments

The genomes of almost all of these cell lines have been shown to contain viral TK DNA sequences by blot hybridization with BamHI-O and SalI-G probe DNA (Table 4). Most of the cellular DNAs contain only one or two restriction fragments complementary to viral sequences whereas the Ltk$^-$ parent cell DNA has none. Close examination of several of our fragment-transformed Ltk$^+$ cell lines has revealed that: (1) the viral DNA is integrated into either cellular or carrier DNA; (2) the site of integration differs in each cell line; and (3) some lines contain multiple tandemly repeated copies of the TK DNA sequences. These points are illustrated and summarized in Figures 5 and 6. Pellicer et al.(20) have shown previously that the 3.5kb BamHI fragment is integrated at one copy per cell in the LH-7 transformant cell line and this DNA was used as a standard for comparison with DNA from the transformants that we have generated. Three Ltk$^+$ lines that received the 29kb XbaI-D fragment and three that received the 3.5kb BamHI-0 fragment from HSV-1(MP) DNA have been studied in detail. Figure 5 shows blot hybridization with pHSV106 DNA probe to each of these cell DNA's after cleavage with BamHI or EcoRI. LH1-X3, LH1-B1 and LH1-B3 all show a single band in the BamHI digests with an intensity equivalent to that obtained with LH-7 DNA whereas BamHI digestion of LH1-X1 gives two such bands. Similarly, LH1-B2 and LH1-X2 give either one and two hybridizing bands respectively in the

BamHI digests, but each band exhibits 10-20 times the intensity of that obtained with equivalent amounts of DNA from the single copy transformant cell lines. This result has been observed consistently with several DNA preparations from both cell lines, and we conclude that they contain multiple copies of the TK DNA sequences. The LH1-B1, LH1-B2 and LH1-B3 cell DNAs (all transfected with the 3.5kb BamHI-O fragment) show unambiguous evidence for integration because they have lost their flanking BamHI sites and the probe now hybridizes to

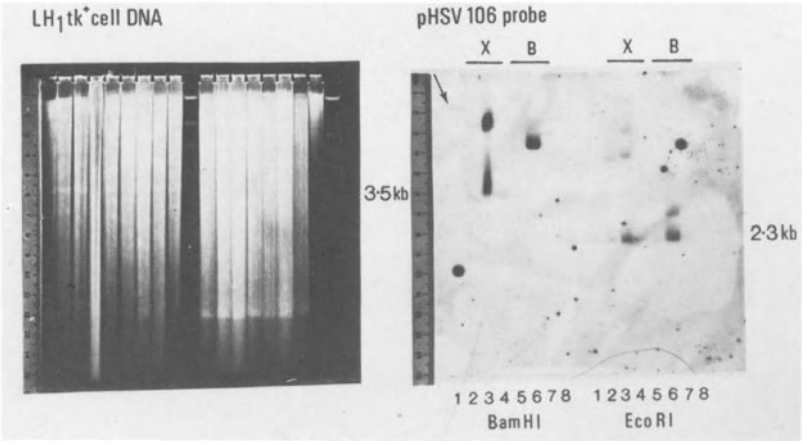

Figure 5: Evidence for multiple tandem repeats in the LH1-B2 and LH1-X2 cell lines. The figure shows a blot hybridization experiment with ^{32}P-labelled pHSV106 DNA to both BamHI and EcoRI digests of various Ltk$^+$ cellular DNAs. The left hand panel contains a UV-light photograph of the ethidium bromide stained cellular DNA pattern after electrophoresis through a 1.4% agarose gel. The right hand panel contains an autoradiograph from the same gel after hybridization with nick translated pHSV106 DNA as a probe. Two sets of samples with 10-15µg of cleaved cell DNA were loaded into each gel slot as follows: 1, LH-7; 2, LH1-X1; 3, LH1-X2 (passage 3); 4, LH1-X3; 5, LH1-B1; 6, LH1-B2 (passage 3); 7, LH1-B3; 8, Ltk$^-$. Slot 9 received 300µg of cleaved phage lambda DNA. The positions of the unintegrated linear 3.5 kb BamHI-O fragment and of the 2.3 kb internal EcoRI-N fragment are indicated with arrows. Comparison of the relative band intensity with that obtained with single copy LH-7 DNA (arrowed) reveals the approximate copy number in the other cell lines. Note that the abberrant migration in slot 3 did not influence the result and that consistently similar findings have been obtained with several different DNA preparations from each of these cell lines.

Table 4. TK^+ Cell Lines Established by Transfection with Viral DNA Fragments

Designation and Origin			Source, Size and Map Location of Input DNA Fragment			Detection of Integrated TK Sequences		
						Number of Sites	Total Copy No.	Positive BamHI Fragment
LH-7(S)	Ltk^-	HSV-1(F)	BamHI-P	3.5kb	0.292-0.316	1	1	14 kb
LH1-X1	Ltk^-	" (MP)	XbaI-D	23 kb	0.291-0.452	2	2	3.5 & 8.5kb
LH1-X2 p3	Ltk^-	" (MP)	XbaI-D	23 kb	0.291-0.452	2	15	3.5 & 8.0kb
LH1-X2 p21	Ltk^-	" (MP)	XbaI-D	23 kb	0.291-0.452	2	2	3.5 & 8.0kb
LH1-X3	Ltk^-	" (MP)	XbaI-D	23 kb	0.291-0.452	1	1	3.5kb
LH1-Xh1	Ltk^-	" (MP)	XhoI-E	8.2kb	0.278-0.333	ND		
LH1-B1	Ltk^-	" (MP)	BamHI-O	3.5kb	0.292-0.316	1	1	17 kb
LH1-B2 p3	Ltk^-	" (MP)	BamHI-O	3.5kb	0.292-0.316	1	15	6.3kb
LH1-B2 p21	Ltk^-	" (MP)	BamHI-O	3.5kb	0.292-0.316	1	3 to 4	6.3kb
LH1-B3	Ltk^-	" (MP)	BamHI-O	3.5kb	0.292-0.316	1	1	7.8kb
LH2-H1	Ltk^-	HSV-2(333)	HinIII-H	17.5kb	0.278-0.333	ND		
LH2-H2	Ltk^-	" (333)	HinIII-H	17.5kb	0.278-0.333	1	1	20 kb
LH2-H3	Ltk^-	" (333)	HinIII-H	17.5kb	0.278-0.333	ND		
LH2-H4	Ltk^-	" (333)	HinIII-H	17.5kb	0.278-0.333	ND		
LH2-Bg1	Ltk^-	" (333)	BglII-G	17.0kb	0.203-0.315	ND		
LH2-Bg2	Ltk^-	" (333)	BglII-G	17.0kb	0.203-0.315	1	3 to 4	8.1kb
LH2-S1	Ltk^-	" (333)	SalI-G	5.6kb	0.281-0.319	1	1	3.6kb
LH2-S2	Ltk^-	" (333)	SalI-G	5.6kb	0.281-0.319	1	1 to 2	13 kb
LH2-Bs1	Ltk^-	" (333)	BstII-H	6.1kb	0.299-0.339	1	1	12 kb
LH2-Bs2	Ltk^-	" (333)	BstII-H	6.1kb	0.299-0.339	1	2 to 3	8.1kb
SH2-Bg1	S-4Etk^-	" (333)	BglII-G	17.0kb	0.203-0.315	ND		
SH2-Bg2	S-4Etk^-	" (333)	BglII-G	17.0kb	0.203-0.315	ND		
LEA-B1	Ltk^-	EHV-1	BamHI-B	15 kb	0.315-0.425	ND		
LEA-B2	Ltk^-	"	BamHI-B	15 kb	0.315-0.425	ND		

single BamHI bands of 17kb, 6.4kb and 7.5kb respectively. Cleavage with other enzymes confirms that this additional DNA must consist of cellular sequences. Similarly, the LH-7 DNA contains a hybridizing fragment integrated into an L-cell BamHI fragment that is 14kb in size. Although integration of the original 3.5kb BamHI DNA fragment does not regenerate the BamHI sites, the internal 2.4kb EcoRI portion appears to remain intact in all three cell lines. Since the multiple copies of viral TK sequences in LH1-B2 and LH1-X2 give rise to only one or two distinct species of BamHI fragments (each larger than the 3.5kb probe DNA) we conclude that either all of the copies integrated independently into identical cellular (or carrier) sequences or, more likely, that a single integrated TK fragment was amplified to create a cluster of adjacent tandemly repeated copies (Figure 6). Further mapping of LH1-B2 DNA shows that the tandem repeat unit is at least 21.5kb in size (defined by the sum of two BstEII multicopy fragments hybridizing to the BamHI probe) and possibly much larger. The LH1-X2 line contains two separate families of multicopy tandem repeats: one retains the BamHI site at 0.292 and the other appears to have lost this site during the integration event. LH1-X1 DNA exhibits a very similar pattern to that of LH1-X2 but both integrated fragments are single copy. The LH1-X series cells were also tested for the presence of the EcoRI-F sequences which represent a 16kb portion of the input XbaI-F fragment mapping from 0.313-0.417. This analysis is complicated because certain viral sequences within this region (even after cloning) cross hybridize specifically to a single BamHI band of 20kb and a slightly larger EcoRI band in all mouse and hamster cell DNAs that we have tested, including that from Ltk^- cells. However, the LH1-X1 and LH1-X2 cell DNAs but not the LH1-B series gave several additional bands that hybridize with this probe. The most intense EcoRI species in LH1-X2 is only 7kb in size implying that only a portion of the adjacent linked

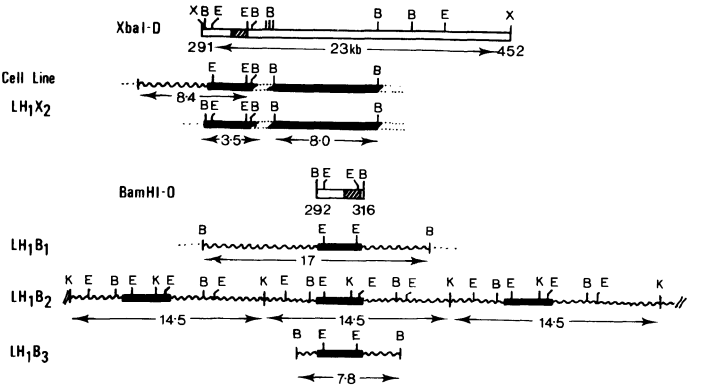

Figure 6: Arrangement of integrated viral DNA sequences in four Ltk+ cell lines derived by transfection with the isolated XbaI-F or BamHI-O fragments from HSV-1(MP) DNA. Open bars indicate the input fragments with hatched bars representing the TK genes. Solid bars denote integrated viral sequences and the wavy lines denote Ltk- cellular sequences. Dotted lines indicate uncertainties in map boundaries. Note that the size of the tandem repeat unit given here for LH1-B2 DNA is a minimum value: it defines only the nearest KpnI sites and could be very much larger.

EcoRI-F sequence is present within the most prominent TK repeat cluster. Figure 6 summaries our current understanding of the structure of integrated viral sequences and provides restriction enzyme cleavage maps within the adjacent cell sequences for the LH1-X2, LH1-B1, LH1-B2 and LH1-B3 cell lines. We emphasize that the usefulness of these panels of cell lines for studying the expression of adjacent viral sequences carried along with the TK gene will be limited until detailed maps of integrated sequences are established in each case.

Cross-Homology Amongst Viral TK DNA Sequences

During the experiments described above we attempted on several occasions to detect HSV-2 TK DNA sequences using the HSV-1 TK DNA probes, but without success. The only time that we achieved this with the heterologous probe

involved an experiment in which 300μg of EcoRI cleaved LH2-Bgl cell DNA was prefractionated by RPC-5 chromatography and each sample eluting at a different salt concentration was further resolved by agarose gel electrophoresis. Blot hybridization revealed a single faint band of 6kb eluting in the middle fractions from RPC-5. In general, we estimate that under our stringency conditions for blot hybridization, total HSV-1 DNA probes hybridize to HSV-2 sequences to an extent that generates radioactive bands with 1/5 the intensity of that observed for the homologous HSV-1 sequences. This kind of experiment performed with an HSV-1 TK DNA probe against HSV-1, HSV-2 and equine abortion virus (EAV) DNAs revealed cross-homology corresponding to only 1/20th of the intensity with HSV-2 TK DNA and at about 1/100th the intensity with a 7.5kb BamHI/EcoRI fragment of EAV DNA. This latter DNA species maps at 0.370 to 0.425 map units in the EAV genome (B. Henry, R. Robinson, G. Hayward, and D. O'Callaghan, manuscript in preparation) and lies within the BamHI-B fragment that was positive in our earlier biochemical transfection assays: presumably it contains the TK gene of that virus.

Use of Cloned TK Genes for Linked Co-Selection of Other Viral Sequences

We have been interested in using the TK gene as a coselection marker for introducing other defined herpesvirus DNA fragments into mammalian cells in culture under conditions favoring expression of the associated viral sequences. Wigler et al. (10) added TK gene DNA together with an excess of unlinked mouse globin DNA to Ltk^- cells. Under these conditions most of the tk^+ transformant cells also contain transfected globin DNA; however, expression of the acquired globin gene proved to be incorrect and at a minimal level. O'Malley et al. (11) obtained more promising results when ovalbumin gene

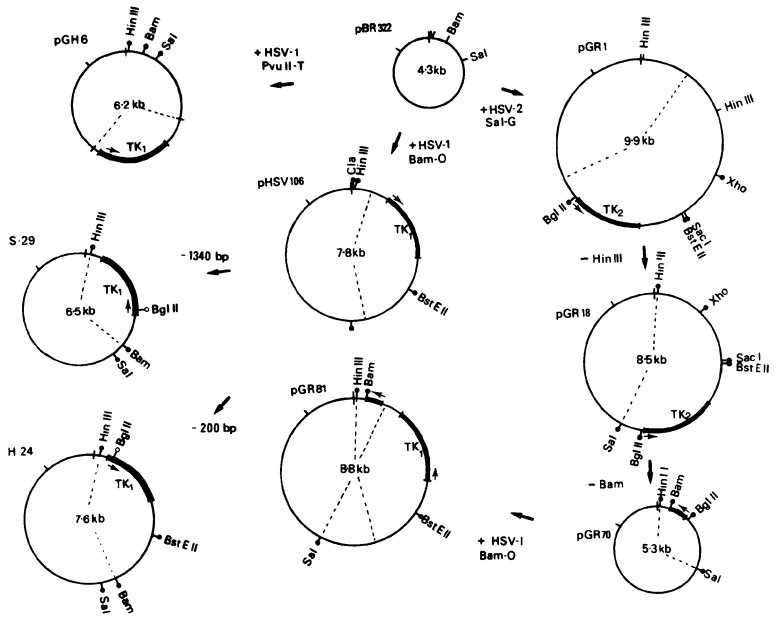

Figure 7: Structure and derivation of various pBR322-TK plasmids. pHSV106 contains an insert of the 3.5 kb BamHI-O fragment from HSV-1(MP) in the Tc^R gene of pBR322. The S29 and H24 deletion derivatives of pHSV106 were constructed by exoIII and S1 digestion from either the SalI or HinIII sites followed by addition of HindIII linkers and reinsertion of the BamHI/HindIII fragment into pBR322. pGH6 received the 1.9 kb PvuII fragment from pHSV106 inserted by blunt-end ligation at the PvuII site in pBR322. The 5.6 kb SalI-G fragment from HSV-2(333) was placed in the Tc^R gene of pBR322 to give pGR1, and pGR18 is a deleted variant in which the portion of pGR1 between the viral HindIII in pBR322 were eliminated. A similar elimination of internal portions of pGR18 between two viral BamHI sites created pGR70 which was then converted into a TK donor plasmid (pGR81 containing a single usable BamHI site) by insertion of the HSV-1 BamHI-O fragment at the BglII site.

DNA was covalently linked to the HSV TK sequences. In this case the transfected tk^+ mouse cell lines expressed chick ovalbumin protein at variable efficiencies. We have proceded on the assumption that direct linkage to the TK gene of the viral sequences to be transfected will favor their expression in cells selected for TK gene expression. Accordingly, we have

cloned various HSV-1 and HSV-2 fragments into appropriate pBR322 derived plasmids that contain the TK gene. One of the first steps was to delete an internal HindIII fragment from pGR1 DNA in an effort to construct a smaller plasmid with greater flexibility. The resulting pGR18 plasmid provides a cloning vehicle with an intact HSV-2 tk gene and single sites for inserting HindIII, BamHI, BglII, SalI, XhoI, BstEII, SacI, or PvuI fragments (see Figure 7). The pHSV106 plasmid can be used directly for inserting only BstEII fragments within the viral sequences or inserting HindIII, ClaI, SalI or PvuI fragments within the pBR322 sequences. At the present time a nearly complete library of HSV-1 BglII fragments ligated into the BglII site in pGR18 has been generated. In addition, selected individual HSV-2 DNA fragments, especially those from morphological transforming regions have been cloned in either pGR18 or pHSV106. A panel of cell lines transfected with these plasmids and possibly incorporating some of the linked coselected viral sequences has been established (Table 5).

Table 5. Transfection of LMtk⁻ Cells with pGR18 Derived Plasmids for Linked Co-selection of Viral Fragments

Transfected Plasmids	Fragment		Colony counts in HAT Medium	Cell line
pGR 126	HSV-1	Bgl II-G	18, 21	LH_1p126
pGR 127		Bgl II-I	41, 26	LH_1p127P
pGR 127		Bgl II-I	16, 22	LH_1p127I
pGR 128		Bgl II-K	28, 17	LH_1p128
pGR 129		Bgl II-M	54, 33	LH_1p129
pGR 130		Bgl II-N	53, 47	LH_1p130
pGR 131		Bgl II-O	54, 36	LH_1p131
pGR 132		Bgl II-P	56, 45	LH_1p132
pGR 135	HSV-2	Bgl II-J	27, 20	LH_2p135
pGR 136		Bgl II-N	17, 14	LH_2p136
pGR 137		Bgl II-P	32, 36	LH_2p137
pGR 138		Bgl II-Q	34, 53	LH_2p138
pGR 139		Bgl II-G	45, 24	LH_2p139
LMtk⁻ DNA only			0, 0	
No treatment			0, 0	

Nucleotide Sequence of the HSV-1 TK gene

The complete nucleotide sequence of the non-coding TK DNA strand is presented in Figure 8. This represents the entire TK gene plus 5' flanking regions extending to the PvuII site and 3' flanking regions extending approximately 360bp beyond the putative translation stop codon (map units 0.313 to 0.302). The sequence was established for both strands by the Maxam and Gilbert procedure (21). Details of the strategy employed and interpretation of the sequencing gel results is presented elsewhere by McKnight (12a). Important features of the sequence in the vicinity of the 5' and 3' ends of the gene are indicated in Figure 8. Recall that BglII, HincII and EcoRI cleavage but not PvuII cleavage inactivates the TK activity in both assay systems. An initial search for TATAAA-like sequences signals directed 5'-3' on the non-coding strand revealed a putative RNA polymerase II transcription initiation signal (boxed) at nucleotides 175 to 180 roughly 55bp 3' to the EcoRI site (map coordinate 0.3125). A duplicate set of typical eukaryotic signals for addition of polyA (22) are observed at nucleotides 1486 to 1492 and 1499 to 1505 just beyond the SmaI site at the 3' end of the gene (map coordinates 0.3045). The occurence of two AATAAAA sequences here (boxed) is believed to be a unique observation and future studies may show that this structure has some significance in the processing of TK mRNA.

Identification of the 5' end of the TK m-RNA

In order to unambiguously locate the 5' terminus of the tk gene we generated S1 maps of the protected DNA in mRNA: DNA hybrids. PolyA containing RNA was isolated by the procedure of Anderson et al (23) from three different cell types: (a) Vero cells 6 hr after infection with

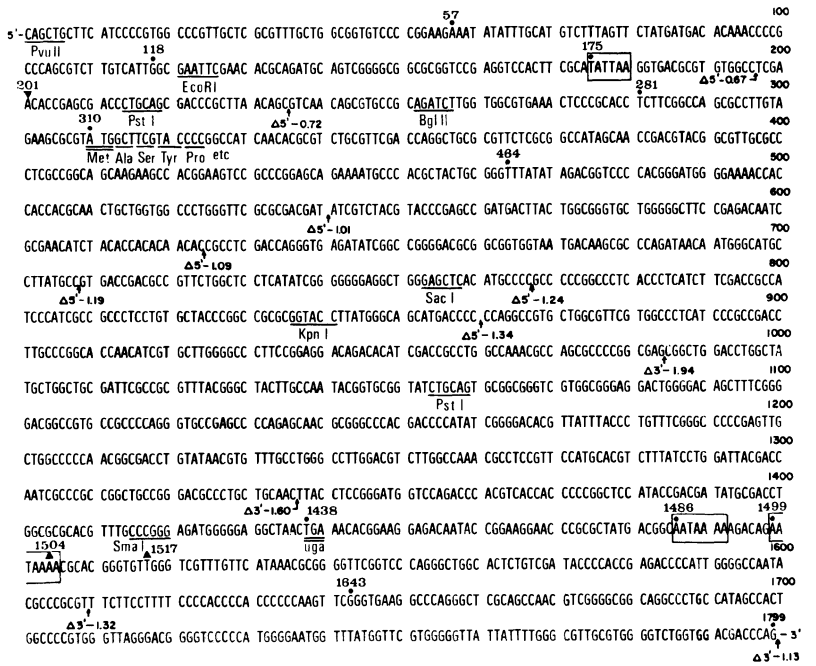

Figure 8: The primary nucleotide sequence of 1799 bases of HSV-1 (MP) DNA to the left of the PvuII site at 0.313. This DNA had been cloned in the pHSV106 plasmid and includes the entire thymidine kinase gene. Only the sequence on the non-coding or r-strand is given. The termini of several of the deletion plasmids used in mapping work are indicated by arrows. Key restriction enzyme recognition sites are underlined and possible control elements near the 5' and 3' ends of the HSV-1(MP) thymidine kinase gene are boxed. The most likely translation initiator and terminator codons are double underlined. See text for descriptions of other marked features.

HSV-1(MP) virus at a multiplicity of 15 plaque forming units/cell, (b) Xenopus oocytes 24hr after injection with pHSV106 DNA, and (c) The mouse LH1-B1 cell line that had been biochemically transformed with the BamHI-O DNA fragment from HSV-1(MP). A small 131 base pair pHSV106 DNA fragment cleaved on one side with BglII and on the other with EcoRI was labelled with ^{32}P-dATP at the 5' ends by polynucleotide kinase. This DNA fragment was

then denatured and the separated TK coding strand hybridized in solution in the presence of excess RNA. S1 nuclease was used to remove single-stranded tails of any RNA:DNA hybrids formed. After hydrolysing the RNA

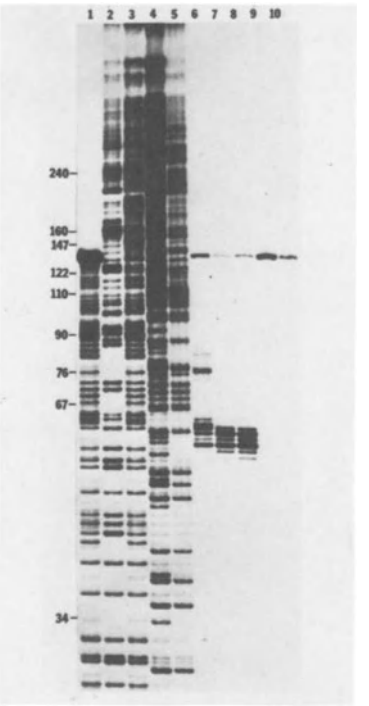

Figure 9: Sequence of the DNA coding strand and S1 nuclease map of the 5' terminus of TK mRNA. The figure shows an autoradiograph of a 20% polyacrylamide sequencing gel that was used to size S1 nuclease digested DNA fragments. To provide a direct comparison the coding strand of the TK gene was terminally ^{32}P-labelled and sequenced as shown in lanes 2-5 (G, A, T, and C reactions, respectively). To locate the 5' end of the appropriate polyA selected RNA isolated from infected cells the coding strand of a BglII-EcoRI fragment (131bp) was terminally labelled at the BglII site and isolated by strand separation. The identity of part of this probe DNA was confirmed by sequencing using the A reaction (modification with pyridinium formate and degradation with piperidine, Lane 1). The remaining portion of 131bp coding strand fragment was hybridized to TK mRNA and digested with S1 nuclease. Lanes 6-8 were loaded with hybridized probe DNA that was digested with 0.25, 2.5 and 12.5 units of S1/100µl respectively. Lane 9 was loaded with a small amount of intact probe DNA and lane 10 with probe DNA digested with 0.25 units of S1/100µl without hybridization to mRNA.

and electrophoresing the protected DNA on a sequencing gel (Figure 9) we were able to count the number of nucleotides between the labelled BglII site and the 5' terminus of the predominant RNA species. As shown in Figure 10, the size of the protected DNA strand obtained in all three situations described above was 50 ± 2 nucleotides. Therefore, from the results of S1 mapping of the transcript we deduce that the 5' terminus of

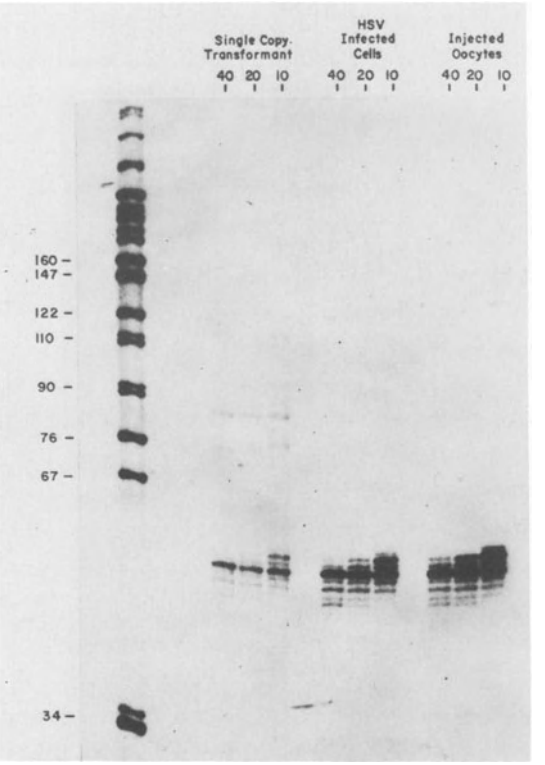

Figure 10: Comparison of the 5' termini of TK mRNA synthesized in transformed, infected or microinjected cells. The labelling, hybridization and sequencing protocols were essentially the same as described in Figure 9 except that the RNA: DNA hybrids were digested with 10, 20 and 40 units of S1/100µl. The sources of RNA were as follows: (1) PolyA$^+$ selection from polysomes of a single copy Ltk$^+$ cell line (LH1B1); (2) PolyA$^+$ selection from polysomes of HSV-1(MP) infected Vero cells (at 6 hr postinfection) and (3) Extracts of Xenopus oocytes 24 hr after microinjection with the pHSV106 plasmid.

TK mRNA occurs at approximately position 201. This site lies 26 nucleotides downstream from the "TATAAA"-like sequence (actually TATTAA in this case) in reasonable agreement with the average location of RNA start points in other sequenced viral and cellular promotor regions utilized by RNA polymeraseII. In addition to demonstrating that the 5' terminus of TK mRNA synthesized in oocytes and biochemically transformed cells is exactly the same as that obtained in virus infected cells, these experiments directly confirm the polarity of TK mRNA synthesis determined by Smiley et al (24).

The TK mRNA in Infected Cells is Not Spliced

The TK gene DNA sequence contains potential donor and acceptor RNA splicing signals. However, although splicing appears to be the predominant pattern in nearly all structural genes it may not be an absolute requirement and certainly not all potential sites are utilized. We have been unable to find any evidence of splicing by Berk and Sharp analysis (25) within the major mRNA species synthesized from this region of the HSV-1 genome at early stages after infection. The 1800bp sequenced portion of the BamHI-O fragment from pHSV106 was recloned in both orientations in the single stranded bacteriophage vector M13mp5 and uniformly labelled DNA representing each of the two strands was then separately annealed in solution to RNA extracted from Vero cells 6 hr after infection with HSV-1(MP). SI nuclease digestion of the resulting RNA:DNA hybrids followed by denaturation and gel electrophoresis showed that only a single DNA band of approximately 1300 nucleotides hybridized to the *l*-strand probe and as expected no specific hybrid formed with the *r*-strand probe (Figure 11). However, we caution that a very small spliced portion at either end of the message would not have been detected by this procedure.

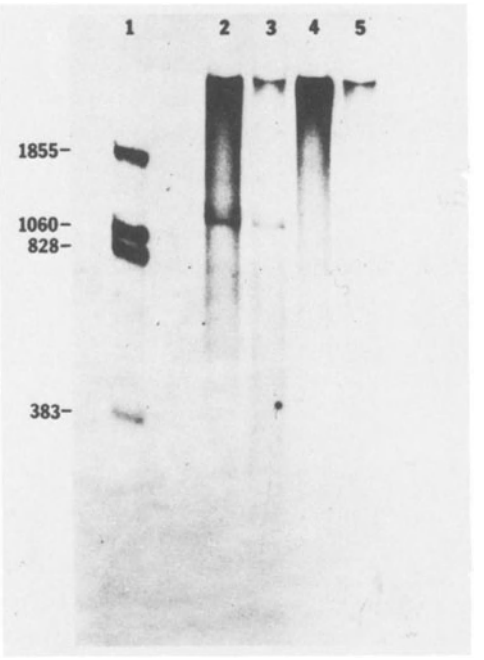

Figure 11: S1 nuclease sizing of TK mRNA. Autoradiograph of an alkaline 1% agarose gel after electrophoresis of S1 digested RNA/DNA hybrid molecules. The numbers adjacent to the marker DNA bands in lane 1 indicate sizes in nucleotides. Lanes 2 and 3 were loaded with uniformly ^{32}P-labelled M13/tk l or coding strand DNA that had been hybridized to TK mRNA from infected Vero cells then digested with 2.5 and 25 units of S1 nuclease/100µl, respectively. Lanes 4 and 5 were loaded with M13/tk r or non-coding strand DNA after similar hybridization and S1 treatment.

Location of an Open Reading Frame

An analysis of the location of potential translation terminating codons in the tk gene sequence is presented in Figure 12. The results are consistent with the notion of a non-spliced mRNA. A single contiguous open reading frame of 1128 nucleotides exists in the *r*-strand or non-coding sequence between the initiator methionine codon ATG at position 310 (+110 nucleotides from the mRNA start site) and the TGA triplet at 1438. All three reading frames on the *l*-strand contain several terminator codons within this region. In addition, a potential

ribosome binding site with a sequence partially complementary to the 3' end of 18S RNA occurs between nucleotides 281 and 290. The resulting primary polypeptide would presumably begin Met, Ala, Ser, Tyr, Pro, etc. and continue for 376 amino acids. Unfortunately, no amino acid sequencing data are available at present to confirm these predictions, but they are consistent with the size of 42,000 daltons that has been assigned to the TK polypeptide by SDS polyacrylamide gel electrophoresis (26). In addition,

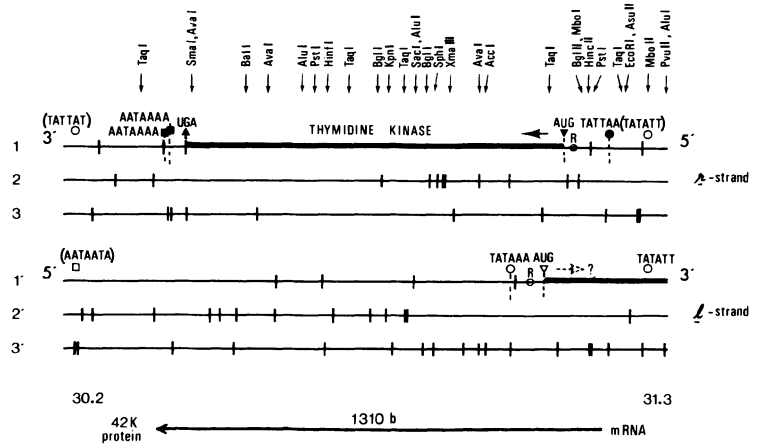

Figure 12: Location of open reading frames on both the l- and r-strands in the vicinity of the thymidine kinase gene. The diagram shows the location of terminator codons (vertical bars) in all three reading frames. Thickened lines indicate two potential coding regions associated with promotor-like sequences: one is the thymidine kinase gene on the r-strand and the other the 5' end of an unknown gene product which may be translated to the right of 0.311 on the l-strand. The locations of actual (solid motifs) or potential (open motifs) transcription and translation regulatory signals associated with adjacent open reading frames are flagged in the diagram. The relative locations of many restriction enzyme sites that are either confirmed or predicted by the sequence data are shown above the diagram. Sites for cleavage with BclI, BstEII, ClaI, HaeII, HindIII, PvuI, SacII, XbaI and XhoI are absent within the 1800bp sequenced region.

the termination of translation for the TK polypeptide is known to be suppressed in vitro by an opal (UGA) suppressor tRNA (27).

Analysis of the Putative TK Gene, Promotor Region

The "TATAAA" concensus sequence is believed to play a role primarily in the alignment of initiation of mRNA synthesis. However, a second conserved oligonucleotide sequence (GG $\begin{matrix}C\\T\end{matrix}$CAAT) usually at approximately 80 nucleotides upstream from the 5' start point has also been proposed as part of the promotor region in several cellular and viral structural genes (27, 28). The sequence GGCGAAT begins at -83 in the TK gene promotor region (position 118 in Figure 8) and includes the EcoRI site which we have shown to inactivate TK activity. In a more precise analysis of the function of this portion of the TK DNA one of us (S.L.M.) has recently established and tested a refined series of deletions extending across the 5' flanking DNA of the TK gene. mRNA mapping assays from microinjected oocytes reveal that normal TK activity levels require that the first 95 nucleotides in front of the mRNA start site remain intact. Deletions inside this point cause a sharp decrease in the competence of the plasmid DNAs to direct the synthesis of TK mRNA in Xenopus oocytes. We believe that this work defines for the first time the 5' outer boundaries of a pol II promotor sequence.

Other Potential Promotor-like Sequences

A putative duplex stem-loop structure between the TATAAA signal and the mRNA start site has been suggested for the adenovirus type 2 "late" viral promotor (29) and the appropriate TK sequence can also be imagined to form such a structure. Rather surprisingly, a search for similar

features in both the leftward and rightward directions from two other "TATAAA"- like sequences (one on each strand) near the 5' end of the tk gene reveals plausible (GG $\begin{smallmatrix}C\\T\end{smallmatrix}$CAAT)-like concensus sequences 50 nucleotides away on the 5' side and potential stem-loop structures directly adjacent on the 3' side in both cases. A

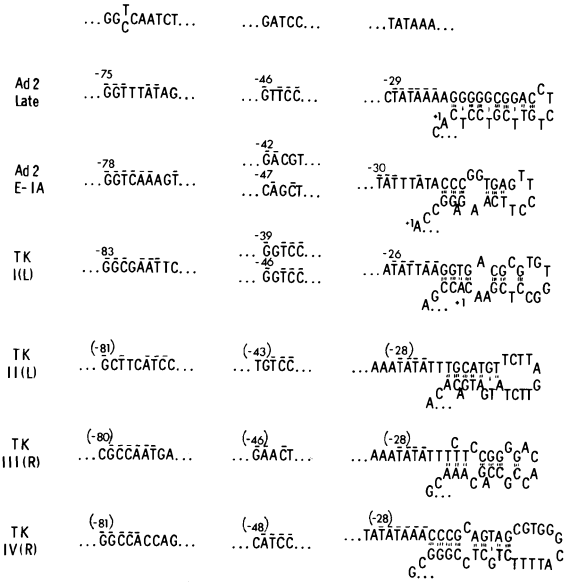

Figure 13: Comparison of relevant sequences around the four Hogness box like signals found near the 5' end of the HSV-1 thymidine kinase gene. All show features typical of either active or modified pol II promotors. The key concensus sequences for other cellular and viral promotors and the potential stem-loop structure exhibited by the major Ad-2 late promotor are given for comparison. The non-coding strand for promotor-like regions I and II is the r-strand (equivalent to mRNA transcribed leftwards from the l-strand). Regions III and IV occur on the l-strand (equivalent to mRNA transcribed rightwards). Region I is believed to be the active promotor for thymidine kinase in both infected and biochemically transformed cells. The Hogness box signals in regions II and III overlap creating a single ten base pair palindrome lying between the PvuII and EcoRI sites which is a potential candidate for the regulatory signal recognized when thymidine kinase transcription (β-class) is induced by immediate-early gene products (α-class).

comparison of these structures with "early" and "late" Ad-2 promotors, the actual TK promotor, and a generalized concensus sequence for cellular structure genes is shown in Figure 13. Note that the two TATATT containing regions overlap at positions 57 and 66 between the PvuII and EcoRI sites creating a ten base pair palindrome AAATATATTT (see Figure 8). If these sites do not represent actual functional promotors it is tempting to speculate that they might be modified promotor sequences adapted to mediate the induction of TK activity in viral infected cells by the VP175 immediate-early protein (30, 31). A fourth plausible promotor-like sequence occurs inside the TK gene region surrounding a classical TATAAA sequence at position 469 to 464 in the opposite strand. The reading frame is open for all 360 nucleotides that have been sequenced beyond the most proximal ATG initiator codon from this site (see Figure 12). Possible consensus sequences upstream plus a reasonably plausible stem-loop structure are included for comparison in Figure 13. If an *r*-strand transcript does exist here it would overlap with the 5' end of the TK gene but proceed in the opposite direction. However, we wish to emphasize that no evidence exists at present for such a transcript or polypeptide: they are merely theoretical possibilties based on sequence data alone.

Non-Coding Sequences Near the 3' End of the TK Gene

The precise site of polyA addition onto TK mRNA synthesized in oocytes has also been mapped by the S1 hybrid protection procedure using appropriate ^{32}P end-labelled DNA fragments (S. McKnight, unpublished observations). These results indicate that two distinct addition sites are used, each mapping 18 nucleotides to the 3' side of the duplicated AATAAAA signals (ie. at nucleotides 1504 and 1517).

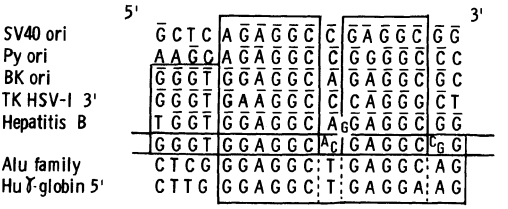

Figure 14: Comparison of the "Alu core"-like sequence found at the 3' end of the TK gene with similar sequences found in polyoma, BK, SV40 and Hepatitis-B viruses and the concensus Alu-core sequence from human cellular DNA. Boxes indicate an apparent concensus sequence for all of the viral Alu-core sequences and a hypothetical extended concensus sequence for those from the three human viruses.

Beyond the 3' end of the TK coding region there are terminators in all three reading frames in the r-strand for at least 300 nucleotides immediately following the polyA signals. Evidently this is a non-coding region (at least for proteins) and it contains the following unusual sequences: (1) A long pyrimidine tract (26 of 28 nucleotides between positions 1609 and 1636); (2) An Alu-family core sequence at position 1643-1660; (3) A 10 or 12 base pair palindrome TCCCCCATGGGGAA at 1724-1736; and (4) An AT-rich box TTATTATTTT at 1758-1767 surrounded by GC-rich sequences but lacking the other concensus sequences typical of promotors. A comparison of the potential Alu core sequence at the 3' end of the HSV tk gene with that found at or near the replication origins in SV40, Polyoma and BK viruses is shown in Figure 14. The complete cellular Alu family sequences are 300 base pairs long and occur in 300,000 copies in human and hamster genomes: they are thought to be associated with replication origins and abundant pol III transcripts (32). Note that the 14-base pair core exists as an inverted duplication in SV40 and that the homology amongst these sequences in the three human viruses (HSV, BK and Hepatitis-B) extends over an additional three nucleotides (-GGT-) compared to the others. There is no

evidence to suspect the existence of a replication origin at this point in HSV DNA but one might expect to find a "late" leftwards promotor near here for the series of capsid polypeptides encoded between 0.2 and 0.3 in the genome (33).

ACKNOWLEDGEMENTS

The work performed at Johns Hopkins Medical School was supported by grants NO1 CA22130 and NO1 CP71022 from the N.I.H. Funds for research carried out by S.L.M. were provided by the Carnegie Institute of Washington. S.L.M. is a Postdoctoral Fellow of the Helen Hay Whitney Foundation for Medical Research. G.R.R. is a predoctoral trainee in the Medical Scientist Training Program at Johns Hopkins (NIH GM 07309). We thank A. El Kareh and S. Silverstein for TK antisera, LMtk$^-$ cells and LH-7 cells, G. Gentry for a gift of ara-T, P. Leitman for supplying ^{125}ICdR, W. Summers for conducting IdC assays on oocyte extracts, and D. Thomas and G. Milman for assistance and advice in the ^{125}ICdR autoradiographic assays. The excellent technical assistance of D. Ciufo, M. McClane and R. Kingsbury is gratefully acknowledged. We thank D. Brown for initiating contacts between our laboratories.

REFERENCES

1. Munyon, W., Kraiselburd, E., Davis, D. and Mann, F. (1971). J. Virol., 7, 813-820.
2. Jamieson, A.T. and Subak-Sharpe, J.H. (1974). J. gen. Virol., 24, 481-492.
3. Davis, D.B. and Kingsbury, D.T. (1976). J. Virol., 17, 788-793.
4. Kraiselburd, E., Gage, L.P., and Weissbach, A. (1975). J. Mol. Biol. 97, 533-542.
5. Bacchetti, S. and Graham, F.L. (1977). Proc. Natl. Acad. Sci., 74, 1590-1594.
6. Minson, A.C., Wildy, P., Buchan, A., and Darby, G.

(1978). Cell, 13, 581-587.
7. Sugino, W.M., Chadha, K.C. and Kingsbury, D.T. (1977). J. gen. Virol., 36, 111-112.
8. Elion, G.B., Furman, P.A., Fyfe, J.A., De Miranda, P., Beauchamp, L. and Schaeffer, H.J. (1977). Proc. Natl. Acad. Sci. USA, 74, 5716-5720.
9. Wigler, M., Silverstein, S., Lee, L.S., Pellicer, A., Cheng, Y.C., and Axel, R. (1977). Cell, 11, 223-232.
10. Wigler, M., Sweet, R., Sim, G.K., Wold, B., Pellicer, A., Lacy, E., Maniatis, T., Silverstein, S. and Axel, R. (1979) Cell, 16, 777-785.
11. Lai, E.G., Woo, S.L.C., Bordelon-Riser, M.E., Fraser, T.H., and O'Malley, B.W. (1980). Proc. Natl. Acad. Sci. USA, 77, 244-248.
12. Preston, C.M. (1979). J. Virol, 29, 275-284.
12a. McKnight, S.L. (1980). Nucl. Acids Res. 8, 5949-5964.
13. Reyes, G.R., LaFemina, R., Hayward, S.D. and Hayward, G.S. (1979). Cold Spring Harbor Symp. Quant. Biol. 44, 629-641.
14. Maitland, N.J. and McDougall, J.K. (1977). Cell 11, 233-241.
15. McDougall, J.K., Masse, T.H. and Galloway, D.A. (1980) J. Virol., 33, 1221-1224.
16. Colbere-Garapin, F., Cousterman, S., Horodniceanu, F., Kourilsky, P. and Garapin, A.C. (1979). Proc. Natl. Acad. Sci. USA, 76, 3755-3759.
17. Enquist, L.W., Vande Woude, G.F., Wagner, M., Smiley, J.R. and Summers, W.C. (1979). Gene, 7, 335-342.
18. Wilkie, N.M., Clements, J.B., Boll, W., Mantel, N., Lonsdale, D. and Weissmann, C. (1979). Nucl. Acids Res., 7, 859-877.
18a. McKnight, S.L. and Gavis, E.R. (1980). Nucl. Acids. Res. 8, 5931-5948.
19. Summers, W.C. and Summers, W.P. (1977). J. Virol., 24, 314-318.
20. Pellicer, A., Wigler, M., Axel, R. and Silverstein, S. (1978). Cell, 14, 133-141.
21. Maxam, A.M. and Gilbert, W. (1977). Proc. Natl. Acad. Sci. USA, 74, 560-564.
22. Proudfoot, N.J.. and Brownlee, G.G. (1976). Nature 263, 211-214.
23. Anderson, K.P., Stringer, J.R., Holland, L.E. and Wagner, E.K. (1979). J. Virol., 30, 805-820.
24. Smiley, J.R., Wagner, M.J., Summers, W.P. and Summers, W.C. (1980). Virology 102, 83-93.
25. Berk, A.J. and Sharp, P.A. (1977). Cell, 12, 721-732.
26. Cremer, K., Bodemer, M., Summers, W.C. (1978). Nucl. Acids Res., 5, 2333-2344.
27. Cremer, K.J., Bodemer, M., Summers, W.P., Summers, W.C. and Gesteland, R.F. (1979). Proc. Natl. Acad. Sci. USA, 76, 430-434.
28. Busslinger, M., Portmann, R., Irminger, J.C. and Birnstiel, M.L. (1980). Nucl. Acids Res., 8, 957-977.

29. Benoist, C., O'Hare, K., Breathnach, R. and Chambon, P. (1980). Nucl. Acids Res., 8, 127-142.
30. Ziff, E., and Evans, R. (1978). Cell 15, 1463-1475.
31. Leiden, J.M., Buttyan, R. and Spear, P. (1976). J. Virol., 20, 413-424.
32. Kit, S. and Dubbs, D.R. (1977). Virology, 76, 331-340.
33. Jelinek, W.R., Toomey, T.P., Leinwand, L., Duncan, C.H., Biro, P.A., Choudary, P.V., Weissman, S.M., Rubin, C.M., Houck, C.M., Deininger, P.L., and Schmid, C.W. (1980). Proc.Natl. Acad. Sci. USA, 77, 1398-1402.
34. Wagner, E.K., Anderson, K.P., Costa, R.E., Devi, G.B., Gaylord, B.H., Holland, L.E., Stringer, J.R., and Tribble, L.L. (1981). (This volume, Chap. 4).
35. Morse, L.S., Buchman, T.G., Roizman, B. and Schaffer, P.A. (1977). J. Virol. 24, 231-248.

16. Assignment of Epstein-Barr Virus-determined Nuclear Antigen (EBNA) Gene to Chromosome 14 in Human Lymphoblastoid Cells

K. Yamamoto[1], F. Mizuno[2], T. Matsuo[1], A. Tanaka[3], M. Nonoyama[3], and T. Osato[1]

Summary

Hybrid clones and subclones between human lymphoblastoid FV5 cells and MCB2 fibroblasts were examined for the presence of Epstein-Barr virus (EBV) DNA, the expression of the virus-determined nuclear antigen (EBNA), and the presence of human chromosomes, in the course of serial passage in vitro. Among 14 hybrid clones examined, three were positive for EBNA and EBV DNA and had human chromosome 14, but the remaining 11 clones were totally negative for both EBV markers and did not reveal the presence of this particular chromosome. Furthermore, ten subclones isolated from one of the three positive clones contained only chromosome 14 as the human chromosome. In all of these subclones EBNA, EBV DNA and chromosome 14 were segregated concordantly. These results seem to indicate an apparent linkage relationship between human chromosome 14 and the EBNA antigen gene in human lymphoblastoid cells.

Y. Becker (ed), Herpesvirus DNA.

Introduction

Epstein-Barr virus (EBV) genome has been shown to be closely associated with cell genome of human lymphocytes transformed by EBV *in vitro*, lymphoblastoid cell lines with B-cell markers and Burkitt lymphoma and nasopharyngeal carcinoma biopsy specimens (1-4). It appears certainly of importance to clarify which human chromosome(s) is required for the maintenance and expression of the viral genetic information. Klein *et al.* (5) described that EBV DNA-carrying human Burkitt/mouse fibroblast hybrids contained a relatively small number of human chromosomes and there was no dramatic change in such number when EBV genomes were lost. These results suggested that a very small number of human chromosomes, perhaps only one, is involved in the maintenance and expression of EBV genetic information. Similar results were also obtained by Glaser *et al.* (6,7). More recently, however, both research groups (8-10) have presented contrasting data suggesting that the persistence of EBV genetic information may not require the presence of specific human chromosome(s) in their hybrid cell systems.

We have also been trying for several years (11-13) to determine with which human chromosome(s) the resident EBV genome and the expression of the virus-determined nuclear antigen (EBNA) (14) are specifically associated, through somatic hybrids between human and mouse cells (15). In order to achieve clear-cut results, EBNA-positive lymphoblastoid cells that contained only one to two EBV genome equivalents per cell (16,17) were used. Data showed that the resident EBNA antigen gene is closely associated with human chromosome 14 in our hybrid combination (18).

Experimental Approach

On the basis of the successful application to assign SV40 T antigen gene to specific human chromosomes (19,20),

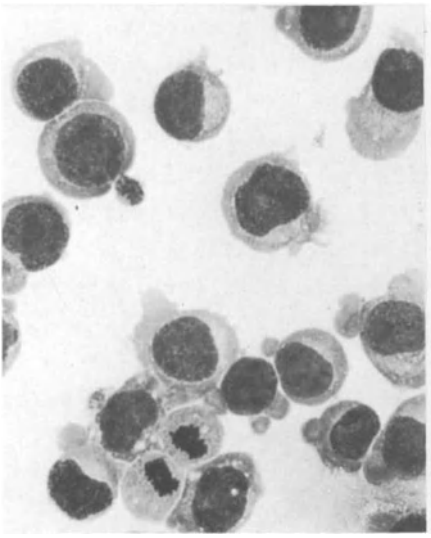

Fig.1. *Human FV5 cells (16) of lymphoblastoid morphology.* Giemsa stain. x 400

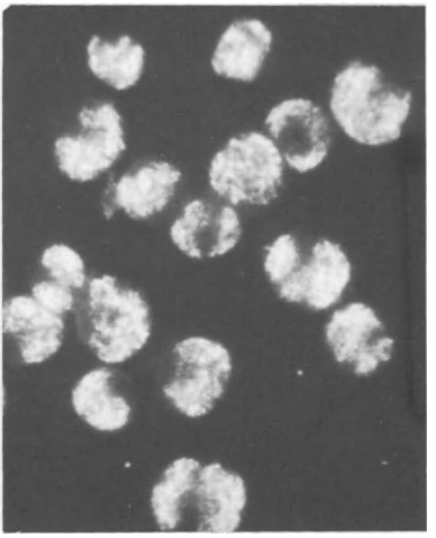

Fig.2. *EBNA immunofluorescence in FV5 cells (16,17).* Stained with EBV-seropositive normal human serum containing complement, followed by fluorescein isothiocyanate-conjugated antihuman β1C/β1A goat serum. x 400

we carried out the present work by using somatic cell hybrids between human (FV5) and mouse (MCB2) cells and taking advantage of the preferential loss of human chromosomes in the hybrid cells (15). The FV5 cells

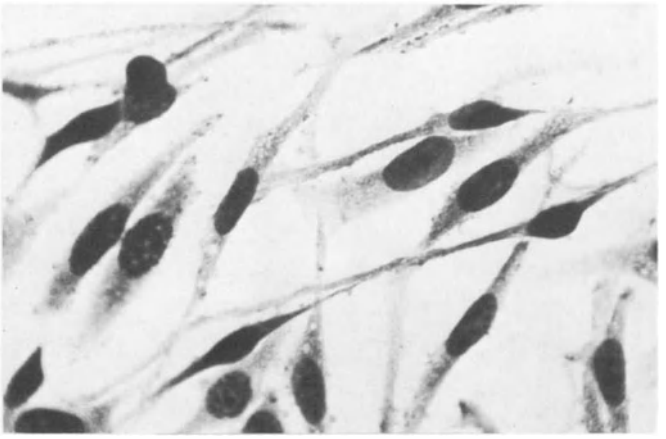

Fig.3. *Mouse MCB2 cells (Yamamoto et al., unpublished data) of fibroblastic morphology.* Giemsa stain. x 400

(Fig. 1) are cloned cells derived from the nonproducer human lymphoblastoid FVNC cell line previously established in our laboratory (16), the cells which are intensely positive for EBNA immunofluorescence (Fig. 2), but contain only one to two EBV genome equivalents per cell (17). The monolayer MCB2 cells (Fig. 3) are cloned cells of BUdR-resistant MCB fibroblast cell line derived from a methylcholanthrene-induced DDD mouse tumor in our laboratory (Yamamoto et al., unpublished data). The cells are totally negative for EBV genome and EBNA immunofluorescence. Somatic hybrids between FV5 and MCB2 cells were obtained according to the method described elsewhere (21). A number of hybrid clones and subclones were isolated from several different colonies (22). Detection of EBV DNA (2) and EBNA (14) and chromosome analysis (23,24) were all carried out with these hybrid clones and subclones at the same passage levels.

Results

Formation of somatic hybrids between human lymphoblastoid FV5 and mouse fibroblastic MCB2 cells

Human lymphoblastoid FV5 cells were fused with thymidine kinase-deficient mouse MCB2 fibroblasts in the presence of UV-inactivated Sendai virus and then incubated in hypoxanthine/aminopterin/thymidine (HAT) selective medium. After 2-3 weeks of incubation, a number of discrete cell colonies became evident (Fig. 4). The cells grew in an attached form on culture flasks and they were polygonal in morphology (Fig. 5), in contrast to their parental round FV5 and spindle-sphaped MCB2 cells. These polygonal cells contained both human and mouse chromosomes, which were distinguished by the selective affinity of 33258 Hoechst for mouse centromeres and the differences of the quinacrine banding patterns (23). Many clones and subclones were then isolated from several hybrid colonies in semisolid agar medium (22).

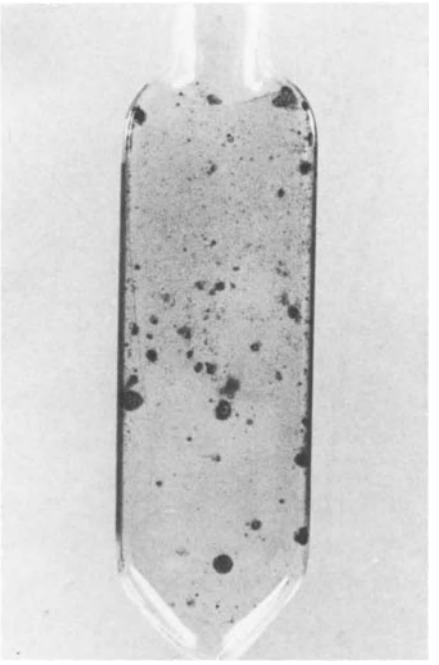

Fig.4. *FV5/MCB2 hybrid cell colonies grown in HAT medium.* Giemsa stain. x 2/3 Cell hybridization was carried out according to Okada (21). FV5 cells (3 x 10^6) were mixed with BUdR-resistant MCB2 cells (1 x 10^6) in the presence of UV-inactivated Sendai virus (500 HAU/ml). The mixture was kept at 4°C for 15 min and then incubated at 37°C for 20 min with frequent shaking (100 strokes/min). After washing, they were fed in growth medium (MEM containing 10% fetal calf serum and 10% tryptose phosphate broth) for 24 h and further incubated in HAT selective medium (growth medium supplemented with 1 x 10^{-4}M hypoxanthine, 4 x 10^{-7}M aminopterin and 1.6 x 10^{-5}M thymidine). Hybrid cell colonies were obtained in about three weeks and then seeded into semisolid agar medium (22). A number of hybrid clones and subclones were isolated from several different colonies.

EBNA expression in FV5/MCB2 hybrid clones and subclones

EBNA immunofluorescence (14) investigations were first carried out with 14 hybrid clones. The percentages of the positive cells in these clones were extensively examined at 3, 18 and 36 months after their isolation and the results are summarized in Tables 1 and 2. Among 14 examined, 11 clones were obviously EBNA-positive at 3 months, as illustrated in Fig. 6. The proportions of EBNA-positive cells in these clones ranged from 30 to 100%.

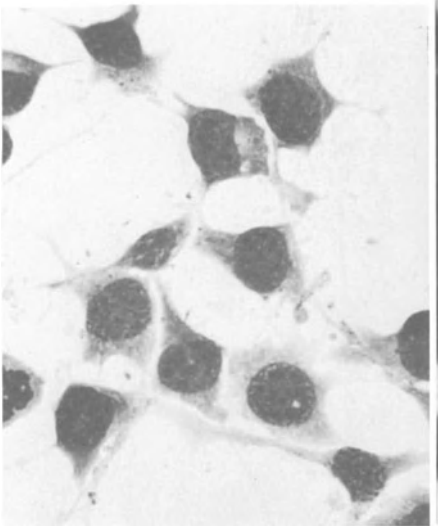

Fig.5. *Interspecific hybrid cells between human lymphoblastoid FV5 cells and mouse fibroblastic MCB2 cells grown in an attached form on culture flask.* Note polygonal cell morphology. Giemsa stain. x 400

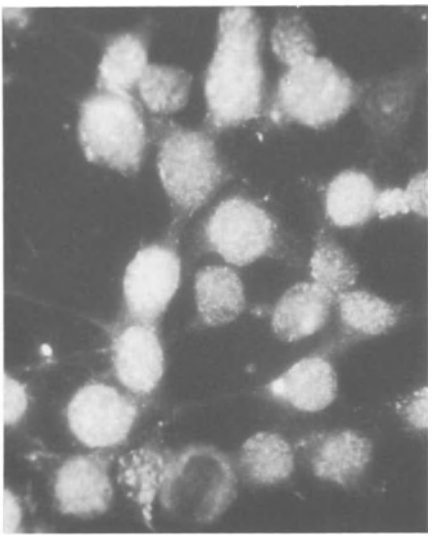

Fig.6. *Intense EBNA immunofluorescence in all nuclei in FV5/MCB2 clone 19.* x 400

When they were further examined at 18 months, most of the previously positive clones were completely negative and only clones 17, 18 and 19 were still positive in all cells. At 36 months after isolation, all of the hybrid clones tested became eventually EBNA-negative. One of the three positive clones, clone 19, was further seeded into semi-solid agar medium at 18 months. The resulting 10 subclones were also positive for EBNA in all cells. One of the 10 subclones became negative at 3 months after isolation, two additional subclones were negative at six months and all remaining positive subclones were also converted into totally negative after 10 months (Table 3).

Detection of EBV genome in FV5/MCB2 hybrid clones and subclones

Tables 2 and 3 also describe the results of EBV cRNA/cell DNA hybridization test (2) with 14 hybrid clones and 10 subclones. Raji cell line as a positive control

Table 1. Expression of EBNA in FV5/MCB2 hybrid clones

Months after isolation of FV5/MCB2 clones	FV5/MCB2 clones	
	EBNA-positive*	EBNA-negative
3	3,5,7,8,10,13 14,16,17,18,19	1,12,24
18	17,18,19	1,3,5,7,8,10,12, 13,14,16,24
36	none	1,3,5,7,8,10, 12,13,14,16, 17,18,19,24

* Percentages of EBNA-positive cells in hybrid clones ranged from 30 to 100.
The anticomplement immunofluorescence was carried out for the detection of EBNA (14). Cells grown on coverslips were washed once with balanced salt solution (BSS) and dried at room temperature and fixed in acetone-methanol (1:1) at -20°C. The coverslips were treated with heat-inactivated standard EBV-seropositive serum from a normal person (anti-EBNA of 1:640), in parallel with inactivated seronegative serum (anti-EBNA of $< 1:5$), with complement. They were washed four times with BSS, stained with fluorescein isothiocyanate-conjugated anti-human β1C/β1A goat serum (Hyland Laboratories, Costa Mesa, USA) at 37°C for 50 min, washed again four times and mounted in 50% BSS-glycerol. All the stained preparations were examined under a Leitz Orthoplan fluorescence microscope.

contained 50 EBV genome equivalents per cell (2), whereas human parental FV5 cells involved one to two EBV genomes per cell as reported (17). Neither the negative control Molt-4 cells nor the MCB2 mouse parental fibroblasts had EBV DNA. When the hybrid cells were examined at 18 months after isolation of clones and throughout the incubation period of subclones, EBNA-positive clones and subclones, all of which showed the immunofluorescence in all nuclei, were also positive for only one to two EBV genome equivalents per cell as well as their parental lymphoblastoid FV5. No detectable EBV DNA was evident in any EBNA-negative clones examined. Also, the loss of EBNA was accompanied by the loss of EBV DNA.

*Table 2. Relation between the presence of EBV genome, the expression of EBNA, and the presence of chromosome 14 in FV5/MCB2 hybrid clones**

FV5/MCB2 clone	EBNA-positive, %	EBV genome equiv. per cell	Human chromosomes in FV5/MCB2 clones																							
			A			B		C							D			E			F		G			
			1	2	3	4	5	6	7	8	9	10	11	12	13	14	15	16	17	18	19	20	21	22	X	Y
1	0	<1	−	−	−	−	−	−	−	−	−	−	−	−	−	−	−	−	−	−	−	−	−	−	−	−
3	0	ND	+	+	−	−	+	−	−	−	−	−	−	−	−	−	−	−	−	−	−	−	−	−	−	−
5	0	ND	−	−	−	−	−	−	−	−	−	−	−	−	−	−	−	−	−	−	−	−	−	−	−	−
7	0	<1	−	+	+	−	−	−	−	−	−	−	−	−	−	−	−	−	−	−	−	−	−	−	−	−
8	0	ND	−	−	−	−	−	−	−	−	−	−	−	−	−	−	−	−	−	+	−	−	+	−	−	−
10	0	<1	−	−	+	+	+	−	−	−	+	−	+	−	−	−	−	−	−	−	−	−	−	−	−	−
12	0	<1	−	−	−	−	−	−	−	−	−	−	−	−	+	−	−	−	−	−	−	−	+	+	−	−
13	0	<1	−	−	−	−	−	−	+	−	−	−	−	−	−	−	−	−	−	−	−	−	−	−	−	−
14	0	ND	−	+	−	−	−	+	−	−	−	−	−	−	−	−	−	−	−	−	−	−	−	−	−	−
16	0	<1	+	+	+	−	−	−	−	−	−	−	−	−	−	−	+	−	+	−	+	+	−	−	−	−
17	95-100	1-2	−	+	+	−	−	−	+	−	−	−	−	−	−	+	+	−	+	−	−	−	−	−	−	−
18	95-100	1-2	+	+	+	−	−	−	+	−	−	−	−	−	−	+	+	−	+	−	−	−	+	−	−	−
19	95-100	1-2	−	−	−	−	−	−	−	−	−	−	−	−	−	+	−	−	−	−	−	−	−	−	−	−
24	0	ND	−	−	−	−	−	−	−	−	−	−	−	−	−	−	−	−	−	−	−	−	−	−	−	−

ND, not determined.
* Results obtained 18 months after isolation of clones.

Table 2. EBV-specific cRNA/cell DNA hybridization has been described previously (2). Cells were treated with Pronase (1 mg/ml) and 1% sodium dodecyl sulfate, followed by extraction of DNA with phenol. The DNA was denatured with alkali and fixed onto nitrocellulose filters, which were then baked at 80°C under reduced pressure, and incubated with EBV-specific radioactive cRNA (1.5 x 10^5 cpm per filter) in 6x saline-citrate (SSC, 0.15 M NaCl-0.01 M Na citrate) at 66°C for 20 h. The filters were washed with 2x SSC, treated with RNase (20 mg/ml) and washed again with the same buffer. The radioactivity of the hybridized material was measured in a scintillation counter and the DNA on the filters was measured by the diphenylamine test. The counting data were normalized to 50 μg of DNA and the number of EBV genome equivalents per cell was calculated from the value of 50 genome equivalents per cell for nonproducer Raji cells. Nonspecific background hybridization to Simpson cell DNA was subtracted before the calculation was made.

Karyological analysis of FV5/MCB2 hybrid clones and subclones

The chromosome examinations of the FV5/MCB2 hybrid cells were carried out by the quinacrine mustard-33258 Hoechst double staining (23), in parallel with the immunofluorescence and the nucleic acid hybridization at the same passage levels. The chromosome constitution of all 14 hybrid clones was consistent with a fusion product containing one mouse chromosome set and one incomplete human set. At 3 months of their isolation, the number of human chromosomes was already small, ranging from 3 to 13. As described above, three of 14 clones was still positive for EBV DNA and EBNA at 18 months and these hybrid clones were further analysed in detail karyologically. The results are summarized in Table 2. Human chromosomes identified in clone 17 were Nos. 2,3,7,14,15 and 17 and chromosomes 1,2,3,7,14,15,17 and 21 were involved in clone 18. On the other hand, in clone 19, chromosome 14 alone was present in all of the metaphases examined (Fig. 7). The human chromosome involved in common in these three EBV marker-positive clones was therefore chromosome 14. Fig. 8 shows partial karyotypes of No. 14 chromosomes from four individual cells of the parental FV5, clone 17, clone 18 and clone 19, respectively. In contrast, human chromosomes 1,2,3,4, 5,6,7,9,11,13,15,17,18,19,20,21 and 22 were involved in the 11 negative clones. Chromosome 14, however, was not evident in any negative clones tested.

Table 3. Concordant segregation of EBNA, EBV genome, and chromosome 14 in FV5/MCB2 hybrid subclones

FV5/MCB2 subclone	EBNA, EBV genome, and chromosome 14 in FV5/MCB2 subclones			
	1 mo	3 mo	6 mo	10 mo
19-1	+/+/+	−/−/−	−/−/−	−/−/−
19-2	+/+/+	+/+/+	−/−/−	−/−/−
19-5	+/+/ND	+/+/ND	+/+/ND	−/−/ND
19-8	+/+/ND	+/+/ND	+/+/ND	−/−/ND
19-13	+/+/ND	+/+/ND	+/+/ND	−/−/ND
19-15	+/+/+	+/+/+	−/−/−	−/−/−
19-18	+/+/+	+/+/+	+/+/+	−/−/−
19-19	+/+/ND	+/+/ND	+/+/ND	−/−/ND
19-22	+/+/ND	+/+/ND	+/+/ND	−/−/ND
19-25	+/+/+	+/+/+	+/+/+	−/−/−

Months after isolation of subclones are given in the headings. Results are expressed as presence or absence of: EBNA/chromosome 14/EBV DNA. ND indicates the presence of EBV DNA was not determined.

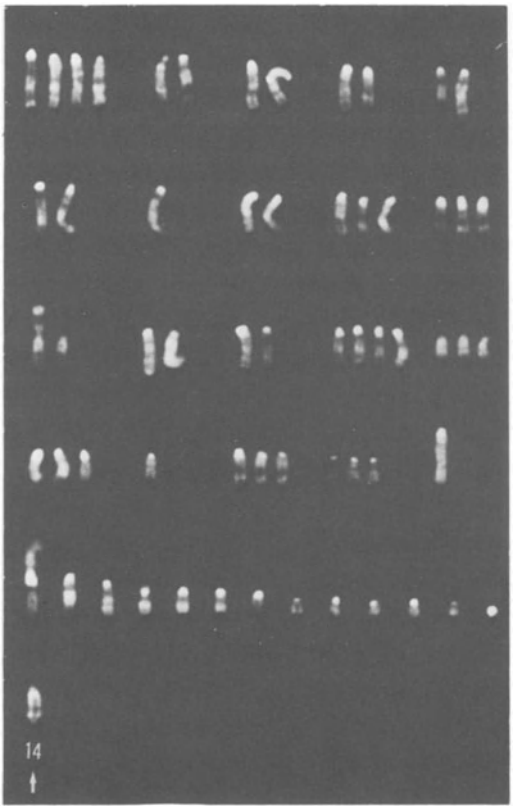

Fig.7. *Karyotype of FV5/MCB2 clone 19.* This hybrid clone contains only chromosome 14 (arrow) as human chromosomes and all other chromosomes originate from the mouse MCB2. Detection of each parental chromosome in interspecific cell hybrids was made according to the method described elsewhere (23). Hybrid cells between human FV5 and mouse MCB2 were treated with colchicine at a final concentration of 0.05 μg/ml for 30 min. After trypsinization, they were treated with 0.075 M KCl solution at 37°C for 10 min, fixed by three changes of methanol-acetic acid (3:1) and then spread on slides and air-dried. The slides were stained with a mixed solution of quinacrine mustard (50 μg/ml) and 33258 Hoechst (0.5 μg/ml) dissolved in McIlvaine's buffer, pH 7.0, for 10 min, rinsed and mounted in the same buffer, pH 4.5. Well-spread metaphase plates were photographed with an Olympus fluorescence microscope and the chromosome analysis was made with 50 metaphases per sample, on the basis of the selective 33258 Hoechst affinity for mouse chromosome centromeres and the specific quinacrine banding patterns of human and mouse chromosomes.

Further chromosome investigations were carried out with subclones of clone 19, as shown in Table 3. When examined one month after their isolation, 10 subclones

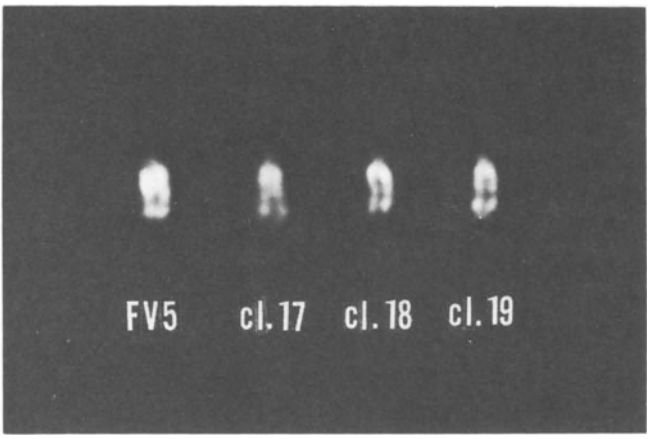

Fig.8. *Partial quinacrine banded karyotypes of No. 14 chromosomes from four individual cells of FV5, FV5/MCB2 clone 17, clone 18 and clone 19.*

tested were all EBV marker-positive in consistent association with chromosome 14 alone. At three months, in one of these subclones, 19-1, the human chromosome was segregated concomitantly with the loss of EBNA and EBV-genome. Subsequently, at six months two additional subclones, 19-2 and 19-15, became simultaneously negative for EBNA, EBV DNA and chromosome 14. The remaining 7 subclones were also eventually negative not only for EBV markers but for this particular human chromosome, when examined after 10 months of their isolation.

Enzyme analysis of FV5/MCB2 hybrid clones and subclones

The electrophoretic enzyme analysis (25) of the FV5/MCB2 hybrid cells was carried out to confirm the results obtained by the quinacrine mustard-33258 Hoechst double staining. Fig. 9 shows that EBV genome-positive and EBNA-positive clones and subclones were also positive for the human nucleoside phosphorylase, known to be assigned to human chromosome 14 (24), and the heteropolymer between human and mouse enzymes. When the extract of the human parental FV5 cells and that of the mouse MCB2 were simply mixed, only the enzyme bands corresponding to these two species were seen.

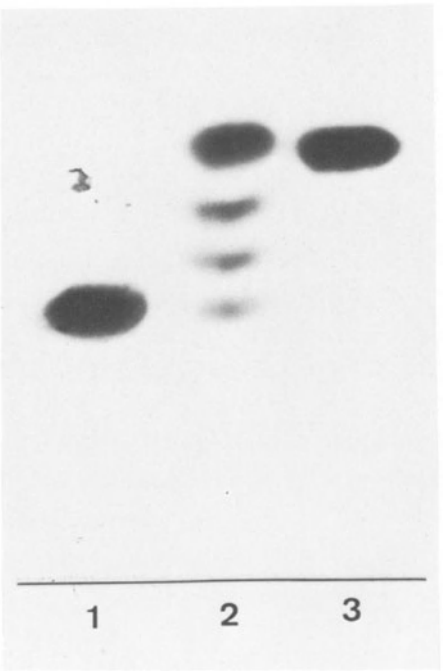

Fig.9. *Zymogram of nucleoside phosphorylase in cellulose acetate gel electrophoresis (24,25).* Channel 1 shows the pattern of the human parental FV5; Channel 2 shows the expression of both parental enzymes and of the heteropolymer between the human and the mouse enzyme in FV5/MCB2 clone 19; Channel 3 shows the pattern of the mouse parental MCB2. After centrifugation of the sonicate of each cell sample (1×10^8), the extract was applied to a cellulose acetate gel and electrophoresed in 0.02 M phosphate buffer, pH 7.0, at 4°C at 200 volts for 90 min. The gel was then incubated in the reaction mixture {(0.2 ml inosine (5 mg/ml); 10 μl xanthine oxidase (4 units/ml); 0.2 ml MTT (2 mg/ml); 0.2 ml phenazine methosulfate (0.4 mg/ml); 1.4 ml Tris-$MgSO_4$ buffer, pH 7.4)} at 37°C for 15 min.

Discussion

Along the line of a pioneer work on SV40 T antigen gene locus determination (19), several reports have recently described the relation between the presence of EBV genome, the expression of EBNA and the presence of human chromosomes in somatic cell hybrids between human lymphoblastoid cells and mouse cells, taking advantage of the preferential loss of human chromosomes in such hybrid cells

(5-10,18). Klein et al. (5) previously suggested that EBV DNA may be associated with a limited number of human chromosomes, perhaps only one, since their hybrids that had lost detectable viral genomes and EBNA still contained a considerable number of human chromosomes. Glaser et al. (6), on the other hand, identified at least 13 out of 23 human chromosomes by karyologic and enzyme analyses in the EBV DNA-negative and EBNA-negative hybrid cells. They suggested that EBV genome may be associated with at least one of human chromosomes 3,4,5,6, and 10. They have further examined another mouse/Burkitt hybrid cell combination and described that the expression of EBNA is probably related to the presence of chromosomes 7 and/or 17 (7). More recently, however, investigators of both groups (8-10) have reached a conclusion that no specific human chromosome(s) can either be associated with the maintenance of EBV genome or the expression of EBNA in their hybrid combinations, such as Burkitt lymphoma cell/mouse fibroblast and nasopharyngeal carcinoma cell/mouse fibroblast, and that the persistence of EBV genetic information may not require the presence of a specific human chromosome(s).

In contrast to these reports, our findings obtained from several years investigations (11-13,18) strongly suggest that EBNA antigen gene locus is closely associated with human chromosome 14. In order to achieve clear-cut results, we used EBNA-positive lymphoblastoid cells containing only one to two EBV genome equivalents per cell, whereas other investigators studied cells harboring multiple copies of EBV genome. In our particular cells, the expression of EBNA was considered to be attributed to the function of such a very small number of resident EBV genomes.

Detailed karyotype analysis of 14 hybrid clones by the banding procedure showed that human chromosome 14 was consistently involved in common in all three EBV genome-positive and EBNA positive clones, but not in the remaining

11 negative clones. This was confirmed by the electrophoretic enzyme assay, in which the EBV marker-positive hybrid clones, but not negative ones, displayed the heteropolymer between the human and mouse nucleoside phosphorylase. The particular human enzyme was known to be specifically linked to chromosome 14. No correlation was evident between the presence of any other human chromosomes, the presence of EBV genome and the expression of EBNA. Furthermore, EBV genome, EBNA and chromosome 14 were concordantly segregated in 10 positive subclones, which had contained chromosome 14 alone as human chromosomes. The result excluded the possibility that the expression of EBNA may have also occurred by transfer of EBV genome to mouse chromosomes in our hybrid combination.

All our findings thus seem to indicate that the resident EBNA antigen gene can be closely associated with human chromosome 14 and the presence of this particular chromosome alone is probably sufficient for the maintenance and expression of EBV-oncogenic information in human lymphoblastoid cells.

Several reports have recently described the addition of a portion of chromosome 8 to the terminal end of chromosome 14 in lymphomas, including Burkitt tumors (26-28). It is deemed worthy of investigation to clarify whether or not the close association of EBNA antigen gene with human chromosome 14 is related to the mechanism of EBV-induced oncogenesis.

Acknowledgements

We thank Drs. W. Henle, G. Henle, Y. Okada, M. Sasaki and M.C. Yoshida for helpful discussions and pertinent comments. We also thank Miss J. Kusajima for secretarial services. This work was supported in part by grants from the Ministry of Education, Science and Culture (201033, 201050 and 201059) and the Ministry of Health and Welfare (52-6) of Japan and from the U.S. National Cancer Institute (ROI-CA-21665-02).

References

(1) zur Hausen, H. and Schulte-Holthausen, H.: Presence of EB virus nucleic acid homology in a "virus-free" line of Burkitt tumour cells. Nature, 227, 245-248 (1970)
(2) Nonoyama, M. and Pagano, J.S.: Detection of Epstein-Barr viral genome in nonproductive cells. Nature, 233, 103-106 (1971)
(3) zur Hausen, H., Schulte-Holthausen, H., Klein, G., Henle, W., Henle, G., Clifford, P. and Santesson, L.: EBV DNA in biopsies of Burkitt tumours and anaplastic carcinomas of the nasopharynx. Nature, 228, 1056-1058 (1970)
(4) Nonoyama, M. and Pagano, J.S.: Homology between Epstein-Barr virus DNA and viral DNA from Burkitt's lymphoma and nasopharyngeal carcinoma determined by DNA-DNA reassociation kinetics. Nature, 242, 44-47 (1973)
(5) Klein, G., Wiener, F., Zech, L., zur Hausen, H. and Reedman, B.: Segregation of the EBV-determined nuclear antigen (EBNA) in somatic cell hybrids derived from the fusion of a mouse fibroblast and a human Burkitt lymphoma line. Int. J. Cancer, 14, 54-64 (1974)
(6) Glaser, R., Nonoyama, M., Shows, T.B., Henle, G. and Henle, W.: Epstein-Barr virus: Studies on the association of virus genome with human chromosomes in hybrid cells. In: de Thé, G., Epstein, M.A. and zur Hausen, H., eds., Oncogenesis and Herpesviruses II, Part 1 (IARC Scientific Publications, No. 11, Lyon), pp.457-466 (1975)
(7) Glaser, R., Croce, C.M. and Nonoyama, M.: Studies on the association of the Epstein-Barr virus genome with chromosomes in human (Burkitt)/mouse hybrid cells. Abst. of 3rd International Symposium on Oncogenesis and Herpesviruses, p.83 (1977)
(8) Spira, J., Povey, S., Wiener, F., Klein, G. and Andersson-Anvret, M.: Chromosome banding, isoenzyme studies and determination of Epstein-Barr virus DNA content on human Burkitt lymphoma/mouse hybrids. Int. J. Cancer, 20, 849-853 (1977)
(9) Glaser, R., Nonoyama, M., Hampar, B. and Croce, C.M.: Studies on the association of the Epstein-Barr virus genome and human chromosomes. J. Cell Physiol., 96, 319-326 (1978)
(10) Steplewski, Z., Koprowski, H., Andersson-Anvret, M. and Klein, G.: Epstein-Barr virus in somatic cell hybrids between mouse cells and human nasopharyngeal carcinoma cells. J. Cell Physiol., 97, 1-8 (1978)
(11) Yamamoto, K., Matsuo, T. and Osato, T.: Studies on human chromosomes closely associated with Epstein-Barr virus gene expressions. I. Analysis of human-mouse somatic cell hybrids. Abst. of 24th General Meeting of the Society of Japanese Virologists, p.2006 (1976)

(12) Yamamoto, K. and Osato, T.: Studies on human chromosomes closely associated with Epstein-Barr virus gene expressions. II. Retation between the virus-determined nuclear antigen (EBNA) and human chromosome D-14 in human-mouse somatic cell hybrids. Abst. of 25th General Meeting of the Society of Japanese Virologists, p.241 (1977)
(13) Mizuno, F., Yamamoto, K., Matsuo, T., Tanaka, A., Nonoyama, M. and Osato, T.: Studies on human chromosomes closely associated with Epstein-Barr virus gene expressions. III. Relation between EBV DNA and human chromosome D-14 in human-mouse somatic cell hybrids. Abst. of 26th General Meeting of the Society of Japanese Virologists, p.236 (1978)
(14) Reedman, B.M. and Klein, G.: Cellular localization of an Epstein-Barr virus (EBV) associated complement-fixing antigen in producer and non-producer lymphoblastoid cell lines. Int. J. Cancer, 11, 499-517 (1973)
(15) Weiss, M.C. and Green, H.: Human-mouse hybrid cell lines containing partial complements of human chromosomes and functioning human genes. Proc. Nat. Acad. Sci. U.S.A., 58, 1104-1111 (1967)
(16) Osato, T., Mizuno, F., Yamamoto, K. and Nonoyama, M.: Alteration in Epstein-Barr virus-human lymphoid cell interactions caused by the presence of type-C viral genome. In: de Thé, G., Epstein, M.A. and zur Hausen, H., eds., Oncogenesis and Herpesviruses II, Part 2 (IARC Scientific Publication No. 11, Lyon), pp.27-35 (1975)
(17) Osato, T., Yamamoto, K., Matsuo, T., Aya, T., Mizuno, F. and Nonoyama, M.: Interaction between Epstein-Barr virus and type-C virus in human cells. In: de Thé, G. and Ito, Y., eds., Nasopharyngeal Carcinoma: Etiology and Control (IARC Scientific Publication No. 20, Lyon), pp.413-420 (1978)
(18) Yamamoto, K., Mizuno, F., Matsuo, T., Tanaka, A., Nonoyama, M. and Osato, T.: Epstein-Barr virus and human chromosomes: Close association of the resident viral genome and the expression of the virus-determined nuclear antigen (EBNA) with the presence of chromosome 14 in human-mouse hybrid cells. Proc. Nat. Acad. Sci. USA, 75, 5155-5159 (1978)
(19) Croce, C.M., Girardi, A.J. and Koprowski, H.: Assignment of the T-antigen gene of simian virus 40 to human chromosome C-7. Proc. Nat. Acad. Sci. USA, 70, 3617-3620 (1973)
(20) Croce, C.M.: Assignment of the integration site for simian virus 40 to chromosome 17 in GM54VA, a human cell line transformed by simian virus 40. Proc. Nat. Acad. Sci. USA, 74, 315-318 (1977)

(21) Okada, Y.: Analysis of giant polynuclear cell formation caused by HVJ virus from Ehrlich's ascites tumor cells. I. Microscopic observation of giant polynuclear formation. Exp. Cell Res., 26, 98-107 (1962)
(22) Mizuno, F., Aya, T. and Osato, T.: Growth in semisolid agar medium of human cord leukocytes freshly transformed by Epstein-Barr virus. J. Nat. Cancer Inst., 56, 171-173 (1976)
(23) Yoshida, M.C., Ikeuchi, T. and Sasaki, M.: Differential staining of parental chromosomes in interspecific cell hybrids with a combined quinacrine and 33258 Hoechst technique. Proc. Japan Acad., 51, 184-187 (1975)
(24) Ricciuti, F. and Ruddle, F.: Assignment of nucleoside phosphorylase to D-14 and localization of X-linked loci in man by somatic cell genetics. Nature New Biol., 241, 180-182 (1973)
(25) van Someren, H., Beijersbergen van Honegouwen, H., Los. W., Wurzer-Figurelli, E., Doppert, B., Vervloet, M. and Meera Khan, P.: Enzyme electrophoresis on cellulose acetate gel II. Zymogram patterns in man-Chinese hamster somatic cell hybrids. Humangenetik, 25, 189-201 (1974)
(26) Manolov, G. and Manolova, Y.: Marker band in one chromosome 14 from Burkitt lymphomas. Nature, 237, 33-34 (1972)
(27) Jarvis, J.E., Ball, G., Rickinson, A.B. and Epstein, M.A.: Cytogenetic studies on human lymphoblastoid cell lines from Burkitt's lymphomas and other sources. Int. J. Cancer, 14, 716-721 (1974)
(28) Zech, L., Haglund, U., Nilsson, K. and Klein, G.: Characteristic chromosomal abnormalities in biopsies and lymphoid-cell lines from patients with Burkitt and non-Burkitt lymphomas. Int. J. Cancer, 17, 47-56 (1976)

17. Organization of the human cytomegalovirus genome

J.L.M.C. Geelen and M.W. Weststrate

SUMMARY

The general organization of the human cytomegalovirus DNA is characterized by: the presence of terminal and internal inverted repeats, the presence of terminal reiterated sequences, and the presence of nicks and gaps. The DNA exists in four isomeric forms which are present in equimolar amounts. Strain variation was analysed by cross blot hybridization of restriction endonuclease cleaved DNA. The submolar fragments and three areas in the long unique sequence were identified as regions of high variability. The submolar fragments and one of the three variable areas of the genome are transcribed immediate early post infection.

INTRODUCTION

Human cytomegalovirus (CMV), a member of the herpesvirus group, is an ubiquitous pathogen with a variety of clinical manifestations (28). Until recently the study of the molecular properties of the genome was greatly hampered due to problems in the isolation and purification of intact, infective CMV DNA. Recent improvements in the extraction procedures (8,9) have made it possible to obtain sufficient amounts of DNA from extracellular virus. In this chapter we describe the general properties of the DNA and the experiments to asses the structural and the functional organization of the genome.

Y. Becker (ed), Herpesvirus DNA.

CONFORMATION, SIZE AND BASE COMPOSITION

CMV DNA is a linear double-stranded molecule with a molecular weight of approximately 150×10^6 D (8,9). The buoyant density in CsCl is 1.717 g/cm^3 (4,9,13) corresponding to an average G + C content of 58%. By partial denaturation mapping six unique A + T and G + C rich localizations can be detected, five of which appear to be in a specific sequence, and the sixth one may be at either end of the molecule (18).

The molecular weight of the CMV genome has for some time been somewhat controversial. For a long time a value of 100×10^6 D was generally accepted. This molecular weight was based on cosedimentation with HSV DNA (13) and on electron microscopy (22). The first indication that the complete genome of CMV could be larger than 100×10^6 D was obtained by Kilpatrick and Huang (18), when alignment of their denaturation maps resulted in a molecular weight of 150×10^6 D. This has recently been confirmed by Geelen *et al.* (8,9), who showed by length measurements that most DNA molecules extracted from purified virus consisted of molecules of $\pm 150 \times 10^6$ D. A few molecules of $\pm 120 \times 10^6$ D, possibly representing defective molecules (20) were found. The DNA preparations analysed were infective. A similar molecular weight of 150×10^6 D has since then been found by DeMarchi *et al.* (6, sedimentation velocity and kinetic complexity), Lakeman and Osborn (19, sedimentation velocity) and by restriction enzyme analysis (Weststrate, Geelen, and Van der Noordaa, submitted for publication). The sum of the molecular weights of the restriction enzyme fragments, as determined by electron microscopy and mobility in agarose gels, resulted in molecular weights of 154×10^6 D (*Bgl*II), 155×10^6 D (*Hin*dIII) and 153×10^6 D (*Xba*I) for CMV DNA (AD169).

FRAGMENTATION IN ALKALI

The presence of nicks and gaps in herpesvirus DNA has been described for HSV DNA (7,27), PRV DNA (1) and EBV DNA (10). These nicks and gaps are apparently randomly distributed over the DNA, as analysed by sedimentation in sucrose gradients of alkali treated DNA (27) or by electron microscopy of exonuclease treated DNA (1,10). When CMV DNA (AD169) is incubated in alkali and centrifuged on a neutral high salt gradient (23) a sedimentation profile as shown in Fig.1 is obtained.

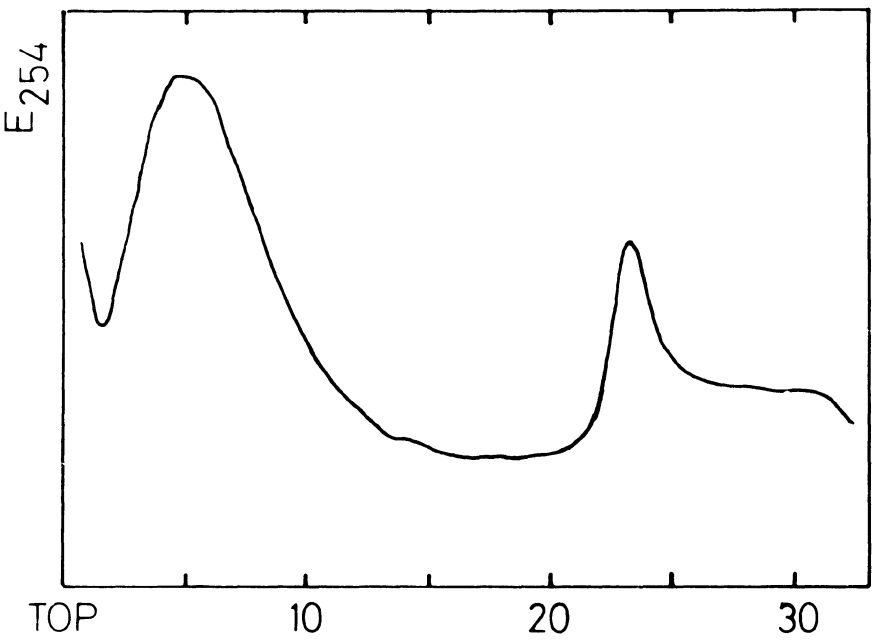

Fig.1. Sedimentation profile of alkaline denatured CMV DNA. 10 µg DNA was incubated for 5 min at room temperature in 0.1 N NaOH, neutralized with KH_2PO_4 and centrifuged for 1 h at 30,000 rpm in a Beckman SW 41 rotor on a 5-20% linear high salt sucrose gradient as described by Sheldrick et al. (23).

From this figure it can be concluded that approximately 15% of the single-stranded DNA molecules are intact. As, except for the intact molecules, no distinct size class can be observed, the nicks and gaps appear randomly distributed over the genome. This conclusion has further been confirmed by analysis of exonuclease treated DNA. When the DNA is incubated with exonuclease III and examined in the electron microscope single-stranded regions bounded by double-stranded areas are observed (Geelen and Maris, unpublished observations). When these preparations are cleaved with the restriction endonuclease *Hin*dIII, and electrophoresed on agarose gels a smear is obtained, as is shown in Fig.2. However after repair of the DNA using T4 DNA polymerase and T4 ligase and subsequent incubation with exonuclease III and *Hin*dIII, a normal *Hin*dIII digest pattern is obtained, while only the terminal fragments are affected by the exonuclease (Weststrate, unpublished).

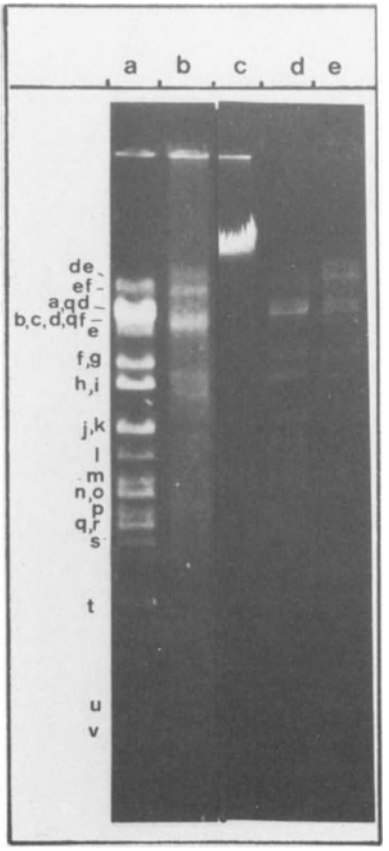

Fig.2. Analysis of the distribution of nicks and gaps in CMV DNA (AD169) by exonuclease incubation and HindIII cleavage. The samples were electrophoresed on 0.7% agarose gels as described by Weststrate et al. (submitted for publication). lane a: HindIII digest; lane b: exonuclease III incubation, followed by HindIII cleavage; lane c: CMV DNA repaired by T4 polymerase + T4 ligase; lane d: HindIII digest of c; lane e: exonuclease III incubation of c, followed by HindIII cleavage.

SEQUENCE ARRANGEMENT OF CMV DNA

The sequence arrangement of CMV DNA can be derived from restriction enzyme analysis and by electron microscopic examination of denatured and reannealed single-stranded DNA molecules (Sheldrick *et al.*, to be published). When alkali denatured CMV DNA (AD169) is centrifuged in neutral high salt sucrose gradients, and the intact single-stranded molecules examined in the electron microscope two types of fold back structures are observed: the C2-form (two single-stranded circles joined by a duplex) and the L-form (one single-stranded circle and a duplex region, joining the circle to the single-stranded DNA). Based on the dimensions of the single- and double-stranded areas of these two forms, a structure as shown in Fig.3 has been derived (Sheldrick, Berthelot and Laithier, to be published).

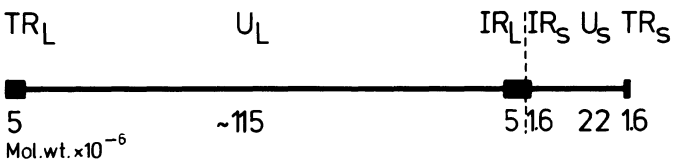

Fig.3. Structural organization of CMV DNA (AD169; Sheldrick, Berthelot and Laithier, to be published).

As can be seen from this figure the sequence arrangement in CMV DNA is of the same general plan as in HSV DNA, but with regions of different relative and absolute size. In HSV DNA besides this general arrangement small reiterated sequences are found at the termini of the unique sequences (12). To analyse whether reiterated sequences are present at the termini of CMV DNA, an approach as described by Grafstrom *et al.* (11) was used. The DNA was incubated with exonuclease III, adjusted to 2xSSC, reannealed, and examined under the electronmicroscope. Up to 20% of the molecules were found to be circularized (Fig.4).

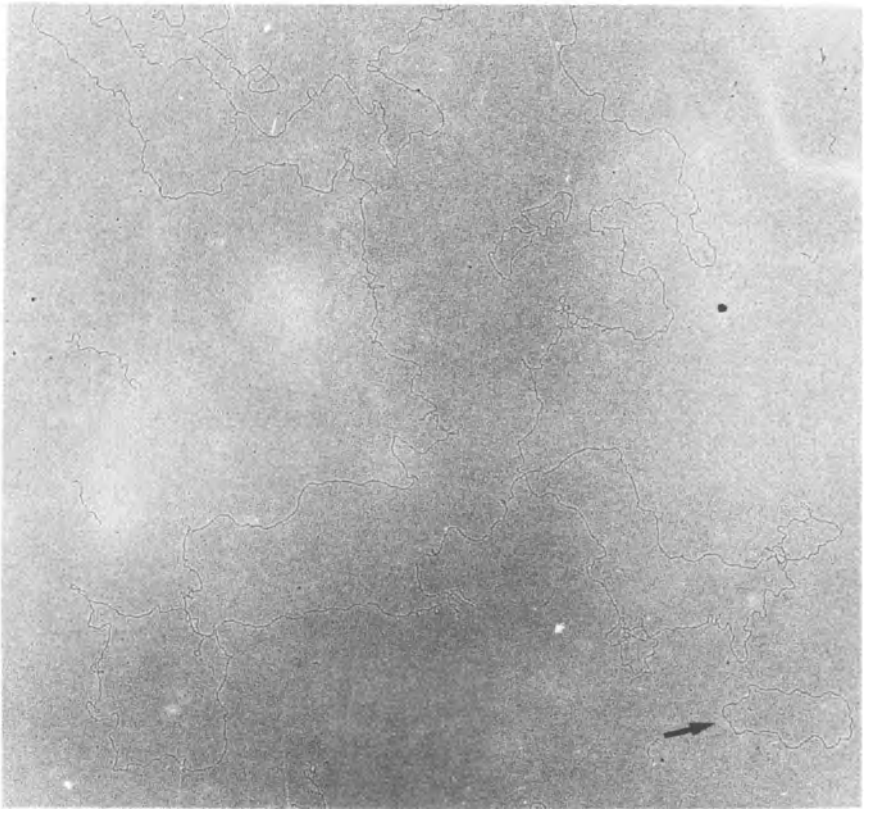

Fig.4. Electron micrograph of circularized CMV DNA. The DNA was circularized as described by Grafstrom et al. (11) and spread as described by Davis et al. (5). The arrow indicates a PM_2 DNA molecule ($6.7x10^6$ D, ref.8).

Besides the unit length circles, two size classes of smaller circles were observed (respectively $132x10^6$ and $28x10^6$ D, see Fig.5)

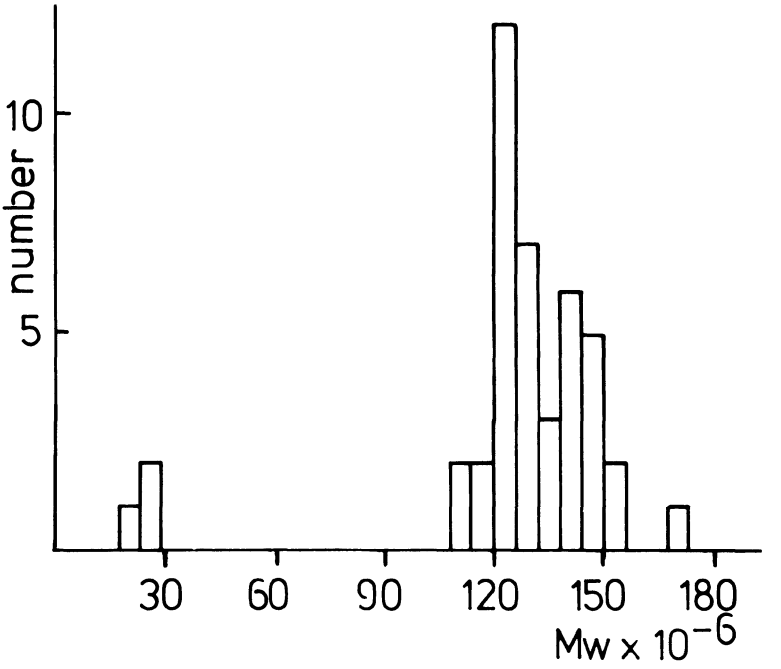

Fig.5. Size distribution of circularized CMV DNA (AD169).

The appearance of circles smaller than unit size may be explained in two ways. The presence of defective molecules (20,26) with the same terminal configuration as the complete genome or a preferential scission at the junction of the two unique sequences of CMV DNA. If the terminal reiterated sequences are repeated at the junction, then, as can be seen in Fig.3, circles of $\pm 125 \times 10^6$ D (long unique sequence) and of $\pm 25 \times 10^6$ D (short unique sequence) could be formed.

ISOMERIC ARRANGEMENT AND RESTRICTION ENZYME CLEAVAGE PATTERNS OF CMV DNA (AD169)

CMV DNA contains contiguous internal reverted repeats of the terminal repeats (Sheldrick *et al.*, to be published) and has terminal redundancies as shown by exonuclease digestion and circularization (Geelen and Weststrate, 3rd Herpes Virus Workshop, Cambridge, 1978). In this sequence arrangement recombination between the ends of the molecules and their reverted repeats may occur readily and give rise to a population of molecules containing four isomeric arrangements, differing in the relative orientation of the two unique sequences (24). Evidence for the existence of four isomeric arrangements has been obtained by restriction enzyme analysis of the DNA. When CMV DNA is cleaved with the restriction enzymes *Hin*dIII of *Bgl*II (enzymes which do not cleave in the repeated regions) four 0.5 M terminal fragments and four 0.25 M fragments overspanning the junction are found. All other fragments are present in concentrations of 1 M relative to the concentration of intact DNA (Weststrate *et al.*, submitted for publication). Cleavage of AD169 DNA with the restriction enzymes *Bgl*II, *Hin*dIII and *Xba*I results in 32, 27 and 21 fragments respectively (Fig.6). The arrangement of these fragments on the genome has been determined using cross blot hybridization and identification of linkage groups by double digestions (Weststrate *et al.*, submitted). In constructing the physical maps for the above mentioned enzymes another variation was observed: electrophoresis of the *Xba*I fragments results in a characteristic set of submolar fragments (Fig.6, j-n), with molecular weights differing in multiples of 300,000 D. By cross blot hybridization it was shown that all these fragments were interrelated and should be located at the same position in the CMV genome. This heterogeneity was after prolonged electrophoresis also observed in the *Hin*dIII e fragment, but not in the *Bgl*II a fragment (in which the *Hin*dIII e fragment is located). This is probably due to the lack of resolving power of 0.7% aga-

rose gels for fragments with a molecular weight of more than 20×10^6 D. The physical maps for the enzymes *Bgl*II, *Hin*dIII and *Xba*I are shown in Fig.7.

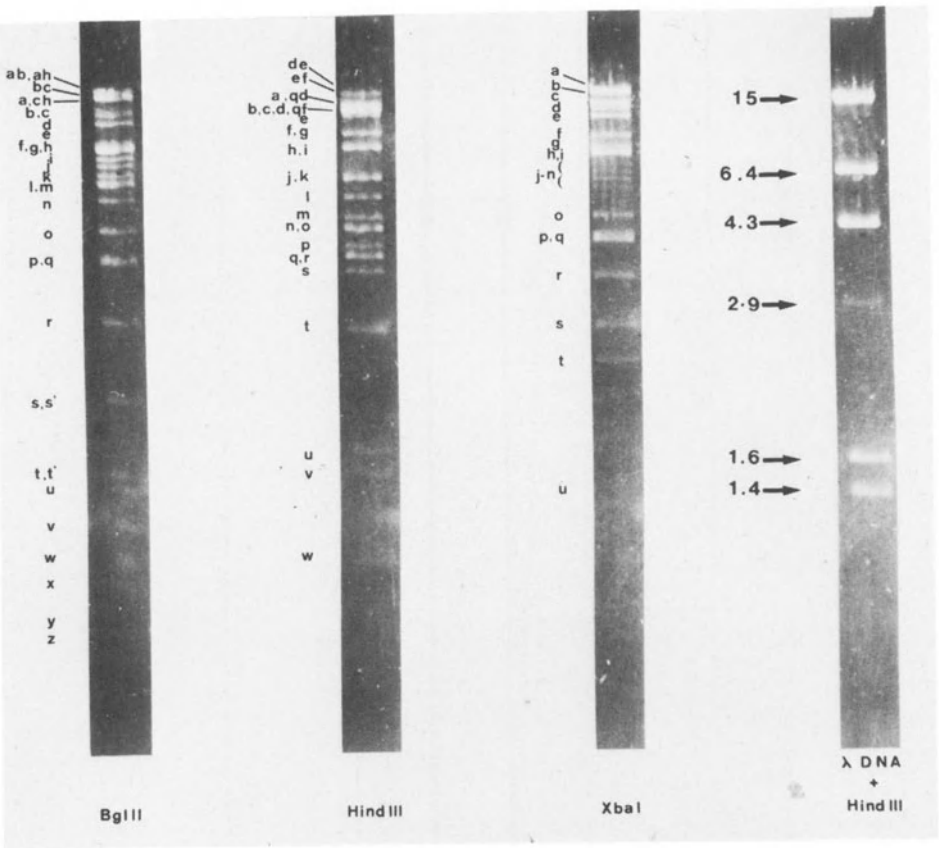

Fig.6. Restriction enzyme cleavage patterns of CMV DNA (AD169). CMV DNA (1 µg) was cleaved with the restriction endonuclease BglII (Bacillus globigii), HindIII (Haemophilus influenzae)or XbaI (Xanthomonas badrii) and electrophoresed on 0.7% agarose gels.

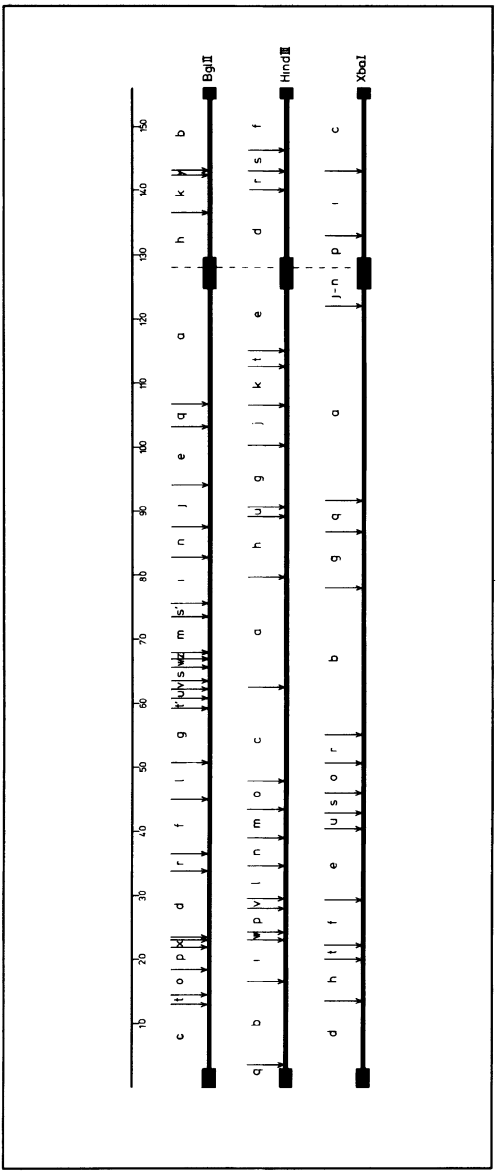

Fig.7. Physical maps for the BglII, HindIII and XbaI cleavage sites on CMV DNA, strain AD169. Only one orientation is shown.

STRAIN VARIATION

It has well been documented, that upon cleavage with restriction endonucleases of DNA isolated from various human isolates electrophoresis patterns are obtained, which, although they show a large number of comigrating fragments, are characteristic for most isolates (14,17). One exception to the high level of homology between the human isolates described up to now, is the Colburn strain, which is probably a simian CMV-related virus (15). The homology between the different CMV isolates is not restricted to the comigrating fragments, as can be seen in Fig.8. In the experiment shown in this fi-

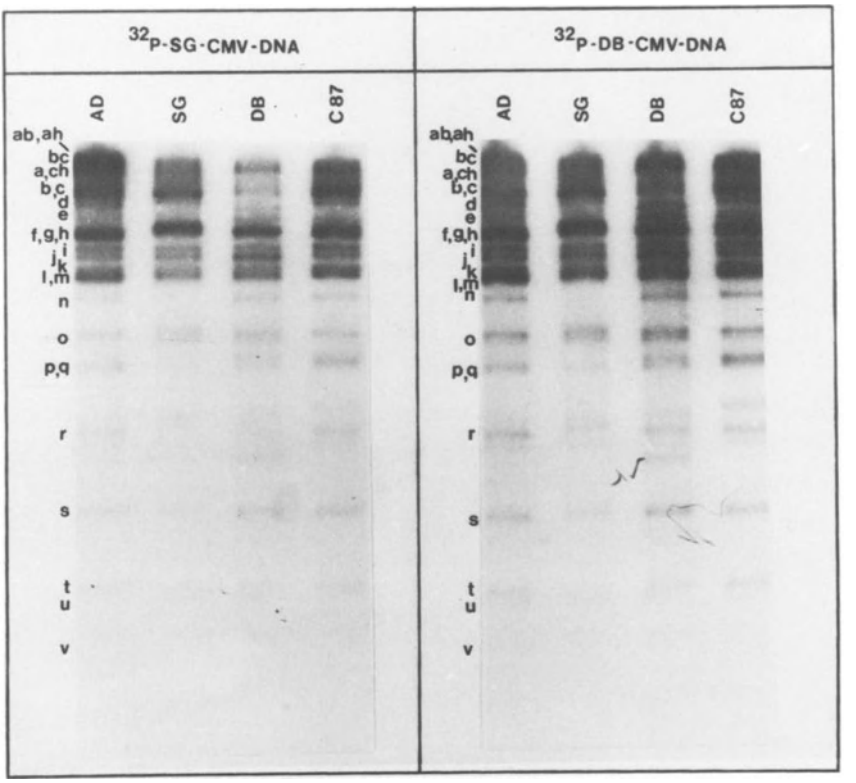

Fig.8. Hybridization patterns of CMV DNA, isolates AD169, C87, DB, and SG, after digestion with BglII, electrophoresis and transfer to nitrocellulose sheets, with ^{32}P-labelled SG DNA (A) or ^{32}P-labelled DB DNA (B). Hybridization was performed as described by Jeffreys and Flavell (16).

gure DNA of four isolates (AD169, C87, DB and SG) was cleaved with the restriction endonuclease *Bgl*II, electrophoresed on agarose gels, transferred to nitrocellulose sheets (25) and hybridized to two different ^{32}P-labelled CMV DNA probes. As no differences could be detected in the hybridization patterns with the two different probes, this is once again an indication for the high level of homology between the human CMV isolates.

The strain variation was further analysed by cross blot hybridization of restriction endonuclease cleaved DNA. By this technique homology between comigrating fragments can be detected. The strains analysed by this technique and their origin are described in Table 1.

Table 1. Human cytomegalovirus isolates and their origin.

CMV isolate	origin	isolated by
AD169	adenoid	Rowe *et al.* (21)
C87	kidney	Benyesh-Melnick *et al.* (2)
DB	urine	Slaterus, Amsterdam
SG	urine	Slaterus, Amsterdam
PT	urine	Kapsenberg, Bilthoven

An example of a cross blot analysis of AD169, C87 and PT DNA is shown in Fig.9. From this figure it can be seen that C87 resembles AD169 much more than the PT isolate, as more *Xba*I fragments of C87 are comigrating and cross hybridizing with the AD169 *Xba*I fragments than with the PT isolate.

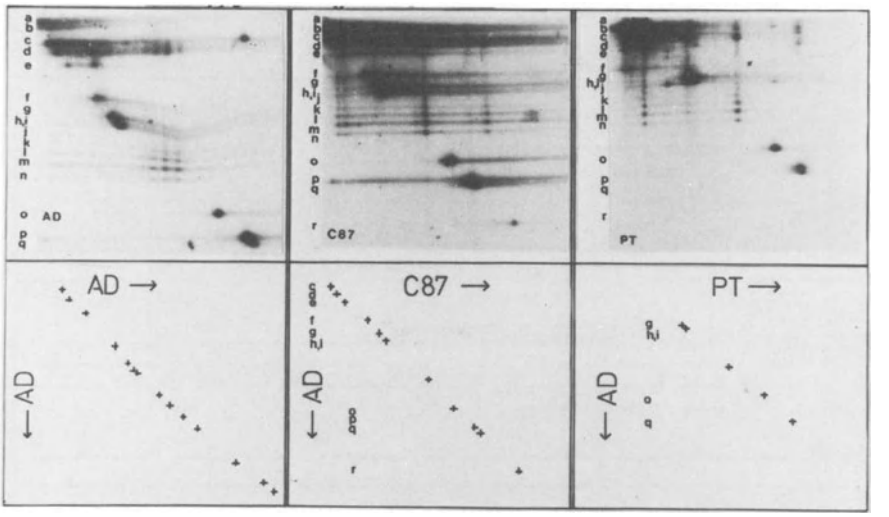

Fig.9. Cross hybridization of XbaI cleaved DNA. ^{32}*P-labelled AD169 (A), C87(B), or PT DNA (C) were cleaved with XbaI, electrophoresed on 0.7% agarose gels, and transferred under hybridization conditions (65*^{o}*C, 5xSSC + 0.1% SDS + 0.2% PVP + 0.2% BSA + 0.2% Ficoll) perpendicular to nitrocellulose sheets containing immobilized unlabelled XbaI fragments of AD169 DNA. After the transfer-hybridization, the nitrocellulose sheets were washed as described by Jeffreys and Flavell (16). The lower panels are a graphic interpretation of the upper panels.*

Secondly it can be seen that the heterogeneity found in the *Xba*I pattern of AD169 DNA (see above, fragments j-n) is not present in C87 or PT DNA. This heterogeneity was also not observed in SG or DB DNA (data not shown).
When it is assumed, that fragments comigrating and cross hybridizing among different isolates are located at the same position on the genome, then these fragments can be mapped on the AD169 physical map as is shown in Fig.10.

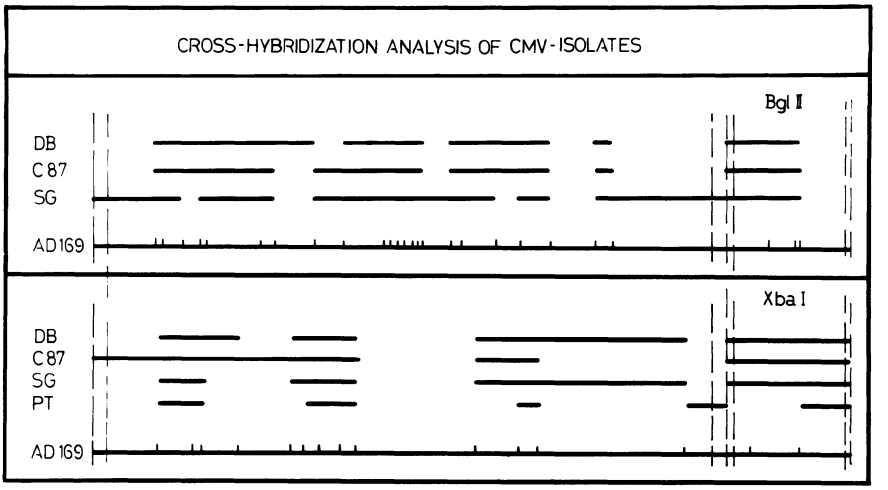

Fig.10. Location of restriction endonuclease fragments of C87, DB, SG and PT DNA, which are comigrating and cross hybridizing with AD169 DNA fragments, on the physical maps of AD169 DNA. The upper panel shows the BglII data and the lower panel the XbaI data.

From this figure it can be seen, that, although variations occur at many sites of the genome most differences are found at the termini of the genome and three areas in the long unique sequence (the *Bgl*II fragments f, m and e).
To analyse whether these areas are functionally related, the location of transcripts on the CMV genome was analysed.
As in HSV1 (3) in the expression of the CMV genome three periods can be identified:

immediate early transcription: transcripts presumably made by a pre-existing host RNA polymerase,

early transcription: made before onset of the DNA replication,

late transcription: transcripts made after onset of the viral DNA replication.

To locate these transcripts on the CMV DNA ^{3}H-uridine labelled immediate early and early viral RNA was hybridized to nitrocellulose bound fragments generated by *Bgl*II, *Hin*dIII and *Xba*I cleavage. Immediate early post infection the expression of the genome is very limited: only the terminal fragments and one fragment in the long unique sequence (*Bgl*II f fragment) were found to hybridize. At early (0-8 hr p.i. or transcribed in the presence of phosphonoacetic acid [PAA], an inhibitor of the viral DNA polymerase) times post infection hybridization is found to all fragments, although some fragments are overrepresented and other are underrepresented. The transcription data for the immediate early and early transcripts are summarized in Fig.11.

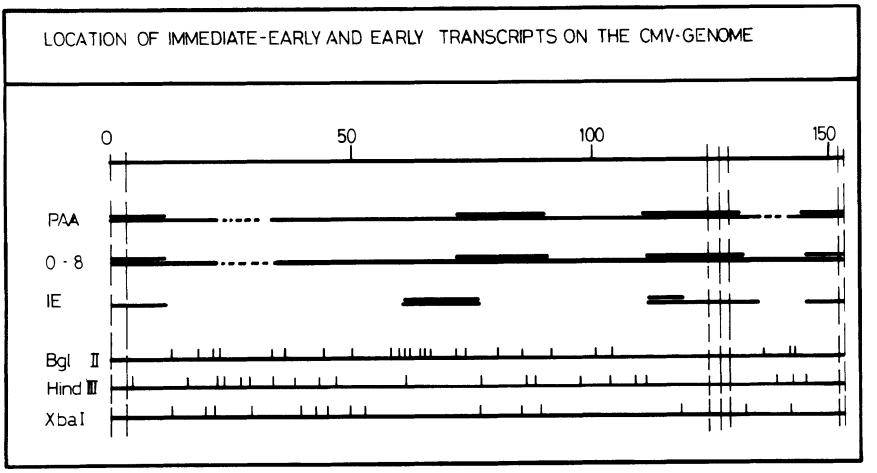

Fig.11. Location of immediate early (IE) and early (0-8 hr p.i., and PAA) transcripts on the CMV DNA (strain AD169).
The IE transcripts were transcribed in the presence of 200 µg/ml cycloheximide (3).

DISCUSSION

The molecular weight of human cytomegalovirus DNA (strain AD169) was shown to be $\pm 150 \times 10^6$ D by length measurements. This molecular weight was further confirmed by restriction endonuclease analysis. Summation of the molecular weights of fragments generated by cleavage with the *Bgl*II, *Hin*dIII, or the *Xba*I restriction endonucleases leads to values of approximately 153×10^6 D. In the DNA nicks and gaps are found. These nicks and gaps are apparently randomly distributed, as upon centrifugation of alkali denatured DNA on sucrose gradients only the full length single-stranded molecules are detected as a distinct size class. A second indication for the random distribution is, that after labelling *in vitro* using DNA polymerase I followed by restriction endonuclease cleavage all fragments are labelled according to their molecular weight.

The general plan for the organization of CMV DNA resembles the organization of HSV DNA: terminal reiterated sequences were detected by the circularization of exonuclease treated DNA, and the presence of terminal and internal inverted repeats was determined by hybridization of single-stranded molecules (Sheldrick, Berthelot and Laithier, to be published). This general plan was confirmed by restriction endonuclease analysis of the DNA: four 0.5 M terminal fragments and four 0.25 M internal fragments were identified (*Bgl*II, *Hin*dIII). No submolar fragments were present in the *Xba*I cleavage pattern, as this enzyme cleaves within the repeats. In the mapping data heterogeneity is observed in the *Hin*dIII e and the *Xba*I j-n fragments, but not in the *Bgl*II a fragment (in which the *Hin*dIII e fragment is located). This is probably due to the lack in resolving power of 0.7% agarose gels for very large fragments (*Bgl*II a is more than 20×10^6 D).

The *Xba*I fragments j-n are all located at the same position on the physical map of AD169 DNA and differ in molecular weight in multiples of 300,000 D. The nature of these reiterated sequences is still under investigation.
The homology of the DNAs of AD169, C87, DB, PT and SG was analysed by cross blot hybridization using AD169 as reference. Most comigrating fragments cross hybridized and were then considered to be located at the same position on the genome. Although variations (loss or extra cleavage site) were observed in most parts of the genome, the strongest variation was found in the submolar fragments and the *Bgl*II fragments f, m and e. To see, if there is a functional relationship between these areas of high variability, the location of immediate early and early transcripts on the genome was determined using an approach as described by Clements *et al.* (3). By combination of the transcription and the strain variation data a possible correlation (except the *Bgl*II e and f fragments) has been observed between strain variability and the immediate early expressed areas of the genome. To establish this correlation, it will be necessary to analyse more strains with restriction endonucleases with multiple recognition sites resulting in a more detailed mapping of the location of the immediate early transcripts on the CMV DNA.

Acknowledgements.
We thank W.Maris, B.Schrever and I.Zwaan for their excellent technical contributions, and drs. P.Wertheim and J.v.d.Noordaa for helpfull discussions.
This work was partly supported by the Koningin Wilhelmina Fonds.

REFERENCES

1. BEN-PORAT,T., F.J.RIXON, M.L.BLANKENSHIP.(1979) Analysis of the structure of the genome of pseudorabies virus. *Virology* 95, 285-294.
2. BENYESH-MELNICK,M., H.S.ROSENBERG, AND B.WATSON. (1964) Viruses in cell cultures of kidneys of children with congenital heart malformations and other diseases. *Proc.Soc. Exp.Biol.Med.* 117, 452-459.
3. CLEMENTS,J.B., R.J.WATSON, AND N.M.WILKIE. (1977) Temporal regulation of herpes simplex virus type 1 transcription: location of transcripts on the viral genome. *Cell* 12, 275-285.
4. CRAWFORD,L.V., AND A.J.LEE. (1964) The nucleic acid of human cytomegalovirus. *Virology* 23, 105-107.
5. DAVIS,R.W., M.SIMON, AND N.DAVIDSON. (1971) Electron microscope heteroduplex methods for mapping regions of base sequence homology in nucleic acids. *Meth.Enzym.* 21, 413-428.
6. DeMARCHI,J.M., M.L.BLANKENSHIP, G.D.BROWN, AND A.S.KAPLAN (1978) Size and complexity of human cytomegalovirus DNA. *Virology* 89, 643-646.
7. FRENKEL,N., AND B.ROIZMAN. (1972) Separation of the herpes virus deoxyribonucleic acid on sedimentation on alkaline gradients. *J.Virol.* 10, 565-572.
8. GEELEN,J.L.M.C., C.WALIG, P.WERTHEIM, AND J.VAN DER NOORDAA. (1978) Human cytomegalovirus DNA. I. Molecular weight and infectivity. *J.Virol.* 26, 813-816.
9. GEELEN,J.L.M.C., C.WALIG, P.WERTHEIM, AND J.VAN DER NOORDAA. (1978) Characterization of human cytomegalovirus: Infectivity and molecular weight. In *Oncogenesis and Herpesviruses III*. (G.de-Thé, W.Henle, and F.Rapp,eds.). *IARC Scientific Publications, Lyon. pp. 97-103.*
10. GIVEN,D., D.YEE, K.GRIEM, AND E.KIEFF. (1979) DNA of Epstein-Barr virus. V. Direct repeats of the ends of Epstein-Barr virus DNA. *J.Virol.* 30, 852-862.
11. GRAFSTROM,R.H., J.C.ALWINE, W.L.STEINHART, AND C.W.HILL. (1974) Terminal repetitions in herpes simplex virus type 1 DNA. *Cold Spring Harbor Symp.Quant.Biol.* 39, 679-681.
12. HONESS,R.W., AND D.H.WATSON. (1977) Unity and diversity in the herpesviruses. *J.gen.Virol.*37, 15-37.
13. HUANG,E.-S., S.-T.CHEN, AND J.S.PAGANO. (1973) Human cytomegalovirus. I. Purification and characterization of viral DNA. *J.Virol.* 12, 1473-1481.
14. HUANG,E.-S., B.A.KILPATRICK, Y.-T.HUANG, AND J.S.PAGANO. (1976) Detection of human cytomegalovirus and analysis of strain variation. *Yale J.Biol.Med.* 49, 29-43.
15. HUANG,E.-S., B.A.KILPATRICK, A.LAKEMAN, AND C.A.ALFORD. (1978) Genetic analysis of a cytomegalovirus-like agent isolated from human brain. *J.Virol.* 26, 718-723.
16. JEFFREYS,A.J., AND R.A.FLAVELL. (1977) A physical map of the DNA regions flanking the rabbit β-globin gene. *Cell* 12, 429-439.

17. KILPATRICK,B.A., E.-S.HUANG, AND J.S.PAGANO. (1976) Analysis of cytomegaloviruses with restriction endonucleases *Hin*dIII and *Eco*RI. *J.Virol.* 18, 1095-1105.
18. KILPATRICK,B.A., AND E.-S.HUANG. (1977) Human cytomegalovirus genome: partial denaturation map and organization of genome sequences. *J.Virol.* 24, 261-276.
19. LAKEMAN,A.D., AND J.E.OSBORN. (1979) Size of infectious DNA from human and murine cytomegalovirus. *J.Virol.* 30, 414-416.
20. RAMIREZ,M.L., M.VIRMANI, C.GARON, AND L.ROSENTHAL. (1979) Defective virions of human cytomegalovirus. *Virology* 96, 311-314.
21. ROWE,W.P., J.W.HARTLEY, S.WATERMAN, H.C.TURNER, AND R.J.HUEBNER. (1956). Cytopathogenic agent resembling human salivary gland virus recovered from tissue culture of human adenoid. *Proc.Soc.Exp.Biol.Med.* 117, 452-459.
22. SAROV,I., AND FRIEDMAN,A. (1976) Electron microscopy of human cytomegalovirus DNA. *Arch.Virol.* 50, 343-347.
23. SHELDRICK,P., M.LAITHIER, D.LANDO, M.L.RYHINER. (1973) Infectious DNA from herpes simplex virus: infectivity of double-stranded and single-stranded molecules. *Proc.Natl. Ac.Sci.* 70, 3621-3625.
24. SHELDRICK,P., AND N.BERTHELOT. (1974) Inverted repetitions in the chromosome of herpes simplex virus. *Cold Spring Harbor Symp.Quant.Biol.* 39, 667-678.
25. SOUTHERN,E.M. (1975) Detection of specific sequences among DNA fragments separated by gel electrophoresis. *J.Mol.Biol.* 98, 503-518.
26. STINSKY,M.F., E.S.MOCARSKI, AND D.R.THOMSEN. (1979) DNA of human cytomegalovirus: size heterogeneity and defectiveness resulting from serial undiluted passage. *J.Virol.* 31, 231-239.
27. WILKIE,N.M. (1973) The synthesis and substructure of herpesvirus DNA: the distribution of alkaline labile single strand interruptions in HSV-1 DNA. *J.gen.Virol.* 21, 453-476.
28. WRIGHT,H.T. (1973) Cytomegaloviruses. In *The herpesviruses* (A.Kaplan, ed.) p.353-388, *Academic Press Inc., New York.*

18. DNA of Tupaia Herpesviruses

G. Darai*, R.M. Flügel, B. Matz* and H. Delius#

INTRODUCTION

Tupaia (the tree shrew), a member of the family Tupaiidae, is regarded as one of the most primitive prosimians bridging the gap between insectivores and primates (1,2). The phylogenetic placement of the Tupaia has led to much interesting discussion (3-5), especially after recently published reports (6-9), on the first discoveries of fossil tree shrews of the eocene and miocene periods. Our aim was to test animals suitable for laboratory experiments in medicine and biology which are more closely related to primates than to rodents. From this point of view several laboratories are engaged in studying Tupaia in different fields of science. For the past four years, we have been studying tumor induction in Tupaia by means of chemicals, radiation and viruses. A number of herpesviruses have been isolated from different animal species including subprimates and primates (10-12), as well as from a malignant lymphoma of owl monkeys (13), a spontaneous myelomonocytic leukemia of orangutan (14), Burkitt's lymphoma (15), and nasopharyngial carcinomas of man (16).

HISTORY AND BIOLOGICAL PROPERTIES OF TUPAIA HERPESVIRUSES

The isolation and electron microscopic characterization of a herpes-like virus, THV-1, from a degenerating lung tissue culture of an apparently healthy Tupaia has been reported (17,18). A second tree shrew (THV-2) herpesvirus was isolated and characterized by Darai et al. (19). THV-2 was isolated from a degenerating cell culture derived from a tumor of an adult *Tupaia belangeri* approximately 8 years old (19). The histopathological examination revealed that this tumor was a high-grade malignant lymphoma centroblastic with multiple metastases. The third Tupaia herpesvirus,

Y. Becker (ed), Herpesvirus DNA.

THV-3, was isolated from a tumor of an adult tree shrew about 9 years of age. This tumor was histopathologically characterized as being similar to human Hodgkin's disease, lymphocytic depletion type with multiple metastases. A fourth tree shrew herpesvirus, THV-4, was released from a degenerating spleen culture of a moribund, 11-year-old animal. All four Tupaia herpesviruses can be efficiently propagated on Tupaia embryonic fibroblast cells, yielding a virus titer of about 8×10^6 to 5×10^7 PFU/ml five days after infection (19). All four herpesviruses can be plaque-assayed on Tupaia embryonic fibroblasts, and these cells were used to plaque-purify THV-1 to THV-4. The history and biological properties of the Tupaia herpesviruses are compiled in Table 1.

PHYSICAL PROPERTIES OF TUPAIA HERPESVIRUS DNA

Preparation of viral DNA

The virus was grown and harvested as described previously by Darai et al. (19) and was purified as described for the equine herpesvirus by centrifugation in neutral sucrose followed by a cesium chloride floating gradient (20). Intact DNA of the different tree shrew herpesviruses was extracted as follows: The resuspended virus pellets were lysed with sodium dodecyl sulfate (0.5% final concentration) and after 15 min at 37°C, proteinase K was added (50 µg/ml) and the preparations were incubated at 37°C overnight. Subsequent manipulations of all DNA preparations were performed by using sterile pipettes (bore diameter 3 to 5 mm). The remaining procedures used for the DNA preparation were previously described (21), but the dialysis step was omitted. DNA concentrations were determined from the absorbance at 260 and 280 nm. THe preparations had an A_{260}/A_{280} ratio of 1.9 to 2.0.

Determination of buoyant density

Radioactive THV DNA was extracted and prepared from Tupaia

Table 1. History and Biological Properties of Tupaia Herpesviruses

	THV-1	THV-2	THV-3	THV-4
Isolation	Isolated from a degenerating lung tissue culture from an apparently healthy Tupaia*	Isolated from a degenerating cell culture from a malignant lymphoma of a moribund Tupaia**	Isolated from a degenerating cell culture from a Hodgkin's sarcoma of a moribund Tupaia**	Isolated from a degenerating cell culture from spleen of a moribund Tupaia***
Host range	Tupaia embryonic fibroblasts Tupaia embryonic kidney cells Primary rabbit kidney cells Human foreskin fibroblasts Marmoset skin fibroblasts Tupaia, rabbit, and human leukocytes		8.0×10^6 to 2.0×10^7 PFU/ml 1.0×10^7 to 5.0×10^7 PFU/ml 1.0×10^4 to 7.0×10^5 PFU/ml 1.0×10^4 to 3.0×10^4 PFU/ml 1.0×10^2 to 2.0×10^2 PFU/ml 1.0×10^4 to 5.0×10^5 PFU/ml	
CPE	Enlargement of infected cells, inclusion bodies in nucleus and cytoplasma			
Reproductive cycle	Relatively slow reproductive cycle, maximal infectivity was reached 4 to 6 days p.i., total cell degeneration of infected Tupaia fibroblasts 6 to 8 days p.i.			
Pathogenicity	Lethal for juvenile and young adult Tupaia by i.v. (100%) and i.p. (25%) application			not done
Latency	Infectious virus recovered from spleen of infected animals, which survived the acute infection			not done
Oncogenicity	Induced hyperplasia of thymus -thymoma- in New Zealand rabbits			in progress

*Mircovic et al., Proceedings of the 10th International Congress of Microbiology, 181-189, 1970. **Darai et al., J. gen. Virol., 43, 541-551, 1979. ***Darai et al., VIIIth Congress of the International Primatological Society, 1980.

embryonic fibroblast cultures separately infected with each of the four THVs and labelled with ^{3}H-thymidine. After purification of the THV particles by low and high speed centrifugation, the DNA was extracted and analyzed by preparative isopycnic CsCl centrifugation. A more precise determination of the buoyant density of THV DNA by analytical ultracentrifugation gave a value of ρ = 1.724 µg/ml corresponding to a G+C content of 65.4% when calculated according to Schildkraut et al. (22).

Thermal denaturation profiles

Two determinations of the ultraviolet absorbance-temperature profile of the DNA in 0.1 x SSC resulted in a T_m value of 81.0°C. This corresponds to a G+C content of the DNA of 65%. The values are in agreement with those obtained from buoyant density analyses as described above.

Measurement of the contour length of THV DNA in the electron microscope

The molecular weight of THV DNA was determined by electron microscopic measurement of the contour length of the DNA using PM2 DNA as an internal length standard. Based on a molecular weight of 26.4 x 10^6 for T7 DNA (23), the measurement of 38 molecules of THV DNA resulted in a molecular weight of 129 to 133 x 10^6 daltons. An example for the double-stranded DNA of THV-2 is given in Fig. 1. Single-stranded DNA of THV was prepared for electron microscopy by heating the viral DNA in formamide and isolating the single strands from agarose gels as described by Koller et al.(24). Figure 2 documents that single-stranded THV DNA does not display any extended stem-loop structures.

Restriction endonuclease cleavage patterns of THV DNA

Analysis of the DNA of the four THV strains with the restriction endonucleases Kpn I, Hpa I, Cla I, Hind III, Bgl II and Eco RI showed the characteristic DNA fragment patterns. Here we present the DNA patterns of those enzymes which demonstrated similarities and dissimilarities between

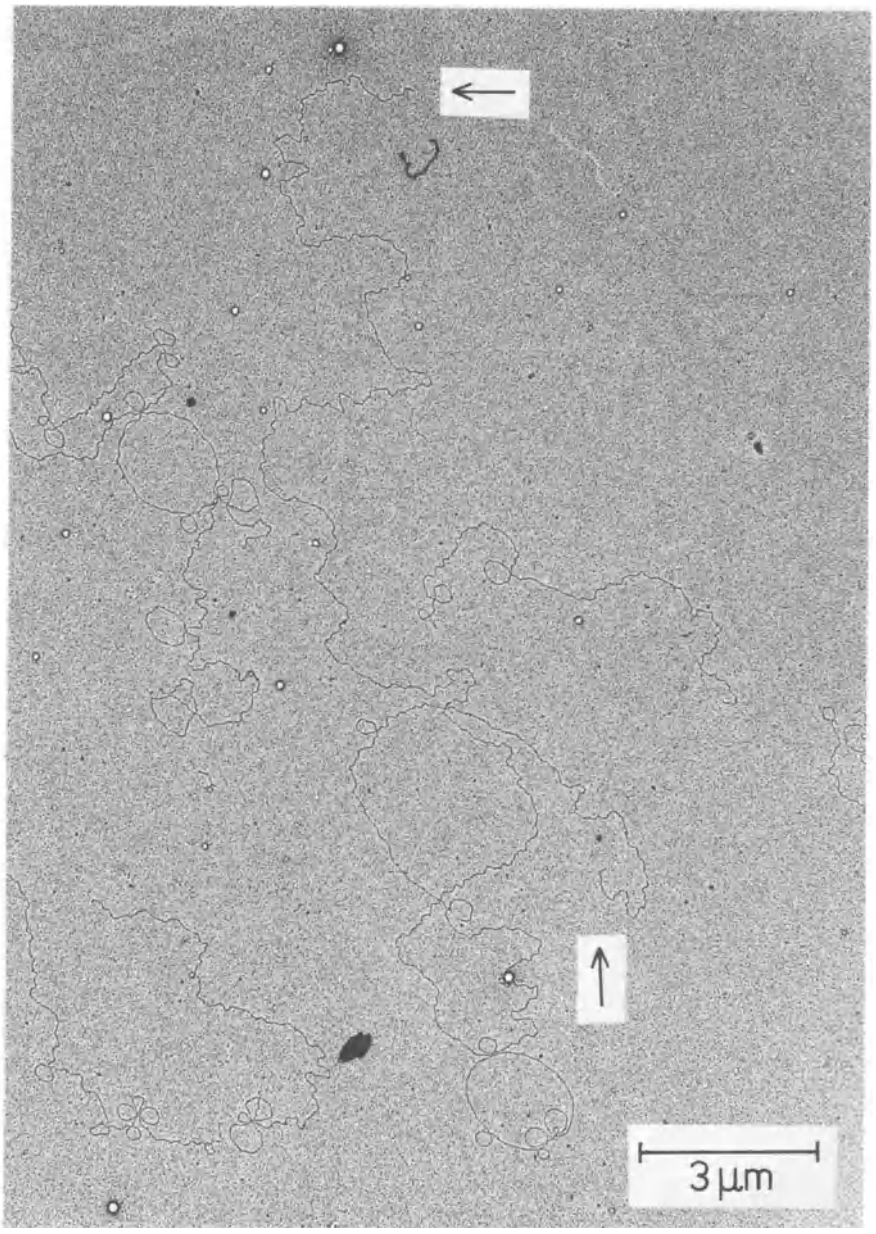

Figure 1: Cytochrome spreading of THV-2 DNA, double-stranded, linear form. The arrows mark the ends of the molecule.

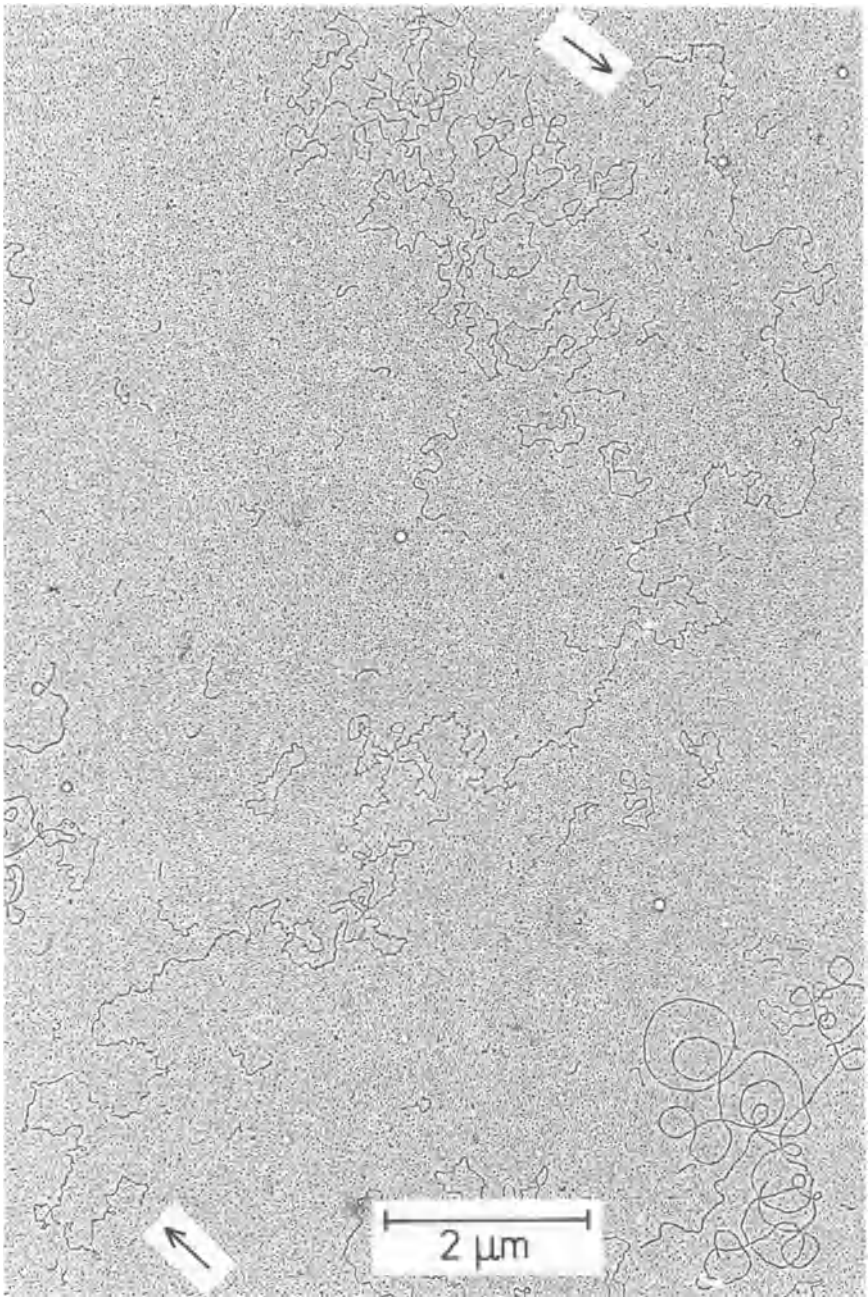

Figure 2: Cytochrome spreading of single-stranded THV-2 DNA. The arrows mark the ends of the molecule. The small circles are DNA of bacteriophage M13.

the different Tupaia herpesviruses (Figs. 3-7). The results are summarized in Table 2. No minor bands were detectable.

Table 2. Analysis of DNAs of Tupaia herpesviruses 1 to 4 using different restriction endonucleases and electrophoresis on agarose gels

Restriction enzyme		Apparent number of DNA bands* THV-1	THV-2	THV-3	THV-4
Cla I	AT↓CGAT	18	16	13	15
Eco RI	G↓AATTC	13	14	15	14
Hind III	A↓AGCTT	10	12	10	8
Hpa I	GTT↓AAC	11	15	10	17
Kpn I	GGTAC↓C	23	22	21	20
Bgl II	A↓GATCT		>25		
Others**			>50		

* Detectable at an agarose concentration of 0.5%; DNA fragments of $<1 \times 10^6$ daltons are not included.

** The following enzymes produced more than 50 DNA fragments: Alu I, Ava I, Hae II, Hinc II, Hind II, Mbo II, Pst I, Pvu II, Bal I, Hpa II, Sac I, Xba I, Mst I, Taq I, Bst EII, Xho I, Bgl I, Sac II, Bam HI, Sal I and Sma I.

Molecular weights of the DNA fragments of THV-1 to 4, produced by digestion with restriction enzymes Hind III and Eco RI are given in Tables 3 and 4, using DNA of bacteriophage λ, HSV-1, human adenovirus type 2 and *M. hyorhinis* Bst EII fragments A and B with molecular weights of 75 and 50 x 10^6 respectively, as markers (21). The terminal fragments of THV-2 and THV-4 DNAs were determined by treatment with *E. coli* exonuclease III prior to restriction enzyme cleavage. The terminal fragments of THV-2 DNA are marked by asterisks in Tables 3 and 4. The infectivities of THV-1 to 4 DNAs were tested on Tupaia embryonic fibroblasts using calcium chloride technique developed by Graham et al. (25). DNA from each THV was able to transfect Tupaia embryonic fibroblasts as detectable by specific plaques with the same morphology as those of wild-type THV.

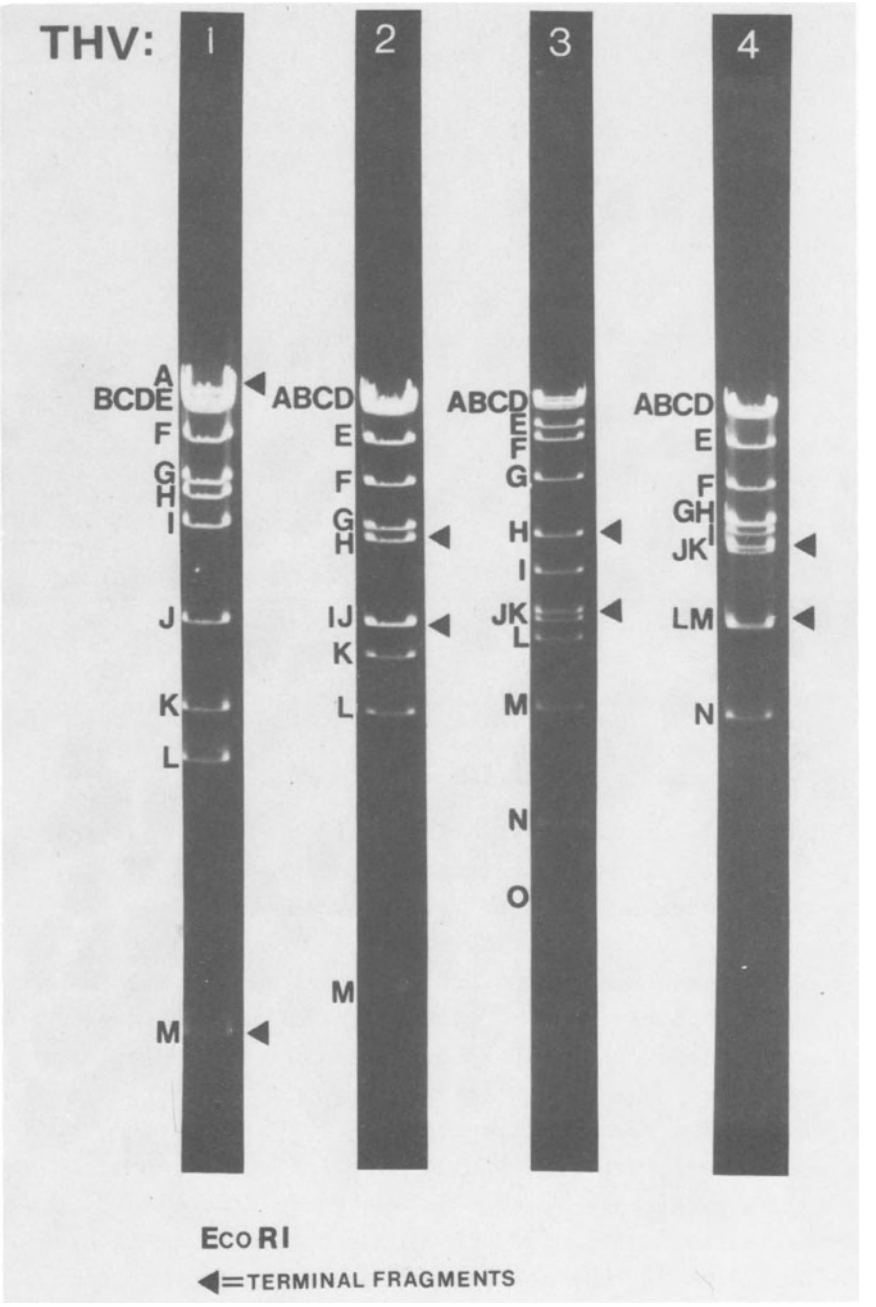

Fig. 3: Eco RI cleavage pattern of DNAs of Tupaia herpesviruses 1 to 4

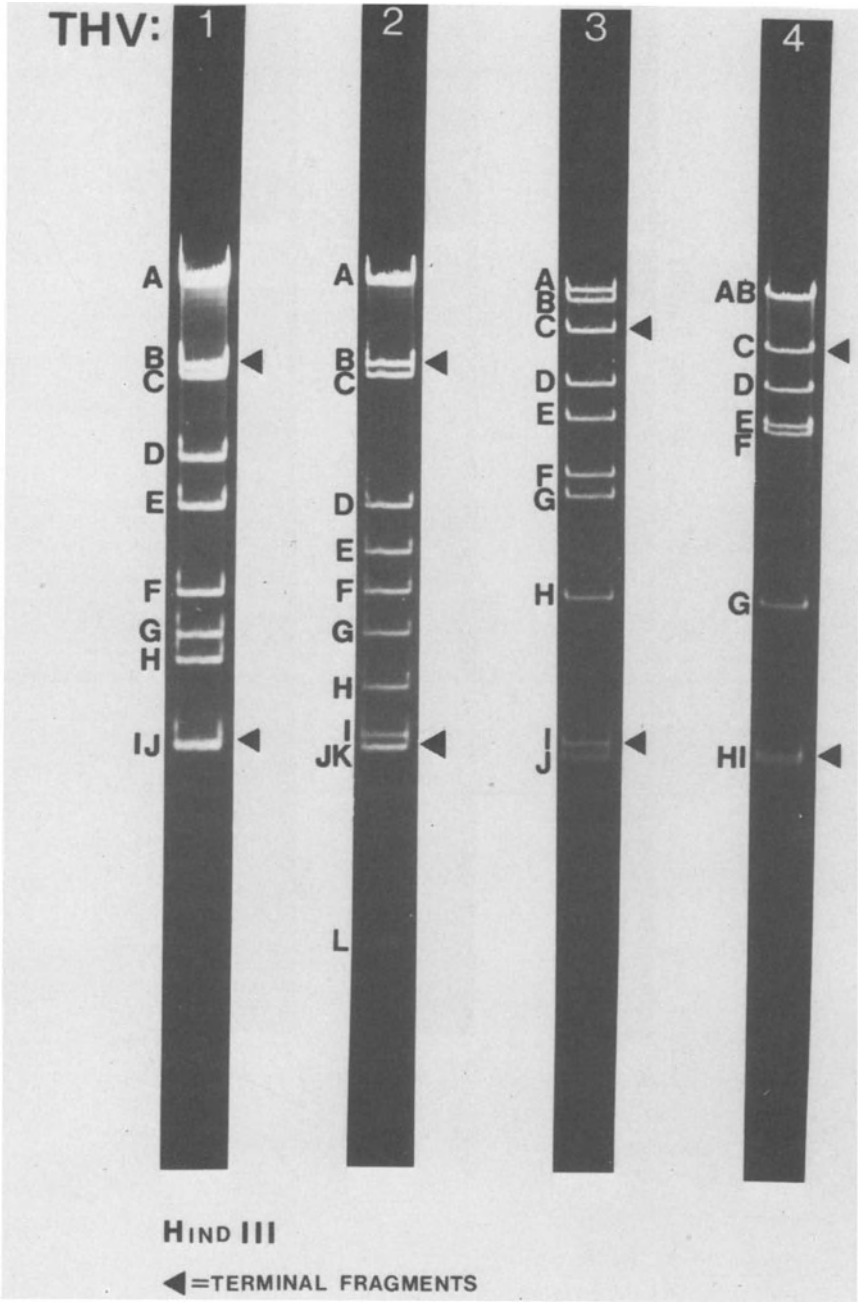

Fig. 4: Hind III cleavage pattern of DNAs of Tupaia herpesviruses 1 to 4

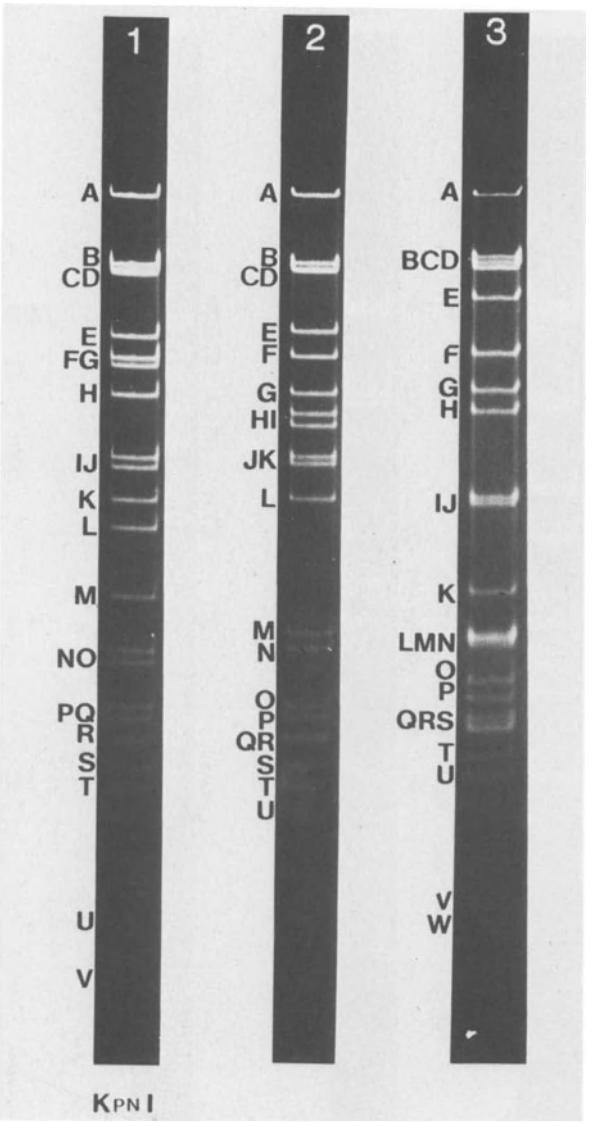

Fig. 5: Kpn I cleavage pattern of DNAs of Tupaia herpesviruses 1 to 3

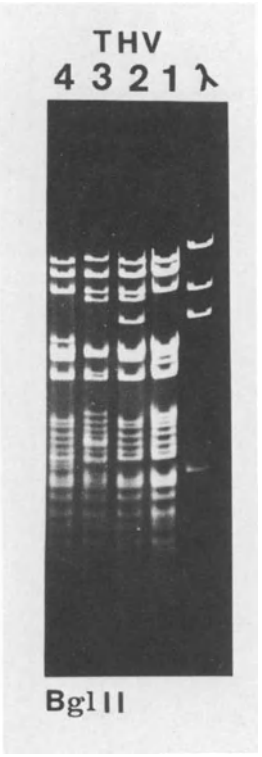

Fig. 6: Bgl II cleavage pattern of DNAs of Tupaia herpesviruses 1 to 4

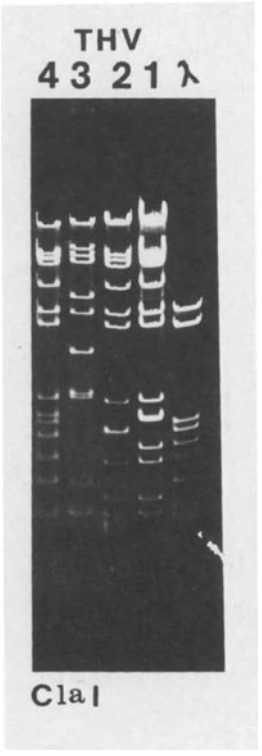

Fig. 7: Cla I cleavage pattern of DNAs of Tupaia herpesviruses 1 to 4

Table 3. Molecular weights of DNA fragments of Tupaia herpesviruses produced by restriction endonuclease Eco RI

Fragment Number	THV-1	THV-2	THV-3	THV-4
A	20*	16.5	16.5	17.5
B	16.5	15.5	15.5	16.5
C	15.5	15.0	15.0	14.5
D	15.0	15.0	14.5	14.5
E	15.0	12.0	12.5	11.4
F	12.0	9.6	11.7	9.2
G	9.6	7.7	9.6	8.2
H	9.2	7.2*	7.2*	7.9
I	7.2	5.0	6.1	7.7
J	5.0	4.8*	5.1*	7.2*
K	3.5	4.4	4.7	7.1
L	3.0	3.5	4.5	5.5*
M	1.4*	1.5	3.5	5.3
N		0.2	2.5	3.9
O			1.95	
Total	132.9	117.9	130.85	136.5

*Terminal fragments were determined by exonuclease III treatment of the DNA prior to restriction enzyme cleavage.

Table 4. Molecular weights of DNA fragments of Tupaia herpesviruses produced by restriction endonuclease Hind III

Fragment Number	THV-1	THV-2	THV-3	THV-4
A	~60	~60	35.0	33.5
B	15.0*	15.0*	21.0	33.0
C	13.5	13.5	20.0*	17.0*
D	9.1	7.3	13.3	13.5
E	7.3	5.8	11.5	11.0
F	4.8	4.8	8.7	10.3
G	4.0	4.0	7.8	5.8
H	3.6	3.3	4.8	2.9*
I	2.6*	2.75	2.75*	2.7
J	2.5	2.6*	2.5	
K		2.55		
L		1.0		
Total	122.4	122.6	136.35	129.7

*Terminal fragments were determined by exonuclease III treatment of the DNA prior to restriction enzyme cleavage.

DISCUSSION

Regarding the structure of their genomes, the tree shrew herpesviruses are unique when compared with the DNA of other known herpesviruses from different species. There are many similarities in the size and restriction enzyme cleavage patterns of the DNA of the four Tupaia herpesviruses. The properties of the DNA are summarized in Table 5. Minor bands were not detectable. Larger reiterations do not seem to occur in the THV genomes; instead, the THV DNA molecules of 118-136 daltons seem to consist of a long unique DNA sequence. This conclusion was verified by electron microscopic examination of single-stranded THV DNA under conditions favoring intra-strand hybridization. Self-annealed single strands of THV DNA did not form stem-loop structures. This result rules out the existence of isomeric forms of THV DNA. In addition, blot hybridization experiments revealed extensive homology among the DNA of the four different Tupaia herpesviruses. We cannot exclude very short repeats at this stage of our investigations. Recently, grouping of herpesviruses was attempted on the basis of their genome structure and size. When the large size of their genomes, which range from 118-136 x 10^6 daltons, and the unique sequence arrangements within the genomes are considered, it seems appropriate to emphasize that Tupaia herpesviruses constitute the first members of a new herpesvirus subgroup.

The channel catfish herpesvirus (CCV) is so far the only herpesvirus with DNA characterized by a simple reiteration of one set of DNA sequences (8-10 x 10^6 daltons) in the same orientation as the termini (26). THV DNA differs from CCV DNA not only in the molecular weight, but also in the apparent lack of repeats in the THV DNA. The relatively high molecular weight of THV DNA and its simple sequence arrangement when compared to the more complicated CCV DNA might indicate that on the evolutionary scale Tupaia herpesviruses diverged earlier from its host - the tree shrew - than other herpesviruses did. Thus, it is possible to consider Tupaia herpesviruses as one of the 'phylogenetically'

Table 5. Properties of DNA of Tupaia herpesviruses

		THV-1	THV-2	THV-3	THV-4
Buoyant density in CsCl ($gxml^{-1}$)			1.724		
Thermal denaturation (^{0}C, in 0.1xSSC)		←	81.0	→	
(G+C) content (%)			64.5		
Molecular weight (Megadalton)					
1) Restriction enzyme analysis					
	Eco RI	132.9	117.9	130.85	136.5
	Hind III	122.4	122.6	136.35	129.7
2) Contour length measurement		129 ± 3	133 ± 2	130 ± 2	132 ± 3
Transfectivity		+	+	+	+
Stem-loop structures		-	-	-	ND
Existence of isomeric forms		-	-	-	-
Intertypic sequence homology		+	+	+	+

oldest members in the herpesvirus family.

REFERENCES

1. Fiedler, W., Hofer, H., Schulz, A.H. and Starck. D. Primatology 1:1-252, 1956.
2. Moore, W.G., and Goodman, M. Bull. Math. Biophys. 30:279-289, 1968.
3. Goodman, M. Science 153:1550, 1966.
4. Lehmann, H., Romero-Herrera, A.E., Joysey, K.A. and Friday, A.E. Ann. N.Y. Acad. Sci. 241:380-391, 1974.
5. Dene, H., Goodman, M. and Prychodko, W. J. Mamm. 49:697-706, 1978.
6. Chopra, S.R.K., Kaul, S. and Vasishat, R.N. Nature 281:213-214, 1979.
7. Chopra, S.R.K. and Vasishat, R.N. Nature 281:214-215, 1979.
8. Maier, W. Z. f. zool. Systematik u. Evolutionsforschung 15:311-318, 1977.
9. Martin, R.D. Nature 281:178-179, 1979.
10. Agrba, V.A., Yakovleva, L.A., Lapin, B.A., Sangulija, I.A., Timanovskaya, V.V., Markaryan, D.S., Chuvirov, G.N. and Salmanova, E.A. Exp. Pathol. 10:318-332,1975.
11. Meléndez, L.V., Daniel, M.D., Hunt, R.D. and Garcia, F.G. Lab. Animal Care 18:374-381, 1968.
12. Meléndez, L.V., Hunt, R.D., King, N.W., Barahona, H.H., Daniel, M.D., Fraser, C.E.O. and Garcia, F.G. Nature New Biol. 235:182-184, 1972.
13. Hunt, R.D., Meléndez, L.V., King, N.W., Gilmore, C.E., Daniel, M.D., Williamson, M.E. and Jones, T.C. J. Natl. Cancer Inst. 44:447-465, 1970.
14. Rasheed, S., Rongey, W.R., Bruszweski, J., Nelson-Rees, W.A., Rabin, H., Neubauer, R.H., Esra, G. and Gardner, M.B. Science 198:407-408, 1977.
15. Epstein, M.A., Henle, G., Achong, B.G. and Barr, Y.M. J. Exp. Med. 121:761-770, 1965.
16. Zur Hausen, H., Schulte-Holthausen, H., Klein, G., Henle, W., Henle, G., Clifford, P. and Santesson, L. Nature 228:1056-1058, 1970.
17. McCombs, R.M., Brunschwig, J.P., Mircovic, R. and Benyesh-Melnick, M. Virology 45:816-820, 1971.
18. Mircovic, R., Voss, W.R. and Benyesh-Melnick, M. Proceedings of the 10th International Congress of Microbiology, Mexico City, 181-189, 1970.
19. Darai, G., Matz, B., Schröder, C.H., Flügel, R.M., Berger, U., Munk, K. and Gelderblom, H. J. gen. Virol. 43:541-551, 1979.

20. Abodeely, R.A., Lawson, L.A. and Randall, C.C. J. Virol. 5:513-527, 1970.

21. Gross-Bellard, M., Oudet, P. and Chambon, P. Eur. J. Biochem. 36:32-38, 1973.

22. Schildkraut, C.L., Marmur, J., and Doty, P. J. Mol. Biol. 4:430-443, 1962.

23. Stüber, D. and Bujard, H. Mol. gen. Genet. 154:299-303, 1977.

24. Koller, B., Delius, H., Bünemann, H. and Müller, W. Gene 4:227-239, 1978.

25. Graham, F.L. and van der Eb, A.J. Virology 52:456-467, 1973.

26. Chousterman, S., Lacasa, M. and Sheldrick, P. J. Virol. 31:73-85, 1979.

19. Organization and Replication of Pseudorabies Virus DNA

Tamar Ben-Porat and Albert S. Kaplan

STRUCTURE OF THE GENOME OF PSEUDORABIES (Pr) VIRUS

The genome of Pr virus, swine herpesvirus, consists of a linear, double-stranded DNA molecule, molecular weight approximately 90 x 10^6 (5, 21). Pr viral DNA has a relatively high G+C content (73 moles %) (2) and is asymmetric with respect to its G+C content (21); it gives rise to characteristic partial denaturation maps, indicating that the DNA is not circularly permuted (21).

The structure of Pr virus DNA is complex, as is that of other herpesviruses. It consists of two unique sequences, one, a short unique sequence (MW, 6 x 10^6), is found between a sequence of MW of 10 x 10^6 which is repeated on its other side in inverted complementary form - the inverted repeat (Powell, Clement, and Wilkie, personal communication; (5, 24). The extreme end of the molecule, the terminal repeat, is not represented internally in the inverted repeat (5).

In addition to the large inverted repeat, the genome of Pr virus also contains several minor repeated sequences, as demonstrated by the appearance of single- or double-stranded lariats in self-annealed, denatured, or exonuclease-digested molecules (5). The lack of formation of unit-size circles by exonuclease-digested DNA is particularly noteworthy. Over 2,000 Pr viral DNA molecules digested with *E. coli* exonuclease III or phage T5 exonuclease for various periods of time (1 to 15 min) and self-annealed under various conditions were examined, but under

Y. Becker (ed), Herpesvirus DNA.

none of these experimental conditions did unit-size circular Pr DNA molecules appear, although under the same conditions, HSV-1 DNA did form circles. Attempts to produce circles by varying the conditions of extraction or to detect the presence of a protein that would hold the ends of the virion DNA together did not yield positive results (5). Thus, either some unknown factor prevents circularization of Exo-III-treated Pr virus DNA *in vitro* or Pr virus DNA is not terminally redundant, despite the fact that it forms circles *in vivo* and replicates in the form of concatemers in a head-to-tail alignment (see below). We consider this latter possibility to be unlikely.

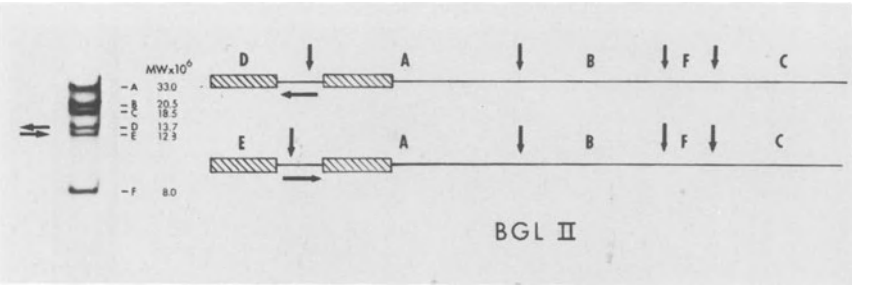

Fig. 1. Bgl-II Restriction Enzyme Map of Pr Virus DNA Bgl-II does not cleave the inverted repeats (striped rectangle) but does cleave the unique short sequence of Pr virus DNA, giving rise to fragments D and E which are present in one-half molar quantities because each is produced by digestion of one of the two isomeric forms of Pr virus DNA. The Bgl-II restriction enzyme map of Pr virus DNA was communicated to us prior to publication by Powell, Clements and Wilkie and has been confirmed in our laboratory.

Pr virus DNA exists in two isomeric forms in which the short unique sequence is present in two different orientations with respect to the long unique sequence. This is illustrated by the digestion pattern of Pr virus DNA with Bgl-II restriction endonuclease which gives rise to two different size fragments, D and E; these fragments are present in equimolar (0.5 M) amounts and originate

from the two different isomeric forms of the DNA (Fig. 1). The existence of two isomeric forms of Pr virus DNA was first demonstrated by Powell, Clements and Wilkie (personal communication) and was confirmed in our laboratory.

Pr virus DNA fragments upon alkaline denaturation (3) as does HSV DNA (14, 25). The number of sites at which the Pr virus DNA fragments is approximately the same as the number of sites at which the DNA fragments upon denaturation with formamide or the number of sites at which Exo III can initiate digestion (5). On the average, there are 3.5 nicks or gaps per double-stranded molecule; however, some molecules have as few as one nick or gap. No single-stranded interruption can be found at a nonrandom site along the molecules. Thus, there are no significant numbers of alkali-sensitive bonds in Pr virus DNA and no nicks or gaps at nonrandom sites on the DNA molecules.

The complex structure of the genomes of the herpesviruses raises some interesting questions regarding the mechanism by which they replicate. There has been considerable speculation about the functional significance of the nicks and gaps in the viral DNA, as well as about structural isomers of herpesvirus DNA and the mechanisms by which they arise. A resolution of these problems will probably be obtained only when the mechanisms by which the DNA of these viruses replicates have been elucidated. We summarize here our data concerning the mode of replication of the DNA of Pr virus. We also present evidence that Pr virions containing either one of the two isomeric forms of the DNA molecules are infectious.

MODIFICATIONS OF INFECTING VIRUS DNA BEFORE INITIATION OF VIRUS DNA SYNTHESIS

Despite the relatively high ratio of physical to infectious particles in populations of Pr virions, usually

20:1, a large proportion of the virions will participate in the infective process in cells infected at high multiplicity. Approximately 50% of the virions adsorb to the cells; 30 to 90% (depending on the experiment) of the DNA in the adsorbed virions become associated with the cell nuclei and practically all of that DNA will replicate (6). If one studies the structure of the DNA molecules present in the infecting virions that become associated with the cell nucleus, one is likely therefore to observe those processes involving virus DNA which will participate in replication. The fate of infecting viral DNA was studied before the initiation of DNA synthesis by electron microscopy and by digestion with restriction endonucleases.

1. Analysis by Electron Microscopy

To examine the structures of the virus DNA before the onset of DNA synthesis, the DNA from the nuclei of cells infected with [^{14}C]- or [^{3}H]-thymidine-labeled virions was extracted. Virus DNA was separated from cellular DNA by isopycnic centrifugation in CsCl and was examined in an electron microscope. The following three types of molecules were observed: (i) unit-size molecules with single-stranded ends; (ii) unit-size circular molecules; and (iii) concatemeric molecules composed of a maximum of 2 unit-size molecules (14).

The formation of these structures indicates that upon entering the nucleus, the DNA is digested by an exonuclease and forms circles or concatemers as a result of annealing of its cohesive ends. However, since this process could not be duplicated after *in vitro* digestion of the ends by exonucleases (see above), it is not clear whether the formation of circles or concatemers *in vivo* occurs by this mechanism.

2. Analysis by Restriction Endonuclease Digestion.

To determine whether changes in the structure of the infecting virus DNA could be detected, cells were infected with [^{32}P]-labeled purified virions and the virus DNA present in the cell nucleus before the start of virus DNA synthesis was analyzed by digestion with various restriction endonucleases. The restriction enzyme pattern of the DNA revealed that by 2 hours post infection approximately 70% of the virus DNA molecules had lost their free ends. Instead of the fragments representing the free ends, each digest contained a new fragment consisting of the two end fragments joined together. These results show that before the start of DNA synthesis, virus DNA forms circles or concatemers and that a relatively large proportion of the infecting virus DNA undergoes this process (4, 9).

SEDIMENTATION CHARACTERISTICS OF VIRUS DNA SYNTHESIZED AT VARIOUS TIMES AFTER INFECTION

The following two phases of viral DNA replication can be distinguished: (i) Up to 3 hours post-infection newly-synthesized DNA is associated mainly with molecules that sediment heterogeneously with S values up to approximately twice that of mature viral DNA (54 S). That these structures represent virus DNA in its first round of replication can be deduced from the following: The fork movement in replicating Pr virus DNA is approximately 1 μm/min (1) and most virus DNA replication occurs unidirectionally (see below) along the 45 μm long molecule. Under the experimental conditions we use, virus DNA synthesis starts at 2:15 hours post-infection. Thus the DNA will be in its first round of replication up to 3 hours post infection. (ii) At later times after infection, most of the newly-synthesized DNA is associated with structures sedimenting with S values up to 100 times that of mature virus DNA (3). In addition, both at early and late times

after infection some of the newly-synthesized DNA sediments more slowly than does mature virus DNA. The smaller-than-unit-size molecules are artifacts of isolation and result from the fragility of replicating Pr virus DNA (7).

STRUCTURES OF REPLICATING DNA DURING THE FIRST ROUND OF VIRUS DNA REPLICATION

1. Analysis by Electron Microscopy

Examination in an electron microscope of virus DNA molecules present within the infected cells after virus DNA synthesis has begun (2.75 to 3 hours post-infection) revealed several different types of DNA structures: (i) Molecules containing large replicative loops were observed on unit-size circular, unit-size linear, and longer

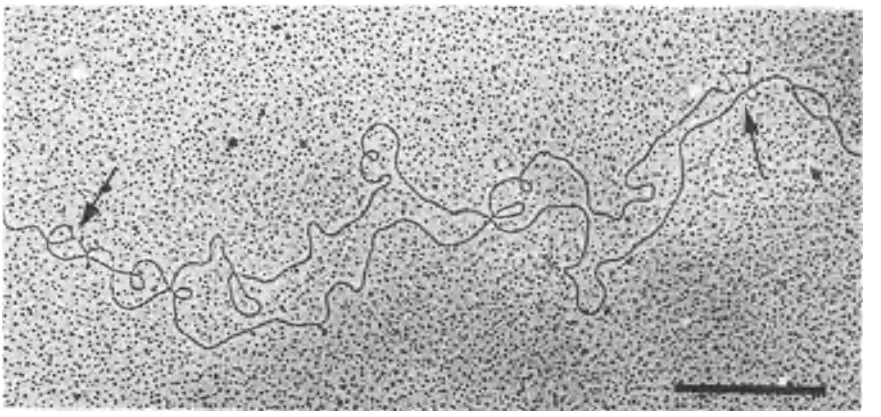

Fig. 2. Replicative Loop in Virus DNA
The virus DNA was isolated at 2.75 hours post infection. This replicative loop measures 10 μm. The arrows indicate the regions of the forks and of single-strandedness. The bar represents 1 μm.

than-unit-size molecules. An example of a typical replicative loop with single-stranded regions in the *trans*-position is shown in Fig. 2. (ii) Y-shaped molecules with branches

of varying sizes were observed on unit-size, as well as on longer-than-unit-size, molecules. (iii) Replicative loops and branches were also seen on many smaller-than-unit-size molecules; however, these were shown to be breakage products resulting from the fragility of the replicating Pr DNA (7).

2. Analysis by Restriction Endonuclease Digestion

Replicating herpesvirus DNA molecules are fragile and fragment upon isopycnic centrifugation in CsCl or KI, a procedure essential to their separation from cellular DNA. The correct interpretation of the structures observed by electron microscopy is therefore difficult and it is necessary to corroborate these observations by other methods. The DNA synthesized during the first round of replication was therefore analyzed by restriction enzyme digestion.

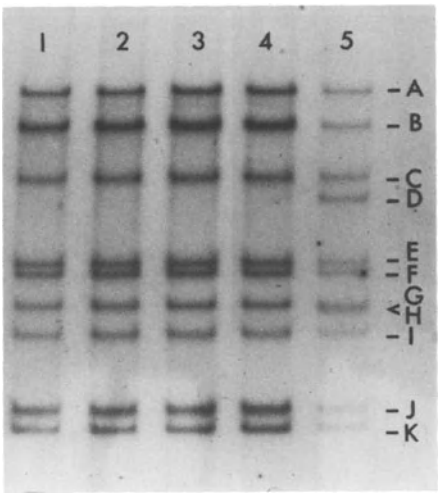

Most of the Pr DNA molecules undergoing the first round of replication are "endless;" the normal end restriction fragments are underrepresented and, instead, a new fragment appears, which is composed of the two end fragments

Fig. 3. Autoradiogram of Kpn-I Digested Pr Virus DNA Labeled During the First Round of Replication

Viral DNA synthesized by the cells from the time of infection was labeled with ^{32}P and purified. The DNA was digested with Kpn-I restriction enzyme and the fragments separated on agarose gels. Tracks 1-4, DNA harvested at 2 hr 30 min, 2 hr 40 min, 2 hr 50 min and 3 hr, respectively; track 5, mature virion DNA.

joined together. This is illustrated in Fig. 3, which shows that Kpn-I end fragments D and H are not detectable while band B (which has the molecular weight expected of the joined H and D fragments) is overrepresented. That band B does indeed contain the joined fragments H and D was shown by excising the DNA in band B and annealing it to filter strips to which the separated Kpn-I fragments of Pr virus DNA had been fixed.

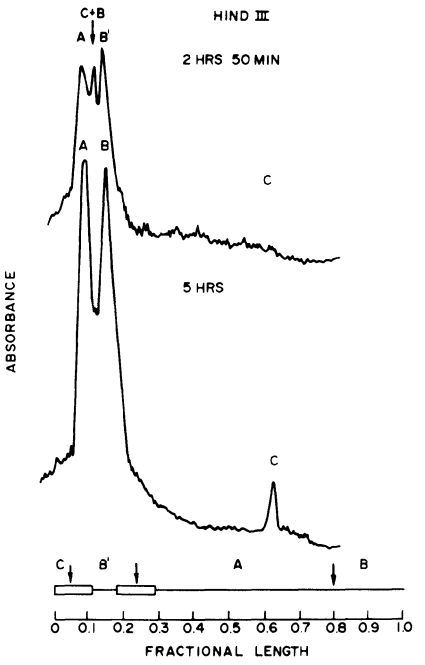

That Pr DNA is "endless" during its first round of replication is illustrated also in Fig. 4 which shows a Hind-III digest of newly synthesized DNA that had accumulated in the infected cells during the first round of DNA replication. End fragment C (the end fragment containing the main origin of replication, see Fig. 6) is virtually absent and a new fragment appears with a molecular weight equal to that of the two end fragments (B + C) joined together.

Fig. 4. Microdensitometer Tracing of an Autoradiogram of Hind III Digested Pr Viral DNA Labeled for Various Times
The experiment was performed as described in the legend to Fig. 3. The DNA was digested with Hind III restriction enzyme.

Thus, most of Pr DNA is endless during its first round of replication. The DNA is either in the form of circles or large concatemers. However, since most of the DNA syn-

thesized during the first round of replication has an S value only approximately twice that of mature DNA (see above), which is inconsistent with very large concatemeric structures, we conclude that most of the DNA replicates in the form of circles. In some experiments, however, some free, labeled ends appear (8), indicating that replication can also be initiated on linear molecules, either of unit-length size or larger-than-unit size.

LOCATION OF ORIGIN OF REPLICATION

1. Analysis by Electron Microscopy

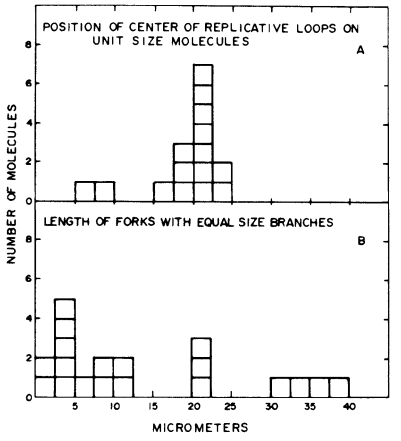

The position of replicative loops on linear, unit-size molecules and the lengths of the branches on forked unit size molecules observed to date are summarized in Fig. 5. Most of the centers of the replicative loops occupy a position approximately 20 μm from one of the ends (Fig. 5A), indicating that initiation of viral DNA replication occurs preferentially at that position. The

Fig. 5. Summary of the Positions of the Centers of Replicative Loops on Unit-size Molecules and of the Lengths of Branches on Forked Molecules.

Infected cells were collected at 2 hr 40 min post infection. The DNA was extracted, viral DNA was separated from cellular DNA by isopycnic centrifugation in cesium chloride and spread for electron microscopy. Only unit-size molecules with "eyes" at least 0.5 μm in length and molecules with equal-size branches were included in this figure.

lengths of the branches on forked molecules are summarized in Fig. 5B. Many of the branches are relatively short. This is inconsistent with internal initiation at approximately 20 μm from one of the ends; therefore, initiation of DNA replication must occur also near or at the end of the molecule.

Because the structures observed in DNA undergoing its first round of replication did not appear if the infected cells were incubated with an inhibitor of DNA synthesis (FUdR), it is likely that these structures are replicative in nature. Thus, the electron microscopic evidence suggests that there are two origins of replication on Pr virus DNA and that replication occurs on circular, as well as on linear-unit size and longer-than-unit size, molecules.

2. Analysis by Restriction Endonuclease Digestion

The origins of replication of Pr virus DNA were determined by restriction enzyme digestion and the gel transfer hybridization technique. Because the DNA of the herpesviruses replicates as concatemers (3) and because replication therefore probably bears no temporal relationship to maturation, it is possible to locate the origin of replication of the virus DNA only if one labels the DNA during its first round of replication.

Fig. 6 illustrates the relative specific activity of different regions of the viral genome synthesized at various times during the first round of replication of Pr virus DNA, as determined by gel transfer hybridization. A gradient of specific activity along the genome is observed during the earliest stage of DNA replication, with the regions of greatest specific activity being near the end of the molecule bearing the inverted repeat. Thus, the main origin of replication is near (or at) that end of the molecule. As replication continues, the specific activity of the fragments, as expected, equalizes and the gradient of specific activity moves from the end of the molecule

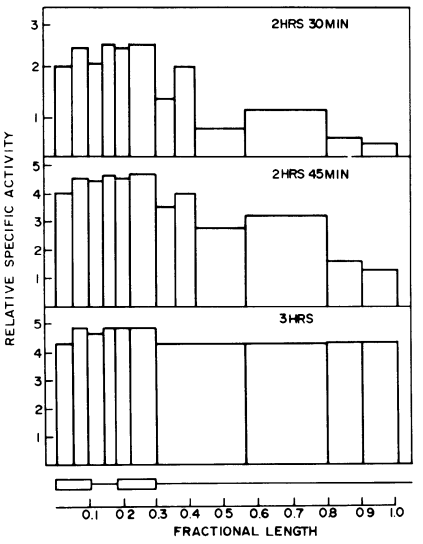

bearing the inverted repeat to the other end. The labeling of the DNA was not due to repair synthesis because most of the labeled DNA acquires a higher buoyant density when the infected cultures are incubated in the presence of BUdR. Thus, it appears that replication is initiated mainly near (or at) the end of the molecule bearing the inverted repeats and proceeds unidirectionally to the other

Fig. 6. Determination of the Origin of Replication of Pr Virus DNA. The viral DNA was labeled for various times during the first round of DNA replication. The labeled DNA was annealed to separated restriction fragments of Pr virus DNA bound to filter strips. After appropriate exposure times, autoradiograms of the filter strips were scanned, the amount of radioactive DNA that had annealed to the different DNA fragments was quantitated, and the specific activity in DNA fragments derived from different parts of the viral genome was determined.

end (8). The fact that all DNA fragments are labeled (although to a different specific activity) as early as 15 min after initiation of DNA synthesis indicates that there probably is more than one origin of replication. However, the region of the genome in which the second internal origin of replication (20 μm from one of the ends) is detected by electron microscopy is only barely preferentially labeled. It is possible, therefore, that DNA synthesis is initiated at that position on relatively few molecules (8).

STRUCTURE OF REPLICATING DNA PRESENT IN THE CELLS AT THE TIME OF EXPONENTIAL VIRUS DNA SYNTHESIS

1. Analysis by Electron Microscopy

During the phase of rapid virus DNA synthesis (4 hours post infection), the newly synthesized molecules are associated with structures which sediment with S values up to 100 times greater than those of mature viral DNA; they have been partially characterized (3). Electron microscopic observations of purified intracellular viral DNA at 4 hours post infection have revealed the presence of large "tangles" of DNA with very compact, densely aggregated centers (3) similar to those found in T4 and T7 bacteriophage-infected cells (13, 16, 20). Jacob and Roizman (18) confirmed the presence of such structures in HSV-infected cells. Longer-than-unit-size, linear viral DNA molecules were also observed (3).

The large tangles with which newly synthesized viral DNA is associated are not disrupted by treatment with ionic or nonionic detergents, nor are they affected by digestion with RNase or proteases (3). These structures are quite complex and do not lend themselves easily to analysis by electron microscopy. Consequently we have resorted to other methods in order to analyze these structures.

2. Analysis by Restriction Endonuclease Digestion

These experiments were designed to answer the following questions: (i) Is the DNA in the tangles in the form of true concatemers, i.e., is it composed of linear arrays of unit-size molecules? (ii) If so, what is the arrangement of the DNA in the concatemers (head to tail or head to head)?,

If the replicative viral DNA sedimenting with high S values is in the form of true concatemers; i.e., structures in which several viral chromosomes are linked in linear

arrays, the terminal regions of the viral genome should be linked to each other. Upon digestion with restriction enzymes, the bands consisting of the two end fragments of the viral DNA should be underrepresented and if the concatemers, as expected, consist of linear arrays of DNA molecules arranged head to tail, a new fragment consisting of the two joined end fragments should appear.

To determine the arrangement of Pr virus DNA in the concatemers, [^{32}P]-labeled concatemeric viral DNA was obtained by labeling the cells with ^{32}P up to 4 hours post-infection and by isolating the rapidly sedimenting viral DNA by centrifugation in a neutral sucrose gradient (approximately 70% of the labeled viral DNA sediments with a value > 200 S). The viral DNA was further purified by isopycnic centrifugation in CsCl and digested with restriction endonucleases.

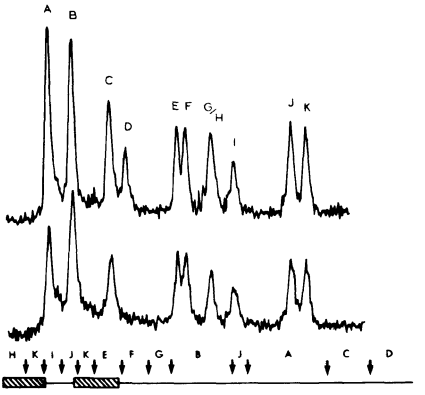

Fig. 7 shows the scan of autoradiograms of rapidly sedimenting [^{32}P]-labeled concatemeric viral (bottom panel) and of mature viral DNA (top panel) digested by Kpn-I. It is clear from a comparison of this profile with that of mature viral DNA that band D (MW, 8.5 x 10^6) and band H (MW, 5.3 x 10^6) both of which are end fragments, are underrepresented whereas band B (MW, 13.8 x 10^6) is overrepre-

Fig. 7. Profile of Restriction Fragments Generated by Kpn-I from Mature and Concatemeric Pr Virus DNA

^{32}P-labeled Pr DNA extracted from mature virions (top panel) and ^{32}P-labeled concatemeric DNA associated with rapidly sedimenting structures (bottom panel) was digested with Kpn-I, electrophoresed and autoradiographed.

sented in the concatemeric DNA. The joined end fragments (MW, $5.3 \times 10^6 + 8.4 \times 10^6 = 13.7 \times 10^6$) would have a molecular weight similar to that of fragment B. Indeed, band B in concatemeric DNA digests contains sequences complementary to fragment B as well as to the two end fragments D and H (19a). Thus, concatemeric DNA consists of arrays of unit size molecules in head-to-tail arrangements.

Several variations of the same experiments have been performed and the concatemeric DNA has been analyzed by a variety of enzymes. In all cases the concatemeric DNA was found to consist of tandem arrays of unit-size molecules in head-to-tail alignment (1a, 4a). Jacob *et al.* (17) have also arrived at similar conclusions concerning the arrangement of HSV-1 molecules in the concatemers.

3. Mechanism of Maturation of Concatemeric DNA

The maturation of Pr virus DNA from the replicative concatemeric form to molecules of genome length was examined using nine DNA^+ temperature-sensitive (ts) mutants of Pr virus, each belonging to a different complementation group. At the nonpermissive temperature, cells infected with each of the mutants synthesize concatemeric DNA. Cleavage of the concatemeric DNA to genome length viral DNA is defective in all the DNA^+ ts mutants tested, indicating that several viral gene products are involved in the DNA maturation process (Table 1 and 19a).

In none of the ts mutant-infected cells are capsids with electron dense cores (containing DNA) formed. Empty capsids with electron translucent cores are, however, formed in cells infected with six of the nine temperature-sensitive mutants; in cells infected with three of the mutants, no capsid assembly occurs. Because these three mutants are deficient both in maturation of DNA and in the assembly of viral capsids, one can conclude that maturation

Table 1. *Characteristics of DNA$^+$ ts Mutants*

Viral Mutant	DNA Synthesis	Cutting of Concatemers	Empty Capsid Formation	Full Capsid Formation	Late Polypeptide PAGE Profiles
1	1.43[a]	-	-	-	±
N	0.70	-	+	-	+
J	0.80	-	-	-	+
101	0.85	-	+	-	+
106	0.77	-	+	-	+
109	0.93	-	-	-	+
1E12-1	0.50	-	+	-	+
1E13-1	0.50	-	+	-	+
UH3	0.70	-	+	-	+

[a] Virus DNA synthesized by mutant divided by virus DNA synthesized by wild type infected cultures.

of viral DNA is dependent upon the assembly of capsids (Table 1 and 19a).

In cells infected with two of the DNA$^+$ mutants, in which empty capsids accumulate, normal maturation of viral DNA occurs after shift-down of the cells to the permissive temperature in the presence of cycloheximide (indicating that the temperature-sensitive proteins involved in DNA maturation become functional after shiftdown) and concomitant with cleavage of concatemeric DNA, full capsids with electron dense cores appear. Furthermore, the number of empty capsids decreases with a concomitant increase in the number of full capsids showing conclusively that the empty capsids are precursors to full capsids (19a).

Fig. 8 summarizes the mode of replication and maturation of Pr virus DNA.

FUNCTIONAL IDENTITY OF THE TWO ISOMERIC FORMS OF THE VIRUS DNA

Based on indirect evidence we had been led to conclude tentatively that virions containing both isomeric forms are

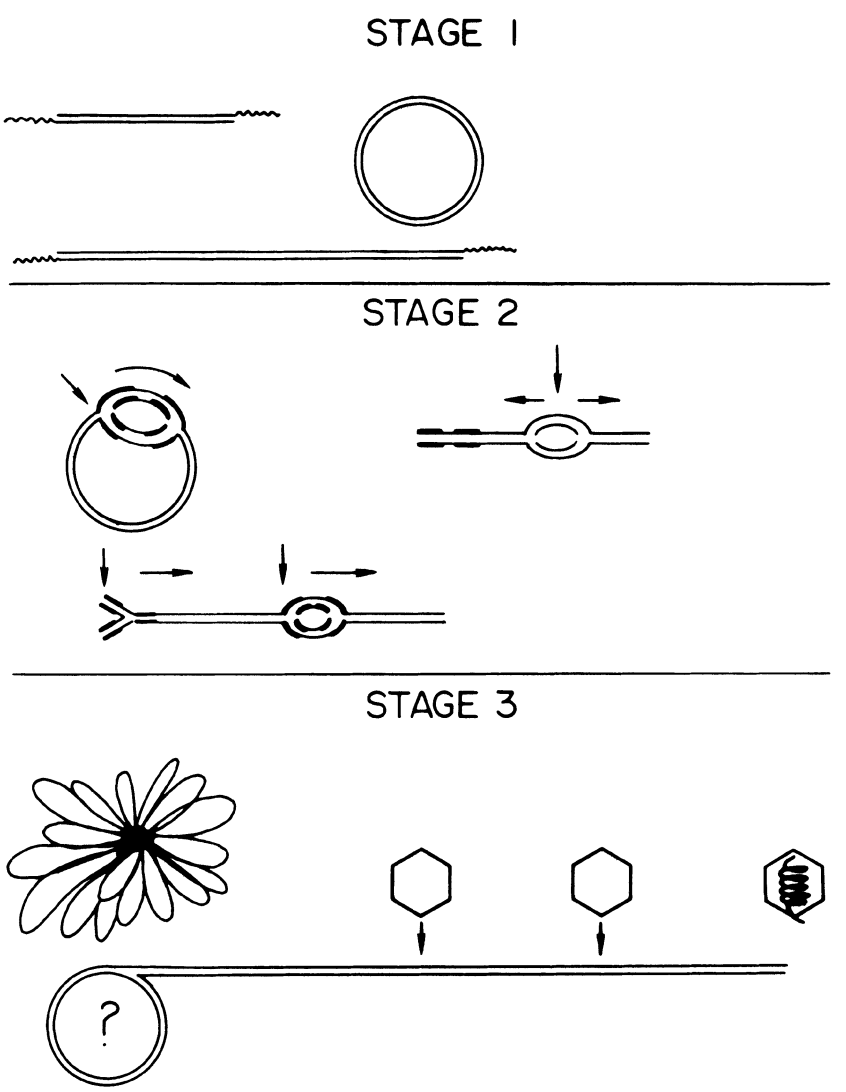

Fig. 8. Diagram of the Different Stages of Pr Virus DNA Replication

Stage I: Before replication, the DNA acquires single-stranded ends and circular concatemeric molecules are formed.

Stage II: The main origin of replication (indicated by vertical arrows) is near or at the end of the molecule which bears the inverted

repeat. Most of the replicating molecules are in circular form or in the form of small concatemers. Electron microscopic studies have indicated that a second origin of replication may exist 20 μm from one of the ends.

Stage III: Replicating DNA is in the form of tangles containing arrays of linear molecules in head-to-tail alignment. Currently available information is consistent with replication via a rolling circle. Genome size DNA is cleaved from the concatemers by a mechanism which requires the assembly of viral capsids. Concomitant with cleavage, the DNA is encapsidated into these empty capsids.

infectious. This conclusion was based on the following evidence: (i) The synthesis of immediate-early proteins (the first virus proteins synthesized during the infective process) occurs only in virus-infected cells which go on to produce a plaque (11). (ii) Immediate-early RNA is transcribed from the middle of the inverted repeat region (12), a region that is the same in both isomers of Pr virus DNA and the transcription of immediate-early RNA would therefore probably occur from either one of the isomeric forms. Taken together, these observations lead to the prediction that virions containing either isomeric form of the DNA are infectious.

Digestion of Pr virus DNA with Bgl-II restriction endonucleases gives rise to two different size fragments, D and E, which are present in one-half molar amounts each and which originate from the two different isomeric forms of the DNA (see Fig. 1). Since the presence of either the D or the E Bgl-II fragments is diagnostic for the presence in a population of DNA molecules of one of the two isomeric forms of the DNA, one can determine which isomeric form of the DNA is present in a given DNA preparation. We have used this method to determine whether virions containing only one of the two isomeric forms of the DNA or either one are infectious.

1. Analysis of the DNA Present in Virions that Adsorb to

Cells and of the DNA that Penetrates the Cell Nucleus.

To determine whether virions containing either isomeric form of the viral DNA can adsorb to the cells and whether both isomeric forms of the DNA penetrate the cell nucleus, [^{32}P]-labeled virions were purified and allowed to adsorb to susceptible cells. The DNA present in the unadsorbed virus, as well as the DNA that had either remained in the cytoplasm or had become associated with the cell nucleus, was isolated and digested with Bgl-II restriction enzyme. Table 2 summarizes the results of this experiment.

The relative distribution of the radioactive DNA in the initial virion population (column 4) in unadsorbed virus (column 5) and in the DNA that becomes cell-associated but is associated with the cytoplasmic fraction of the cells is similar. The virus DNA associated at 50 min post infection with the nucleus is virtually indistinguishible from the DNA that is associated with the total DNA population of the virions and fragments D and E are equally represented in that DNA. We conclude from these data that virions containing either isomeric forms of the DNA adsorb equally well to the cell and that their DNA is equally likely to penetrate the cell nucleus (9).

The results in Table 2 (column 7) show also that by 2 hours post infection (before the start of DNA synthesis) a large proportion of the DNA that had penetrated the cell nuclei had lost its free ends. Fragments C, D, and E (all end fragments, see Fig. 1) are considerably underrepresented and, instead, a new fragment comigrating with fragment A (which consists of the joined C and D or C and E fragments) appears. As mentioned above, Pr virus DNA, upon entering the cells, forms circles and small concatemeric molecules. The data in Table 2 show that a relatively large proportion of the DNA that had reached the nuclei undergoes this process and, more importantly, that both configurations of the DNA participate equally well in this process (8).

TABLE 2.

Analysis of Bgl-II Digests of DNA Present in Virions that Adsorbed to Cells and of DNA that Penetrated the Cell Nuclei[a]

Bgl-II band	MW	Percent of total DNA expected in fragment	Total virions	Unadsorbed virions	Adsorbed virions		
					Cytoplasm 50 min P.I.	Nuclei 50 min P.I.	Nuclei 2 hrs P.I.
A	33.0	35.5[b]	31.2[c]	30.9[c]	30.3[c]	34.3[c]	45.5[c]
B	20.5	22.0	21.5	23.1	22.8	23.8	24.2
C	18.5	19.9	19.5	20.1	21.7	19.7	13.1
D (0.5 M)	13.7	7.4	9.4	8.8	8.4	7.3	2.9
E (0.5 M)	12.3	6.6	8.8	8.0	8.0	5.7	2.5
F	8.0	8.6	9.6	9.1	8.8	9.2	11.8

[a]RK cells were infected with purified ^{32}P-labeled virions and the virions allowed to adsorb to the cells for 50 min. Unadsorbed virus was removed and the cells further incubated for various times when they were harvested, the cytoplasmic and nuclear fractions separated, the DNA extracted and digested with Bgl-II restriction endonuclease. The digest was electrophoresed in agarose gels, the gels exposed for autoradiography and the autoradiograms were scanned. The percentage of the total radioactive DNA present in each of the bands was determined by planimetry from appropriately exposed gels.

[b]Calculated from the molecular weights of each fragment.

[c]The percentage of total radioactivity in each band was determined by planimetry of scans of the autoradiograms.

2. Virions Containing Either Isomeric Form of the DNA are Infectious

At high multiplicities of infection most of the virus DNA that reaches the cell nucleus will participate in replication (6). Since both isomeric forms of the DNA do reach the cell nucleus (see Table 2), it was to be expected that both isomeric forms would replicate at high multiplicities of infection, as indeed was found to be the case.

The question whether virions which contain either isomeric form are infectious can be answered, however, only by determining which configuration of the DNA replicates under conditions of low multiplicities of infection, i.e., in the absence of helper functions which may be provided by the infectious form of the DNA. Two types of experiments were performed to answer this question.

a. Analysis of DNA that Matures First from Concatemeric DNA

In cells infected with some DNA^+ mutants (of which tsN is a representative) virus DNA concatemers will accumulate and maturation will occur shortly after shiftdown to the permissive temperature, even in the absence of DNA or of protein synthesis (19a). To determine whether both isomers of the DNA are equally represented in the DNA that matures first in cells infected with tsN at low multiplicity; i.e., whether both isomeric forms are represented in the concatemers, the experiment, the results of which are illustrated in Fig. 9, was performed.

In the virus DNA that accumulates in cells infected with tsN at the nonpermissive temperature (Fig. 9A) no free ends (fragments C, D and E, see Fig. 1 for map) can be detected. Band A is overrepresented because the joined end fragments C + D and C + E have approximately the same molecular weight as fragment A and comigrate with it. After a period of incubation of one hour at the permissive temperature, free ends appear because virus DNA has matured (Fig. 9B). Of interest is the fact that bands D and E appear in equimolar amounts, indicating that both

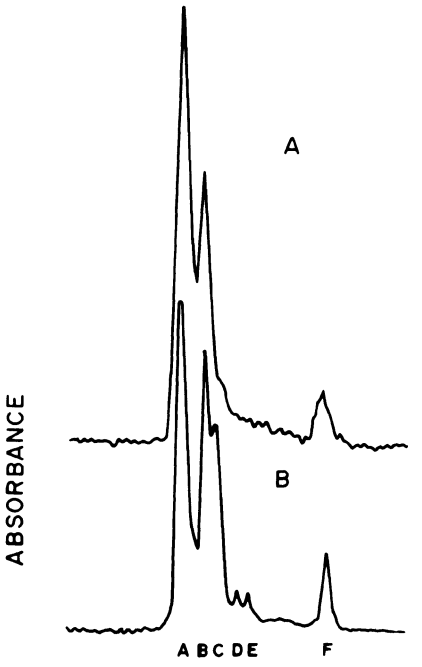

isomeric forms are represented equally in the DNA that is cleaved first from the concatemeric DNA. Thus, in populations of cells in which each was infected with a maximum of only one virus particle, DNA concatemers accumulate at the nonpermissive temperature in which both isomers of the DNA are equally represented (9). If one assumes that isomerization of the DNA occurs by a mechanism that necessitates DNA maturation; i.e., that concatemeric forms of the DNA consisting of both isomers will not be generated from a single form in the

Fig. 9. Bgl-II Restriction Enzyme Pattern of Virus DNA Accumulating at the Nonpermissive Temperature in Cells Infected with TsN at a Low Multiplicity and After Shiftdown to the Permissive Temperature. RK cells were preincubated in medium without phosphate + 5-fluorouracil (FU) (to inhibit cellular DNA synthesis) for 48 hours. The cultures were further incubated in the same medium containing ^{32}P (100 μc/ml) for 24 hours when they were infected with tsN (m.o.i., 0.01 PFU/cell) and incubated at 41° in medium without phosphate + FU + ^{32}P (100 μc/ml) up to 6 hours post infection. The medium was changed to one containing FUdR (2 μg/ml) + cycloheximide (100 μg/ml) (inhibiting practically all further synthesis of DNA or protein) and the cultures were shifted down to 32°. Part of the cultures was harvested immediately thereafter (panel A) and part further incubated at 37° for one hour (panel B). The virus DNA was extracted, purified, digested with Bgl-II restriction endonuclease, and the fragments were separated on agarose gel. The autoradiograms obtained were scanned.

absence of DNA cleavage, and that isomerization is not a direct consequence of the cleavage process, these results indicate that both isomeric forms of the DNA initiate infection and replicate. To corroborate this finding further the experiments summarized below were performed.

b. Participation of Both Isomeric Forms of Pr Virus DNA in the First Round of Replication in Cells Infected at Low Multiplicity

During the first round of replication most molecules in the process of replication are "endless," i.e., no labeled free ends appear in the replicating DNA. In some experiments, however, some labeled free ends appear (8). To determine whether only one or both isomeric forms of the DNA replicate in cells infected at low multiplicity, cells were infected with 0.01 PFU/cell (0.2 physical particles/cell) and the virus DNA was labeled with ^{32}P. The labeled virus DNA was isolated and digested with Bgl-II restriction enzyme. Labeled fragments D and E were clearly identifiable in the digest (9). That the ^{32}P that was incorporated into viral DNA because of DNA replication rather than repair synthesis was shown by the fact that, if the cells are incubated in the presence of BUdR, most of the ^{32}P incorporated into virus DNA becomes density labeled (9). We conclude from these data that in the cells infected with virions containing either isomeric form of the DNA, the first round of viral DNA replication takes place and that they both are infectious (9).

CONCLUDING REMARKS

The complex structure of the DNA of the herpesviruses raises several interesting questions: (i) How do the DNA isomers arise? (ii) When and how do the inverted repeats interact (because, to maintain their identity, they must do so at some stage)? (iii) Are the DNA isomers functionally equivalent? (iv) What are the functions of the inverted repeats?

With the conviction that the answer to questions i and ii may be obtained by examining the mode of replication of

the DNA, we have analyzed the replicative structures of Pr virus DNA during the early and late stages of infection. Indeed, with the availability of this information, these questions can now be approached experimentally. Question iii has been effectively answered; we have shown that virions containing either one of the two isomeric forms of the DNA are infectious. The last question concerning the functions of the inverted repeat is, of course, the most interesting. At present, however, it remains simply a matter for speculation.

REFERENCES

1. Ben-Porat, T., Blankenship, M. L., DeMarchi, J. M., and Kaplan, A. S. (1977). J. Virol. 22, 734-741.

1a. Ben-Porat, T., Jean, J.-H., Blankenship, M. L., and Tokazewski, S. (1978). in: Oncogenesis and Herpesviruses III, pp. 63-73.

2. Ben-Porat, T., and Kaplan, A. S. (1962). Virology 16, 261-266.

3. Ben-Porat, T., Kaplan, A. S., Stehn, B., and Rubenstein, A. S. (1976). Virology 69, 547-560.

4. Ben-Porat, T., Ladin, B., and Veach, R. A. (1980). in: Microbiology - 1980, in press.

4a. Ben-Porat, T., and Rixon, F. J. (1979). Virology 94, 61-70.

5. Ben-Porat, T., Rixon, F. J., and Blankenship, M. L. (1979). Virology 95, 285-294.

6. Ben-Porat, T., Stehn, B., and Kaplan, A. S. (1976). Virology 71, 412-422.

7. Ben-Porat, T., and Tokazewski, S. A. (1977). Virology 79, 292-301.

8. Ben-Porat, T., and Veach, R. A. (1980). Proc. Natl. Acad. Sci. U.S.A., in press.

9. Ben-Porat, T., Veach, R. A., and Ladin, B. F. (1980). Virology, submitted for publication.

10. Delius, H., and Clements, J. B. (1976). J. Gen. Virol. 33, 125-134.
11. DeMarchi, J. M., Ben-Porat, T., and Kaplan, A. S. (1979). Virology 97, 457-463.
12. Feldman, L., Rixon, F. J., Jean, J.-H., Ben-Porat, T., and Kaplan, A. S. (1979). Virology 97, 316-327.
13. Frankel, F. R. (1968). Cold Spring Harbor Symp. Quant. Biol. 33, 485-493.
14. Frenkel, N., and Roizman, B. (1972). J. Virol. 10, 565-572.
15. Hayward, G. S., Jacob, R. J., Wadsworth, S. C., and Roizman, B. (1975). Proc. Natl. Acad. Sci. U.S.A. 72, 4243-4347.
16. Huberman, J. A. (1968). Cold Spring Harbor Symp. Quant. Biol. 33, 509-524.
17. Jacob, R. J., Morse, L. S., and Roizman, B. (1979). J. Virol. 29, 448-451.
18. Jacob, R. J., and Roizman, B. (1977). J. Virol. 23, 394-411.
19. Jean, J.-H., and Ben-Porat, T. (1976). Proc. Natl. Acad. Sci. U.S.A. 73, 2674-2678.
19a. Ladin, B. F., Blankenship, M. L., and Ben-Porat, T. (1980). J. Virol., submitted for publication.
20. Paetkau, V., Langman, L., Bradley, R., Scraba, D., and Miller, R. C., Jr. (1977). J. Virol. 22, 130-141.
21. Rubenstein, A. S., and Kaplan, A. S. (1975). Virology 66, 385-392.
22. Sheldrick, P., and Berthelot, N. (1974). Cold Spring Harbor Symp. Quant. Biol. 39, 667-678.
23. Skare, J., and Summers, W. C. (1977). Virology 76, 581-595.
24. Steveley, W. S. (1977). J. Virol. 22, 232-234.
25. Wilkie, N. M. (1973). J. Gen. Virol. 21, 453-467.

ACKNOWLEDGEMENT

The work of the authors has been supported by the National Institutes of Health, U.S.A., Grant No. 10947.

20. Equine Herpesviruses: Biochemical studies on genomic structure, DI particles, oncogenic transformation and persistent infection

Dennis J. O'Callaghan*, Berch E. Henry, Joe H. Wharton, Steven A. Dauenhauer, Ralph B. Vance, John Staczek, Sally S. Atherton and Robin A. Robinson

INTRODUCTION

Three species (types) of the Herpetoviridae family are naturally occurring infectious agents of equidae and are designated equine herpesvirus (EHV) types 1, 2, and 3. Although the three viruses share some antigens and their genomes exhibit some genetic homology, they are immunologically distinct by cross neutralization tests and have virus type unique physicochemical and biological properties that are sufficient to merit separation of the triad into separate species (see 1). Like their counterparts in man, equine herpesviruses cause natural infections that vary in severity and clinical manifestations from inapparent infection to localized infections of the genitalia and eye to severe systemic infections that may involve the central nervous system (1, 2).

EHV-1 (equine abortion virus; equine rhinopneumonitis virus) is the etiologic agent of several diseases that may present as equine abortion disease, severe rhinopneumonitis, exanthema of the genitalia, or a persistent infection that may lead to paresis and encephalitis (see 1). This virus replicates in a variety of cell types with a high yield of extracellular virus and has been adapted to the Syrian hamster which has proved to be ideal as a host for the preparation of large quantities of virus and subviral components and as an in vivo model of herpesvirus replication (see 1, 3, 4, 5, 6, 7, 8).

EHV-2 (equine cytomegalovirus; ECMV) constitutes a group of slow growing viral isolates that are serologically related and are distinguishable from the classic type-1 virus. Because of its growth characteristics, its tendency to remain cell associated and its ability to cause the formation of large intranuclear inclusion and extensive cytomegaly, this virus has been called equine cytomegalo-

Y. Becker (ed), Herpesvirus DNA.

virus (9). EHV-2 has been isolated as an adventitious agent from uninoculated primary equine cell cultures as well as from both apparently normal horses and horses with widely divergent disease syndromes (1). EHV-2 is similar to cytomegaloviruses that cause diseases in other animal species including man, as the virus has a tendency to cause persistent infections of the host and little is known of the factors in the virus-host interactions that determine pathogenicity.

EHV-3 (equine coital exanthema virus) causes a true venereal disease that is characterized by vesicles, pustules, and ulcers on the genitalia of equidae and is known to be transmitted by coitus. All isolates appear to be antigenically identical and can be distinguished from EHV-1, which also may cause lesions on the genitalia, by their inability to be neutralized by antiserum against EHV-1 and by their in vitro host range which is restricted to equine cells (1, 10).

A significant amount of our basic understanding of the molecular structure and physicochemical properties of herpesviruses and of the biochemical events of herpesviruses replication has come from studies employing the equine herpesviruses (1, 4). These three viruses offer the investigator interesting experimental systems for comparative studies on the biology and biochemistry of related herpesviruses. Indeed, a variety of virus-host relationships is exhibited by the equine herpesviruses as not only do they vary in biological activities within the range of the cytocidal response (1, 9), but EHV-1 and ECMV have been shown to have oncogenic potential and the capacity to establish persistent infection (11, 12, 13, 14), and virus preparation rich in defective interfering (DI) particles have been shown to alter the events of virus replication and cytopathology *in vivo* and *in vitro* (11, 12, 15, 16, 17).

In this chapter we present in brief form our initial findings on the structure of the genomes of equine herpesviruses, document the potential of EHV-1 and ECMV to persistently infect and oncogenically transform mammalian cells, and summarize preliminary experiments designed to

identify the specific viral DNA sequences harbored by EHV-1 transformed cells, tumor tissues, and tumor cell lines.

I. MOLECULAR STRUCTURE OF THE GENOME OF EHV-1

Studies in numerous laboratories have confirmed the initial observations that the genomes of some herpesviruses are terminally redundant and contain inverted repetitions of terminal sequences that bracket regions of unique sequences (18, 19). It is now well documented that the genomes of herpes simplex viruses (HSV) contain inverted repetitions from both ends of the molecule at a position that divides the molecule into a long (L) segment and a short (S) segment and that four molecular arrangements of DNA sequences result due to the orientation of the L and S components (see 20). Recent electron microscopic investigations have shown that the genome of pseudorabies virus (PRV), a porcine herpesvirus, also consists of an S and an L component, but of these two regions of unique DNA sequences, only the S region is bracketed by a repeat that is present in complementary inverted form on each side (21, 22, 23). Thus, only the S region inverts in molecular orientation, and two isomers of this 90.6×10^6 dalton molecule exist. This molecular structure for PRV DNA has been confirmed very recently by restriction endonuclease mapping techniques (24). Interestingly, equine herpesvirus type 1 DNA has been found to have this type of structure in which a single pair of palindromic sequences bracket the S unique (Us) sequences and mediate the inversion of the S component relative to the fixed orientation of the L component (P. Sheldrick, personal communication; see 21).

As part of our overall goal to elucidate the detailed structural maps of the three equine herpesviruses so that some of the biochemical and biological properties of these viruses may be understood at the molecular level, we have initiated studies employing restriction enzyme mapping techniques to discern the structure of the EHV-1 genome. The experimental approach involved: 1) primary enzyme cleavage of unlabeled or radiolabeled (^{3}H-TdR or $^{32}PO_4$) EHV-1 DNA to ascertain the number, size, and molar concen-

tration of restriction enzyme generated fragments, 2) identification of end fragments by determining which fragments are susceptible to digestion with lambda 5'-exonuclease, and 3) ordering of the fragments by use of secondary digestion of primary fragments and Southern blot hybridization of individual $^{32}PO_4$-labeled fragments to digests of total viral DNA (20, 27, 28, 29, 30, 31).

A. *Number, Size, and Molarity of EHV-1 DNA Fragments.* The results of experiments in which radiolabeled EHV-1 DNA isolated from highly purified virions (25, 26) was cleaved with EcoR I, Bgl II, Xba I, and Bam HI restriction endonucleases and the resultant digests characterized for fragment number, size, and molarity are presented in Table 1. Cleavage of ^{32}P-labeled viral DNA with EcoR I resulted in the generation of 17 fragments ranging in molecular weight from 23.4 to 1.3×10^6 daltons. Three of these fragments, designated as G, H, and I, were found to co-migrate in a single large cluster which had a molecular weight of 6.2×10^6 daltons while all others were shown to be single fragments. Similar digestion of EHV-1 DNA with Bgl II yielded 16 DNA fragments that ranged from 24.5 to 1.0×10^6 daltons. All of these fragments were found to be single peaks with the exception of fragments G, H and fragments O, P which migrated as doublets of molecular weights 5.1×10^6 daltons and 1.0×10^6 daltons, respectively. Xba I treatment of viral DNA resulted in the generation of 15 major fragments ranging in molecular weights from 18.6×10^6 to 1.7×10^6 daltons and all of these were shown to be single bands. In addition, a cluster of minor fragments was present which possessed molecular weights of less than 1.0×10^6 daltons. Finally, cleavage of EHV-1 DNA with Bam HI gave 16 fragments of molecular weights 13.7×10^6 to 2.8×10^6 daltons, and all of these were single fragments with the exception of a 9.8×10^6 dalton doublet consisting of fragments B and C.

Calculation of the molar ratios of the various restriction enzyme fragments of EHV-1 DNA revealed the presence of 1.0 molar (M) and 0.5 M fragments (Table 1). Specifically, all bands generated by treatment with Bgl II,

Table 1

Restriction Enzyme Fragments of EHV-1 DNA:
Determination of Size, Molarity and Terminal Fragments[a]

EcoR I		Bgl II		Xba I		Bam HI	
Fragment	Molarity	Fragment	Molarity	Fragment	Molarity	Fragment	Molarity
23.4	1.0	*A 24.5	1.0	A 18.6	1.0	A 13.7	1.0
A 12.4	0.5	B 9.2	1.0	B 12.9	1.0	B,C 9.8	2.0
B 11.7	0.5	C 8.3	1.0	*C 8.7	1.0	D 6.2	1.0
D 9.1	0.5	D 7.3	1.0	D 8.2	1.0	E 5.4	1.0
E 8.4	0.5	E 6.6	1.0	E 6.1	1.0	F 4.6	1.0
F 8.2	1.0	F 6.3	1.0	F 6.0	1.0	G 4.3	1.0
G,H,I 6.2	3.0	G,H 5.1	2.0	*G 4.4	1.0	H 4.1	1.0
*J 4.9	1.0	I 4.3	1.0	H 3.8	1.0	I 4.0	1.0
K 4.2	1.0	J 3.8	1.0	I 3.4	1.0	J 3.6	1.0
L 3.9	1.0	K 2.6	1.0	J 2.9	1.0	K 3.4	1.0
M 3.4	1.0	L 2.4	1.0	K 2.6	1.0	L 3.3	1.0
N 2.7	1.0	M 1.9	1.0	L 2.5	1.0	M 3.2	1.0
O 2.2	1.0	*N 1.4	1.0	M 2.5	1.0	N 3.2	1.0
P 1.7	1.0	O,P 1.0	2.0	N 2.1	1.0	O 3.0	1.0
Q 1.3	1.0			O 1.7	1.0	P 2.8	1.0

a $^{32}PO_4$-labeled or ^{3}H-TdR labeled EHV-1 DNA isolated from purified virions (1, 25) was incubated with an excess of the appropriate restriction enzyme for a period of time sufficient to assure complete cleavage, and the resultant fragments were separated by electrophoresis in cylindrical 0.6% agarose gels at 40V for 40 hours (28). The gels were stained with ethidium bromide and examined or were sliced into 1mm fractions which were assayed for radioactivity. Digests of unlabeled or ^{3}H-labeled lambda bacteriophage DNA were employed as size markers to determine the molecular weight of the fragments. Molarity calculations were based upon these estimated molecular weights, values for the amount of radioactivity present in each fragment relative to total cpm, and a genome size of 92×10^6 daltons. Molecular weights of fragments are given in daltons $\times 10^6$.

Designates terminal fragment. Identified by digestion of purified EHV-1 DNA with an excess of lambda 5'-exonuclease for various times and determining which fragments generated by subsequent restriction were absent or reduced in size as compared to digests untreated with exonuclease.

Xba I and Bam HI were 1.0 M while those produced by cleavage with EcoR I were found to be of both types. The 0.5 M EcoR I fragments consisted of bands B, C, D and E while the remaining 12 fragments were 1.0 molar. The presence of these 0.5 M fragments in restriction enzyme digests of EHV-1 DNA was consistent with the model that the S component can invert and yield two sets of terminal fragments (21; P. Sheldrick, personal communication).

B. *EHV-1 DNA End Fragment Determination.*
Purified unlabeled EHV-1 DNA was digested with lambda 5'-exonuclease and subsequently cleaved with EcoR I, Bgl II and Xba I restriction enzymes. End fragments were judged to be those fragments which were absent or exhibited altered migration patterns on agarose gels after ethidium bromide visualization (Table 1). Experiments of this type revealed that three end fragments were present in EcoR I digests of EHV-1 DNA, two of which (D and E) were 0.5 M while the third band, H, was 1 M. The remaining three enzyme digests contained only two end fragments each, and these corresponded to Bgl II bands A and M and Xba I bands C and G (see Table 1). All of these end fragments also were found to be 1 M. These data in conjunction with those showing the generation of 0.5 M fragments further indicated that inversion of a portion of the EHV-1 genome occurs during virus replication.

C. *Secondary Digestion of EHV-1 DNA Restriction Enzyme Fragments.*
Purified ^{32}P-labeled EcoR I, Bgl II and Xba I primary fragments were isolated, cleaved with each of the other two restriction enzymes, and the molecular weights of the resultant secondary fragments were determined. The results from the six double restriction enzyme combinations are given in Tables 2-4.

D. *Southern Blot Hybridization of EHV-1 DNA Fragments.*
Experiments employing blot hybridization of ^{32}P-labeled Bam HI EHV-1 DNA fragments to unlabeled EcoR I, Bgl II and

Table 2

Double Reciprocal Digestion of EHV-1 DNA With EcoR I and Bgl II Restriction Enzymes[a]

EcoR I Fragment (M.W.x10^6)	Bgl II Cleavage Products (M.W.x10^6)	Bgl II Fragment (M.W.x10^6)	EcoR I Cleavage Products (M.W.x10^6)
A (23.4)	9.2,5.1,5.1,2.4,1.0,0.6	A (24.5)	12.4,11.7,9.1,8.4,3.4
B (12.4)	12.4	B (9.2)	9.2
C (11.7)	11.7	C (8.3)	5.2,1.8,1.3
D (9.1)	9.1	D (7.3)	5.6,1.6
E (8.4)	8.4	E (6.6)	4.4,2.2
F (8.2)	4.4,1.9,1.9	F (6.3)	3.5,2.2,0.6
G (6.2)	5.6,0.6	G (5.1)	5.1
H (6.2)	5.2,1.0	H (5.1)	5.1
I (6.2)	2.4,1.8,0.9,0.8	I (4.3)	2.4,1.9
J (4.9)	3.5,1.4	J (3.8)	2.4,1.4
K (4.2)	2.2,2.0	K (2.6)	2.0,0.6
L (3.9)	2.0,1.9	L (2.4)	2.4
M (3.4)	3.4	M (1.9)	1.9
N (2.7)	2.4,0.3	N (1.4)	1.4
O (2.2)	2.2	O (1.0)	1.0
P (1.7)	1.7	P (1.0)	1.0
Q (1.3)	1.3		

Primary restriction enzyme fragments of $^{32}PO_4$-labeled EHV-1 DNA were generated and fractionated by electrophoresis as described in Table 1. One mm slices were assayed by Cerenkov counting and slices containing each fragment were pooled and solubilized in 5 M sodium perchlorate at 60°C. After dialysis at 4°C againts TE (0.01 M Tris pH 7.4; 0.001 M EDTA) buffer, the agarose was removed by centrifugation (20,000xg for 20 min), and the DNA was extracted from the supernatant with phenol, precipitated with ethanol and dialyzed exhaustively against TE buffer. Each recovered fragment was digested with a second restricton enzyme, and the cleavage products were separate by electrophoresis in 0.7% agarose. Gels were sliced longitudinally and these sections were dried onto filter paper strips which were allowed to expose X-ray film with the aid of Cronex Lighting plus intensifying screens (Dupont Co.). Autoradiograms were also prepared of primary fragments obtained with each of the pair of restriction enzymes as well as of DNA digests generated by cleaving DNA with both enzymes (double-digests). The autoradiograms were developed, and the molecular weigh of fragments in the secondary digests and double digests were estimated by employing EHV-1 primary fragments and lambda DNA fragments as markers.

Table 3

Double Reciprocal Digestion of EHV-1 DNA With EcoR I and Xba I Restriction Enzymes[a]

EcoR I Fragment (M.W.x10^6)	Xba I Cleavage Products (M.W.x10^6)	Xba I Fragment (M.W.x10^6)	EcoR I Cleavage Products (M.W.x10^6)
A (23.4)	14.0,6.1,2.9,0.5	A (18.6)	14.0,4.6
B (12.4)	12.4	B (12.9)	12.4,11.7
C (11.7)	11.7	C (8.7)	8.7,8.4
D (9.1)	8.7	D (8.2)	6.1,2.1
E (8.4)	8.4	E (6.1)	6.1
F (8.2)	4.6,3.6	F (6.0)	3.2,1.7,0.6
G (6.2)	3.2,2.6	G (4.4)	4.3
H (6.2)	2.4,0.9,0.9,0.8,0.7	H (3.8)	3.6
I (6.2)	6.1	I (3.4)	3.4
J (4.9)	4.3,0.6	J (2.9)	2.9
K (4.2)	3.4	K (2.6)	2.6
L (3.9)	3.4	L (2.5)	2.1
M (3.4)	2.1,0.8	M (2.5)	2.5
N (2.7)	2.1,0.6	N (2.1)	2.1,1.5,0.8,0.5
O (2.2)	2.2	O (1.7)	1.3
P (1.7)	1.7		
Q (1.3)	1.3		

[a] Primary restriction enzyme fragments were generated from $^{32}PO_4$-labeled EHV-1 DNA isolated from purified virions and each fragment was isolated and cleaved with the second enzyme. The methods for these procedures and for identification of secondary fragments by autoradiographic techniques are summarized in Table 2.

Table 4

Double Reciprocal Digestion of EHV-1 DNA With Bgl II and Xba I Restriction Enzymes[a]

Bgl II Fragment ($M.W.x10^6$)	Xba I Cleavage Products ($M.W.x10^6$)	Xba I Fragment ($M.W.x10^6$)	Bgl II Cleavage Products ($M.W.x10^6$)
A (24.5)	12.9,8.7,2.1,0.8	A (18.6)	6.5,5.1,4.3,1.9,0.8
B (9.2)	6.5,2.7	B (12.9)	12.8
C (8.3)	2.5,1.8,1.7,0.9,0.8,0.7	C (8.7)	8.7
D (7.3)	4.9,2.4	D (8.2)	3.5,2.4,1.7,0.6
E (6.6)	3.8,1.9,0.8	E (6.1)	2.7,2.4,1.0
F (6.3)	3.6,2.5	F (6.0)	4.9,1.1
G (5.1)	5.1	G (4.4)	3.6,0.8
H (5.1)	2.7,2.4	H (3.8)	3.7
I (4.3)	4.3	I (3.4)	1.9,1.5
J (3.8)	3.5	J (2.9)	2.7
K (2.6)	1.6,1.0	K (2.6)	2.4
L (2.3)	2.3	L (2.5)	2.5
M (1.9)	1.9	M (2.5)	2.5
N (1.4)	0.8,0.6	N (2.1)	2.1
O (1.0)	1.0	O (1.7)	1.7
P (1.0)	1.0		

[a] The methods for the generation and isolation of $^{32}PO_4$-labeled primary restriction enzyme fragments, for the generation of secondary fragments, and for the separation of secondary fragments and their detection by autoradiography are summarized in Table 2.

Xba I digests of viral DNA were performed in order to establish the relative positions of several fragments whose locations were ambiguous. The results obtained by this method confirmed the fragment linkage as determined by double reciprocal experiments (data not shown).

E. *Cleavage Map of the EHV-1 Genome.*

The tentative cleavage map of the EHV-1 genome based on the initial series of experiments with three restriction enzymes is presented in Fig. 1, and the salient features of the structure of this genome are summarized here and discussed briefly.

The size of the genome is 92×10^6 daltons as the total molecular weight of viral DNA fragments generated with a variety of restriction endonucleases yielded this value. This molecular weight is in excellent agreement with determinations made from physicochemical and electron microscopic studies (1, 32).

The data support the model (21) that the genome consists of an L component and an S component and that two molecular forms of the molecule exist due to the ability of the S region to invert relative to the L. It was found that the four 0.5 M EcoR I fragments were located in the S region and that these fragments bracketed a 1 M EcoR I M fragment, giving the S region a maximum size of 24.2×10^6 daltons. Since the EcoR I E fragment was 8.4×10^6 in size and was 0.5 M, the site for this cleavage was judged to be located within the unique region (Us) of the S component and the size of the terminal repeats that bracket the Us region must be less than 8.4×10^6.

More information about the size of the S region can be deduced from the Xba I cleavage data. Since the cleavage site for the Xba I C fragment was in the Us region (C fragment is larger than 8.4×10^6 daltons), the site for this 1 M fragment had to lie at the same distance from the S region terminus in both isomers. Thus, the most likely explanation for the data is that Xba I cleavage sites in the S region lie 8.7×10^6 daltons from each terminus such that inversion of the region would not alter the size of

the fragments generated. The best estimate of the size of the S region from these data is that it encompasses these two 8.7×10^6 fragments as well as the internal 2.1 and 0.8×10^6 fragments and thus is approximately 20.3×10^6 daltons. The size of the terminal repeats of the S region appear to be in the range of 7 to 8×10^6 daltons as determined by electron microscopic studies (Sheldrick, personal communication), and data from these experiments confirm that these repeat sequences are less than 8.4×10^6 daltons.

Lastly, it should be mentioned that preliminary hybridization experiments with a variety of terminal fragments indicate that common sequences are present at both termini. This suggests that at some time during the replication of EHV-1 DNA the genome circularizes, and it may be during this process that the inversions of the S region occur (see 20, 33).

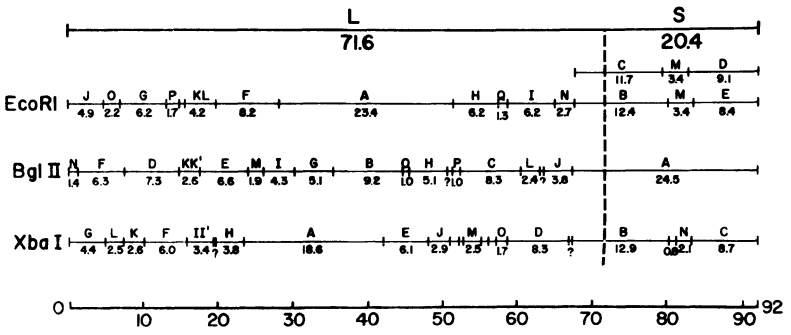

Fig. 1. cleavage map of the EHV-1 genome

II. DEFECTIVE INTERFERING PARTICLES OF EHV-1

The appearance of DI particles in populations of animal viruses passaged at high multiplicity is a well established phenomenon and has been observed for most groups of animal viruses, including the herpesviruses (see 1, 15, 16, 17, 24, 35, and 36). Recent studies in our laboratory have shown that DI particles of EHV-1 are generated by serial, high multiplicity passage both in the hamster and in cell cul-

ture and that these particles differ from standard virus in biochemical and biological activities (15, 16, 17). In both systems, the genome of DI particles has been shown to be similar in size to that of the standard virus but to have a greater buoyant density (DI = 1.724g/cm^3; std = 1.716g/cm^3) and to be genetically less complex than standard DNA (15, 17). Since interference of standard EHV-1 replication was shown to require expression of the DI genome (15) and since virus preparations rich in EHV-1 DI particles transform cells and/or initiate persistent infection (11, 12, 13; see below), it was of considerable interest to identify the DNA sequences present in the defective DNA.

Studies are now in progress to map the DNA sequences present in the genome of EHV-1 DI particles, and preliminary results will be summarized here. Since DI particles could not be separated from standard virions by rate velocity sedimentation or isopycnic banding centrifugation techniques, the initial approach to identify sequences present in the DNA of DI particles has concerned restriction enzyme analyses of total DNA isolated from purified virus preparations shown to be rich in the 1.724g/cm^3 DNA species as judged by isopycnic determinations in the analytical ultracentrifuge. As shown previously, the amount of defective DNA, the 1.724g/cm^3 DNA species, appears in a cyclic manner during serial, high multiplicity passage of EHV-1 in L-M cells and may account for more than 70% of total DNA in preparations of purified particles that are a mixture of standard virions and DI particles (15). Initial experiments in which total DNA from purified particles containing both DNA species was cleaved with restriction enzymes indicated that fragments located in the S region of the standard genome were greatly over represented, suggesting that defective DNA originates from the S region. The most meaningful information was obtained from experiments in which these mixed DNA preparations were cleaved with Bgl II, as no cleavage sites for this enzyme are present in the S region (see Fig. 1). Digestion of DNA isolated from purified particles of DI passage D15b which

contained approximately 75% defective DNA as judged by analytical ultracentrifugation techniques revealed the presence of high molecular weight DNA fragments which were larger than the $24.5x10^6$ A fragment and which were not present in any preparations of standard virus DNA (Fig. 2). Analyses of radiolabeled (^{3}HTdR or $^{32}PO_4$) viral DNA from other DNA preparations that were 65-75% defective DNA indicated that approximately 70% of the total radioactivity was present in these very large Bgl II fragments which have minimal molecular weights in the range of 28 to $36x10^6$ daltons (Fig. 3). Experiments being conducted at the time of this writing reveal that secondary digestion of these large Bgl II fragments with EcoR I yields EcoR I fragments present in the S region of the standard genome.

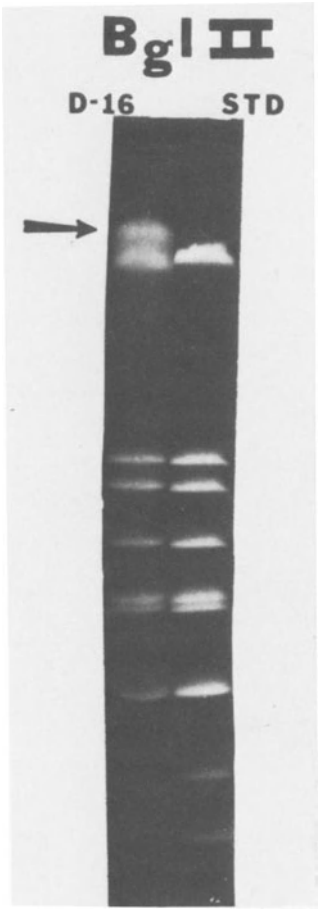

Fig. 2. Bgl II fragments of EHV-1 standard (ρ=1.716g/cm^3) and DNA isolated from DI passage D-16b shown by isopycnic banding in the analytical ultracentrifuge to be 67.7% defective DNA (ρ=1.724g/cm^3). DNAs isolated from purified viral particles were cleaved with Bgl II and the resulting fragments were separated by electrophoresis as described in Table 1. Arrow points to a family of high molecular fragments (+28-36x10^6 daltons) found only in defective DNA. Due to presence of standard DNA in mixed virus preparation of D-16b, all Bgl II fragments were present, and the number and size of these fragments are given in Table 1.

Presently, it is not known whether some L region DNA sequences are present in this defective DNA, but it is possible that this defective DNA originates entirely from the S region as has been shown some defective DNAs of HSV-1 (36, 37). However, recent analysis of the structure of defective DNA of pseudorabies virus has shown that one species of defective DNA is comprised of sequences from both the L and S segments, and experiments are now in progress to map the fine structure of this EHV-1 defective DNA.

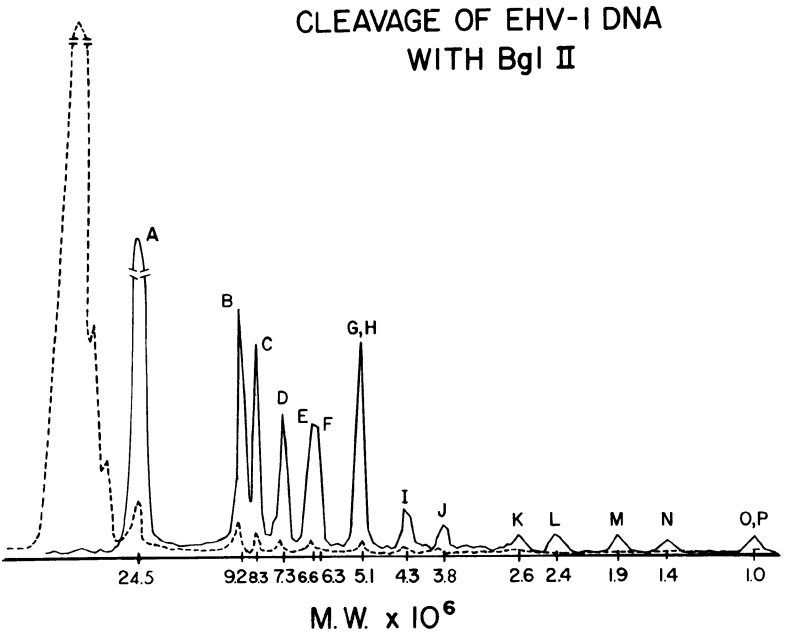

Fig. 3. Typical radioactivity profile of Bgl II fragments of ^{3}H-TdR-labeled or $^{32}PO_4$-labeled EHV-1 standard DNA (———) or DNA from passages of DI particles containing 60-75% defective DNA (----). LM cells maintained in either thymidine deficient medium (^{3}H-TdR labeling) or phosphate deficient medium ($^{32}PO_4$ labeling) were infected with standard virus (10PFU/cell) or with supernatant from a DI passage (<1 PFU/cell; 20-100 particles/cell), and at 3-6 hr postinfection ^{3}H-TdR (25μ Ci/ml, 60 Ci/mM) or $^{32}PO_4$ (25-50 μCi/ml) was added (15). At 48 hr or 96 hr, extracellular particles were purified (25) and the amount of defective DNA was measured by CsCl isopycnic banding in the analytical ultracentrifuge as described previously (15). Fragments generated by Bgl II digestion were separated in agarose gels which were fractionated, and the gel slices were solubilized and analyzed for radioactivity (Table 1). The fragments larger than the Bgl II A fragment were present only in DNA from virus containing DI particles, and the proportional of total cpm in these fragments was dependent on the amount of defective DNA.

III. PROPERTIES OF THE GENOME OF EQUINE CYTOMEGALOVIRUS

As discussed in the Introduction, equine herpesvirus type 2 possesses the biological hallmarks of a cytomegalovirus and differs from EHV-1 in several properties. Despite these biological differences, EHV-1 and ECMV appear to share DNA sequences and both have the ability to oncogenically transform primary hamster embryo cells (see below). Therefore, we have initiated studies designed to compare the genomic structures of these two herpesviruses and to determine eventually whether the DNA sequences present in EHV-1 and ECMV transformed cells are virus type unique or type shared.

Table 5

Physicochemical Properties of ECMV DNA

ρ	= 1.7165g/cm^3[a]
% G+C	= 57.7[a]
Sw^{20}	= 61.8[b]
Molecular weight	= 121.7x10^6 daltons[b]

[a] Buoyant density was determined by isopycnic banding in the Beckman Model E analytical ultracentrifuge by methods described previously (1, 15, 32). % G+C was calculated from the buoyant density using the relationship of Sueoka (38).

[b] Sedimentation coefficient was determined by rate velocity sedimentation analyses in sucrose density gradients. Molecular weight was calculated from the sedimentation coefficient using the relationship $S = 0.063\ M^{0.37}$ (39).

In initial experiments, unlabeled or ^{3}H-TdR labeled ECMV DNA, extracted from nucleocapsids or from virions released from infected equine cells, was employed in experiments to determine its physicochemical properties (Table 5). CsCl isopycnic banding of ECMV DNA in the analytical ultracentrifuge revealed that this DNA has a buoyant density of 1.7165g/cm^3 which corresponds to a guanine + cytosine content of 57.7%. These values are similar to those of EHV-1 DNA which has a density of 1.716 g/cm^3 and a G+C content of 57% (1, 15, 32). Several series of experiments employing rate velocity centrifugation in neutral sucrose gradients to estimate the size of the viral genome indicated that ECMV DNA cosedimented with ^{14}C-labeled

T4 bacteriophage DNA and sedimented more rapidly than ^{14}C-labeled EHV-1 DNA. The best average value for the sedimentation coefficient of ECMV DNA was 61.8S, which corresponded to a molecular weight of 121.7x10^6 daltons according to the equation of Doty et al. (39; see Table 5).

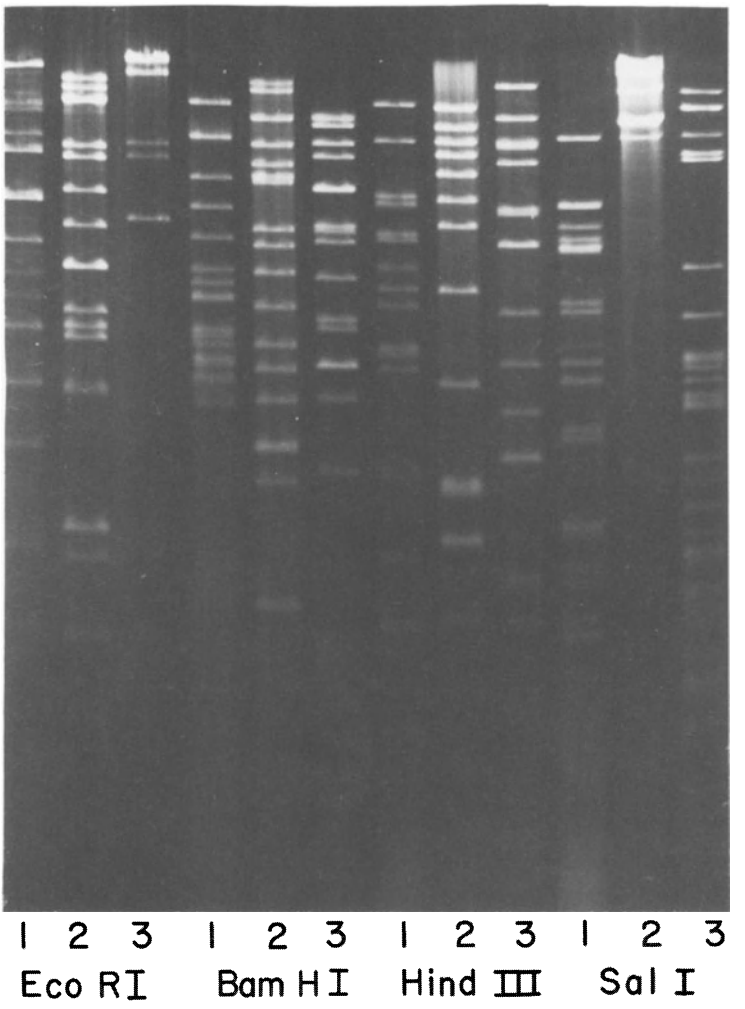

Fig. 4. Comparison of the genomes of equine herpesvirus type 1, type 2 (equine cytomegalovirus), and type 3 (equine coital exanthema virus) by restriction endonuclease digestion. Viral DNA's isolated from purified virions or nucleocapsids were digested with the enzymes listed above, and the resulting fragments were separated in a 0.6% agarose gel and stained with ethidium bromide as described in Table 1. Virus type is indicated by number.

The finding that the ECMV genome has an estimated molecular weight of 121×10^6 daltons suggested that this DNA may differ significantly in structure from the EHV-1 genome which has a molecular weight of 92×10^6 daltons (Fig. 1). Comparison of the genomes of these two equine herpesviruses by analysis with restriction endonucleases supported this possibility as the cleavage patterns of these two DNAs differed markedly (Fig. 4).

To more accurately determine the size of the equine cytomegalovirus genome, $^{32}PO_4$-labeled viral DNA was prepared and digested with restriction enzymes, and the number, size and molar concentration of the fragments were determined to estimate the molecular weight of the fragments. EcoR I fragments of bacteriophage lambda and the large molecular size Sal I fragments of bacteriophage BF23 were employed as standards (40). As can be seen (Fig. 5; Table 6), cleavage with EcoR I yielded 21 fragments.

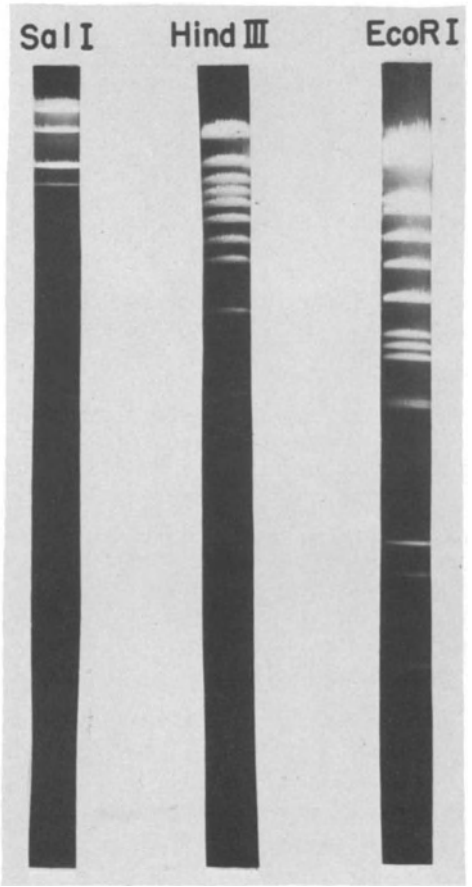

Fig. 5. Sal I, Hin d III and EcoR I fragments of ECMV DNA separated in 0.8% agarose gels and stained with ethidium bromide as described in Table 1. The size and molar concentration of these fragments are listed in Table 6.

that ranged in size from 18.2 to 0.8×10^6 daltons and gave a total molecular weight of 126×10^6 daltons. Cleavage of ECMV DNA with Sal I and Hind III generated fragments with total molecular weights of 126.1 and 126.5×10^6 daltons, respectively (Table 6).

Table 6

EcoRI, Hind III, and Sal I Digests of ECMV DNA[a]

EcoRI			Hind III			Sal I		
Fragment	M.W.[b]	[M][c]	Fragment	M.W.[b]	[M][c]	Fragment	M.W.[b]	[M][c]
A	18.2	1	A	44.0	1	A	45.5	1
B	15.8	1	B	13.8	1	B	29.0	1
C,D	13.3	2	C	12.0	1	C	17.0	1
d	12.9	0.5	D	10.7	1	D,E	11.9	2
E	9.6	1	E	9.2	1	F	10.8	1
F	8.4	1	F	7.7	1	Total = 126.1×10^6		
G	6.4	1	G	6.3	1			
H	5.3	1	H	5.4	1			
I,J	4.4	2	I	4.1	1			
K	3.7	1	J	2.8	1			
L	3.5	1	K	2.1	1			
M	3.4	1	L	2.0	1			
N	3.0	0.5	M	1.9	1			
O	2.9	0.5	N	1.7	1			
P,Q	1.7	2	O	1.6	1			
R	1.6	1	P	1.2	1			
S	1.1	1	Total = 126.5×10^6					
T	0.8	1						
Total = 126.1×10^6								

[a] *$^{32}PO_4$-labeled ECMV DNA digests were separated by electrophoresis in 0.6% or 0.8% gels which were sliced and counted by scintillation spectrometry. EcoR I fragments of ^3H-lambda DNA, Sal I fragments of BF23 bacteriophage DNA and various restriction fragments of EHV-1 DNA (see Table 1) were employed as molecular markers.*

[b] *Molecular weight (M.W.) is recorded x 10^6 daltons.*

[c] *[M] represents the molar concentration of each fragment relative to the entire genome.*

Thus, the molecular weight values from restriction enzyme analyses are in excellent agreement with the value of 122×10^6 daltons obtained by physicochemical methods. This value for the size of the equine cytomegalovirus genome exceeds that of the EHV-1 genome by one-third and is consistent with the finding that the molecular weights of cytomegalovirus DNAs are significantly greater than those of the rapidly cytocidal herpesviruses.

IV. ONCOGENIC TRANSFORMATION AND PERSISTENT INFECTION MEDIATED BY EQUINE HERPESVIRUSES.

Previous reports from our laboratory have shown that abortive infection of primary LSH hamster embryo (HE) cells with UV-irradiated EHV-1 results in oncogenic transformation (13). Recent studies have confirmed this and have shown that infection of HE cells with EHV-1 preparations enriched for DI particles may lead to a state of persistent infection characterized by a mixed cell response in which persistent infection of some cells is accompanied by oncogenic transformation (11, 12). In addition, experiments in progress indicate that infection of primary HE cultures with equine cytomegalovirus (EHV-2) at very high multiplicities of infection also may lead to oncogenic transformation concomitant with persistent infection. Here, we present some of the biological and biochemical properties of the cell lines resulting from equine herpesvirus-cell interactions in which the cytocidal response does not occur and give our initial findings on the quantitation and identification of the viral DNA sequences present in these transformed cells, tumor tissues, and tumor cell lines.

A. *Biological Properties of Cells Transformed and Persistently Infected with EHV-1 and ECMV.*

Infection of HE cells, a permissive host for EHV-1, with approximately 500 UV-irradiated standard EHV-1 particles per cell resulted in the formation of foci of cells with altered morphology and growth properties. Three independently established cell lines, designated LSEH-3, LSEH-4,

and LSEH-8, have been employed to investigate the biological and biochemical properties of EHV-1 transformation obtained by abortive infection with UV-irradiated virus (Table 7).

These cells exhibited an altered, network-like morphology marked by the predominance of fibroblastic type cells. In contrast to normal HE cells which survived only several passages in culture, LSEH-3, 4, and 8 cells became immortal, grew to high saturation density in low (0.5%) serum containing medium, formed colonies in soft agar at high plating efficiencies, and acquired resistance to superinfection with EHV-1 at multiplicities that exceeded 10 PFU/cell. These cell lines did not produce infectious virus or contain particles as determined by a variety of assays including the infectious center technique and electron microscopic examination. All attempts to induce virus by exposure to iododeoxyuridine, hydroxyurea (26), and temperature shifts have failed.

These cells have been shown to be oncogenic in both newborn and adult LSH hamsters, and inoculation with as few as 1,000 cells resulted in one hundred percent incidence of tumors. Histopathological and electron microscopic studies have identified these tumors as malignant fibrous sarcomas that readily invade the musculature and undergo metastasis to organs, especially the lungs. Cultured sarcoma cells were highly tumorigenic, and tumor type and development were not dependent on the passage of the transformed or tumor cell line employed, the age and sex of the animal, or the inoculation site. In addition, tumor tissue and cell lines established from the sarcomas did not contain infectious EHV-1 and all attempts to induce virus production were unsuccessful. However, it is important to note that more than 80% of the cells in all LSEH transformed and tumor cell lines have been shown to express structural and nonstructural EHV-1 proteins by immunofluorescent techniques employing antisera to virions and infected cell extracts. In support of these data, it has been shown that the sera of animals bearing tumors resulting from inoculation with either transformed cells

(LSEH-3, 4, 8) or tumor cells (LSEH-3T, 4T, 8T) contained EHV-1 neutralizing antibody (plaque reduction assays), indicating that viral DNA sequences are present and are expressed in these cells (see below).

Infection of primary HE cells with standard EHV-1 resulted in marked cytopathology, production of high yields of infectious virus, and the eventual lysis of these permissive cells. In contrast, infection of HE cell cultures with EHV-1 preparations containing DI particles (1, 15, 16) led to a mixed cell response in which a portion (3 to 20%) of the cells became persistently infected and released infectious virus, while other cells became oncogenically transformed (Table 7). The mixed cells became immortalized, continued to release virus and were resistant to superinfection with standard EHV-1 added at multiplicities of 1 to 20 PFU/cell.

Six cell lines (designated DI-5, 6, 7, 8, 9, and 10) established independently by infection with EHV-1 DI passage D-7b (65% defective DNA) have undergone more than seventy-five passages without loss of virus producing cells and without significant variation in the percent of cells that produce virus (Table 7). These cell lines have the properties of transformed cells as they formed colonies in soft agar, survived continued passage, grew to high saturation density, replicated in low (0.5%) serum containing medium and exhibited a short generation time. Inoculation of newborn LSH hamsters with these mixed cell cultures resulted in a fatal, fulminant hepatitis, characteristic of EHV-1 infection in the hamster (1, 3). In contrast, similar inoculation of animals that were four weeks of age or older (and therefore were immunocompetent) led to the development of malignant sarcomas at the site of inoculation and the eventual metastases of these tumors to other organs. These tumors were transplantable and tumor cell lines (DI-5T, 6T, 7T, 8T, 9T, and 10T) established from these sarcomas did not release virus or contain viral particles. However, a minimum of 60% of the cells in each tumor cell line contained viral antigens detectable by immunofluorescent techniques employing antisera to EHV-1

structural or nonstructural proteins. In addition, the sera of animals bearing tumors resulting from the inoculation with virus negative tumor cell lines contained significant levels of EHV-1 neutralizing antibody (plaque reduction assays). These findings indicate that EHV-1 DNA sequences were present and expressed in these tumor cells and that the nonproducer transformed cells were selected for in immunocompetent animals inoculated with the mixed cell population.

It should be noted that persistently infected HE cell lines have been established with other EHV-1 virus preparations rich in DI particles and that in some cases the biological properties of the persistently infected cultures varied. For example, the DI-3 cell line, which was established with EHV-1 DI passage X-16, was also comprised of both persistently infected cells (8%) and nonproducer cells, but 4-6 week old LSH hamsters inoculated with these cells underwent a runting syndrome. The animals grew poorly, failed to mature and exhibited pathological changes in the spleen characterized by extramarginal erythropoiesis and decreased cellularity in both the red and white pulp. Only 50% of these runting animals eventually developed sarcomas at the site of inoculation, and these tumors developed at a rate much slower than those derived from DI-5 to DI-10 cells. The pathogenesis and possible role of DI particles in this runting disease process are presently being investigated.

Lastly, we have recently shown that equine cytomegalovirus also has oncogenic potential and have established ECMV transformed cell lines by infecting primary HE cultures with ECMV at very high multiplicities of infection (approximately 1500 particles per cell). These cell lines, designated EC-1, 2, and 3, survived prolonged culture, grew to high saturation densities in low (0.5%) serum containing medium, formed colonies in soft agar, and caused malignant sarcomas within 4 weeks after inoculation into 4-6 week old syngeneic hamsters (Table 7). Two of these transformed cell lines, EC-2 and EC-3, have been shown to contain persistently infected cells, although only 5% or less of the

Table 7

Biological Properties of Hamster Embryo Cells Transformed By EHV-1 and ECMV

Conditions[a]	Cell Line	% Virus Producers[b] Inf.	Ctr.	EM	Resistant To Superinfection[c]	Colony Formation Soft Agar[d]	Inoculation 4wk. Hamster[e]	% Cells With Viral Antigen Transformed Cell	Tumor Cell[f]
Infection w.	LSEH-3	0		0	Yes	60%	100% Sarcoma	+80	+75
UV-irrad.	LSEH-4	0		0	Yes	78%	100% Sarcoma	+80	+75
Std. EHV-1	LSEH-8	0		0	Yes	80%	100% Sarcoma	+80	+75
Infection	DI-5	3-7		5	Yes	+50%	100% Sarcoma	+70	+60
w/EHV-1	DI-6	3-10		2	Yes	+55%	100% Sarcoma	+70	+60
DI-D7b	DI-7	5-17		5	Yes	+50%	100% Sarcoma	+70	+60
	DI-8	4-11		2	Yes	+55%	100% Sarcoma	+70	+60
	DI-9	7-8		ND[g]	Yes	+55%	100% Sarcoma	+70	+60
	DI-10	13-20		ND	Yes	+50%	100% Sarcoma	+70	+60
Infection	DI-3	8		7	Yes	ND	100% Runting	+70	ND
EHV-1 DI-X16							50% Sarcoma		
Infection	EC-1	0		0	Yes	+50%	100% Sarcoma	ND	ND
with ECMV	EC-2	2		0.5	Yes	+50%	100% Sarcoma	ND	ND
	EC-3	5		0.8	Yes	+50%	100% Sarcoma	ND	ND

a) Primary HE cultures were infected as listed: 500 particles/cell UV-irradiated EHV-1, 100 to 3,000 particles/cell EHV-1 D-7(65% defective DNA), 100 to 3,000 particles EHV-1 DI-X16(+70% defective DNA), or 1500 particles/cell ECMV. Foci of transformed cells were picked and maintained in culture. b) Percent of cells producing virus was measured by 1) infectious center assay in which test cells were plated onto monolayer of permissive LM cell or equine dermis cell and 2) electron microscopic examination of thin sections of transformed cells. c) Cells at different passages were tested for resistance to superinfection with exogenous, homologous virus at multiplicities of 1 to 20 PFU/cell; EC cells were resistant to both EHV-1 and ECMV. d) Minimal percent of cells capable of forming colonies in soft agar. e) Subcutaneous inoculation of 4-6 week old LSH hamsters with 1 to 5×10^6 cells. f) Cells on coverslips were fixed with acetone or methanol and reacted with either hamster antisera to EHV-1 virions or antisera (absorbed with 3×10^{11} virions per ml) to extracts of HE infected cells. The cells were rinsed, then were reacted with fluorescein conjugated rabbit anti-hamster immunoglobulin, dried, and examined in a Leitz Ortholux fluorescent microscope. Tumor cell lines established from tumor tissues expressed viral antigens, but all tumor cell lines were virus non-producers. g) ND = not done; these studies are in progress.

total cells in these cultures released infectious virus or contained viral particles. Of interest were the findings that tumor cell lines (EC-1T, 2T, 3T) did not release or contain virus and that all lines of transformed cells and tumor cells were resistant to superinfection with either ECMV or EHV-1. The biochemical properties of these transformed and tumor cell lines are now being investigated.

It should be noted that secondary hamster fibroblast cultures infected at multiplicities of 10 PFU/cell with ECMV failed to exhibit cytopathologic effects and support virus replication. Therefore, the experiments described in this section support the idea that altered herpesvirus-cell interactions such as abortive infection obtained with UV-irradiated EHV-1, infection with EHV-1 rich in DI particles, or ECMV infection of semi-permissive cells under conditions of very high multiplicity may result in cellular responses that lead to establishment of persistent infection and oncogenic transformation.

B. *Detection, Quantitation and Identification of Viral DNA Sequences in EHV-1 Transformed Cells, Tumor Tissues, and Tumor Cell Lines.*

To examine the role of viral DNA in the initiation and maintenance of oncogenic transformation of mammalian cells, the amount and the percent of EHV-1 genomic sequences in the LSEH and DI transformed cells, tumor tissues, and tumor cell lines were determined by DNA-DNA hybridization analyses. Reassociation reactions were designed to allow ^{32}P-labeled EHV-1 DNA to reanneal in the presence of 50 molar excess LSEH or DI cell DNA under stringent hybridization conditions that could detect a single copy of unique viral DNA sequences only 2.8 kilobases (Kb) in size. As shown in Table 8, detectable amounts of viral DNA have been found in all cells assayed to date. LSEH transformed and tumor cells contained only a small percentage of the genome in very small amounts. The DI-transformed cells, which include persistently infected producer cells (Table 7), contained numerous copies of the entire EHV-1 genome, whereas the virus negative DI tumor cells (DI-5T, 7T, 8T,

Table 8

Quantitation of EHV-1 DNA Sequences in EHV-1 Transformed Cells, Tumor Tissues, and Tumor Cells[a]

Cellular DNA	Passage No.	N	% Viral Genome	Genome Equivalents
HEF	2-4	50	0.0	0.0
LSEH-3	20-25	50	3.8	1.0
LSEH-4	20-25	50	20.9	2.2
LSEH-8	20-25	50	3.3	0.3
LSEH-3T	1-5	50	2.9	1.2
LSEH-4T	1-5	50	5.1	2.5
LSEH-4T	Tumor Tissue	50	12.2	4.0
LSEH-8T	1-5	50	2.2	3.0
LSEH-8T	Tumor Tissue	50	2.5	3.0
DI-5	20-25	0.16	100	25.3
DI-8	20-25	0.16	100	26.6
DI-10	20-25	0.16	100	43.7
DI-5T	1-5	50	42.2	2.2
DI-7T	1-5	50	44.2	2.5
DI-8T	1-5	50	42.6	3.1
DI-10T	1-5	50	56.7	3.8

[a] EHV-1 DNA (0.5μg) was labeled to high specific activity ($+10^8$ cpm/μg) with α-^{32}P dCTP by in vitro nick translation (41), separated from free nucleotides by passage through Sephadex G-50, extracted with phenol, precipitated with ethanol, resuspended in 0.4 NaOH, sheered to 500-600 base length fragments by boiling for 20 min., neutralized with 3M Tris-HCl (pH 3), and dialyzed against several changes of hybridization buffer (0.1M Tris-HCl, pH 8.1, 25mM EDTA, 1M NaCl). Cell DNAs were extracted with phenol once and chloroform-butanol twice from pronase-digested cell pellets, precipitated with ethanol, dissolved in hybridization buffer supplemented with 0.3M NaOH, heated at 100°C for 20 min to depolymerize RNA, neutralized, dialysed extensively against hybridization buffer, and adjusted to a final concentration of 6.25 mg/ml in 20% formamide. Hybridization reactions containing viral probe DNA and cell DNAs at a molar ratio (N) of 50 to 1 were sealed in capillary tubes, denatured at 117°C for 10 min., and allowed to reanneal at 63°C for at least 360 hrs. Radioactive double-and-single-stranded DNAs were separated by hydroxyapatite chromatography, and TCA precipitable counts were measured by liquid scintillation spectroscopy. Reassociation kinetics were plotted and quantitated by methods previously described (42).

and 10T) harbored less than 57% of the genome in amounts of only a few genome equivalents per cell. Additional hybridization analyses of both LSEH transformed cells and DI tumor cells maintained for numerous passages indicated that both the percent of the EHV-1 genome and the number of copies of viral DNA per cell were reduced with passage of these cells in vitro. To identify the DNA sequences harbored in these cells and to ascertain whether the retention of viral DNA sequences was a selective or random process, experiments employing the Southern blot hybridization technique (31) were initiated.

In the first series of experiments, EHV-1 DNA fragments ranging in size from 1.8 to 13.9 Kb and representing map positions 0.28 to 0.48 and 0.72 to 1.0 were radiolabeled (41) and used as probes for hybridization to blots of DNA from LSEH and DI transformed and tumor cells. The restriction enzyme digests of cell DNAs were fractionated by electrophoresis in preparative agarose gels that allowed 250 μg of restricted DNA to be employed per well. The data of these initial studies indicated that an EHV-1 DNA sequence mapping from 0.33 to 0.38 was common to all seven cellular DNAs analyzed (Table 9). Interestingly, none of the LSEH transformed and tumor cells established by transformation with UV-irradiated standard virus contained sequences from the S region, whereas the DI transformed and tumor cells, which were established using virus rich in DI particles, contained all sequences from the S region as well as sequences from the L region. It remains to be determined whether these S region sequences will be lost with continued passage of the DI-tumor cells which are not virus producers.

The analyses of the LSEH-4 cells at different levels of passage confirmed that some viral DNA sequences were lost from EHV-1 transformed cells during passage, and the identification of a common region of the viral genome in all these cells suggests that retention of viral DNA sequences is a selective process. However, it will be necessary to map the viral sequences in the DNAs from all the other EHV-1 transformed and tumor cell lines before

Table 9

Identification of Viral DNA Sequences in EHV-1 Transformed and Tumor Cells by Blot Hybridization with Selected ^{32}P-labeled Bgl II and EcoR I Viral Fragments[a]

		L Region Fragments										S Region Fragments				
	^{32}P-Bgl II	B	D	G	H	I	J	O	P			A				
	^{32}P-EcoR I									A	F	G	N	B	C	D	E	M
	Passage	EHV-1 DNA Sequences Detected in Cell DNA																
Cell DNA	Number	Bgl II								EcoR I				Bgl II	EcoR I			
LSEH-4	25-28	B	D	G		I				A	F	G		none	none			
LSEH-4	66		D	G		I				A	F			none	none			
LSEH-4	125			G		I				A				none	none			
LSEH-4T	1-5			G		I				A				none	none			
DI-5	26-28	B	D	G	H	I	J	O	P	A	F	G	N	A	B	C	D	E M
DI-5T	1-5	B		G						A				A	B	C	D	E M
DI-10T	1-5	B		G			J			A			N	A	B	C	D	E M

a) Cell DNAs were digested with EcoR I and Bgl II overnight, and the fragments separated by electrophoresis in 0.8% agarose gels were transferred to nitrocellulose sheets which were dried and incubated for 6-18 hr at 41°C in annealing mix (3xSSC, 50% formamide, 200 µg/ml yeast RNA, 20 µg/ml denatured E. coli DNA), supplemented with 0.027% each of bovine serum albumin, polyvinylpyrrolidone, and Ficoll. Blot hybridization with Bgl II and EcoR I fragments of EHV-1 DNA labeled by nick translation with α-^{32}P-dCTP (41) was performed by saturating filters with annealing mix containing 1x10^6 cpm/ml of viral probes. After incubation at 41°C for 48 hr. unannealed probe DNA was removed from filters by several washes with 2xSSC at 20°C followed by repeated washes for 24 hrs in 6xSSC, 0.5% SDS at 68°C. Final washes of filters were in 2xSSC at 20°C. Filters were exposed for 1-10 days at -70°C to Kodak RP-Royal X-omat film in the presence of a Dupont Cronex "Lighting" plus intensifying screen.

confirming this hypothesis. Indeed, it will be of special interest to ascertain whether viral DNA sequences and proteins are present in the ECMV transformed and tumor cells and whether such ECMV sequences and gene products are those shared by these two viruses and possibly by cells transformed by equine herpesviruses. Experiments designed to answer these basic questions are being carried out by employing a) RPC-5 column chromatography of milligram amounts of cell DNAs to enrich for regions of host DNA containing integrated viral DNA, b) plasmid vectors to clone viral DNA sequences to provide quantities of DNA sufficient for mapping studies and for selection of viral transcripts in these cells and c) techniques for in situ radiolabeling of cell membrane proteins to allow the identification of viral polypeptides expressed in EHV transformation.

Acknowledgments

Support for these investigations was obtained from Research Grant AI-02032 and General Medical Research Support Grant S-507-RR-05386 awarded by the National Institutes of Health and Research Grant PCM-7822700 awarded by the National Science Foundation. We acknowledge Postdoctoral Fellow Awards from the American Cancer Society and National Cancer Institute to JHW, a Clinical Postdoctoral Fellowship to RBV, and two research travel awards to BEH from the Southern Regional Education Board.

We thank Dr. Gary Hayward for helpful discussions and collaboration in mapping studies, Ms. Linda Hill for technical assistance, Ms. Nan Mansfield for preparation of photographs and Ms. Cheryl Tucker for secretarial help.

References

1. O'Callaghan, D.J., G.P. Allen, and C.C. Randall. 1978. Structure and Replication of the equine herpesviruses pp 1-31. in Equine Infectious Diseases IV. ed. J. Bryans and H. Gerber. Veterinary Publications Inc., Princeton, New Jersey.

2. Gutekunst, D.E., W.A. Malmquist, and C.S. Becvar. 1978. Antigenic relatedness of equine herpesvirus types 1 and 3. Arch. Virol. 56:33-45.

3. O'Callaghan, R.J., C.C. Randall, and G.A. Gentry. 1972. Herpesvirus replication in vivo. Virology 49:784-793.

4. O'Callaghan, D.J. and C.C. Randall. 1976. Molecular anatomy of herpesviruses: recent studies. Prog. Med. Virol. 22:152-210.

5. O'Callaghan, D.J., H.W. Rogers, and C.C. Randall. 1972. Amino acid composition of equine abortion (herpes) virus. Virology 47:842-844.

6. Kemp, M.C., M.L. Perdue, H.W. Rogers, D.J. O'Callaghan and C.C. Randall. 1974. Structural polypeptides of the hamster strain of equine herpesvirus type 1: Products associated with purification. Virology 61:361-375.

7. O'Callaghan, D.J., M.C. Kemp, and C.C. Randall. 1977. Properties of nucleocapsids isolated from an in vivo herpesvirus infection. J. Gen. Virol. 37:585-594.

8. Kemp, M.C., J.C. Cohen, D.J. O'Callaghan and C.C. Randall. 1975. Equine herpesvirus induced alterations in nuclear RNA and DNA polymerase activities. Virology 68: 467-482.

9. Wharton, J.H., B.E. Henry, and D.J. O'Callaghan. 1978. Biological and physicochemical properties of equine cytomegalovirus. Proc. Ann. Meeting Amer. Soc. Microbiology, Las Vegas, Nev.

10. Bryans, J.T. and G.P. Allen. 1973. In vitro and in vivo studies of equine coital exanthema pp 322-336. Proc. 3rd Int. Conf. Eq. Inf. Dis., Paris. Karger, Basel.

11. Robinson, R.A., B.E. Henry, and R.B. Vance, and D.J. O'Callaghan. 1979. Herpesvirus oncogenesis: Properties of cells transformed by inactivated virus or defective interfering particles. Proc. Amer. Assoc. Cancer Res. 20: 139.

12. O'Callaghan, D.J., B.E. Henry, R.B. Vance, C.C. Randall, and R.R. Robinson. 1978. Oncogenic transformation with standard and defective interfering particles of equine herpesvirus type 1. Proc. Int. Herpesvirus Workshop, Cambridge, England.

13. O'Callaghan, D.J., C.C. Randall, R. Duff, G. Allen, J. Jackson, and J.W. Blasecki. 1977. Oncogenic transformation of inbred hamster cells by equine herpesvirus type 1. Proc. 3rd Int. Symposium on Oncogenesis and Herpesviruses, Cambridge, Mass.

14. Allen, G.P., D.J. O'Callaghan, and C.C. Randall. 1978. Oncogenic transformation of nonpermissive murine cells by viable equine herpesvirus type 1 (EHV-1) and EHV-1 DNA. pp 509-516. in Oncogenesis and Herpesviruses III ed. G. de The, W. Henle, and F. Rapp. Int. Agency for Research on Cancer, Lyon, France.

15. Henry, B.E., W.W. Newcomb, and D.J. O'Callaghan. 1979. Biological and biochemical properties of defective interfering (DI) particles of equine herpesvirus type 1. Virology 92:495-506.

16. Henry, B.E., W.W. Newcomb, and D.J. O'Callaghan. 1980. Alterations in viral protein synthesis and capsid production in infection with DI particles of herpesvirus. J. Gen. Virol. in press.

17. Campbell, D.E., M.C. Kemp, M.L. Perdue, C.C. Randall, and G.A. Gentry. 1976. Equine herpesvirus in vivo: Cyclic production of a DNA density variant with repetitive sequences. Virology 69:737-750.

18. Sheldrick, P. and N. Berthelot. 1974. Inverted repetitions in the chromosome of herpes simplex virus. Cold Spring Harbor Symp. Quant. Biol. 39:667-678.

19. Grafstrom, R.H., J.C. Alwine, W.L. Steinhart, and C.W. Hiel. 1974. Terminal repititions in herpes simplex virus type 1 DNA. Cold Spring Harbor Symp. Quant. Biol. 39:679-681.

20. Roizman, B. 1979. The structure and isomerization of herpes simplex virus genome. Cell 16:481-494.

21. Sheldrick, P. and N. Berthelot, unpublished. Cited in Honess, R.W. and D.H. Watson. 1977. Unity and diversity in the herpesviruses. J. Gen. Virol. 37:15-37.

22. Stevely, W.S. 1977. Inverted repetition in the chromosome of pseudorabies virus. J. Virol. 22:232-234.

23. Ben-Porat, T., F.J. Rixon, and M.L. Blankenship. 1979. Analysis of the structure of the genome of pseudorabies virus. Virology 95:285-294.

24. Rixon, F. and T. Ben-Porat. 1979. Structural evolution of the DNA of pseudorabies-defective viral particles. Virology 97:151-163.

25. Perdue, M.L., M.C. Kemp, C.C. Randall, and D.J. O'Callaghan. 1974. Studies of the molecular anatomy of the L-M cell strain of equine herpesvirus type 1. Proteins of the nucleocapsid and intact virion. Virology 59: 201-216.

26. Cohen, J.C., M.L. Perdue, C.C. Randall, and D.J. O'Callaghan. 1975. Replication of equine herpesvirus type 1: Resistance to hydroxyurea. Virology 67:56-67.

27. Clements, J.B., R. Cortini, and N.M. Wilkie. 1976. Analysis of herpesvirus DNA substructure by means of restriction endonucleases. J. Gen. Virol. 30:243-256.

28. Hayward, G.S., R.J. Jacob, S.C. Wadsworth, and B. Roizman. 1975. Anatomy of herpes simplex virus DNA: evidence for four populations of molecules that differ in the relative orientations of their long and short components. Proc. Nat. Acad. Sci. U.S.A. 72:4243-4247.

29. Skare, J. and W.C. Summers. 1977. Structure and function of herpesvirus genomes. II. EcoR I, Xba I, and Hind III endonuclease cleavage sites on herpes simplex virus type 1 DNA. Virology 76:581-595.

30. Wilkie, N.M. 1976. Physical maps for herpes simplex virus type 1 DNA for restriction endonucleases Hind III, Hpa I and Xba d. J. Virol. 20:222-233.

31. Southern, E.M. 1975. Detection of specific sequences among DNA fragments separated by gel electrophoresis. J. Mol. Biol. 98:503-517.

32. Soehner, R.L., G.A. Gentry, and C.C. Randall. 1965. Some physicochemical characteristics of equine abortion virus nucleic acid. Virology 26:395-405.

33. Jean, J.H. and T. Ben-Porat. 1976. Appearance in vivo of single-stranded complementary ends on herpesvirus DNA. Proc. Nat. Acad. Sci. U.S.A. 73:2674-2678.

34. Huang, A.S. 1973. Defective interfering viruses. Annu. Rev. Microbiol. 27:101-117.

35. Frenkel, N., R.J. Jacob, R.W. Honess, G.S. Hayward, H. Locker and B. Roizman. 1975. Anatomy of herpes simplex virus DNA: III. Characterization of defective DNA molecules and biological properties of virus populations containing them. J. Virol. 16:153-167.

36. Frenkel, N., H. Locker, W. Batterson, G.S. Hayward, and B. Roizman. 1976. Anatomy of herpes simplex virus DNA: VI Defective DNA originates from the S component. J. Virol. 20:527-531.

37. Graham, R.J., Z. Bengeli, and G.F. Vande Woude. 1978. Physical map of the origin of defective DNA in herpes simplex virus type 1 DNA. J. Virol. 25:878-887.

38. Sueoka, N. 1961. Variation and heterogenity of base composition of deoxyribonucleic acids: A compilation of old and new data. J. Mol. Biol. 3:31-40.

39. Doty, P., B.B. McGill, and S.A. Rice. 1958. The properties of sonic fragments of deoxyribose nucleic acid. Proc. Nat. Acad. Sci. U.S.A. 44:432-438.

40. Lange-Gustafson, B. and M. Rhoades. 1979. Physical map of bacteriophage BF23 DNA: Restriction enzyme analysis. J. Virol. 30:923-928.

41. Maniatis, T., A. Jeffrey, and D.G. Kleid. 1972. Nucleotide sequence of the rightward operator of phage lambda. Proc. Nat. Acad. Sci. U.S.A. 72:1184-1188.

42. Fujinaga, K., K. Sekikawa, H. Yamazaki, and M. Green. 1975. Analysis of multiple viral genome fragments in adenovirus 7-transformed hamster cells. Cold Spring Harbor Symp. Quant. Biol. 39:633-636.

21. Organization of integrated herpesvirus DNA Sequences in Equine herpesvirus type 1 transformed and tumor cell lines

Robin A. Robinson and Dennis J. O'Callaghan

INTRODUCTION

With the developments of the techniques of restriction endonuclease mapping, *in vitro* labeling of DNA to high specific activities by nick-translation, and Southern blot hybridization, the detection of specific viral genes integrated into cellular genomes and the elucidation of integration sites and of the arrangement and orientation of integrated viral sequences to each other and to flanking host sequences have become feasible for papovavirus, retrovirus and adenovirus tumor systems. Utilizing these powerful molecular tools, Ketner and Kelly (1) and Botchan et al. (2) have examined the nature and arrangement of SV40 DNA sequences integrated into mouse and rat cell genomes. Neither cellular nor viral DNA sequences were concluded from these studies to be specific for integration of SV40 DNA. Subsequently, similar studies characterized both integrated and free viral sequences in polyoma and BK virus transformed cells (3, 4, 5). Numerous findings of specific retrovirus proviral sequences of both endogenous and exogenous origin and of their molecular organization in eukaryotic genomes have accumulated in recent years using the Southern blotting procedure. These studies have led to the identification of the *src* gene and its gene product (see 6). In addition, mapping by these techniques have permitted the examination of adenovirus sequences integrated in adenovirus transformed hamster and rat cells (7, 8).

Studies using these methods to detect viral sequences and to determine the integration patterns within various herpesvirus transformed cells, tumor tissues, and tumor cells have been stymied by the overwhelming genetic complexity and molecular size of herpesvirus genomes. Hence, elucidation of herpesvirus oncogenic transforming genes by transfection of mammalian cells with specific herpesvirus

Y. Becker (ed), Herpesvirus DNA.

DNA restriction fragments isolated from agarose gels has superceded direct efforts to examine integration of herpesvirus sequences in transformed cells. These transfection studies have revealed that HSV-1 sequences with map units 0.30 to 0.45 (9) and that HSV-2 (333 strain) sequences with map units 0.584 to 0.628 (10) have morphological transforming activity. Independently, Jariwalla et al. (11) have reported that tumorigenic transformation was induced by a HSV-2 (S-1 strain) sequence mapping between 0.43 and 0.58 map coordinates on the physical map of strain 333 of HSV-2 DNA.

The emergence of conflicting data from the HSV-2 DNA transfection experiments, the failure to date to obtain oncogenically transformed cell lines using HSV fragments in transfection experiments, the presence of contaminating sequences in restriction fragments isolated from gels, and the limited information obtained in transfection studies have convinced us that using specific restriction endonucleases that cleave at limited sites in the cellular genome together with blot hybridization is a more direct approach to identify viral and host DNA sequences involved in herpesvirus oncogenesis. The availability of numerous well-characterized equine herpesvirus type 1 (EHV-1) transformed and tumor cell lines established in our laboratory (12, 13, 14) and the construction of libraries of specific EHV-1 DNA restriction fragments cloned into plasmids and bacteriophage DNAs have provided excellent reagents for studying the role(s) that specific herpesvirus sequences, integrated or free forms, play during oncogenic transformation.

In this report, we have employed restriction endonucleases (EcoRl and Bgl II) together with blot hybridization using a library of 18 selected EHV-1 cloned restriction fragment probes to analyze the herpesvirus sequences present in hamster embryo cells (HEF) oncogenically transformed by UV-irradiated EHV-1 and in progeny tumor cells. Results from these studies indicate that a specific region of the EHV-1 genome with map coordinates 0.32 to 0.38 is conserved in all of the EHV-1 transformed and tumor cells

examined to date. We conclude that specific EHV-1 DNA sequences can integrate during transformation at multiple sites within the HEF cell genome to render the cell oncogenic.

I. EXPERIMENTAL APPROACH AND RECONSTRUCTION EXPERIMENTS. A diagrammatic representation of our rationale in these experiments is outlined in Figure 1. EHV-1 transformed or tumor cell DNA, containing subgenomic fragments of the EHV-1 genome, was digested to completion with a sequence-specific restriction endonuclease. The digestion products were fractionated according to size by electrophoresis in agarose gels, and the DNA was alkali denatured and neutralized *in situ* followed by transfer to nitrocellulose filter paper (15). The fragments of restricted cellular DNA that contain viral DNA sequences were detected by hybridization with specific ^{32}P-labeled cloned EHV-1 DNA restriction fragments.

DNA-DNA reassociation analyses of cell DNAs from EHV-1 transformed cells, tumor tissues, and tumor cells showed that many of these cell lines contained only a few copies of subgenomic EHV-1 DNA sequences which were less than 3×10^6 daltons in size (12). Therefore, it was necessary to determine the maximum size probe that could detect at least a single copy of viral sequences 2×10^6 daltons in size within 20-25 µg of cellular DNA. Reconstruction experiments were carried out under conditions described in Table 1. Briefly, 25 µg aliquots of LSH normal hamster DNA, digested with restriction endonucleases, were mixed with 0.31 copies/cell of an EHV-1 DNA sequence (specific restriction fragment) of approximately 2.0×10^6 daltons in size and electrophoresed in 0.7% agarose gels. The specific viral DNA fragment to be detected was hybridized with various ^{32}P-labeled EHV-1 cloned DNA restriction fragments which contained sequences complementary to those of the fragment to be detected. The results of these experiments are presented in an autoradiogram in Figure 2. After a four-day exposure of x-ray film to the hybridized filter, viral sequences were readily detected with probes

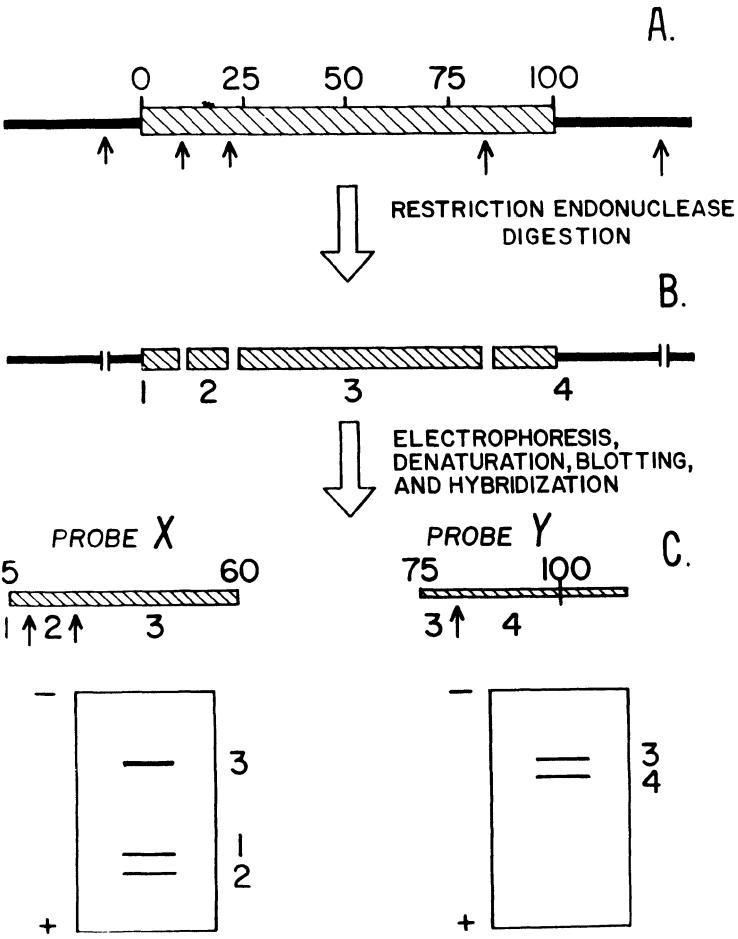

Fig. 1. A schematic representation of restriction enzyme analysis of integrated viral DNA by blot hybridization. (A) Transformed cell DNA contains host sequences (——) and inserted viral DNA (▨). Arrows indicate the sites of restriction endonuclease cleavage in both host and viral sequences. (B) Restriction endonuclease digestion of this cell DNA produces fragments of DNA, two of which (2 and 3) contain only viral sequences. (C) After electrophoresis and blotting of the digested DNA followed by hybridization to a specific ^{32}P-labeled viral DNA (probes x and y), detection of DNA fragments containing viral sequences only and viral-cellular joint sequences is visualized by autoradiography of the exposed x-ray film. Alignment of detectable fragments corresponds to the location of restriction endonuclease sites in the host cell DNA.

Table 1

Probe Specificity Reconstruction Experiment

^{32}P-EHV-1 DNA Fragment Probes[a]	Blotted DNAs[b]	Homology[c]
1. Bgl II - F (6.3×10^6; .015-.084)	Xba I - L (2.5×10^6; .048-.075)	39.7%
2. Bgl II - C (8.3×10^6; .570-.660)	Xba I - O (1.7×10^6; .622-.640)	21.3%
3. Bam HI - A (13.7×10^6; .486-.635)	Xba I - O (1.7×10^6; .622-.640)	12.4%
4. Xba I - A (18.6×10^6; .256-.458)	Bgl II - M (1.9×10^6; .263-.284)	10.2%
5. Bgl II - A (24.5×10^6; .734-1.00)	Xba I - N (2.1×10^6; .887-.910)	8.6%
6. EHV-1 genomic DNA (92.0×10^6)	Xba I - N (2.1×10^6; .887-.910)	2.3%
7. EHV-1 Bgl II DNA fragments (MW markers)		

[a] Viral DNA probes were isolated from cloned restriction fragment DNA preparations. These DNAs were labeled to high specific activities (1×10^8 cpm/μg) by *in vitro* nick-translation as described previously (16). Molecular weights in daltons and map coordinates are enclosed in brackets.

[b] Viral DNA fragments to be detected with these probes in blot hybridization experiments were prepared from cloned EHV-1 DNA restriction fragments.

[c] The amounts of sequence homology between the viral DNA to be detected and the probe are listed in this column.

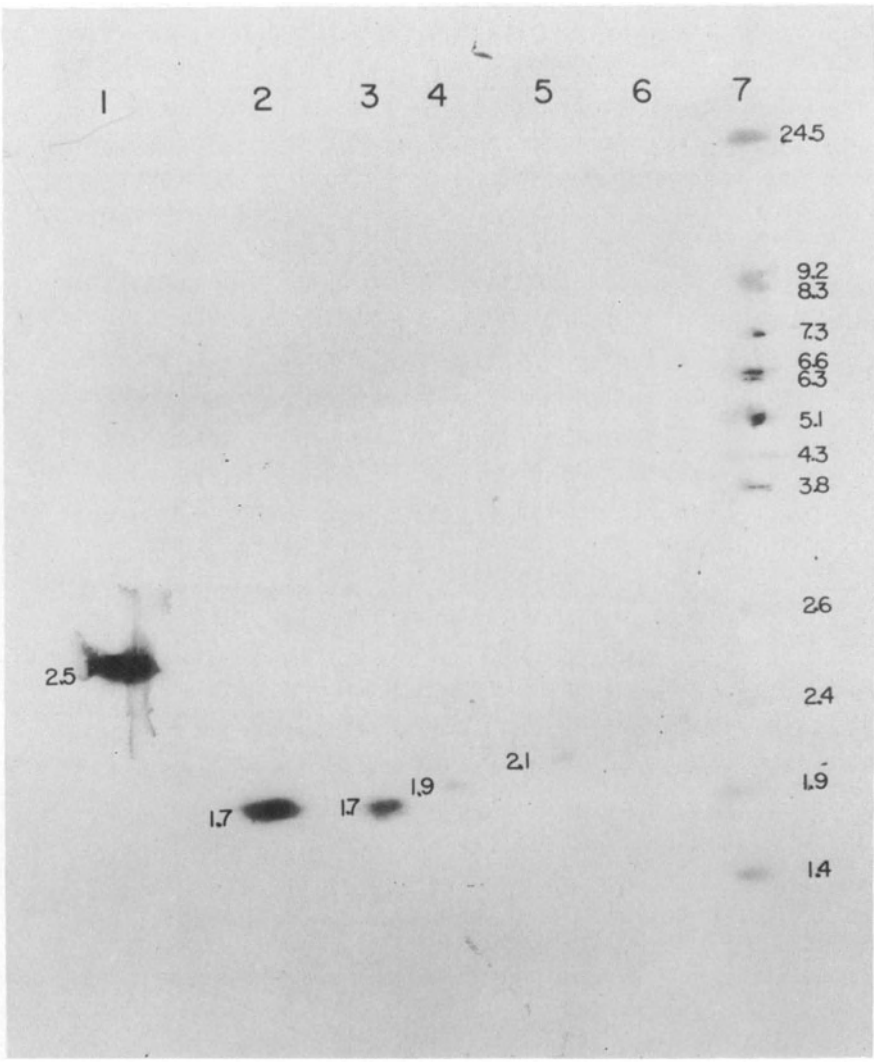

Fig. 2. Detection of EHV-1 DNA sequences contained in reconstruction experiments of viral DNA mixed with hamster cell DNA. 25 µg of normal primary hamster cell DNA was combined with 40-50 picograms of a specific EHV-1 DNA fragment, digested to completion with either EcoRI or Bgl II restriction endonucleases, fractionated by electrophoresis in 0.7% agarose gels at 1.5 V/cm for 36 hr, stained with ethidium bromide (0.5 µg/ml), visualized by UV-light to ensure enzyme digestion of DNA occurred, alkali denatured and neutralized in situ, and transferred to nitrocellulose filters in 5 x SSC as previously described (15). Nick-translation of probes listed in Table 1 with α-^{32}P-deoxy-nucleotides (300 Ci/mM) was done as previously described (16).

1, 2, and 3, which were less than 15 x 10^6 daltons in size. A 10 day exposure revealed that probes 4 and 5 were able to detect the viral fragment in the cell DNA, but the nonspecific background signal was extremely high and unsuitable for reproducible results. Under no circumstances could the genomic length probe detect the viral fragment using these hybridization and labeling conditions. These reconstruction experiments indicated that cloned EHV-1 restriction fragments of less 15 x 10^6 daltons in molecular weight should be used as labeled probes to achieve the maximal sensitivity of this technique.

II. LIBRARY OF CLONED RESTRICTION FRAGMENT PROBES.
The above reconstruction experiments suggested that usage of viral restriction fragments as hybridization probes provided the most feasible approach for detecting subgenomic portions (< 2 x 10^6 daltons) of the viral genome integrated in amounts of only a few copies per cell. To accomplish this end, recombinant DNAs were constructed between EHV-1 DNA restriction fragments and DNAs of plasmid and/or phage vectors. E. coli strains HB101 and C600SF8 were transformed with ligations of EcoRI or Bam HI EHV-1 DNA restriction fragments and plasmid pBR322. The lysogenic phage, Charon 4A, containing Xba I or Bgl II EHV-1 DNA restriction fragment inserts was grown in E. coli strains CSH18 and DP50. Details for the preparation and the screening of these clones are described in Robinson et al (17) employing recombinant DNA methodology (see 18). The cloned restriction fragments chosen as probes are listed in Figure 3, and the rationale for their selection is presented below:

(i) all restriction fragments used as probes have molecular weights less than 15 x 10^6 daltons,
(ii) the total coding capacity of this probe library is equivalent to the genome of EHV-1,
(iii) many of the probes have overlapping coding regions in order to map more precisely viral sequences, and
(iv) well-defined cleavage maps exist for these restriction fragments (14, 19).

All restriction fragments used as probes were screened routinely for purity by restriction endonuclease analyses and by blot hybridization. Each of these probes was labeled to specific activities > 1 x 10^8 cpm/μg by nick-translation (16) and was used in separate experiments to examine the distribution of specific EHV-1 sequences in EcoRI- or Bgl II-cleaved DNA from transformed and tumor cell lines.

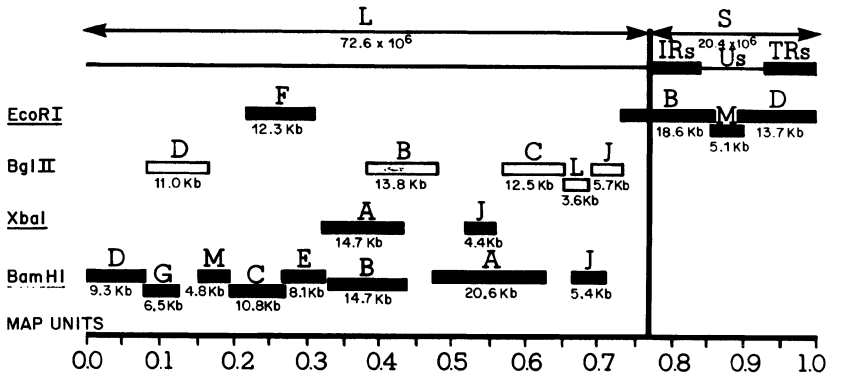

Fig. 3. The library of cloned EHV-1 DNA restriction fragments used as probes in blot hybridizations to detect viral DNA sequences in EHV-1 transformed and tumor cells. EcoRI and Bam HI restriction fragments of EHV-1 DNA were cloned into the plasmid vector pBR322, and Xba I and Bgl II restriction fragments of EHV-1 DNA were cloned into the lambda phage, Charon 4A, as previously described (18).

III. ARRANGEMENT OF VIRAL DNA SEQUENCES IN EHV-1 TRANSFORMED AND TUMOR CELL DNAs DIGESTED WITH EcoRI.

The EHV-1 transformed and tumor cell lines LSEH-8 and LSEH-8T contain 0.3 and 3.0 copies representing 3.3 and 2.2% of the virus genome, respectively (12). These results are suggestive that a reduction in viral genetic material integrated during transformation and an amplification of the retained viral sequences are active processes during *in vivo* tumorigenesis. However, the percentage of the virus genome represented in these cells and the number of viral copies are average estimates and cannot be considered as absolute values to be reflected in blot hybridization experiments.

The DNAs of these cell lines were digested with the restriction endonuclease EcoRI, which does not cleave internally the DNA of EHV-1 cloned fragment probes 6, 8, 9, 11, 13, 16, 17, and 18. Single EcoRI sites are found in the DNA of EHV-1 cloned fragment probes 1, 2, 3, 7, 14, and 15. Double and triple EcoRI cleavage sites are present internally in the DNA of EHV-1 cloned fragment probes 5, 10 and 4, 12, respectively. After digestion, the restriction fragments were electrophoresed through 0.7% agarose gels, transferred to nitrocellulose filter paper, and hybridized to each of the ^{32}P-labeled EHV-1 cloned fragment probes separately.

Autoradiographs of hybridized filters containing EcoRI digests of LSEH-8 and LSEH-8T DNAs are shown in Figures 3 and 4, respectively. Within the LSEH-8 transformed cell genome, two fragments, 10.1 and 12.4 megadaltons (md), were detected with the ^{32}P-labeled Bam HI-E (.271 - .329) and -B (.329 - .436) probes. EcoRI cleaves the Bam HI-E fragment at a single site (.304), yielding fragments of molecular weights 2.3 md and 3.0 md (19); therefore, if both fragments are part of the integrated viral sequence, two fragments would be detected for each integrated copy. However, since similar size fragments were detected with the Bam HI-B probe, which is adjacent to the 2.3 md fragment of the EcoRI digest of Bam HI-E fragment and has no EcoRI cleavage sites, only viral sequences encoded by .31 to .329 and .329 to .38 are integrated into the hamster genome. This is confirmed by the absence of detectable viral sequences in hybridizations with the EcoRI-F probe (.215 - .304) and the Bgl II-B probe (.386 - .486). Each fragment, 10.1 md and 12.4 md, represents a separate integrated viral sequence with flanking host sequences. A similar pattern of integration is seen in the EcoRI digests of the tumor cell DNA. With only the Bam HI-B probe, two fragments, 12.8 md and 13.8 md, were detected in the LSEH-8T tumor cell genome. However, the increased size in molecular weight can be attributed to an increase in copy number and to a loss of viral sequences. Generally, these conclusions were borne out in Cot analyses previously described (12).

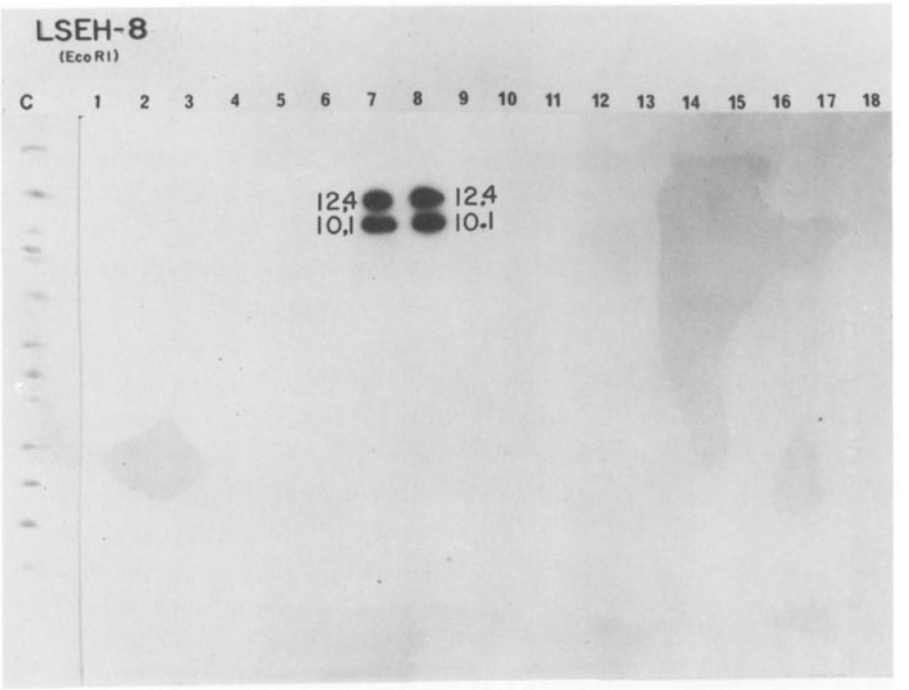

Fig. 4. Detection of fragments of DNA containing EHV-1 DNA sequences following cleavage of LSEH-8 transformed cell DNA with the restriction endonuclease EcoRI. The digestion products were fractionated by electrophoresis in 0.7% agarose gels for 40 hr at a potential of 1.75 V/cm, alkali denatured in situ, transferred to nitrocellulose filters, immobilized to the filters by heating 2 hr at 80°C in vacuo, and hybridized to 1-2 x 10^7 cpm/ml of each ^{32}P-labeled EHV-1 DNA probes. Conditions for blot hybridizations were similar to those described previously (15). The hybridized filters were washed and allowed to expose Kodak X-Omat XR-1 film for 6-10 days. The lane labeled "C" represents EcoRI or Bgl II digests of ^{32}P-labeled EHV-1 DNA and served as molecular weight markers. Lanes 1 through 18 refer to EHV-1 DNA probes used and are as follows: 1, Bam HI-D; 2, Bam HI-G; 3, Bgl II-D; 4, Bam HI-M; 5, Bam HI-C; 6, EcoRI-F; 7, Bam HI-E; 8, Bam HI-B; 9, Bgl II-B; 10, Bam HI-A; 11, Xba I-J; 12, Bgl II-C; 13, Bgl II-L; 14, Bam HI-J; 15, Bgl II-J; 16, EcoRI-B; 17, EcoRI-M; 18, EcoRI-D.

IV. ARRANGEMENT OF VIRAL DNA SEQUENCES IN EHV-1 TRANSFORMED AND TUMOR CELL DNAs DIGESTED WITH Bgl II.

To map more precisely the viral sequences integrated in the genomes of these cell lines and to define the boundaries of their integration sites, LSEH-8 and LSEH-8T DNAs were digested with a different restriction endonuclease, Bgl II. This enzyme does not cleave internally the DNA of EHV-1 DNA fragment probes 3, 9, 12, 13, 15, 16, 17, and 18. Single Bgl II restriction sites are present internally in the EHV-1 DNA fragment probes 1, 2, 4, 5, 7, 8, and 11. Multiple cleavage sites for Bgl II are located internally in the EHV-1 DNA fragment probes 6, 10, and 14. The results of blot hybridizations utilizing our library of probes with Bgl II restricted cell DNAs are presented in Figures 6 and 7.

The viral sequences hybridizing to the Bam HI-E fragment were detected in two fragments of the Bgl II-digested LSEH-8 genome. Both of these fragments (2.8 md and 4.0 md) are smaller than the Bam HI-E fragment and probably represent the 4.1 md Bgl II-digestion product of the Bam HI-E fragment. Two fragments (6.1 md and 7.0 md) were detected with Bam HI-B fragment probe within the LSEH-8 genome. These viral sequences map from .330 to .386 map units and are conjoined with two different sets of host flanking sequences. It can be concluded from these data taken together with the EcoRI results that the LSEH-8 genome contains two sets of integrated viral sequences mapping from .31 to .38.

In the LSEH-8T tumor cell genome, only viral sequences complementary to the Bam HI-B fragment were detected. All three fragments (4.6 md, 6.1 md, and 7.0 md) were smaller than the Bam HI-B fragment. These data confirm EcoRI results of LSEH-8T tumor cell DNA, as viral sequences mapping from .33 to .38 are integrated at two different sites within the host genome. If the 4.6 md fragment is interpreted as representing two fragments of colinear viral sequences with different host flanking sequences, then these data are consistent with the gene amplification concept proposed below.

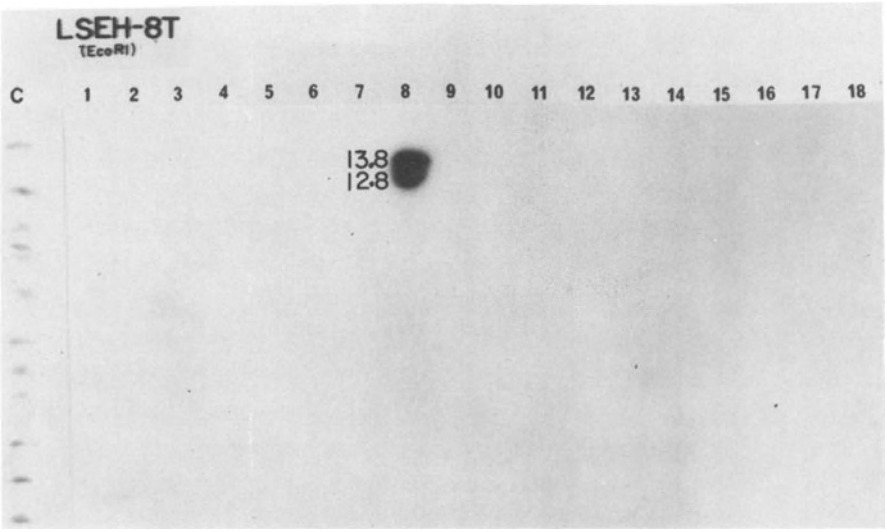

Fig. 5. Detection of fragments of DNA containing EHV-1 DNA sequences following cleavage of LSEH-8T tumor cell DNA with the restriction endonuclease EcoRI. The products of digestion were analysed as described in the legend to Figure 4.

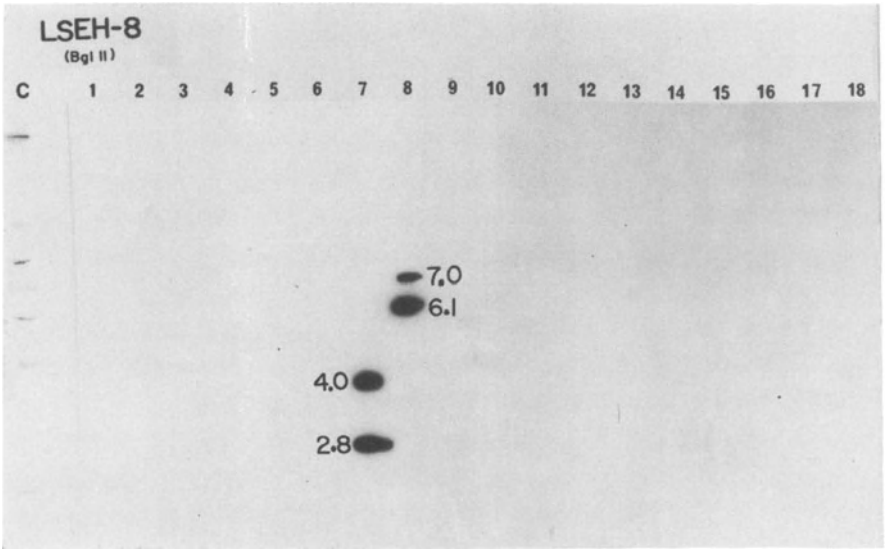

Fig. 6. Detection of fragments of DNA containing EHV-1 DNA sequences following cleavage of LSEH-8 transformed cell DNA with the restriction endonuclease Bgl II. The products of digestion were analyzed as described in the legend of Figure 4.

The EcoRI and Bgl II data for the EHV-1 transformed and tumor cell genomes demonstrate that the EHV-1 DNA sequences exhibit specific and unique patterns of distribution with respect to the cleavage sites of these enzymes. In addition, the patterns of distribution of the viral sequences within the transformed cell genome differed from that of the tumor cell genome. Despite the fact that multiple copies of similar viral sequences were retained in these cell lines, a limited number of viral-specific sequences was detected in each cell line. From these results, restriction maps of integrated viral sequences and adjoining cellular sequences were constructed and are summarized in Figure 8. To substantiate these findings, cloned EHV-1 restriction fragment are being examined in transfection experiments for their morphological and oncogenic transforming activities.

V. DISCUSSION

After transformation with EHV-1, HEF cells acquire viral DNA sequences that are representative of only a small portion of the virus genome (12). The data presented here demonstrate that a specific set of viral sequences mapping from .31 to .38 are conserved within the genome of the LSEH-8 transformed cell. Viral sequences mapping from .33 to .38 are retained in these cells during tumorigenesis and are a subset of those viral sequences present in the transformed cell. These data provide evidence that EHV-1 DNA can be linked covalently to cellular DNA during oncogenic transformation and that this integration occurs at several sites within the host genome. Thus, these data and results from blot hybridization experiments using DNA from many other EHV-1 transformed and tumor cell lines (unpublished observations) suggest that an EHV-1 DNA sequence corresponding from .32 to .38 of the viral genome may contain specific sequences involved in the process of recombination with the cellular DNA during transformation. Several questions of particular interest that our laboratory is attempting to answer at present are:

(1) Are multiple sites within the host genome receptive for

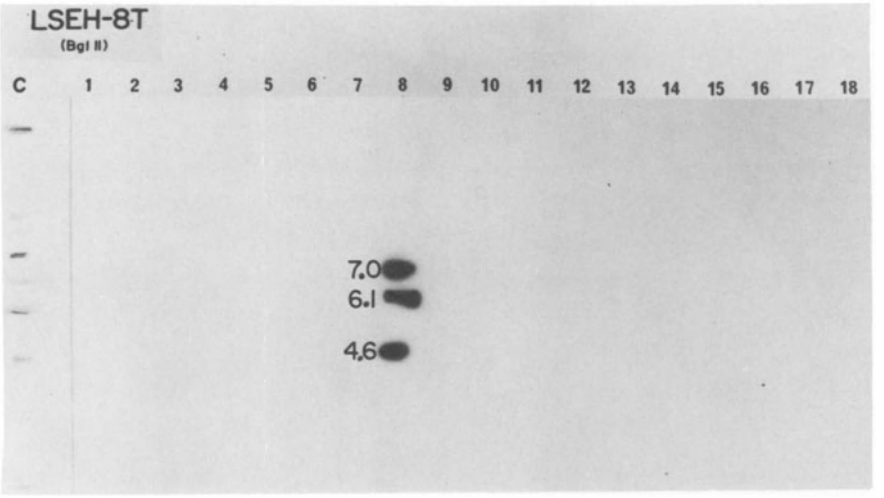

Fig. 7. Detection of fragments of DNA containing EHV-1 DNA sequences following cleavage of LSEH-8T tumor cell DNA with the restriction endonuclease Bgl II. The products of digestion were analyzed as described in the legend to Figure 4.

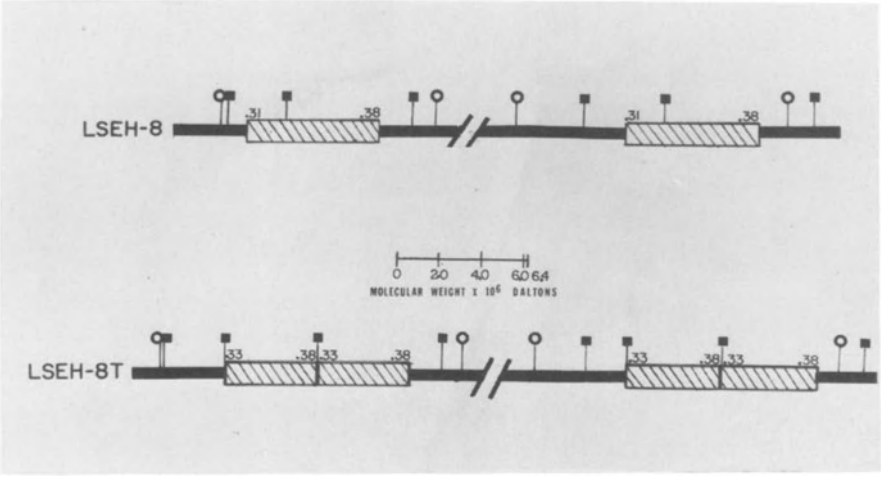

Fig. 8. Maps of viral DNA sequences integrated into the genomes of EHV-1 transformed and tumor cells. The maps were constructed as described in the text. The heavy solid lines represent flanking cellular DNA sequences; the hatched boxes represent integrated EHV-1 DNA. (▬) indicates the regions of the EHV-1 map which contain the junctions between cellular and viral DNA sequences. The symbols represent the two restriction endonucleases used: (■) Bgl II and (O) EcoRI. The molecular weights of these segments are given in daltons.

integration of viral sequences?

(2) Are specific viral sequences integrated directly into the host genome or retained selectively from integrated copies of the whole viral genome?

(3) In cells with multiple copies of viral DNA, are the viral sequences integrated in tandem relative to one another?

Another feature of the integrated viral sequences suggested by these studies is that during tumorigenesis a small subset of identical viral sequences are excluded from each integration site and subsequently that the remaining viral sequences undergo gene duplication in a head-to-head fashion. A model depicting this arrangement of integrated viral sequences is presented in Figure 8. Results of blot hybridizations using other restriction endonuclease digests of these cell DNAs were similar to those obtained with EcoRI and Bgl II DNA digests and strengthened this interpretation concerning the distribution pattern of viral sequences in these host genomes. This type of genetic rearrangement in which specific DNA sequences are amplified is not unique to viral DNA during transformation, as the dihydrofolate reductase gene of murine cells has been shown to undergo repeated gene duplication in response to treatment with methotrexate (20).

The other major finding resulting from these blot hybridization studies is that the pattern of restriction fragments containing EHV-1 sequences is different for independently derived EHV-1-transformed cell line. Although the exact location of integrated viral sequences within the host genome appears to differ among all cell lines examined to date, it cannot be concluded that the cellular sites for integration of viral sequences are completely random. By the use of recombinant DNA techniques, we are cloning host sequences containing the viral inserts. DNA sequencing of the nucleotides at the joint regions between host and viral sequences present in these clones will enable us to answer some of the questions concerning the mechanism and nature of integration of tumor virus genes into eukaryotic chromosomes. Specifically, we hope to de-

termine whether any set(s) of host nucleotide sequences are receptive specifically for herpesvirus transforming genes.

Acknowledgments

Support for these investigations was obtained from Research Grant AI-02032 and General Medical Research Support Grant S-507-RR-05386 awarded by the National Institubes of Health and Research Grant PCM-7822700 awarded by the National Science Foundation.

We thank Dr. J. Craig Cohen for helpful technical assistance and enlightening discussions and Ms. Cheryl Tucker for secretarial assistance in the preparation of this manuscript.

References

1. Ketner, G. and T.J. Kelly. 1976. Integrated SV40 sequences in transformed cell DNA: analysis using restriction endonucleases. PNAS, U.S.A. 73: 1102-1106.

2. Botchan, M., W. Topp, and J. Sambrook. 1976. The arrangement of SV40 sequences in the DNA of transformed cells. Cell 9: 269-287.

3. Birg, F., R. Dulbecco, M. Fried, and R. Kamen. 1979. State and organization of polyoma virus DNA sequences in transformed rat cell lines. J. Virol. 29: 633-648.

4. Prasad, I., D. Zouzias, and C. Basilico. 1976. State of the viral DNA in rat cells transformed by polyoma virus. I. virus rescue and the presence of nonintegrated viral DNA molecules. J. Virol. 18: 436-444.

5. Chenciner, N., M.P. Grossi, G. Meneguzzi, A. Covallini, R. Manservigi, G. Barbanti-Brodano, and G. Milanesi. 1980. State of viral DNA in BK virus-transformed rabbit cells. Virology 103: 138-148.

6. Duesberg, P.H., P.K. Vogt, K. Bister, D. Troxler, and E.M. Scolnick. 1978. Oncogenic (onc) genes of sarcomas, leukemias, and carcinoma viruses, p. 95-111. In Avian RNA tumor viruses. Piccin Editore, Padva.

7. Sutter, D., M. Westphal, and W. Doerfler. 1978. Patterns of integration of viral DNA sequences in the genomes of adenovirus type 12-transformed hamster cells. Cell 14: 569-585.

8. Galloway, D.A., E. Lukanidin, W.C. Topp, and J. Sambrook. 1979. Transformation of rat cells by the hybrid virus Ad2^{+} HEY. J. Gen. Virol. 42: 339-356.

9. Camacho, A. and P. Spear. 1978. Transformation of hamster embryo fibroblasts by a specific fragment of the herpes simplex virus genome. Cell 15: 993-1002.

10. Reyes, G.R., R. LaFemina, S.D. Hayward, and G.S. Hayward. 1979. Morphological transformation by DNA fragments of human herpesviruses: evidence for two distinct transforming regions in HSV-1 and HSV-2 and lack of correlation with biochemical transfer of the thymidine kinase gene. Cold Spring Harbor Symp. Quatn. Biol. 44: in press.

11. Jariwalla, R.J., L. Aurelian, and P.O. Ts'o. 1980. Tumorigenic transformation induced by a specific fragment of DNA with herpes simplex virus type 2. PNAS, U.S.A. 77: 2279-2283.

12. Robinson, R.A., B.E. Henry, R.G. Duff, and D.J. O'Callaghan. 1980. Oncogenic transformation by equine herpesviruses (EHV) I. properties of hamster embryo cells transformed by UV-irradiated EHV-1. Virology 101: 335-362.

13. Robinson, R.A., R.B. Vance and D.J. O'Callaghan. 1980. Oncogenic transformation by equine herpesviruses (EHV) II. Co-establishment of persistent infection and oncogenic transformation of hamster embryo cells by EHV-1 defective interfering particles. J. Virol. in press.

14. O'Callaghan, D.J., B.E. Henry, J.H. Wharton, S.A. Dauenhauer, R.B. Vance, J. Staczek, S.A. Atherton, and R.A. Robinson. 1980. Equine herpesviruses: biochemical studies on genomic structure, DI particles, oncogenic transformation and persistent infection. In: Herpesvirus DNA: Recent Studies on the Internal Organization and Replication of the Viral Genome, Becker, Y. (ed.), The Hague, Martinus Nijhoff BV.

15. Southern, E.M. 1975. Detection of specific sequences among DNA fragments separated by gel electrophoresis. J. Mol. Biol. 38: 503-517.

16. Rigby, P.W.J., M. Diekmann, C. Rhoades, and P. Berg. 1977. Labeling deoxyribonucleic acid to high specific activity in vitro by nick translation with DNA polymerase I. J. Mol. Biol. 113: 237-251.

17. Robinson, R.A., P.W. Tucker, and D.J. O'Callaghan. 1980. Recombinant DNA cloning of equine herpesvirus DNA restriction fragments in plasmid and phage vectors. (Manuscript Submitted).

18. Blattner, F.R., A.E. Blechl, K.D. Thompson, J.E. Richards, J.L. Slightom, P.W. Tucker, and O. Smithies. 1978. Human and mouse DNA. I. cloning of fetal gammaglobin and mouse alphaglobin DNA: preparation and screening of shotgun collections. Science 202: 1279-1283.

19. Henry, B.E., S.A. Dauenhauer, J.H. Wharton, and D.J. O'Callaghan. 1979. Molecular structure of the genomes of standard virus and DI particles of EHV-1 and -2. Proc. Fourth International Herpesvirus Workshop. Cold Spring Harbor Symposium. 1979: 7.

20. Schimke, R.T., F.W. Alt, R.E. Kellems, R.J. Kaufman, and J.R. Bertino. 1977. Amplification of dihydrofolate reductase genes in methotrexate resistant cultured mouse cells. Cold Spring Harbor Symp. Quant. Biol. 62: 649-657.

22. Organization and expression of the DNA of Marek's disease virus and of herpesvirus of turkeys

Meihan Nonoyama and Kanji Hirai*

SUMMARY

Intact DNA of Marek's disease virus (MDV) is a linear, nicked, double-stranded DNA with a molecular weight of approximately 100 x 10^6. The buoyant density of MDV DNA in CsCl density gradient is 1.705 g/cm^3. However, serially passaged MDV resulted in the production of virus with lower density DNA (1.700 g/cm^3). The data suggests that the repeated cycle of infection with MDV results in accumulation of defective virus particles.

Treatment of the standard MDV DNA with a density of 1.705 g/cm^3 with restriction enzymes Sma, Sal 1 and Bam Hl yield fragments present mostly in equal molar abundance, and the sum of the molecular weights of the fragments produced by cleavage with each enzyme is approximately 100 x 10^6. Some of the fragments are present in greater than molar quantities which may indicate that MDV DNA has repeated sequences. The end fragments of the standard MDV DNA were identified by treatment with lambda exonuclease and the Southern blotting hybridization technique. Heterogeneity in the size of Sal 1 fragments was only found at one end of the DNA, but not the other end, suggesting that one end has a variable number of copies of a reiterated sequence, possibly a tandem repeat unit with the molecular weight of 0.5 x 10^6.

Digestion with Sal 1 of the "defective DNA", banded at a density of 1.700 g/cm^3 in CsCl, revealed that the fragments at one end of the standard MDV DNA were missing in the defective DNA, which is probably generated from the rolling circle type of replication.

* On leave from Department of Molecular Biology, Tokai University School of Medicine, Bohseidai, Isehara 259-11, Japan.

Y. Becker (ed), Herpesvirus DNA.

Herpesvirus of turkeys (HVT), which prevents Marek's disease in chickens, shares only 1 to 4% DNA homology with MDV, indicating that a close DNA homology between these two viruses is not necessary for effective vaccination against the disease.

The status of latent virus genome in a nonproductive chicken lymphoblastoid cell line, MKT-1, has been studied. A large proportion of the resident MDV DNA in MKT-1 cells was found to be another example of the plasmid form of latent herpesvirus DNA.

A study of transcription of the latent MDV genome in MD tumor tissue and MKT-1 cells has shown that the virus-specific RNA sequences were transcribed from less than 15% of the viral DNA template. The polysomal fractions of MKT-1 cells and of spleen tumor contained only a portion of the virus-specific RNA sequence found in whole cell extracts, indicating the existence of a post-transcriptional control mechanism within the MD-transformed cells.

When MKT-1 cells were synchronized by a double thymidine block to examine events in the replication of latent MDV DNA, it was found that the latent MDV DNA in the transformed cells replicates during the early S phase of the cell cycle, prior to the onset of active cellular DNA synthesis.

INTRODUCTION

Marek's disease (MD), a highly contagious lymphoproliferative disease of chickens, is a unique model for the study of herpesvirus oncogenesis. It is one of a few naturally occurring lymphoproliferative diseases associated with horizontally transmitted herpesvirus. The disease is readily produced in chickens, the natural host, by inoculation with cell-free MDV or cell-associated MDV, as well as by exposure to other birds with the disease.

Vaccination against virus induced tumor was first demonstrated in MDV (infection) in chickens (6). Herpesvirus of turkeys (HVT) antigenically cross-react with MDV and shares common antigens as judged by gel precipitation, immunofluorescence and neutralization tests (34,55). It is suggested, however, that protection against MD by HVT inoculation may be due to cell mediated immunity initiated by HVT infection (35). The role of MD tumor-associated surface antigen (MATSA) in induction and prevention of MD is not clear. MATSA

is shown to be induced on the surface of MDV-transformed cells (30,56). HVT and attenuated MDV also induce MATSA on spleen and peripheral blood lymphocytes of infected chickens (24,37,41). Since this antigen is not induced on the surface of MDV infected cultured cells (56), it appears that the antigen is specifically induced in lymphocytes infected with HVT or MDV and is possibly a virus-induced cell coded protein.

Knowledge of the organization and structure of MDV DNA is necessary for an understanding of the biochemistry of cell transformation and virus replication. Genetic relatedness of HVT and MDV also should be investigated further to understand the mechanism of vaccination.

In the first section of this chapter, we will discuss experiments on the defective DNA in an MDV preparation (51), the structural analysis of MDV DNA (28), and the genetic relatedness of MDV and HVT (27). The second section will discuss the state and replication of latent MDV genomes (25,50), as well as the transcriptional regulation in MD tumor cells and transformed cells (44,45).

1. STRUCTURAL ANALYSIS OF MDV DNA

1.1 General Properties of MDV DNA

MDV DNA has been found in chicken tumor cells and in some chicken lymphoblastoid cell lines (31,32). MDV is usually propagated in chick embryo fibroblast (CEF) cells. MDV DNA is a linear, nicked, double-stranded DNA with a molecular weight of approximately 100×10^6. The S value of MDV has been determined to be 55S in neutral glycerol gradient. The buoyant density of MDV is 1.705 g/cm^3 in neutral CsCl which is consistent with a guanine plus cytosine content of 45-47% (17,26). However, we have observed from time to time heterogenicity of virus DNA in our 55S virus DNA preparation in CsCl equilibrium centrifugation, one banding at 1.705 g/cm^3, and the other at 1.700 g/cm^3. Virus specific cRNA prepared from a DNA preparation which consisted of homogenous virus DNA of 1.705 g/cm^3 hybridized equally to DNA of 1.700 g/cm^3 density but not to cell DNA. These experiments indicate that DNA of 1.700 g/cm^3 is not derived from cell DNA, but contains homologous sequences to virus DNA of 1.705 g/cm^3. An accumulation of defective virus was obtained for study by isolating a single focus of MDV to expand into a high passaged virus preparation.

Cell-free MDV was released by sonication of MDV infected cells and propagated in CEF. A single focus of MDV was isolated and grown by continuous passage. At the 6th passage virus was isolated and the DNA was purified as 55S. Virus DNA was also isolated as 55S at the 25th passage. Both virus DNA preparations were centrifuged to equilibrium in CsCl. As shown in Figure 1, the 6th passage virus DNA showed a symmetrical peak at 1.705 g/cm^3, whereas the 25th passage

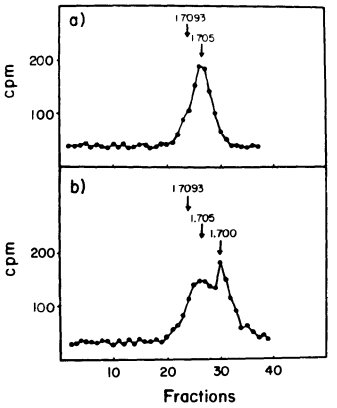

FIGURE 1. Buoyant density determination of MDV DNA from low and high passaged cultures: The GA strain of MDV was propagated in secondary CEF cells. A single focus of MDV was isolated from a cell-free virus preparation obtained by sonication (9) and propagated by continuous passage in secondary CEF. The cultures at the 6th and 25th passages were labeled with ^{3}H-thymidine (1 µCi/ml) and was harvested when 70-80% of the culture showed CPE. Virus was extracted by using 1.0% NP 40 and 0.5% Triton x 100. The extracted virus was further purified through a sucrose gradient and the DNA was isolated as 55S by glycerol gradient centrifugation as described previously (50). Both samples were centrifuged to equilibrium in CsCl at 35,000 rpm at 18^{o}C for 48 hours in a Beckman T-50 rotor and fractions were collected. ^{3}H-labeled lambda DNA was used as a density marker at 1.7093 g/cm^3 in a separate tube. (a) 6th passage (b) 25th passage.

virus DNA contained both 1.705 and 1.700 g/cm^3 DNA. Since cell-associated MDV is used to infect CEF cultures and the effectiveness of infectivity varies each time, the time of appearance of defective virus is not always the same even if the same ratio of infected cells

to uninfected CEF is used. However, repeated passages of virus stock eventually result in the appearance of defective virus.

1.2 MDV DNA digested with restriction endonucleases

In order to map MDV DNA, the standard viral DNA banding at 1.705 g/cm^3 in CsCl equilibrium centrifugation was analysed. Several restriction enzymes were used to determine which enzyme produces fewer fragments; most enzymes yielded more than fifteen fragments. For example, EcoRl produced at least 16 fragments, Hind III 20, and Bgl II 22 fragments. Although EcoRl produced 16 fragments, the total molecular weight of MDV/EcoRl fragments was 62×10^6, which is smaller than the conventional figure (1×10^8 daltons). This suggests that many EcoRl fragments contain molar ratios of two or three. We have recently found several enzymes which might prove helpful for MDV DNA physical mapping. MDV DNA was digested with Sma, Sal 1 or Bam Hl endonucleases and the individual digests were electrophoresed on 0.5% agarose gels. The gel was stained with ethidium bromide and then visualized over a UV light source. Twelve bands were produced by the Sma enzyme (Fig. 2), of which the largest fragment had a molecular weight of 15.8×10^6. Most bands contained molar ratios of unity, except the G and L fragments (7.3 and 2.4×10^6, respectively; Table 1). Eighteen bands were produced by the Sal 1 endonucleases. The molecular weight differences between fragments B and C, C and D, and D and E are $0.5 - 0.6 \times 10^6$ daltons, which represent the tandem repeat molecules. This smear area was found by later studies to represent the end fragments of MDV DNA, having submolar ratios.

There are fourteen bands produced by the Bam Hl enzyme, with varying molar ratios. Fragments I and K have multiple molar ratios. The total molecular weight of the Bam Hl digest is 99.1×10^6 (Table 1). Since the possible defective MDV DNA was obtained in high passaged cultures, both standard and defective virus DNA were analyzed by a restriction enzyme. Standard virus DNA and virus DNA, most of which had a low density, was digested with restriction enzyme Sal 1 and subjected to electrophoresis in 0.4% agarose gel. It was found that Sal 1 digests of the possible defective virus contained 16 fragments, whereas wild type virus DNA generated 18 fragments ranging from 1×10^6 to 13.8×10^6 daltons. However, the two fragments, H and I were not observed in the higher passaged virus DNA preparation.

TABLE 1 Estimation of molecular weight and molar ratio of MDV DNA digested with Sma, Sal 1 and Bam H 1 endonucleases

	Sma		Sal 1		Bam H 1	
Frag. No.	M.W.[a]	Suggested Molar Ratio	M.W	Suggested Molar Ratio	M.W.	Suggested Molar Ratio
A	15.8	1	13.8	1	14.5	1
B	12.8	1	12.5	1	12.2	1
C	11.4	1	11.9	1	9.9	1
D	11.1	1	11.3	1	7.9	1
E	9.4	1	10.8	1	6.7	1
F	7.9	1	8.9	2	6.1	1
G	7.3	2	8.3	1	4.7	1
H	5.7	1	7.4	1	3.6	1
I	5.5	1	6.6	1	3.4	5
J	3.4	1	5.4	1	2.9	1
K	3.2	1	4.9	1	2.4	4
L	2.4[b]	4	3.5	1	2.0	2
M			2.6	1	1.6	N.D.
N			2.3	1	1.2[b]	N.D.
O			2.1	1		
P			1.8[b]	2		
Total	110.4		96.8		99.1	

a. Molecular weight in megadaltons was calculated from a comparison of its mobility with that of lambda DNA EcoRl fragments.

b. Molecular weight below 1 x 10^6 daltons did not include here.

N.D. Not Done

No new bands appeared in the possible defective virus DNA.

1.3 Identification of the end fragments of MDV DNA

To find the end fragments of MDV DNA, lambda exonuclease was used on MDV DNA prior to endonuclease digestion. Lambda exonuclease preferentially attacks 5' -phosphoryl terminals of intact DNA. The standard MDV DNA, banding at 1.705 g/cm^3 in CsCl equilibrium centrifugation, was predigested with the exonuclease and then cleaved with Bam Hl endonuclease. The results are illustrated in Fig. 3A. The A and D

fragments are more sensitive to the exonuclease digestion and are therefore located near the ends of MDV DNA. Although the D fragment did not disappear as readily as the A fragment, densitometer tracings of each fragment were taken for comparison between exonuclease-treated and untreated DNA. The areas of the absorbance peaks of the A and D fragments were found to have absorbance losses up to 74% and 62%, respectively, in comparison with other fragments which lost between 15% and 48%.

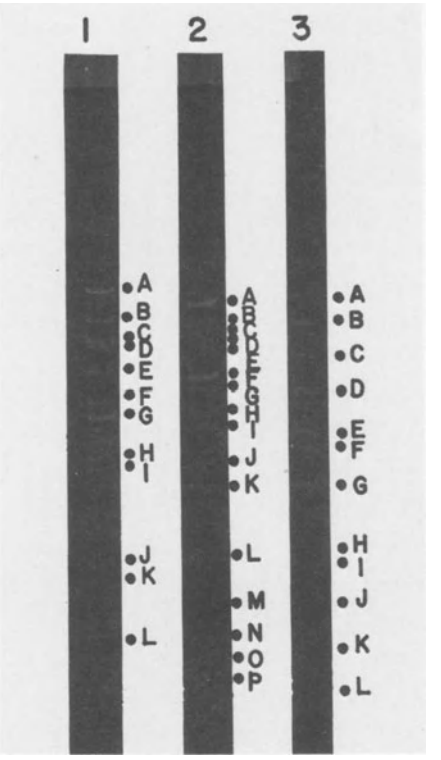

FIGURE 2. Restriction endonuclease-cleavage pattern of MDV DNA: One µg of MDV DNA, banding at 1.705 g/cm^3 in CsCl density gradient, was digested with endonucleases 1) Sma, 2) Sal 1, and 3) Bam Hl respectively. The digested DNA fragments were separated by 0.5% agarose gel electrophoresis at 80V for 16 hr, stained with ethidium bromide and photographed under UV light as described previously (27). DNA bands were designated alphabetically.

The Sal 1 enzyme was also employed in the lambda exonuclease study. Several fragments, A, B, C, D, E, H and I, were found significantly sensitive to the exonuclease with B, C, D and E fragments generally appearing as a smear area (Fig. 3B). The B, C, D and E fragments probably represent one end of the MDV DNA molecule which may contain tandem repeat sequences. The H and I fragments, then, represent the other end fragments. Digestion of MDV-defective virus DNA with Sal 1 revealed only H and I fragments missing. No other fragments were found in the Sal 1 digest. If defective virus DNA was deleted in an interior segment of MDV DNA, that should produce extra fragment(s) on the gel. Thus, H and I fragments may be located on the other end of the molecule.

To identify which of the Bam Hl and Sal 1 fragments corresponded to each other, both end fragments (A and D) of the Bam Hl were isolated and nick-translated with ^{32}P-dCTP, and then hybridized with Sal 1 fragments on blotting nitrocellulose paper. The Bam A fragment is only hybridized to Sal 1 smear regions (fragments B, C, D, E), whereas the Bam D fragment is preferentially hybridized to Sal 1, H and I fragments.

Fragments of Sma also were included in this blotting hybridization procedure. The results indicate that Bam A fragments hybridize to Sma B which suggests that Sma B may be the end fragment. It is noted that Bam A also hybridized to Bam C less extensively. This may indicate Bam A and C have homologous DNA sequences, which implies that MDV DNA might have repeat or inverted repeat sequences.

1.4 DNA homology between MDV and HVT (Herpesvirus of Turkeys)

HVT is used as a commercial vaccine against tumor induction caused by MDV infection in chickens. It is important to know the degree of DNA homology between these two viruses for future study of the oncogenic property of MDV.

1.4a Reassociation kinetics between virus DNAs

To compare the DNA homology, 55S HVT and MDV DNAs were isolated from purified virions and reassociation kinetics was tested between HVT DNA and MDV DNA.

No acceleration of the reaction was observed when ^{3}H-HVT DNA or ^{3}H-MDV DNA was reassociated with an excess amount of MDV DNA or HVT DNA, whereas reassociation of the probe DNA with homologous virus DNA

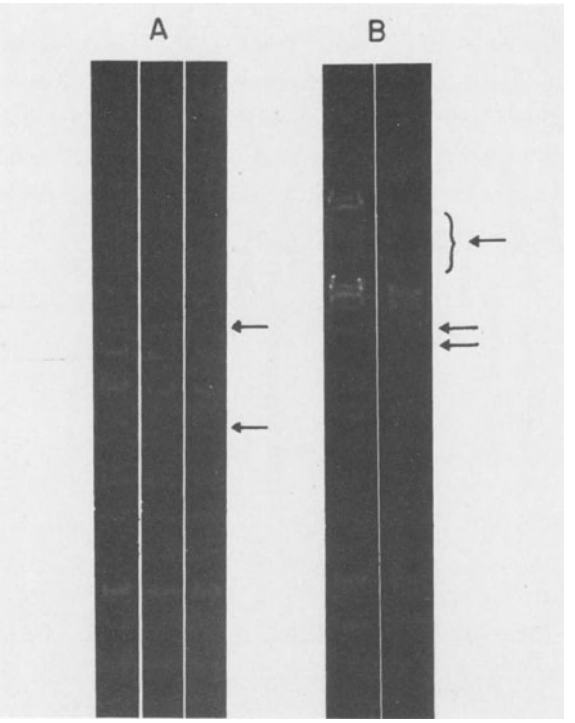

FIGURE 3. Identification of terminal fragments of MDV DNA: One µg of MDV DNA was treated with exonuclease and subsequently digested with A) Bam H or B) Sal 1, electrophoresed as described in the legend of Fig. 2. A) MDV DNA cleaved with Bam Hl endonuclease: Left, no exonuclease digestion; center, exonuclease treatment for 5 min; right, for 10 min. The upper and lower arrows indicate the A and D fragments. B) MDV DNA cleaved with Sal 1 endonuclease: left, no exonuclease digestion; right, exonuclease treatment for 10 min. The upper arrow indicates the location of the smear region (fragments B, C, D, and E). The two lower arrows indicate H and I.

was accelerated. The result indicated that no appreciable homology exists between HVT and MDV DNA as judged by reassociation kinetics.

1.4b Electrophoretic patterns obtained by digestion of virus DNA with various restriction endonucleases.

The relationship of the two virus DNAs was further tested by comparing electrophoresis patterns of the restriction enzyme fragments for each

DNA.55S virus DNA was isolated and digested with Hind III, Xba, Sal 1, Bam Hl or Xho restriction enzymes. The digested products were separated by electrophoresis in 0.5% agarose gel. The electrophoretic profiles of MDV DNA and HVT DNA were different as seen in Figure 4. Most of the DNA fragments produced by endonucleases from MDV and HVT DNA did not have identical electrophoretic mobility in agarose gel.

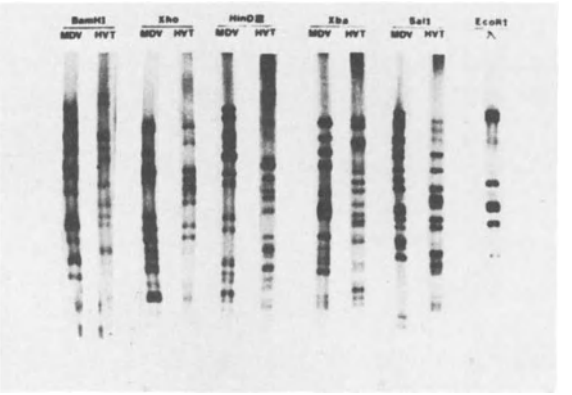

FIGURE 4. Autoradiograms of electrophoretic profiles of MDV DNA and HVT DNA cleaved with restriction endonucleases: 3,000 cpm of MDV ^{32}P-DNA and HVT ^{32}P-DNA were cleaved with various restriction enzymes as indicated and electrophoresed in 0.4% agarose horizontal gels at 80V for 16 hours. The gels were dried and autoradiographed with intensifying screens (DuPont Cronex).

1.4c Detection of DNA homology by Southern blotting hybridization.

Attempts to detect homology between these two DNAs led to the use of the more sensitive Southern blotting hybridization technique. MDV and HVT DNAs were both digested with restriction endonuclease EcoRl and run separately by electrophoresis on a 0.5% agarose slab gel. The DNA fragments on the gel were then transferred to nitrocellulose filters according to Southern's method (47) and hybridized with a ^{32}P-labeled viral DNA probe. The results are shown in Figure 5. As expected the MDV DNA fragments all hybridized with ^{32}P-MDV DNA (Figure 5, columns 2 and 4). In the HVT DNA gel, three visible bands can be seen with molecular weights of 5.6, 4.9 and 4.7 megadaltons (Figure 5, column 3) which indicated hybridization of these three fragments with ^{32}P-MDV DNA. Reciprocal experiments were conducted using ^{32}P-

labeled HVT DNA as a probe. In Figure 5, column 5, four MDV DNA fragments can be seen which hybridized to ^{32}P-HVT DNA. The molecular weights of these fragments are 7.1, 4.5, 3.9 and 3.5 megadaltons. However, these four fragments, and the three just mentioned, are seen as only faint bands after longer periods of exposure when compared to the intensity of the bands from positive controls. It is roughly estimated from densitometer tracings, considering the amount of virus DNA on the filter (MDV DNA 0.75 µg and HVT 0.25 µg), that homologous sequences between MDV and HVT DNA are within the range of 1 to 4% This is equivalent to 2.5 to 6 coding genes unless the sequences are scattered.

2. LATENCY OF MDV GENOMES

Lymphoid tumors from MDV infected chickens contain copies of the MDV genome but are usually free of MDV antigens and virus particles (31). However, certain established cell lines derived from MD lymphomas produce virus particles (or viral antigens) in a small percentage of the cell population (3, 23, 36).

It is important to study the status of latent MDV genomes and other characteristics of the MD lymphoid cell lines to understand herpesvirus-induced neoplasia.

2.1 The number of virus genomes in tumor tissues and established lymphoblastoid cells.

All tumors from chickens inoculated with MDV contained multiple copies, from 3 to 12 of the MDV genome per cell, which confirms data reported by Nazerian et al. (1973). It should be mentioned that the tumor tissues contained a variety of cell types, therefore the value obtained for the average number of genomes per cell is not absolute, but merely an indication of the presence of MDV DNA. In contrast, MKT-1 is an established, nonproductive, lymphoblastoid cell line carrying MDV genomes, the average number of which remains a constant 15 genomes per cell.

2.2 Analysis for the state of latent MDV genome.

Since MKT-1 cells contain multiple virus genomes per cell and are virus nonproductive, they provided a system analogous to that of Raji cells in EBV studies. The majority of EBV genomes in Raji cells are

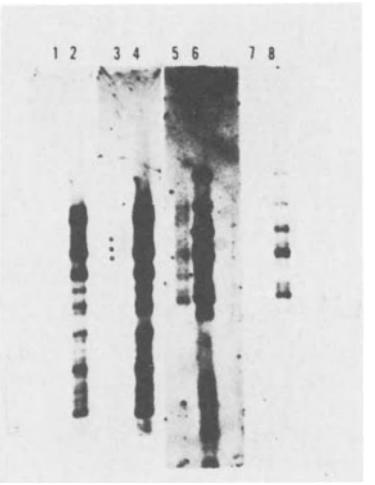

FIGURE 5. Southern Blotting Hybridization between MDV DNA and HVT DNA: MDV DNA (0.45 µg) or HVT DNA (0.25 µg) was digested with EcoRl and electrophoresed in 0.5% agarose gel at 80V for 16 hours. The DNA fragments were transferred to nitrocellulose filter paper. The filters were baked at 80°C for 2 hours under vacuum and hybridized with ^{32}P-labeled viral DNA (1 x 10^7 cpm). Hybridized fragments were exposed to autoradiography film (RP/R2) with intensifying screens (DuPont Cronex). 1) ^{32}P-MDV DNA + 0.25 µg HVT DNA exposed for 1/2 day, 2) ^{32}P-MDV DNA + 0.75 µg MDV DNA exposed for 1/2 day, 3) ^{32}P-MDV DNA + 0.25 µg HVT DNA exposed for 4 days, 4) ^{32}P-MDV DNA + 0.75 µg MDV DNA exposed for 4 days, 5) ^{32}P-HVT DNA + 0.75 µg MDV DNA exposed for 4 days, 6) ^{32}P-HVT DNA + 0.25 µg HVT DNA exposed for 4 days, 7) ^{32}P-HVT DNA + 0.75 µg MDV DNA exposed for 1/2 day, 8) ^{32}P-HVT DNA + 0.25 µg HVT DNA exposed for 1/2 day.

not covalently integrated into cellular DNA and exist as plasmid DNA (2,48).

To examine whether MDV DNA in MKT-1 cells can be separated from cell DNA, cells were gently lysed with proteinase K and Sarkosyl, and the viscous lysate was centrifuged through a glycerol gradient, 5 to 10%, with a 20% cushion. Each fraction was tested for MDV DNA by cRNA hybridization. High molecular weight cellular DNA was found at the 20% glycerol cushion. As shown in Fig. 6, 70-80% of the MDV DNA was separated from the high molecular weight cellular DNA and was found in two peaks. The fast sedimenting DNA was recentrifuged

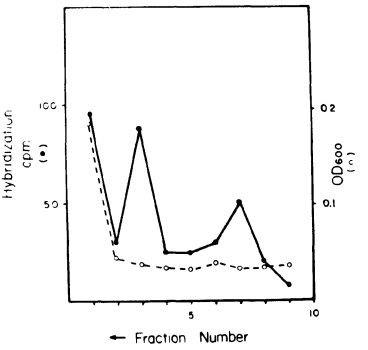

FIGURE 6. Separation of MDV DNA from high molecular weight cell DNA: $2x10^6$ cells were lysed by pronase (1 mg/ml) and Sarkosyl (1%) and the viscous lysate centrifuged through a 5 to 10% glycerol gradient with a 20% cushion of glycerol at 12,500 rpm for 12 hours at 4^oC in a JS 13 rotor. The gradient was fractionated into 10 tubes and virus DNA was detected by cRNA hybridization. ●——● = hybridization; O·····O = OD_{600} diphenylamine reaction for location of cellular DNA.

through a 10 to 30% glycerol gradient. The DNA sedimented about 50% faster than T2 DNA indicating that the sedimentation value was approximately 100S. The slow sedimenting DNA was similarly analyzed and found to be 65S with a minor peak at the 55S region. The 100S molecule was examined further to determine sedimentation value in an alkaline condition and found to be 200S. The 100S molecule, analyzed by ethidium bromide-CsCl equilibrium centrifugation, banded at the identical position as that of closed circular molecules. Thus, the results obtained with MKT-1 cells are very similar to those with Raji cells, as reported by Tanaka and Nonoyama (48); and Adams and Lindahl (2). The 100S molecule of EBV DNA in Raji cells assumes the form of a covalently closed circular DNA (29). The small amount of 55S linear DNA could be a by-product caused by manipulation. MDV DNA in MKT-1 cells seems to assume the same form as EBV DNA in Raji cells. The results have not proven whether or not some MDV genomes are integrated covalently into cellular DNA, although recentrifugation of high molecular weight cell DNA did separate at least 50% of the MDV DNA from cell DNA.

2.3 Transcription of latent virus DNA

It is important to know how latent virus DNA actually functions in transformed cells and tumors. Therefore, the amount of virus mRNA and the fraction of virus DNA transcribed in MKT-1 cells and tumors were examined by DNA-RNA hybridization kinetics (11).

2.3a Transcription of virus genomes in MKT-1 cells with or without IUDR treatment.

When the kinetics of hybridization of ^{3}H-MDV DNA with unlabeled RNA extracted from CEF whole cells infected with MDV was done, it was found that the extent of hybridization is greater than 45%, suggesting that most of the virus genome may be transcribed. Polyribosomal RNA isolated from infected CEF hybridized to the same extent with the MDV DNA probe, indicating that all the species of viral RNA are transferred to polyribosomes. Figure 7 shows the kinetics of hybridization between MDV DNA and whole cell RNA or polyribosomal RNA of MKT-1 cells, both with and without IUDR treatment. The data indicate that untreated MKT-1 cells contain viral specific sequences that are homologous to only 15% of MDV DNA and approximately 70% of these virus RNA species are found in the polyribosomal fraction. When MKT-1 cells were treated for two days with 50 µg/ml of IUDR and further incubated for three days in fresh medium, virus genome transcription was induced, with the extent of hybridization reaching almost 40%. This indicates that almost the entire genome appears to be transcribed, assuming that the coding strand was transcribed.

To determine whether the viral RNA sequences found in IUDR treated MKT-1 cells were encoded by the same DNA sequences as in MDV infected CEF, RNA from both cultures were mixed and hybridized to ^{3}H-MDV DNA. If the viral RNA transcripts from the two cultures were encoded from different DNA sequences, the hybridization of labeled MDV DNA with this RNA mixture would be greater than 45%, i.e., greater than the observed value for MDV infected CEF RNA. If the viral specific RNA sequences from the two sources were identical, hybridization should not exceed 45%. Since the hybridization reached a plateau of 45%, this indicates that the viral specific RNA in MKT-1 cells treated with IUDR was encoded by the same DNA sequences as the viral specific RNA in CEF productively infected with MDV.

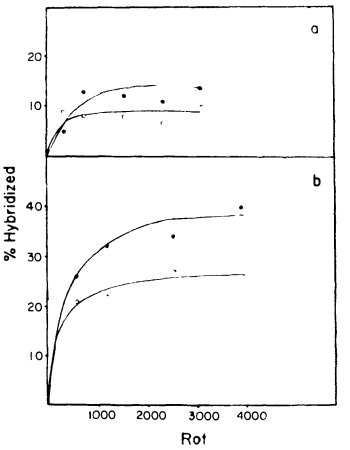

FIGURE 7. Hybridization kinetics between MDV DNA and MKT-1 whole cell and polysomal RNA: a) Without IUDR Treatment : Hybridization mixtures each contained 3 mg/ml unlabeled RNA and approximately 0.01 µg/ml ^{3}H-MDV DNA (20,000 cpm) in a final volume of 0.5 ml. 100 µl samples were taken at various intervals up to 3 days. The percent of ^{3}H-MDV DNA hydrized at each interval was determined by S1 nuclease digestion. b) With IUDR Treatment: Hybridization mixtures each contained 5 mg/ml unlabeled RNA and approximately 0.01 µg/ml ^{3}H-MDV DNA (20,000 cpm) in a final volume of 0.5 ml. 100 µl samples were taken at various intervals up to 3 days. ●——● = Whole cell RNA; O——O = Polyribosome RNA

Rot = mole nucleotide RNA x seconds x liter^{-1}

The virus specific RNA found in the polyribosomes also increased following treatment of MKT-1 cells with IUDR (Fig.7), but the percent of virus specific RNA in the polyribosomal fraction remained approximately 70% of the virus RNA species from whole cells. It may be concluded that after treatment of MKT-1 cells with IUDR, although most of the MDV genome appears to be transcribed, there still remains a post-transcriptional control mechanism (or block) which excludes certain RNA transcripts from association with polyribosomes.

2.3b Transcription of virus genomes in tumors.

All MD tumors tested contained virus RNA as well as virus genomes. It should be noted that the virus genome transcription in these tumors

is restricted to 10-15% of the virus DNA, which is similar to the virus genome transcription obtained in MKT-1 cells. Transcription of the MDV genome in tumor tissues was examined further in regard to detection of viral specific RNA found in the polyribosomal fraction.

Polyribosomes were isolated from a portion of a lymphoid tumor of the spleen, induced by inoculation with MDV, and RNA was extracted. Another portion of the tumor was used to extract total cellular RNA. As shown in Figure 8, this spleen tumor contained RNA sequences homologous to 12% of the MDV DNA, showing the same degree of transcription of the viral genome as MKT-1 cells (Figure 7) and other tumors tested. The polyribosomes from this spleen tumor contained RNA sequences homologous to only 5-6% of the viral DNA. Therefore, the viral RNA transcripts in the polyribosome fraction of the spleen tumor represent only a portion of the RNA sequences found in the whole tumor.

To determine whether the viral specific RNA found in tumor tissues and MKT-1 cells were encoded by the same DNA sequences, total cellular RNA extracted from the above spleen tumor was mixed with RNA extracted from MKT-1 cells and hybridized to ^{3}H MDV DNA. If the viral RNA transcripts from these two sources were synthesized from different DNA sequences, the hybridization value of the mixture would be greater than 12-14%, i.e. greater than, or possibly the sum of, the values observed for the spleen tumor and MKT-cells. If the viral RNA sequences from the two sources were identical, the hybridization should exceed 14%. As the hybridization reached 12%, this indicates that the viral RNA transcripts in the spleen tumor were encoded by the same DNA sequences as the viral RNA transcripts in MKT-1 cells. Thus, these experiments indicate that transcriptional and post-transcriptional controls of latent virus genome in MKT-1 cells reflect those in MD tumors.

2.4 Virus DNA replication in synchronized MKT-1 cells

When MKT-1 cells were subjected to a double thymidine block, a high percentage of the cell population was synchronized. By using ^{3}H-thymidine uptake as a measure of the degree of synchronization, it is evident that about 70 to 80% of the cells were in synchrony and that cellular DNA synthesis took place between 2 and 4 hours after the removal of excess thymidine. In order to determine whether there is a specific period during the S phase when viral DNA replicates in MKT-1

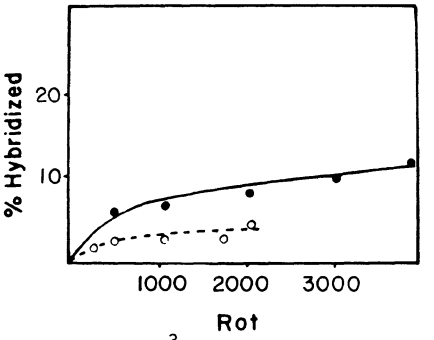

FIGURE 8. Hybridization of ^{3}H-MDV DNA with unlabeled RNA from an MD spleen lymphoma: RNA was extracted from a spleen lymphoma. Hybridization conditions were the same as described in Figure 7. ●——● = Hybridization with whole cell RNA; O----O = Hybridization with polyribosomal RNA.

cells, total cellular DNA was extracted from unlabeled MKT-1 cells at hourly intervals after thymidine removal and reassociated with a ^{3}H-MDV DNA probe. By assigning the number of virus genomes per cell at time 0 as 1 and expressing the rest of the sample relative to this, it can be seen that there was a 1.55 fold increase in the relative number of virus genomes during the first 2 hours after removal of thymidine. This finding indicates that latent virus DNA genomes replicate in the early state of the S period before cellular DNA synthesis actively begins. However, if all the latent virus genomes replicated in the early S phase before cellular DNA synthesis began the amount of virus DNA should have doubled, which was the case in EBV latent genome replication in Raji cells (13). The 1.6 fold increase of virus genomes in MKT-1 cells instead of a 2.0 fold increase may be due to some cellular DNA synthesis which had already occurred by the time of virus DNA replication. Part of the reason for not attaining a 2-fold increase may also be attributed to incomplete synchrony of MKT-1 cells. Thus, the data indicate that MDV DNA replication in MKT-1 cells occurs at a similar phase of the cell cycle as EBV DNA in Raji cells.

DISCUSSION

MDV DNA shares some common properties with the DNAs of other herpes-

viruses and is a linear, nicked, double-stranded DNA with a molecular weight of 100 to 110 x 10^6 (4, 17, 26). The genome of HVT DNA is slightly smaller than that of MDV DNA and is also a linear, double-stranded molecule with single-stranded break (17). The buoyant density of MDV DNA (1.705 g/cm^3) in a neutral CsCl gradient was slightly less than that of HVT DNA (1.707 g/cm^3) (17).

Serially-passaged MDV resulted in the production of virus with a lower density DNA (1.700 g/cm^3) (51). It has been reported that the undiluted passaging of HSV-1 resulted in the evolution of virus populations containing defective DNA molecules and exhibiting altered biological properties (52). The defective DNA in various strains of HSV-1 showed a density increase (52) or a density decrease in CsCl (42). The density increase in the defective HSV DNA is due to the fact that the defective DNA is composed of sequences in tandem arrangement present in the S region of standard virus DNA, which are GC rich (12). The term "defective virus", therefore, is tentatively used for the serially passaged MDV throughout the text. However, the defective nature of this virus remains to be proven by infectivity. Some of our MDV preparations accumulated defective virus rapidly in 6 to 7 passages. Generally serial passage of virus with a high multiplicity causes a rapid accumulation of defective virus as found in several herpesviruses, such as HSV (7,52), pseudorabies virus (40) equine herpesvirus,human cytomegalovirus (38) and herpesvirus saimiri (10). Due to the passage of a cell-associated virus, the appearance of defective MDV may not follow the general pattern. The accumulation of defective virus does not result from a high multiplicity of infection with cell-associated virus, since in the initially infected cells the ratio of defective virus and infectious virus remains the same regardless of the multiplicity of infection. Thus the low multiplicity of infection causes an increase in virus replication and reinfection until the total population of cell is infected, thereby establishing a higher probability of producing defective virus.

Under conditions where the ratio of the number of uninfected CEF to MDV-infected CEF was high, the synthesis of MDV DNA became detectable at 6 to 9 hours post-infection (h.p.i.) and reached a maximum at about 15 h.p.i. while enhanced incorporation of ^{3}H-thymidine into cellular DNA occurred later than initiation of MDV DNA synthesis and was detectable at 24 h.p.i. (18). Since oncogenic DNA

viruses in general stimulate cellular DNA synthesis (39), the stimulation of cellular DNA synthesis by MDV infection is an important feature and further investigations are required.

Electrophoresis of the digestion products of MDV DNA cleaved with restriction endonucleases revealed the presence of major and minor bands (17,27) which may indicate that MDV might have repeated or inverted repeat sequences. However, the treatment of MDV DNA with Sma, Sal 1 and Bam Hl yields fragments present mostly in equal molar ratio, and the sum of the molecular weights of the fragments produced by cleavage with each enzyme is approximately 100 x 10^6 (Table 1), which agrees with the reported molecular weight of MDV DNA (17,26). Digestion of MDV DNA with Sal 1 yields at least four fragments, B, C, D and E, present in submolar amounts. The molecular weight differences found in these fragments were 0.5 to 0.6 x 10^6. The differences may be due to the variation in the number of copies of a reiterated sequence, possibly tandem repeat units with molecular weight of 0.5 x 10^6. The treatment of MDV DNA with lambda exonuclease before cleavage with Sal 1 resulted in the disappearance of these Sal 1 fragments, as well as the H and I fragments, indicating that these fragments are near the termini of the MDV genome. As illustrated in Fig. 9, the B, C, D and E fragments may represent one end of the MDV DNA molecule while the H and I fragments represent the other end. It should be clarified further whether the tandem repeat units are located at the termini of MDV DNA or exist as internal repeated sequences in the possible terminal fragments.

A blotting hybridization study revealed that Bam A and Sma B fragments of MDV DNA preferentially hybridized with the Sal 1 terminal fragments, B, C, D and E, indicating that all of these fragments are located at the same end of the viral DNA. Heterogeneity in the size of the Sal 1 fragments was found only at one end of the DNA, but not at the other end. However, the degree of homology between terminal fragments of both ends of the MDV DNA should be examined. Recently an electronmicroscopic study (8) revealed that single strands of MDV and HVT DNAs showed single and double looped, fold-back structures, indicating the presence of inverted repeats as found in the structure of HSV DNA (43). However, fragments in 0.25 and 0.5 molar quantities were not found in any digested products of MDV DNA. This may imply that the structure of MDV DNA does not assume

the four different arrangements as in that of HSV DNA (]4, 46, 54). The presence of internal repeated sequences in MDV DNA was also shown by the fact that the terminal fragment, Bam A of MDV DNA, had some homologous DNA sequences with the internal fragments, Bam C. The internal repeated sequence could be located at the junction between S and L regions as illustrated in Fig. 9.

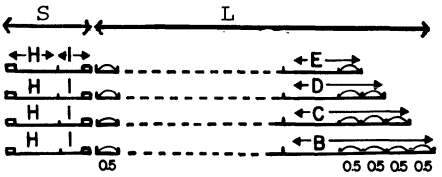

FIGURE 9. Maps showing the arrangement of terminal Sal 1 fragments of MDV DNA: The S and L regions of MDV DNA were tentatively located on the map, based on the data demonstrated by Cébrian, et al. (8). Open bars indicate that the terminal (TRs) or internal (IRs) inverted repeated sequences at the S region. The numbers (0.5) indicate the size, 0.5×10^6, of the tandemly repeated sequences in the L regions, and of the inverted sequences possibly located at the junction of the S and L regions.

Digestion of the defective MDV DNA did not generate any new bands and only two fragments, Sal 1 H and I, disappeared probably because the end of the missing portion is located close to the Sal 1 cleavage site. The Sal 1 H and I fragments are located at one end of the MDV DNA molecules and may be in the S region as illustrated in Fig. 9. The lighter density of the defective DNA might be due to the loss of the H and I fragments, which are probably GC rich. The mechanism for generation of defective DNA can be explained by the rolling circles after circularization of wild type virus DNA with Sal 1 H plus I fragments as a tail. The concatemers resulting from the proposed rolling circle type of replication might be cut apart and packaged in virions by a mechanism involving recognition of these defective DNA, as suggested in the mechanism for origin of defective HSV DNA (5).

The restriction endonuclease cleavage patterns of different strains of MDV or HVT were almost identical, but not between MDV and

HVT (17,27). Therefore, the pattern can be used for identification of these herpesvirus DNAs. The difference in restriction endonuclease cleavage patterns may not indicate the lack of DNA sequence homology between these two viruses. DNA-DNA reassociation kinetics and blotting hybridization techniques indicate that the DNA of these two viruses share 1 to 4% homology, equivalent to 1.5 to 6 coding genes (17,27). However, it is premature at present to speculate about whether these coding genes are related to the mechanism of vaccination with HVT against MD. Kaschka-Dierich, et al.,(21) reported that they could not find any homology between these two virus DNAs using blotting hybridization with the viral complementary RNA. It is possible that the homologous sequences between these two virus DNAs might not be transcribed in vitro by bacterial polymerase under certain conditions.

The latent state of oncogenic herpesvirus DNA, such as EBV (1, 33) and herpesvirus saimiri (53) has been well documented. Studies on the status of latent EBV DNA in nonproductive Raji cells, derived from a Burkitt's lymphoma patient, revealed that the majority of virus genomes, if not all, are not covalently integrated into cellular DNA (33, 48) and exist as a circular plasmid DNA (2,29). Although some virus DNA in the transformed cells may likely be integrated linearly into cellular DNA, definite evidence has not been obtained mainly due to the technical difficulty in separation of the viral DNA from cellular DNA. Since at least 80 to 90% of the MDV genomes in non-productive MKT-1 cells exist as circular plasmid DNA, the latent state of MDV seems to be similar to that of EBV DNA in Raji cells. At present it is difficult to prove technically that the rest of the latent MDV genome may be integrated into cellular DNA unless a more sensitive technique such as blotting hybridization is used. Recently, it has been reported that a large proportion of MDV DNA in MD lymphoblastoid cell lines is integrated into the cellular DNA (22). This conclusion is based mainly on data from analysis in CsCl density gradients which might produce confusing results due to the similar densities of viral and cellular DNA, as well as the presence of defective virus DNA of 1.700 g/cm^3. It is possible, however, that the latent MDV genome may exist in a different status in different cell lines. Since the circular state of herpesvirus DNA in transformed cells was demonstrated in cells transformed by EBV or herpesvirus

saimiri, as well as by MDV, the circular plasmid form may be responsible for maintenance (or initiation) of herpesvirus transformation.

Several lymphoid tumors from MDV-infected chickens and nonproductive MKT-1 cells contain copies of the MDV genome but are free of MD antigens and virus particles (31, 32, 50). These cells serve as a model to examine the mechanism(s) involved in the control of expression of MDV genetic information in transformed cells where there is no evidence for viral replication (44, 45).

Analysis of DNA-RNA hybridization revealed that in productively infected CEF 45% of the MDV DNA template of 90% of the viral genome was transcribed if only the coding strand of double-stranded DNA is copied. Whereas, in all tumors tested and in MKT-1 cells transcription was restricted to 12 to 14% of the viral DNA template. Thus, the expression of viral DNA in the transformed cells is controlled by the synthesis of RNA from a restricted portion of the viral genome. When MKT-1 cells were treated with IUDR, viral early antigens were produced and 42% of the viral DNA template was transcribed, but productive infection did not follow. The artificial mixture of RNAs extracted from MKT-1 cells and spleen tumor cells hybridized with the same portion of MDV DNA indicating that the viral RNAs transcribed in the MKT-1 cells and spleen tumor tissues are encoded by the same DNA sequences. The virus specific RNA sequences found in the polysomes of MKT-1 cells were encoded from 8 to 10% of the viral DNA and in the spleen tumor only 5%. In contrast, all virus-specific RNA sequences transcribed from 45% of the MDV DNA were found in the polyribosome fraction in CEF productively infected with MDV. This result suggests the existence of a post-transcriptional control mechanism by which RNA sequences are selected for transfer to polyribosomes for translation. The transfer of a restricted portion of viral specific RNA to polyribosomes was also demonstrated in nonproductive EBV infected lymphoblastoid cell lines (15) and in hybrid cells (49). The persistence of HVT genomes, as well as the MDV genome, has been found in a lymphoblastoid cell line established from HVT vaccinated chickens (19). The presence of MATSA, which is expressed on MDV transformed cells (30, 56), was demonstrated on the spleen and peripheral blood lymphocytes of HVT vaccinated chickens (24,37,41), as well as on these HVT-associated transformed cells. Thus, it is important to study the state

and genetic expression of resident HVT genomes in the transformed cells.

The finding (25) that the resident MDV genomes in MKT-1 cells replicate in the early stage of the S period, prior to the onset of active cellular DNA synthesis, suggests that this event is under a stringent control mechanism by which the latency of viral genomes is controlled. The latent EBV genomes in nonproductive RAji cells also replicate during the early S phase. This implies that the same mechanism of viral latency may be operative in both MDV and EBV transformed cells.

ACKNOWLEDGMENTS

We thank Dr. Mary SMith for valuable suggestions in the preparation of this manuscript.

This work was supported by a contract (No. 1 CP33205) from the National Cancer Institute under the Virus Cancer Program.

REFERENCES

1. Adams, A., Lindahl, T., and Klein, G. (1973). Proc. Natl. Acad. Sci. USA 70, 2888-2892.
2. Adams, A. and Lindahl, T. (1975) Proc. Natl. Acad. Sci. USA 72, 1477-1481.
3. Akiyama, Y. and Kato, S. (1974). Biken's J. 17, 105-116.
4. Bachenheimer, S.L., Kieff, E.D., Lee, L.F. and Roizman, B. (1972). In: Oncogenesis and Herpesviruses (Ed. P.M. Biggs), IARC Scientific Publications No. 2, pp. 74-81.
5. Becker, Y., Asher, Y., Weinberg-Zahlering, E., Rabkin, S., Friedmann, A., and Kessler, E. (1978). J. Gen. Virol. 40,319-335.
6. Biggs, P.N., Payne, L.N., MIlne, B.S., Churchill, A.E., Chubb, R.C., Powell, D.G., and Harris, A.H. (1970) Veterinary Record 87, 704-709.
7. Bronson, D.L., Dressman, G.R., Biswal, N. and Benyesh-Melnick, M. (1972). INtervirology 1, 141-153.
8. Cebrian, J., Kaschka-Dierich, C., Berthelot, N. and Sheldrick, P. (1979). The Fourth Cold Spring Harbor Meeting on Herpesviruses, Cold Spring Harbor (abstract).
9. Cho, B.R., (1977). Avian Diseases 22, 170-176.
10. Fleckenstein, B., Bornkamm, G.W. and Ludwig, H. (1975). J. Virol. 15, 395-406.
11. Frenkel, N. and Roizman, B. (1972). Proc. Natl. Acad. Sci. USA. 69, 2654-2658.
12. Frenkel, N., Locker, H., Batterson, W., Hayward, G.S. and Roizman, B. (1976). J. Virol. 20, 527-531.
13. Hampar, B., Tanaka, A., Nonoyama, M. and Derge, J. (1974). Proc. Natl. Acad. Sci. USA 71, 631-633.
14. Hayward, G.S., Jacob, R.J., Wordworth, S.C. and Roizman, B. (1975). Proc. Natl. Acad. Sci. USA, 72, 4243-4247.
15. Hayward, S.D. and Kieff, E.D. (1976). J. Virol. 18, 518-525.

16. Henry, B. E., Newcomb, W. W., and O'Callaghan, D. J., (1979). Virology 92, 495-506.
17. Hirai, K., Ikuta, K., and Kato, S., J. Gen. Virol. in press.
18. Hirai, K., Ikuta, K., and Kato, S., Avian Diseases, in press.
19. Hirai, K., Kitamoto, N., Ikuta, K., and Kato, S., (1979). The Fourth Cold Spring Harbor meeting on Herpesviruses. Cold Spring Harbor (abstract).
20. Jacob, R. J., Morse, L. S., and Roizman, B., (1979) J. Virol. 29 448-457.
21. Kaschka-Dierich, C., Bornkamm, G. W., and Thomssen, R., (1979) Medical Microbiology and Immunology 165, 223-239.
22. Kaschka-Dierich, C., Nazerian, K., and Thomssen, R., (1979). J. Gen Virol. 44, 271-280.
23. Kato, S., and Akiyama, Y., (1975). In Oncogenesis and Herpesviruses II (Eds. G. de-The, M. A. Epstein and H. zur Hausen). IARC Scientific Publications No. 11, Lyon, pp.101-108.
24. Kitamato, N., Ikuta, K., Kato, S., and Yamaguchi, S., (1979) Biken's J. 22, 11-20.
25. Lau, Y. R., and Nonoyama, M., J. Virol. in press.
26. Lee, L. F., Kieff, E. D., Bachenheimer, S. L., Roizman, B., Spear, P. G., Burmester, B. R., and Nazerian, K., (1971). J. Virol. 7, 289-294.
27. Lee, Y. S., Tanaka, A., Silver, S., Smith, M., (1979). Virology 93, 277-280.
28. Lee, Y. S., and Nonoyama, M., manuscript in preparation.
29. Lindahl, T., Adams, A., Bjursell, G., Bornkamm, G., Kaschta-Kierich, C., and Jehn, U., (1976). J. Mol. Biol.102, 511-530.
30. Matsuda, H., Ikuta, K., Maiyamoto, H., and Kato, S., (1976). Biken's J.19, 119-123.
31. Nazerian, K., Lindahl, T., Klein, G., and Lee, L. F., (1973). J. Virol. 12, 841-846.
32. Nazerian, K. and Lee, L. F., (1974) J. Gen. Virol., 25, 317-321.
33. Nonoyama, M., and Pagano, J. S., (1972). Nature New Biology 238, 169-171.
34. Onuma, M., Mikami, T., and Hayashi, T.T.A., (1974). J. Natl. Cancer Inst. 52, 805-813.
35. Payne, L. N., Powell, P. C., Rennie, M. C., and Ross, L. J. N., (1978). Avian Pathology, 7, 427-432.
36. Powell, P. C., Payne, L. N., Frazier, J. A., and Rennie, M. T., (1974). Nature 251, 79-80.
37. Powell, P. C., and Rennie, M., (1978). Vet. Rec. 103, 232-233.
38. Ramirez, M. L., Virmani, M., Garon, C., and Rosenthal, L. J., (1979). Virology 96, 311-314.
39. Rapp, F., and Li, J. L. H., (1974). Cold Spring Harbor Symp. Quant. Biol. 39, 747-763.
40. Rubenstein, A. S., and Kaplan, A. S., (1975). Virology 66, 385-392.
41. Schat, K. A., and Calnek, B. W., (1978). J. Natl. Cancer Inst. 61, 855-857.
42. Schroder, C. H., Stegmann, B., Lauppe, H. F., and Kaerner, H. C., (1975). Intervirology 6, 270-284.
43. Sheldrick, P., and Berthelot, N., (1974). Cold Spring Harbor Symp. Quant. Biol., 39, 667-678.
44. Silver, S., Smith, M., and Nonoyama, M., (1979) J. Virol. 30, 84-89.
45. Silver, S., Tanaka, A., and Nonoyama, M., (1979) Virology, 93, 127-133.

46. Skare, J. and Summers, W.C. (1977) Virology, 76, 581-595.
47. Southern, E.M. (1975). J. Mol. Virol. 98, 503-512.
48. Tanaka, A., and Nonoyama, M. (1974). Proc. Natl. Acad. Sci. USA, 71, 4658-4661.
49. Tanaka, A., Nonoyama, M. and Glaser, R. (1977) Virology 82, 63-68.
50. Tanaka, A., Silver, S. and Nonoyama, M. (1978) Virology 88, 19-24.
51. Tanaka, A., Lee, Y-S. and Nonoyama, M., submitted.
52. Wagner, M., Skare, J. and Summers, W.C. (1974). Cold Spring Harbor Symp. Quant. Biol. 29, 683-686.
53. Werner, F.J., Bornkamm, G.W. and Fleckenstein, B. (1977). J. Virol. 22, 794-803.
54. Wilkie, N.M. and Cortini, R. (1976). J. Virol. 20, 211-22.
55. Witter, R.L., Nazerian, K., Purchase, H.G. and Burgoyne, G.H. (1970) Am. J. Vet. Res. 31, 525-538.
56. Witter, R.L., Stephens, E.A., Sharma, J.M. and Nazerian, K. (1975). J. Immunol. 115, 177-183.

INDEX